SEISMIC INTERPRETATION OF THE SOUTHERN UPLANDS TERRANE

by

ZAYD A. R. KAMALIDDIN

B. Sc. University of Baghdad, M. Sc. Glasgow University

Thesis submitted for the degree of Ph. D. (by research) at the University of Glas-gow, Department of Geology and Applied Geology, 1991.

ProQuest LLC.
789 East Eisenhower Parkway
P.O. Box 1346
Ann Arbor, MI 48106 – 1346

To Ikbal, Rasha and Ali with all my love

DECLARATION

The material presented in this thesis is the result of research carried out between October 1988 and August 1991 in the Department of Geology and Applied Geology, University of Glasgow, under the supervision of Dr J. J. Doody.

This thesis is based on my own independent research and any published or unpublished material used by me has been given full acknowledgement in the text.

Zayd Kamaliddin

J. J. Doody

(Supervisor)

Department of Geology and Applied Geology,

University of Glasgow, Glasgow.

ACKNOWLEDGEMENTS

It will be very difficult for me to thank all the people who helped me finish this work because simply I do not know where to start.

Professor Leake is not only thanked for allowing me the use of the departmental facilities, but also for his moral support and encouragement when I was on the verge of abandoning this project.

The members of staff who stood by our side, my wife and I, and provided us with the moral and financial support which helped us through our very difficult times. To each one of them I would like to say thank you, you are part of this work and your help will never be forgotten. The same goes for my fellow-Arab postgraduate students who are all thanked for their support financially and otherwise.

Dr. J.J Doody **(Ben)** is thanked for supervising this work and for his enthusiastic and constructive discussions. Without his constant *pressure* and help this work would not have materialised. I would like especially to thank him for the time he devoted in the last few months in helping to finish the project. To him I owe a great deal.

This project benefitted considerably from discussions with Professor Bluck and Dr. Haughton who provided me generously with their scientific advice and new ideas. Dr. C. Farrow is thanked for his consistent help and advice regarding the computing facilities.

I would like to present my sincere appreciation and gratitude to Professor Russel, Dr. Jardine, Dr. Gribble and Dr. Rikabi for their help and support.

The co-operation and sincere help of the quarry managers and the numerous land owners is much acknowledged and appreciated.

Many thanks are due to Mr. R.T. Cumberland who never hesitated in providing me with any help required during both this project and an earlier M.Sc. pro-

ject. The most complicated figures of this thesis are a great testimony to his creativity. I am indebted to Mr. R. Morrison for supplying, almost, everything he can. Messers G. Gordon and E. Speirs are both thanked, the former for maintaining the seismic recording sets and the latter for providing me with the vehicles for my fieldwork.

I would like to thank all my family, my wife Ikbal, my daughter Rasha and my son Ali, for their keen support, consideration and love. Ikbal is also thanked for waking up, early on cold mornings, to prepare food for my fieldwork.

Finally, I cannot end these acknowledgments without remembering and thanking the two persons to whom I owe simply everything, my father Rasool and my mother Frida. I thank you both, extending all my love and respect hoping that one day we meet.

CONTENTS

LIST OF FIGURES

SUMMARY

The Southern Uplands Network (SUN) project comprised 5 wide-angle seismic profiles recorded in the Southern Uplands of Scotland using quarry blast sources. Four profiles trend N-S across regional strike and the fifth is parallel to it. A sixth profile was recorded, in the north of the Midland Valley, along the axis of the Strathmore Syncline to establish the basin-basement relationships in that area.

A large and good quality dataset was acquired which was then processed using the available facilities and computer software to obtain the final models by deploying the appropriate interpretation methods.

P-wave velocities of 5.25-5.65 km/s were modelled for Lower Palaeozoic sediments in the Southern Uplands. P-wave velocities of 4.3-4.5 km/s were assigned to minor Upper Old Red Sandstone deposits.

Crystalline basement of 6.0-6.1 km/s was detected beneath the NE Southern Uplands, suggesting continuation of Midland Valley basement southwards at a depth of 2.8-3.2 km. However, the SUN suggests that this basement does not extend along strike in the Southern Uplands towards the SW, where an "intra-sedimentary" refractor (5.8 km/s) is detected, perhaps of Ordovician age, at 1.0-2.0 km depth. It may be the missing forearc proposed by some authors.

Throw on the Southern Uplands Fault is varied. In the NE it downthrows northward; in the SW downthrow southward is inferred.

Three E-W trending faults (the Leadhills Line, Kingledores Fault and Hartfell Line) offset crystalline basement beneath the Southern Uplands. Previously these

were interpreted as tract bounding faults, characteristic of an accretionary prism. SUN reveals a more important tectonic role for them, perhaps being locations for amalgamation of terranes forming the Southern Uplands. SUN did not image any accretionary prism tract bounding faults. The observed faults suggest a stepped, rather than dipping, crystalline basement underlying the Southern Uplands. These faults also offset the intra-sedimentary refractor.

Previous work established Midland Valley basement as essentially flat, with faults mapped at surface soling out at detachments above this basement, and that it extends south unaffected by the Southern Uplands Fault. SUN shows this basement to be offset by faults in the southern Midland Valley (e.g. Henshaw, Pentland, Kerse Loch and Southern Uplands Fault). In the northern Midland Valley NW-SE trending faults also offset basement causing a step-like pattern. Top crystalline basement exists at 2.0-4.9 km depth here being shallower in the NE. SUN confirmed velocity ranges already established for the Midland Valley upper crust.

It is argued that the SUN provides strong evidence against the Southern Uplands being a complete accretionary prism. The following models may be invoked:

[1] Accretionary prism slice thrust over Midland Valley-type crystalline basement.

[2] Juxtaposition of a number of terranes along major faults interpreted by SUN.

[3] A thrust stack.

INTRODUCTION

The Southern Uplands Network (SUN) project was designed to cover the Southern Uplands with a network of seismic refraction profiles trending across the regional strike. The main problems to be tackled in this project were to:

[1] Establish the nature and structure of the crystalline basement to the Southern Uplands.

[2] Ascertain if this basement is an extension of the Midland Valley basement.

[3] Determine the role and nature of the Southern Uplands Fault. Is it a terrane boundary, or of some other significance?

[4] Determine the behaviour of faults within the Southern Uplands and southern Midland Valley ?terranes.

These are problems which have inspired many workers to envisage a wide variety of models for the Southern Uplands area. Of particular interest is the effect on this basement of the major faults which are mapped at the surface, such as the Kingledores Fault and the Hartfell and Leadhills Lines (in the Southern Uplands), and the Pentland and Kerse Loch faults in the southern Midland Valley.

Within the Southern Uplands the E-W trending faults were considered as only tract bounding faults and not as major dislocations in the region. The recorded profiles, have uncovered valuable information about these structural features, some of which extend deeper than previously thought. The nature of some of these structures will be evaluated within the constraints of the available data.

Many previous workers presented different models for the Southern Uplands. The dataset acquired by this project presents a valuable opportunity to resolve uncertainties and/or to put forward new ideas where old models prove to be invalid.

In the NE corner of the Midland Valley, in the Strathmore Syncline, an additional unreversed profile was recorded with the aim of developing a previous model presented by the author for the area to the immediate south of the syncline. This profile trends parallel to the axis of the syncline and it was anticipated that, since it is the first seismic profile in this area, the main structural and seismic relationships could be established, such as the major faults within the syncline and the velocity structure of the main stratigraphic units. This profile enabled the author to establish a new view of the basement in the north of the Midland Valley by integrating the results with those available from previous work.

A network of wide-angle seismic profiles was recorded across the designated areas and the data were processesd using the facilities available at the Geology & Applied Geology Department, Glasgow University. The processed data were then modelled by the application of methods such as WHB inversion, planar layer, plus-minus and raytracing and the final models then presented.

For ease of reference and due to the large amount of figures presented in this work, they are presented at the end of the thesis, rather than being dispersed through the thesis and so greatly fragmenting the text. It is important to note that shots located in the south of the project area are plotted at the left end of the figures and those in the north are drawn at the right end. All the digital seismic sections are plotted with a reduction velocity of 6 km/s. Station numbers are presented in multiples of 5 and where extra recording points were used they are given the preceding station number with "a" as a suffix.

CHAPTER ONE

GENERAL REVIEW OF GEOLOGY AND GEOPHYSICS

1.1. Introduction

Development of the plate tectonic concept has led to the production of many models for the synthesis of the Southern Uplands within the general framework of the British Caledonides. These models varied from a simple accretionary prism hypothesis to a more complicated scenario of a group of amalgamated terranes constituting the region. The purpose of the Southern Uplands Network "SUN" is to add to the understanding of the upper crustal structure and the velocity distribution in the Southern Uplands of Scotland. Determination of the type, origin, velocity and depth of the basement underlying the assumed accretionary prism is of the utmost importance in understanding whether this prism was formed by simple subduction or was emplaced in its present position by strike-slip movement or thrusting. It is also hoped that using data acquired by the SUN project, the main structures and faults in the Southern Uplands and in the south of Midland Valley can be further assessed and a dependable model of their nature can be presented.

Because of the large number of models available and their diversity, a general review of the most important seems to be inevitable before any attempt to study this region can be made. In addition to this account, the geological and geophysical setting of the area will be presented without any particular emphasis on any certain location within the Southern Uplands since the seismic data acquired during this project cover the whole region in general.

There is general agreement that the Southern Uplands *'terrane'* in its present-day geographic configuration is the product of the closure of the Iapetus Ocean, and the consequent Caledonian orogeny.

1.2. Closure of a Proto-Atlantic Ocean (Iapetus) and its implications:

After the geosynclinal synthesis of Jones (1938), which was the first major model for the British Caledonides, modelling of this orogenic event has progressed from a relatively simple conceptual framework of two converging plates, *Laurentia* and *Baltica* represented by the Canadian and Baltic Shields respectively, with a single suture, to more complicated models involving several plates, many terranes and large strike-slip motions. These two major continents were separated, presumably, during the Proterozoic and joined along the suture line in the Silurian - Devonian times.

Wilson (1966) had suggested that a proto-Atlantic Ocean was bounded by an American continent which included most of Scotland and northern Ireland, and a European continent which included the rest of Britain. This ocean closed in the late Ordovician to form a single continent, then much later, began to open again during the late Mesozoic but along a different suture to form the present-day Atlantic. This interpretation initiated a great deal of research to explain the relationships between ancient America and Europe and the Ordovician closure of the Iapetus ocean.

Following Wilson's ideas, Dewey (1969, 1971), who was the first to propose a model for the development of the Iapetus in terms of plate tectonics, extended the hypothesis suggesting that Scotland north of the Southern Uplands and the northern part of Ireland were part of the north American continent where the Midland Valley was considered to be a continental margin, transitional between continental and oceanic crust. The Girvan-Ballantrae ophiolite, in the SW Midland Valley, was interpreted as an upthrust relic of an ancient northward-dipping

Benioff zone composed of oceanic crust and mantle with a marginal basin origin (Fig. 1.1a).

Further to the south, the Southern Uplands was believed to have been a remnant of the proto-Atlantic ocean, formed during late Ordovician-Silurian times and composed of oceanic crust covered by flysch sediments. Bordering this ocean fragment in the south, the European continent was believed to be similarly bounded by earlier and later Benioff zones dipping in a southeasterly direction.

Fitton & Hughes (1970) adopted Dewey's model with some modifications where they envisaged a southerly dipping Benioff zone which originated in an oceanic trench centred upon the Moffat (Southern Uplands) geosyncline and extended beneath an island arc situated in the Lake District and Wales.

Powell (1971) criticised both models presenting powerful geophysical evidence (magnetic and gravity) suggesting that the Southern Uplands is underlain by continental, not oceanic, crust of Lewisian type basement with a normal continental thickness of 30 km, and therefore it could not represent a proto-Atlantic remnant ocean. This led to the alternative interpretation of gravity data by Gunn (1973) which indicated that the Midland Valley of Scotland to the north corresponds to a gravity high, and that this, rather than the Southern Uplands, could be the remnant of the proto-Atlantic ocean, where two subduction zones occur, one dipping to the northwest located in the Highland Border ophiolites and the other, dipping in southeasterly direction and located in the Girvan-Ballantrae area (Fig. 1.1b).

Church & Gayer (1973) suggested that the Girvan-Ballantrae ophiolites and those in northern Newfoundland originated on the northwestern side of the Iapetus ocean in association with a northwest-dipping Benioff zone (Fig. 1.1c).

Mitchell & McKerrow (1975) compared the Scottish Caledonides with the Tertiary Burma orogen and suggested that while the proto-Atlantic ocean was still in existence in the late Ordovician, Benioff zones were dipping northward beneath

the Southern Uplands and Girvan composed of oceanic crust. Turbidites were shed from the north and piled into a thick series of thrust sheets, as subduction resulted in northward movement of the oceanic crust. Final continental collision took place in the Lower Devonian and three structural belts were formed instead: (1) Highlands beneath which there was continental crust, (2) the Midland Valley with thick sediments and volcanics underlain by oceanic or thin continental crust, and (3) the Southern Uplands underlain by oceanic crust.

Williams (1975) carried out a cluster analysis of the distribution of faunal colonies and deduced that the Iapetus ocean was still in existence in early Ordovician times but mixing of faunal animals took place at late Ordovician when the two continents were sutured together. By studying pelagic animal distribution, McKerrow *et al.* (1976) estimated the rate of subduction during the Ordovician and the width of the Iapetus ocean at that time, which was envisaged to be 2000-3000 km at the end of the Ordovician. They concluded that final continental collision took place after the Lower Devonian rocks were formed. These estimates contrast with those of Phillips *et al.* (1976) who estimated the width of the Iapetus ocean to be only 600-800 km in early Ordovician.

Wright (1976) endorsed a more tectonically vigorous regime of alternating subduction of oceanic crust in two opposing directions (cyclic), to the northwest and to the southeast, causing orogenic phases associated with each individual cycle. The Caledonian orogen marked the closure of the Iapetus ocean and consequent continental collision in Silurian to mid-Devonian times. No palaeomagnetic evidence is available to support this hypothesis. Moseley (1976), who in questioning the validity of the model of an accretionary prism for the Southern Uplands had summarised the different models available, envisaged a late Silurian continental collision with the Southern Uplands underlain by continental crust.

Dewey & Shackleton (1984) predicted a late Silurian to mid-Devonian diachronous closure of the Iapetus ocean with a sinistral strike-slip motion of 1000

km for the Midland Valley and the Southern Uplands involving a triple-junction complex in the North Sea area between an *Avalonia* microcontinent and a semi-consolidated Laurentian/Baltic continent.

Soper & Hutton (1984) proposed a similar model for the closure of the Iapetus ocean invoking a triple-junction for the final continental collision involving the originally sutured continents, Laurentia and Baltica, and a third southerly oriented arm represented by *Cadomia* with sinistral sense of motion (Fig. 1.1d), these events taking place in late Silurian-early Devonian times. In their model they envisaged two subduction zones, one towards the north and the other towards the south, and they concluded that sinistral displacements represent a distinct tectonic regime later than the main Caledonian events, a conclusion which was also endorsed by Watson (1984). This accretion of Cadomia onto the already sutured Laurasian plate produced the *nonmetamorphic Caledonides* of Britain during the early Devonian.

This model was supported by Gibbons & Gayer (1985) who were the first workers to suggest that the British Caledonides consists of a collage of suspect terranes juxtaposed together by strike-slip motion instead of a simple continent-continent collision. However the timing of the final continental collision of *Avalonia* (England, Wales, South Ireland, eastern Newfoundland, Nova Scotia, coastal New Brunswick and coastal New England) into Laurentia-Baltica was later reviewed by Soper *et al.* (1987) and McKerrow (1988a, 1988b) and McKerrow & Soper (1989) and was ascribed to late Lower Devonian times rather than end-Silurian.

Hutton (1987), following the ideas of Soper & Hutton and Gibbons & Gayer, stressed the importance of sinistral strike-slip movements which took place after the suturing of the ancient continents in the end Silurian to mid Devonian times and so rearranged the group of *dissociated terranes* that comprises the British Isles. An Ordovician closure of the Iapetus ocean is suggested followed by the

formation of a Silurian successor basin across the Laurentia and Gondwanaland microcontinents to the south. Furthermore, he proposed that by the end of the Silurian, Gondwanaland, rotating in a clockwise manner, carried Laurentia into collision with Baltica creating a major sinistral strike slip zone disrupting the palaeogeography of the British Isles, although Lefort *et al.* (1988) suggest the middle Devonian-Carboniferous times for the final suturing of these continents.

Hutton concluded that this zone contains many different terranes representing a *suture zone* rather than a single Iapetus suture. An important aspect of Hutton's interpretation for this project is that he considers the Southern Uplands as a group of terranes brought together by large scale strike-slip movements, instead of the usual synthesis of scraped off crustal slivers stacked together by thrusting to form an accretionary prism (e.g. Leggett *et al.* 1979b).

Using faunal distribution analysis, the presence of these three continents and their Ordovician separation was also envisaged by the work of Cocks & Fortey (1982) and Fortey & Cocks (1988) who also suggested the presence of other oceans such as the *Tornquist Sea* to the east of England and the *Rheic Ocean* to the south.

Mason (1988) agrees with the Dewey & Shackleton model for the presence of a triple junction in the North Sea involving the three continents (see also Jacob *et al.* 1985) and with Hutton's suggestion of the presence of dissociated terranes. He also agrees about the Middle Silurian suturing of Laurentia and Baltica and argues that this suturing left the North Sea region as an embayment at their margin and allochthonous terranes docked into this embayment from the southwest from Silurian to Devonian times (e.g. Grampians, Southern Uplands and North England). Therefore diversity of petrology, geochemistry, sense of subduction, and times of construction and obduction of the British fragments means they can only be marginal to a much wider ocean (Proto-Tethys), rather than the Iapetus that separated Laurentia and Baltica from Gondwanaland. He suggests that the

name Iapetus should be confined to the region between the former two continents and not be extended into Britain and North America across the North Sea triple junction.

Soper (1988) developed the Soper & Hutton (1984) model. He acknowledged the importance of the concept of terrane accretion (see Bluck 1985), and that more than two continents were involved in the final collision with additional number of terranes entrapped in between and juxtaposed by strike-slip motion. He suggested a model which is summarised below:

[1] The Caledonian-Appalachian orogen had a Y-shaped configuration whose arms, which intersect near Britain in the North Sea (Fig. 1.1e), mark collision sutures between elements derived from three continental plates: Laurentia, Baltica and Gondwana.

[2] Laurentia and Baltica collision took place in late Silurian-early Devonian times producing the *Scandian orogeny*, while northward accretion of the Cadomia terrane (a terrane detached from Gondwana and consisting of two amalgamated terranes; Armorica and Avalonia) onto Laurentia-Baltica occurred in early Devonian times.

[3] The late Caledonian structures of north Britain indicate sinistral, not dextral, transpression movement in disagreement with the interpretation of Phillips *et al.* (1976).

[4] Subduction of Iapetus oceanic lithosphere beneath the southern margin of Laurentia took place in early to mid-Silurian times, or even later.

[5] Large sinistral displacements on faults within the Southern Uplands (e.g. the Kingledores fault) implies that the now juxtaposed northern, central and southern belts of the complex (see later) were once widely separated.

[6] There are two distinct Caledonian convergence regimes: the main Caledonian orogeny of the NW Highlands and the later transpression event.

[7] Terrane accretion is a primary cause of orogenies. The final model of his interpretation is illustrated in Figure 1.1f.

From the above mentioned models, the following criterion should be emphasised in relation to this project:

[1] Three continents existed in late Pre-Cambrian to Palaeozoic times and were separated by one large ocean named Iapetus (Harland & Gayer 1972) and possibly two other smaller oceans (the Rheic Ocean and Tornquist Sea).

[2] Oblique continental convergence (Lambert & McKerrow 1976, Phillips *et al.* 1976, Johnson *et al.* 1979, Stone *et al.* 1987, Kemp 1987) led to suturing along a line which trends NE-SW through Britain and its postulated location is in the vicinity of the Solway Firth (Phillips *et al.* 1976, Leggett *et al.* 1979, Dewey 1982, Soper 1988, McKerrow & Soper 1989). Allen (1987) does not agree with this location and suggests a more southerly location of the suture line in northern England to the immediate south of the study area, while Gunn (1973) suggested that the Midland Valley marks the position of the Iapetus suture.

[3] A number of lithospheric fragments or terranes were involved in this collision and were juxtaposed together along strike-slip faults by sinistral strike-slip motion. Elders (1987, 1989), using petrographic studies of granite clasts in conglomerates from the Southern Uplands, suggested that the region was situated SE of Newfoundland in the late Ordovician. Also sedimentary provenance of conglomerate clasts along both margins of the Midland Valley indicate that different terranes were present to the north and south of the Midland Valley and that later movements brought the terranes into their present configuration (Upton *et al.* 1984, Bluck 1983, 1984).

McKerrow (1988) inferred that a total of 1500 km of sinistral strike-slip motion took place in late Ordovician times bringing the Southern Uplands to its present position. This movement is divided between the three major faults

in northern Britain: the Great Glen, Highland Boundary, and Southern Uplands Faults. He also argued that sinistral shear might have taken place within the Grampian, Midland Valley and Southern Uplands terranes thus reducing the net movement along the faults to as little as 300 km. Shackleton (1979) and Soper (1988) agree with this figure, while McKerrow & Cocks (1986) estimate this strike-slip movement to be only 100-200 km and Bluck (1984) to be <500 km. It is thought that these movements persisted until the early Devonian. It is worth mentioning here that Phillips *et al.* (1976) suggested dextral rather than sinistral movement of about 1000 km for Scotland during the closure of the Iapetus.

These conclusions were supported by work done using palaeomagnetic measurements in Laurentia and Baltica and in the Caledonian-Appalachian orogen. Trench *et al.* (1989) using APWP data from the Grampian, Midland Valley and Southern Uplands terranes confirmed that these three terranes behaved as a single entity from Siluro-Devonian times and were positioned at low southerly latitude in Ordovician times close to the southern Laurentian margin (see also Briden *et al.* 1988).

1.3. The Southern Uplands: An Accretionary Prism ?

From the previous account the important question is: where does the Southern Uplands terrane fit in this scenario of colliding continents and transported terranes?

Before answering this question it is important to present a simplified account of the accretionary prism concept. An accretionary prism is formed when a thick sedimentary cover exists on an ocean plate entering a subduction zone. Packets of sediments are sequentially accreted onto the edge of the fore-arc. Continuing accretion is from beneath, under the toe of the aggrading prism, in slices bounded by gently continent-dipping thrust faults. As the process continues at the toe, the

earlier formed slices are steepened by backward rotation, and the slices undergo internal deformation by folding and cleavage formation. Prolonged accretion gives rise to a ridge feature, the trench slope break, which may become emergent above sea level.

Geometrical configurations of accretionary prisms can be varied depending on the following factors:

[1] Angle and rate of subduction.

[2] Amount of sediments present in the trench.

[3] Tectonic history.

Many diverse ideas were suggested concerning the evolution of the northern continental margin during the closure of the Iapetus ocean and the formation of the Southern Uplands (e.g oceanic relic, accretionary prism, suspect terrane) on the NW margin of the Iapetus suture during the Lower Palaeozoic. Dewey (1969) presented the first plate-tectonic model for the British Caledonides dividing them, along the Highland Boundary Fault, into a metamorphosed *orthotectonic zone* to the north and a *paratectonic zone* to the south. The latter was considered to be unmetamorphosed until the discovery of low-grade regional metamorphic rocks of prehnite-pumpellyite facies (Oliver & Leggett 1980). Dewey regarded the Southern Uplands as the final remnant of the Iapetus ocean which was composed of oceanic crust. He later revised this model suggesting that the region lay to the south of the trench (Dewey 1971, 1974 and also Church & Gayer 1973). On the other hand, Gunn (1973), followed by Jeans (1973), considering the possibility that the Southern Uplands is underlain by continental basement, interpreted the region as part of the southern continental margin during the closure of the Iapetus ocean.

Phillips *et al.* (1976), who invoked the idea of a NW dipping subduction zone positioned beneath the Southern Uplands accretionary prism, concluded that oblique collision caused dextral strike-slip motion bringing the Southern Uplands next to the Lake District, although both have different collision histories. Final

continental collision took place in Late Ordovician times. However, Johnson *et al.* (1979), agreeing with the oblique collision hypothesis, expressed many doubts (based on geophysical and sedimentological evidence) about the need for such large scale dextral displacement along the Solway Line to juxtapose the Southern Uplands with the Lake District. They also disagreed on the timing of the continental collision suggesting that it took place in Late Silurian-Devonian times.

McKerrow *et al.* (1977) interpreted the Southern Uplands as an accretionary prism formed on the northern margin of the Iapetus ocean composed of different zones which were originally separated and then brought tectonically together by sheet transportation to form an imbricate thrust structure. The emergent "*Cockburnland*" rise in the north of the region supplied sediments to the Midland Valley in the north and the ocean to the south during early Silurian. They visualized the structure as dominated by listric faults which converge downwards to a basal detachment. The thrusts have propagated in sequence from north to south, and as younger thrusts develop beneath older ones the later are ramped-up and the whole stack of thrust sheets is uplifted and eroded.

Leggett *et al.* (1979a, 1979b) developed this model and, agreeing on the original separation of the different zones, divided the Southern Uplands into 10 tracts which have considerable along-strike continuity and are separated by major reverse strike faults (Fig. 1.2a). However, they expressed doubts about the simple accretionary prism model and accordingly envisaged the possibility of other models such as marginal ocean basin with a remnant arc to the southeast or transform margin. They concluded that the crust below the Southern Uplands is different to that below the Midland Valley to the north and the Lake District to the south, and that strike-slip movements may have been connected with the development of the accretionary prism.

Leggett (1980) and Leggett *et al.* (1982), emphasising the fore-arc accretionary prism model for the Southern Uplands, presented a detailed account of the

synthesis of the Southern Uplands prism. The main aspects of their model were that the accretionary prism was formed by the accretion of ocean floor and/or trench sediments, which were scraped off above the northward subducting Iapetus ocean crust as discrete fault-bounded tracts. Agreeing with McKerrow *et al.* (1977) about the original geographic separation of these tracts, they suggested that accretion ended by late Silurian. Furthermore this prolonged accretion, which indicates slow continental convergence, had produced during late Ordovician and early Silurian a trench slope break (Cockburnland, see also Oliver & Leggett 1980), which shed sediments north to the Midland fore-arc basin and the trench in the south. Deposition of this fore-arc succession was controlled by the Southern Uplands Fault and is now buried under Upper Palaeozoic cover.

They further argued that since accretion did not start until mid-Ordovician, the problem of what happened in the fore-arc before onset of accretion in the Southern Uplands is still open to speculation. However they proposed three possibilities: (1) the subducting margin was non-accretionary, i.e. any sediments accumulating on the trench or coming into the trench on the downgoing plate were subducted; (2) the subducting ocean plate may have mechanically eroded the over-riding Laurentian margin prior to the Southern Uplands accretionary phase; or (3) strike-slip movements on major faults sub-parallel to the margin may have removed older (Cambrian and early Ordovician) fore-arc sediments. Kelling *et al.* (1987), in agreement with this model and in an attempt to solve some of these problems, invoked a late Ordovician active continental margin arc juxtaposed against the Southern Uplands fore-arc trench with SE prograding fans and other fan systems to account for the unusual sedimentological characteristics which appear anomalous in terms of a simple fore-arc accretionary prism model.

Finally, Leggett *et al.* (1980) and Leggett *et al.* (1982) concluded that the Southern Uplands rocks were derived originally from an ocean-floor/trench environment and were not deposited *in situ* on a continental basement. Therefore,

the Southern Uplands accretionary prism could be allochthonous (see also Upton *et al.* 1983), i.e. a model of obduction of the accretionary terrane over thinned continental basement as a result of the closure of the Iapetus ocean.

These arguments were developed later by Leggett *et al.* (1983), who suggested that continental basement below the Southern Uplands came from the south rather than the north (underthrusting), i.e. it is the northern extension of the English basement and this will explain the missing Ordovician arc-trench gap (Fig. 1.2b). However, this basement does not continue across the Southern Uplands Fault. Leggett *et al.* also indicated that while subduction continued during the late Silurian and much of the early Devonian, the Southern Uplands continued to be uplifted by underthrusting. They concluded that the Midland Valley, the Southern Uplands and the Lake District terranes were subjected to minimal strike-slip movement after the closure of the Iapetus (see also Trench *et al.* 1989). Bluck (1985), in questioning the nature of the basement underlying the Southern Uplands, shed doubts on the above model arguing that seismic data (Hall *et al.* 1983) and geochemical studies (Thorpe *et al.* 1984) require a much shallower crust than that suggested by the model (more than 10 km) and also envisaged a different crust underlying England compared to Scotland.

Bluck (1983, 1984 and 1985) disagreed with all previous workers who interpreted the Midland Valley as a fore-arc basin dividing the Southern Uplands accretionary prism to the south from a basement-arc terrane to the north where detritus eroded from the metamorphosed Dalradian terrane were dispersed over the Midland Valley fore-arc region and accumulated in the trench. He argued that the presence of a proximal fore-arc sequence (at Girvan) demands an arc to the immediate north of it in the Midland Valley and a fore-arc to the south of it in the position of the Southern Uplands. He also suggested that since the arc-trench gap always exceeds 45 km and normally exceeds 90 km, a complete fore-arc basin must be missing where a trench sequence (Southern Uplands) and a coeval proxi-

mal fore-arc basin sequence (Girvan) lie adjacent to each other (Fig. 1.2c). Therefore the Southern Uplands accretionary prism must have been thrust over the missing basin as well as the continental crust of the Midland Valley arc during late Silurian (see also Bevins *et al.* 1986).

According to Leggett (1980, 1982), the Cockburnland Ordovician trench break supplied sediments to the Midland Valley fore-arc basin to the north and the trench to the south. However, Bluck rejected this idea suggesting that this structure is impossibly narrow (26 km) to have supplied all these sediments.

Finally, Bluck concludes that the Southern Uplands were either covered by other formations which supplied the debris to the north, or they were not in that position during late Silurian and may have been emplaced either by strike-slip faulting (see also McKerrow 1986) and/or by thrusting from the SE. Furthermore accretionary prisms should be underlain by oceanic crust, while the evidence available indicates that the Southern Uplands are overlying continental basement and therefore must be allochthonous.

Needham & Knipe (1986) combined Bluck's model of the obduction of the Southern Uplands wedge onto continental basement and Leggett's idea of underthrusting of English basement where they suggested that, after the Silurian, the region became a large-scale pop-up structure between a fore-thrust, the Iapetus suture, and a back thrust, which emplaced the Southern Uplands northward over the Midland Valley continental basement. Their model was based on the criteria proposed by Knipe & Needham (1986) to explain the deformational processes responsible for the evolution of accretionary prisms.

McCurry & Anderson (1989) adopted a model which incorporates some of the previous hypothesis, though with a modified mechanism involving overthrusting as well as underthrusting to the NW and also suggested that continental and oceanic crusts approached each other from the north and south respectively, in the vicinity of the downward projection of the Ordovician-Silurian contact of the

Southern Uplands.

Up to this stage all models discussed considered the Southern Uplands as essentially an accretionary prism accreted in a fore-arc situation. McKerrow (1987) who presented the different views concerning this model indicated that there are several difficulties in the acceptance of a simple subduction-accretion model such as the location of the arc associated with the accretion model. Also Barnes *et al.* (1987) have indicated that structural evidence strongly suggests that the three belts comprising the Southern Uplands have different tectonic histories and therefore they cannot be all explained by the simple accretionary prism framework. In the following section some of the other models, which do not regard the Southern Uplands as an accretionary prism, will be presented.

1.4. The Southern Uplands: Alternative Models

[1] Murphy & Hutton (1986) argued that an accretionary model cannot be accepted only on the basis of structural evidence since a SE prograding turbidite wedge, imbricated by south eastwards thrusting, can produce a similar basic structure to that of the Southern Uplands. They suggested further that it is erroneous to consider the belts of the Southern Uplands as a continuous entity given that Cockburnland lay as a palaeogeographic divide between the Northern Belt with its oceanic affinity and the Central and Southern Belts of no obvious oceanic affinity. Leggett *et al.* (1979a) attributed this to selective decollement of the oceanic rocks. Murphy & Hutton interpreted the Kingledores Fault as a major dislocation along this boundary which replaced the Cockburnland arc terrane. They concluded that the Central and Southern belts are composed of SE prograding Silurian turbidite fan system that was cut by a SE-directed imbricate thrust stack, i.e. a Silurian successor basin (Fig. 1.2d), and it is bounded to the SE by a remnant arc at the NW edge of Cadomia while the Northern Belt may be part of an accretionary prism of Ordovician age.

[2] Hutton & Murphy (1987) developed the previous model and interpreted the Silurian of the Southern Uplands and south of the Iapetus suture in Ireland as representing the fill of a broadly symmetrically filled basin which derived its detritus from Ordovician arc complexes to either side of that basin, thus developing a successor basin. The southern arc is considered to be that of Lake District-Wexford while the northern arc is the missing Cockburnland which was once present between the Northern and Central Belts. This arc was cut out by end Silurian sinistral deformation along the Kingledores Fault. Therefore they consider the Northern Belt and the combined Central and Southern Belts as two separate tectonostratigraphic terranes which were juxtaposed in the late Silurian-early Devonian times. However, imbrication of the Central and Southern Belts took place as the successor basin was compressed by continued convergence between the Cadomian and Laurentian continents.

[3] Stone *et al.* (1987) interpreted the Southern Uplands as an imbricate thrust belt initiated in a backarc position, but developing during the Silurian (see also Barnes *et al.* 1989) as a foreland basin migrating southward ahead of the rising thrust stack with a mature continental landmass to the north and a rifted continental fragment containing an active volcanic arc to the south during the Ordovician and early Silurian (see also Merriman & Roberts, 1990).

[4] Morris (1987), in pursuit of the backarc hypothesis, developed a model based on the suggestion that an arc massif once occupied the zone between the North Belt and the Central Belt. His first assumption was that the North Belt is not part of the Southern Uplands accretionary prism and is composed of two compositionally distinct clastic units which are separated by a strike slip fault. Criticising the model of Stone *et al.* (1987) and suggesting a more northly arc massif, he divided the Southern Uplands into three tectonostratigraphic units, a backarc (the Northern Belt), an arc (Cockburnland), and a fore-arc basin to the SE (Central and Southern Belts). The backarc basin was closed and deformed at the end of the Ordovician

and subsequently overthrust northwestwards by the allochthonous thrust stack imbricated Central and Southern Belts fore-arc sequence at the end Silurian.

In criticising the last three models, Kelley & Bluck (1989) using mica dating and Bluck (pers. comm.) suggest that a provenance area for the Southern Uplands micas and associated igneous clasts is a contemporary arc-basement situated in the Midland Valley region. Therefore they conclude that the suggestion that parts of the Southern Uplands sequence were deposited in a backarc setting is not supported by this evidence (i.e. the arc yielding these sediments lay north of the Southern Uplands). However, Elders (1989) argued that since clasts dated in both cases were obtained from different areas, the dates obtained by Kelley & Bluck merely indicate that different depositional systems were operative in the Southern Uplands and the possibility of strike slip movements still exists.

Contrary to the above hypothesis, Styles *et al.* (1989) used petrographic studies of volcanic materials to suggest a missing volcanic arc terrane lay to the south of the Southern Uplands and was the principal contributor of these clasts.

[5] Heinz (1989) studied volcanic clasts and greywackes from the Southern Uplands and the Midland Valley. Chemical analysis of these clasts led him to the conclusion that the Northern Belt was developed in an Ordovician backarc basin behind an active island arc (Cockburnland). To the north of this basin, a continental region of complex composition was eroded and represented the source area for the greywackes and clasts. An Ordovician closure of the Iapetus ocean was also suggested causing folding and thrusting of the backarc basin. By the Silurian the tectonic regime had changed mainly to strike slip movements and a new basin developed in the collision area (the Central and Southern Belts of the Southern Uplands), where the erosional debris of the inactive island arc were deposited. Towards the end of the Silurian, compressional movements caused folding and thrusting of the Central and Southern Belts while the island arc disappeared due to sediment overthrusting or strike slip movements and therefore its presence can

only be inferred from the detritus it provided. Contrary to the Heinz model, Mitchell (1989) envisaged a fore-arc setting for the Northern Belt with subduction taking place towards the south in Ordovician times while Cockburnland represented the island-arc.

1.5. Geology and Structure of the Southern Uplands

The Southern Uplands is the region bounded by the Southern Uplands Fault in the north, the English Border to the south, the North Channel in the west, and the North Sea to the east. It is conventionally divided into three belts (Peach & Horne 1899), although more than ten major fault-bounded tracts are known (Leggett 1979 a,b). The Belts are termed the Northern, Central and Southern Belts. The oldest rocks exposed in the region are of Arenig age (Lower Ordovician) and the most recent are sedimentary rocks of the Triassic system. Detailed accounts of the Southern Uplands stratigraphy and structure are given in Greig *et al.* (1971), Walton (1983), McKerrow (1986) and Stone *et al.* (1987). Figure 1.3 shows a geological map of the region while Figures 1.4 and 1.5 show the stratigraphic and structural relationships between the adjacent Belts (or tracts) respectively. Refer to Figure 1.2a for the correlation of the different tracts.

These Figures show clearly that the region is dominated by Lower Palaeozoic rocks which become progressively younger towards the SE while younger sediments form a low-lying fringe on the SE side of the area, but in places they occur in valleys and broad depressions within the region itself. The igneous suites of the Southern Uplands are represented by remnants of oceanic basalts of Arenig age forming the base of greywacke sequence in the NW part of the Northern Belt and are considered to be slivers from the Arenig zone which partially floored the extending Southern Uplands basin (Stone *et al.* 1987). An extensive dyke swarm is concentrated in the southern half of the Central Belt and northern edge of the Southern Belt. Dykes decrease in abundance northwards, becoming generally rare in the Northern Belt. Field relationships indicate that these dykes were intruded

synchronously with assembly of younger parts of the Southern Uplands thrust stack.

Leggett *et al.* (1978, 1979) interpreted the basalts, cherts and shales to be of ocean floor lithologies, while Leggett (1980) interpreted the greywackes as both ocean floor and trench deposits. The mode of deposition was either by longitudinal fans (mostly from the NE) or by fans and mass-flow deposits flowing from the NW down the inner trench wall (McKerrow 1986).

In the SW granitic intrusions of Lower Palaeozoic age are present. The most important intrusions are found at Loch Doon, Cairnsmore of Fleet, and Criffell in Galloway. The first is intruded into Ordovician rocks, along with smaller intrusions. The rocks surrounding the Cairnsmore of Fleet mass are mainly Silurian, but also include some of Ordovician age, while the Criffell complex is intrusive in Silurian strata. The SUN seismic lines avoid these intrusions.

Metamorphism of the Palaeozoic rocks of the Southern Uplands was the product of regional metamorphism of the lowest grade ranging from zeolite to prehnite-pumpellyite facies (Oliver & Leggett 1980) which was diachronous starting in Ordovician times in the Northern Belt, continuing in the early Silurian times in the Central Belt and terminating with the end of accretion in the late Silurian times in the Southern Belt (Oliver *et al.* 1984). Oliver (1988), who presented a review on the metamorphism of the paratectonic zone, suggested that the main metamorphic processes involved were tectonic burial in the accretionary complex. The main occurrences of metamorphic minerals are in the Northern and Central Belts.

In contrast to younger formations, the Ordovician and Silurian beds are strongly folded, the predominant trend of the structure being between NE and ENE. The rocks are mainly greywackes, basalts, cherts, shales, and fine-grained siltstones. The structure of the Southern Uplands is dominated by reverse strike faults and belts of homoclinal, steeply-dipping NW-younging greywackes, which

seems to be due to horizontal compression in a NNW-SSE direction. Reversed strike-fault and subsequent wrench-faults are widely developed in association with the main folding and there is widespread evidence of the late re-activation of many faults under different stress conditions. Major strike faults are those which bound tracts of differing stratigraphy and have indeterminable, though possibly very large, displacements. However, the extension of some of these faults across the Southern Uplands is uncertain due to lack of exposure. Leggett *et al.* (1982) considered these tracts as discrete packets of accreted ocean floor and/or trench sediments scraped off above the northwards subducting Iapetus ocean crust. They also interpreted the major faults as original decollement surfaces during accretion of the tracts which were initiated as low-angle thrusts. The stratigraphical polarity within individual sequences is predominantly towards the NW, although successive fault-bounded slices are generally younger towards the SE. The tracts may be several hundred to several thousand metres in thickness and some can be traced for 100 km or more along strike (Bevins *et al.* 1986).

The Southern Uplands, including part of the southern Midland Valley, structures were divided into three *tectonic domains* by Weir (1979). The northern domain near Girvan is characterised by asymmetrical folds and NW-translating thrusts; the middle domain, which comprises the Northern Belt and part of the Central Belt, is characterised by a series of listric faults, the main thrust faults being associated with outcrops of *Moffat shales*; the southern domain includes the Southern Belt, where folds are abundant and associated with steep strike faults.

The term *Line* was used by Floyd (1976) to describe some of the major faults, due to the prominence of linear outcrops of basal lithologies (basalt, chert and graptolitic shale) marking the traces of imbricate zones on Geological Survey maps. The geology of each belt is now described.

1.5.1. The Northern Belt

The Northern Belt stratigraphical and structural relationships are the essential basis of the accretionary prism model for the Southern Uplands as a whole, (Leggett *et al.* 1979 a,b and Barnes *et al.* 1987). This Belt consists entirely of Ordovician rocks (Arenig to Ashgill) where early Ordovician spilites and cherts pass up into thick greywacke turbidites and rudites. This Belt includes tracts 1-3 which are a strike-parallel sequences of greywackes divided by discontinuous narrow outcrops of fossiliferous black mudstone and chert (Moffat Shale). Basalts are also present and occur only in this belt. They include submarine lavas, mass-flow agglomerate and occasional air-fall tuffs.

Tract 1 - Coulter/Noblehouse sequence: the most northerly tract, lying immediately south of the Southern Uplands Fault and consists of basalts, followed by red cherts and a thick greywacke development. It contains the *Corsewall* and *Marchburn Formations*.

Tract 2 - Afton-Abington sequence: consists of basalts, cherts, black shales and greywackes. This sequence is bounded to the north by the *Grassfield Fault* and to the south by the *Leadhills Line* or *Fault*. The latter is thought to be a strike fault and Morris (1987) envisages it as a reverse or thrust fault zone which dips 30-40 degrees NW in the Southern Uplands and prefers the name *Northern Belt Median Fault*. The tract contains the *Kirkcolm* and *Galdenoch Formations*.

Tract 3 - Lowther-Tweeddale sequence: this tract occurs between the Leadhills Line and Kingledores Fault. It consists of grey and blue slates and siltstones, and associated fine-grained micaceous greywackes. Leggett *et al.* (1979b) suggest that a major fault cut this tract and may extend SW to the *Fardingmullach Line*. This tract contains the *Portpartrick* and *Shinnel Formations*, where the latter formation may represent the highest Ordovician (Ashgill) or early Silurian age. It is interesting that acid, intermediate and basic magmatic debris of Llandeilo-Ashgill age are found in this tract.

It was thought that the Northern Belt pattern continues into the Central Belt, but evidence of major sinistral displacements on the Kingledores Fault separating the two Belts (Anderson & Oliver 1986) weakened this assumption. However, it was seen from section 1.4 that the Northern Belt is now the focus of some new interpretations for the Southern Uplands where it is considered as an entirely separate entity from the Silurian of the Central and Southern Belts. The main deformation of this unit is believed to be pre-Silurian in age (Hutton 1987).

1.5.2. The Central Belt

Llandovery rocks, the oldest of the Silurian System, form most of the Central Belt. Here greywackes are commonly underlain by thick late Ordovician/early Silurian graptolitic shales (Moffat shales). It includes tracts 4-9. This belt is bounded by the Kingledores Fault to the NW which separates it from the Ordovician of the Northern Belt, and the *Riccarton Line* to the SE which separates it from the Wenlock series of the Southern Belt. The rocks are highly folded and their outcrop is modified in many places by the presence of Ordovician inliers, while in the east exposure is much interrupted by areas of upper Palaeozoic rocks.

The Central Belt has two distinct parts. The northern part is characterised by the proximal turbidite facies of the *Gala Group*, in which the sandstone is usually quartzose in composition although locally pyroxenous. Moffat Shale inliers occur but are much less continuous than those farther north, defining relatively indistinct tracts. The southern part of the Belt is composed of an extremely uniform, relatively distal turbidite facies (*Hawick Group*) in which sandstone is compositionally distinct from the Gala Group sandstone by virtue of containing primary carbonate detritus.

Tract 4 - Talla Sequence: This tract lies south of the Kingledores Fault and is composed of greywackes belonging to the *Pyroxenous Group* and the *Kilfillam Formation*. McKerrow (1986) indicated that the granite clasts in rudites of this

tract are older than the Scottish granites and could have originated from Newfoundland. The southern boundaries of this tract are marked by a major fault in the SW and a line of *Birkhill Shale* (top division of the Moffat Shales) in the NE.

Tract 5 - Hartfell Sequence: A full succession of the Moffat Shales is present in this tract and greywackes overlie the Birkhill Shales while the greywackes of the *Garheugh Group* crop out in the SW. The southern boundary of this tract is marked by the *Hartfell Line.*

Tract 6 - Dobbs Linn Sequence: Here most of the Moffat Shales are carbonaceous, but grey mudstones are present at some levels while the Gala Greywackes are rich in garnet detritus. A major shatter belt marks the southern boundary of this tract south of Moffat *(Moffat Valley Fault).*

Tract 7 - Craigmichan Sequence: This sequence is exposed in a complex zone of imbrication to the north of the *Ettrick Valley Fault* which marks its southern boundary. Thick developments of Moffat Shales are present overlain by greywackes of the Gala Group.

Tract 8 - Ettrickbridgend Sequence: South of the Ettrick Valley Fault, Gala Greywackes are interbedded with thin shales representing this tract. To the SW, a prominent line of Moffat Shale crops out north of a major reverse fault, the *Hawick Line* marking the southern boundary of this tract.

Tract 9 - Hawick Sequence: This tract is represented by the outcrop of the *Hawick Rocks*, a distinctive group of greywackes with red mudstone interbeds with their composition varying from greywacke to calcareous sandstone. The southern boundary of this tract is marked by the *Riccarton Line* which is a major reverse fault. There is debate about the age of the Hawick Rocks, but in recent years the Upper Llandovery has been considered as their probable age (Walton 1983).

1.5.3. The Southern Belt

This Belt consists of Silurian greywackes-turbidites, interbedded with thin, later Silurian graptolitic shales and it is represented by tract 10. Two lithostratigraphic units are exposed, the *Riccarton Beds* and the *Raeberry Castle Beds*, both of Wenlock age (McKerrow 1986 and Barnes 1987), although Leggett *et al.* (1982) and Walton (1983) suggest that the Raeberry Castle Beds are of Llandovery age. However, Kemp (1986, 1987) presented a detailed account on the tectonostratigraphy of the Southern Belt and divided it into an early Wenlock *Ross Formation* and a mid-late Wenlock Raeberry Castle Formation.

Bedding within the Southern Belt is essentially subvertical although there is some variation both along and across strike with subvertical thrust faults. In the southern Central Belt and the Southern Belt, unlike the Northern Belt and the northern Central Belt, there are no basal lithologies (basalts, cherts and black shales) along the major faults.

Tract 10 - Riccarton Sequence: This tract consists of greywackes of the *Riccarton Group*. They are recognised by the presence of abundant thin horizons of graptolitic, dark grey to greyish black laminated argillaceous siltstone. Leggett *et al.* (1979b) suggest that this group may have been deposited in three distinct sequences in three separate fault blocks of Wenlock age. They also assign the Raeberry Castle Formation to the Llandovery. It is mainly composed of fine grained greywacke and calcareous sandstone. The Raeberry Castle Formation is characterised by its diverse association of turbidite facies and may represent a distinct tract by itself.

1.6. Post Silurian Rocks

1.6.1. Lower Old Red Sandstone (ORS)

Lower ORS sediments are found in the eastern margin of the Southern Uplands in two belts of poorly cemented and unsorted greywacke-conglomerates.

Another outcrop of Lower ORS is located further to the SE consisting of red feldspathic sandstones and conglomerates, with a few thin cornstones, some partings of red marl, and a volcanic succession of andesitic lavas and coarse tuff, which is at least 600 m thick. On the SE border, great thicknesses of augite-hypersthene-andesite lavas are present. Many small intrusions of Lower ORS age are found in the central part of the region, but the most important are the granitic masses located at Loch Doon, Cairnsmore of Fleet, and Criffell in Galloway.

The Loch Doon granite is intruded into Ordovician rocks along with many smaller intrusions while the second is intruded in Silurian and Ordovician strata. The Loch Doon outcrop occupies an area extending from Loch Doon to Loch Dee, a distance of over 18 km. It has a maximum width of 10.5 km and is surrounded by a girdle of altered sediments. The granites are divided into three main types, a basic rock (norite), an intermediate rock (tonalite) and an acid rock (granite). The Cairnsmore of Fleet mass occupies an oval-shaped outcrop 17 km long and 11 km wide lying between the Loch Doon and Criffell bodies. The Criffell igneous complex forms an elevated tract of land. The longer axis of the mass has a NE trend, coinciding with the regional strike of the Silurian rocks. The emplacement of the plutonic rocks has resulted in a pronounced deflection of the strike of the adjacent country rocks at the ends of the complex. Other, smaller, intrusions of similar types occur outside the area occupied by the large masses described above. However, one of the characteristic features of Lower ORS igneous activity is the prevalence of a similar magma over a wide area. In the SW, as in the NE, all the plutonic rocks are intimately related, and the occurrence of the same types in widely separated localities suggests that they belong to the same petrographical province.

In addition to the above plutonic bodies dykes are also abundant in the Galloway district, where they cut both the plutonic rocks and the surrounding sediments. Emplacement of the granitic bodies has caused metamorphism of the surrounding sedimentary rocks varying widely in extent and intensity. The altered

rocks are Ordovician/Silurian greywackes, grey and black shales, chert, and igneous rocks, and dykes of ORS age.

1.6.2. Upper Old Red Sandstone

The Upper ORS rests with marked unconformity on older rocks. It consist mainly of red, yellow or buff fluvial sandstone, with lenses of conglomerates which are thinner and less coarse than the conglomerates of the lower divisions. The upward passage into the Carboniferous is everywhere transitional, with the topmost sandstone passing upward into the mudstones and shales of the Carboniferous.

The conglomerates are composed mainly of greywacke pebbles, with scattered fragments of porphyrites and other igneous rocks derived from minor intrusions in the Lower Palaeozoic. Wind-rounded sand grains in the sandstones seem to indicate a semi-arid continental climate. Generally the Upper ORS occupies a tract of undulating country along the eastern side of the region extending from the Southern Uplands Fault in the north to the English Border in the south. A continuation of the major eastern outcrop occurs in the central and southern parts of the region east of the Solway Firth.

1.6.3. Carboniferous

The Carboniferous System in the Southern Uplands is restricted to a few areas and is formed mainly of sediments laterally varying in thickness and locally intercalated with penecontemporaneous volcanic rocks. The strata range from thick beds of sandstone, mudstone and limestone to thinner developments of coal, seatclay, ironstone and cementstone, together with basalt and tuffs of volcanic origin. The largest outcrop of Carboniferous strata extends from the southern margin of the Southern Uplands, north of the Solway Firth, trending north-eastwards along the English Border for 130 km where it fringes the great areas of Carboniferous outcrop in the northern counties of England. These outcrops contain the

thickest development of Carboniferous strata totalling some 3500 m, and in most places the strata rest conformably on older rocks. The most eastern extension of Carboniferous strata is marked by a smaller outcrop in the SE corner of the region.

In addition to these main outcrops are numerous remnants of ancient volcanoes which are thought to have been active during Carboniferous times. These small outcrops of igneous rocks have been intruded into strata of Silurian and Upper ORS age. In Sanquhar, south of the Southern Uplands Fault, Carboniferous beds rest directly on Ordovician in places. This outlier comprises a rectangular outcrop of about 45 square kilometres in which the rocks at the surface are mainly Upper Carboniferous.

Carboniferous rocks are also exposed in five small areas on the shore of the Solway Firth. They are faulted against the Silurian rocks of the Southern Uplands to the north, while elsewhere an unconformity represents the main stratigraphical relationship between the Carboniferous and the Silurian. Finally, a small exposure of Carboniferous strata is found in the extreme west along the shoreline west of Stranraer which includes 750 m of strata consisting mostly of pink, red and brown sandstones and conglomerates with subordinate bands of shales and mudstone.

The regional strike of the structures of the Carboniferous rocks is NE, the strata dipping gently to the SE. The beds have been disrupted by numerous north-easterly faults with downthrow predominantly to the SE. There has been little intrusive activity apart from the emplacement of the numerous small volcanic necks.

1.6.4. Permo-Triassic

The Permo-Triassic rocks are called collectively New Red Sandstone. The Permian System is considered to comprise all the late Palaeozoic desert-sandstones and breccias, as well as the associated lavas and intrusive rocks. The Triassic

rocks occur only in an area of some 140 square kilometres near the eastern end of the Solway Firth along the English Border. The main Permian exposures are located in the extreme west around Stranraer and are about 1200 m thick, and in the central part of the Southern Uplands, around Dumfries (1000 m thick) and south of Moffat where the sequence is partly unconformable on Lower Palaeozoic rocks and partly faulted against them.

1.7. The Southern Uplands Fault (SUF)

The SUF is considered to be the main structural boundary between the Midland Valley in the north and the Southern Uplands in the south. It consists of three discontinuous segments slightly offset from one another (Walton 1983). The south-west segment forms the *Glen App Fault*, the central sector is the SUF proper and in the north-east it is continued *en echelon* by either the *Lammermuir Fault* or the *Pentland Fault* (Cameron & Stephenson 1985). In the SW, Leggett *et al.* (1979b) indicated that the *Stinchar Fault* may represent the SW continuation of the SUF and not the Glen App Fault. However, Anderson (1965) suggested that the SUF should not be treated as a single master fault, but as a number of faults comprising a major structure, i.e. a fault zone.

The SUF separates the steeply dipping, folded and faulted rocks of the Southern Uplands from the more gently deformed strata in the Midland Valley. In the SW, in the Glen App area, the fault lies within the outcrop of the Lower Palaeozoic rocks and the line of separation between the Southern Uplands and the Midland Valley, in terms of the sediments and their deformation, is that section of the *Straiton Fault* south of Girvan. The downthrow of the fault is thought to be towards the north but there are some anomalies suggesting a downthrow towards the south (e.g at Sanquhar basin and along the Glen App Fault section). Kelling (1961) estimated that the Ordovician rocks had suffered a southerly throw of 1000 m in the SW section, while the throw is minimal at the extreme east of the region.

The age of the fault may be Ordovician or Silurian, although Greig *et al.* (1971) suggest a Lower ORS age, and later large dip-slip movements are envisaged which may be as late as Middle ORS age. Movements along the fault affected Carboniferous sedimentation, confining deposits to the Midland Valley. Cameron & Stephenson (1985) indicated that displacement along the SUF began as early as Lower to Middle Devonian and was renewed, in some instances with the throw reversed, during the Carboniferous and later. They also suggested that the downthrow was originally to the NW but later movements on the fault caused displacements in an opposite sense to the earlier displacement. A pre-Carboniferous throw of 900 m in the SW is also envisaged.

Weir (1979) interpreted the SUF as the initial location of a Benioff zone established after the Arenig, and having a continuous history of activity through the remainder of the Lower Palaeozoic. Leggett *et al.* (1983) indicated that there had been little, if any, movement along the SUF, while McKerrow (1988) suggested that sinistral strike slip movement of 500 km took place along the fault in late Silurian or early Devonian times, but Elders (1987) suggests a 300 km displacement only. McKerrow & Elders (1989) envisaged a more northerly trace for the SUF, in the east and west. In the SW this trace may coincide with the Stinchar Fault, which is 5 km NW of the conventional line, while in the east, if tracts 1 and 2 are assumed to continue along strike below the Carboniferous, the fault trace will trend further north, just south of Edinburgh. They concluded that, since the Ordovician, 400 km of strike-slip displacement took place along the SUF and this movement persisted after the Silurian. However, Winchester & Max (1989), questioned the scale of the strike-slip movement along the SUF and suggested that if such movement had occurred it must have been of a small magnitude whereas, contrary to the above, Evans *et al.* (1991), who integrated isotope data, petrography of detrital clasts, and palaeocurrent flow analyses deduced that the SUF must be a locus of major sinistral strike-slip movement.

The SUF is assumed to be a normal fault, but transcurrent movement has been suggested to explain the variability of the downthrow. Thirlwall (1989) suggested that significant transcurrent or across-strike displacements took place on the SUF in late Silurian-early Devonian.

1.8. The Kingledores Fault

In Scotland the Kingledores Fault separates the Ordovician Northern Belt from the Silurian Central Belt. Its possible continuation in the North Channel and Ireland is referred to as the *Orlock Bridge Fault* and the, further west, the *Slieve Glah Shear Zone*. In the latter area it separates rocks with contrasting metamorphic histories, according to Murphy & Hutton (1986), who also considered it as a major dislocation rather than a simple tract bounding fault (Leggett *et al.* 1979 a,b) of end Silurian age.

Leggett *et al.* (1983) envisaged the fault as the most significant structure in the Southern Uplands since it separates groups of tracts with similar sequences (in age and lithology), namely the Northern and the Central Belts and it can be also recognised over longer distances than the average tract bounding fault. They also interpreted the fault as being sinistral strike-slip of late Silurian-early Devonian age, a view supported later by McKerrow (1986), Elders (1987), Hutton (1987), Morris (1987) and Hutton & Murphy (1987), while Thirlwall (1989) suggested transcurrent movements of only few kilometres to have taken place along the fault.

However, Anderson & Oliver (1986), who described the fault along its 400 km track in great detail, observed that there is an obvious systematic decrease in the width of the fault zone from SW to NE, and that the Scottish outcrops are less impressive than those in Ireland. Their explanation for these observations was that the fault may branch or splay so that the movement is taken up on several surfaces but only the Belt boundary remains recognisable, or the fault may be exposed at progressively higher levels eastwards.

They also considered the Southern Uplands as an accretionary prism from which at least four tracts are missing by sinistral strike-slip movement along the Kingledores Fault, or that the fault amalgamates two similar, but initially separate and distinct, accretionary prism terranes of southerly prograding turbidites by sinistral strike-slip movement. They concluded that large sinistral strike-slip movements took place along the fault with a magnitude in access of 400 km in late Silurian or early Devonian times.

More recently, McCurry & Anderson (1989) envisaged the fault as a nearly vertical structure penetrating the crust to the basement at a depth of approximately 18 km.

1.9. The Midland Valley of Scotland

Part of the SUN project covers the southern margins of the Midland Valley especially the Ballantrae area in the SW along line 4, and the Edinburgh-Haddington region in the SE of the Midland Valley along lines 1, 2, and 3. It is appropriate here to present a summary of the most important geological and physical aspects of these regions.

The Strathmore Syncline is another part of the Midland Valley which is covered by the SUN project. It is located in the extreme NE part of the Midland Valley. A single profile was recorded nearly parallel to the axis of the syncline to integrate the results with those obtained by the author during a previous project.

1.9.1. The SW of the Midland Valley of Scotland

This region is well described by Cameron & Stephenson (1985). The most important feature of this area is the Ballantrae igneous complex which is composed mainly of basic and ultrabasic rocks of Arenig age representing the remnants of an older obducted plate. They form the basement to the northward overstepping Caradocian sediments of the Girvan district. The main rock exposures are a group of spilitic lavas and pyroclastic rocks with associated cherts and

fossiliferous shales, and a number of major and minor intrusions. A characteristic feature of the spilites is the presence of very well developed fine-grained pillow lavas which indicate that they were extruded underwater. Serpentinite crops out in two broad zones oblique to the shoreline south of Girvan while gabbro and dolerite, albitized, granulitized and foliated in varying degrees, occur in many small areas within the serpentinite. The whole succession forms a typical ophiolite assemblage. The sedimentary rocks, associated with the complex are mostly cherts, conglomerates and black shales.

Ordovician and Silurian conglomerates present in the area share a suite of quartzite, basic-ultrabasic and granitic clasts similar to those of the Southern Uplands which implies a similarity in provenance arguing against lateral displacement of the Midland Valley relative to the Southern Uplands. Bluck (1983), with evidence for a missing forearc sequence in Ordovician times, inferred that the Southern Uplands accretionary prism was not in its present position during the Silurian, and that the Midland Valley basement extended beneath the Southern Uplands as far as the Southern Belt. The accreted Southern Uplands was said to have been thrust from the SE over the projected Midland Valley and Girvan forearc sequence.

Silurian rocks in the area are in contact with the Ordovician south of Girvan and are separated into two main sub-parallel NE-SW trending outcrops by the Kerse Loch Fault. Outcrops of Lower ORS composed of conglomerates, lavas and sandstones rest unconformably on a group of Silurian rocks in the southern Midland Valley and Girvan area. Carboniferous rocks are also found with minor occurrences of Permian rocks.

Cameron & Stephenson (1985) indicated that at Girvan the *Kerse Loch Fault* represents a line of faulting across which there is an abrupt increase in thickness, indicating differential subsidence. This fault trends WSW subparallel to the SUF. McLean & Qureshi (1966), McLean & Deegan (1978) and Francis (1983), also

suggested that continuous movement along the fault controlled the sedimentation of the Carboniferous, and gave rise to spectacular thickness variation on the different sides of the fault.

1.9.2. The SE of the Midland Valley of Scotland

The region is described in Cameron & Stephenson (1985), while a detailed account of the Haddington district is found in McAdam & Tulloch (1985). In this area, the Carboniferous and Devonian sedimentary and igneous rocks of the Midland Valley are separated from the Ordovician and Silurian strata of the Southern Uplands by the most easterly fracture of the SUF, the Lammermuir Fault.

The main outcrop of Lower ORS strata is at the Pentland Hills which comprises an upthrust outcrop of folded Silurian strata and Devonian conglomerates, sandstones and lavas. They are sharply defined on the SE side by the Pentland Fault. These Lower Devonian rocks are known to rest with angular unconformity on the Silurian rocks. Thicknesses of 600 m of Upper Devonian rocks are also present at the Edinburgh area and are highly reduced on the NW side of the Pentland Hills where they overstep Lower Devonian and Silurian sediments and lavas.

Sedimentary rocks of the Carboniferous age are represented by the *Lothian Oil-Shale Fields*. They belong to the Dinantian succession and are one of its thickest parts in the Midland Valley. Beds of volcanic ash and lava occur at several horizons within the unit. The strata have a regional dip to the west and are folded into a series of minor domes and basins trending N-S to NE-SW. These folds are cut by a series of E-W to NE-SW trending faults. Dentith (1987) interpreted these faults as being of listric nature soling out at shallow depth (2-3 km), and forming a flower structure across which there is a downthrow to the north. There are also important Dinantian volcanic rock outcrops in the Haddington area, in the extreme SE corner of the Midland Valley.

The seismic profiles cross many E-W trending faults in the SE part of the Midland Valley such as the *Pentland Fault* which is considered as a post-Carboniferous reverse fault south of Edinburgh, the *Dunbar-Gifford Fault* south of Haddington, the *Colinton Fault*, south of Ratho.

1.9.3. The Strathmore Syncline

The asymmetric Strathmore Syncline is dominated by the abundant exposure of Lower ORS strata which crop out along its entire length (Fig. 1.6). The ORS consists of terrestrial clastic sediments which accumulated in fluvial fans, braided streams and lakes and were deposited on a surface of folded and eroded Lower Palaeozoic sediments. These rocks attain their maximum thickness of 7500 m in the Strathmore Syncline, though their thickness is much reduced in the eastern part of the region (4000 m). South of the syncline the *Sidlaw Hills* lavas trend in a NE direction and are composed of olivine-basalts with minor andesites dipping gently towards the NW beneath younger sediments of Lower ORS age.

Kamaliddin (1988) interpreted a N-S trending seismic refraction profile (Figure 2.1) with Collace quarry, which was used to record Line 6 in this project, as its northern shot. He concluded that Lower ORS rocks, which are exposed at the surface in the Strathmore Syncline, have a velocity of 5.3-5.8 km/s and thickness of 5.2 km. A basement refractor of a velocity of 6.04 km/s was interpreted at a depth of 5.2 km. It was suggested that this refractor is not horizontal where it is displaced upwards towards the axis of the Strathmore Syncline. It was one of the aims of this project to establish the stratigraphic and geophysical relationships along the axis of the syncline in NE-SW direction to be integrated with the previous results mentioned above. The depth of the basement refractor and whether it is horizontal or stepped was another objective.

1.10. Previous Geophysical Studies

Many geophysicists have contributed valuable work to increase our understanding of different geophysical, geological, and palaeotectonic aspects of the region. These interpretations, which include seismic studies as well as gravity and magnetic profiling, will be discussed below.

1.10.1. Seismic Studies

[1] Jacob (1969) analysed events (mostly quarry blasts) recorded at EKA, a seismological array of continuous operation located in the central part of the Northern Belt at Eskdalemuir (see Figure 1.10 for location), and indicated that there is a gradual increase in velocity from 5.54 km/s at the surface to 5.94 km/s at 12 km depth, then the velocity jumps to 6.4 km/s.

[2] Powell (1971), using a variety of geophysical investigations including magnetic, seismic, resistivity and gravity, strongly criticised Dewey's conclusion that the Southern Uplands represents the remnant of the proto-Atlantic ocean. He suggested that there was as much as 30 km of continental crust in the region and that the Lower Palaeozoic sediments and the Caledonian granites extend to depths of about 12-15 km. Underneath these the pre-Palaeozoic basement is taken to consist of high-grade schists and gneisses, probably of Lewisian type.

[3] In 1974, the Lithospheric Seismic Profile across Britain (LISPB) was completed (see Fig. 2.1 for location). It is a reversed 1000 km N-S seismic refraction line which crossed the eastern half of the study region in the vicinity of Edinburgh. The results of this project were interpreted by Bamford (1979) and Bamford *et al.* (1976, 1977, 1978) and summarised below:

(i) A poorly constrained superficial layer of upper Palaeozoic and younger sediments with velocity of 4.0-5.0 km/s and thickness of 2-3 km.

(ii) A second layer with velocity of 5.8-6.0 km/s was interpreted as a Lower Palaeozoic succession to a depth of 7-8 km. In the Highlands this layer has velocities of 6.1-6.2 km/s and is interpreted as a combination of Caledonian

metasediments and intrusions.

(iii) A refractor with velocity of 6.4 km/s was inferred as the top of crystalline basement existing at a depth of more than 8 km. Beneath the Southern Uplands, this layer has a velocity of 6.3 km/s to an undefined depth. It is important to note that Jacob's 6.4 km/s layer is not recognised under the Southern Uplands by the LISPB profile.

Figure 1.7 shows the final interpretation of the LISPB profile across Britain. Three principle discontinuities are indicated by velocity changes. The lowest (Moho) separates the mantle with a velocity of 8 km/s from lower crust with a velocity of 7 km/s. Above this is a layer with velocities exceeding 6.4 km/s north of the SUF but less than 6.3 km/s south of it. This layer was interpreted as pre-Caledonian basement, with a major difference across the SUF. Above it, and to the north of the Midland Valley, is the main part of the upper crust, with velocities of 6.0-6.05 km/s in the Northern Highlands. This layer is interpreted as Caledonian metamorphic rocks. South of the Highland Boundary Fault under the Midland Valley and Southern Uplands the corresponding layer has velocities of 5.8-6.0 km/s. A comparison between the crustal models proposed by Bamford (1979) and Powell (1971) is shown in Figure 1.8.

In their study of the distribution of Poisson's Ratio (σ) in the region, Assumpcao & Bamford (1978) concluded that the LISPB ratios are generally close to the conventional value of 0.25 except, for their Lower Palaeozoic layer in the Southern Uplands ($\sigma = 0.231$) and for crystalline basement under the Midland Valley ($\sigma = 0.224$). They suggest that these low values indicate that the region of the SUF is a major point of interest and tectonic activity.

[4] El-Isa (1977) analysed data recorded at Broughton (BTN), 10 km SE of the SUF (see Figure 1.10 for location), using a temporary 9-seismometer Geostore array with the intention of recording quarry blasts from either side of the fault. Local events and dedicated shots were also recorded and analysed. The data

suggested that the velocity in the Lower Palaeozoic of the Southern Uplands varies with azimuth and is anisotropy dependent. His model involved a velocity change, at zero depth, from 5.0 km/s parallel to the regional strike to 4.4 km/s at right angles to it. The presence was also suggested of a high velocity layer (V_p > 5.8 km/s) at no more than a few kilometres depth beneath the array and dipping to the NW.

This work was combined with a later study into the physical properties of Lower Palaeozoic sediments using ultrasonic measurements on small rock cores to presures of 5 kbars (Adesanya 1982). It was concluded that the high velocity observed in the Southern Uplands (V_p> 6.0 km/s) was not due to Palaeozoic greywackes but crystalline rocks.

[5] Information from the Southern Uplands Seismic Profile (SUSP) was interpreted by Warner *et al.* (1982). The line is a reversed 120 km seismic refraction profile trending parallel to the SUF along the Northern Belt, from Dunbar to Sanquhar. A three layered upper crustal model was envisaged (Fig. 1.9). Figures 1.10 and 2.1 show the location of the SUSP profile.

(i) Lower Palaeozoic greywackes extend from the surface to a depth of no more than 1 km, with a velocity range of 5.75-5.80 km/s.

(ii) A refractor with velocity of 6.0 km/s and occurs at a depth of 1 km is suggested to be an igneous or metamorphic body. The presence of this refractor at nearly right angles to the LISPB 5.8 km/s refractor supports the hypothesis, of the velocity being higher along strike.

(iii) At depths of 2-4 km, another refractor with velocity of 6.31 km/s was detected.

[6] Hall *et al.* (1983), in their re-interpretation of the SUSP, BTN, EKA and LISPB combined with new seismic evidence (Fig. 1.10), suggested that, contrary to the LISPB conclusion of the presence of a major discontinuity near the SUF, the basement under the Southern Uplands is seismologically indistinguishable from

that below the Midland Valley, that it continues for at least 15-20 km southwards below the Southern Uplands and that another crustal block underlies the EKA seismological array further to the south. This basement is of continental affinity and occurs at shallow depth (1-5 km). They suggested that the high velocity crust of the Midland Valley continues south of the SUF, but deepens rapidly to the SE of SUSP and BTN and that a 10-20 km wide high velocity block underlies EKA and extends NE-SW, while another block underlies LISPB shot 2 (Fig. 1.11 a and b) in the Southern Belt terminating at the boundary with the Central Belt.

Figure 1.10 also shows that a total of 5 fast (V_p = 6.0 km/s) and slow (V_p = 5.6 km/s) velocity blocks are predicted to exist in the Southern Uplands. Figure 1.11a shows the time-distance plot for the data used in their interpretation with the different blocks illustrated, while Figure 1.11b shows a velocity-depth plot for the Southern Uplands.

However, Oliver *et al.* (1984) and Oliver & McKerrow (1984), who suggested the presence of greenschist facies rocks at shallow depth in the Southern Uplands, criticized the Hall *et al.* model of fast and slow blocks. They argued that velocity anisotropy in foliated rocks (e.g. slate, chlorite schist and micaschist) could produce velocity anisotropy such as that measured at BTN. Also different levels of the prehnite-pumpellyite-greenschist facies transition could equally give the same effects as that shown on the LISPB time-distance plot (Fig. 1.11a), although the author notes that it is unlikely that such a transition would be sharp enough to explain the data. They also indicated that the faults between the fast and slow blocks match up with faults already mapped between various tracts, therefore a thick Southern Uplands accretionary prism is inferred.

[7] The Western-Isles-North Channel (WINCH) deep seismic reflection profile was studied by Hall *et al.* (1984). The profile runs through the North Channel across the extensions of the Midland Valley and into the Firth of Clyde. Their conclusion was that there are no observed margins to the Midland Valley equivalent to the

bounding faults on land and that there are no contrasts in seismic character on either side of the SUF. That is, the fault is discernible as a low-angle feature within the basement and the Midland Valley basement may continue southwards below the Southern Uplands (Fig. 1.12). However, Brewer *et al.* (1983) indicated that the upper crust over much of the WINCH profile is seismically transparent and many of the major geological boundaries cannot be imaged (e.g. the Moine Thrust, the Highland Boundary Fault and the Southern Uplands Fault). They concluded that there is insufficient impedance contrast across these faults, or they are too steep to be properly imaged, or there is no contrast in seismic character across them.

Beamish & Smythe (1986) combined the WINCH data with other seismic reflection and geoelectric sounding data to model the Iapetus suture which was imaged as a thin slab of high conductivity dipping NW at 15–25° extending down to and through the Moho at 28 km depth with a velocity of 6.2-6.5 km/s. Stone *et al.* (1987) commenting on this slab considered it as a deep crustal fracture not necessarily related to the Southern Uplands thrust system while McKerrow & Soper (1989) see it as one of the many crustal shear zones produced during plate convergence and that it is unlikely that a plate boundary can be imaged as a single inclined reflector. They concluded that the basement is apparently present at very shallow depths of 1-2 km adjacent to the SUF deepening to about 10 km below the Solway Firth with a velocity of 6.1 km/s.

[8] More recently, Klemperer & Matthews (1987) compared the WINCH image of the Iapetus suture along the western side of Britain with the North East Coast Line (NEC) which is a BIRPS multichannel seismic reflection profile off the east coast of the Midland Valley and the Southern Uplands trending sub-parallel to the WINCH and imaging to 50 km depth. They concluded that two fundamental differences between the two profiles are present. The first is the dip of the Iapetus suture which appears to increase from 25° in the west (on WINCH) to 40° in the

east (NEC). Secondly, the crust beneath the North Sea is strongly layered north of the suture and less reflective south of the suture whereas in the west the opposite situation exists.

Freeman *et al.* (1988) presented a comprehensive interpretation of the NEC data. Their model included a reflective sedimentary cover sequence, a seismically transparent middle crust, a reflective lower crust (see also Matthews 1986, who envisaged a layered lower crust west of Britain) and a transparent mantle (see also Cook *et al.* 1988). Freeman *et al.* suggested the juxtaposition of a number of terrane types from two continental margins including the recognition of a sub-crustal subduction complex and the inference of collision-related decoupling of the crust and mantle (Fig. 1.13). The Iapetus suture (IS) was interpreted as a flake of high velocity and/or high density material dipping 40°N implying that the northern continent formed the hanging wall of the main suture and that subduction finally ended with continental crust of the southern margin of the Iapetus ocean underthrusting the northern margin.

Another reflector (IN) was identified as a major tectonic boundary between rocks of Midland Valley affinity and the highly diffractive crust below the Southern Uplands (see Fig. 1.13). Two deeper parallel reflectors termed P_1 and P_2 and having a separation of 3.4 km were observed and persist over about 55 km horizontal distance transecting the Moho downwards into the mantle to 6-7 km below the Moho. Freeman *et al.* interpreted the structure bounded by these two reflectors as of Caledonian origin representing oceanic crust which has been attenuated dominantly by simple shear along the Moho during the collision event. The top margin of the shear zone is produced by southerly transport of Midland Valley type continental crust over the top of the subduction complex. The bottom margin is the present day Moho and marks a plane of decoupling of crust and mantle corresponding to a relatively untectonised tail of oceanic crust.

No conclusive answer was given by Freeman *et al.* as to the nature and extension of the SUF, but they assumed that if the fault reaches the Moho it will coincide with the boundary between the Midland Valley and Southern Uplands terranes or, alternatively, it may root at the northerly termination of the P_1 and P_2 reflectors. Finally they correlated the (IN) reflector rather than the IS reflector (Klemperer & Matthews 1987) with the WINCH Iapetus suture.

[9] Re-assessing available models and integrating them with new data (see Figure 2.1 for location), Davidson *et al.* (1984) and Davidson (1986) re-interpreted the velocity configuration in the southern parts of the Midland Valley. Their conclusion was that the LISPB interpretation of the geological nature of the a_o refracting layer as Lower Palaeozoic clastic sediments is erroneous, and it is interpreted better as a quartz-feldspar rich crystalline layer of igneous or metamorphic origin which passes beneath the surface expression of the SUF at approximately 2.5 km depth. It is assumed to continue southeastwards under at least the Northern Belt, so the SUF marks only the late Caledonian structural juxtaposition of the Ordovician trench sediments with the Silurian interarc sequence.

Furthermore, the Kerse Loch Fault does not displace the a_o refractor. It is suggested that a major basement strike-slip zone, producing a flower fault pattern whose branching petals include the Kerse Loch and the Southern Uplands faults. A decollement zone due to major rheology contrast across the basement/cover interface may be another solution. However, the a_o/a_1 interface was considered as a metamorphic facies change, from amphibolite to granulite.

[10] As part of a persistent effort at Glasgow University to add to the understanding of the physical properties and structure of the crust in the Midland Valley and the adjacent regions, Al-Mansouri (1986) recorded several seismic refraction lines in the SW corner of the Midland Valley and southwards across the SUF (Figure 2.1). In addition to these profiles, laboratory velocity measurements up to 200 bars confining pressure of samples of the Ballantrae complex and greywackes of the

Northern Belt were undertaken. The results indicated that the high velocities, previously interpreted as crystalline basement (> 6.0 km/s) could be obtained from the Northern Belt mafic greywackes.

However, Al-Mansouri determined a wide range of values from his greywacke samples. The average value for the Lower Palaeozoic rocks of the Southern Uplands was 5.77 km/s. A basement with a velocity of 6.0 km/s is said to occur at 1.7-2.0 km depth with rapid velocity increase to 6.35-6.40 km/s at a depth of 6 km. This basement extends from the Midland Valley under the Northern Belt at about 1.8-2.3 km depth and deepens under the Central and Southern Belts, being overlain by thicker Lower Palaeozoic sediments. Travel-time delays of 0.2 s across the Southern Uplands, Kerse Loch and Stinchar Faults were attributed to vertical zones of low velocity rocks in the fault zone, postulated to be either serpentinite or sheared, fractured rocks.

It should be mentioned here that Adesanya (1982), who carried out a similar project, obtained different velocities for the Lower Palaeozoic of the Southern Uplands and Girvan area. Hammer line velocities in rocks exposed at Girvan ranged from 2.9-4.0 km/s in greywackes and 2.2-3.8 km/s in shales. Velocities of 5.3 km/s and 4.9 km/s parallel and perpendicular to strike, respectively, were obtained from seismic refraction profiles executed at EKA. Core velocities from shale and greywackes were also determined parallel and perpendicular to strike. The values for the shale are 4.31 km/s and 3.63 km/s respectively and for the greywackes are 5.15 km/s and 5.04 km/s respectively.

It is noticeable that discrepancies occur between core velocities obtained by the two workers for the Lower Paleozoic rocks where Al-Mansouri obtained a mean value of 5.7 km/s while Adesanya suggested a range of values of which the highest does not exceed 5.2 km/s. Similar differences are also observed in data collected along seismic refraction lines by the two workers.

[11] Regional seismic data recorded across the Midland Valley (MAVIS) were interpreted by Dentith (1987). The dataset comprised two sub-parallel E-W profiles across approximately the whole width of the Midland Valley and intersected by a N-S profile. Controlled shots were used in the project and the acquired data were integrated with previous seismic work (Sola 1985). A four layer model was suggested for the region:

[1] Layer 1 with P-wave velocity of 3.0-5.0 km/s and thickness of 0-2 km is interpreted as Carboniferous and Upper ORS.

[2] Layer 2 with P-wave velocity of 5.4 km/s and thickness of approximately 2 km, is interpreted as Lower ORS and Lower Palaeozoic.

[3] Layer 3 with P-wave velocity of 6.04 km/s and thickness of approximately 3 km is interpreted as crystalline basement.

[4] Layer 4 with P-wave velocity of 6.43 km/s is interpreted as higher velocity crystalline basement.

This division of the Midland Valley upper crustal cover allowed the subdivision of the LISPB layer 2 into two layers of about 5.4 and 6.0 km/s respectively. This was in addition to the confirmation of the subdivision of the LISPB layer 1 envisaged by Davidson (1986). Dentith agreed also with LISPB interpretation of layer 3.

1.10.2. Gravity, Magnetic and Electrical Studies

[1] McLean (1966) carried out a detailed gravity survey of Ayrshire and concluded that the Kerse Loch Fault and the sub-parallel Straiton Fault end against or trail into a NNE-SSW structural high. This structure is apparently continuous from the core of Arenig rocks, SW of Girvan to the Arenig outcrop in the NE of the area.

[2] McLean & Qureshi (1966) made one of the first regional geophysical studies (regional gravity data) of the crust of the Midland Valley and its approaches and

deduced that the crust beneath the Midland Valley could be 5 km thinner than under the Grampians and the Southern Uplands.

[3] From aeromagnetic anomalies and a gravity high over the western part of the Southern Uplands (Galloway), Powell (1970) modelled a dense Lewisian basement under the Lower Palaeozoic sediments.

[4] El-Batrouk (1975), from regional interpretation of Bouguer anomalies in the Southern Uplands, suggested that the granite plutons are connected at depth of a about 7.5 km by a saddle-like structure as a single massive batholith along the Caledonian trend.

[5] The electrical conductivity of the crust beneath Scotland and north England has been investigated by several magnetotelluric surveys. Jones & Hutton (1979a, 1979b) indicated marked lateral variations in conductivity structures across southern Scotland. One dimensional inversion of these data suggests that there is a conductive zone beneath the Midland Valley between 12 and 44 km depth. Beneath the Southern Uplands there is a zone of similar conductivity between depths of about 28 and 70 km. They concluded that these layers are the same because of their similar resistivities.

[6] Hutton *et al.* (1980) extended the previous work with thirty new stations forming a traverse approximately coincident with the LISPB profile. Two dimensional modelling of both magnetotelluric and geomagnetic response functions indicated sharp changes in the depths of seismic boundaries. For example, the Great Glen, Highland Boundary and Southern Uplands Faults, have their counterparts in the electrical model. Ingham & Hutton (1982a, 1982b) extended the data into the Midland Valley and attributed the presence of a good conductor beneath the Southern Uplands to many effects such as the presence of hydrated rocks and dehydration at the amphibolitic/granulitic transition in the upper part of the conducting zone, solid conduction in basaltic and ultramafic rocks at deeper depths, and possibly partial melting below 70 km. They also envisaged that there is a

fundamental difference in the lower crustal structure to the north and south of the SUF.

[7] Hipkin & Hussain (1983) produced two north-south trending gravity profiles across Scotland (Fig. 1.14). The effects of known sedimentary layers (Devonian) have been removed to highlight anomalies of deeper (older) origin. A positive anomaly of 20-30 mgal was expected in the Midland Valley relative to the areas to the north and the south, corresponding to the LISPB 6.4 km/s layer occurring at about 7 km depth and terminating at the SUF, and falling to about 15 km depth some 20 km north of the Highland Boundary Fault.

This change in gravity observed to the north coincides with the Moine-Dalradian contact mapped at the surface, but in the south no equivalent changes were observed. A gravity "low" with an amplitude of -100 mgal, elongated to the SE of and parallel to the SUF north-east of Sanquhar basin was interpreted as a granitic body at shallow depth with density of 2650 kg m^{-3}, giving a density contrast with the country rock of -70 kg m^{-3} (Lagios & Hipkin 1979).

1.11. Summary

The Caledonian orogeny represents a cycle of events in which two previously separated continents, Avalonia and Laurentia, collided closing the ocean that once existed between them (Iapetus) and during their collision a number of small terranes became trapped. The ocean opened about the beginning of the Cambrian period and finally closed in Silurian-Devonian times. The suture marking the former site of the ocean crosses Britain near the Scottish border and continues into Ireland via the Solway Firth. Scotland and the NW of Ireland are derived from the marginal portions of the North Atlantic continent, while the rest of Britain and Ireland were derived from the European continent.

Concerning the issue of the Southern Uplands, the majority of workers agree that it represents an accretionary prism formed in a fore-arc environment on the

northern margin of the Iapetus ocean. This interpretation will explain two important characteristics of the region: (1) The predominant NW (continent-ward) younging of strata and (2) The progressive appearance of younger sequences in the fault blocks towards the SE (ocean-wards). However, the principle controversy is about the position of the arc associated with this prism. Some authors think that it lay to the north of the Southern Uplands Fault while others suggest that during the Silurian it lay along the line of the Kingledores Fault and has been removed by faulting. A third view suggests that it lay to the south during Ordovician and early Silurian times and is now covered by the sediments of the Southern Belt.

Leggett (1987), in assessing the various models available and the validity of using analogues, concluded that each accretionary prism assumes its distinctive fingerprints and there is no well studied modern/Neogene margins which can be taken as a model for the past.

Strong arguments still exist (see section 1.4) that the Northern Belt should be treated as an entirely separate entity from the Silurian of the Central and Southern Belts, and the idea of a more complicated tectonostratigraphic history for the Southern Uplands cannot be disregarded.

The LISPB model for Northern Britain suggests that the Midland Valley basement terminates abruptly at the SUF, while more recent work (Hall *et al.* 1983; Upton *et al.* 1983; Al-Mansouri 1986 and Davidson 1986) suggest otherwise and that this basement continues at least for another 15-20 km south of the SUF.

Bamford (1979) did not identify the rock type associated with the interpreted 6.3 km/s different basement. In fact, there are few clues as to the nature of the underlying basement in both the Midland Valley and the Southern Uplands and the discrimination between them on the basis of results obtained from a single across-strike profile seems to be conjectural. Leggett *et al.* (1983) pointed out that it is possible that continental collision may have thrust some of the accretionary

prism over the southern edge of the Midland Valley crust. This may indicate limited projection of the 6.4 km/s layer under the Southern Uplands. Furthermore, the LISPB uppermost layers (the top 2-3 km) were beyond the LISPB resolution, which was designed to study deeper structures, but this could produce a misleading image for solution of deeper problems.

However, it is possible using a medium range seismic network like the SUN, that problems such as the depth and perhaps the thickness of the basement can be estimated. Also it is possible using such project to determine the downward extension of the main faults and their effect on the underlying basement.

CHAPTER TWO

DATA ACQUISITION, FIELD PROCEDURES AND INSTRUMENTATION

2.1. Introduction

Quarry blasts were used as sources to record a network of seismic profiles across the Southern Uplands and adjacent areas. This network is called SUN: Southern Uplands Network. A seismic refraction project of this type will involve many aspects which should be accounted for to obtain the maximum benefit from the work done, such as quality of the data being acquired, site locations and their accessibility, recorder gains and how they can be optimally set, time availability and other limitations which can affect greatly the progress of such a project.

From this and previous work carried out by the author many aspects of operations are discussed which were found to greatly affect data quality but which had not been assumed to be significant by other workers. In addition to a discussion of all these factors and procedures, a description of the profiles recorded and the field recording equipment deployed will be presented. Finally, a brief account of the playback and digitization system will be given. Information concerning quarries used in this project is listed in Appendix 1.

2.2. Description of the Profiles

Data acquisition started in March 1989 and was finished by the end of December 1990. The total length of the lines recorded is approximately 288 km of which 203 km was reversed. A total of 265 stations were occupied, of which 40%

were occupied more than once due to several reasons such as bad weather conditions, change of blasting time without advance notice, or to improve data quality. A station spacing of 2 km was maintained throughout the project although, this was highly controlled by the accessibility of the site locations, a factor which also affected the lateral offset of the recording sites from the planned positions of the stations, but this was also kept within a range of 2 km.

Figure 2.1 shows the geographic locations of the six SUN profiles which are numbered, within the Southern Uplands, in increasing order from east to west. Quarries are named after nearby towns. Five profiles cover the Southern Uplands. The sixth lies at the northern edge of the Midland Valley parallel to the axis of the Strathmore Syncline and was recorded to expand the knowledge obtained by a previous project (see Kamaliddin 1988). Of the five Southern Uplands profiles, three are reversed and two are single end shooting due to the scarcity of quarries. The geographic coordinates, the names and type of coupling of the recorded stations are listed in Appendix 2. Refer to Figures 1.2a and 1.5 for all fault locations mentioned in this chapter.

Apart from line 5, all the profiles covering the Southern Uplands trend approximately N-S, crossing the regional strike. Quarries at the northern end of each line are within the Midland Valley to provide data across the SUF as well as to achieve deeper penetration. The fifth profile, which was recorded from Glenluce quarry, trends parallel to the regional strike, south of and parallel to the Kingledores Fault. This line was recorded to provide extra control on the velocity configuration in the uppermost layer of the area and to estimate the velocity change with azimuth, and thus correlate any change with previous geophysical work in the region (see section 1.10).

2.2.1. Line 1: Melrose - Bangley

This profile is 40 km long and trends in a SE-NW direction. It marks the

eastern limit of the project covering the eastern part of the Southern Uplands. The profile was recorded from Craighouse quarry (Melrose) in the SE, which lies about 1 km NE of Melrose and is situated in intrusive igneous rocks (trachytes). At its NW end, Bangley quarry (Haddington), which is located about 24 km east of Edinburgh, was used to record the line towards the SE. The quarry is located on extrusive igneous rocks (tuffs) of Lower Carboniferous age. It was not possible to extend the profile further to the north of Bangley quarry shooting from Melrose due to high noise levels in the vicinity of the Firth of Forth. Nor was it possible to extend it to the south of Melrose because of the low energy released by Bangley quarry.

The main structures traversed by this line are the Kingledores Fault, which occurs approximately 17 km north of Melrose quarry and the SUF "zone" which is present at a distance of 27-31 km north of Melrose quarry. This zone is comprised of two main faults, the Lammermuir fault, which marks the recognized surface trace of the SUF and a fault 2-4 km further north trending parallel to the Lammermuir fault, known as the Dunbar-Gifford Fault. The main lithological units traversed by the profile are, from SE to NW, rocks of Upper ORS age which are exposed in the southern third of the profile followed by rocks of the Ordovician and Silurian periods exposed at the middle section of the line representing rocks of the Central and Northern Belts of the Southern Uplands. Towards the northern third of the line, beyond the SUF, Midland Valley rocks of Carboniferous age occur.

2.2.2. Line 2: Melrose - Ratho

This line is 64 km long trending in a SSE-NNW direction extending between Melrose quarry in the SSE and Craigpark quarry (Ratho) in the NNW which is situated on quartz-dolerite intrusive rocks 13 km SW of Edinburgh. This profile meets line 1 at Melrose quarry in the south. The distance between the two end quarries of this line is 59 km, but recording of Ratho quarry was extended SE of

Melrose quarry for a further 5 km making use of the high energy released by this quarry.

Unfortunately Melrose quarry did not live up to expectations and the maximum distance at which headwaves could be received from this quarry did not exceed a range of 40-42 km, leaving 25% of the line unreversed. This gap did not pose serious problems to the project since it lies in the Midland Valley where good velocity data is available from previous projects (e.g. Davidson 1986, Dentith 1987). It was also planned to record this line from Broad Law quarry, as a within line shotpoint, but for reasons beyond the author's control this was not achieved.

The profile intersects the surface trace of the Hartfell Line at 9 km NNW of Melrose quarry and the Kingledores Fault at a high angle 21 km NNW of the quarry. The SUF zone occurs at a distance ranging from 28.5 km to 30.5 km from the same quarry, while the Leadhills Line is thought to be present between the last two faults. The line also crosses the *Pentland* and *Colinton* Faults at approximately 16 km and 4 km SE of Ratho quarry respectively within the Midland Valley (i.e. 43 km and 55 km from Melrose quarry). The main lithological units exposed along the line are similar to those observed along line 1 where Midland Valley Carboniferous and Upper ORS rocks are present at the northern end of the line, while rocks of similar ages and lithologies are exposed at the SE end of the line. Strata of the Silurian and Ordovician ages are exposed along the rest of the line.

2.2.3. Line 3: Aberdour - Moffat

This line was designed to provide deeper penetration of the crust beneath the Southern Uplands using large offsets. Therefore a more northerly-situated quarry (Aberdour) was chosen to record the line from its northern end. This quarry lies north of the Firth of Forth and had proved to be an excellent source during a pre-

vious project. In addition to Aberdour quarry, Ratho quarry which is situated 17 km SW of Aberdour, was also used to provide data in the same direction. Both quarries were recorded towards Moffat which is about 80 km south of Aberdour. It was anticipated that Ratho quarry, which was recorded to a large offset when used in recording Line 2, would provide the same recording range along this line. This proved to be true, making this line the longest of the project (66 km). The line was displaced about 3 km towards the west, from its straight orientation towards Moffat, at 17 km south of Aberdour in order to record it from Ratho. This was because the decision to use the latter quarry was made after the recording of the line from Aberdour had already started.

It was planned to record the line from Moffat quarry at its SW end to provide reversed coverage. This was not achieved because of the infrequency of the blasts at this quarry and poor communications with the quarry management resulted in the very rare blasts at this quarry being missed.

The main known structures traversed by this profile are, from north to south, the Pentland Fault occurring at 16 km south of Ratho quarry, the SUF 27 km south of Ratho, the Kingledores fault which lies at a distance of 40 km south of Ratho and, finally, the Hartfell Line which occurs at about 52 km SW of Ratho. The lithologies exposed along the line are Carboniferous and Upper Devonian rocks which are found north of the SUF, followed by the Ordovician rocks of the Northern Belt just south of the SUF. To the south of this the Silurian rocks of the Central and Southern Belts are exposed.

It is important to note that SUN lines 1-3 all intersect, nearly at right angles, the SUSP profile and trend sub-parallel to the LISPB profile (see Figure 2.1). Also it is worth noting that the profiles traverse the slow (S2) and fast (F3) zones of Hall *et al.* (1983) while line 3 crosses the site of the Broughton Array (El-Isa (1977), south of the SUF.

2.2.4. Line 4: Glenluce - Tormitchell

This line trends in a S-N direction at the SW margin of the Southern Uplands and thus marks the western limit of the project. The two quarries used in recording this reversed line are: Barlockhari quarry (Glenluce) in the south and Tormitchell quarry sited 6 km SE of Girvan, in the north. The former is situated on dioritic intrusive rocks and the latter on basaltic lavas (extrusive). The quarries are 38 km apart and the line was extended at both ends, for 3 km south of Glenluce recording from Tormitchell, and for 12 km north of Tormitchell recording from Glenluce, making a total of 53 km of data coverage.

The primary target of this line was to obtain enough data to be able to correlate the velocity configuration in this part of the region with that obtained by the SUN profiles 1-3 in the east, and with results obtained from previous geophysical work which was mostly concentrated in the east (see section 1.10). The second objective for this line was to investigate the lateral change and extension of structures, and perhaps, the stratigraphy, towards the west. Using the high energy released by Glenluce quarry, the basement beneath the SW part of the Midland Valley was to be studied, together with any possible downward extension of the major faults north of the SUF in the vicinity of Girvan and, thus, to tie this work with a previous refraction project executed by Al-Mansouri (1986). This was made possible by the relatively large distance between Glenluce quarry, in the south, and the Girvan district, in the north, where the necessary crossover distance was obtained to detect arrivals from the Midland Valley basement.

The main structures crossed by the profile are the Kingledores Fault at a distance of 2 km from Glenluce quarry, the Glenn App Fault at 30 km, the Stinchar Fault with its surface expression situated 3 km north of the Glenn App Fault and, finally, the Kerse Loch Fault at approximately 43 km in the vicinity of Girvan. It is assumed by many authors (e.g Leggett 1980, Leggett *et al.* 1979, McKerrow 1986) that the Leadhills and the Fardingmullach Lines may extend as far towards

the west as the Rhins of Galloway, thus intersecting this profile at short offsets north of Glenluce. The profile traverses rocks of Silurian and Ordovician age along most of its length, except at its northern extension in the SW part of the Midland Valley where the main exposures are rocks of Carboniferous and Upper ORS age.

2.2.5. Line 5: Glenluce - Newton Stewart

This is the only profile in the Southern Uplands which trends parallel to the regional strike. It is oriented in a SW-NE direction south of and parallel to the Kingledores Fault and lies entirely within the Central Belt where rock exposures are greywackes of Silurian age. The profile was recorded from Glenluce quarry and is 22 km long and was designed to provide extra control on the velocities of the top regional layer. It was terminated shortly before the subsurface extension of the granitic bodies present in the area (see section 1.5) to eliminate any misleading velocity values which may be caused by these bodies.

2.2.6. Line 6: Boysack - Collace

This is the only line recorded completely within the Midland Valley. It lies in the NE corner of the region parallel to the axis of the Strathmore Syncline and was designed to tie with a previous line recorded from Collace quarry toward Aberdour in the SW. The only problem which hindered the recording of this profile was the infrequency of the blasts of the two quarries used, namely Boysack quarry at its NE end, which blasted only twice, and Collace quarry at its SW end, which blasted only 5 times of which 4 were missed. The line trends in a NE-SW direction parallel to the Highland Boundary Fault and is 45 km long traversing sedimentary and igneous rocks which are entirely of Lower Devonian age (ORS and associated volcanic rocks). Both quarries are situated in Lower Devonian andesite lavas. There are many minor NW-SE trending faults which intersect the line nearly at right angles. These faults mainly affect Lower Devonian strata and

the associated volcanic rocks of the Ochil and Sidlaw Hills which lie to the south of the line.

Due to the little amount of data recorded from Collace quarry (only 7 scattered traces), the profile will be treated as an unreversed profile, neglecting Collace data in the processing procedures and it will be only used in constraining the interpreted model. However, an unfiltered digital section will be presented in chapter 5 to show the data acquired from Collace.

2.3. Field Work

In planning and executing a seismic project of this scale involving uncontrollable parameters such as weather conditions, noise sources, the area being investigated (which is limited by the locations of active quarries) and, most importantly, the time and type of the blast, two important factors must be considered before and during the time of recording and these are:

[1] Recording site location

[2] Instrument gain setting

2.3.1. Recording Site Location

During the planning stages of a profile, a line is usually drawn on the map connecting the two end quarries, in the case of reversed coverage, and a station is marked at each successive location using a constant spacing (e.g. 1, 2 or 5 km) depending on the degree of resolution desired. This procedure will place many stations in areas of high cultural noise or at inaccessible locations. Such stations have to be shifted to more appropriate sites. During this project, when such situations were encountered, care was taken so that the maximum shift did not exceed a radius of 2 km perpendicular to the line or 0.5 km along the line. This was done in very rare cases but the average shift of the stations was approximately 1 km at right angles to the line and 300 m along it. Three stations along line 3 (10, 32 and 33) were not recorded because it was impossible to reach them from any direction.

Concerning stations which were close to permanent sources of noise (such as large towns or factories), the only solution was to record the station several times (up to 8 times) in the hope that one of these recordings will be obtained where the noise levels are at their minimum and the quarry blasts with maximum charge in order to get a reasonable seismic trace. In such cases, if the wind speed was at its minimum and the quarry face being removed is perpendicular to the line and facing away from the station (see section 2.3.2), then the amount of energy received will be increased and such stations could be recorded, despite their closeness to permanent sources of noise. This is provided the gains used are kept within reasonable limits so that recordings are not saturated.

Dentith (1987) and Kamaliddin (1988) suggested that rock outcrops are better recording sites than drift. This proved to be true in the Midland Valley where the main exposures are volcanic rocks. Rocks which are subjected to large scale deformational processes, like in the Southern Uplands, attenuate seismic energy at a higher rate than those of the Midland Valley, presumably because there are more cracks, joints and other microstructures which will contribute to energy dissemination. Another possible factor is that, in the Southern Uplands, the drift cover is thin and therefore any local noise will be transmitted directly to the bedrock which is basically a better energy transmitter. In the Midland Valley thicker drift areas have far more local noise sources than the Southern Uplands which are easily transmitted to the geophones in these drift sites. However, in practice, drift sites within the Southern Uplands were better recording sites, than rock sites and firm compact soil was sought as a preferable recording site, contrary to the practices utilised in the Midland Valley.

Figures 2.2 a and b show the frequency analysis of noise and seismic signal at two stations located along line 4, and recorded from Tormitchell. The left hand spectrum is from a geophone inserted in soil (station tm08) while the right hand spectrum is from a geophone coupled to a rock outcrop (station tm8x). It is clearly

seen from Figure 2.2a that the noise occupies a wider frequency range (2-15 Hz) at the rock site than the noise frequency range seen at the drift site (2-5 Hz). In Figure 2.2b the case is reversed, the seismic signal frequency content is much lower at the rock site (2-19 Hz) than at the drift site (2-36 Hz). Figure 2.2c shows the seismic traces used for this comparison. The two traces were recorded on the same day using the same shot. It must be admitted here that the frequency range obtained at the drift site may contain a wider spectrum of frequencies of both signal and local noise since drift sites, in the Southern Uplands, were found to be better "conductors" of seismic energy than rocks. It remains that the important factor in locating the onset on seismic traces is still the S/N ratio and signal amplitude and both were better for traces recorded in drift.

As mentioned above, this is just one experience of many such cases and hence there is no firm rule for geophone coupling concerning this particular issue, and tests must be carried out prior to any project. In recording line 3, from Ratho quarry towards the south, station 38 south of Moffat was coupled to igneous rocks at a disused quarry. The seismic trace obtained at this site was excellent compared to other traces collected at rock exposures in the Southern Uplands, taking into account, also, the large offset obtained (66 km). This indicates that igneous rock exposures of younger age (Tertiary), in the Southern Uplands, have suffered less deformation than the surrounding Silurian, sedimentary rocks and therefore, they have the same good conducting qualities as those of the Midland Valley, while rock exposures of sedimentary origin, which are more likely to have suffered large deformations are poor conductors of seismic energy. This may be explained by the fact that these Tertiary igneous rocks were intruded after the main deformational phases which were active until the end of the Silurian-Devonian period.

2.3.2. Instrument Gain Setting

The gain scale of the recorders is divided into 6 settings corresponding to a range of 88-118 dB i.e. 6 dB per interval. Gain setting of the recording sets is

equally as important in determining the quality of detectable seismic energy as the site location and the way geophones are inserted. It must be high enough to adequately record events at a station at a given distance from a shot of a given size, but must be low enough to prevent saturation of the recording system by noise and/or the event. The most important factors controlling the gain value at a station on a given recording day are:

[1] Wind speed is a major source of noise. It was noticed that beyond a range of about 20 km from the quarry any small increase in the wind speed will cause higher distortion of the seismic wave form compared to traces recorded at ranges less than 20 km. Therefore stations closer to the quarry can be recorded on windy days thus permitting the use of low gains, while furthest stations can be recorded in preference on calm days where maximum gains could be used. However, apart from the first 10-20 km of a profile, it is not advisable to do any recording when wind speed is predicted to 30 mph.

[2] Orientation of the quarry face being removed. This proved to be a decisive factor in recording good quality seismic data for large offsets and in employing lower gains where noise sources on a particular day are too high to use the desired gains. However, high gains should be used if the face being removed is at a low angle to or facing the direction of the stations being recorded. This is because much of the energy released by the blast towards the recorders is consumed in fracturing and moving the rocks outwards. Lower gains can be used if the face being removed is at right angles to the profile and facing away from it because most of the energy released towards the recorders will be transmitted through the solid rock.

An excellent example of the quarry face effect is seen along Line 3. This line was recorded from two quarries at its northern end, namely Aberdour and Ratho quarries. Aberdour uses an average charge of 3.5 tonnes of high explosives while Ratho employs a mixture of high explosives and fertilizers with average

blasts of 1.4 tonnes. The distance between the two quarries is 17 km which means that the stations (6-25) which are recorded from both quarries are always 17 km further from the source in the case of Aberdour quarry than those recorded from Ratho quarry. In the case of Aberdour quarry the face being blasted always faced the profile, while in the case of Ratho quarry, the face was always away from the line.

Comparing Figures 4.30a and 4.31a (stations 6-25 of line 3) it can be clearly seen that data quality obtained from Ratho is much better than that obtained from the Aberdour, especially towards the southern end of the profile and this applies to the range obtained from both quarries where a maximum of 57 km was obtained from Aberdour quarry while a range of 66 km was obtained from Ratho quarry and this could have been increased by another 4-6 km if not for other factors. The weather conditions at the time of recording the southern section of this line from both quarries were very similar. The 17 km difference in range of a given station from the two sources is not the factor in the quality difference, because seismograms recorded at the same distance from the sources are of different quality.

Another comparison with Ratho quarry data can be made along Line 2. Recording from Melrose quarry, which uses nearly double the charge of Ratho and where the quarry face is towards the profile, a maximum range of 42 km was obtained with moderate quality (Fig. 4.28a). In comparison, energy from Ratho quarry in the reversed direction, with its face away from the profile, reached 64 km with nearly half the charge.

If the wind speed and the quarry face are at their ideal situation, sufficiently large ranges could be achieved despite the size of the blast. Along line 2 an offset of 64 km was obtained using a blast of only 1.7 tonnes, which according to Dentith (1987) and Kamaliddin (1988) is sufficient only for a maximum range of about 40 km. In the case of line 2, the wind speed was less than 5 mph and the quarry face was at right angles to the line and away from it. This allowed the

recording of the end stations of this line with relatively good S/N ratios (see Fig. 4.29). Furthermore, if it was not for the lack of recording sets, an extra 10 km of data could have been recorded with the same quality. Also along line 3 an offset of 66 km was obtained using a total charge of 1.3 tonnes with excellent quality.

However, and in conclusion to the above discussion, it is unlikely that a profile longer than 75-80 km could be executed even if all the given parameters were to be optimised, when using quarry blasts of the sizes used here. Also the possibility of obtaining reasonable results diminishes if the wind speed exceeds 45 mph, no matter how good the other parameters are.

[3] The size of charge being blasted is another important factor in determining the quality and range of seismic data and therefore the amount of gain used. Quarries usually divide the total charge on a number of holes ranging from 8-40 so as to greatly reduce the power of the blast to prevent harmful vibrations reaching neighbouring farms and towns. Davidson (1986), Dentith (1987) and Kamaliddin (1988) all claimed that the most important component of a given blast is the quantity of explosives present in the first fired hole. This proved to be largely true, but it was noticed that, if all other conditions are kept constant, while the total charge is increased by 30-50% for a given quarry, an increase of 10% of the total length of the profile in terms of detectable seismic data will be observed along with some improvement in the quality of it. Thus, lower gains could be used in such cases subject to other conditions.

[4] The depth of the shotpoint holes can affect the range of detectable seismic data and therefore higher gains must be used if the holes are too shallow (<10 m). This is simply because in planning shallow holes much of the blast energy will be directed upwards which is less useful for seismic purposes.

[5] Permanent sources of noise such as factories, main roads and towns where the use of very low gains or the shift of the station to other locality (if possible) is unavoidable.

[6] Tractors etc. working in the fields are a bad noise source, especially during spring and summer when quarries work at their maximum capacity, thus limiting the use of this productive period.

[7] Time of the blast and location of the site. Lower gains should be used at stations near towns if the blasting time is around midday (which it is usually is!) when cultural noise increases. Higher gains can be used on rainy days when movement of people and vehicles is less.

Kamaliddin (1988) presented a table of gain settings versus offset (reproduced in Table 2.1) as a general guide for this purpose. The primary factor was considered to be the size of the charge being blasted. These values were suggested assuming varied quarry face orientation and did not give much importance to other factors. However, during this project it became evident that the charge size is not the only prime factor in determining the gain used. There are another two important factors which influence data quality and detection range: the orientation of the quarry face being blasted and wind speed. Thus the values referred to above could be modified to those of Table 2.2 when other conditions are favourable.

Table 2.1 Recommended gain values used for an instantaneous charge of 90-150 kg.

Distance in km	Gain
0-5	1
6-10	1-2
11-16	2-3
17-30	3-4
>30	4-6

Table 2.2 Recommended gain values used when quarry face is at right angles to the profile and facing away from it. Wind speed is less than 12 mph using instantaneous charge of 90-150 kg.

Distance in km	Gain
0-20	1-2
20-40	2-4
40-80	4-6

Table 2.2 shows the gain settings when all other factors are at optimum. For different situations gain values should be set 1-2 units higher than the suggested values, if weather conditions and local noise permit such increase. In practice, only 1 unit increase is usually possible and this will affect data quality to a limited extent. A 2 units increase in poor weather conditions or when a small charge is fired will certainly distort the data.

However, every quarry has its own "fingerprint", this special fingerprint will be an additional influence on data quality and recording range. For example, it is believed that quarry blasts using a mixture of fertilisers and high grade explosives are poor sources, but an explosion of 1.3 tonnes of such a mixture was recorded 66 km away from Ratho quarry (station 38 along Line 3) with excellent results. Conversely, Melrose quarry which uses only high grade explosive in its blasts did not provide reasonable data further than 40 km offset using a total charge of 1.6 tonnes. Usually the researcher will become familiar with such quirks after recording a few blasts and hence the gain values given in Tables 2.1 and 2.2 can be adjusted accordingly, but these adjustments usually will not exceed +/- 1 gain unit.

Finally, Dentith (1987) and Kamaliddin (1988) suggested that a linear relationship exists between the charge size and the maximum range that headwaves reach, but from the above discussion it is evident that this relationship is approximate and it can only be accepted as a general guide line for estimation purposes.

2.3.3. Recommended Field Procedures

During this project and a former M. Sc. one, more than 1000 sites were occupied under varied weather and other conditions. From the experience gained in recording these stations the following practices are highly recommended to increase both productivity and signal quality. However, if the number of people working on such a project is increased to more than one the productivity will be increased accordingly but not necessarily in the same proportion, since other factors such as the number of recording sets available and the knowledge of the area and roads are important.

[1] An average upper crustal refraction profile is about 50 km long, although in some special cases it may reach 75 km, with an average recording point separation of 2 km. This will make it impossible to record the profile in one or two field days and it is advisable to divide it into three equal segments. Sequential recording of these segments is not necessary, and the decisive factor on which part of the line to be recorded on a certain day is the wind speed and quarry face being blasted (see section 2.3.2). So by recording far stations on "good" days and near stations on "bad" days a line 50 km long can be recorded in approximately 8-9 field days instead of an average of 16 days, thus doubling productivity.

[2] Quarry practices should be checked prior to a decision on the use of its blasts because some, although using relatively large charges, have certain practices which significantly reduce the maximum distance at which recording can be done. For example, Bangley quarry uses an average total charge of 1.3 tonnes with approximately 130 kg in each hole which was theoretically sufficient for the offset anticipated, but an additional delay is put in each hole reducing the charge to half its power and, accordingly, the maximum distance to which the headwaves travelled was reduced. This caused a great deal of problems in recording line 1.

Another practice which affected data quality and range was what is termed by quarry managers as *top and bottom initiation*. This means that the detonators

are placed either at the top or at the bottom of each hole and hence the direction of the energy wave is controlled by this method. Top initiation means that the detonators are fired at the top of the holes and therefore the energy is directed towards the bottom reducing local vibrations and increasing the amount of rock fragments produced. It was expected that top initiation would improve both data quality and range, but this was not supported by evidence derived from Ratho quarry when it switched from bottom initiation to top initiation. To the author's surprise both data quality and range were reduced. This could not be confirmed since few shots were recorded using the top initiation. A rough comparison between the two methods can be obtained, as far as data quality is concerned, by comparing data obtained along line 2 using bottom initiation (Fig. 4.29) and data obtained along line 3 (Fig. 4.31a), from station 11 onward, where the second practice was used.

[3] Field tests should be carried out to decide whether rock or drift sites are better recording sites before starting any project. Dentith (1987) and Kamaliddin (1988) worked in the Midland Valley and suggested that rock sites are always better in acquiring good signal/noise ratio and maximising the distance at which headwaves are observed. This was not the case in the Southern Uplands where rock sites were very noisy, probably because they were mostly of sedimentary origin and have been subjected to extensive weathering and deformation, thus their seismic transmission qualities have been reduced. It was noticed that, unlike rocks in the Midland Valley, most rock exposures in the Southern Uplands are highly cracked.

[4] Geophones should be placed away from forests and, even, individual trees which are substantial sources of noise due to movement of their roots. Loose soil reduces detectable seismic energy markedly, because the low compaction of soil will cause poor coupling of the seismometers and therefore low transmission of energy. In cultivated fields, seismometers should be firmly inserted below the

ploughed section of soil in the more solid earth, thus reducing to a great extent noise caused by continuous movement of small fragments of soil in the geophone hole and ensuring firm coupling of the geophones. However, deep burial of geophones is not as important as their protection from wind and obtaining firm contact with the soil. So even on windy days geophones can be inserted directly in the soil cover provided that they are well covered thus avoiding loose contact if the ground was dug and they were buried in gravelly soil. Finally, the geophones should be placed away from flowing water in rivers, streams etc. because of noise created by the flowing water.

[5] It was found that the best protection from wind effect is the firm insertion and burial of the geophones when a hole is used whereas when geophones are placed directly on the surface of the ground, a plastic cover will be very useful as a means of protection. Some tests were made to see if buckets could provide the same protection when buried on top of the geophone as an extra cover but the results were not encouraging, probably because these buckets act like drums covering the buried geophones and any minute earth movement will be amplified. A well packed soil cover proved to be the best method for protection in all cases.

[6] Small gullies and valleys should be avoided as recording sites since they act as wind tunnels and any small change in wind speed will be amplified in these locations. Therefore sets left to operate on remote start in calm weather will be highly affected if wind conditions deteriorate subsequently.

[7] On the recording day farmers should be asked if empty fields will be used later in the day. Important recordings were lost because animals were let into empty fields after the stations were setup and the animals chewed the wires or changed the orientation of the radio antenna thus distorting M.S.F reception. Also, tractors working in the fields later in the day destroyed potentially valuable data.

[8] Accessibility of stations should be checked before starting any project and adjustment to the orientation of the line should be made (if possible) so that most

of the stations are easily approached even in bad weather. This will help to avoid gaps along the profiles.

[9] It is highly recommended that the shotpoint is the first station to be set during a recording day. This is to avoid missing the blast altogether due to an unagreed change in the firing time due to unpredicted difficulties in loading the explosives or the manager's decision to advance the blast 1 or 2 hours. Several (hard) working days were wasted due to such incidents.

[10] An average person, familiar with the area being investigated and its roads, can either establish three stations or collect five in one hour. This is important in planning the amount of work to be done on a certain recording day since the quarries in this area usually blast around 1 pm +/- 30 min. This means that the person/group have approximately 3-4 hours to establish about 10 stations. Allowances should be made for the time needed to reach the quarry, set the shotpoint recorder, and go to the line segment being recorded that day. It is important to decide on the number of stations, their locations and the best roads to be used before setting out to avoid confusion and loss of valuable time.

[11] Avoid using high gains (more than 4 gain units) at noisy sites beyond 40 km range because this make it more difficult to locate weak events which are usually received at such distances, since high gains will cause local noise to saturate the system due to the high sensitivity of the sets.

[12] Since conducting a project of this type will involve quarry blasts and not expensive dedicated shots, it is better to record noisy traces several times until a good seismic record is obtained (or the different recorded traces are stacked) to avoid any possibility of large error value when only one noisy filtered trace is used.

[13] Quarries which blast a total charge of 100-500 kg are considered inadequate for medium-large scale refraction projects since the maximum offset usually obtained from such quarries is only about 20 km, meaning that only the top 1-2

km of the crust is covered by these blasts. Quarries used during this project have an average blast of 2 tonnes which provided data up to 66 km with reasonable results, allowing deeper coverage of the upper crustal layers to be achieved. Also there is always the possibility that such quarries have one or two larger shots each year (4-5 tonnes) which could be recorded to large offsets (50-80 km).

Tables 2.3 to 2.10 are logs of recording of each quarry and give an idea of the progress of the project. The number of stations refers to **successful** recordings per day. Typically 7-9 stations were setup and some lost due to a variety of factors such as M.S.F (timing signal) reception, change of weather and other conditions.

Table 2.3 Aberdour Quarry Recording Log

Date	Time hr min sec	Total Charge kg	No. of Stations Recorded
19/5/89	12:31:49.93	2800	7
3/11/89	14:59:56.87	3600	7
13/6/90	12:32:51.38	1500	8
3/9/90	14:10:50.83	5100	3

Table 2.4 Bangley Quarry Recording Log

Date	Time hr min sec	Total Charge kg	No. of Stations Recorded
15/3/89	12:29:25.68	875	3
12/4/89	12:31:24.98	1650	2
20/4/89	12:31:46.90	960	3
4/5/89	12:27:33.69	1200	3
25/5/89	12:26:44.32	1000	5
3/5/90	12:30:32.23	1000	4

Table 2.5 Boysack Quarry Recording Log

Date	Time hr min sec	total Charge kg	No. of Stations Recorded
28/4/89	15:01:36.80	3525	7
22/5/90	15:12:20.79	4600	15

Table 2.6 Collace Quarry Recording Log

Date	Time hr min sec	Total Charge kg	No. of Stations Recorded
2/6/89	14:37:04.88	2600	7

Table 2.7 Glenluce Quarry Recording Log

Date	Time hr min sec	Total Charge kg	No. of Stations Recorded
22/8/89	15:59:19.38	1000	12
29/8/89	13:03:09.71	1200	4
21/11/89	12:31:37.21	1200	3
23/2/90	12:46:58.23	1300	4
20/6/90	12:35:30.45	900	2
28/11/90	13:38:17.167	1200	7

Table 2.8 Melrose Quarry Recording Log

Date	Time hr min sec	Total Charge kg	No. of Stations Recorded
21/3/89	12:04:28.31	1200	2
12/4/89	12:03:27.82	1600	5
19/4/89	12:04:33.64	1000	3
3/5/89	12:02:43.93	1200	5
24/5/89	12:02:30.75	1100	6
7/6/89	12:05:33.51	1200	2
21/6/89	12:02:16.40	1100	6
18/8/89	12:04:29.66	1000	7
31/8/89	12:04:32.06	1200	6
7/9/89	12:03:34.89	1000	3
28/12/89	12:03:34.34	1000	2
24/5/90	12:04:47.25	1400	1
28/5/90	12:04:41.00	1300	5

Table 2.9 Ratho Quarry Recording Log

Date	Time hr min sec	Total Charge kg	No. of Stations Recorded
21/3/89	12:51:03.22	1800	1
30/8/89	14:58:33.64	2170	9
4/10/89	12:56:21.43	1595	9
24/10/89	12:48:15.25	1960	7
1/12/89	12:49:21.58	1700	6
16/3/90	14:01:43.94	2170	4
26/4/90	12:55:19.48	1265	6
4/5/90	12:59:54.00	1600	8
6/6/90	12:57:46.44	1125	7
15/6/90	12:57:31.16	1300	5

Table 2.10 Tormitchell Quarry Recording Log

Date	Time hr min sec	Total Charge kg	No. of Stations Recorded
11/7/89	17:02:47.32	1000	6
12/7/89	17:00:08.72	1500	5
12/12/89	13:59:45.28	1500	7
24/4/90	14:59:41.77	1375	5
1/6/90	12:07:16.80	1375	1

2.4. Field Recording Equipment

The Glasgow FM "Mark 2" recorder was used to record the data throughout the project. 22 sets were available to the author, out of which 15-18 were deployable at a given time. These sets are from an original 50 machines developed in 1983 from prototypes designed in 1981 by Dr J. Hall and Mr G. Gordon in the Department of Geology and Applied Geology, Glasgow University. A vertical 4.5 Hz L15B Mark geophone was used to detect the seismic energy. Figure 2.3 shows the recording arrangement of the sets. The recorders are based on a standard cassette deck amended to permit simultaneous recording on all four tracks. Therefore the C120 cassette tapes used allow an one hour recording window. A band-pass filter of 1.5-60 Hz is used to filter the pre-amplified seismic data, from which

the data is then passed through an integral amplifier/modulator and recorded on two channels. The first channel covers a gain range of 88-118 dB with selectable 6 dB intervals while the second is fixed at 18 dB down from the selected high gain channel.

The 60 kHz MSF time signal, broadcast from Rugby, is detected by a tuned radio receiver and is recorded on the third channel. The fourth channel is an auxiliary channel and was not used in this project. The recorders have a remote-start facility and electronic clock allowing deployment up to 24 hours in advance. Recorder geophone specifications are given in Appendix 3.

2.5. Playback and Digitization System

Initially recordings were replayed using an analogue playback facility which comprised a cassette deck mechanism with the tape head wired for replay only. Each seismic channel is then passed through a demodulator and analogue filters which proved to be of great use in initial assessment of noisy traces. These filters were usually set to pass frequencies between 3 and 40 Hz, but in traces where noise level is high and of constant frequency the bandpass was reduced to 3-21 Hz giving excellent results.

The output of each channel is then amplified and passed to a Bryans 40000 UV oscillograph which has two useful facilities. The first is the ability to adjust the paper speed thus allowing the separation of the first arrivals from other arrivals (if there is a reasonable frequency and amplitude difference) and the expansion of the onsets over longer time periods permitting onsets to be identified. The second facility is the ability to adjust the amplifier gains allowing a weak onset to be magnified.

The MSF channel is also demodulated but passed directly to the oscillograph via an amplifier. A Schmitt trigger is used to enhance the MSF signal to give it a box shape on the analogue playback for easy time correlation. The signal is finally

passed to a decoder which displays the time in days, hours, minutes and seconds, allowing quick discovery of the approximate position on the tape of an event. Figure 2.4 summarizes the stages involved in producing analogue traces and digitization.

Analogue-to-digital conversion is the technique by which the amplitude of a waveform is expressed in numbers at a specific values of time. The Programmable Data Processor (PDP) 11/23 PLUS microcomputer was used for converting analogue data to digital form. The software was programmed by R.T. Cumberland. The data are passed from the playback system through anti-aliasing analogue filters (3-40 Hz). An ADV11-C analogue-digital conversion board was used which can accept up to sixteen single ended bipolar inputs or 8 differential inputs, either unipolar or bipolar. Data sampling was set at 200 samples/second. However, occasional power supply problems in the field could cause changes of recording tape speed. In the laboratory the tape will be played at "normal" speed, hence a sampling rate differing from the nominal 200 samples per second will take place. Doody (1985) used a program to overcome this problem which was later developed by F. S. Ahmed and used in this project. Program **RESAMP** determines the average number of samples between the start of each successive MSF second pulse and then resamples resulting in an equal sampling rate within each second (i.e. 200 samples/s).

For traces at less than 45 km offset digitisation is carried out for 15 seconds from just prior to the start of event and for traces at >45 km range digitization is applied for 20 seconds. Program MSFPLOT, written by R. Reid, was then used to relate the start of the digitized file to the shot instant for further digital processing and display purposes after it has been converted to integer form and transferred to the Departmental network of Sun workstations.

2.6. Summary

In this chapter a description of the profiles recorded and the main lithologies and structures traversed by them was given to provide a general overview of the project and what might be obtained in the light of the new seismic data in terms of structure and geology. An outline of the field procedures used in the project and the problems faced in collecting the data was also presented. A detailed account of the best techniques needed to acquire a good dataset is provided. In general data quality was good and if more time was available for field work, the quality could have been improved even more. However, the relatively slow rate of data acquisition was due to four main factors which are: weather conditions (40%), MSF reception (35%), the failure of the seismic sets to operate on remote start (20%), and operator error (5%).

The sets used proved to be a reliable tool for such seismic project, although their maintenance became a real problem at the late stage of the project because of their extensive and sometime cruel use for long periods by many people and, for many sets, their productive life time was extended to its limit. M.S.F reception comprised another major problem but in this case nothing can be done since shifts in the M.S.F transmission and reception can happen at any time during the recording day, but this problem was avoided to some extend by using two sets as a back up at each site thus reducing the possibility of data loss.

The main advantages in using quarry blasts as sources for seismic projects is the availability of them as cheap and repetitive source of energy, while the main disadvantages of using quarry blasts are that seismic projects will be restricted by the locations of these quarries and their individual engineering practices, especially the delay in their firing procedures to reduce shock waves created by the explosives because of environmental regulations. This creates a long wavetrain which will highly distort secondary arrivals, thus reducing the possibility of using them as sources for vital information for the study of subsurface lithologies.

CHAPTER THREE

THEORY AND METHODS OF SEISMIC INTERPRETATION

3.1. Introduction

Aspects of seismic data processing and interpretation used in this project are discussed and the theories presented. All procedures of data processing such as frequency analysis and filtering are presented along with a summary of the statistical method by which different velocity segments are plotted on the time-distance graphs and the criteria by which error estimations associated with the arrival times are determined. The determination of the sub-surface velocity structure is crucial in any geological modelling using the seismic method. The overestimation or underestimation of the velocities of the different layers could lead to inaccurate estimates of interface depth. In the Midland Valley and the Southern Uplands interfaces are sub-horizontal and, therefore, it must be noted that observed velocities are apparent depending on the direction of the rays and their relation to the dips. Further, the effect of anisotropy cannot be neglected. To determine the various velocities and depths present with reasonable accuracy and subsequently to establish the final geological model, either a good dataset is available or the appropriate filters are used to improve the seismic traces. Theories of the interpretation methods applied are also discussed. It should be mentioned here that these interpretational methods are applicable to both P-wave and S-wave data.

3.2. Frequency Analysis and Filtering

Seismic traces are composed of a mixture of signal and noise with frequencies occupying a wide spectrum. They are non-periodic functions, but for the purpose of their analysis they can be treated as periodic waveforms with an infinitely long period. They can be expressed either in the time domain (i.e. their amplitude as a function of time) or in the frequency domain (i.e. by the amplitude and phase of a finite number of sine waves).

In order to isolate certain wanted events spectral analysis for all the lines was carried out to find the dominant frequencies. This was done in two stages. The first was to determine the main range of frequencies for first arrivals and the preceding noise. Frequency filtering was carried out accordingly. Secondary arrivals were more difficult to locate and therefore the P-wave arrivals derived from the first stage were used as guide lines for the second stage in which any possible correlation between these already filtered events and other secondary arrivals present in the digital sections was determined. Subsequently, frequency analysis was undertaken to obtain the appropriate filters to be used for onset determinations.

Program **PLOT** was the main software used for such processing. It was written by R. Reid and K. Davidson at Glasgow University. It is designed to handle digital seismic data: to simply process the data for display, or to undertake spectral analysis, or to frequency filter data based on parameters obtained in the frequency filter design program, **FWFIR.** Graphics were then obtained using the **UNIX 'S'** plotting package. All the data of this project were processed by these programs.

Program PLOT is provided with a windowing function which makes it possible to apply frequency analysis on any desired length of the traces for any desired length of time. Two windows were chosen to determine the noise and signal frequency spectra for the primary arrivals: the first window covers the time from the

start of the digitised trace to the actual arrival time to give the noise spectrum, and the second window covered 0.5 s after the first window thus giving the onset frequency spectrum. For the secondary arrivals a 0.5 s window was also used beginning at their onset. This proved to be an adequate procedure in most cases. It should be noted that the onsets of S-waves are less easy to determine than those of P-waves. A full discussion of the implications of frequency analysis will be presented in chapter 4.

There are two main categories of filters: those which are designed on the basis of the waveform are termed *optimum filters* and those which are *independent* of the waveform, of which *frequency filters* are an example. A frequency filter discriminates against predefined unwanted frequencies. It is designed on an arbitrary basis without direct reference to the signal or noise, and without reference to the actual effectiveness of the filter. The optimum filter is designed on the basis of the character of the waveform or on the basis of the actual input and desired output signal (Wiener filtering). Digital processing of seismic data has been described by many authors (e.g. Robinson & Treitel 1964, 1980; Hatton *et al.* 1986).

The main effect of a filter is defined by its *impulse response* which is the output of the filter when a spike function is input (Fig. 3.1) and is sometimes called the *operator*. It is the impulse response which is mathematically convolved with the input signal to give the filtered trace. In order to carry out frequency filtering Fourier transformation is used to convert the signal from the time domain to the frequency domain and vice versa. This is done by converting a time function, g(t), into its amplitude, A(f), and phase spectra, 0(f), or into the frequency spectrum G(f) such that

$$G(f) = A(f)e^{i\theta(f)} \tag{3.1}$$

g(t) and G(f), the time and frequency domain representation of the waveform, are known as a Fourier pair and are interchangeable.

To design a filter, a transfer function is specified in the frequency domain which is then used to design an impulse response of finite length in the time domain. To illustrate this, consider a low-pass filter whose cut-off frequency is fc. The ideal output of the filter is represented by the amplitude spectrum shown in Figure 3.2a. Frequencies greater than fc have zero amplitude and below fc have constant unit amplitude. This is the transfer function of the ideal low-pass filter which is then converted into the time domain by Fourier transformation giving the impulse response shown in Figure 3.2b. This filter will only pass frequencies between 0 and fc. The impulse response of this filter is a sinc function and therefore it is infinitely long and must be truncated to produce a realisable filter operator (Fig. 3.2c). This operator when convolved with an input waveform will result in a gradual cut-off low-pass filter (Fig. 3.2d).

Program FWFIR provides several options of frequency filters to be used and these are low-pass, high-pass, band-pass and band-stop filters. Several window functions are used to control the truncation of the operator such as rectangular, triangular, Hamming, generalized Hamming, Hanning, Kaiser (10-sinh) and Chebyshev windows.

This program produces the coefficients of the desired filter, which are stored for use by the filter option in program PLOT. The Hamming window, which was used in this project, is a particular empirical weighting function. The truncated autocovariance function, $a(L)$, is multiplied by the window to produce a modified apparent autocovariance function $a_m(L)$.

The autocovariance is apparent because only a finite length of data was used in obtaining it. It is modified by the window and also because only lags between 0 and L_m are used. The general equation for the window is:

$$W(L) = 0.54 + 0.46 \cos \pi \frac{L}{L_m}$$

Frequency filters may be of *minimum phase* or *zero phase*. Assume t0 is

some point on the input waveform during the convolution operation such that t<0 represents the future and t>0 the past segment of this waveform. Minimum phase filters have a memory component only and thus operate on the present and past of the waveform, with all values for t<0 = 0. This means the output waveform has no phase shift relative to the input. In contrast, zero phase filters have anticipation and memory, the operator being symmetrical about a point t, equal to half the operator length. This has the advantage of more of the input waveform being considered during each convolution operation, but results in a phase shift equal to t/2 relative to the input waveform.

A band-pass filter may be thought of as a set of cosine waves of equal amplitude which are in phase and which are restricted to frequencies within the frequency band that is to be passed. The output of the filter process will only contain cosine waves that are common to both the input trace and the filter. Filters are not ideal. They cannot reject everything below and above the pass band desired. There is a ramp-off of the pass band at both ends, so increasing the rate of cut off frequencies will decrease the side lobe levels at the expense of a softer reject slope.

3.3. Errors Associated with Arrival Times

A standard error of +/- 0.03 s was calculated for the travel times at all stations. The main components of this error are:

[1] Errors in locating the shotpoint and the receivers were estimated to be +/- 40 m and +/- 10 m respectively. The removed face of an active quarry changes frequently and these changes are not updated on Ordnance Survey maps which are used to locate all shots and receivers. Also locating the receiver position involves some error due to recently changed topographic and man-made features such as new fencing, new buildings and the removal of forests and old fences already present on the maps used to position the receivers. All this will give a total error

of +/- 0.01 s assuming an average surface velocity of 5 km/s along the profile.

[2] Onsets on analogue playback records can be read to an accuracy of only +/- 0.01 s. This is due to errors in locating the onset arrivals (especially on noisy traces) and difference in the speed of the playback system when producing analogue output for onset picking which causes a difference in spacing between M.S.F seconds pulses.

[3] Shifts caused by the playback filters produce an estimated error of 0.01 s. Since this error effects all the traces by the same amount and does not effect the digital sections, it is not included in the calculations and it is mentioned here only for illustration.

[4] The seismic set used to record the shot instant is placed about 20 m from the actual position of the shotpoint. This will cause an estimated error of 0.007 s assuming that the surface velocity at the quarry is 3.00 km/s. This will vary subject to the actual surface velocity.

3.4. Statistical Determination of Time-Distance Segments

A variety of causes (e.g. refractor topography, near surface layers) can cause scatter of the onset readings plotted on a time-distance graph which define the different velocity segments and these readings are invariably scattered about the *best-fit line* for a particular segment.

To statistically determine the velocities of these segments, linear regression analysis was undertaken to determine best-fit gradients and, thus, velocities and time intercepts. Linear regression software forms part of the UNIX 'S' package. In this method the best fit line to the data is determined by considering two variables, one independent (distance in this case) and the other dependent (time), and minimizing the deviation of the points from the line. The equation of the best fit line is

$$y_i = mx_i + c + e \qquad (3.2)$$

where

x_i = offset of the i-th observation, the independent variable

y_i = travel-time of the i-th observation of the arrival, the dependent variable

m = slope

c = intercept

e = error

The best fit line is one which satisfies the condition

$$\sum_{i=1}^{n}(\delta y_i - y_i)^2 \text{ is a minimum} \tag{3.3}$$

where

n = number of observations

The sum of the squares of the vertical deviations about the line is minimised. Error is considered negligible on x values while the dependent variable y has random-error term (e).

Apart from cases where velocity segments are curved and the WHB method had to be used (only in the cases of the first segments), the regression function was undertaken to determine velocity values obtained from the time-distance graphs, together with the time intercepts and the errors associated with these values. The error values were calculated by adding and subtracting the reciprocal of the standard error derived from the function to the reciprocal of the gradient to obtain the minimum and maximum velocity variation respectively.

3.5. The Refraction Method

3.5.1. Planar Layer Interpretation

Dobrin (1960) and Kearey & Brooks (1984) discussed the principles of refraction in detail. Consider a seismic ray incident on an interface between two layers of different velocity. The transmitted ray will obey Snell's Law and will be

refracted according to the following equation:

$$\frac{\sin i}{\sin r} = \frac{V1}{V2} \tag{3.4}$$

where

i = angle of incidence relative to the normal to the interface

r = angle of transmission relative to the normal

V1= velocity in the first layer

V2= velocity in the second layer

An ideal case of the raypaths of energy refracted at a horizontal interface and travelling through layers of constant velocity is shown in Figure 3.3. The direct ray travels horizontally through layer 1 at a velocity V1. The resulting travel-time curve is a straight line of slope 1/V1 and zero intercept. The angle θ is such that the ray AB is critically refracted, i.e. the ray is refracted such that it is transmitted along the interface between the two layers. Therefore, sin r is equal to 1. Consider the path ABCD of the ray critically refracted at the interface between layers 1 and 2. The travel time, T(AD), along this path is

$$T(AD) = T(AB) + T(BC) + T(CD) \tag{3.5}$$

$$= \frac{Z1}{V1\cos\theta} + \frac{X - 2Z1\tan\theta}{V2} + \frac{Z}{V1\cos\theta} \tag{3.6}$$

Since $\sin r = 90^{o}$

$$\sin\theta = \frac{V1}{V2} \quad (\textit{Snell's Law}) \tag{3.7}$$

and

$$\cos\theta = \left[1 - \frac{V1^2}{V2^2} \right]^{½} \tag{3.8}$$

we can rewrite equation 3.6 as

$$T(AD) = \frac{X}{V2} + \frac{2Z\ (V2^2 - V1^2)^{½}}{V1\ V2} \tag{3.9}$$

From the time-distance plot the intercept time (T_i1) on the time axis is given by

$$T_i1 = \frac{2Z\ (V2^2 - V1^2)^{½}}{V1\ V2} \tag{3.10}$$

and therefore

$$Z1 = \frac{T_i1\ V1\ V2}{2\ (V2^2 - V1^2)^{½}} \tag{3.11}$$

Thus, the depth to layer 2 can be determined by the use of the intercept time if V1 and V2 are known. Similarly depth to layer 3 can also be determined if V3 is known.

$$Z2 = 0.5 \left[T_i2 - 2\,Z1\, \frac{(V3^2 - V1^2)^{½}}{V3\ V1} \right] \frac{V3\ V2}{(V3^2 - V2^2)^{½}} \tag{3.12}$$

In reality refractors cannot be treated as perfectly horizontal or planar, so the time-distance plot does not give the true refractor velocity but another quantity, called apparent velocity, which is a function of the true velocity of the refracting layer and its structure along the recording profile.

In the case of *dipping refractors* reverse shooting becomes essential to determine the dip of the refractor along the profile. The gradients and intercept times for the forward and reverse curves are different (Fig. 3.4). Derivations of the equations for the dipping interface are given in Dobrin (1960) and Kearey & Brooks (1984). Only the main equations will be presented here. The angle of dip can be determined by the relation.

$$\alpha = \frac{1}{2}(\sin^{-1}V_1 m_d - \sin^{-1}V_1 m_u) \tag{3.13}$$

where

α = refractor dip along the profile

m_d = slope of the downdip segment

m_u = slope of the updip segment

The perpendicular distance Zu in an updip direction to the interface can be calculated from the intercept time, T_iu.

$$T_i u = \frac{2Zu\cos i_c}{V_1} \tag{3.14}$$

Therefore

$$Zu = \frac{V_1 T_i u}{2\cos i_c} \tag{3.15}$$

where i_c = is the angle which the incident ray makes with the normal

The perpendicular distance Zd in the downdip direction can be derived similarly, and the actual depth at the up dip direction shot is

$$Du = \frac{Zu}{\cos\alpha} \tag{3.16}$$

and at the down dip shotpoint:

$$Dd = \frac{Zd}{\cos\alpha} \tag{3.17}$$

Faults may offset the refractor arrival velocity segments of the travel-time curve observed from opposite sides of the fault (Fig. 3.5). Therefore two intercept times will be present, T_i1 and T_i2. The difference between them will relate to the throw of the fault. The equation for determining the throw of the fault is

$$\delta Z = \frac{\delta T V1V2}{(V2^2 - V1^2)^{1/2}} \tag{3.18}$$

where

δZ is the throw of the fault, and

δT is the difference between the time intercepts.

The above equation is valid only if the fault throw is much less than the depth to the refractor.

3.5.2. Plus-Minus Method

Hagedoorn (1959) realised the uncertainities and imprecisions involved in the assumption of *planar* interfaces for the interpretation of refraction data. He introduced the plus-minus method which is based on the calculation of a *plus time* for each receiver, analogous to an intercept time, for conversion to refractor depth and a *minus time* for the estimation of refractor velocity. Dips of refractor topography are assumed to be less than 5 degrees and reversed coverage is essential for the application of this method. Figure 3.6 illustrates the geometry of an undulatory refractor.

The plus time is the sum of the travel-times to a receiver from the two sources, S1 and S2, minus the travel-time between S1 and S2 (T(S1S2)). For a receiver K

$$Tplus(K) = T(S1K) + T(S2K) - T(S1S2) \tag{3.19}$$

$$= (T(S1R) + T(RZ) + T(ZK)) + (T(S2W) + T(WT) + T(TK)) - (T(S1R) + T(RW) + T(S2W)) \tag{3.20}$$

$$= T(ZK) + T(TK) + T(RK) + T(WT) - T(RW) \tag{3.21}$$

$$= T(ZK) + T(TK) - T(ZT) \tag{3.22}$$

This is equivalent to the intercept time (Tint) for a shot fired at K. Therefore, Z(K), the refractor depth below K, is given by

$$Z(K) = \frac{Tplus(K)\, V2\, V1}{2\,(V2^2 - V1^2)^{1/2}} \tag{3.23}$$

The minus time is defined as the difference in travel-times between arrivals from sources S1 and S2 arriving at a receiver K. V2 is obtained from the minus times.

$$Tminus(K) = T(S1K) - T(S2K) \tag{3.24}$$

$$= (T(S1R) + T(RZ) + T(ZK)) - (T(S2W) + T(WT) + T(TK)) \quad (3.25)$$

Refractor relief is assumed to be negligible between Z and T

$$\langle KPZ = \langle KPT = 90^{o}$$

$$KZ = KT$$

Therefore

$$Tminus(K) = (T(S1R) + T(RZ)) - (T(S2W) + T(WT)) \quad (3.26)$$

and similarly

$$Tminus(L) = (T(S1R) + T(RU)) - (T(S2W) + T(WV)) \quad (3.27)$$

A straight line with a gradient equal to half the refractor velocity is obtained when plotting the minus time against the receiver position.

$$Gradient = \frac{X}{Tminus(L) - Tminus(K)} \quad (3.28)$$

$$= \frac{X}{T(S1R)+T(RU)-T(S2W)-T(WV)-T(S1R)-T(RZ)+T(S2W)+T(WT)} \quad (3.29)$$

$$= \frac{X}{T(RU) - T(WV) - T(RZ) + T(WT)} \quad (3.30)$$

$$= \frac{X}{T(ZU) + T(VT)} \quad (3.31)$$

For low relief ZU = VT = KL = X and therefore

$$T(ZU) + T(VT) = \frac{2X}{V2} \quad (3.32)$$

Hence the gradient of a minus time graph can be expressed as

$$Gradient = \frac{V2}{2} \quad (3.33)$$

3.5.3. The Wiechert-Herglotz-Bateman (WHB) Method

Work carried out in the Midland Valley of Scotland by Davidson (1986), Dentith (1987) and Kamaliddin (1988), showed that the first segments of regional

time-distance graphs were curved. This was an indication of vertical and lateral variation of seismic velocity within the regional topmost layer. They proposed that such data were suitable for inversion to a velocity-depth model using a solution to the WHB integral (e. g. Grant & West 1965).

In this project, Melrose and Glenluce quarries are situated in the Southern Uplands, the first is located on ORS rocks and the second on Lower Palaeozoic rocks. The rest of the quarries are all situated in the Midland Valley on rocks of the Devonian age. First velocity segments obtained from quarries located on ORS rocks are curved in most of the cases, while data obtained from Glenluce quarry (Lower Palaeozoic) showed minimal curvature suggesting that since ORS rocks are younger than those of the Southern Uplands, this behaviour is probably due to the type of rocks and the diagenetic stages they are subjected to. The following equations show the theory behind the WHB method.

$$Z(V) = \frac{1}{\pi} \int_{x=0}^{x=X} \cosh^{-1}(V\ dt/dx)\ dx \qquad (3.34)$$

where

$V = (dx/dt)_{x=X}$

This represents the velocity V, at a depth Z, Z being the turning point of a ray arriving at the surface at a range X from the source. The method assumes that velocity always increases downwards without lateral velocity variation.

3.6. The Reflection Method

In this survey several reflected events were detected and analysed. The theory of reflection is discussed in detail by Dobrin (1960) and Kearey & Brooks (1984). Only a brief review of the basic concept will be presented here.

The amount of energy of a ray incident on an interface which will be reflected or transmitted through the interface will be determined by the *acoustic*

impedance (Z) across the particular interface. The acoustic impedance of a rock is the product of its density and its appropriate velocity i.e. $Z = \rho V$. Therefore, the smaller the contrast in acoustic impedance across a rock interface the greater is the proportion of energy transmitted through the interface, which is usually the case in reflection where only small amount of energy is reflected.

The time-distance curve, for a single reflector below a constant velocity layer, of reflected rays is a hyperbola whose axis of symmetry is the time axis and is governed by the following equation

$$Tx^2 = To^2 + \frac{X^2}{V^2} \tag{3.35}$$

where Tx is the two-way travel time, To is the two-way travel time at zero offset, X is the source receiver offset and V is the overlying layer velocity. It must be mentioned here that in the case of a dipping layer the curve will be an asymmetric hyperbola.

3.7. The Raytracing Method

In geologically complex regions one does not expect the velocity distribution to be uniform in either the lateral or vertical directions. Therefore the velocities and depths, and hence the geological models, obtained by the above mentioned methods should be approached cautiously. These models should be treated as a general framework for future refinment by other methods which do not involve the simplified assumptions made for the previous methods.

The *raytracing method* is a more sophisticated method for modelling. As used here, this involves tracing rays through two-dimensional laterally inhomogeneous media involving curved interfaces, block structure, vanishing layers and isolated bodies. This proved to be an adequate interpretive method for modelling the data.

The **SEIS83** computer raytracing package is a slightly modified version of the **SEIS81** package (Cerveny & Psencik 1981) and consists of the raytracing

program SEIS83, the program RAYPLOT to plot the rays, and the programs SYNTPL and SEISPL which, respectively, calculate and plot synthetic seismograms based on the output of SEIS83. The program employs two-point raytracing using the modified shooting method of initiating a ray, where a raypath is defined and travel times computed from the source to a specified receiver geometry with rays leaving the source between predetermined angles. The dynamic raytracing system is used to determine the geometrical spreading of the generated rays by solving a system of two linear ordinary differential equations by a modified *Euler's method.*

Execution is an iterative process, where a trial ray is generated and traced through the model back to the surface. When successive rays terminate at the surface on either side of a receiver, the difference between the positions of the ray termination at the surface and the intended receiver point is calculated and a new initial ray angle chosen. This process is repeated a specified number of times, or until the ray terminates within a pre-selected distance of the receiver.

A grid of velocity values which may vary laterally and vertically is input for each layer. A continuous velocity function is obtained by using one of the following methods: fitting bicubic splines to these data, linear interpolation between grid points, or by piece-wise bilinear interpolation.

3.8. Poisson's Ratio

The dataset acquired included several sets of shear waves and thus it was feasible to isolate such events, by filtering processes, to determine their velocities and therefore the Vp/Vs value and Poisson's ratio (σ) using the expression:

$$\sigma = \frac{0.5\,(Vp/Vs)^2 - 1}{(Vp/Vs)^2 - 1} \qquad (3.36)$$

Poisson's ratio is defined as the ratio of strain normal to strain parallel to

uniaxial stress applied to a unit cube of rock. For rocks it is generally 0.25. The knowledge of the distribution of Poisson's ratio might be expected to add significantly to the understanding of the physical properties of the underlying rocks.

3.9. Other Data Reduction Methods

In addition to the methods discussed in the previous sections there are other methods which are equally valid for the interpretation of the acquired data. They were not applied in this work, because it is thought that their application would not result in any significant improvement to the final models. Some of these methods are discussed briefly below:

[1] *Time-term method* of interpretation in which delay times for recording sites over a given refractor are obtained and a least squares value of its velocity is also determined (Willmore & Bancroft 1960). A series of simultaneous equations are constructed from the travel time data and solved to give values with standard errors for all the source and receiver sites, and the refractor velocity. The method is subject to the same assumptions as other interpretation methods using delay times.

The resulting values for the individual delay times can then be converted into local refractor depths using the same procedure as in the plus-minus method. This method is best suited to arrays of intersecting profiles where shots are recorded along more than one of the profiles.

The application of the plus-minus method in this project was considered satisfactory enough and therefore the above method was not applied although the acquired data in the NE of the Southern Uplands along lines 1, 2 and 3 could be regarded as arrays suitable for such interpretation.

[2] *Generalized Reciprocal Method.* In the plus-minus method dips are assumed essentially to be less than 10 degrees, i.e. there is an inherent smoothing of the

interpreted refractor geometery where the refractor is assumed to be planar between the points of emergence from the refractor of the forward and reverse rays. This problem is solved in the generalised reciprocal method (Palmer 1980) where it combines the forward and reverse rays which, rather than arriving at the same detector, leave the refractor at approximately the same point and arrive at different positions separated by a distance δx. The optimal value of δx is selected on the basis of various tests associated with the method.

[3] *Single-ended Profile Method.* This method was devised to interpret low velocity surface layers represented by refracted arrivals in single-ended reflection spread data, for use in the calculation of static corrections (Cunningham 1974). It can be applied in many other situations. In the case of conventional reversed shooting (Fig. 3.3) only the central portion of the refractor (B to C for example) is sampled by the refracted rays while the parts of the refractor directly below and near the end shotpoints are not sampled. This procedure was introduced to accommodate such needs.

To apply the standard methods for conventional reversed profiles discussed above, the apparent velocity of the unreversed section of the profile must be determined and this is done by using the equation below:

$$\frac{\delta t}{\delta x} = \frac{1}{V_{2d}} - \frac{1}{V_{2u}}$$

Where V_{2u} and V_{2d} are the updip and downdip apparent velocities, δt is the difference in travel time of refracted rays from the adjacent shots recorded at the same offset distance x. These velocities could be determined by using both the single-ended travel-time curves and the above equation.

The original intention of recording line 3 was to obtain large offsets, thus sampling deeper refractors, using Aberdour quarry (see Chapter 2). Control of the

near-surface velocity structure was to have been achieved by recording from Ratho quarry. However, Ratho quarry provided data to even greater offset than Aberdour quarry. The single- ended profile method requires receiver separation coverage from both shots to be equal to the separation of the two shotpoints used and continuity of refractor being interpreted is also a requirement. Unfortunately the first condition was not achieved along line 3 and therefore this method of interpretation was not appplied to the acquired data.

[4] *Split-profile Method.* This method is applied for full planar layer interpretation in the presence of dip where data is recorded in both directions from a central shotpoint. Johnson (1976) used the apparent velocity to find the incident and dip angles for each successive layer. By starting the calculation for the first, shallowest refractor and finding its dip, then the second and so on to build up the model. The general equation for this method is:

$$t(k) = \frac{X \sin\beta_1}{V_1} + \sum_{i-1}^{k=1} \frac{H_i}{V_i} \cdot (\cos\alpha_i + \cos\beta_i)$$

Where

k designates the interface along which the wave is refracted,

Hi = the vertical thickness of the i-th layer beneath the source,

Vi = the velocity of the i-th layer,

α_i = the angle with respect to the vertical made by the downgoing ray in the i-th layer,

β_i = the angle with respect to the vertical made by the upgoing ray in the i-th layer,

X = distance.

3.10. Summary

Processing procedures discussed in this chapter proved to be an adequate and essential tool by which the data were refined and prepared for interpretation. While most interpretational methods discussed involve simplifying assumptions, the combined application of these methods will provide reasonable means to produce a well constrained model provided that data quality and coverage is adequate. It is difficult to assume, in an area like Scotland with all its complex geological history, that there is lateral homogeneity in lithology and thus no lateral change in velocity. This is most likely to lead to many errors in the final geological model. Raytracing which is considered as an advanced method of interpretation could lead, with aid of the raw models obtained by the other methods, to a very well constrained and refined end-model.

CHAPTER FOUR

DATA PROCESSING, ANALYSIS AND IMPLICATIONS

4.1. Introduction

Programs PLOT and FWFIR, which represent part of the processing software package available on the SUN workstation network, were used to process the digitized data. They provide facilities to carry out frequency analysis and subsequent filtering of the seismic traces. In this chapter, the results and the implications of such undertakings will be described with some preliminary interpretations of the data deduced from this processing.

4.2. Frequency Analysis - Primary Waves

Frequency analysis was carried out to find the dominant P-wave frequencies in the area covered by the project. The results obtained from this process were satisfactory and a discrimination between signal and noise frequencies was obtained for use in the filtering process. Figures 4.1-4.10 show the results of lines 1, 2, 3, 4, 5 and 6 respectively. These are followed by 5 noise plots (Figures 4.11-4.15) showing a sample of noise frequencies along each line, which were chosen to show the variation in noise frequency levels in the region.

Two windows were deployed for spectral analysis of the data. The first covers the noise spectrum and starts from zero time on the digital section to the actual arrival time of the event and the second is 0.5 s long and starts from the event time. On some of the signal plots, a high frequency level with peaks at a range of

34-38 Hz is observed. These peaks do not represent actual seismic energy, nor field noise, but they are induced by the ageing playback system.

Summary results of frequency analysis are presented in Table 4.1 and illustrate the different seismic energy peaks present along the different profiles.

Table 4.1 Frequency analysis results for signal and noise spectra along the recorded profiles. Values refer to major components of spectra.

Line	Noise range in Hz	Signal Range in Hz
1:Melrose-Bangley	<18	6-14
1:Bangley-Melrose	<20	5-20
2:Melrose-Ratho	<18	5-15
2:Ratho-Melrose	<18	5-18
3:Aberdour-Moffat	<20	5-18
3:Ratho-Moffat	15-25	6-20
4:Glenluce-Tormitchell	<20	8-22
4:Tormitchell-Glenluce	<20	5-20
5:Glenluce-Newton Stewart	<10	8-22
6:Boysack-Collace	<15	6-15

As expected, both signal and noise frequencies coexist at most of their fre-

quency spectra, especially at less than 20 Hz, which made it difficult to discriminate against unwanted frequencies by frequency filtering.

A study of Table 4.1 and Figures 4.1-4.15 shows that although signal frequencies occupy a relatively wide range, the "effective" peaks are found at a much narrower spectrum within these ranges (described in section 4.2.1) which makes it possible to choose a narrower bandpass filter, or a "low cut" lowpass filter, to extract the embedded seismic energy in these ranges.

4.2.1. Implications of Primary Wave Frequency Analysis

Table 4.1 shows that noise levels in the Southern Uplands and in the Strathmore Syncline region are dominantly lower than 20 Hz with the exception of line 3 when recorded from Ratho quarry towards Moffat (15-25 Hz) where the first 6 traces (up to 13 km distance) showed higher noise levels (>20 Hz), probably because of the higher energy released by this quarry. This was not observed along line 2 when recorded from the same quarry. This general range of noise frequencies gives some indication of the big task of attempting to frequency filter these data since most of the signal frequencies occupy exactly the same range as the noise (5-20 Hz). Fortunately, because of the high energy released by the quarries used and the careful choice of the recording sites and sometimes the recording day, it was relatively easy to acquire data with high P-wave signal/noise (S/N) ratio which did not need extensive filtering to locate the onsets. In cases where extensive filtering was needed, the stations were re-recorded if the filtering results were unsatisfactory, and the old and new recordings filtered, their waveforms correlated and arrival times compared to deduce the most realistic onset time. Also, the correlation of waveforms of traces recorded on the same day from the same blast proved to be a good approach to such problems where such traces display similar waveforms and in most cases phases.

Kamaliddin (1988) suggested that quarry practices are the most decisive fac-

tor in the amount of energy detected and the frequency bands measured along a profile. He suggested also that frequency changes, such as attenuation, along major lithological boundaries are not observed. In his work, Kamaliddin used 4 quarries recording 3 lines, while in this work 7 quarries were used recording 6 lines, i.e. nearly double the amount of information is available and hence a more detailed study could be made to interpret such relationships with a greater degree of confidence.

Data acquired along line 1 recording from Melrose quarry (Fig. 4.1) show a frequency range of 6-14 Hz with frequency peaks at 7-9 Hz whereas a noticeable frequency drop occurs at 28 km distance. Along the reversed section of the profile, recording from Bangley quarry (Fig. 4.2), signal frequency range is 5-20 Hz with the highest peaks occurring at 19 Hz with few exceptions and with minimal attenuation along the section. This means, although recording along the same profile and therefore the same lithology, frequencies detected differ to a great extent with respect to the quarries from which they are derived.

Considering line 2 recording from Melrose quarry (Fig. 4.3), a narrower frequency range is obtained (5-15 Hz), but frequency peaks remain at broadly similar levels as along line 1 when recording from the same quarry. However, noticeable frequency attenuation is observed from the trace 1 to trace number 13 at 26 km offset, then a slightly higher range of peaks appear (10-12 Hz) decaying at the same rate to the end of the dataset. Recording along line 2 from the opposite direction (Ratho quarry, Fig. 4.4) yielded a frequency range of 5-18 Hz which is within the average limit obtained for the Southern Uplands (5-20 Hz) but frequency peaks are at about 10-12 Hz with attenuation occurring at 22 km. These latter peaks are relatively higher than those recorded from the reversed direction.

Summarizing the above, data acquired along lines 1 and 2, when recording from Melrose quarry, yielded similar frequency peaks while reversed recordings of the two profiles provided different peak levels suggesting that frequencies are

quarry rather than lithology dependent. Frequency changes do not seem to be related to any lithological or structural boundaries. In the four cases discussed above, changes at a lithological boundary occur only in one case, along line 2 recording from Melrose, but this coincides with a change of velocity segment.

Line 3 was recorded by the single-ended profile method which provided the opportunity to study the quarry-frequency relationship from another viewpoint, where the raypaths approach the lithological and structural boundaries nearly at the same angle and the effect of dip is negligible. Signal frequency range obtained along this profile recording from Aberdour quarry (Fig. 4.5) is 5-18 Hz with peaks at 9-11 Hz. It is worth mentioning here that exactly the same frequency range was obtained by Kamaliddin (1988) when he used this quarry to record two profiles, the first towards the NE from Aberdour and the second towards the NW. Line 3 was also recorded from Ratho quarry (Fig. 4.6) in the same direction and the frequency range obtained is 6-20 Hz, but peak levels occur at 10-12 Hz. Note that the same range of frequency peaks was obtained when line 2 was recorded from Ratho quarry, but with a frequency drop at 28 km. The relatively higher peak levels obtained from Ratho quarry along the same line is also another indication of the dominance of source over path attenuation effects.

Recording from Glenluce quarry (Fig. 4.7), along line 4, a frequency range of 8-22 Hz was obtained with frequency peaks occurring at two intervals: at a range of 0-15 km dominant frequencies are 6-10 Hz; beyond this frequencies of 16-22 Hz dominate. However, the frequency range obtained from Tormitchell quarry (Fig. 4.8) is 5-20 Hz with frequency peaks at 8-18 Hz and rapid attenuation continuing to 23 km distance and thereafter frequency peaks remain at a constant level of 7-9 Hz.

Using Glenluce quarry to record line 5 (Figure 4.9) resulted in a P-wave frequency range of 8-22 Hz which is exactly the same range obtained along line 4 from the same quarry. Frequency peaks also occur at a similar level of 8-10 Hz

collaborating the above argument of the control of quarry practices on P-wave frequencies detected.

As mentioned above, Glenluce quarry was used to record lines 4 and 5. These profiles are nearly perpendicular to each other (Figure 2.1). An attempt to correlate P-wave frequencies to azimuth of the recorded lines was not successful since no changes in frequency ranges nor peaks are observed (Figures 4.7 and 4.9). The same attempt was made to correlate detected frequencies and azimuth along lines 1 and 2, recording from Melrose quarry (Figures 4.1 and 4.3), and lines 2 and 3 recording from Ratho quarry (Figures 4.4 and 4.6) with no positive results. The best possible answer to these observations is that since the quarry characteristics are the dominant factor in controlling frequencies emitted these changes, if any, cannot be observed. Further, the azimuth of the quarry face relative to the line of recorders does not seem to have any influence on the range of frequencies observed. These observations can be verified by recording concentric profiles around quarry and analyse the data to detect any frequency changes with azimuth.

In conclusion to the above, two main observations can be made. The first is that the initial source content dominates attenuation effects and the second is that only source characteristics can control what is emitted. It can be assumed with confidence that source characteristics such as the type of explosives used, the depth of holes, the method of blasting, the number of delays placed and the type of rock the quarry is situated in are the sole factors which control frequencies transmitted by a particular blast. The last factor, that is rock type, may be explained by the fact that these rocks may act as an initial "filter" permitting only certain bands of frequencies to be transmitted while the rest of the seismic energy is either stopped or highly attenuated. Furthermore, the attempt of discriminating between the different lithological units on the basis of frequency changes is invalid.

4.3. Frequency Analysis - Shear Waves

An entirely different approach was used to analyse the frequency content of the shear waves. Since detecting the exact onset of such arrivals is a difficult matter, their approximate positions had to be determined by lowpass filtering prior to any frequency analysis. Assumpcao & Bamford (1978) employed lowpass filters with a Hanning window to locate the S-wave onsets. They suggested, correctly, that this will reduce the high-frequency background noise and at the same time does not diffuse the S-wave onsets with the *ringing* often caused by narrowband filter.

In this project a similar approach was followed except that the Hamming window was used, rather than the Hanning, because the former gave the best results of all other windows to process the whole dataset. The same window length as used for spectral analysis of the P-wave data was used to process the S-waves, where 0.5 s was added to the interpreted S-wave arrival time. Once the range of S-wave frequencies was determined, the filters were further constrained to produce the best possible filtered digital section for locating the onsets.

Therefore, both frequency analyses and filtering were used interchangeably to locate the most probable S-wave onsets. Instead of using frequency analysis as a guideline for filtering processes, it was used to confirm the presence and hence the validity of the S-wave arrivals in the already filtered digital sections while preliminary filtering was essential to locate the most likely time windows at which the S-wave onsets are located to proceed from there to frequency analyse them. Figures 4.16-4.25 show frequency analysis of the detected S-waves.

4.3.1. Implications of Shear Waves Frequency Analysis

Table 4.2 shows the different S-wave peak levels obtained from Figures 4.16-4.25.

Table 4.2 Frequency analysis results of S-wave arrival spectra along the recorded profiles.

Line	Power peak	Remarks
1:Melrose-Bangley	4-8 Hz	attenuation continuous to 16 km
1:Bangley-Melrose	4-8 Hz	attenuation continuous to 15 km
2:Melrose-Ratho	5 Hz	S-waves are consistent to 42 km
2:Ratho-Melrose	4-7 Hz	attenuation continuous to 18 km
3:Aberdour-Moffat	5 Hz	attenuation continuous to 25 km
3:Ratho-Moffat	4-6 Hz	attenuation between 0-20 & 50-66 km
4:Glenluce-Tormitchell	5-8 Hz	attenuation continuous to 38 km
4:Tormitchell-Glenluce	8-10 Hz	attenuation continuous to 22 km
5:Glenluce-Newton Stewart	5-10 Hz	S-waves are consistent to 21 km
6:Boysack-Collace	5-7 Hz	attenuation between 16-30 km

From Table 4.2, it can be seen that all S-wave frequencies detected lie within the general low frequency range (<10 Hz) which was envisaged for the Midland Valley by previous workers (e.g. Davidson 1986, Dentith 1987) and which is also the general expected range for S-waves. The relation of quarry practices and, perhaps, lithology to the quality of S-waves obtained and the maximum offset at which they are detected will be discussed in section 4.6.

4.4. Filtering of Primary Waves

Digital frequency filtering was used in processing the data according to the results obtained from frequency analysis (Figs. 4.1-4.10). The principal aim of any digital filtering process is to improve the S/N ratio of an input seismic trace and this is defined as the energy ratio of a desired event divided by all remaining energy (noise) at that time. It was mentioned earlier, that P-wave onsets were, in most cases, of good quality and arrival times were read directly from the playback analogues, but in some cases the use of filters was necessary to locate the first break.

From tests carried out by Dentith (1987) and Kamaliddin (1988) to determine the best combination of filter type and length to be applied to the seismic data and from tests undertaken during this work, it was decided that a Hamming window of length 1 s produces the best results, although all other windows except the rectangular window produced nearly the same results.

The filter parameters, whether bandpass or lowpass and what range of frequencies to be cut, had to be decided upon on individual basis regarding what trace(s) of a certain profile had to be improved by filtering. Usually particular velocity segments of a profile show more noise than other segments of the same profile. This is because of several reasons, such as bad weather conditions at the time of recording a particular segment, or firing a small charge on a certain recording day resulting in poor data quality. So emphasis was made to produce the best results for **the segments where filtering was needed most**. Other segments that did not need further improvements because of their better quality were disregarded for parameter selection. Care was taken not to distort the overall good quality by extensive filtering of the noisy traces. That is, for data presentation purposes, filtering was carried out to illustrate the best possible results without presenting the individual filtered traces which were treated in a different manner to the rest of the dataset because of their high noise levels.

In this work both zero and minimum phase filters were tested on the same dataset and it was found that, as far as the P-wave onsets are concerned, no significant difference in performance was observed. Therefore, minimum phase filters were used because they produce no phase shift and therefore easier correlation with their unfiltered counterparts can be made. Figures 4.26-4.35 show the unfiltered and, when applicable, the filtered digital sections of the recorded profiles. As mentioned above, only some of the profiles were filtered. In these cases the figure is split into two: part "a" is the unfiltered data; part "b" its corresponding filtered section.

4.5. Filtering of Secondary Arrivals

As discussed earlier, filtering was essential to locate and confirm the presence of S-wave arrivals. In many cases these attempts were successful. In other cases the background noise and the low frequency range of the secondary arrivals were beyond the capabilities of the filters available. Frequently filtering produced good secondary arrivals but, unfortunately, they were not consistent (especially reflections) and it was not possible to correlate these over more than one or two seismic traces. Sometimes, even those which were consistent and thought to represent good reflectors, were not realistic when subjected to further calculations and interpretations. Figures 4.36-4.45 show the results of the filtering processes undertaken to obtain the secondary arrivals.

To extract the interpretable second arrival data, only lowpass filters were deployed. It was found that correlating the results of two or three such filters with different parameters increases to a great extent the possibility of locating such arrivals. In most of the cases where second arrivals overlap and the high frequencies dominate, it was difficult to locate these arrivals. Zero phase filters proved to be of great help in isolating the most likely position of the first break because of their tendency to reduce high energy events and by comparing such results with the results of equivalent minimum phase filters, a satisfactory interpretation was possible. Compare Figs. 4.42 a, b and c, where the effect of combining three filters to successfully isolate the secondary arrivals is clear. The filters used were minimum phase and zero phase lowpass filters set at 6 Hz and a minimum phase lowpass filter of 10 Hz. Notice also the effect of the zero phase filter and how it affects the high frequencies present. The zero phase filters were used as subsidiary filters where high frequencies are accompanying the S-wave arrivals which may be attributed to noise only or noise and S-wave arrivals. They proved to be very effective in giving an indication of where the onsets start by reducing the high frequencies to a great extent. The minimum phase filters were more effective in

preserving the "sharpness" of the S-wave onset, thus by comparing the two results a good estimate of the first break was made possible. Sometimes when S-wave arrivals are at their higher frequency level (approx. 10-12 Hz) and accompanied by noise, the aid of a 10 Hz minimum phase lowpass filter was needed.

A drawback of using zero phase lowpass filters, was that if high frequencies (>25 Hz) are present within the single trace, it tends to distort all frequencies present including valuable data. However, the procedure described above for filtering digital sections gave very good results, but it must be admitted that shear wave arrival data quality along some of the profiles was excellent (e.g. line 4).

The main observations deduced from frequency filtering the S-waves and studying their behaviour were that the different velocity segments on the digital sections do not necessarily match the P-wave configuration, and one should not expect the same segmentation pattern of S-wave and P-wave. Secondly, S-waves, recorded at relatively large offsets (>20 km), are highly attenuated although their signature could be traced for a further 10-20 km but with no possible interpretation.

4.6. Quarry Blasts as Sources of S-Waves

Quarry blasts were proved to be an adequate source of S-waves provided that good care is taken in recording the data. The availability of such data allows an attempt to be made to find whether S-waves occurrence is connected to the quarry engineering practices and/or lithology crossed.

Figures 4.36-4.45 show the filtered S-wave arrivals interpreted along the recorded lines. These data were acquired from a large number of shots using the different quarries. It was hoped that "good quarries" will produce better secondary arrivals than the others but no such criteria could be established. Grouping the quarries into good and bad is based on two factors: the orientation in relation to the profile of the quarry face being removed and the average amount of charge the

quarry usually blasts, the former being the most important. According to these principles, Boysack, Ratho and Glenluce are the best quarries used in this project and therefore the best quality of S-waves should be expected. Alternatively no such good arrivals are expected from Melrose, Bangley and Tormitchell quarries while Aberdour quarry can be considered as a special case where it uses a large charge (average 3.5 tonnes), but the removed quarry face is always towards the profile (line 3) which is not the ideal case.

Lines 2 and 3 were recorded from Ratho quarry (Figures 4.39 and 4.41). Good consistent S-wave data were obtained along line 3 for about 66 km, while along line 2 data quality is poorer and for a shorter range (33 km) with no apparent consistency. Weather conditions were the same when the two lines were recorded. This may indicate that S-wave arrivals are not connected to the quarry characteristics. The lithology traversed by the two profiles is mostly the same except that along line 2 the last 12 stations (41 km from the shot and onwards) are located on Upper ORS rocks, which may be the cause for the difference in S-wave quality.

Good S-wave arrivals were not expected from Melrose quarry since it is considered as a poor blaster, because the face being removed always faces the lines being recorded. Using this quarry, lines 1 and 2 (Figs. 4.36 and 4.38) were recorded towards the north. S-wave data were obtained for 18 km with poor quality along line 1 while, along line 2, good data were acquired for 38 km, i.e. more than double the distance with better quality. The same poor quality is observed from the reversals of these profiles where Bangley quarry (poor blaster) and Ratho quarry (good blaster) were used to record the lines from the opposite direction. This is another indication that quarries are not responsible for S-wave data quality recorded and it may be the lithology which is the main factor.

Line 3 was recorded, in the same direction, from Aberdour and Ratho quarries. The first is considered as a poor blaster and the second a good blaster. Data

obtained from Aberdour quarry is very poor and inconsistent compared with good consistent data obtained from Ratho. This may represent an argument against the connection of S-wave quality and lithology since it suggests that quarry practice is also a factor, but the first 9 traces recorded along the profile, using Aberdour quarry, were recorded in high winds while the poor quality along the rest of the line may be attributed to the fact that the quarry always faces the profile and so no good quality data could be expected. This is also evident from the P-wave arrivals which show very poor quality. Therefore a conclusion based on the results of this line alone is not adequate.

Data recorded along lines 4 and 5 (Figs 4.42a, 4.43 and 4.44) are considered to be the best S-wave data acquired in this project. S-wave arrivals from the two quarries used, Glenluce and Tormitchell, are excellent with relatively the same consistency. This may be considered as an additional proof that the main factor determining the quality and range of S-wave arrivals is lithology rather than quarry practices.

4.7. Summary

P-wave frequencies were in the range of 5-20 Hz with noise levels occupying nearly the same spectrum. Filtering of P-waves was necessary to improve some of the traces in the vicinity of permanent noise sources. Minimum phase lowpass and bandpass filters were to enhance P-waves. Lowpass filters proved to be the most effective process in dealing with S-waves and they were used in combinations including both zero phase and minimum phase of high cut 6 and 10 Hz. S-wave frequencies were always less than 10 Hz. Their most dominant peaks were in the range of 4-8 Hz which agreed with values obtained by other workers. A relation between quarry practice and S-wave arrivals data quality was not established, but there are some indications that S-wave quality and consistency and, perhaps, range are dependent on the lithology traversed by the profiles. However, it is difficult to envisage such relation, because in the case of P-wave data the

evidence available indicates that quarry characteristics are the dominant control on P-wave data detection.

CHAPTER FIVE

DATA INTERPRETATION

5.1. Introduction

This chapter will be devoted to the interpretation of the data gathered for the **SUN** project. The main objective of the project was to obtain a well constrained seismic model for the Southern Uplands, permitting a regional geological interpretation. A network of 4 lines was recorded across strike and a fifth line was recorded parallel to the regional strike of the Southern Uplands. It was hoped that this network would provide good estimates of velocities and depths to key interfaces which could be integrated with other available data to produce the seismic model.

The region is still a matter of controversy regarding its geological history, tectonic setting and geophysical structure (see Chapter 1). Well constrained seismic data are scarce. Therefore much of the interpretation here had to be undertaken with great caution developing old ideas, rejecting models which the acquired data proved to be erroneous and producing new ideas for future development. Mention of projects relevant to any line(s) being discussed will be made and the appropriate figure(s) presented (e.g. LISPB, SUSP and those of Al-Mansouri (1986)), to illustrate the similarities and contradictions between the different sets of data.

An additional profile was recorded in the NE corner of the Midland Valley of Scotland from which headwaves from a basement refractor were obtained. The

results and interpretation of this profile will be also presented.

The WHB interpretation of the first arrival segments, where applicable, will be discussed first, since a knowledge of near surface velocity structure is critical to the interpretation of deeper structure. Data presentation includes the time-distance graphs and the interpreted digital seismic sections. These will be arranged in groups where the first of each group will be the time-distance graph of the line while the following figure(s) will represent the seismic section(s) with all interpreted arrivals marked. On these figures, a_0 refers to top layer arrivals; a_1 to headwaves from lower sedimentary layers; a_2 to headwaves from crystalline basement; and, finally, a_3 are high velocity headwave arrivals detected along line 3. Station numbers appear at the top of the seismic sections which are plotted with a reduction velocity of 6 km/s. Arrivals which are considered abnormal due to local ambiguities were excluded from regression to obtain the most realistic velocities.

The dataset obtained includes good S-wave information along most of the lines, especially along line 4 (Figs. 4.39 a-c and 4.40), which provide extra knowledge and constraints on the lithology of the region.

Finally, due to special circumstances which affected the author's work to a great extent in the later stages of this project, the intended extent of interpretation had to be reduced and, therefore, raytracing was applied to lines 2 and 4 only. These two lines were chosen because they represent two structurally different settings of the Southern Uplands. Hence to raytrace these lines should permit good tectonic and lithological correlation to be made between the east and west of the Southern Uplands.

5.2. Velocity determination

As outlined above, two procedures were used to determine the velocities of the obtained time-distance segments. The WHB method was used to invert time-distance data to velocity-depth models of the topmost layers, while regression was

used to calculate both direct arrival velocities where the WHB inversion could not be used and headwave velocities.

Table 5.1 shows the WHB results while Tables 5.2-5.11 show all obtained velocities including average velocities obtained by the WHB inversion for each line, detection range and the corresponding time intercepts.

Table 5.1 WHB results obtained from the SUN project. Depth ranges are as inferred from Figures 5.1-5.6.

Line	Velocity range in km/s	Depth range in km
Line 1: Melrose shot	4.5-5.2	0.6-1.3
Line 1: Bangley shot	3.8-4.4	0.2-1.0
Line 3: Aberdour shot	3.9-4.5	0.4-1.3
Line 3: Ratho shot	4.5-5.1	0.3-1.3
Line 6: Boysack shot	4.7-5.3	0.6-1.9
Line 6: Collace shot	4.9-5.4	0.2-2.4

Table 5.2 P-wave velocities obtained along line 1, Melrose-Bangley.

Arrival	Range (km)	Velocity (km/s)	Intercept (s)
a0	0-10	4.50	0.00
a2	12-18	6.06 +/- 0.03	0.54 +/- 0.02
a0	18-22	5.18	0.07
a2	24-31	5.92 +/- 0.06	0.51 +/- 0.07
a2	32-41	5.71 +/- 0.12	0.37 +/- 0.16

Table 5.3 P-wave velocities obtained along line 1, Bangley-Melrose.

Arrival	Range (km)	Velocity (km/s)	Intercept (s)
a0	0-8	4.05	0.00
a2	10-17	5.99 +/- 0.20	0.58 +/- 0.09
a0	19-23	5.02 +/- 0.09	-0.17 +/- 0.09
a2	24-31	5.00 +/- 0.05	-0.34 +/- 0.08

Table 5.4 P-wave velocities obtained along line 2, Melrose-Ratho.

Arrival	Range (km)	Velocity (km/s)	Intercept (s)
a0	0-6	4.33	0.00
a0	8-20	5.38 +/- 0.03	0.24 +/- 0..01
a2	22-31	6.10 +/- 0.04	0.75 +/- 0.05
a2	33-42	6.29 +/- 0.08	1.00 +/- 0.08

Table 5.5 P-wave velocities obtained along line 2, Ratho-Melrose.

Arrival	Range (km)	Velocity (km/s)	Intercept (s)
a0	0-4	3.58	0.00
a1	4-14	5.35 +/- 0.05	0.36 +/- 0.02
a2	16-25	5.95 +/- 0.07	0.86 +/- 0.05
a2	27-36	6.06 +/- 0.21	0.88 +/- 0.19
a2	38-50	6.02 +/- 0.07	0.84 +/- 0.07
a2	52-64	6.20 +/- 0.07	1.12 +/- 0.14

Table 5.6 P-wave velocities obtained along line 3, Aberdour-Moffat.

Arrival	Range (km)	Velocity (km/s)	Intercept (s)
a0	0-10	4.05	0.00
a1	10-16	5.23 +/- 0.45	0.61 +/- 0.27
a2	18-29	6.02 +/- 0.01	1.02 +/- 0.08
a2	31-38	6.21 +/- 0.15	1.11 +/- 0.14
a2	40-45	6.02 +/- 0.03	1.02 +/- 0.05
a3	47-51	6.25 +/- 0.08	1.13 +/- 0.11
a3	53-55	6.21	1.00

Table 5.7 P-wave velocities obtained along line 3, Ratho-Moffat.

Arrival	Range (km)	Velocity (km/s)	Intercept (s)
a0	0-13	4.70	0.00
a1	14-26	5.40 +/- 0.01	0.25 +/- 0.01
a3	28-34	6.25 +/- 0.08	0.90 +/- 0.07
a3	36-38	6.25	0.85
a2	41-50	6.17 +/- 0.06	0.72 +/- 0.08
a2	52-66	6.09 +/- 0.06	0.78 +/- 0.14

Table 5.8 P-wave velocities obtained along line 4, Glenluce-Tormitchell

Arrival	Range (km)	Velocity (km/s)	Intercept (s)
a0	0-14	5.46 +/- 0.02	0.00
a1	16-28	5.62 +/- 0.03	0.06 +/- 0.03
a2	28-42	6.02 +/- 0.03	0.39 +/- 0.06
a2	46-50	5.88 +/- 0.01	0.30 +/- 0.01

Table 5.9 P-wave velocities obtained along line 4, Tormitchell-Glenluce.

Arrival	Range (km)	Velocity (km/s)	Intercept (s)
a0	0-11	5.26 +/- 0.02	0.00
a1	13-24	5.75 +/- 0.01	0.21 +/- 0.01
a1	26-34	5.68 +/- 0.06	0.07 +/- 0.03
a1	37-42	5.65 +/- 0.03	-0.02 +/- 0.06

Table 5.10 P-wave velocities obtained along line 5, Glenluce-Newton Stewart.

Arrival	Range (km)	Velocity (km/s)	Intercept (s)
a0	0-10	5.68 +/- 0.06	0.00
a1	12-23	5.99 +/- 0.05	0.10 +/- 0.01

Table 5.11 P-wave velocities obtained along line 6, Boysack-Collace.

Arrival	Range (km)	Velocity (km/s)	Intercept (s)
a0	0-18	4.85	0.00
a2	19-25	5.65 +/- 0.40	0.51 +/- 0.30
a2	27-40	5.52 +/- 0.03	0.30 +/- 0.04
a2	41-45	5.62 +/- 0.03	0.30 +/- 0.04

The above tables present the velocity constraints on upper crustal lithological units as determined by WHB inversion and regression. From these tables it can be seen that the Midland Valley layer 1 (Carboniferous and Upper ORS) has a P-wave velocity range of 3.8-5.2 km/s and the Midland Valley layer 2 (Lower ORS and/or Lower Palaeozoic) a range of 4.7-5.4 km/s while the Midland Valley crystalline basement has a range of 6.0-6.1 km/s. These values are determined from

Melrose, Bangley, Ratho, Aberdour, Glenluce, Tormitchell and Boysack quarries. All these velocities lie within the ranges envisaged from previous seismic surveys carried out in the region.

Within the Southern Uplands, 5 main lithological units are detected from Melrose, Bangley, Ratho, Aberdour, Glenluce and Tormitchell and these are as follows:

1- Upper and/or Lower ORS rocks exposed at the surface in the Melrose area where a P-wave velocity range of 4.30-5.20 km/s is determined. This range of values is nearer to that of the Midland Valley layer 1 than that of layer 2, which does not support the suggestion of Rock & Rundle (1986) that a large thickness of Lower ORS rocks may underlie the Upper ORS exposed at Melrose.

2- Lower Palaeozoic rocks with a P-wave velocity range of 5.4-5.5 km/s. The velocity of this layer has been and is a matter of debate and a detailed discussion of its most likely velocity will be presented in section 5.7.

3- Sedimentary refractor in the SW of the region with an approximate P-wave velocity of 5.7 km/s. There is no previous information about this unit and modelling this refractor is dependent on information acquired by this project only.

4- Crystalline basement refractor with a P-wave velocity range of 5.71-6.29 km/s. It is thought that these velocity limits do not represent the true basement velocity variation, but they are due to dip effect. The true basement velocity is believed to lie within a range of 6.0-6.1 km/s.

5- A high velocity body detected along line 3 with an average P-wave velocity of 6.25 km/s.

5.3. Interpretation Using the WHB Inversion

The WHB velocity-depth inversion method was applied to 6 sets of data along lines 1, 3 and 6. The results are examined in detail following the summary of section 5.2.

5.3.1. Application of the WHB Inversion - General Procedures

This method was applied to the first velocity segments (the direct arrivals) of the time-distance graphs where the curvature of these segments was indicative of rapid velocity change. The program was written by J. Hall and modified by K. Davidson and M. Dentith. Five curves were fitted to the data representing the best fit curve, the straightest, the most curved, the maximum and minimum fit to the error bars discussed in section 3.3 respectively (top plots of Figures 5.1-5.6). These curves were intended to produce the maximum variation in velocity-depth curves obtainable within the errors of the data. The program can read data at irregular intervals where the time-distance segments are well constrained and it is only applicable for situations where there are no velocity inversions and no lateral velocity variation. This limited the use of this program to a great extent since the recorded profiles are intersected by many faults which offset the smoothed curves and hence it was not possible to apply the program in such cases.

Direct arrivals along lines 1, 3 and 6, were appropriate for velocity-depth inversion. Along line 2, the first velocity segment obtained from Ratho shot was concave upwards which may indicate velocity inversion and/or lateral velocity decrease away from the shotpoint. While from the other end, recording from Melrose, the direct arrival segment was offset by a fault, so regression was used to calculate the gradients of the offset velocity segments. Along line 4, the first velocity segment derived from Glenluce was offset by two faults while data obtained from Tormitchell quarry, in the north, showed minimal curvature and the first layer velocity was determined by regression. Similarly, regression was applied to data obtained from Glenluce quarry along line 5.

As noted above, use of the WHB assumes that there is no lateral velocity change in the top layer. It cannot be expected that such an assumption will be completely valid in the study area. Dentith (1987) suggests that since the curvature of the time-distance segment is a function of both lateral and vertical velocity

variation, the resultant velocity-depth curve is also a function of these variations. He also envisaged that data recorded in the direction of lateral velocity increase predict higher velocities at a given depth than occur below the source location. He concluded that to derive the true velocity-depth curve a pair of curves must be recorded exactly parallel to lateral velocity change.

Quarries used in this project are all located on igneous rocks (mostly sills) within the sedimentary sequence over which the profiles were recorded. This affected arrivals at receivers within 2-4 km range, which showed higher velocities than those determined using stations positioned on sedimentary rocks. This is explained by the igneous rocks having an initially higher velocity than the sediments and that they have been less influenced by weathering and therefore their velocity is reduced to a lesser extent. Due to this, the near-quarry recordings were omitted from the WHB calculations.

5.3.2. Results Obtained by the WHB Inversion

In this project, only the first station of lines 1 (recording Melrose shot), 3 (recording Ratho shot), and 6 (recording both shots) suffered the acceleration mentioned in the previous section and therefore were not used in the WHB analysis. This effect was not observed on data recorded along line 1 from Bangley and line 3 from Aberdour. Bangley quarry is located on basaltic tuffs of the Carboniferous age which are likely to have relatively low velocity compared to other igneous rocks such as sills. These rocks are also confined to a small area within a thick Carboniferous basin south of the Firth of Forth. This may explain why the "near quarry" effect is not observed here. At Aberdour the first station recorded along the profile was 3.5 km away from the shot, across the Firth of Forth, and so remote from the igneous body quarried at Aberdour.

Figures 5.1-5.6 show the results obtained by applying the WHB method for lines 1, 3, and 6. Most of the quarries used in this project were located in the

Midland Valley where much control on the topmost layer is available from work of Davidson (1986), Al-Mansouri (1986), Dentith (1987) and Kamaliddin (1988). These constraints were used in addition to results obtained in this project.

Figure 5.1 shows the velocity-depth inversion obtained along line 1 from Melrose quarry. These WHB values were the only results obtained within the Southern Uplands since inversion of data from the other Southern Uplands quarry (Glenluce) was not possible (see above). Velocity-depth curves acquired along lines 1 and 3 recording from Bangley, Aberdour and Ratho quarries (Figures 5.2-5.4 respectively) constrained the Midland Valley layer 1 velocity-depth relationship. Figures 5.5 and 5.6, using Boysack and Collace shotpoints, constrained the Midland Valley layer 2, which is the surface layer along line 6.

A velocity range of 4.5-5.2 km/s was obtained along line 1, using the Melrose shot, the corresponding depth range was 0.6-1.3 km (Fig. 5.1). The rocks exposed at the surface in the area are of Upper Devonian age (Fig. 1.3). These rocks are equivalent to the Midland Valley layer 1. At a short distance to the north of Melrose quarry, Lower ORS rocks are exposed at the surface corresponding to the Midland Valley layer 2. Rock & Rundle (1986) have indicated that these rocks were erroneously interpreted as Upper ORS, and could reach 600 m thickness. An average velocity of 4.5 km/s was obtained for this layer. This represents the higher velocity limit of the Midland Valley average layer 1 velocity of 4.0-4.5 km/s which may indicate that these rocks are indeed Upper ORS rocks and not Lower ORS, but at depth they may be underlain by Lower ORS rocks. Peter Haughton (pers. comm.) indicated that there is a high possibility that the Lower ORS rocks exposed in the region dip gently beneath the Upper ORS and therefore there may be a succession of the Midland Valley layers 1 and 2 in the Melrose area.

Results obtained from the reversal of this line, using the Bangley shot, gave a velocity range of 3.8-4.4 km/s at depths of 0.2-1.0 km (Fig. 5.2). This range of

velocity was expected since the line, at this location, traverses thick Carboniferous sediments of the SE Midland Valley.

Along line 3 results obtained from Aberdour quarry gave a velocity range of 3.9-4.5 km/s at depths of 0.4-1.3 km (Fig. 5.3). WHB results obtained from Ratho quarry, 17 km SW of Aberdour along the same line, yielded a velocity range of 4.5-5.1 km/s while depth values ranged between 0.3 and 1.3 km (Fig. 5.4). Notice the difference in maximum velocity values between the two shots. These differences were expected since the velocity segment of the first arrivals derived from Aberdour shot covers the Firth of Forth area where thick Carboniferous beds are present. Dentith (1987) envisaged a thickness in excess of 3 km for the Carboniferous layers along the MAVIS I south line in the Firth of Forth area. Since the Aberdour velocity segment is observed entirely across these Carboniferous strata, lower velocities are to be expected.

In contrast, the Ratho shot results showed higher velocity values. The profile crosses Upper and Lower ORS lithologies 9 km south of Ratho shot where velocities are higher than those obtained from the thick Carboniferous strata.

Figure 5.5 shows top layer velocities obtained along line 6 when recording from Boysack shot. A velocity range of 4.7-5.3 km/s is obtained over rocks of Lower ORS age which cover almost the entire Strathmore Syncline. Notice the similarity between these results and the results obtained along lines 1 and 3 when Melrose and Ratho shots were used respectively (summarised in Table 5.1). The similarity in lithology traversed by the three lines (mostly Lower ORS rocks) have contributed largely to these results. Note how the presence of Carboniferous strata along lines 1 (Bangley shot) and line 3 (Aberdour shot) has affected the velocity ranges obtained where lower values were calculated. However, the depth range obtained along line 6 was 0.6-1.9 km corresponding to Lower ORS strata. Kamaliddin (1988), recording Collace quarry towards Aberdour in the SE, obtained an average velocity value of 4.5 km/s at a depth of 0.8 km. His profile

was recorded perpendicular to line 6 and traversed the Tay Firth (line KAZ1, Figure 2.1) where 600 m thickness of Carboniferous strata are present. The velocities obtained in that area are highly affected by the low velocity of these rocks.

Results obtained from Collace quarry are shown in Figure 5.6. A velocity range of 4.9-5.4 km/s was obtained at a depth range of 0.2-2.4 km. These results are obviously the highest, in terms of velocity and depth, obtained by this method in the entire project. They again reflect the higher velocity of layer 2 sampled by line 6 and they also reflect the large thickness of the Lower ORS in the Strathmore Syncline area.

5.3.3. Discussion and Summary

In Table 5.1 the WHB method results obtained in this project were summarised while Table 5.12 shows a comparison between these and previous results obtained via WHB.

Table 5.12 Comparison of previous WHB P-wave results and those of SUN grouped by exposure across which the results were obtained.

Carboniferous & Upper ORS		
Project	Velocity range in km/s	Depth range in km
Davidson (1986)	3.2-4.0	0.0-2.0
Al-Mansouri (1986)	3.6-4.1	0.0-0.5
Dentith (1987)	3.0-4.6	0.5-3.0
Kamaliddin (1988)	3.3-4.6	0.0-1.2
SUN Project (1991)	3.9-4.5	0.4-1.3
Lower ORS		
Project	Velocity range in km/s	Depth range in km
Dentith (1986)	4.6-5.0	0.9-3.0
Kamaliddin (1988)	4.6-5.2	0.8-2.3
SUN Project (1991)	4.5-5.4	0.9-2.4

A study of Table 5.1 shows that the velocities obtained range from 3.9 (Aberdour shot) to 5.4 km/s (Collace shot). It is clear that these values are dependent on the rocks exposed at the surface at a specific locality where they are sam-

pled by the WHB method. These rocks are mainly of two groups: Carboniferous and Upper Devonian (usually referred to as Midland Valley layer 1), which show lower velocity values, and Lower Devonian rocks (Midland Valley layer 2) which crops out in many parts of the Midland Valley and some parts of the Southern Uplands (e.g. Melrose area) and which show the higher WHB velocities.

Table 5.12 compares the SUN results and those obtained by previous seismic projects. Lower WHB velocity values of 3.2-3.8 km/s are usually obtained across thick Carboniferous basins such as the Midlothian Coalfield and the Clackmannan district in the central Midland Valley, where a thick Carboniferous basin exists. High WHB velocities are usually obtained where the Lower Devonian beds are either at surface or occur at shallow depth.

Finally, it is more likely that the rapid increase of velocity with depth is associated with certain type of rocks rather than a specific region. Along line 4 the two quarries used (Glenluce and Tormitchell) are both located on Lower Palaeozoic rocks where no such effect is observed (Fig. 5.19) while on all other cases where the quarry is located on Devonian or Carboniferous rocks, the velocity increase is evident.

5.4. Planar Layer Interpretation of P-waves

The planar layer methods discussed in Chapter 3 will be applied, where possible, to the data to obtain preliminary geophysical and geological models to be further developed by raytracing of selected profiles, so providing a regional model for the Southern Uplands. Note that the un-interpreted digital sections are presented in Figures 4.26a, 4.27a, 4.28a, 4.29, 4.30a, 4.31a, 4.32, 4.33a, 4.34 and 4.35. Refer to Tables 5.1-5..11 for all velocity values determined in this project. Appendix 4 contains the observed travel times and gains used at the SUN recording sites.

5.4.1. Line 1: Melrose-Bangley

This line represents the most eastern limit of the SUN network. It trends SE-NW across the regional strike. Data obtained along this profile are the poorest in quality, due to the low energy released by the two quarries and the high noise levels encountered, especially at the northern end near the Firth of Forth.

The time-distance graph is presented in Figure 5.7 while the interpreted digital sections are illustrated in Figures 5.8 and 5.9. A schematic model for this line is presented in Figure 5.10. Refer to Tables 5.2 and 5.3 for the relevant velocities. Arrivals obtained from Melrose can be divided into 5 segments. The first represents direct arrivals (a_0) from the Lower ORS rocks exposed at the surface in the Melrose area. The second segment represents crystalline basement (a_2) at a crossover distance of 12 km. This is followed by third segment of lower velocity (interpreted as a_0) at a distance of 18 km which is stepped in time from the previous one. At this location, 18 km from Melrose quarry, the extension of the Hartfell Line, marking the boundary between tracts 5 and 6, may cross line 1. McKerrow (1986) had indicated that the Hartfell Line could extend 15-20 km east of the Lower ORS exposure near Melrose, while Leggett *et al.* (1979b) suggested that the Line terminates west of the outcrop by the same distance.

Further north, the Kingledores Fault intersects the line at a distance of 23 km from Melrose. Beyond this point basement arrivals (a_2) were detected again. Line 1 crosses the SUF 31 km from Melrose, beyond which a further group of basement arrivals were detected. This group has a slightly lower velocity and this is thought to be due to northward thickening of the Midland Valley layer 1 causing the underlying basement refractor to dip northwards (see Figure 5.10). This is in agreement with the plus-minus model for this line (section 5.6.1).

Using the velocities of the first two segments (Table 5.2) and equation 3.11 the thickness of the Lower ORS at the southern end of the profile was determined to be 1.81 +/- 0.36 km. No other thicknesses were measurable with the Melrose

data because of the presence of the low velocity segment in the middle of the profile. It is thought here that this low velocity is caused by a drop in the basement refractor due to the presence of the bounding faults thus arrivals are derived from the thicker part of the low velocity layer 1. Thus since Melrose arrivals at either side of the Hartfell Line are from different lithological units, the throw of this fault could not be determined. Similarly no throw was determined for the Kingledores Fault. The throw of the SUF was calculated to be 0.55 +/ 0.07 km, downthrowing towards the north. Equation 3.18 was used in these calculations where V1 was taken to be the average velocity of the top sedimentary cover north and south of the fault (4.30 km/s) and V2 is the average velocity of the basement observed on either side of the fault (5.81 km/s). A δt of 0.09s across the SUF was used.

Recording from the northern shotpoint at Bangley, 5 velocity segments were observed also. The first (a_0) represents the Midland Valley layer 1. At a distance of 8.5 km from the shot the line intersects the SUF. No arrivals from the Midland Valley layer 2 were detected before the SUF, which is due to the thickness of layer 1 in that area, representing the Carboniferous sedimentary basins in the Firth of Forth area. Basement arrivals beyond the fault (a_2) are earlier in time than predicted by arrivals at closer stations, indicating that basement is shallower south of the SUF, i.e. the fault downthrow is towards the north. This segment of a_2 is offset from the next by the Kingledores Fault at a distance of 17 km from the shotpoint.

Beyond the Kingledores Fault a low velocity segment (a_0) is observed from Bangley. This agrees with the low velocity observed from Melrose in this location and suggests basement downthrows to the south across this fault. It is likely that the Kingledores Fault and Hartfell Line, which intersect the line at 18 and 22 km from Bangley quarry respectively, are the bounds of a downfaulted basement block (Fig. 5.10) which is overlain by a thicker layer 1 sequence than to the north

and south. The graben appears to be sufficiently deep that the quickest path for basement headwaves to pass through this zone is to travel directly through the low velocity sediments.

Figure 5.7 shows that at 23 km from Melrose quarry observed arrivals are advanced in time in both directions. Since this cannot be explained by a simple fault the model in Figure 5.10 is presented to explain this. Arrivals obtained from Melrose quarry are regarded as acceptable within the graben context while the first trace obtained from the Bangley data south of the Kingledores Fault may pass through a basement "rise" just south of the fault causing its early arrival. This rise was not detected from the other direction because of lack of coverage (two stations covering 6 km distance). However, the other 2 arrivals detected from Bangley quarry along the low velocity segment are not affected by this rise as the first trace of the zone and therefore they are not as early in time as the first.

It should be mentioned here that the model presented in Figure 5.10 incorporates data from the MAVIS project, especially regarding the thicknesses and depths of the Lower ORS north of the SUF where arrivals from these rocks are not detected along line 1.

No geological information is available to explain the presence or the nature of the low velocity section detected along this line. However, Hall *et al.* (1983) suggested the presence of fast and slow velocity zones underlying at least the NE of the Southern Uplands mainly from re-interpretation of the LISPB profile (Figure 1.10). The low velocity zone detected along line 1 resembles a NE extension of the S2 zone of Hall *et al.*, but the velocities obtained along line 1 are 5.02 and 5.18 km/s while Hall *et al.* obtained 5.6 km/s. Along SUN lines 2 and 3 (see later) which are closer to LISPB, the step pattern seen along line 1 is present, but with smaller magnitude. The basement steps seen along lines 2 and 3 may represent the edges of the zone where downthrow is less. If the zone detected along line 1 is not an extension of the S2 zone observed on LISPB, then it may be

a local example of basement blocks being displaced vertically.

Finally, an arrival of relatively low velocity (5.00 km/s) is detected beyond a distance of 24 km from the Bangley shotpoint. It is interpreted as a down-dip apparent velocity from crystalline basement with a substantial dip toward the south. The arrival is observed across the Lower ORS basin of the Melrose area (see Figures 1.3 and 2.1). It is most likely that this basin is fault controlled since it is elongated in a direction perpendicular to the regional strike and has very straight edges. However, the observed velocity suggests that a significant and progressive deepening of the basement takes place along the profile and beneath the Lower ORS basin.

For the reasons mentioned above, no throws or thicknesses were determined from the Bangley dataset along line 1. However, an attempt to obtain a reasonable estimate of the thickness of layer 1 north of the SUF was made for possible future correlation with the other profiles further west. The throw of the SUF along line 1 (recording from Melrose quarry) was determined to be 0.55 +/- 0.07 km. Assuming that the SUF throw is the same when sampled from both directions and substituting the value of this throw in Equation 3.18, the time difference which the fault should cause from the Bangley direction can be estimated. V1 was taken to be the average velocity of the top layers north and south of the fault (4.30 km/s) and V2 to be the average velocity of the two basement segments on either side of fault (5.81 km/s). The deduced time difference was 0.09s which was added to the time intercept of the first basement headwaves (recording from Bangley) to "cancel" the effect of the fault in order to have some estimate of the thickness of layer 1 north of the SUF.

Using the corrected time intercept and V1=4.05 km/s and V2=5.99 km/s in equation 3.11 a thickness of 1.90 +/- 0.38 km was determined for layer 1 north of the SUF. It is worth mentioning that the crystalline basement velocities obtained along this profile are lower than those detected along lines 2 and 3 which are

usually >6.0 km/s.

5.4.2. Line 2: Melrose-Ratho

This line is oriented in a SSE-NNW direction. Partial coverage (2/3 of the line) was obtained from Melrose quarry in the SE, while full coverage was obtained from the more powerful quarry, Ratho, in the NW from which arrivals were detected to 6 km beyond Melrose quarry, some 64 km from the shotpoint. Figure 5.11 shows the time-distance plot while Figures 5.12 and 5.13 show the interpreted digital data. Refer to Tables 5.4 and 5.5 for the velocity values obtained along this profile.

The time-distance graph of Melrose data shows three groups of arrivals. The first are direct arrivals from the topmost section of the Upper and/or Lower ORS rocks (a_0) which are at surface in the area of Melrose quarry. The second group of arrivals are direct arrivals from the Lower Palaeozoic rocks (a_0) and are detected from a distance of 8 km from Melrose quarry. These two groups of arrivals are separated from each other by the Hartfell Line. The third group of arrivals are interpreted as crystalline basement arrivals (a_2) and are separated from the second by the Kingledores Fault at a distance of 22 km from Melrose quarry. This group is itself divided into two segments by the SUF at a distance of 32 km from Melrose quarry. The last two segments may either represent the same basement sampled from two different depth levels, or they represent two different basements where the first is a "Southern Uplands basement" and the second is a "Midland Valley basement". However, change of velocity due to dip is another possible explanation.

If we assume that the two basement segments are from the same interface, then the throw of the SUF can be determined, presenting the first seismic opportunity to accomplish this. Figure 5.11 shows that arrivals from this basement are divided into several segments along line 2 with slightly different velocities

separated by time steps due to faults. An estimate of the true refractor velocity has to be made prior to any throw calculations. The basement segment south of the SUF, at a distance of 22-31 km from Melrose quarry, is reversed from Ratho. A true basement velocity of 6.08 km/s was determined from here. Using equation 3.18, a throw of 0.84 +/- 0.10 km was computed for the SUF* where V1 was to be the average velocity of the two top layers (4.85 km/s) and a δT of 0.11s was measured for the time difference across the fault plane. No throws were calculated for the other faults which intersect the line (recording from Melrose quarry) because these faults separate arrivals from different layers, so equation 3.18 does not apply. This also prohibited the determination of the thicknesses of the two top sedimentary units because no correct time intercept can be measured and, hence, calculations will involve overestimation or underestimation of these thicknesses.

Time-distance data from the reversed direction (Ratho quarry) show 3 groups of arrivals also. The first, which is the first two traces up to a distance of 4 km from the quarry, are direct arrivals from the Lower Carboniferous rocks which crop out at this location with typical Carboniferous strata velocity of 3.58 km/s. This group is separated from the second by the Colinton Fault (Fig. 1.5) at a distance of 4 km from Ratho quarry. The second group of arrivals are interpreted as headwaves from the Lower ORS rocks (a_1). These arrivals (5 traces) show a concave upward velocity segment which may indicate progressive decrease of velocity with depth, or, a lateral change of velocity, but is here interpreted as due to an acute steepness of the Lower ORS refractor causing progressive delay of arrivals. The last two traces which showed maximum delay were not included in the regression.

The Pentland Fault, 15 km from Ratho separates the Lower ORS headwave arrivals from the third group, which are interpreted as crystalline basement arrivals

*A throw of 0.82 km was determined when line 1 was recorded from the same shot (see the previous section), across the SUF at a different location.

(a_2). Basement arrivals are seen to the end of the profile and offset by 3 faults resulting in 4 velocity segments (see Table 5.5). The first basement segment has a low velocity (5.95 km/s) which, if compared with the high velocity obtained for the same segment from the reversed direction (6.29 km/s), strongly suggests that these velocities are caused by a dipping interface, i.e the Midland Valley basement along line 2 dips down in a southerly direction. Poorer data quality may be the reason for the higher apparent velocity (6.20 km/s) of the last segment obtained in this direction.

A true basement velocity of 6.08 km/s was determined (see above) and used for V2 in determining all fault throws shown in the Ratho data. V1 was taken to be the average velocity (4.46 km/s) of the top two layers and equation 3.18 was used in the calculations. A throw of 0.51 +/- 0.06 km was calculated for the SUF which intersects the profile at 26 km from Ratho quarry. The downthrow of the fault is towards the north consistent with that determined from Melrose. The Kingledores Fault intersects the profile at a distance of 36 km from Ratho quarry. Using δT of 0.02s, a throw of 0.16 +/- 0.02 km was computed. Arrivals at either side of the fault show substantial scatter making the determination of the direction of the downthrow difficult, but a southerly directed downthrow is more likely. At 50 km from Ratho quarry, the Hartfell Line intersects the profile downthrowing to the south. A throw of 0.26 +/- 0.03 km was calculated for this fault using a δT of 0.04s.

At this stage it seemed feasible to use the Ratho data to obtain some estimate of the Midland Valley basement depth for future modelling (raytracing). The Colinton Fault (Fig. 1.5) offsets layer 1 arrivals from those of layer 2 while the Pentland Fault offsets layer 2 from layer 3 arrivals preventing any depth calculations. An approximate basement depth was computed to compare with results from the MAVIS profiles which trend in the vicinity of Ratho.

The Colinton Fault (Fig. 5.11) shows no time difference across the fault plane indicating that it has a small throw and therefore small error will be involved in the calculation of the thickness of layer 1 if the fault throw is ignored. Equation 3.11 was used where V1 and V2 are the velocities of the first two segments mentioned above. A thickness of 0.87 +/- 0.10 km was obtained for layer 1 (Carboniferous and Upper ORS) ignoring the throw of the Colinton fault for the reason mentioned above. Equation 3.12 was used to calculate the thickness of layer 2 (Lower ORS and ? Lower Palaeozoic), yielding a value of 2.64 +/- 0.53 km. V1 and V2 are as in the previous case while the true basement velocity obtained above was used for V3 (6.08 km/s).

The throw of the Pentland Fault was not considered in determining the above thickness of layer 2 where the time intercept used was that of the fault-delayed velocity segment. Therefore, the throw of this fault should be deduced from the total thickness of the sedimentary cover in order to obtain a more realistic depth to the basement. However, along line 3 (see later), the throw of the Pentland Fault was determined to be 0.68 km, throwing the basement down towards the south as in the case of line 2. Subtracting this throw from the total thickness of the sedimentary cover obtained above will result in a basement depth of 2.8 km north of the Pentland Fault while south of the fault, a deeper basement is envisaged.

Dentith (1987) raytraced a basement refractor at a depth of 4.0 km north of Edinburgh along the MAVIS I south profile and at a depth of 2.5 km along the MAVIS II profile which trends N-S across the centre of the Midland Valley. Sola (1985) raytraced the same basement at a depth of 2.5 km to the immediate north of the SUF, in the centre of the Midland Valley. Therefore, the basement depth calculated along line 2 is considered in good agreement with the available information about the region. The velocity values obtained are in good agreement with the previous projects.

5.4.3. Line 3: Aberdour-Moffat

This profile is the longest recorded in this project (66 km), trending in a N-S direction from Aberdour quarry to south of Moffat. It is the only line which was obtained by the single-ended method using two shots located at its northern end namely Aberdour and Ratho. Contrary to what was anticipated, the smaller Ratho quarry provided the more powerful blasts so that a larger offset and better quality data were obtained than from Aberdour.

Figure 5.14 shows the time-distance plots of the profile while the digital traces are presented in Figures 5.15 and 5.16. Velocities and codes of arrivals are listed in Tables 5.6 and 5.7. Observing data recorded from Aberdour quarry, 4 sets of arrivals are recognised. The first are direct arrivals from the Midland Valley layer 1 rocks (a_0) exposed at the surface, detected up to a range of 10 km. This is followed by a second group of arrivals (a_1) at a crossover distance of 10 km from Aberdour quarry representing layer 2 (Lower ORS) headwave refractions (refer to Figure 5.17 for all velocities and lithologies).

Crystalline basement headwaves (a_2) were detected beyond a crossover distance of 16 km. This set is divided into 5 velocity segments by 4 major faults. These segments fall into 2 subsets, north and south of the SUF which intersects the profile at a distance of 46 km from the shot, with basement velocity being abnormally high immediately south of the fault.

The last 2 basement velocity segments south of the SUF are believed to be refracted from a high velocity lithological unit (a_3) considered by some authors as an "unresolved" structure (e.g. Warner *et al.*, 1982 and El-Isa, 1977). This high velocity can be interpreted in terms of either velocity increase with depth in basement, or due to arrivals from a different lithological unit such as a basic igneous body or remnants of oceanic crust trapped after the closure of the Iapetus Ocean (Bluck pers. comm.).

This profile was unreversed, but the velocities obtained all lie within the accepted ranges which are present in the region. Therefore, it was decided that the horizontal layer equations are valid for an initial interpretation of this line.

Equations 3.11 and 3.12 were used to calculate the thicknesses of layers 1 and 2. A thickness of 1.95 +/- 0.39 km was obtained for the Carboniferous and Upper Devonian layer 1 and 1.57 +/- 0.31 km for the Lower Devonian and (?) Lower Palaeozoic layer 2. Adding these two thicknesses, a depth of 3.52 km is obtained for the Midland Valley basement. Dentith (1987) obtained a depth of 4 km for the basement along the MAVIS south line which intersects this profile 3 km south of Aberdour in the Firth of Forth. Along MAVIS 3, which nearly coincides with line 3 between Aberdour and Ratho, he obtained a basement depth of 4.4 km. All his models were obtained by raytracing. The above interpretation is thus in good agreement in terms of velocities and depths with the MAVIS models.

It was mentioned above that basement data recorded from Aberdour are stepped in time due to the effect of 4 faults. At a distance of 31 km from Aberdour a fault occurs, termed in this project as the *Henshaw Fault.* Using equation 3.18 a throw of 0.34 +/- 0.04 km was calculated for this fault with δT=0.05s, V1 is the average velocity of the top two layers (4.64 km/s) and V2 is the average velocity of the 3 basement segments (6.09 km/s) north of the SUF. It throws down to the north. The same equation and velocities were used to calculate the throw of the Pentland Fault which intersects the profile at a distance of 39 km from Aberdour. With δT=0.10s a throw of 0.68 +/- 0.08 km was calculated downthrowing to the south.

At a distance of 46 km from Aberdour the SUF offsets the basement which has 2 different velocities on either side of the fault (6.02 km/s north and 6.25 km/s south of the fault). This difference could lead to the conclusion that there are 2 different basements separated by the SUF. Conversely, this difference could be interpreted in terms of change of dip or rays passing within the same basement but

at deeper levels.

No throw for the SUF was calculated from the Aberdour data because of the presence of 2 different lithological units on either side of it. The last fault which intersects the profile is the Leadhills Line 52 km from Aberdour. An upthrow of 0.54 +/- 0.06 km to the south was deduced using a time difference of 0.08s. V1 used was the same as in the previous cases while V2 was the average velocity of the segments on either side of the fault (6.23 km/s).

Data obtained from the Ratho shot indicate the presence of 4 groups of arrivals. The first is interpreted as direct arrivals from the Carboniferous and Upper ORS rocks (layer 1) which are exposed in the area. At a distance of 13 km from Ratho quarry the Henshaw Fault offsets layer 1 from layer 2 followed by the SUF which intersects the line at a distance of 27 km from Ratho quarry separating the second group of arrivals (a_1) from the third which are interpreted as high velocity crystalline basement headwaves (a_3). Finally, at a distance of 41 km from Ratho quarry normal basement velocities were detected representing the a_2 refractor. Crystalline basements arrivals are divided into 4 segments by the effect of 3 faults.

To obtain the thickness of layer 1 it was essential to know the time intercept of the second velocity segment. This was not possible in the case of Ratho data because the Henshaw fault offsets layers 1 from 2 throwing the latter upwards to the south. Fortunately the throw of this fault is known from the Aberdour data (0.34 km). Using this throw and substituting V1 and V2 obtained along the Ratho data into equation 3.18, a time difference of 0.04s due to this fault was obtained. This time difference was then added to the time intercept of a_1 to "cancel" the effect of the fault. Equation 3.11 was used to calculate the thickness of layer 1 which was 1.37 +/- 0.27 km.

Equation 3.12 was then used to determine the thickness of layer 2 which was calculated to be 2.90 +/- 0.58 km where V1 and V2 were the velocities of the top

2 layers, while V3 was the average velocity of the basement segments (6.19 km/s). Therefore, if the above thicknesses are correct then the depth to the Midland Valley basement will be 4.26 km between Ratho and the SUF. This value agrees with the MAVIS I south data (4.30 km), but it does not agree with the depth obtained along line 2 (2.8 km), 20 km to the east. A possible explanation for this is that the Midland Valley basement is composed of vertically displaced blocks, at least along the southern margins of the region, due to the presence of faults such as the Pentland and Henshaw Faults.

At distances of 35, 39 and 51 km from Ratho quarry the Leadhills Line, Kingledores Fault and Hartfell Line intersect the profile respectively. Using equation 3.18, where V1 is the average velocity of the top two layers (5.05 km/s) and V2 is the average velocity of the 4 observed basement segments (6.19 km/s), throws of 0.39 +/- 0.05, 0.52 +/- 0.06 and 1.35 +/- 0.27 km were deduced for these faults respectively. The δT applied were 0.05, 0.06 and 0.16s. The first 2 faults downthrow to the north and the last to the south.

Figure 5.17 shows the geological model derived by planar layer interpretation along line 3 and the velocities employed. The main feature of this model is the faulted step-like behaviour of the basement, especially in the Southern Uplands. These basement faults coincide with the locations of faults within the Southern Uplands, that have been long considered as tract bounding faults and so as evidence of an accretionary prism. The downward extension of these faults to offset the underlying basement sheds great doubt on the nature of these faults as tract bounding faults within an accretionary prism.

The presence of a high velocity region (10-12 km wide) within this basement, with a velocity of 6.25 km/s, immediately to the south of the SUF is another important feature of this model. Is it the 6.3 km/s basement seen along the SUSP profile at nearly the same depth? Or is it an intrusion of a basic igneous body within the normal basement? The SUSP model outlines an area of uncertainty at

the same location where the high velocity region is found by SUN (dashed refractor of Figure 1.9). El-Isa (1977) also indicates the presence of a high velocity structure underlying the Broughton array (Fig. 1.10). He attributes this change of velocity to anisotropy but admitted that further studies are needed. However, Bluck (pers. comm.) offers another alternative explanation of the nature of this region in suggesting that it may be an oceanic crustal relic trapped after the final closure of the Iapetus Ocean. All these will be discussed in the next chapter.

To further investigate the nature of the basement refractor detected along line 3 and to find any possible correlation with the SUSP profile, an adaptation of the plus-minus method was applied to the profile although it is not reversed. Depths were measured relative to a reference point at station 20 to the immediate south of the SUF, 47 km south of Aberdour. Actual depth at the reference point was assumed to be the 3.6 km of the planar layer model presented in Figure 5.17. The time difference, δT was used as equivalent to the plus times of the respective stations since no real plus times could be obtained so that:

$Z_r = 2\ \delta t \times F$

where

Z_r = Relative depth

δt = time difference between the observed arrivals at the station and the time extrapolated from the reference station.

$$F = \frac{V2V1}{2\,(V2^2 - V1^2)^{1/2}}$$

Velocities had to be obtained from other SUN lines. A refractor velocity of 6.04 km/s was obtained from the minus times along SUN line 2 (see section 5.6.2). Data recorded from Glenluce quarry, along line 4, provide the best control on the velocity of the Lower Palaeozoic rocks exposed in the Southern Uplands. Such control is not available along line 3 since only ORS arrivals are detected

from the sedimentary cover. A velocity of 5.46 km/s was used as V1 (see Table 5.8). These velocities were applied to the equation presented above to determine the relative depths below the respective receivers. Figure 5.18 shows the resultant depth model.

Studying the above Figure, no possible correlation between the refractor and the SUSP at their point of intersection south of the SUF could be observed, but south of the Kingledores Fault the two models have the same depth (1 km). This model also suggests that the Hartfell Line has a much larger downthrow (2.5 km) than that obtained by the planar layer model (1.4 km). It is important to emphasise that the changes in refractor depth are the main features of this model. Absolute depths are uncertain by the nature of the modelling.

Finally, preliminary planar layer interpretation of data obtained along lines 1, 2 and 3 indicate that the SUF, as many other workers have predicted, downthrows the basement towards the north. Most importantly the "tract bounding faults" all extend downwards to offset the Southern Uplands basement, which means that their accretionary prism origin must be questioned. Additionally, some faults (the Henshaw and Pentland Faults) within the southern Midland Valley basement cause the same step-like behaviour as seen in the Southern Uplands basement.

5.4.4. Line 4: Glenluce-Tormitchell

Figure 5.19 shows the time-distance graph obtained along line 4 while Figures 5.20 and 5.21 show the interpreted digital sections of the profile and Tables 5.8 and 5.9 include all the velocities derived along this line. Recording from Glenluce, 3 sets of arrivals are observed. The first represents direct arrivals from the topmost section of the Silurian-Ordovician rocks (a_0) observed up to 14 km offset. Faults traversed by the line cause steps in the data. The first is the Kingledores Fault which intersects the profile at a distance of nearly 2 km from Glenluce quarry. The second is interpreted here as the Fardingmullach Fault

which intersects the profile at about 6 km from Glenluce quarry. Most of the published literature indicate the possibility of this line/fault continuing as far as the western coast of the Southern Uplands at the Rhins of Galloway (e.g Evans *et al.*, 1991).

The velocity of the direct arrivals was obtained by regression (see Table 5.8). This velocity (5.46 km/s) was averaged through the Silurian and Ordovician sedimentary cover south and north of the Kingledores Fault respectively. Al-Mansouri (1986) obtained a similar velocity of 5.31 km/s for the Lower Palaeozoic rocks in the same area.

The second set of arrivals (a_1) is detected at a distance of 16 km and are interpreted as headwaves from an (?) intra Lower Palaeozoic refractor. These arrivals are offset from the previous set by the Leadhills Line at a distance of 14-16 km. Beyond 28-30 km, arrivals from the Midland Valley basement (a_2) were detected. These arrivals were consistent to the end of the recorded profile and were offset by the Kerse Loch Fault at 42-46 km distance from Glenluce quarry. Beyond this fault the basement has lower velocity of 5.88 km/s which is interpreted as a downdip effect of the same basement. No time step is observed due to the SUF, the westward continuation of which should pass at a distance of 30-35 km from Glenluce quarry.

No throw was calculated for the Leadhills Line because it is located at a position where two different velocity segments meet (14 km from Glenluce) and therefore equation 3.18 does not apply.

A time delay of 0.10s was measured for the Kerse Loch Fault which offsets the Midland Valley basement in the vicinity of Girvan. Averaging the basement velocity across the fault plane yielded 5.95 km/s and using equation 3.18, a throw of 1.95 +/- 0.39 km was obtained for the fault which downthrows the basement toward the north where the northern segment of this basement dips towards the north beneath the Midland Valley. Al-Mansouri (1986) estimated a throw of 0.8-

1.0 km for each of the SUF and Kerse Loch Faults with a downthrow towards the south, but he argues against this model where the geology of the region and data recorded along his M1 line suggest otherwise (see Figure 2.1). It must be emphasised here, that the throw obtained for the Kerse Loch Fault from SUN data is approximate, since no control is available on the overburden velocities, but it highlights the substantial throw of the fault and the degree of its downward extension to basement.

The data recorded along line 4 suggest that the Midland Valley basement is truncated against a sedimentary refractor beneath the geographical location of the SUF where both interfaces occur at the same depth. This is because, at a distance of 28 km from Glenluce, the time-distance graph shows a decrease in gradient, rather than a time step, which is indicative of a higher velocity layer being sampled (Midland Valley basement). Al-Mansouri (1986), along his line M1, modelled a change in velocity rather than an actual fault in the region where the SUF is supposed to be located (Figure 5.22), but he envisaged the direction of the throw of the fault to be in an opposite sense to that accepted by most geologists, i.e throwing down to the south. This may be a another example of the complexity of the area and the difficulties encountered in interpreting the exact behaviour of the fault where it cannot be properly visulised.

Using equation 3.11, the thickness of the topmost section of the Lower Palaeozoic rocks was calculated to be 0.80 +/- 0.09 km where V1 and V2 used were 5.46 and 5.62 km/s respectively while using equation 3.12, a thickness of 2.20 +/- 0.44 km of the Lower Palaeozoic sediments was determined assuming that either the Midland Valley basement (V3=6.02 km/s) in the SW of the Southern Uplands does not terminate at the SUF, but extends further south below this refractor, as many previous workers suggested, or a similar basement with nearly the same velocity underlies this refractor. If this assumption is valid, then this basement is at a depth of about 3.00 km below line 4. Al-Mansouri (1986) inter-

preted the basement along his M1 line (see Fig. 2.1) to be at a depth of 4.0 km shallowing towards the north (Fig. 5.22), while the SUSP model has a 6.0 km/s horizontal basement underlying the Southern Uplands (Fig. 1.9) at a depth of 1 km.

Two sets of arrivals were obtained from the reversal of line 4 (Tormitchell shot, Figure 5.19). The first set represents direct arrivals through the Ordovician rocks that crop out near Tormitchell quarry (within the Midland Valley). WHB inversion was not applied to this section because arrivals show a linear relationship. Regressing the data yielded a velocity of 5.26 km/s. Al-Mansouri (1986) obtained a higher velocity of 5.65 km/s along his M1 line which trends subparallel to and west of line 4 traversing the Ballantrae ophiolitic complex. Al-Mansouri had no direct arrival control on the Ordovician rocks near Tormitchell because they are not within the range of the direct arrivals of M1 his line. His velocity values were determined by raytracing.

The second set of arrivals (a_1) obtained along line 4 using Tormitchell is offset from the first by the Glen App Fault, at a distance of 10-12 km from the quarry. It is offset by two fault zones itself: the Leadhills Line and the combined effect of the Fardingmullach and the Kingledores Faults respectively. These faults define three time-distance segments. Their velocities, which are listed in Table 5.9, show that these three segments represent a single refractor of an average velocity of 5.69 km/s which was interpreted as the same intra Lower Palaeozoic refractor detected from the reversal of this line (note the similar velocity obtained from Glenluce shot for this refractor indicating low dip). Using equation 3.11, a thickness of 1.35 +/- 0.27 km was obtained for the Ordovician rocks. In calculating this thickness the throw of the Glen App Fault was not considered since it is not measurable because it separates two different sets of arrivals, although its effect may have caused some over-estimation of the thickness of the Ordovician strata.

As mentioned above the data indicate the presence of three faults other than the Glen App Fault which are interpreted as the Leadhills Line, which intersects the profile at a distance of 22-25 km from Tormitchell quarry, and the Fardingmullach/Kingledores fault zone which intersects the profile at a distance of 34-36 km from the shot. As argued above the latter two faults define a faulted block extending over a range of 3 km and throwing the southern section up towards the south. Figure 5.19 shows that the velocity segments defining the main refractor are sub-parallel and therefore the application of equation 3.18 can be undertaken. A throw of 1.94 +/- 0.39 km was calculated for the Leadhills Line and 1.16 +/- 0.23 km for the Fardingmullach-Kingledores fault-block using (δT_i) in both cases and the refractor velocity V2 was taken to be the average velocity of the three time-distance segments with a value of 5.69 km/s. The downthrow of these faults is towards the north.

Figure 5.19 shows that the faults discussed above define fault zones of approximately 2-3 km width rather than distinctive fault planes. In the case of the Fardingmullach-Kingledores fault zone it is relatively easy to predict the structural configuration which is probably comprised of a fault zone 3 km wide and bounded by the two major faults. Also, Anderson & Oliver (1986) envisaged a systematic decrease in the width of the Kingledores Fault towards the NE from a maximum in the SW which may well explain the relatively large width of the fault zone along line 4. In the case of the Leadhills line the situation is more ambiguous and this may be explained in terms of a shattered zone of 2 km width.

The SUF adds to the above structural complexities because it acts as a seismic barrier prohibiting further analysis of the main refractor to the north, since its amount of throw cannot be determined from the available data. Therefore the actual behaviour of the refractor itself cannot be envisaged and whether it extends north of the SUF is a matter of speculation. However, it is possible to infer the sense of the throw of the SUF if one accepts the argument outlined above where it

was suggested that the Midland Valley basement occurs at the same depth as the sedimentary refractor south of the fault. If this is the case then the Southern Uplands basement should occur below this refractor, requiring the throw of the SUF to be down to the south in agreement with Al-Mansouri (1986).

Due to the above it was difficult to visualize the exact behaviour of the main refractor, given the additional ambiguities observed in the data recorded from the other direction (Glenluce quarry). Therefore, the application of the other planar layer methods discussed in Chapter 3 was suspended at this stage and further interpretation of this line was carried out using more adequate procedures, such as the plus-minus method and raytracing.

An example of the difficulties faced when the planar layer methods were applied to this profile is that, for instance, the dipping layer method assumes continuity of dip of the refractor along the complete seismic line in order to determine depth estimates. This is clearly not the case on line 4, given the fault interpretation placed on the 5.7 km/s refractor. Using the Glenluce shot, where faulting brings the 5.7 km/s refractor closer to the surface, in the south, there will be an underestimate of refractor depth using this assumption. From Tormitchell, which lies in the Midland Valley and is beyond the SUF from where reversed coverage of the 5.7 km/s is obtained, depth estimates will be under- or over-estimated depending on the relation of the depth of the 5.7 and 6.0 km/s refractors at the SUF.

To investigate the nature of the 5.7 km/s refractor detected along line 4, data used by Al-Mansouri (1986) were re-interpreted. These data consisted of 8 air-gun shots fired on a NE-SW profile in the Solway Firth during the Caledonian Suture Seismic Project. The shots were named M05 through to M12. The recording profile (his line M4, Figure 2.1) trends N-S and consisted of 7 seismometers. It is intersected by SUN line 5 and parallel to SUN line 4. Receiver offsets along this profile varied between 42 and 69 km. Al-Mansouri did not present any

interpretation of the acquired data. It was found feasible here to use these data to provide extra constraints on the deeper section of the crustal layers in the area covered by SUN lines 4 and 5 due to the relatively large offsets achieved by line M4. The original seismograms could not be examined. Instead time-distance information tabled by Al-Mansouri (1986) were used.

The time-distance plots of the 8 shots are presented in Figure 5.23. The data define one refractor which is intersected by the Kingledores Fault and, perhaps, the Fardingmullach Fault at about 53 km from the shotpoints. Regressing both segments of the refractor for all 8 time-distance sets resulted in the velocities listed in Table 5.13. Data obtained from shots M09 and M10 are considered abnormal due to the low velocities obtained for the first segments. These are probably due to poor data quality and consequent misidentification of the first arrivals. The other six velocity sets were averaged to obtain two average velocities for the two segments south and north of the fault(s), being 5.88 +/- 0.07 and 5.92 +/- 0.17 km/s respectively.

Table 5.13 Velocities derived from regressing eight data sets obtained from Al-Mansouri (1986) along his line M4. V1 and V2 refer to velocities obtained when the first and second velocity segments of each time-distance graph were regressed respectively.

Shotpoint	V1 in km/s	V2 in km/s
M05	5.99 +/- 0.20	6.21 +/- 0.07
M06	5.88 +/- 0.01	5.88 +/- 0.17
M07	5.92 +/- 0.02	6.09 +/- 0.50
M08	5.88 +/- 0.01	5.78 +/- 0.02
M09	5.52 +/- 0.03	5.55 +/- 0.12
M10	5.55 +/- 0.09	5.85 +/- 0.03
M11	5.81 +/- 0.03	5.71 +/- 0.06
M12	5.78 +/- 0.10	5.85 +/- 0.03

Given the overlap of their error bounds, these average velocities are thought to represent a single refractor, which is the refractor interpreted along SUN lines 4

and 5. The most important implications of these results are:

[1] they support the presence of the main refractor interpreted in the area along SUN lines 4 and 5.

[2] that this refractor has substantial thickness, since no deeper refractor was detected despite the maximum 69 km offset.

[3] the relatively higher velocity values obtained along the M4 line are because these velocities are derived from the deeper parts of the same lithological unit.

To have some estimate of the minimum depth of crystalline basement in the SW of the Southern Uplands the maximum offset recorded (69 km) was assumed to be the minimum crossover distance for arrivals to be detected from this basement. Substituting this value in the equation below, a minimum depth of 5.53 km for the basement was calculated in the SW of the SUN project area.

$$X_{cross} = 2Z \left[\frac{V2+V1}{V2-V1} \right]^{1/2}$$

where

V1=5.70 km/s, the velocity of the sedimentary refractor.

V2=6.0 km/s, the average Midland Valley velocity.

In this work, a model of a deeper basement in the SW is favoured, since the SUSP and WINCH data suggest the presence of such basement at depths ranging between 5-10 km (see Figures 1.9 and 1.12) and because that previous seismic velocity information can explain the differences in velocities between the SUSP and line 4 as due to anistropy of the refractor. Also, Al-Mansouri (1986) suggested that the Lower Palaeozoic sediments in the SW of the Southern Uplands have great thicknesses.

The 5.7 km/s refractor detected along line 4 extending south of the SUF to the end of the recorded data south of Glenluce shot occurs at a depth of 1.35 km

below Tormitchell in the north and 0.80 km below Glenluce in the south. It is offset by several faults and it steps upwards towards the south of the Southern Uplands.

If this refractor is not crystalline basement but rather a sedimentary interface it cannot be envisaged within the traditional context of an accretionary prism, where large thicknesses of accreted sediments are expected and which are usually underlain by high velocity (>6.0 km/s) oceanic crust. Because of the complexity of accretionary prisms, it is unlikely that regionally persistent refractor would be detected within one. Therefore the only refractor detected in the area is taken to be below the prism (the 5.7 km/s refractor) which occurs at a very shallow depth (average 1 km). This depth leads to the conclusion that in the SW of the Southern Uplands only **part** of the accretionary prism is present, the rest of the accreted pile of sediments (usually 10-15 km thick) is missing probably due to either the thrusting of only a slice of it or strike-slip movement.

It is argued here that the 5.7 km/s refractor represents a sequence onto which an accretionary prism, or part of one, has been obducted. It may be the missing forearc suggested by many workers (e.g. B. Bluck pers. comm.) and which is said to have existed between the Southern Uplands accretionary prism, in the south, and the Midland Valley island arc in the north. If this model is correct, then this obducted part of the accretionary prism should extend, along strike, towards the NE. In this work, no evidence is seen to prove the extension of the 5.7 km/s refractor towards the NE. A possible answer for this is that the 5.7 km/s refractor shallows and eventually is truncated, along strike towards the NE, in the area between lines 3 and 4, or it is faulted out in the area. The LISPB model, for the more eastern part of the Southern Uplands (Fig. 5.24), involves a refractor of 5.8 km/s at a shallow depth south of the SUF, but underlain by a very deep basement (>10 km). Results obtained along SUN lines 1, 2 and 3 do not support the presence of such sedimentary refractor in the NE while they confirm the presence of a

much shallower crystalline basement than seen on LISPB.

In conclusion, planar layer interpretation along line 4 did not prove to be an adequate procedure to analyse and interpret the available data because of its basic assumption that interfaces should be considered as essentially planar. Application of the dipping layer method was not carried out because it was not possible to trace the interface across the SUF with any certainity.

The application of these methods were presented here to illustrate the maximum information which could be "extracted" by such methods given the available data. It is apparent that the structural complexity of the area contributed largely to the failure of these procedures to give a reasonable model. But it must be admitted that they provided a good estimate of the general velocity distribution and the seismic nature of the main refractors present in the area as well as defining the main faults information, which is essential for further development and interpretational procedures.

5.4.5. Line 5: Glenluce-Newton Stewart

Glenluce quarry was used to record this unreversed line in a NE direction. It trends parallel to the regional strike south of the Kingledores Fault. Figure 5.25 shows the time-distance graph while the interpreted digital section is shown in Figure 5.26 and Table 5.10 presents the velocities obtained along the line. The data define two velocity segments. The first is interpreted as direct arrivals from the topmost section of the Silurian strata of the Central Belt which are exposed south of the Kingledores Fault. The second segment which has higher velocity (see Table 5.10) is interpreted as headwave arrivals from the same sedimentary refractor detected along line 4 occurs beyond a crossover distance of 11 km from the shotpoint. Direct arrivals along this line show higher velocity than those recorded along line 4 from the same quarry, even though the latter arrivals are mostly detected along the older and presumably faster Ordovician rocks, starting 4

km north of Glenluce. The headwave arrivals, along line 5, also show higher velocity than those along line 4.

The main aim of this profile was to investigate any possible relationships between velocity and azimuth in the Southern Uplands which have been suggested by previous workers. El-Isa (1977) had indicated that systematic variations of velocity with azimuth are present below the EKA array in the central Southern Uplands, concluding that they are due to anisotropy. He also suggested that, in the same area, velocity increases rapidly down to a depth of 1.6 km and thereafter it increases at a slow rate. Adesanya (1982), using data from the same area, reached the same conclusion regarding the along-strike velocity increase, also attributing this increase to anisotropy. Adesanya envisaged a 3% variation in velocity with it being highest parallel to strike.

It is almost certain that we are dealing with the same lithological units along the SUN lines in the Southern Uplands where this azimuth related increase in velocity is caused either by anisotropy or dip or both, although anisotropy is preferred by previous workers (see above) and the refractor interpreted along line 5 must be the same as that modelled along line 4 (5.7 km/s refractor).

Along line 5 a depth of 0.88 +/- 0.10 km was calculated for the 5.99 km/s refractor. The SUSP model (see section 1.10.1) suggests the presence of a top layer (presumably of Ordovician greywacke) with a velocity of 5.7-5.8 km/s to a depth of about 1 km. This layer is underlain by a 6.0 km/s basement layer which is 2-3 km thick. The SUSP profile (Fig. 2.1) is north and parallel to line 5 and trends just south of the SUF. Both headwave velocity and depth values obtained along line 5 are in agreement with the SUSP 6.0 km/s refractor existing at 1 km depth. However, it was established (see above) that the refractor interpreted along lines 4 and 5 is the same. Therefore, this will imply that the line 4 refractor is the same as that of line 5 and the SUSP 6.0 km/s refractors.

The main geological implication of the line 5 interpretation and the correlation with the SUSP 6.0 km/s refractor is that either the SUSP refractor is a sedimentary refractor rather than crystalline basement where its higher velocity is due to the direction of recording, or, contrary to what was suggested in the previous section, the "intra Palaeozoic refractor" is in fact crystalline basement in accord with the SUSP interpretation.

In section 5.6 (see later) the plus-minus method is applied to line 4 and a true refractor velocity of 5.81 km/s was computed in the SW of the Southern Uplands. Accepting the 3% change in velocity in relation to azimuth mentioned above (Adesanya 1982), the obtained headwave velocity along this profile (5.99 km/s) represents a 3% increase in the true refractor velocity detected along line 4. Finally, depths to the refractor below Glenluce quarry calculated along lines 4 and 5 (0.8 and 0.9 km respectively) are in close agreement with each other and the SUSP 1 km "basement" refractor.

5.4.6. Line 6: Boysack-Collace

This profile was designed to highlight the velocity structure along the strike of the Strathmore Syncline. The acquired data were integrated with a previous N-S profile (Kamaliddin 1988) recorded in the vicinity (line KAZ1, Figure 2.1), and which indicated the possibility of a stepped basement underlying the Strathmore Syncline. Full coverage of line 6 was obtained from Boysack quarry, while reversed coverage from Collace quarry was only partially achieved (see section 2.2.6) due to reasons beyond the author's control.

Figure 5.27 shows the time-distance plot for data recorded along this line while Figures 5.28 and 5.29 show the recorded digital data from both shotpoints. It should be noted here that the digital section of data recorded from Collace quarry is un-interpreted due to the little amount of data it contains (7 traces). However, the data obtained from Collace quarry will be used to provide extra con-

straints on the depth to the main refractor detected along the profile (see later).

Arrivals detected from Boysack quarry define two velocity groups. The first group represents direct arrivals from Lower ORS rocks (a_0). The second group of arrivals are interpreted as headwave arrivals from a basement refractor which is dissected by two faults defining three velocity segments. Table 5.11 shows the velocities of these segments and their relevant ranges. From the above Table, it is evident that these three segments represent the same refractor with an average observed velocity of 5.60 km/s which is considered here as due to dipping crystalline basement. Equation 3.11 was used to interpret the depth of the refractor where V1 was taken to be 4.85 km/s (average velocity of topmost layer) and V2 was taken to be 6.04 km/s (true velocity). This value was taken from Kamaliddin (1988) in the absence of reversed coverage on line 6. A thickness of 2.00 +/- 0.40 km was calculated for the topmost layer in the NE below Boysack quarry which is interpreted as Lower ORS or Midland Valley layer 2 (see Dentith 1987 and Kamaliddin 1988). See Figure 5.30.

Note that Kamaliddin (1988) interpreted the 6.04 km/s basement to be at a depth of 4.9 km below Collace quarry. He also suggested that this basement is "stepped upwards" in a northerly direction towards the axis of the Strathmore Syncline from an average depth of 5.2 km beneath the adjacent areas of the Midland Valley.

Two major faults intersect the profile at approximately 26 and 40 km from Boysack quarry, trending in a NW-SE direction. The same time difference of 0.10s was seen across both faults which downthrow to the NE. Using equation 3.18 a throw of 0.92 +/- 0.11 km was calculated for each fault. V1 was 4.85 km/s the velocity of the topmost layer, and V2 was determined by averaging the velocities of the three headwave segments which was calculated to be 5.60 km/s.

Geological maps indicate that these faults are nearly perpendicular to the profile which trends sub-parallel to the axis of the syncline. No names for these

two faults were found in the available literature and, for convenience, the faults will be named after the nearest major geographic features. Therefore, the fault nearest to Boysack quarry at 26 km distance will be termed the *Auchterhouse Hill Fault* and the second fault which is at 40 km distance from Boysack quarry will be called the *Northballo Hill Fault.*

The faults cause steps upward towards Collace quarry i.e the refractor shallows in a SW direction. Assuming that this refractor is a faulted, horizontal interface and is at 2.00 km depth under Boysack quarry, the throws of the two faults mentioned above predict a thickness of only 0.16 km of ORS strata beneath Collace quarry. Figure 5.6 shows the WHB results of the Collace data. It clearly indicates that a thickness of 0.16 km for the Lower ORS is not realistic since the WHB data suggest a more substantial thickness of lower velocity material.

An attempt was made to determine the minimum thickness of Lower ORS cover below Collace quarry by assuming that the offset of furthest trace recorded from Collace shotpoint (22.33 km) represents the minimum crossover distance for such a refractor to be detected. Inspecting Figure 5.6 makes this assumption acceptable since most of the 7 traces recorded from this quarry maintain nearly the same curvature indicating the high probability that they are direct arrivals from the Lower ORS top layer. A minimum thickness of 2.73 km was calculated for the Lower ORS layer. The above excludes the model of a simple horizontal faulted refractor of 5.6 km/s progressively upfaulted towards the SW. Therefore, a more complicated model must be invoked. Furthermore as pointed out in section 1.9.3, geological studies in the region indicate that substantial thicknesses of Lower ORS are present in the Strathmore Syncline and the 0.16 km thickness calculated above cannot be accepted within these ranges.

To provide a geologically acceptable model which could be the best representative of the data acquired, the refractor detected along line 6 was assumed to represent a stepped crystalline basement (in accord with available literature) with

blocks having varied dips. As a result of this assumption the velocities obtained for these headwave segments are used to determine the in-line dips given the assumed refractor velocity. Using the available equations (Dobrin 1976), the angle of dip of each segment was determined using 4.85 km/s for V1 the top layer velocity obtained from the WHB results. The true refractor velocity (V2) was taken to be 6.04 km/s after Kamaliddin (1988). The two velocities provided a value for the angle of incidence from which the angle of dip for each segment was determined. The resulting model is presented in Figure 5.30.

If the velocities assumed above are correct then the following conclusions can be deduced from the model along line 6:

[1] contrary to our previous knowledge, the Lower ORS sequence seems to *thin* in a NE direction in contrast to what was previously believed to be SW thinning ORS basin.

[2] the model implies that, beneath the Strathmore Syncline, the crystalline basement is faulted.

A faulted basement is contrary to all previous seismic work (except Kamaliddin (1988)) carried out in the Midland Valley which suggests a horizontal basement with little or no relief (see Chapter 1). It is important to mention here that the above conclusions are valid only if the assumption that the observed refractor is crystalline basement proves to be true. This could be confirmed by completing the reversed coverage of the profile.

The new model agrees with the ideas of Haughton & Bluck (1988), who envisaged that the Strathmore Syncline is more complex than previously recognised, and that it may be composed of a number of small strike-slip controlled basins which were generated along a suture now concealed by the post-ORS Highland Boundary Fault. Haughton & Bluck also supported the theory that a volcanic ridge in the central Midland Valley of Scotland separated the Lower ORS basin into a northerly Strathmore Basin and a southerly Lanark Basin implying that two

different basements may underlie the Midland Valley.

An interesting point is that the raised block modelled in Figure 5.30 and which lies directly beneath Collace quarry is equivalent to a similar block modelled by Kamaliddin (1988) under the same quarry along his KAZ1 line (Fig. 2.1), which is nearly perpendicular to line 6. In both cases the block has the same depth below Collace quarry (4.9 km). Finally, these basement steps modelled along line 6 could be the controlling factors on deposition in the basins proposed by Haughton & Bluck (1988) who suggested that such basins were probably structurally controlled.

The above model casts doubt on the previous models which define one single basement to underlie the entire Midland Valley. However, a new line of thought is emerging which suggests that the basement underlying the Midland Valley could be composed of at least two basements (Bluck pers. comm.). Also, Read (1989) presented sedimentological evidence of a major subsurface system of en-echelon fractures which trends ENE-WSW along the southern margin of the Strathmore Syncline. Kamaliddin (1988) determined a major fault 12 km south of the Tay Graben trending NE-SW which may represent the eastern continuation of the surface expression of this fracture system including, according to Read, many major faults which cross the central part of the Midland Valley of Scotland trending in a SW-NE direction.

The model suggested along line 6 and the data obtained from Kamaliddin (1988) support this new approach of a more complicated basement underlying the Midland Valley of Scotland.

Work carried out by Haughton (pers. comm.) indicates the presence of large thicknesses of Lower ORS in the proximity of very thin Lower ORS strata is not unusual in the Strathmore Syncline. He suggests that the syncline may not be, as interpreted before, a single sedimentary basin filled with large thicknesses of sediments, but rather composed of many smaller basins which were deposited adjacent

to and on top of each other causing large differences in thicknesses along short distances (see also Haughton & Bluck 1988).

5.5. Interpretation of Detected Shear Waves

The SUN dataset contains good S-wave arrivals detected along most of the profiles. In this section the interpretation of these data will be presented and discussed. Filtering procedures to enhance and obtain the best possible S-wave onsets were discussed in Chapter 4. Results of Vp/Vs values and Poisson's ratios (σ) determined for the respective velocity segments along each line are presented in Tables 5.14-5.19. Appendix 4 contains the observed travel times determined for these arrivals.

Figures 5.8, 5.9, 5.12, 5.13, 5.15, 5.16, 5.20, 5.21, 5.26 and 5.28 show the interpreted S-wave arrivals along lines 1, 2, 3, 4, 5 and 6 respectively. Codes are the same as those of the P-waves (see section 5.1) except that "a" is substituted with "s".

Table 5.14 S-wave velocities, Vp/Vs ratios and Poisson's ratio (PR) determined along line 1.

Melrose shot					
Code	Range (km)	Vp	Vs	Vp/Vs	PR
s2	12-18	6.06	2.71	2.24	0.37
Bangley shot					
Code	Range (km)	Vp	Vs	Vp/Vs	PR
s0	0-8	4.05	1.73	2.34	0.39
s2	10-17	5.99	3.46	1.73	0.25
s0	19-23	5.02	2.72	1.84	0.29
s2	24-33	5.00	2.72	1.83	0.29

Table 5.15 S-wave velocities, Vp/Vs ratios and Poisson's ratio (PR) determined along line 2.

Melrose shot					
Code	Range (km)	Vp	Vs	Vp/Vs	PR
s0	0-6	4.33	1.85	2.33	0.39
s1	8-20	5.38	3.17	1.69	0.23
s2	22-29	6.10	3.09	1.97	0.33
s2	33-42	6.29	3.14	2.00	0.25
Ratho shot					
Code	Range (km)	Vp	Vs	Vp/Vs	PR
s0	0-4	3.58	2.02	1.77	0.27
s1	4-8	5.35	2.64	2.03	0.34
s2	16-25	5.95	3.06	1.94	0.32
s2	27-36	6.06	3.08	1.97	0.33

Table 5.16 S-wave velocities, Vp/Vs ratios and Poisson's ratio (PR) determined along line 3.

Aberdour shot					
Code	Range (km)	Vp	Vs	Vp/Vs	PR
s0	0-10	4.05	2.44	1.66	0.21
s1	10-15	5.23	2.40	2.18	0.37
s2	18-30	6.02	3.52	1.71	0.24
Ratho shot					
Code	Range (km)	Vp	Vs	Vp/Vs	PR
s0	0-13	4.70	2.86	1.64	0.21
s1	14-26	5.40	2.89	1.87	0.30
s3	28-34	6.25	3.57	1.75	0.26
s3	36-38	6.25	3.55	1.76	0.26
s2	40-50	6.17	3.87	1.59	0.17

Table 5.17 S-wave velocities, Vp/Vs ratios and Poisson's ratio (PR) determined along line 4.

Glenluce shot					
Code	Range (km)	Vp	Vs	Vp/Vs	PR
s0	0-14	5.46	3.25	1.68	0.23
s1	16-28	5.62	3.33	1.69	0.23
s2	28-38	6.02	3.51	1.72	0.24
s2	46-50	5.88	3.47	1.69	0.23
Tormitchell shot					
Code	Range (km)	Vp	Vs	Vp/Vs	PR
s0	0-11	5.26	3.08	1.71	0.24
s1	13-24	5.75	3.42	1.68	0.22
s1	26-34	5.68	2.79	2.03	0.34
s1	37-42	5.65	2.99	1.89	0.30

Table 5.18 S-wave velocities, Vp/Vs ratios and Poisson's ratio (PR) determined along line 5.

Glenluce shot					
Code	Range (km)	Vp	Vs	Vp/Vs	PR
s0	0-10	5.68	3.13	1.81	0.28
s1	12-21	5.99	3.52	1.70	0.23

Table 5.19 S-wave velocities, Vp/Vs ratios and Poisson's ratio (PR) determined along line 6.

Boysack shot					
Code	Range (km)	Vp	Vs	Vp/Vs	PR
s0	0-18	4.85	3.03	1.60	0.18
s2	22-25	5.65	3.04	1.86	0.29
s2	27-40	5.52	2.98	1.85	0.29
s2	41-45	5.62	2.78	2.02	0.34

Figures 5.31-5.35 show the σ values determined. The above tables show that σ values obtained along lines 1 (Bangley shot) and 2 (Melrose shot) are abnormally high and it is thought that these high values are due to the presence of these quarries on igneous rocks where the initial high velocity caused by the igneous

bodies result in high σ values. This is one of the main disadvantages of using quarry blasts in seismic surveys.

Along line 3, using Aberdour quarry, a normal σ value (0.21) was obtained for direct arrivals (Table 5.16). The effect outlined above was not observed because the first station is 3.5 km from the quarry away from the igneous body. It seems that the effect of the near quarry igneous rocks cannot be taken as a general rule since Ratho, Glenluce and Tormitchell quarries also showed normal σ values (close to 0.25).

In Chapter 2 a discussion of the relationship between quarries used and the quality of S-waves detected from these quarries was presented but no conclusions were reached. In this project it was noticed that Ratho, Glenluce, Boysack and Tormitchell quarries provided the best P-wave data quality where sharp onsets with relatively higher amplitudes compared to those of the accompanying noise were observed. It seems that such quarries also produce good S-wave energy despite the argument presented above. Tables 5.16-5.18 show the S-wave interpretations obtained from data recorded from these quarries where better results were obtained.

S-waves arrivals from sedimentary (s1) and basement (s2) refractors were obtained along lines 2 (Table 5.15), 3 (Table 5.16) and 4 (Table 5.17, Glenluce shot). In the first two cases the s1 headwaves showed higher σ values than those of s2 detected on the same line, while in the third case the situation is balanced. Along line 4 (Tormitchell shot) only s1 arrivals were detected while along line 6 only s2 arrivals were detected and, therefore, no comparison between the s1 and s2 σ values can be made. Finally, along most of the lines the s2 refractors yielded high σ values which is an indication of more basic crystalline basement.

S-wave velocities are usually constrained by comparing them with the $\sqrt{3}$ value of their equivalent P-wave velocities. Using this procedure for S-headwaves it was found that these velocities are within an average of +/- 500 m/s of that

predicted by equivalent P-wave velocities, which gives some indication of the accuracy of these results where such discrepancies are considered within the acceptable limits.

For comparison Poisson's ratio distribution in northern Britain along the LISPB profile as envisaged by Assumpcao & Bamford (1978) is presented in Figure 5.36. They suggested that in northern Britain σ values are close to 0.25, except in the upper crust south of the SUF (0.231). SUN results (Figures 5.31-5.35) indicate otherwise where generally higher values along most of the lines were obtained. Furthermore, Assumpcao & Bamford indicated that high σ values are obtained near the shotpoints, decreasing with distance. They explained such near surface high σ values as due to the presence of sedimentary basins, suggesting it is a rule rather than exception, and they concluded that average σ for the sedimentary layers lies roughly in the range 0.25-0.34. SUN results show higher σ values for crystalline basement than the sedimentary rocks.

It must be mentioned here that the SUN provided more detailed results with better resolution for the topmost parts of the crust (Carboniferous, Devonian and Lower Palaeozoic sedimentary rock and upper crystalline basement) than LISPB, in which all of these different lithological units were considered as an average thick sedimentary pile.

5.6. Plus-minus Method Interpretation

As outlined in Chapter 3 the plus-minus method essentially requires reversed coverage of the refractor(s) being interpreted. The acquired data provide such coverage only along three lines (lines 1, 2 and 4) which will be discussed in detail in this section. All plus-times, minus-times and computed depths are listed in Appendix 5.

5.6.1. Line 1: Melrose-Bangley

The direct application of this method along this line has to be restricted to the northern part of the Southern Uplands where reversed coverage of the crystalline basement refractor is available (24-31 km from Melrose). Further south the presence of a lower velocity segment (a_0) in mid-line does not permit the extrapolation of the basement refractor towards the north, across the SUF, extrapolation is only possible if this basement is assumed to extend into the Midland Valley.

Figure 5.37 shows the depth model obtained along this line. Equation 3.23 was used to calculate the depths where V1 used was 4.5 km/s south of the SUF and 4.05 km/s north of it representing the a_0 arrivals from the relevant quarries. V2 was determined from the minus times to be 5.93 +/- 0.10 km/s. Figure 5.7 shows that the reversal of this line, recording from Bangley, is 6 km short from covering the southern shot at Melrose, therefore, no proper reciprocal time could be obtained to determine the plus times. The reciprocal time at both ends of a profile should be equal. Thus the time at Bangley quarry where full coverage is available was taken to be equal to this value.

Figure 5.37 shows that, at this location, the SUF seems to have little effect on the basement, although basement is slightly deeper north of the fault. The crystalline basement within the Southern Uplands is at an approximate depth of 1.5 km in contrast to north of the SUF, where it occurs at a depth of a 1.5-2.0 km. This deepening of the basement north of the SUF is supported by the planar layer interpretation for this line discussed in section 5.4.1.

The SUSP profile (Fig. 1.10), intersects the profile just south of the SUF. Along the SUSP a 6.0 km/s refractor was interpreted at a depth of 1 km. Along line 1 the same refractor velocity was obtained at a depth of 1.5 km.

5.6.2. Line 2: Melrose-Ratho

Figure 5.11 shows that two segments, to the immediate north and south of

the SUF, are reversed from both end shots which made this line suitable for the application of the plus-minus method. Plotting the minus times versus distance yielded a true refractor velocity of 6.04 +/- 0.01 km/s (notice the similarity between this velocity and that obtained by the planar layer method for the same refractor which was 6.08 km/s).

Since the two velocity segments mentioned above are bisected by the SUF, it was expected that their minus plot may yield two different velocity gradients corresponding to different basements, but the plot was linear with no indication of velocity change.

The profile is not completely reversed by the Melrose shot and therefore the reciprocal time cannot be determined from this shot. Therefore, the reciprocal time recording from Ratho was used to calculate the plus times using equation 3.22. Equation 3.23 was used to calculate the depths under the respective receivers. The top layer velocity used in the depth calculations was 5.35 km/s.

Extrapolation of the 6.04 km/s refractor to the SSE was undertaken to obtain the plus times outside the reversed section of the profile and hence depth estimates. The final model is presented in Figure 5.38. The main observations which can be made about this model are:

[1] most importantly, the similar velocity obtained on both sides of the SUF.

[2] the effect of the SUF on the basement refractor downthrowing it to the north with a substantial throw which is larger in magnitude (approx. 1.4 km) than that obtained by the planar layer method (0.88 km).

[3] the Hartfell Line downthrows to the south with a throw of about 1 km which is larger than that obtained by the planar layer method (0.26 km).

[4] no obvious throw of the Kingledores Fault can be detected from the plus-minus model.

[5] the deepening of the basement refractor towards the south is consistent with

most of the previous models for the Southern Uplands. For example, Beamish & Smythe (1986) predicted basement of similar velocity to a depth of perhaps 10 km in the Solway Firth area. However, data obtained along this line does not suggest, like other workers had envisaged, that this deepening is due to a general dip of basement, but rather it is due to a step-like deepening across a number of E-W striking major faults which have been regarded as "tract bounding faults" of the overlying accretionary prism.

5.6.3. Line 4: Glenluce-Tormitchell

In section 5.4.4 it was argued that the data along this line are not adequate for extensive planar layer interpretation and hence the main interpretation of this line was delayed to this section and to further analysis by raytracing. Figure 5.19 shows that only the central part of the profile is reversed from both end shots (14-28 km from Glenluce quarry). The minus times were calculated and plotted against offset to compute the refractor velocity which was found to be 5.81 +/- 0.06 km/s. Using this velocity and averaging the direct velocity segments from both end shots to obtain an average V1 velocity of 5.36 km/s, the plus times for the refractor were calculated and their equivalent depths plotted versus distance. Figure 5.39 shows the final model derived by the application of the plus-minus method.

Extrapolation of the refractor towards the south was carried out to obtain estimates of the plus times for stations outside the reversed section which were converted to the equivalent depths. However, north of the reversed section towards Tormitchell, difficulties arise since the profile crosses the Southern Uplands Fault. It would be erroneous to assume that the main refractor continues without any disruption both in depth and velocity beneath this fault, since it is regarded as a major geological boundary in the region.

The available constraints on the velocity structure north of the SUF in the

area between the fault and Tormitchell quarry are derived from data obtained in this work, which constrain the topmost section of the sedimentary cover and data obtained from Al-Mansouri (1986) who raytraced his M1 profile west of line 4. Al-Mansouri's data constrain the lower parts of the sedimentary cover as well as additional information on basement velocity distribution. From Figure 5.19 it can be seen that there is a dominant refractor of a velocity of 6.02 km/s starting at a distance of 28 km from Glenluce, where the profile crosses the Glen App Fault, and extends to north of Tormitchell. This refractor is interpreted as Midland Valley basement.

Accordingly, extrapolation was made using this velocity (6.02 km/s) towards the north to obtain the plus times and depths below this part of the line. To use the most realistic velocity (V1) of the sedimentary cover north of the SUF (Lower Palaeozoic rocks exposed south of Tormitchell quarry) a mean velocity was calculated by integrating the velocity obtained from direct arrivals from Tormitchell (5.26 km/s) and Al-Mansouri's value of 5.77 km/s at a depth of 2.5 km overlying the Midland Valley basement. Assuming that these two velocities represent the minimum and maximum velocity values of the sedimentary layer overlying the basement an average velocity of 5.51 km/s was obtained and used in calculating the depths.

Figure 5.39 shows the undulatory behaviour of this refractor where it is located at an average depth of 2 km. Notice the effect of the Kingledores/Fardingmullach fault zone and the Kerse Loch Fault at 3-6 and 44 km from Glenluce quarry respectively, while no noticeable change in the refractor depth was observed at the Leadhills Line, 14 km from Glenluce quarry.

From the discussions presented in sections 5.4.4 and 5.4.5 three major conclusions can be outlined:

[1] the likelihood that the SW of the Southern Uplands is within a different tectonic regime than the NE given the presence of the 5.8 km/s layer. Similar

lithological units may exist in both areas, but the thicknesses and depths to these units cannot be correlated as far as the available data permit.

[2] the Midland Valley basement, in the NE, seems to continue across the SUF as far south as the Central Belt, while in the SW along line 4 it is uncertain how far south this basement continues. The available results suggest that it either terminates at the SUF, or it deepens below a sedimentary refractor detected along this line and the acquired data could not detect its presence.

[3] it was established from previous geophysical work in the area and from data recorded along lines 4 and 5, using Glenluce quarry, that velocities have considerable azimuthal variations within the Southern Uplands. This has implications for the correlation of depths and velocities and geological models envisaged by different projects.

5.7. Interpretation Using the Raytracing Method

Two of the recorded profiles were raytraced in this project. They were chosen because it is thought, from the planar layer and plus-minus interpretations, that there are two different seismic (and thus geological) settings existing within the Southern Uplands. In the NE of the region, which is covered by three of the SUN profiles, a shallow stepped basement is envisaged which is thought to be an extension of the Midland Valley basement extending south to at least the end of lines 2 and 3, north of the Central/Southern Belts boundary. Line 2 data were raytraced to establish the geological model in this area because, in addition to the 66% reversed coverage of good data quality, it provided relatively long range coverage (64 km), traversing most of the lithological units and major faults being investigated.

Line 4 was the only reversed profile recorded in the SW of the Southern Uplands where preliminary interpretations indicated that different lithological relationships may exist. It was argued above that, in the SW of the Southern Uplands,

a sedimentary refractor with a P-wave velocity of 5.8 km/s may underlie the Lower Palaeozoic sediments exposed at the surface, occurring at a depth of approximately 2 km. No crystalline basement arrivals were detected along this line south of the SUF, which supports the suggestion that either the Midland Valley basement terminates at the SUF (which does not agree with the model for the NE of the region), or Midland Valley basement deepens south of the SUF beyond the resolution of the data. Raytracing of this profile was undertaken in the pursuit of providing a model based on the above assumptions.

Both profiles provided information on the southern parts of the Midland Valley.

Raytracing of the SUN data was based upon the initial models derived from the velocities obtained from the WHB inversion and the regression of the various velocity segments aided by the interface geometry and velocities obtained by the plus-minus interpretation.

Codes of the raytraced arrivals and the discrepancies between the calculated and observed times are listed in Appendix 6. A discrepancy of +/- 0.03s was considered to be an acceptable agreement between computed and observed travel times.

5.7.1. Line 2: Melrose-Ratho

This profile provided a great deal of information within the NE part of the Southern Uplands and adjacent area of the Midland Valley. Its importance arises from the fact that it samples most of the lithologies and faults which were the primary objectives of this project. Data obtained from Ratho quarry displayed high quality first arrivals to a reasonably large offset (64 km). It is also the only available seismic profile along which continuous basement arrivals are detected across the SUF with reversed coverage, providing a rare opportunity to establish whether this seismic basement is a single lithological unit or an amalgamation of two

different tectonic entities sutured along the SUF. The profile also allows the study of the SUF and measurement of its throw.

An initial model for raytracing of line 2 was obtained by the integration of the following data:

[1] From Ratho quarry and extending south along the profile, the Midland Valley layer 1 (Carboniferous and Upper ORS) is exposed at the surface where it terminates at the SUF. This and the underlying layer (Lower ORS and Lower Palaeozoic) have been extensively studied by previous projects and their seismic velocities are well constrained. SUN lines 1 and 2 provided extra velocity measurements for layer 1 which were within the established velocity range (see Chapter 1) of 3.0-5.0 km/s. Line 3 provided extra control on layer 2. Arrivals from this layer were detected along this profile with good quality and a velocity range of 5.2-5.4 km/s was assigned.

[2] Data obtained from the southern shot at Melrose covers an ORS basin within the Southern Uplands. No previous seismic work was carried out in this part of the region and velocity modelling had to rely solely on data obtained along lines 1 and 2 which cross the ORS rocks near their meeting point at Melrose. These data suggest a velocity of approximately 4.5 km/s representing the Upper and Lower ORS rocks exposed in the area i.e. a mixture of the Midland Valley layers 1 and 2.

[3] The Lower Palaeozoic rocks are exposed south of the SUF and their velocity was constrained by data obtained along this line (recording from Melrose) and from line 4. A velocity range of 5.4-5.6 km/s was used for this layer.

[4] Good and consistent basement arrivals were obtained from both shots along this line and reversed coverage of this unit was detected to the north and south of the SUF. Although, in this project, basement arrivals are considered as being derived from the same lithological unit on both sides of the SUF, the available velocity and depth information can be divided into two groups; 1) "Midland

Valley basement" where data to constrain it were obtained from previous work and SUN lines 2 and 3 (arrivals were detected only from Aberdour shot along the latter profile); 2) "Southern Uplands basement" is covered by data acquired along SUN lines 1, 2 and 3. It was argued in previous sections that no distinction between these basements was established from data obtained by the SUN project. Modelling of this basement was carried out to test this hypothesis and a velocity range of 6.0-6.2 km/s was initially assigned for all crystalline basement.

[5] The application of the plus-minus method (see section 5.6.2) to data acquired along this line provided good estimate of the velocity of the basement (6.04 km/s) and indicated the possible depth at which this basement top should occur (2-4 km). Also, it supported the model of a single basement underlying the Southern Uplands and Midland Valley. It is important to note that Dentith (1987) and Kamaliddin (1988) assigned exactly the same velocity to the Midland Valley basement.

[6] There is no previous information available about the amount and direction of throws of the faults traversed by line 2. They were constrained by the SUN planar layer and plus-minus interpretations.

Figure 5.40 shows the final P-wave velocity model along this line while Figure 5.41 shows the rays used to calculate the velocity model. From these figures it can be noted that, as the profile traverses different sedimentary rocks north and south of the SUF it was expected that raytracing would reflect such lateral differences. The raytraced velocities in the Midland Valley are in complete agreement with those already established by previous work, where a velocity range of 3.50-3.75 km/s was determined representing the Carboniferous and Upper ORS rocks (Midland Valley layer 1). This range represents the lower limit of the velocity range expected for this layer but reflects, correctly, the effect of the thick Carboniferous basin in the Lothian area (south of Edinburgh).

A velocity range of 5.30-5.50 km/s was raytraced for the Lower ORS rocks (Midland Valley layer 2) which underlie the Carboniferous and Upper ORS north of the SUF. This is also in agreement with the available velocity information of this layer. The velocities and thicknesses of these two layers are in excellent agreement with those of the MAVIS II south line which traverses the region trending E-W north of line 2.

South of the SUF, at Melrose, Upper and/or Lower ORS rocks are exposed where a velocity range of 4.10-4.40 km/s was modelled. Evidently this range of velocity is too low for the Lower ORS rocks, which might suggest that a greater thickness of Upper ORS is present at this location than was originally thought.

The geological model for line 2 derived by raytracing is presented in Figure 5.42 while the synthetic seismograms and the rays used to calculate them are illustrated in Figures 5.43-5.46 respectively.

The most important result of raytracing line 2 was the successful modelling of the crystalline basement where, as anticipated, a uniform velocity basement was raytraced along the whole line extending from the Midland Valley, across the SUF and beneath the Southern Uplands. This basement has a velocity range of 6.00-6.12 km/s which is the typical velocity range modelled by previous work for the Midland Valley basement (6.00-6.04 km/s). The basement top occurs at a depth of about 3 km. Al-Mansouri (1986) envisaged the same basement velocity in the SW of the region (Figure 5.22), although at a slightly greater depth of 3.5-4.0 km, while Sola (1982) modelled a 6.30 km/s basement occurring at a depth of 3 km whose velocity is consistent with that of the LISPB basement, although LISPB predicted a much deeper refractor existing at approximately 15 km depth.

It is argued that the SUN data provide a good estimate of the basement velocity of 6.00-6.12 km/s. This basement extends from beneath the Midland Valley and under the Southern Uplands, extending at least as far as the Central/Southern Belts boundary. This is in partial agreement with Hall *et al.* (1983) and Al-

Mansouri (1986) who both suggested that this basement extension occurs as far south as the Northern Belt.

An important aspect of the basement model presented here is its faulted nature. The effects of the Pentland, Southern Uplands, Kingledores and Leadhills Faults are evident. No previous seismic model suggested that these faults mapped at the surface affected the underlying crystalline basement. This leads to important tectonic implications to be discussed in the next chapter. The model also illustrates two basements with velocities of 6.0 km/s and 6.4 km/s respectively. The latter basement was first recognised within the Midland Valley by the LOWNET study and its presence subsequently confirmed by the LISPB study. No arrivals corresponding to this refractor were detected along the SUN profiles but Davidson (1986) suggested that this basement extends south of the SUF beneath the Southern Uplands and it should be composed primarily of pyroxene granulites. This basement was added to the model of Figure 5.42 to present an overall idea of the possible upper crustal configuration in the area.

The synthetic seismograms along this line (Figures 5.43 and 5.45) show the modelled P-waves and S-waves. Compare these figures with Figures 4.44 and 4.45 showing the filtered S-wave data and Figures 5.12 and 5.13 showing the unfiltered interpreted seismic sections along this line. The main observation which can be made from this comparison is that in the synthetic data S-wave arrivals show lower amplitudes compared to the equivalent P-wave amplitudes which is consistent with acquired real data (Figure 5.12). These S-wave arrivals are immediately followed by S-wave reflections which show higher amplitudes than both the P- and S-wave refractions. There are similar reflections in the real data but not as consistent as the synthetic seismograms. The synthetic seismograms obtained from modelling the Ratho data (Figure 5.45) show similar behaviour to that discussed above (see Figure 5.13 for the Ratho digital data). In addition, the S-wave arrivals show the same consistency in both cases. The synthetic seismograms

show also some P and S wave reflections from the two shots which are not present in the original data which may be due to higher acoustic impedance contrast being modelled than actually present across the main refractors. However, there are some inconsistent reflections observed on the Ratho real data, probably from the layer 1 / layer 2 and basement interfaces, but the synthetic seismograms show much higher amplitudes for these reflections.

A basic problem which was encountered in constructing the raytraced models was the location of all shotpoints (quarries) on sills or igneous bodies of high velocity. This caused the raytraced models to be consistently fast. This may be due to overestimation of the size and extent of the igneous body where more coverage is needed to have the appropriate velocity control. The higher the velocity contrast between the sill at which the quarry is located and the surrounding sedimentary rocks, the faster is the raytraced model. This is best illustrated in arrival times modelled from the Ratho shot along line 2 where the shotpoint is located on a sill surrounded by thick low velocity Carboniferous basins. An attempt was made to overcome this high initial velocity by reducing the velocity at the source but this required abnormally high velocities for layers 1 and 2 to be correctly modelled although modelling of basement arrivals was achieved with greater accuracy. Because of this the attempt was abandoned.

This problem was highly reduced when line 4 was modelled because although the shotpoints are also located on igneous rocks, the surrounding sedimentary rocks have higher velocities than those along line 2 and therefore a lower velocity contrast exists between the modelled shallow layers, which caused a better scatter of the time discrepancies.

Most of the calculated arrival times were within the acceptable limit of +/- 0.03s of the actual travel times. A few computed scattered arrivals are abnormally fast which may indicate local effects such as the presence of near surface low velocity lithologies, such as thicker drift.

The model along line 2 is generally a "fast" model and this cannot be explained only in terms of real near surface low velocities that are not accounted for in the model. The SEIS83 program has its limitations where it was found that rays approaching high angled faults cannot be modelled unless these faults are "smoothed" by lowering their dip angle or even reducing their throws below the magnitude of the initial model. If these alterations were not made to the model no successful rays were obtained in that vicinity. Sometimes this caused the unnecessary raising/lowering of the refractors which in turn caused faster/slower arrival times to be modelled along entire segments of the model. Line 2 model suffered most of this defect where modelling the highly fractured basement required the presence of many faults with high angles of dip and many adjustments had to be made to reach an acceptable model.

The complex velocity structure present in the region may have contributed also to the amount of scatter by delaying or speeding up seismic waves and, perhaps attenuating some phases more than others. However, the amount of scatter is considered here as of secondary importance in comparison to the overall agreement achieved in modelling arrivals from all of the shots.

5.7.2. Line 4: Glenluce-Tormitchell

An initial model was produced for this line by the application of the plus-minus method (section 5.6.3) and by the integration of results obtained from the planar layer method. The initial raytraced model along this line was constrained as follows:

[1] Rocks of Upper ORS and Carboniferous age are exposed north of Tormitchell quarry where no control is provided by line 4 data. Velocities of 4.00-5.00 km/s were taken from the results obtained during this work for similar rocks in the NE parts of the Midland Valley and which agree with the available literature.

[2] Immediately south of Tormitchell quarry rocks of Ordovician age are exposed

(thought to be forearc sediments), while south of the SUF rocks of the same age are exposed but are considered to be accretionary prism sediments. The latter Ordovician sequence terminates at the Kingledores Fault. Silurian rocks of the same velocity are exposed south of the fault. Information about the velocities of these rocks are available from 3 main sources: Adesanya (1982), Al-Mansouri (1986), and the SUN project. An initial velocity range of 5.25-5.65 km/s was used for raytracing. This velocity range is in agreement with the velocities determined for these rocks from raytracing line 2.

[3] Basement arrivals were detected north of the geographic location of the SUF when recording from Melrose. This basement is considered as the Midland Valley basement for which there is a great deal of information constraining its velocity provided by this and previous work. A velocity range of 6.0-6.1 km/s was applied.

Figure 5.47 shows the velocity model derived by raytracing, while Figure 5.48 shows the rays used to calculate this model.

A velocity range of 5.40-5.65 km/s was calculated for the Lower Palaeozoic rocks south of the SUF, which agrees with the initial velocity model produced for line 4 and confirms that these rocks have lower velocity than that determined by Al-Mansouri and LISPB. It agrees with the values obtained by Adesanya and Davidson. Also, these values agree with those raytraced along line 2 and discussed in the previous section. North of the SUF a slightly lower velocity range was determined (5.30-5.55 km/s) which is still within the velocity limits accepted for these rocks. North of Tormitchell Midland Valley layers 1 and 2 are exposed. They were modelled as one layer, which is reflected in the velocities modelled within the top raytracing layer in that area (Figure 5.47).

Raytracing of line 4 also successfully modelled the downward extension of the Leadhills Line and the Kingledores Fault and their effect on the sedimentary refractor south of the SUF. They both offset the sedimentary refractor which

underlies the area south of the SUF.

Hall *et al.* (1984) in their interpretation of the WINCH profile which runs through the North Channel concluded that there are no observed margins to the Midland Valley equivalent to the bounding faults on land and there are no seismic character contrast on either side of SUF. While Brewer *et al.* (1983) suggested that the upper crust over much of the WINCH profile is seismically transparent and many of the major geological boundaries cannot be imaged.

The model derived along line 4 illustrates clearly the basic difference between seismic refraction and seismic reflection surveys. In the case of refraction projects (e.g. SUN) rays approach complex structures and the different layers laterally where they are less affected by interface structures, while in reflection surveys (e.g. WINCH) the rays travel in nearly vertical paths where more scatter of these rays takes place due to these structures. Therefore, the different models presented above do not necessarily mean that either is wrong due to the contradictions in the final interpretation.

The model of line 4 suggests that the Midland Valley basement is truncated against a sedimentary refractor along the SUF at the same level, i.e. there is no depth difference of these refractors across the fault. Raytracing of line 4 confirmed that such a depth relationship exists between the sedimentary refractor in the south with a P-wave velocity of 5.81 km/s (exactly the same velocity value as obtained for this refractor by the plus-minus method) and the Midland Valley basement in the north with a velocity of 6.0 km/s. Both refractors are at a depth of 2 km in the vicinity of the SUF. However, the possibility that the Midland Valley basement extends southward below the intra-sedimentary refractor was discussed earlier. Raytracing line 4 did not clear this point where a 6.4 km/s basement was assumed to underlie both refractors north and south the SUF (Figure 5.49). No attempt was made to test whether the 6.0 km/s basement underlies the intrasedimentary refractor detected along line 4 due to lack of data and seismic

information from previous work.

The SUN data also confirm that there is not much velocity difference between rocks of the Lower Palaeozoic age and those of the Lower ORS where the determined velocities all lie within the same range of 5.20-5.60 km/s. In the NE of the Southern Uplands the SUF juxtaposes the two units across its plane where arrivals across the fault show clearly its effect (lines 1, 2 and 3) and a distinctive time step is observed. Although no such step is seen in the SW of the region the effect of the fault can still be inferred from the fact that different lithologies are juxtaposed by it, as modelled along line 4.

Davidson *et al.* (1984) interpreted a quartz-feldspar rich crystalline basement of igneous or metamorphic origin that passes beneath the surface expression of the SUF at approximately 2.5 km depth. The depth at which this basement exists completely agrees with the SUN results in the NE of the region, while the SUN results do not predict the extension of the Midland Valley basement beyond the SUF in the SW. Davidson *et al.* also suggested that the Kerse Loch Fault does not displace the basement refractor, while the SUN interpretation clearly suggests otherwise.

The geological model obtained along this line is presented in Figure 5.49 while the synthetic seismograms and the rays used to calculate them are illustrated in Figures 5.50-5.53 respectively.

It was mentioned in the previous section that the disadvantage of the quarries being located on igneous rocks was highly reduced along this profile because of the higher velocities of the surrounding rocks. Better scatter of positive and negative discrepancies were obtained, although the same problems of raytracing around fault edges and smoothing of high angle faults where encountered.

Comparing the synthetic seismograms of Figures 5.50 and 5.52 with the interpreted digital sections presented for line 4 (Figures 5.20 and 5.21) and those of the filtered S-wave data in Figures 4.42a and 4.43 shows that in the Glenluce

digital data S-wave amplitudes are larger than their equivalent P-wave amplitudes while in the synthetic model the relationship is not clear since S-wave reflections close behind the S-refractions obscure the data and make it difficult to determine their amplitudes. The situation is clearer from the other end of the line where data obtained from Tormitchell show lower S-wave amplitudes than P-waves while in the synthetic seismograms the case is reversed where consistent S-waves with high amplitudes (compared to their equivalent P-waves) are seen to the end of synthetic record (Figure 5.52).

Very weak reflections were obtained by raytracing this line but this is understandable where the real data show few or no reflections. This may be due to the small velocity contrast along the main reflectors resulting in low acoustic impedance contrast where no significant reflections could be expected in such circumstances.

CHAPTER SIX

TECTONIC IMPLICATIONS, DISCUSSION AND CONCLUSIONS

6.1. Introduction

The aim of a seismic project such as SUN is to investigate upper crustal regional structure and, where possible, the deeper parts of the earth's crust. Then, to correlate the seismic model with the geology and tectonics of the area under consideration so as to predict the most probable geological model.

In this work, a large dataset was obtained covering what is conventionally termed the Southern Uplands accretionary prism, which is still a matter of debate among geologists and geophysicists. Is it a product of simple obduction of an oceanic plate over a continental margin, or is it composed of a number of terranes, which may, or may not, be accretionary prism in origin? The so-called tract bounding faults themselves came under increasing scrutiny because the assumption that they represent major lithological dislocations had not been confirmed previously. The depth to which they extend and the lithostratigraphic units they offset were also unknown. The nature of the crystalline basement underlying the region is still a matter of controversy. Some authors suggest it is an extension of the Midland Valley basement, while others suggest it is a different basement but *seismically indistinguishable* from that of the Midland Valley. The form of this basement is also not clear, whether it is a dipping basement or stepped. The

amount and direction of the throw of the SUF is another dilemma for many geologists who tried to resolve its secrets.

In this chapter, a conclusion of the main ideas and models presented in this work will be presented. Any suggestions and ideas which the author thinks need further consideration and development will be mentioned.

It is hoped that this contribution can present some of the answers to the above questions, while it will certainly pave the way for future seismic projects to increase our knowledge about the Southern Uplands of Scotland.

6.2. Quarry Blasts as Sources for Seismic Surveys

Data acquisition during this project was completely dependent on quarry blasts as a cheap and available source of energy. They proved to be very adequate for this type of project, carried out by one person and for a fairly short time of fieldwork (6-12 months for field data acquisition). The main factors which determined the quality of data obtained are:

[1] Orientation of the quarry face being blasted.

[2] Wind speed.

[3] Size of charge used.

[4] The presence of permanent noise sources near the recording sites.

The main factors which determine the speed of data acquisition are:

[1] Number of people available for fieldwork.

[2] Interval between quarry blasts.

[3] Weather.

[4] Good planning and field procedures.

[5] Establishing "good communications" with the quarry managers.

[6] Accessibility of the recording sites.

6.3. Data Processing - Main Conclusions

In Chapter 4 data processing was discussed. Frequency analysis of the data suggested that the dominant P-wave frequencies, in the study area from quarry blasts, lie in the range of 5-20 Hz, while S-wave frequencies have a range of 4-10 Hz. Unfortunately the noise often contains significant energy at the same frequencies as those of the primary and secondary arrivals. This makes locating onsets of both waves difficult and sometimes impossible. Use of frequency filters, however, did aid the extraction of the lower frequency S-wave arrivals. In this work it was found that the most effective filters for obtaining P-wave arrivals are bandpass (5-20 Hz) and lowpass (low cut 20 Hz) filters. Detection of S-wave onsets was achieved by the successful use of a combination of minimum phase lowpass filters set at 10 and 6 Hz.

6.4. Velocity Distribution - Analysis and Implications

6.4.1. Velocity Distribution in the Southern Uplands Sediments

There are 2 main lithological units exposed in the Southern Uplands. A minor exposure of Lower and Upper ORS occurs in the Melrose area. Lower Palaeozoic rocks (Ordovician and Silurian) are exposed over the rest of the region (see Figure 1.3). Rock & Rundle (1986) have indicated that the Upper ORS age of rocks in the Melrose area is erroneous and they are, in fact, Lower Devonian. The P-wave velocity obtained for these rocks lies in the range of 4.3-4.5 km/s (Figure 5.40) with a thickness of 1.20 km. This range of velocity is too low for the Lower ORS rocks suggesting that these rocks are indeed Upper ORS.

The main rocks exposed in the Southern Uplands are of Palaeozoic age and a P-wave velocity range of 5.25-5.60 km/s was deduced for them by raytracing (Figure 5.41) having a thickness of 1.0-3.2 km being thicker in the NE than the SW. A wide range of velocities has been produced by previous seismic work for these rocks ranging from those obtained by Adesanya (1982), suggesting a P-wave

velocity of 5.2 km/s, to Al-Mansouri (1986) who envisaged a velocity of 5.70 km/s for these rocks (see section 1.10.1).

Figure 5.24 shows the LISPB interpretation across Scotland where a velocity of 5.0 km/s was assigned for the sedimentary cover in the eastern parts of the Southern Uplands which does not agree with the velocities derived by Al-Mansouri (1986), Sola (1982) and SUSP. The LISPB velocity does not even agree with the velocity obtained by raytracing of SUN line 2 (Figure 5.40).

Davidson (1986) recorded a NW-SE trending profile across both the Midland Valley and the Southern Uplands (line KAD of Figure 2.1) where it terminates west of line 2 and intersects line 3 at Broughton. At the latter location Davidson modelled a velocity range of 4.0-5.35 km/s for the Lower Palaeozoic cover underlain by a gneissose crystalline basement with a velocity of 6.0 km/s. Davidson's velocities are the nearest to those raytraced in this project, although the lower velocity limit of 4.0 km/s is much lower than expected for these rocks.

From the above the velocity range obtained by the SUN project for the Lower Palaeozoic rocks of the Southern Uplands can be regarded as a reasonable average of the P-wave velocities determined from most of the previous projects carried out in the region.

6.4.2. Southern Uplands Basement: Velocities and Structure

Crystalline basement arrivals were observed along all the across-strike profiles recorded. However, these arrivals were detected in the NE of the region along lines 1, 2 and 3 while crystalline basement arrivals were detected only north of the SUF along line 4. A velocity range of 6.0-6.1 km/s was obtained for the basement in the NE of the Southern Uplands (Figure 5.40) indicating that this basement has the same velocity as that of the Midland Valley. The data also suggest that the Midland Valley basement is likely to continue south across the SUF where it is offset by the fault along the 3 lines recorded in the NE. However, this

basement occurs at a depth of 2.8-3.2 km in the NE of the region.

In the SW of the Southern Uplands no crystalline basement velocity was detected (>6.0 km/s). Instead, a refractor with a P-wave velocity of 5.8 km/s was successfully modelled (Figure 5.47) which extends north from the southern shot-point along line 4 at Glenluce and terminates at the geographic location of the SUF, north of which arrivals from a normal crystalline basement were detected. The 5.8 km/s refractor is interpreted as an intra-sedimentary refractor and is overlain by the known Lower Palaeozoic sedimentary cover with a velocity range of 5.4-5.6 km/s (Figure 5.47).

The LISPB profile trends sub-parallel to lines 1 and 3 and oblique to line 2 (Fig. 2.1). Bamford *et al.* (1976, 1977, 1978) interpreted a 3-layer model for the Southern Uplands (Fig. 1.7). Their layer 2 was interpreted as Lower Palaeozoic sedimentary cover of a velocity of 5.8-6.0 km/s to a depth of 10-15 km below the Southern Uplands.

Raytracing line 2 (Figure 5.42) proved that crystalline basement exists at a much shallower depth (2.8-3.2 km) than envisaged from LISPB. This is supported by the other SUN profiles recorded in the NE of the Southern Uplands (Figures 5.10 and 5.17). Therefore, it is clear that a revision of the LISPB model should be made since it disagrees with all other models, including that of SUN.

The LISPB Lower Palaeozoic layer of 5.8-6.0 km/s, including the top superficial layer of Figure 1.7, could be subdivided into 2 units: an upper sedimentary unit (Lower Palaeozoic) of an approximate P-wave velocity of 5.4 km/s and a deeper basement refractor of 6.0-6.1 km/s. However, this does not solve the problem of the 6.3 km/s basement refractor which the LISPB results show at a depth of 12-15 km, whereas the SUSP data (Warner 1982) place it at 2-4 km, Sola (1982) at 5.0 km, Al-Mansouri (1986) at 7.5 km and Davidson (1986) at 5-7 km. Unfortunately, the SUN data do not provide much information about this refractor, although along line 2 such a velocity was encountered when the profile was

recorded from Melrose (the last velocity segment of Figure 5.11), but this high velocity was attributed to dip effect.

However, if the above model is correct, then the SUSP 6.3 km/s basement and the LISPB pre-Caledonian <6.3 km/s layer should exist below the 6.1 km/s basement interpreted in the NE of the region. Therefore, there are two basements which underlie the Southern Uplands: a shallow one which is very similar to that which underlies the Midland Valley occurring at a depth of 2.80-3.20 km and could be the same basement and a deeper basement with a velocity of 6.3 km/s. It could be that the latter, is different to that of the Midland Valley 6.4 km/s basement, although a difference of 0.1 km/s does not necessarily mean that these two basements should be of different nature, especially when anisotropic effects in the sedimentary cover are taken into account.

Davidson (1986) modelled a basement of P-wave velocity 6.05 km/s beneath the Midland Valley, decreasing to 6.0 km/s and occurring at a depth of 2.2 km beneath the Southern Uplands. His velocities agree with those modelled by this project but the depth at which this basement occurs is slightly shallower than that seen in the SUN models. Also the SUN interpretation does not envisage any change in basement velocity across the SUF. Finally, Davidson does not observe the 6.3 km/s basement modelled by the SUSP.

Data obtained by previous workers (El-Isa 1977, Adesanya 1982 and Hall *et al.* 1983) and supported by data acquired along the SUN line 5 indicate that, in general within the Southern Uplands, velocities parallel to strike are higher than those perpendicular to it. Addressing this issue, Hall *et al.* (1983) suggested the presence of large scale anisotropy in the structure of the Southern Uplands, with slices of high grade metamorphic or igneous rocks caught up between accretionary wedge sediments in a stack striking parallel to SUSP (SW-NE). Thus SUSP sampled a high velocity wave guide, whilst the LISPB model shows the average effect of the low and high velocity stacked layers. They concluded that this is the reason

why the SUSP velocities are significantly higher than those of the LISPB.

Therefore, attempting any lithological correlation between LISPB and SUSP, or generally between any profiles that are perpendicular to each other within the Southern Uplands, can be misleading and will involve many assumptions unless the amount of anisotropy within the whole region is well established and key horizons are well correlated (e.g the basement).

The SUN profiles in the NE of the Southern Uplands model show a similar basement block pattern to that of Hall *et al.*, but the major difference between the two models is that SUN suggests that the boundaries to such blocks are marked by the major faults which are seen at outcrop trending E-W across the region. Although Hall *et al.* zones are presumably delineated by faults, the locations of these faults are not seen at surface. The SUN interpretation also indicates that only high velocity segments are observed on either side of the faults along 2 of the profiles recorded in the NE (lines 2 and 3; see Figures 5.11 and 5.14 showing the time-distance data for these lines respectively), whereas along line 1 (Figure 5.7) the Kingledores Fault and the Leadhills Line separate a low and high velocity segment*.

No velocities like those modelled by Hall *et al.* along the low velocity zones (5.6 km/s) were interpreted along the SUN profiles in the NE of the Southern Uplands. Furthermore, the LISPB model upon which Hall *et al.* based their interpretation is questioned and refined (see above). Therefore, according to this new interpretation, the Hall *et al.* interpretation should be reconsidered.

A different refractor was modelled in the SW of the Southern Uplands. This refractor has a velocity of 5.8 km/s and is interpreted to be different from the crystalline basement modelled in the NE of the region. Therefore, there are two possibilities which can be envisaged for the Southern Uplands crystalline basement:

*Along line 1 a low velocity segment was interpreted in the middle of the profile south of the Kingledores Fault.

[1] The same basement exists across the entire Southern Uplands, but it either dips towards the SW or it is stepped downward in this direction. Thus it occurs at depths beyond the resolution of line 4 and it underlies the observed 5.8 km/s refractor.

[2] There are two discrete types of basement underlying the Southern Uplands, one in the NE with an average velocity >6.0 km/s, and a second one in the SW with a velocity of 5.8 km/s (probably of Ordovician age). In this case a different tectonic regime must be invoked to explain its presence, such as the missing forearc suggested by some authors. A deeper crystalline basement must underlie this refractor which is perhaps the 6.4 km/s crystalline basement.

Apart from the fact that the Southern Uplands crystalline basement is shallow (2-4 km deep) and it has similar velocity to that of the Midland Valley, it has two other important features. The first is that it is offset by a number of faults and the second is the presence of a high velocity zone in the centre of the Southern Uplands.

The basement assumes a step-like pattern beneath the Southern Uplands. This behaviour is caused by a number of E-W trending faults and the deepening is usually towards the south apparently starting under the Central Belt. This is in agreement with Al-Mansouri (1986) who suggested that this basement extends from the Midland Valley across the SUF and occurs at large depths beneath the Central and Southern Belts, giving way to thicker overlying Lower Palaeozoic sediments. Also it is consistent with the suggestion of Beamish & Smythe (1986) that a shallow basement (1-2 km deep) with a velocity of 6.1 km/s exists near the SUF and deepens to about 10 km below the Solway Firth. Both models envisage the deepening towards the south as due only to basement dip, while the SUN interpretation suggests that faulting is a key factor.

Along line 3 a high velocity zone (Vp=6.25 km/s) was detected. This zone was originally detected by El-Isa (1977) and also by Warner *et al.* (1982). Two

explanations were offered for the presence of this zone in Chapter 5: the first is that the body is a highly basic igneous intrusion and the second is that it is the remnant of an oceanic crust entrapped after the closure of the Iapetus Ocean. The presence of such a zone certainly deserves more study.

6.4.3. Velocity Distribution in the Midland Valley

It has been long established that the upper crustal cover of the Midland Valley is composed of 3 main lithological units defined by 2 refractors. Layer 1 (Carboniferous and Upper Devonian) with a velocity range of 3.0-5.0 km/s, layer 2 (Lower Devonian and ? Lower Palaeozoic) with a velocity range of 5.2-5.8 km/s and layer 3 (crystalline basement) with a velocity range of 6.0-6.1 km/s. The SUN data acquired in the Midland Valley confirmed these ranges.

6.4.4. The Midland Valley Basement: Velocities and Structure

SUN raises an important point about the structural configuration of the Midland Valley basement. The data acquired strongly suggest that this basement is not as flat as envisaged by some authors (Davidson 1986, Dentith 1987), who predicted a flat basement with little or no relief occurring at a depth of 4-5 km. The SUN data seem to oppose this model by revealing that this basement is offset by downward extending faults in at least two areas: near the northern margin of the region below the Strathmore Syncline, and in the south near to the SUF where basement is broken by at least three faults, namely the Kerse Loch Fault in the SW and the Pentland and Henshaw Faults in the SE.

Davidson (1986) suggested that this basement continues undeviated under the Southern Uplands and Kerse Loch Faults. This is proven to be wrong since the effects of these faults are clearly seen along SUN lines 1, 2 and 3 (SUF) and line 4 (Kerse Loch Fault). Dentith (1987) indicated that, within the Midland Valley, faults mapped at surface sole out at detachments in layer 2 or at the layer 2/layer 3 interface. SUN suggests otherwise, since in that same region major faults (such

as the Pentland and Henshaw interpreted along lines 2 and 3) clearly offset the Midland Valley basement, while in the SW of the region (along line 4) the Kerse Loch fault has the same effect.

The SUN data also suggest that there is another set of faults which offset the basement along the northern margin of the region. There two faults offset this basement along SUN line 6 and are named in this project as the Auchterhouse Hill and Northballo Faults.

A depth of approximately 2.8 km was calculated along line 2 for the underlying basement in the SE Midland Valley (Figure 5.42) and this depth is in agreement with depths obtained by Sola (1985) and Davidson (1986). The MAVIS profiles (Dentith 1987) suggest a basement depth of 4 km in the Firth of Forth area along the MAVIS I south line and a depth of 2.4 km along the MAVIS II profile which is perpendicular to the previous profile trending N-S along the centre of the Midland Valley. Along the MAVIS III profile which nearly coincides with the SUN line 3, a basement depth of 4.5 km was predicted and no faults to offset it were interpreted.

It is clear that the above depths cannot be generalised over the whole area since faults interpreted in this work (such as the Henshaw and Pentland Faults) offset the basement and can cause large changes in basement depths over short distances.

An indication of the undulatory behaviour of the Midland Valley basement comes from data recorded along lines 1 and 2 when both lines were recorded from Melrose quarry. Along line 1 (Figure 5.7) basement arrivals north of the SUF show a low P-wave velocity (5.7 km/s) which was interpreted as due to downdip effect on the basement refractor, but when recording line 2 from the same quarry (Figure 5.11), arrivals showed a high basement velocity (6.29 km/s) which was interpreted as indicative of an updip velocity, especially when the reversal of the specific velocity segment showed lower velocity.

Finally, in the SW corner of the Midland Valley a faulted basement with a depth of about 2-3 km is envisaged. Al-Mansouri (1986) modelled the same depth for the Midland Valley basement in that area, but he argued that this basement has a steep downward dip south of the SUF to a depth of 4 km while the SUN interpretation suggests that either the Midland Valley basement terminates at the SUF, or it dips down but to a much greater depth beyond the resolution of the available data beneath the Southern Uplands.

The above evidence strongly suggests that the Midland Valley basement has been subjected to different tectonic events which caused faults to offset it along its margins while the central parts remained relatively un-disturbed. Other evidence of these different tectonic comes from the fact that faults which offset the basement along the southern margin of the Midland Valley trend E-W while those which are along the northern margin trend NW-SE. This may indicate that this basement was subjected to differing stresses which acted upon it in various geological periods. In the north of the region Middle Devonian time is the most likely period of main effect, while in the south the Carboniferous period is envisaged.

It is thought that the faults interpreted in the south of the Midland Valley are associated with dextral strike-slip movement along the bounding faults which outline the margins of the Midland Valley, while those in the north require sinistral strike-slip movement for which we see no evidence. Haughton (pers. comm.) suggests that the whole of the Strathmore Syncline and the Highland Boundary Fault should be considered as a completely different unit to the Midland Valley, where the faults seen to offset the basement in the former area are associated with compressional movement along the Highland Boundary Fault.

A final remark about the emerging tectonic complexity of the Midland Valley basement. Dentith (1987) suggested that many major faults which trend E-W within the region are associated with thin-skinned tectonics where they sole out at or above the crystalline basement. He interpreted the Ochil Fault as a typical

example of such behaviour. Pursuing the Dentith model, Kamaliddin (1988) reached the same conclusion when he recorded a profile across another part of the Ochil Fault (Line KAZ2 of Figure 2.1). If the models deduced from SUN for the Midland Valley basement are correct, then still deeper intra-basement detachments also exist.

The above discussion highlights the complex nature of the Midland Valley basement and suggests that further localised studies should be executed in the region.

6.5. Main Faults

It is clear that several major faults are key to the evolution of the study area. These faults are now assessed in detail.

6.5.1. The Southern Uplands

The SUN results outlined the lateral and downward extension of three major faults within the region namely, from north to south, the Leadhills Line, the Kingledores Fault and Hartfell Line. It also modelled the behaviour of the SUF. The Leadhills and Hartfell Lines were considered as relatively insignificant structural features (termed lines accordingly) until recently when Morris (1987) suggested that the Leadhills Line may be a reverse thrust fault. Anderson & Oliver (1986) presented a comprehensive study of the Kingledores Fault suggesting that it represents a major dislocation in the region while McCurry & Anderson (1989) were the first to suggest that this fault may extend down as to offset the basement at 18 km depth. No detailed studies were presented for the Hartfell Line apart from that it represents the boundary between tracts 5 and 6 of the Central Belt.

Table 6.1 shows the amount of throw of the faults interpreted within the Southern Uplands including the SUF.

Table 6.1 Main faults interpreted in the Southern Uplands. HFL-Hartfell Line; LHL-Leadhills Line; KGF-Kingledores Fault; SUF-Southern Uplands Fault; *-profile does not intersect fault; (?)-throw cannot be determined. Throws determined from planar methods, except RT-throw value obtained by raytracing; amounts of throw are in km.

Line	HFL	LHL	KGF	SUF
1:Melrose-Bangley	?	*	?	0.55
1:Bangley-Melrose	?	*	?	?
2:Melrose-Ratho	?	*	?	0.84
2:Ratho-Melrose	0.26	*	0.16	0.51
2:RT	0.20	*	0.20	0.20
3:Aberdour-Moffat	*	0.54	*	?
3:Ratho-Moffat	1.35	0.39	0.52	?
4:Glenluce-Tormitchell	*	?	?	*
4:Tormitchell-Glenluce	*	1.94	1.16	*
4:RT	*	0.35	0.40	*

Two major faults interpreted in this project trend along the whole regional strike of the Southern Uplands: the Southern Uplands and Kingledores Faults, indicating that they are major dislocations in the region. The former represents the boundary between two terranes, the Midland Valley and Southern Uplands, while the latter at surface represents the lithological boundary between the Ordovician and Silurian of the Southern Uplands. This project provided evidence indicating that both faults extend downwards and offset the crystalline basement below.

SUN results indicate that the downthrow direction of the SUF is towards the north in the NE of the Southern Uplands as modelled along lines 1 and 3 (Figures 5.10 and 5.17). Along line 2, raytracing indicates a reversed situation (Figure 5.42). In the SW of the region although line 4 data show no time step due to the fault, the direction of downthrow can be inferred from the model presented along the profile (Figure 5.49) suggesting a southerly direction in accord with Al-Mansouri (1986) interpretation. The geological model along line 4 (Figure 5.49) shows a crystalline basement with a velocity of 6.4 km/s to underlie the intra-sedimentary refractor. If the Midland Valley basement (Vp=6.0 km/s) is to extend south of the SUF then it should overlie the 6.4 km/s refractor. Resolution by line

4 does not extend deep enough to resolve if deeper basement is 6.0 or 6.4 km/s in velocity. (see section 5.7.2). Kelling (1961) indicated that the SUF may have a downthrow of 1000 m towards the south in the SW of the Southern Uplands. This view was supported by other authors (see section 1.7) who suggested transcurent movement along the fault to explain this change in throw direction. The SUN interpretation for the SUF confirms these models suggesting a varied amount of throw (Table 6.1) along its strike.

It was mentioned in Chapter 1 that the Pentland Fault could represent the north-east en echelon continuation of the SUF proper. SUN results indicate that the Pentland and Southern Uplands Faults have throws of similar magnitudes. Therefore, both are equally likely to be the continuation of the main SUF.

Variation in the amount of throw is deduced for the Kingledores Fault (Table 6.1), being less in the NE than the SW. This is in support of Anderson & Oliver (1986) who suggested that a systematic decrease in the width of the fault zone occurs from SW to NE. The geological models presented for lines 2, 3 and 4 indicate that the direction of the downthrow is towards the north while along line 1 the direction was unobtainable. The fault offsets the basement in the NE of the Southern Uplands while in the SW of the region the fault offsets the 5.8 km/s refractor interpreted along line 4. SUN does not provide further information on its downward extension below this refractor.

The other two major faults interpreted within the Southern Uplands, the Leadhills and Hartfell Lines, do not show the same along-strike continuity when modelled by SUN. The Leadhills Line, although proven by this work to be of greater importance than originally thought since it offsets crystalline basement, occurs only along the western half of the region in agreement with the available geological data (Figure 1.5). It throws down towards the north along the two profiles which intersect it (see Table 6.1).

The Hartfell Line is modelled by SUN only within the eastern part of the Southern Uplands. It throws down towards the north along line 1 while along lines 2 and 3 a southerly downthrow is envisaged. However, raytracing line 2 (Figure 5.42) indicated that downthrow is towards the north. Like the Leadhills Line, the Hartfell Line extends downward offsetting the crystalline basement.

In conclusion, all the faults discussed above should be treated with the same degree of importance since they show similar tectonic behaviour in their relationship with the underlying basement.

6.5.2. The Midland Valley

Two sets of major faults were modelled within the Midland Valley. The first is comprised of four faults (Colinton, Henshaw, Pentland and Kerse Loch Faults) which trend generally E-W along the southern margin of the region and the second set is comprised of two faults (Auchterhouse and Northballo Faults) which trend NW-SE along the northern margin of the region within the Strathmore Syncline. Table 6.2 contains the throws of all the faults interpreted by SUN in the Midland Valley.

North of the SUF, in the Edinburgh area, SUN lines 2 and 3 recognise three main faults intersecting them. The Colinton and Henshaw Faults have not been recognised as confirmed faults on geological maps which show them as dashed lines indicating that they may be lithological contacts rather than faults. SUN models along lines 2 and 3 confirmed that the Colinton Fault is a major fault within the area, although they provided no evidence of its downward extension or whether it offsets crystalline basement. These models showed that the Henshaw Fault (not named on the available geological maps; it acquired its present name in this project) is a major fault offsetting the underlying crystalline basement. The data suggest that both faults downthrow to the north.

Table 6.2 Main faults interpreted in the Midland Valley. AHF-Auchter house Hill Fault; Col-Colinton Fault; HEN-Henshaw Fault; KLF-Kerse Loch Fault; NHF-Northballo Hill Fault; PL-Pentland Fault; (?)-throw cannot be determined. Throws determined from planar layer methods, except RT-value obtained by raytracing; amounts of throws are in km.

Line	AHF	COL	HEN	KLF	NHF	PL
1:Melrose-Bangley	*	*	*	*	*	*
1:Bangley-Melrose	*	*	*	*	*	*
2:Melrose-Ratho	*	*	*	*	*	*
2:Ratho-Melrose	*	?	*	*	*	?
2:RT	*	1.85	*	*	*	0.45
3:Aberdour-Moffat	*	*	0.34	*	*	0.68
3:Ratho-Moffat	*	*	?	*	*	?
4:Glenluce-Tormitchell	*	*	*	1.95	*	*
4:Tormitchell-Glenluce	*	*	*	*	*	*
4:RT	*	*	*	0.30	*	*
6:Boysack-Collace	0.92	*	*	*	0.92	*

A third fault was modelled in the SE of the Midland Valley which is the Pentland Fault. The SUN data suggest it offsets crystalline basement downthrowing it toward the south (line 3), while raytracing line 2 suggests it has the same effect on the layer 1/layer 2 interface while it downthrows basement towards the north (Figure 5.42).

Line 4 intersects the Kerse Loch Fault in the vicinity of Girvan in the SW of the Midland Valley. Contrary to previous seismic interpretations (Davidson 1986 and Al-Mansouri 1986), the SUN model along this profile indicated that it does offset Midland Valley crystalline basement downthrowing it towards the north.

The second set of faults interpreted within the Midland Valley comprised two faults trending NW-SE along the northern margin of the region. The model along line 6 (Figure 5.30) suggests that these two faults downthrow basement towards the SE.

6.6. Is the Southern Uplands an Accretionary Prism?

To establish whether a certain tectonic unit is an accretionary prism or not the following conditions should be fulfilled:

[1] Younging of successive accretionary wedges towards the ocean, coupled with overall younging of the sequence within each wedge towards the continent.

[2] The presence of steeply dipping tract (wedge) bounding faults separating the accreted slices. These should flatten out at depth and merge into a major, gently-dipping decollement.

[3] Thick pile (10-15 km) of accreted sediments.

[4] Deep oceanic crust (basement) should underlie the pile of accreted material with a velocity of approximately 6.3 km/s.

These requirements can be dealt with as follows:

[1] In the Southern Uplands, the regional younging of the lithological units, seen in the region, towards the SE and the younging of sediments within each unit towards the NW could indeed be evidence of an accretionary prism, but it could also be envisaged as an imbricate thrust stack (McKerrow *et al.*, 1977 and Murphy & Hutton, 1986).

[2] SUN models reveal that the supposed tract bounding faults extend down to offset the underlying continental basement (see below). This strongly suggests that they are of significantly younger age.

[3] Apart from the LISPB model, all other interpretations (including SUN) suggest that the Southern Uplands crystalline basement is a shallow one (2-4 km). This precludes a normal thickness of prism sediments (10-15 km) above basement. If the surface sediments are of prism origin, then only a small slice of the original prism occurs in the Southern Uplands. The degree of deformation seen at surface within the Southern Uplands suggests that the slice is not the basal part of the prism where a much higher grade of deformation is expected.

[4] It has been established by the SUN results and previous seismic work (see Chapter 1) that the nature and seismic velocity of the Southern Uplands basement does not agree with that of oceanic crust. In fact, this basement could be an

extension of the Midland Valley continental basement, requiring the accretionary prism to be allochthonous.

6.7. Suggested Models for the Southern Uplands

SUN results suggest that within the Southern Uplands a Midland Valley-type continental crystalline basement underlies the sediments exposed at surface. This basement is stepped by a number of E-W trending faults where they cause a general deepening of the basement towards the south. This basement does not extend toward the SW at the same depth, but it may deepen either due to faulting or dip effect, such that in the SW an intra-sedimentary refractor occurs at nearly the same depth as the basement seen in the NE. This intra-sedimentary refractor should be underlain by the same basement detected in the NE of the region or by higher velocity basement (6.4 km/s), although the first case is favoured here.

The main results and arguments presented in Chapter 5 and in this chapter, strongly indicate that we are not dealing with a straightforward case of an accretionary prism in the Southern Uplands. The author sees three possible models for the region which can be further developed:

[1] What is seen in the Southern Uplands is an accretionary prism "slice" thrust on to continental basement. But the faults which offset this basement and cut the prism must have been induced after the thrusting of the accretionary prism slice. This strongly suggests that we cannot see tract bounding faults of a prism in the Southern Uplands. If these faults are tract boundaries, then later tectonic movements caused them to propagate downwards into basement, which the author believes is unlikely.

An alternative scenario can be invoked to explain the presence of these faults within the thrust slice concept: the wedge shaped accretionary prism with a thicker SW end is thrust over a faulted crystalline basement being deeper in the SW of the region. These already present faults within this basement were later re-

activated and affected the overlying accretionary prism slice. Therefore, where are the *real* tract bounding faults? No seismic evidence for their existence was found.

[2] The Southern Uplands represents an amalgamation of terranes juxtaposed along the major faults modelled by SUN. This will explain most of the questions raised against the accretionary prism hypothesis, but leaves the presence of the intra-sedimentary refractor modelled in the SW open to question as to how it can fit in this tectonic framework.

[3] A thrust stack.

Proposing the above models for the Southern Uplands does not exclude the possible validity of any of the alternative models discussed in section 1.4.

6.8. Suggestions for Further Work

The SUN project has revealed many points of interest to be pursued by new seismic surveys, but it should be noted that any new project of the SUN type is controlled mainly by the availability of quarries, while other seismic profiling across areas of special interest could be carried out using dedicated shots or other sources of energy. There are, of course, other surveying methods which could be carried out either in conjunction with seismic studies or as separate projects, of which gravity, magnetic and electrical methods are the most effective and feasible.

This project has uncovered a number of geological and seismic anomalies in the Southern Uplands and the Midland Valley which certainly deserve further rigorous studies. The author thinks that it is essential that prior to any new seismic project to be executed in the Southern Uplands a detailed velocity model for the region must be produced in order to resolve the variation of velocity obtained when measured in different directions. Particularly to examine if anisotropy is the sole factor for such behaviour. This will ensure better correlation between existing seismic models and new projects and also the production of more reliable geological models for the region.

The nature of the main faults present in the two surveyed regions and their vertical and lateral extension should have a first priority in any future projects since such information will provide a clearer picture of the tectonics and history of the regions. The differences in the seismic and stratigraphic relationships between the NE and SW of the Southern Uplands suggested by this project should also be further investigated. A 3-D model for the high velocity body located in the centre of the Southern Uplands should be produced by the use of the appropriate methods.

Specific projects to investigate some of the above are:

[1] Active quarries present within the Southern Uplands (e.g. Melrose, Moffat, Dalbeattie and Glenluce) can be used to record pairs of profiles at right angles to each other to verify the velocity-azimuth relationship envisaged in the region and to acquire more information about the Lower Palaeozoic velocity structure within the Southern Uplands.

[2] More N-S profiles should be recorded between SUN lines 3 and 4 to investigate the behaviour of the intra-sedimentary refractor in the SW of the region and to trace its likely along-strike extension. Quarries present within the Southern Uplands and the southern parts of the Midland Valley can be used for this purpose.

[3] Ratho quarry is the best source of energy to further investigate the nature of the high velocity zone detected along line 3. Other nearby quarries (Kames and Hillwood) can also be employed for this purpose. A set of lines, perhaps using the fan-shooting method, may prove to be the best approach to accurately delineate the subsurface extension of this zone and its velocity configuration.

[4] Quarries at Dumfries can be used to study the Central/Southern Belt contact and to acquire seismic information in any direction within the central part of the Southern Uplands.

[5] The completion of the reversal of line 3 (from Moffat) may provide important data about the high velocity zone and the main faults traversed by the profile.

[6] Using Tormitchell quarry, 2-3 profiles recorded at different angles to line 4 (towards the SE) may prove to be very useful in the SW of the region since Al-Mansouri (1986) and the author suggest different models for that part of the Southern Uplands.

[7] Dedicated shot(s) can be used to record profiles parallel and perpendicular to the regional strike using the normal incidence and the wide angle reflection methods to study the underlying basement(s) beneath the Southern Uplands. Such data can provide better imaging of the geological and structural features imposed on this basement by the major faults interpreted by the SUN project.

A more thorough investigation could be carried out into the nature of the high velocity body detected along SUN line 3 and the intra-sedimentary refractor detected along line 4, if detailed reflection data are obtained.

[8] Seismic profiling aided by gravity and magnetic modelling will also facilitate the study of the lateral and downward extension of the granitic bodies located in the SW of the Southern Uplands. This will allow an assessment of the probable depth and shape of these causative bodies. Gravity models constrained by P and S-waves velocities will give reasonable estimates of the densities of the underlying rocks which could provide better information about the nature of these rocks and their lithologies.

[9] To avoid the interference caused by the wavetrain of energy caused by quarry blasts use of dedicated shots could produce excellent S-wave data which could provide more detailed information about the lithologies present in the region.

[10] Completion of the reversal of line 6 along the Strathmore Syncline will complete study of the basement configuration in that part of the Midland Valley, especially since 1/3 of the reversal is already acquired by the SUN project.

[11] The Midland Valley basement and the faults proved by SUN to offset it should be further studied. A large number of quarries within the Midland Valley can be used for such projects.

[12] Surveying the Southern Uplands using the electrical methods, such as the resistivity and self potential methods, could provide extra 3-D knowledge about the high velocity body located along SUN line 3 and the granitic bodies in the SW of the region.

REFERENCES

ADESANYA, O. 1982. Seismic Velocities of the Upper Crust of the Southern Uplands. *Univ. Glasgow Ph. D. thesis (unpubl).*

ALLEN, P. M. 1987. The Solway Line is not the Iapetus Suture. *Geol. Mag.*, **124,** 485-486.

AL-MANSOURI, D. 1986. Seismological Studies of Upper-Crustal Structure in the Vicinity of the Girvan-Ballantrae Area, SW Scotland. *Univ. Glasgow Ph. D. thesis (unpubl.).*

ANDERSON, T. B. 1965. The Evidence for the Southern Uplands Fault in North-east Ireland. *Geol. Mag.,* **102,** 383-392.

ANDERSON, T. B. & OLIVER, G. J. H. 1986. The Orlock Bridge Fault: A Major Late Caledonian Sinistral Fault in the Southern Uplands Terrane, British Isles. *Trans. Roy. Soc. Edin., Earth Sciences,* **77,** 203-222.

ASSUMPCAO, M. & BAMFORD, D. 1978. LISPB-V. Studies of Crustal Shear Waves. *Geophys. J. R. astr. Soc.,* **54,** 61-73.

BAMFORD, D. 1979. Seismic Constraints on the Deep Geology of the Caledonides of Northern Britain, In: HARRIS, A. L., HOLLAND, C. H. & LEAKE, B. E. (eds). *The Caledonides of the British Isles-Reviewed. Spec. Pub. Geol. Soc. London,* **8,** 93-96.

BAMFORD, D., FABER, S., JACOB, B., KAMINSKI, W., NUNN, K., PRODEHL, C., FUCHS, K., KING, R., & WILLMORE, P. 1976. A Lithospheric Seismic Profile in Britain-I Preliminary Results. *Geophys. J. R. astr. Soc.,* **44,** 145-160.

BAMFORD, D., NUNN, K., PRODEHL, B. & JACOB, B. 1977. LISPB-III. Upper Crustal Structure of Northern Britain. *J. Geol. Soc. London,* **133,** 481-488.

BAMFORD, D., NUNN, K., PRODEHL, C. & JACOB, B. 1978. LISPB-IV. Crustal Structure of Northern Britain. *Geophys. J. astr. Soc.,* **54,** 43-60.

BARNES, R. P., ANDERSON, T. B. & McCURRY, J. A. 1987. Along-strike Variation in the Stratigraphical and Structural Profile of the Southern Uplands Central Belt in Galloway and Down. *J. Geol. Soc. London,* **144,** 807-816.

BARNES, R. P., LINTERN, B. C. & STONE, P. 1989. Short Paper: Timing and Regional Implications of Deformation in the Southern Uplands of Scotland. *J. Geol. Soc. London,* **146,** 905-908.

BARRETT, T. J., JENKYNS, H. C., LEGGETT, J. K. & ROBERTSON, A. H. F. 1982. Comment and Reply on "Age and Origin of Ballantrae Ophiolite and its Significance to the Caledonian Orogeny and the Ordovician Time Scale". *Geology* 331-332.

BEAMISH, D. & SMYTHE, D. K. 1986. Geophysical Images of the Deep Crust: the Iapetus Suture. *J. Geol. Soc. London,* **143,** 489-497.

BEVINS, R. E., GIBBONS, W., HARRIS, A. L., & KELLING, G. 1986. The Caledonian Rocks of Britain, In: FETTES, D. J. & HARRIS, A. L. (eds). Synthesis of the Caledonian Rocks of Britain. *Series C : Mathematical and Physical Sciences,* **175,** 1-27.

BLUCK, B. J. 1983. Role of the Midland Valley of Scotland in the Caledonian Orogeny. *Trans. Roy. Soc. Edin., Earth Sciences,* **74,** 119-136.

BLUCK, B. J. 1984. Pre-Carboniferous History of the Midland Valley of Scotland. *Trans. Roy. Soc. Edin., Earth Sciences,* **75,** 275-295.

BLUCK, B. J. 1985. The Scottish Paratectonic Caledonides. *Scott. J. Geol.,* **21, (4),** 437-464.

BLUCK, B. J., HALLIDAY, A. N., AFTALION, M., & MACINTYRE, R. M. 1980. Age and Origin of Ballantrae Ophiolite and its Significance to the Caledonian Orogeny and Ordovician Time Scale. *Geology,* **8,** 492-495.

BREWER, J. A., MATTHEWS, D. H., WARNER, M. R., HALL, J., SMYTHE, D. K. & WHITTINGTON, R. J. 1983. BIRPS Deep Seismic Reflection Studies of the British Caledonides. *Nature,* **305,** 206-210.

BRIDEN, J. C., KENT, D. V., LAPOINTE, P. L., LIVERMORE, R. A., ROU, J. L., SEGUIN, M. K., SMITH, A. G., VAN DER VOO, R. & WATTS, D. R. 1988. Palaeomagnetic Constraints on the Evolution of the Caledonian-Appalachian Orogen, In: HARRIS, A. L. & FETTES, D. J. (eds). The Caledonian-Appalachian Orogen. *Spec. Pub. Geol. Soc.,* **38,** 35-48.

CAMERON, I. B. & STEPHENSON, D. 1985. The Midland Valley of Scotland. *British Geological Survey, 3rd Edition.*

CERVENY, V. & PSENCIK, I. 1983. 2-D Seismic Package Research Report, Institute of Geophysics, Charles University, Prague.

CHURCH, W. R., & GAYER, R. A. 1973. The Ballantrae Ophiolite. *Geol. Mag.,* **110,** 497-510.

COCKS, L. R. M. & FORTEY, R. A. 1982. Faunal Evidence for Oceanic Separation in the Palaeozoic of Britain. *J. Geol. Soc. London,* **139,** 465-478.

COOK, F. A., MATTHEWS, D. H. & JACOB, A. W. B. 1988. Crustal and Upper Mantle Structure of the Appalachian-Caledonide Orogen from Seismic Results, In: HARRIS, A. L. & FITTES, D. J. (eds). The Caledonian-Appalachian Orogen. *Spec. Pub. Geol. Soc.,* **38,** 21-33.

CUNNINGHAM, A. B. 1974. Refraction Data from Single-ended Refraction Profiles. *Geophys,* 39, 292-301.

DAVIDSON, K. A. S. 1986. Seismological Studies of Upper Crustal Structure of the Southern Midland Valley of Scotland. *Univ. Glasgow Ph. D. thesis*

(unpubl.).

DAVIDSON, K. A. S., SOLA, M., POWELL, D. W. & HALL, J. 1984. Geophysical Model for the Midland Valley of Scotland. *Trans. R. Soc. Edin. Earth Sci.,* **75,** 175-181.

DENTITH, M. C. 1987. Geophysical Constraints on Upper Crustal Structure in the Midland Valley of Scotland. *Univ. Glasgow Ph. D. thesis (unpubl.).*

DEWEY, J. F. 1969. Evolution of the Appalachian/Caledonian Orogen. *Nature,* **222,** 124-129.

DEWEY, J. F. 1971. A model for the Lower Palaeozoic Evolution of the Southern Margin of the Early Caledonides of Scotland and Ireland. *Scott. J. Geol.,* **7,** 219-240.

DEWEY, J. F. 1974. Continental Margins and Ophiolitic Obduction: Appalachian-Caledonian System, In: BURK, C. A. & DRAKE, C. L. (eds). The geology of continental margins. *Berlin: Springer-Verlag,* 933-950.

DEWEY, J. F. 1982. Plate Tectonics and the Evolution of the British Isles. *J. Geol. Soc.,* **139,** 371-412.

DEWEY, J. F. & SHACKLETON, R. M. 1984. A Model for the Evolution of the Grampian Tract in the Early Caledonides and Appalachians. *Nature,* **312,** 115-120.

DOBRIN, M. B. 1960. Geophysical Prospecting. *2nd Ed. McGraw-Hill.*

DOBRIN, M. B. 1976. Geophysical Prospecting. *3rd Ed. McGraw-Hill.*

DOODY, J. J. 1985. Deep Crustal Seismic Studies of Southwest Britain. *Univ. Wales Ph. D. thesis (unpubl.).*

EL-BATROUK, S. I. 1975. Geophysical Investigation on Loch Doon Granite South-west Scotland. *Univ. Glasgow Ph. D. thesis (unpubl.).*

ELDERS, C. F. 1987. The Provenance of Granite Boulders in Conglomerates of the Northern and Central Belts of the Southern Uplands of Scotland.

J. Geol. Soc. London, **144,** 853-863.

ELDERS, C. F. 1989. Discussion on Detrital Mineral Ages from the Southern Uplands *using* ^{40}Ar–^{39}Ar laser probe. **146,** 401-403.

ELDERS, C. F. 1989. Reply to discussion on the Provenance of Granite Boulders in Conglomerates of the Northern and Central Belts of the Southern Uplands of Scotland. *J. Geol. Soc. London,* **146,** 881-882.

EL-ISA, Z. H. M. 1977. Seismic Studies of Local Events Received at Three Quarries in Southern Central Scotland. *Univ. Glasgow Ph. D. thesis (unpubl.).*

EVANS, J. A., STONE, P. & FLOYD, J. D. 1991. Isotopic Characteristics of Ordovician Greywacke Provenance in the Southern Uplands of Scotland, In: MORTON, A. C., TODD, S. P. & HAUGHTON, P. D. W. (eds). *Developments in Sedimentary Provenance Studies. Geological Society Publication,* **57,** 161-172.

FITTON, J. G., & HUGHES, D. J. 1970. Volcanism and Plate Tectonics in the British Ordovician. *Earth and Planetary Sci. Letters,* **8,** 223-228.

FLOYD, J. D. 1976. The Ordovician Rocks of West Nithsdale. *Univ. St Andrews Ph. D. Thesis(unpubl.).*

FORTEY, R. A. & COCKS, L. R. M. 1988. Arenig to Llandovery Faunal Distribution in the Caledonides, In: HARRIS, A. L. & FETTES, D. J. (eds). The Caledonian-Appalachian Orogen. *Spec. Pub. Geol. Soc. London,* **38,** 233-246.

FRANCES, E. H. 1983. Carboniferous, In: GRAIG, G. Y. (ed), Geology of Scotland, 253-296. *Scottish Academic Press.*

FREEMAN, B., KLEMPERER, S. L. & HOBBS, R. W. 1988. The Deep Structure of Northern England and the Iapetus Suture Zone from BIRPS Deep Seismic Reflection Profiles. *J. Geol. Soc. London,* **145,** 727-740.

GRAIG, G. Y. 1983. Geology of Scotland. *Scottish Academic Press.*

GRANT, F. S. & WEST, G. F. 1965. Interpretation Theory in Applied Geophysics. *McGraw-Hill.*

GIBBONS, W. & GAYER, R. A. 1985. British Caledonian Terranes, In: GAYER, R. A. (ed), The Tectonic Evolution of the Caledonian-Appalachian Orogen. *Wiesbaden, West Germany, Vieweg,* 3-16.

GREIG, D. C., GOODLET, G. A., LUMSDEN, G. I. & TULLOCH, W. 1971. The South of Scotland. *3rd Ed. British Regional Geology, Institute of Geological Sciences.*

GUNN, P. J. 1973. Location of the Proto-Atlantic Suture in the British Isles. *Nature,* **242,** 111-112.

HAGEDOORN, J. G. 1959. The Plus-Minus Method of Interpretating Seismic Refraction Sections. *Geophy. Prosp.,* **7,** 158-183.

HALL, J., POWELL, D. W., WARNER, M. R., EL-ISA, Z. H. M., ADESANYA, O. & BLUCK, B. J. 1983. Seismological Evidence for Shallow Crystalline Basement in the Southern Uplands of Scotland. *Nature,* **305,** 418-420.

HALL, J., BREWER, J. A., MATTHEWS, D. H. & WARNER, M. R. 1984. Crustal Structure Across the Caledonides from the "WINCH" Seismic Reflection Profile: Influence on the Evolution of the Midland Valley of Scotland. *Trans. Roy. Soc. Edin., Earth Sciences,* **75,** 97-109.

HARLAND, W. B. & GAYER, R. A. 1972. The Arctic Caledonides and Earlier Oceans. *Geol. Mag.,* **109,** 289-314.

HATTON, L., WORTHINGTON, M. H. & MAKIN, J. 1986. Seismic Data Processing: Theory and Practice. *Blackwell Scientific publication.*

HAUGHTON, P. D. W. 1988. A Cryptic Caledonian Flysch Terrane in Scotland. *J. Geol. Soc. London,* **145,** 685-703.

HAUGHTON, P. D. W. & BLUCK, B. J. 1988. Diverse Alluvial Sequences from the Lower Old Red Sandstone of the Strathmore Region, Scotland- Implications for the Relationship Between Late Caledonian Tectonics and Sedimentation, In: McMILLAN, N. J., EMBRY, A. F. & GLASS, D. J. Devonian of the World. *Canadian Soc. Pet. Geologists,* **2,** 269-293.

HEINZ, W. 1989. Vulkanoklastische komponenten und deren geodynamische bedeutung fur die entwicklung der Southern Uplands von Schottland. *Tubinger Geowissenschaftliche Arbeiten, Reihe A,* **Nr. 3.**

HIPKIN, R. G. & HUSSAIN, A. 1983. Regional Gravity Anomalies, 1. Northern Britain. *Rep. Inst. Geol. Sci. 82/10.*

HUTTON, D. H. W., 1987. Strike-slip Terranes and a Model for the Evolution of the British and Irish Caledonides. *Geol. Mag.,* **124(5),** 405-425.

HUTTON, D. H. W. & MURPHY, F. C. 1987. The Silurian of the Southern Uplands and Ireland as a Successor Basin to the End-Ordovician Closure of Iapetus. *J. Geol. Soc. London,* **144,** 765-772.

HUTTON, V. R. S., INGHAM, M. R. & MBIPOM, E. W. 1980. An Electrical Model of the Crust and Upper Mantle in Scotland. *Nature,* **287,** 30-33.

INGHAM, M. R. & HUTTON, V. R. S. 1982a. Crustal and Upper Mantle Electrical Conductivity Structure in Southern Scotland. *Geophys. J. R. astr. Soc.,* **69,** 579-594.

INGHAM, M. R. & HUTTON, V. R. S. 1982b. The Interpretation and Tectonic Implications of the Geoelectric Structure of Southern Scotland. *Geophys., J. R. astr. Soc.,* **69,** 595-606.

JACOB, A. W. B. 1969. Crustal Phase Velocities at the Eskdalemuir Seismic Array. *Geophys. J. R. astr. Soc.,* **18,** 189-197.

JACOB, A. W. B., KAMINSKI, W., MURPHY, T., PHILLIPS, W. E. A. & PRODEHL, C. 1985. A crustal Model for a Northwest-southeast Profile Through

Ireland. *Tectonophysics,* **113,** 75-103.

JEANS, P. F. J. 1973. Plate-tectonic Reconstruction of the Southern Caledonides of Great Britain. *Nature Phys. Sci.,* **245,** 120-122.

JOHNSON, S. H. 1976. Interpretation of Split-spread Refraction Data in Terms of Plane Dipping Layers. *Geophysics,* **41,** 418-424.

JOHNSON, M. R. W., SANDERSON, D. J. & SOPER, N. J. 1979. Deformation in the Caledonides of England, Ireland and Scotland. The Caledonides of the British Isles-reviewed. *Spec. Pub. Geol. Soc. London,* **8,** 165-186.

JONES, A. G. & HUTTON, V. R. S. 1979a. A Multi-station Magnetotelluric Study of Southern Scotland-I. Fieldwork Data Analysis and Results. *Geophys. J. R. astr. Soc.,* **56,** 329-349.

JONES, A. G. & HUTTON, V. R. S. 1979b. A Multi-station Magnetotelluric Study of Southern Scotland-II. Monte-Carlo Inversion of the Data and its Geophysical and Tectonic Implications. *Geophys. J. R. astr. Soc.,* **56,** 351-368.

JONES, O. T. 1938. On the Evolution of a Geosyncline. *Quart. J. Geol. Soc. London,* **94,** *lx-cix.*

KAMALIDDIN, Z. A. R. 1988. Seismic Interpretation of Basin-basement Relationships in the Eastern Midland Valley of Scotland Using Quarry Blasts. *Univ. Glasgow M. Sc. thesis (unpubl.).*

KEAREY, P. & BROOKS, M. 1984. An Introduction to Geophysical Exploration. *Blackwell Scientific Publications.*

KELLING, G. 1961. The Stratigraphy and Structure of the Ordovician Rocks of the Rhinns of Galloway. *Quart. J. Geol. Soc. London,* **117,** 37-75

KELLING, G., DAVIES, P. & HOLROYD, J. 1987. Style, Scale and Significance of Sand Bodies in the Northern and Central Belts, Southwest Southern Uplands. *J. Geol. Soc. London,* **144,** 787-805.

KELLEY, S. & BLUCK, B. J. 1989. Short Paper: Detrital Mineral Ages from the Southern Uplands *using* ^{40}Ar–^{39}Ar laser probe. *J. Geol. Soc. London,* **146,** 401-403.

KEMP, A. E. S. 1986. Tectonostratigraphy of the Southern Belt of the Southern Uplands. *Scott. J. Geol.,* **22, (2),** 241-256.

KEMP, A. E. S. 1987. Tectonic Development of the Southern Belt of the Southern Uplands Accretionary Complex. *J. Geol. Soc. London,* **144,** 827-838.

KLEMPERER, S. & MATTHEWS, D. H. 1987. Iapetus Suture Located Beneath the North Sea by BIRPS Deep Seismic Reflection Profiling. *Geology,* **15,** 195-198.

KNIPE, R. J. & NEEDHAM, D. T. 1986. Deformation Processes in Accretionary Wedges-examples from the Margin of the Southern Uplands, Scotland, In: COWARD, M. P. & RIES, A. C. (eds). Collision tectonics. *Geol. Soc. Spec. Pub.,* **19,** 51-65.

LAGIOS, E. & HIPKIN, R. G. 1979. The Tweeddale Granite-a Newly discovered Batholith in the Southern Uplands. *Nature,* **280,** 672-675.

LAMBERT, R. ST. J. & McKERROW, W. S. 1976. The Grampian Orogeny. *Scott. J. Geol.,* **12,** 271-292.

LEFORT, J. P., MAX, M. D. & ROUSSEL, J. 1988. Geophysical Evidence for the Location of the NW Boundary of Gondwanaland and its Relationship with two Older Satellite Sutures, In: HARRIS, A. L. & FETTES, D. J. (eds). The Caledonian-Appalachian Orogen. *Spec. Pub. Geol. Soc.,* **38,** 49-60.

LEGGETT, J. K. 1979. Oceanic Sediments from the Ordovician of the Southern Uplands, In: HARRIS, A. L., HOLLAND, C. H. & LEAKE, B. E. (eds). *The Caledonides of the British Isles-reviewed. Spec. Pub. Geol. Soc. London,* **8,** 495-498.

LEGGETT, J. K. 1980. The Sedimentological Evolution of a Lower Palaeozoic

Accretionary Fore-arc in the Southern Uplands of Scotland. *Sedimentology,* **27,** 401-417.

LEGGETT, J. K. 1987. The Southern Uplands as an Accretionary Prism: the Importance of Analogues in Reconstructing Palaeogeography. *J. Geol. Soc. London,* **144,** 737-752.

LEGGETT, J. K., McKERROW, W. S., MORRIS, J. H., OLIVER, G. J. H. & PHILLIPS, W. E. A. 1979a. The North-western Margin of the Iapetus Ocean. The Caledonides of the British Isles-reviewed. *Spec. Pub. Geol. Soc. London,* **8,** 499-511.

LEGGETT, J. K., McKERROW, W. S. & EALES, M. H. 1979b. The Southern Uplands of Scotland: A Lower Palaeozoic Accretionary Prism. *J. Geol. Soc. London,* **136,** 755-770.

LEGGETT, J. K., McKERROW, W. S. & CASEY, D. M. 1982. The Anatomy of a Lower Palaeozoic Accretionary Forearc: The Southern Uplands of Scotland. *Geol. Soc. Spec. Pub.,* **10,** 495-520.

LEGGETT, J. K., McKERROW, W. S. & SOPER, N. J. 1983. A Model for the Crustal Evolution of Southern Scotland. *Tectonics,* **2,** 187-210.

MASON, R. 1988. Did the Iapetus Ocean Really Exist? *Geology,* **16,** 823-826.

MATTHEWS, D. H. 1986. Seismic Reflections from the Lower Crust Around Britain, In: DAWSON, J. B., CARSWELL, D. A., HALL, J. & WEDEPOHL, K. H. (eds). The Nature of the Lower Continental Crust. *Spec. Pub. Geol. Soc. London,* **24,** 11-22.

McADAM, A. D. & TULLOCH, W. 1985. Geology of the Haddington District. *British Geological Survey, Scotland. Mem. for 1:50 000 Sheet 33W and part of Sheet 41.*

McCURRY, J. A. & ANDERSON, T. B. 1989. Landward Vergence in the Lower Paleozoic Southern Uplands-Down-Longford Terrane, British Isles. *Geology,*

17, 630-633.

McKERROW, W. S. 1986. The Tectonic Setting of the Southern Uplands, In: FETTES, D. J. & HARRIS, A. L. (eds). Synthesis of the Caledonian Rocks of Britain. *D. Reidel Publishing Company,* 207-220.

McKERROW, W. S. 1987. The Southern Uplands Controversy. *J. Geol. Soc. London,* **144,** 735-736.

McKERROW, W. S. 1988a. The Development of the Iapetus Ocean from the Arenig to the Wenlock, In: HARRIS, A. L. & FETTES, D. J. (eds). The Caledonian-Appalachian Orogen. *Geol. Soc. Spec. Pub.,* **38,** 405-412.

McKERROW, W. S. 1988b. Wenlock to Givetian Deformation in the British Isles and the Canadian Appalachians, In: HARRIS, A. L. & FETTES, D. J. (eds). The Caledonian-Appalachian Orogen. *Geol. Soc. Spec. Pub.,,* **38,** 437-448.

McKERROW, W. S. & ELDERS, C. F 1989. Short Paper: Movements on the Southern Uplands Fault. *J. Geol. Soc. London,* **146,** 393-395.

McKERROW, W. S., COCKS, L. R. M. 1976. Progressive Faunal Migration Across the Iapetus Ocean. *Nature,* **263,** 304-306.

McKERROW, W. S., LEGGETT, J. K. 1977. Imbricate Thrust Model of the Southern Uplands of Scotland. *Nature,* **267,** 237-239.

McKERROW, W. S. & COCKS, L. R. M. 1986. Oceans, Island arcs and Olistostromes: The Use of Fossils in Distinguishing Sutures, Terranes and Environments Around the Iapetus Ocean. *J. Geol. Soc. London,* **143,** 185-191.

McKERROW, W. S. & SOPER, N. J. 1989. The Iapetus Suture in the British Isles. *Geol. Mag.,* **126 (1),** 1-8.

McKERROW, W. S. & ELDERS, C. F. 1989. Short Paper: Movements on the Southern Uplands Fault. *J. Geol. Soc. London,* **146,** 393-395.

McLEAN, A. C. 1966. A Gravity Survey in Ayrshire and its Geological Interpretation. *Trans. R. Soc. Edin.,* **66,** 239-283.

McLEAN, A. C. & QURESHI, I. R. 1966. Regional Gravity Anomalies in the Western Midland Valley of Scotland. *Trans. R. Soc. Edin.*, **56,** 267-283.

McLEAN, A. C. & DEEGAN, C. E. 1978. The Solid Geology of the Clyde Sheet (55 N/6 W). *Institute of Geological Sciences, Report 78/9,* 95-114.

MERRIMAN, R. J. & ROBERTS, B. 1990. Metabentonites in the Moffat Shale Group, Southern Uplands of Scotland: Geochemical Evidence of Ensialic Marginal Basin Volcanism. *Geol. Mag.,* **127,** 259-271.

MITCHELL, A. H. G. 1989. Short Paper: Arc Reversal in the Scottish Southern Uplands? *J. Geol. Soc. London,* **146,** 736-738.

MITCHELL, A. H. G., & McKERROW, W. S. 1975. Analogous Evolution of the Burma Orogen and the Scottish Caledonides. *Geol. Soc. Am. Bull.,* **86,** 305-315.

MORRIS, J. H. 1987. The Northern Belt of the Longford-Down Inlier, Ireland and Southern Uplands, Scotland: An Ordovician Back-arc Basin. *J. Geol. Soc. London,* **144,** 773-786.

MOSELEY, F. 1977. Caledonian Plate Tectonics and the Place of the English Lake District. *Geol. Soc. Am. Bull.,* **88,** 768-768.

MURPHY, F. C. and HUTTON, D. H. W. 1986. Is the Southern Uplands of Scotland Really an Accretionary Prism? *Geology,* **14,** 354-357.

NEEDHAM, D. T., KNIPE, R. J. 1986. Accretion- and Collision-related Deformation in the Southern Uplands Accretionary Wedge, Southeastern Scotland. *Geology,* **14,** 303-306.

OLIVER, G. J. H. 1988. Arenig to Wenlock Regional Metamorphism in the Paratectonic Caledonides of the British Isles: A review, In: HARRIS, A. L. & FETTES, D. J. (eds). The Caledonian-Appalachian Orogen. *Spec. Pub. Geol. Soc.,* **38,** 347-363.

OLIVER, G. J. H. & LEGGETT, J. K. 1980. Metamorphism in an Accretionary Prism: Prehnite-pumpellyite Facies Metamorphism of the Southern Uplands of Scotland. *Trans. Roy. Soc. Edin., Earth Sciences,* **71,** 235-246.

OLIVER, G. J. H. & McKERROW, W. S. 1984. Seismological Evidence for Shallow Crystalline Basement in Southern Uplands, Scotland. *Nature,* **309,** 89-90.

OLIVER, G. J. H., SMELLIE, J. L., THOMAS, L. J., CASEY, D. M., KEMP, A. E. S., EVANS, L. J., BALDWIN, J. R. & HEPWORTH, B. C. 1984. Early Palaeozoic Metamorphic History of the Midland Valley, Southern Uplands-Longford-Down Massif and the Lake District, British Isles. *Trans. Roy. Soc. Edin., Earth Sciences,* **75,** 245-258.

PALMER, D. 1980. The Generalised Reciprocal Method of Seismic Refraction Intrpretation. *Society of Exploration Geophysics, Tulsa.*

PEACH, B. N. & HORNE, J. 1899. The Silurian Rocks of Britain, 1, Scotland. *Mem. Geol. Surv. Scotland.*

PHILLIPS, W. E. A., STILLMAN, C. J. & MURPHY, T. 1976. A Caledonian Plate Tectonic Model. *J. Geol. Soc. London,* **132,** 579-609.

POWELL, D. W. 1970. Magnetised Rocks within the Lewisian of W. Scotland and Under the Southern Uplands. *Scott. J. Geol.,* **6,** 297-301.

POWELL, D. W. 1971. A Model for the Lower Palaeozoic Evolution of the Southern Margin of the Early Caledonides of Scotland and Ireland. *Scott. J. Geol.,* **7,** 369-372.

READ, W. A. 1989. Sedimentological Evidence for a Major Subsurface Fracture System Linking the Eastern Campsie and the Eastern Ochil Faults. *Scott. J. Geol.,* **25,** 187-200.

ROBINSON, E. A. & TREITEL, S. 1964. Principles of Digital Filtering. *Geophysics,* **29,** 395-404.

ROBINSON, E. A., 1980. Geophysical Signal Analysis. *Prentice-Hall.*

ROCK, N. M. S. & RUNDLE, C. C. 1986. Lower Devonian Age for the "Great (basal) Conglomerate", Scottish Borders. *Scott. J. Geol.,* **22,** 285-288.

SHACKLETON, R. M. 1979. The British Caledonides: Comments and Summary, In: The Caledonides of the British Isles-reviewed. *Spec. Pub. Geol. Soc. London,* **8,** 299-304.

SOLA, M. A. 1985. The Seismic Structure Under the Central Midland Valley from Refraction Measurements. *Univ. Glasgow Ph. D. thesis, (unpubl.).*

SOPER, N. J. 1988. Timing and Geometry of Collision, Terrane Accretion and Sinistral Strike-slip Events in the British Caledonides, In: HARRIS, A. L. & FETTES, D. J. (eds). The Caledonian-Appalachian Orogen. *Spec. Pub. Geol. Soc.,* **38,** 481-492.

SOPER, N. J. & HUTTON, D. H. W. 1984. Late Caledonian Sinistral Displacement in Britain: Implication for a Three-plate Collision Model. *Tectonics,* **3,** 781-794.

SOPER, N. J. & WOODCOCK, N. H. 1987. Late Caledonian (Acadian) Transpression in North West England: Timing, Geometry and Geotectonic Significance. *Proceedings of the Yorkshire Geological Society,* **46,** 175-192.

SOPER, N. J., GIBBONS, W. & McKERROW, W. S. 1989. Displaced Terranes in Britain and Ireland. *J. Geol. Soc. London,* **146,** 365-367.

STONE, P., FLOYD, J. D., BARNES, R. P. & LINTERN, B. C. 1987. A Sequential Back-arc and Foreland Basin Thrust Duplex Model for the Southern Uplands of Scotland. *J. Geol. Soc. London,* **144,** 753-764.

STYLES, M. T., STONE, P. & FLOYD, J. D. 1989. Short Paper: Arc Detritus in the Southern Uplands: Mineralogical Characterization of a "missing" Terrane. *J. Geol. Soc. London,* **146** 397-400.

THIRLWALL, M. F. 1989. Short Paper: Movement on Proposed Terrane Boundaries in Northern Britain: Constraints from Ordovician-Devonian Igneous Rocks. *J. Geol. Soc. London,* **146,** 373-376.

THORPE, R. S., BECKINSALE, R. D., PATCHETT, P. J., PIPER,, J. D. A., DAVIS, G. R. & EVANS, J. A. 1984. Crustal Growth and Late Pre-Camberian-early Palaeozoic Plate Tectonic Evolution of England and Wales. *J. Geol. Soc.,* **141,** 521-536.

TRENCH, A., DENTITH, M. C., BLUCK, B. J., WATTS, D. R. & FLOYD, J. D. 1989. Short Paper: Palaeomagnetic Constraints on the Geological Terrane Models of the Scottish Caledonides. *J. Geol. Soc. London,* **146,** 405-408.

UPTON, B. G. J., ASPEN, P. & CHAPMAN, N. A. 1983. Upper Mantle and Deep Crust Beneath the British Isles. *J. Geol. Soc. London,* **140,** 105-122.

UPTON, B. G. J., ASPEN, P. & HUNTER, R. H. 1984. Xenoliths and their Implications for Deep Geology of the Midland Valley of Scotland and Adjacent Regions. *Trans. Roy. Soc. Edin., Earth Sciences,* **75,** 65-70.

WALTON, E. K. 1983. Lower Palaeozoic-stratigraphy, In: GRAIG, G. Y. (ed), Geology of Scotland, 105-137. *Scottish Academic Press.*

WALTON, E. K. 1983. Lower Palaeozoic-Structure and Palaeogeography, In: GRAIG, G. Y. (ed), Geology of Scotland, 139-166. *Scottish Academic Press.*

WARNER, M. R., HIPKIN, R. G. & BROWITT, C. W. A. 1982. Southern Uplands Seismic Refraction Profile - Preliminary Results. Geophys. J. R. astr. Soc., **69,** 297.

WATSON, J. V. 1984. The Ending of the Caledonian Orogeny in Scotland. *J. Geol. Soc. London,* **141,** 193-214.

WEIR, J. A. 1979. Tectonic Contrasts in the Southern Uplands. *Scott. J. Geol.,* **15,** 169-186.

WILLIAMS, A. 1975. Plate Tectonics and Biofacies Evolution as Factors in Ordovician Correlation, In: Bassett, M. G. (ed). The Ordovician System. *Proceedings Palaeo. Assoc. symposium : Cardiff, Univ. Wales and Nat. Mus. Wales,* 18-53.

WILLMORE, P. L. & BANCROFT, A. M. 1960. The Time-term Approach to Refraction Seismology. *Geophys. J. R. astr. Soc.,* **3,** 419-432.

WILSON, J. T. 1966. Did the Atlantic Close Then Re-open? *Nature,* **211,** 676-678.

WINCHESTER, A. & MAX, M. D. 1989. Discussion on the Provenance of Granite Boulders in Conglomerates of the Northern and Central Belts of the Southern Uplands of Scotland. *J. Geol. Soc. London,* **146,** 359-360.

WRIGHT, A. E. 1976. Alternating Subduction Direction and the Evolution of the Atlantic Caledonides. *Nature,* **264,** 156-160.

APPENDIX 1. QUARRIES USED-GENERAL INFORMATION

QUARRIES USED - GENERAL INFORMATION

[1] Collace quarry, [NE of Perth].

Manager: Mr. Harley (very cooperative).

Tel: 08215-222.

Frequency: Big blast approximately every 6 months.

Number of holes: Varies.

Charge: 1- 3 tonnes.

Remarks: Good blaster but not dependable. Maximum obtainable range is approximately 50 km*.

[2] Boysack quarry, [Friockheim].

Manager: Same as in 1.

Tel: Same as in 1.

Frequency: Once every 9 months.

Number of holes: 12 - 15 holes.

Charge: 3-4 tonnes.

Remarks: Very good blaster but infrequent. Maximum obtainable range is approximately 60 km.

[3] Goat quarry, [Aberdour].

---

* Maximum detectable ranges quoted are when recording conditions (orientation of quarry face being removed and charge size ..etc.) are favourable.

Manager: Mr. Pittry (very helpful).

Tel: 038-3860517.

Frequency: Every 14-21 days.

Number of holes: 11-30 holes.

Charge: 2-5 tonnes.

Remarks: Frequent and good blaster. Maximum obtainable range is approximately 60 km.

[4] Craighouse quarry, [Melrose].

Manager: Mr. Robertson (very helpful).

Tel: 089682-2085.

Frequency: A blast each week.

Number of holes: 10-20 hole.

Charge: 1-2 tonnes.

Remarks: Very punctual and frequent blaster but a poor source of energy. Maximum obtainable range is approximately 45 km.

[5] Craigpark quarry, [Ratho].

Manager: Mr. Stewart (Very helpful).

Tel: 031 333 1405.

Frequency: Once every 20 days.

Number of holes: 10-14 holes.

Charger: 1-2 tonnes (mixture).

Remarks: Powerful blaster and ideal for projects across the SUF and within the Southern Uplands. Ranges up to 80 km can be obtained in good conditions.

[6] Bangley quarry, [Haddington].

Manager: Mr. David Grant (helpful but formal).

Tel: 0620825811.

Frequency: 1 blast/week.

Number of holes: 10-15 holes.

Charge: 1-2 tonnes (mixture).

Remarks: Very poor blaster and not recommended for future use. Maximum obtainable range is about 40 km.

[7] Tormitchell quarry, [Girvan].

Manager: Mr. Jordan Barr (very helpful).

Tel: 046587-239.

Frequency: Average 2 months period.

Number of holes: 10-20 holes.

Charge: 1-2 tonnes.

Remarks: Very good blaster. Maximum obtainable range is approximately 55 km.

[8] Barlockhari quarry, [Glenluce].

Manager: Mr. McClurg (very helpful).

Tel: 05813-329.

Frequency: A blast every 2-3 months.

Number of holes: 10-14 holes.

Charge: 1-2 tonnes.

Remarks: Excellent blaster and large offsets can be obtained. Using this quarry, projects can be designed to cover both the Southern Uplands to the east of it and

across the SUF into the Midland Valley (quarry conditions are ideal in the later case) with very good data quality. Maximum obtainable range is approximately 65 km.

APPENDIX 2. RECORDING SITES: NAMES AND LOCATIONS

LINE 1 - MELROSE QUARRY - SITE LOCATIONS

Quarry location: Easting 360.05 Northing 636.14
Quarry type: Intrusive igneous rocks (Porphyrite and Trachyte)

SITE NUMBER	SITE NAME	EASTING	NORTHING	GEOPHONE COUPLING
mb01	Georgefield farm	359.72	637.98	Drift
mb02	Grizzlefield farm	358.62	639.88	Drift
mb03	Legerwood farm	357.80	641.44	Drift
mb04	Legerwood farm	357.88	643.53	Drift
mb05	Boon farm	357.13	645.70	Drift
mb06	Thirlestane farm	356.62	647.72	Drift
mb07	Thirlestane farm	356.50	649.47	Drift
mb08	Burncastle farm	354.83	650.82	Drift
mb08a	Bruncastle farm	355.19	652.55	Drift
mb09	Burncastle farm	355.54	653.44	Drift
mb10	Longcroft farm	354.29	655.30	Drift
mb11	Tollishill farm	353.29	657.40	Drift
mb12	Tollishill farm	352.78	659.10	Drift
mb12a	Tollishill farm	352.47	660.19	Drift
mb13	Longyester farm	352.60	660.99	Drift
mb14	Dumbadam farm	352.68	663.97	Drift
mb15	Long Newton farm	351.64	664.91	Drift
mb15a	Skudsbush farm	351.35	666.15	Drift
mb16	Bankrugg farm	350.93	667.39	Drift
mb17	Upper Bolton farm	350.55	668.94	Drift
mb18	West Field farm	350.19	671.18	Drift
mb19	Blackwood farm	349.49	672.44	Drift
mb00	Alderston farm	349.65	675.49	Drift

LINE 1 - BANGLY QUARRY - SITE LOCATIONS

Quarry location: Easting 348.86 Northing 675.15
Quarry type: Basalt (Tuffs) of Carboniferous age.

SITE NUMBER	SITE NAME	EASTING	NORTHING	GEOPHONE COUPLING
bm19	Letham farm	349.57	672.99	Drift
bm18	Westfield farm	350.19	671.18	Drift
bm17	Upper Bolton farm	350.55	668.94	Drift
bm16	Bankrugg farm	350.93	667.39	Drift
bm15	Long Newton farm	351.64	664.91	Drift
bm14	Dumbadam farm	352.68	663.97	Drift
bm13a	Longyester farm	352.94	662.05	Drift
bm13	Longyester farm	352.62	660.97	Drift
bm12a	Longyester farm	352.46	660.18	Drift
bm12	Tollishill farm	352.78	659.10	Drift
bm11	Tollishill farm	353.29	657.40	Drift
bm10	Longcroff farm	354.29	655.30	Drift
bm09	Burncastle farm	355.54	653.44	Drift
bm08	Burncastle farm	354.85	651.14	Drift
bm07	Thirlestane farm	356.50	649.47	Drift
bm06	Thirlestane farm	356.62	647.72	Drift
bm05	Boon farm	357.13	645.70	Drift
bm04	Legerwood farm	357.88	643.53	Drift
bm03	Legerwood farm	357.80	641.44	Drift

LINE 2 - MELROSE QUARRY - SITE LOCATIONS

Quarry location: Easting 360.05 Northing 636.14
Quarry type: Intrusive igneous rocks (Porphyrite and Trachyte).

SITE NUMBER	SITE NAME	EASTING	NORTHING	GEOPHONE COUPLING
mr01	The Park farm	358.98	636.90	Drift
mr02	Woods	356.99	638.18	Drift
mr03	side road	355.35	639.73	Drift
mr04	Mosshouses farm	353.59	640.67	Drift
mr05	Colmsliehil farm	352.07	641.89	Drift
mr06	Threepwood farm	350.39	642.91	Drift
mr07	Allanshaws farm	349.20	644.13	Drift
mr08	Muirhouse farm	347.28	645.36	Drift
mr09	Little Cathpair	345.85	646.68	Drift
mr10	Bankhouse farm	343.85	647.94	Drift
mr11	Pirntaton farm	342.46	649.60	Drift
mr12	Brockhouse farm	341.32	650.87	Drift
mr13	Haltree farm	340.10	651.20	Drift
mr13a	Borthwick Hall	338.60	652.23	Drift
mr14	Carcant farm	336.98	651.97	Drift
mr15	Carcant farm	335.74	653.59	Drift
mr15a	Carcant farm	335.12	654.58	Drift
mr16	Outerston farm	333.50	655.66	Drift
mr17	Outerston farm	332.59	656.59	Drift
mr18	Braidwood farm	330.93	657.07	Drift
mr19	Edgelaw farm	329.29	658.80	Drift
mr20	Newbigging farm	328.02	660.21	Drift
mr21	Newbigging farm	326.25	661.26	Drift

LINE 2 - RATHO QUARRY- SITE LOCATIONS

Quarry location: Easting 313.01 Northing 670.49
Quarry type: Quartz-dolerite intrusive rocks.

SITE NUMBER	SITE NAME	EASTING	NORTHING	GEOPHONE COUPLING
ra28	Dalmahoy farm	314.64	669.10	Drift
ra27	Cocklaw farm	316.40	668.30	Drift
ra26	Rosebank farm	318.28	667.32	Drift
ra25	Middle Kinleith farm	319.20	666.03	Drift
ra24	Kirton farm	321.06	664.20	Drift
ra23	Crosshouse farm	322.94	663.64	Drift
ra22	Penicuik town	324.00	662.34	Drift
ra21	Kirkettle farm	326.25	661.26	Drift
ra20	Newbigging farm	328.02	660.21	Drift
ra19	Edgelaw farm	329.29	658.80	Drift
ra18	Braidwood farm	331.12	657.38	Drift
ra17	Outerston farm	332.59	656.59	Drift
ra16	Outerston farm	333.50	655.68	Drift
ra15a	Caracant farm	335.12	654.58	Drift
ra15	Caracant farm	335.65	653.60	Drift
ra14	Carcant farm	336.98	651.97	Drift
ra13a	Borthwick farm	338.60	652.23	Drift
ra13	Haltree farm	340.10	651.20	Drift
ra12	Brockhouse farm	341.32	650.87	Drift
ra11	Pirntaton farm	342.29	649.24	Drift
ra10	Bankhouse farm	343.85	647.94	Drift
ra09	Little Cathpair farm	345.85	646.68	Drift
ra08	Muirhouse farm	347.28	645.36	Drift
ra07	Allan Shaws farm	349.20	644.13	Drift
ra06	Threepwood farm	350.39	642.91	Drift
ra05	Colmsliehil farm	352.07	641.89	Drift
ra04	Mosshouses farm	353.59	640.67	Drift
ra03	Side road	355.35	639.73	Drift
ra02	Woods	356.99	638.18	Drift
ra01	The Park farm	358.82	636.85	Drift
ra00	Third farm	361.04	635.39	Drift
ra33	Third farm	361.50	634.90	Drift
ra55	Delcove Mains	365.05	632.43	Drift

LINE 3 - ABERDOUR QUARRY - SITE LOCATIONS

Quarry location: Easting 317.45 Northing 686.78
Quarry type: Quartz dolerite sill.

SITE NUMBER	SITE NAME	EASTING	NORTHING	GEOPHONE COUPLING
ab01	Dalmeny House	316.54	678.76	Drift
ab02	Dalmeny House	316.62	677.15	Drift
ab03	Nether Lennie farm	316.38	675.02	Drift
ab04	Gogar Mount farm	315.80	672.02	Drift
ab05	Over Gogar farm	316.20	670.65	Drift
ab06	Warriston farm	315.78	668.81	Drift
ab07	Easter Newton farm	312.60	666.51	Drift
ab08	Buteland House	312.71	664.07	Drift
ab09	Listonshiels farm	313.46	661.99	Drift
ab11	Baddinsgill farm	311.88	657.81	Drift
ab12	Baddinsgill farm	312.21	656.45	Drft
ab13	Baddinsgill farm	312.43	654.75	Drift
ab14	N. Slipper field farm	312.19	652.38	Drift
ab15	S.Slipper field farm	312.19	652.38	Drift
ab16	Ingraston farm	311.68	648.80	Drift
ab17	Newmill farm	311.44	646.79	Drift
ab18	Netherurd Mill farm	311.35	644.70	Drift
ab19	The Mount farm	310.99	642.52	Drift
ab20	Stirkfield farm	310.22	640.39	Drift
ab21	Cloverhill farm	311.10	638.13	Drift
ab22	Corstane farm	310.84	636.44	Drift
ab23	Rachan farm	311.38	634.31	Drift
ab24	Cardon farm	310.21	632.81	Drift
ab25	Mossfennan farm	310.84	629.62	Drift

LINE 3 - RATHO QUARRY- SITE LOCATIONS

Quarry location: Easting 313.01 Northing 670.49
Quarry type: Quartz-dolerite intrusive rocks.

SITE NUMBER	SITE NAME	EASTING	NORTHING	GEOPHONE COUPLING
rt06	Hatton farm	312.87	668.55	Drift
rt07	East Newton farm	312.62	666.50	Drift
rt08	Buteland House	312.71	664.07	Drift
rt09	Listonshiels farm	313.46	661.99	Drift
rt11	Baddinsgill farm	311.88	657.81	Drift
rt12	Baddinsgill farm	312.21	656.45	Drift
rt13	Baddinsgill farm	312.58	654.69	Drift
rt14	North Slipper field	312.19	652.38	Drift
rt15	South Slipper field	312.74	650.28	Drift
rt16	Ingraston farm	311.68	648.80	Drift
rt17	Newmill farm	311.44	646.79	Drift
rt18	Netherurd farm	311.35	644.70	Drift
rt19	The Mount farm	310.99	642.52	Drift
rt20	Stirkfield farm	310.22	640.39	Drift
rt21	Cloverhill farm	311.10	638.13	Drift
rt22	Corstane farm	310.84	636.44	Drift
rt23	Rachan Mill farm	311.38	634.31	Drift
rt24	Cardon farm	310.21	632.81	Drift
rt25	Cardon farm	310.21	632.81	Drift
rt26	Kingledores farm	310.50	628.40	Drift
rt27	The Crook farm	311.06	626.38	Drift
rt28	The Inch farm	310.25	624.59	Drift
rt29	Forestry Commission	308.85	622.57	Drift
rt30	Craiglaw farm	308.90	620.40	Drift
rt31	Nether Fruid farm	310.37	618.70	Drift
rt34	Corehead farm	307.29	612.46	Drift
rt35	Mountain blow farm	308.60	610.11	Drift
rt36	Commonside farm	307.85	607.95	Drift
rt37	The Hope House	307.98	607.05	Drift
rt38	The Dyke farm	307.85	604.30	Quarry

LINE 4 - GLENLUCE QUARRY - SITE LOCATIONS

Quarry location: Easting 221.20 Northing 556.42
Quarry: Dioritic intrusive rocks.

SITE NUMBER	SITE NAME	EASTING	NORTHING	GEOPHONE COUPLING
gt01	High Glenjorrie farm	220.84	558.50	Drift
gt02	Whitecairn farm	221.51	560.49	Drift
gt03	Garvilland farm	221.58	561.90	Drift
gt04	Dranigower farm	221.60	564.75	Drift
gt05	Balmurrie farm	220.78	566.49	Drift
gt06	Balmurrie farm	220.53	567.81	Drift
gt06a	Private forest	221.20	569.10	Drift
gt07	Private forest	221.77	570.39	Drift
gt08	Forestry Comm.	222.68	572.79	Drift
gt8a	Forestry Comm.	222.49	573.62	Drift
gt09	Forestry Comm.	223.11	574.49	Drift
gt10	Chirmorrie farm	220.90	576.70	Drift
gt11	Dochroyle farm	223.29	579.04	Drift
gt12	south Barhill	222.22	580.36	Drift
gt13	White Cairn farm	222.31	582.60	Drift
gt14	Knockytinnal farm	222.95	584.53	Drift
gt15	Bellymore farm	222.97	586.83	Drift
gt16	Docherniel farm	223.63	588.60	Drift
gt17	Benan farm	222.94	591.13	Drift
gt18	Minuntion farm	224.10	592.15	Drift
gt00	Barbae farm	222.94	594.96	Drift
gt33	High Troweir farm	222.99	596.43	Drift
gt44	Penkill farm	223.34	598.63	Drift
gt66	Blair farm	223.74	602.23	Drift
gt77	Chapelton farm	224.00	604.50	Drift
gt88	Minnybrae farm	223.78	606.35	Drift

LINE 4 - TORMITCHELL QUARRY - SITE LOCATIONS

Quarry location: Easting 223.40 Northing 594.60
Quarry type: Basaltic lavas

SITE NUMBER	SITE NAME	EASTING	NORTHING	GEOPHONE COUPLING
tm18	Pinclanty farm	223.23	592.05	Drift
tm17	Benan farm	222.96	590.78	Drift
tm16	Docherniel farm	223.63	588.60	Drift
tm15	Bellymore farm	222.97	586.83	Drift
tm14	Knockytinnal farm	222.95	584.53	Drift
tm13	White Cairn farm	222.31	582.60	Drift
tm12	Barrhill Town	222.30	580.55	Drift
tm11	Dochroyle farm	223.29	579.04	Drift
tm10	Chirmorrie farm	220.90	576.70	Drift
tm09	Forestry Commission	223.11	574.49	Drift
tm08a	Forestry Commission	222.49	573.62	Drift
tm08	Forestry Commission	222.68	572.79	Drift
tm07	Private Forest	221.20	569.10	Drift
tm06a	Forestry Commission	221.20	569.10	Drift
tm06	Balmurrie farm	220.53	567.81	Drift
tm05	Balmurrie farm	220.78	566.49	Drift
tm04	Dranigower farm	221.60	564.75	Drift
tm03	Garvilland farm	221.55	561.95	Drift
tm02	Whitecairn farm	221.51	560.49	Drift
tm01	High Glenjorrie farm	220.84	558.50	Drift
tm00	Barlockhart farm	221.36	555.90	Drift
tm33	South Milton farm	221.44	554.49	Drift
tm44	Castle Sinniness farm	221.39	553.18	Drift

LINE 5 - GLENLUCE QUARRY - SITE LOCATIONS

Quarry location: Easting 221.20 Northing 556.42
Quarry: Dioritic intrusive rocks.

SITE NUMBER	SITE NAME	EASTING	NORTHING	GEOPHONE COUPLING
gn02	Dergoals farm	224.48	558.96	Drift
gn04	Knockishee farm	228.12	560.75	Drift
gn05	Barmore farm	229.87	561.59	Drift
gn06	Ardachie farm	231.90	562.60	Drift
gn09	Cullach farm	237.51	564.79	Drift
gn10	North Barnkirk farm	239.50	566.57	Drift
gn11	Boreland Lodge	240.92	567.48	Drift

LINE 6 - BOYSACK QUARRY - SITE LOCATIONS

Quarry location: Easting 362.81 Northing 749.63
Quarry type: Basalt.

SITE NUMBER	SITE NAME	EASTING	NORTHING	GEOPHONE COUPLING
bc22	Boysack farm	361.42	749.97	Drift
bc20	Helenston farm	358.02	747.10	Drift
bc19	Smithyton farm	356.22	746.98	Drift
bc18	Ascurry farm	354.11	745.86	Drift
bc17	Cockhill farm	352.59	744.80	Drift
bc16	Kirkbuddo House	350.51	743.90	Drift
bc15	Holemill farm	348.40	743.42	Drift
bc14	Fothringham	346.69	743.08	Drift
bc13	Newton farm	345.20	741.90	Drift
bc12	South Tarbra	343.09	741.31	Drift
bc11	Mansefield farm	341.33	740.28	Drift
bc10	Balcalk farm	339.64	739.55	Drift
bc09	North Balluderen	337.59	738.72	Drift
bc08	Balbeuchley House	335.69	737.92	Drift
bc07	Eastfield farm	333.79	737.21	Drift
bc06	West Adamston	332.02	736.34	Drift
bc05	Castle farm	330.17	735.58	Drift
bc04	Forest	327.76	734.30	Drift
bc03	Littleton farm	326.48	733.92	Drift
bc02	Lochton farm	324.58	733.22	Drift
bc01	Balloleys farm	322.88	732.50	Quarry
bc00	Hoolmyre farm	321.80	731.49	Drift

LINE 6 - COLLACE QUARRY - SITE LOCATIONS

Quarry location: Easting 320.76 Northing 731.59
Quarry type: Basalt.

SITE NUMBER	SITE NAME	EASTING	NORTHING	GEOPHONE COUPLING
co01	Balloleys farm	322.88	732.50	Drift
co03	Littleton farm	326.48	733.92	Drift
co04	Woods	327.58	734.40	Drift
co06	West Adamston	332.02	736.34	Drift
co08	Balbeuchley farm	335.69	737.92	Drift
co09	North Balluderen	337.59	738.72	Drift
co11	Mansefield farm	341.33	740.28	Drift

APPENDIX 3. GLASGOW SEISMIC RECORDER SPECIFICATIONS

GLASGOW FM MARK 2 SEISMIC RECORDER

SPECIFICATIONS

Detector: Mark Products L15B 4.5 Hz geophones with 600 ohm coil, or alternative.

Amplifier Gain: adjustable 88-118 dB in 6 dB steps; second output at 18 dB lower than first; clipped 10 V p-p (less for better linearity). Input resistance of 4.7 k-ohm for 0.65 of critical damping of L15B geophones.

Modulator: central frequency is 2 kHz; frequency deviation for 10 V p-p input is +/- 100%: current output is 250 A.

Recording: saturation.

Demodulator: produces 2 V output for maximum modulator input (10 V); 14 dB loss reduces overall system gain to the range 56-104 dB (including both gain output).

Playback filters: Kemo VBF/3.

Oscillograph: Bryans 40000 6-channel.

System frequency response: direct connection of modulator to modulator; 3 dB down points give approximate pass-band of 2-60 Hz.

Noise and distortion: system noise limits dynamic range to 46 dB at maximum gain. Distortion is less than 1% at 70% of clipping level.

Wow and flutter: less than 0.25% .

Power Requirements: Amplifier-modulator 20 mA; 18V. Recorder (during recording) 115 mA; 18V.

Cassette recorder: Tape speed 4.74 cm/s

APPENDIX 4. OBSERVED TRAVEL TIMES

Reduction velocity used in calculating reduced times is 6.0 km/s.

LINE 1: MELROSE SHOT

OBSERVED TRAVEL TIMES - PRIMARY WAVES

SITE	RANGE (km)	FIELD GAIN	TRAVEL TIME (s)	RED TIME (s)
mb01	1.87	1	0.55	0.24
mb02	4.00	1	1.01	0.34
mb03	5.76	2	1.36	0.40
mb04	7.70	3	1.75	0.47
mb05	9.99	3	2.18	0.51
mb06	12.08	3	2.54	0.53
mb07	13.79	5	2.82	0.52
mb08	15.58	5	3.12	0.52
mb08a	17.11	3	3.37	0.51
mb09	17.88	6	3.50	0.52
mb10	20.00	4	3.94	0.61
mb11	22.31	4	4.39	0.67
mb12	24.08	3	4.60	0.59
mb12a	25.22	3	4.79	0.58
mb13	25.94	5	4.89	0.56
mb14	28.79	3	5.41	0.61
mb15	29.97	4	5.60	0.61
mb15a	31.24	3	5.79	0.59
mb16	32.55	5	6.08	0.65
mb17	34.15	3	6.39	0.69
mb18	36.40	5	6.78	0.71
mb19	38.31	5	7.06	0.75
mb00	40.70	3	7.54	0.75

LINE 1: MELROSE SHOT

OBSERVED TRAVEL TIMES - SHEAR WAVES

SITE	RANGE (km)	FIELD GAIN	TRAVEL TIME (s)	RED TIME (s)
mb06	12.08	3	5.26	3.25
mb07	13.79	5	5.99	3.69
mb08	15.58	5	6.60	4.00
mb08a	17.11	3	7.13	4.28
mb09	17.88	6	7.45	4.47

LINE 1: BANGLEY SHOT

OBSERVED TRAVEL TIMES - PRIMARY WAVES

SITE	RANGE (km)	FIELD GAIN	TRAVEL TIME (s)	RED TIME (s)
bm19	2.27	1	0.62	0.24
bm18	4.19	1	1.11	0.41
bm17	6.43	2	1.65	0.58
bm16	8.03	3	1.99	0.65
bm15	10.61	4	2.37	0.60
bm14	11.81	3	2.52	0.55
bm13a	13.72	5	2.90	0.62
bm13	14.67	5	2.95	0.51
bm12a	15.40	5	3.13	0.57
bm12	16.52	3	3.35	0.60
bm11	18.29	3	3.47	0.43
bm10	20.58	4	3.95	0.52
bm09	22.71	3	4.37	0.58
bm08	24.74	3	4.64	0.52
bm07	26.79	5	5.02	0.56
bm06	28.51	3	5.39	0.63
bm05	30.59	4	5.83	0.73
bm04	32.88	4	6.26	0.78
bm03	34.87	6	6.60	0.79

LINE 1: BANGLEY SHOT

OBSERVED TRAVEL TIMES - SHEAR WAVES

SITE	RANGE (km)	RED TIME
bm19	2.27	1.22
bm18	4.19	1.70
bm17	6.43	2.14
bm16	8.03	2.18
bm15	10.61	2.70
bm14	11.81	2.84
bm13a	13.72	3.09
bm13	14.67	3.18
bm12a	15.40	3.29
bm12	16.52	3.41
bm11	18.29	3.14
bm10	20.58	3.66
bm09	22.71	4.03
bm08	24.74	3.41
bm07	26.79	3.66
bm06	28.51	4.16
bm05	30.59	4.49
bm04	32.88	5.01

LINE 2: MELROSE SHOT

OBSERVED TRAVEL TIMES - PRIMARY WAVES

SITE	RANGE (km)	FIELD GAIN	TRAVEL TIME (s)	RED TIME (s)
mr01	1.31	1	0.36	0.14
mr02	3.68	1	0.89	0.27
mr03	5.91	2	1.38	0.40
mr04	7.89	2	1.71	0.39
mr05	9.83	3	2.07	0.43
mr06	11.80	2	2.45	0.48
mr07	13.47	4	2.73	0.48
mr08	15.75	4	3.17	0.55
mr09	17.68	4	3.55	0.60
mr10	20.04	3	3.97	0.63
mr11	22.15	4	4.40	0.70
mr12	23.83	4	4.66	0.68
mr13	25.00	4	4.85	0.68
mr13a	26.81	3	5.13	0.66
mr14	27.98	4	5.37	0.70
mr15	29.92	5	5.66	0.67
mr15a	31.00	4	5.84	0.67
mr16	32.95	4	6.26	0.77
mr17	34.24	3	6.48	0.77
mr18	35.86	4	6.71	0.73
mr19	38.20	4	7.12	0.75
mr20	40.07	3	7.38	0.70
mr21	42.11	4	7.73	0.71

LINE 2: MELROSE SHOT

OBSERVED TRAVEL TIMES - SHEAR WAVES

SITE	RANGE (km)	FIELD GAIN	TRAVEL TIME (s)	RED TIME (s)
mr01	1.31	1	1.00	0.78
mr02	3.68	1	2.07	1.46
mr03	5.91	2	3.45	2.50
mr04	7.89	2	3.44	2.12
mr05	9.83	2	3.83	2.19
mr06	11.80	2	4.37	2.41
mr07	13.47	4	4.81	2.56
mr08	15.75	4	5.69	3.07
mr09	17.68	4	6.32	3.37
mr10	20.04	3	7.21	3.87
mr11	22.15	4	8.20	4.56
mr12	23.83	4	8.60	4.62
mr13	25.00	4	8.92	4.75
mr13a	26.81	3	9.66	5.19
mr14	27.98	4	10.04	5.37
mr16	32.95	4	10.04	5.37
mr16	32.95	4	11.54	6.05
mr17	34.24	3	11.78	6.08
mr18	35.86	4	12.35	6.37
mr19	38.20	4	13.12	6.75
mr20	40.07	3	13.83	7.16
mr21	42.11	4	14.33	7.31

LINE 2: RATHO SHOT

OBSERVED TRAVEL TIMES - PRIMARY WAVES

SITE	RANGE (km)	FIELD GAIN	TRAVEL TIME (s)	RED TIME (s)
ra28	2.14	1	0.64	0.28
ra27	4.04	1	1.13	0.45
ra26	6.15	1	1.51	0.48
ra25	7.63	1	1.78	0.51
ra24	10.22	2	2.28	0.58
ra23	12.07	2	2.68	0.66
ra22	13.68	1	3.09	0.81
ra21	16.13	3	3.57	0.88
ra20	18.19	3	3.95	0.92
ra19	20.04	4	4.23	0.89
ra18	22.44	3	4.65	0.91
ra17	24.01	4	4.89	0.89
ra16	25.28	4	5.14	0.92
ra15a	27.32	3	5.40	0.84
ra15	28.32	3	5.52	0.80
ra14	30.29	4	5.89	0.84
ra13a	31.52	3	6.08	0.82
ra13	33.26	4	6.46	0.92
ra12	33.26	4	6.56	0.82
ra11	36.18	4	6.88	0.78
ra10	38.20	4	7.21	0.84
ra09	40.64	4	7.63	0.86
ra08	42.57	5	7.93	0.83
ra07	44.85	5	8.31	0.84
ra06	46.53	4	8.63	0.87
ra05	48.49	5	8.91	0.83
ra04	50.44	5	9.24	0.84
ra03	52.33	4	9.60	0.87
ra02	54.57	5	9.97	0.88
ra01	56.83	5	10.34	0.87
ra00	59.45	4	10.80	0.89
ra33	60.15	4	10.90	0.87
ra55	64.47	5	11.55	0.81

LINE 2: RATHO SHOT

OBSERVED TRAVEL TIMES - SHEAR WAVES

SITE	RANGE (km)	FIELD GAIN	TRAVEL TIME (s)	RED TIME (s)
ra28	2.14	1	1.17	0.81
ra27	4.04	1	2.11	1.44
ra26	6.15	1	2.71	1.69
ra25	7.63	1	3.33	2.06
ra24	10.22	2	4.26	2.56
ra21	16.13	3	6.63	3.94
ra20	18.19	3	7.47	4.44
ra18	22.44	3	8.55	4.81
ra17	24.01	4	8.88	4.87
ra16	25.28	4	9.21	5.00
ra15a	27.32	3	9.53	5.00
ra15	28.32	3	9.80	5.07
ra14	30.29	4	10.36	5.31
ra13a	31.52	3	10.69	5.44
ra12	34.44	4	11.68	5.94
ra11	36.18	4	12.47	6.44

LINE 3: ABERDOUR SHOT

OBSERVED TRAVEL TIMES - PRIMARY WAVES

SITE	RANGE (km)	FIELD GAIN	TRAVEL TIME (s)	RED TIME (s)
ab01	8.07	2	2.07	0.72
ab02	9.66	1	2.41	0.80
ab03	11.80	3	2.86	0.89
ab04	14.85	2	3.50	1.03
ab05	16.18	3	3.68	0.98
ab06	18.05	3	4.00	1.00
ab07	20.86	3	4.50	1.02
ab08	23.22	4	4.92	1.05
ab09	25.13	4	5.17	0.98
ab11	29.50	5	5.92	1.01
ab12	30.78	4	6.07	0.94
ab13	32.42	4	6.36	0.96
ab14	34.80	4	6.70	0.90
ab15	36.80	4	7.08	0.94
ab16	38.41	4	7.30	0.90
ab17	40.44	3	7.75	1.01
ab18	42.52	4	8.09	1.01
ab19	44.73	4	8.46	1.01
ab20	46.95	5	8.87	0.85
ab21	49.06	4	9.01	0.83
ab22	50.77	4	9.29	0.83
ab23	52.82	4	9.56	0.76
ab24	54.45	4	9.80	0.73
ab25	57.54	5	10.26	0.67

LINE 3: ABERDOUR SHOT

OBSERVED TRAVEL TIMES - SHEAR WAVES

SITE	RANGE (km)	FIELD GAIN	TRAVEL TIME (s)	RED TIME (s)
ab01	8.07	2	4.02	2.67
ab02	9.66	1	4.67	3.06
ab03	11.80	3	5.54	3.75
ab04	14.85	2	6.81	4.34
ab05	16.18	3	6.95	4.25
ab06	18.05	3	7.62	4.61
ab07	20.86	3	8.97	4.89
ab08	23.22	4	9.14	5.27
ab09	25.13	4	9.72	5.53
ab11	29.50	5	10.92	6.00

LINE 3: RATHO SHOT

OBSERVED TRAVEL TIMES - PRIMARY WAVES

SITE	RANGE (km)	FIELD GAIN	TRAVEL TIME (s)	RED TIME (s)
rt06	2.10	1	0.45	0.10
rt07	4.16	1	0.94	0.25
rt08	6.58	1	1.49	0.39
rt09	8.68	1	1.90	0.45
rt11	12.88	5	2.71	0.56
rt12	14.21	3	2.89	0.52
rt13	15.96	3	3.22	0.55
rt14	18.28	3	3.64	0.60
rt15	20.37	3	4.04	0.65
rt16	21.88	3	4.31	0.66
rt17	23.90	2	4.69	0.70
rt18	25.99	3	5.08	0.75
rt19	28.19	4	5.41	0.71
rt20	30.38	4	5.78	0.72
rt21	32.57	4	6.12	0.70
rt22	34.27	4	6.39	0.68
rt23	36.37	3	6.69	0.63
rt24	37.93	4	6.94	0.62
rt25	41.08	4	7.40	0.55
rt26	42.32	3	7.62	0.57
rt27	44.31	3	7.93	0.54
rt28	46.13	4	8.21	0.52
rt29	48.25	5	8.57	0.53
rt30	50.41	3	8.93	0.53
rt31	52.01	4	9.34	0.67
rt34	58.31	4	10.37	0.65
rt35	60.54	5	10.69	0.60
rt36	62.75	4	11.12	0.66
rt37	63.64	4	11.25	0.64
rt38	66.39	5	11.71	0.64

LINE 3: RATHO SHOT

OBSERVED TRAVEL TIMES - SHEAR WAVES

SITE	RANGE (km)	FIELD GAIN	TRAVEL TIME (s)	RED TIME (s)
rt06	2.10	1	1.12	0.77
rt07	4.16	1	2.04	1.34
rt08	6.58	1	3.15	2.06
rt09	8.68	1	3.82	2.37
rt11	12.88	5	4.89	2.74
rt12	14.21	3	5.17	2.80
rt13	15.96	3	5.85	3.19
rt14	18.28	3	6.48	3.44
rt15	20.37	3	7.33	3.94
rt16	21.88	3	7.56	4.31
rt17	23.90	2	8.48	4.50
rt18	25.99	3	9.26	4.92
rt19	28.19	4	9.76	5.06
rt20	30.38	4	10.26	5.20
rt21	32.57	4	10.99	5.56
rt22	34.27	4	11.43	5.72
rt23	36.37	3	11.94	5.88
rt24	37.93	4	12.38	6.06
rt25	41.08	4	12.97	6.12
rt26	42.32	3	13.30	6.25
rt27	44.31	3	13.88	6.50
rt28	46.13	4	14.23	6.54
rt29	48.25	5	14.73	6.69
rt30	50.41	3	15.46	7.06
rt31	52.01	4	16.60	7.94

LINE 4: GLENLUCE SHOT

OBSERVED TRAVEL TIMES - PRIMARY WAVES

SITE	RANGE (km)	FIELD GAIN	TRAVEL TIME (s)	RED TIME (s)
gt01	2.11	1	0.38	0.03
gt02	4.08	1	0.78	0.10
gt03	5.49	1	1.05	0.13
gt04	8.34	1	1.53	0.14
gt05	10.08	3	1.86	0.18
gt06	11.41	2	2.10	0.20
gt06a	12.68	3	2.40	0.29
gt07	13.98	2	2.57	0.24
gt08	16.44	2	2.97	0.23
gt8a	17.25	4	3.13	0.25
gt09	18.17	4	3.30	0.27
gt10	20.28	3	3.71	0.33
gt11	22.72	3	4.10	0.32
gt12	23.96	4	4.36	0.37
gt13	26.20	3	4.71	0.35
gt14	28.16	4	5.08	0.38
gt15	30.46	4	5.48	0.40
gt16	32.27	4	5.76	0.38
gt17	34.75	4	6.19	0.40
gt18	35.85	4	6.36	0.38
gt00	38.58	4	6.80	0.37
gt33	40.05	4	7.06	0.39
gt44	42.26	2	7.42	0.38
gt66	45.88	4	8.12	0.48
gt77	48.16	3	8.51	0.48
gt88	50.00	3	8.82	0.49

LINE 4: GLENLUCE SHOT

OBSERVED TRAVEL TIMES - SHEAR WAVES

SITE	RANGE (km)	FIELD GAIN	TRAVEL TIME (s)	RED TIME (s)
gt02	4.08	1	1.43	0.75
gt03	5.49	1	1.95	1.03
gt04	8.34	1	2.89	1.50
gt05	10.08	3	3.27	1.59
gt06	11.41	2	3.73	1.82
gt06a	12.68	3	4.17	2.06
gt07	13.98	2	4.52	2.19
gt08	16.44	2	5.08	2.34
gt8a	17.25	4	5.50	2.62
gt09	18.17	4	5.71	2.69
gt10	20.28	3	6.42	3.04
gt11	22.72	3	7.17	3.38
gt12	23.96	4	7.55	3.56
gt13	26.20	3	8.11	3.74
gt14	28.16	4	8.64	3.95
gt15	30.46	4	9.48	4.40
gt16	32.27	4	9.94	4.56
gt17	34.75	4	10.67	4.87
gt18	35.85	4	11.10	5.12
gt00	38.58	4	11.74	5.31
gt66	45.88	4	14.65	7.00
gt77	48.16	3	15.33	7.30
gt88	50.00	3	15.83	7.50

LINE 4: TORMITCHELL SHOT

OBSERVED TRAVEL TIMES - PRIMARY WAVES

SITE	RANGE (km)	FIELD GAIN	TRAVEL TIME (s)	RED TIME (s)
tm18	2.55	1	0.50	0.08
tm17	3.84	1	0.77	0.13
tm16	6.00	1	1.15	0.15
tm15	7.78	2	1.48	0.19
tm14	10.08	3	1.92	0.24
tm13	12.00	2	2.31	0.30
tm12	14.05	4	2.67	0.33
tm11	15.56	3	2.89	0.30
tm10	18.04	3	3.36	0.35
tm09	20.06	4	3.72	0.38
tm08a	20.96	5	3.84	0.35
tm08	21.77	4	4.01	0.38
tm07	24.26	4	4.41	0.36
tm06a	25.55	4	4.56	0.31
tm06	26.94	3	4.82	0.33
tm05	28.23	4	5.06	0.36
tm04	29.90	4	5.35	0.37
tm03	32.66	4	5.85	0.41
tm02	34.16	3	6.08	0.38
tm01	36.19	3	6.39	0.36
tm00	38.71	3	6.83	0.38
tm33	40.11	4	7.09	0.40
tm44	41.42	4	7.31	0.41

LINE 4: TORMITCHELL SHOT

OBSERVED TRAVELL TIMES - SHEAR WAVES

SITE	RANGE (km)	FIELD GAIN	TRAVEL TIME (s)	RED TIME (s)
tm18	2.55	1	1.18	0.76
tm17	3.84	1	1.58	0.94
tm16	6.00	1	1.97	0.97
tm15	7.78	2	3.04	1.74
tm14	10.08	3	3.54	1.86
tm13	12.00	2	4.20	2.20
tm12	14.05	4	4.84	2.50
tm11	15.56	3	5.25	2.66
tm10	18.04	3	5.95	2.94
tm09	20.06	4	6.52	3.18
tm08a	20.96	5	6.81	3.32
tm08	21.77	4	7.13	3.50
tm07	24.26	4	7.02	2.97
tm06a	25.55	4	7.74	3.49
tm06	26.94	3	8.23	3.74
tm05	28.23	4	8.76	4.06
tm04	29.90	4	9.30	4.31
tm03	32.66	4	10.13	4.69
tm02	34.16	3	10.72	5.03
tm01	36.19	3	10.75	4.72
tm00	38.71	3	11.59	5.14
tm33	40.11	4	12.07	5.39
tm44	41.42	4	12.50	5.59

LINE 5: GLENLUCE SHOT

OBSERVED TRAVEL TIMES - PRIMARY WAVES

SITE	RANGE (km)	FIELD GAIN	TRAVEL TIME (s)	RED TIME (s)
gn02	4.15	1	0.73	0.04
gn04	8.16	1	1.42	0.06
gn05	10.09	1	1.79	0.10
gn06	12.34	1	2.17	0.11
gn09	18.33	2	3.15	0.10
gn10	20.93	2	3.64	0.16
gn11	22.61	2	3.88	0.11

LINE 5: GLENLUCE SHOT

OBSERVED TRAVEL TIMES - SHEAR WAVES

SITE	RANGE (km)	FIELD GAIN	TRAVEL TIME (s)	RED TIME (s)
gn02	4.15	1	1.49	0.80
gn04	8.16	1	2.81	1.45
gn05	10.09	1	3.38	1.70
gn06	12.34	1	3.87	1.80
gn09	18.33	2	5.55	2.50
gn10	20.93	2	6.29	2.80

LINE 6: BOYSACK SHOT

OBSERVED TRAVEL TIMES - PRIMARY WAVES

SITE	RANGE (km)	FIELD GAIN	TRAVEL TIME (s)	RED TIME (s)
bc22	1.43	1	0.41	0.17
bc20	5.42	2	1.22	0.32
bc19	7.10	2	1.60	0.41
bc18	9.48	2	2.05	0.47
bc17	11.30	3	2.41	0.52
bc16	13.56	3	2.84	0.58
bc15	15.69	3	3.21	0.59
bc14	17.34	3	3.55	0.65
bc13	19.23	3	3.97	0.76
bc12	21.40	3	4.29	0.72
bc11	23.43	4	4.64	0.74
bc10	25.27	3	4.97	0.76
bc09	27.48	4	5.27	0.69
bc08	29.54	4	5.64	0.72
bc07	31.57	4	6.00	0.74
bc06	33.53	4	6.43	0.76
bc05	35.53	4	6.75	0.82
bc04	38.25	4	7.21	0.83
bc03	39.58	3	7.47	0.87
bc02	41.60	3	7.72	0.79
bc01	43.45	5	8.05	0.81
bc00	44.84	4	8.30	0.83

LINE 6: BOYSACK SHOT

OBSERVED TRAVEL TIMES - SHEAR WAVES

SITE	RANGE (km)	FIELD GAIN	TRAVEL TIME (s)	RED TIME (s)
bc22	1.43	1	1.24	1.00
bc20	5.42	2	2.61	1.71
bc19	7.10	2	3.16	1.98
bc18	9.48	2	3.89	2.31
bc17	11.30	3	4.44	2.56
bc15	15.69	3	5.99	3.37
bc14	17.34	3	6.55	3.65
bc12	21.40	3	7.57	4.00
bc11	23.43	4	8.18	4.28
bc10	25.27	3	8.84	4.63
bc09	27.48	4	9.27	4.69
bc08	29.54	4	10.11	5.19
bc07	31.57	4	10.69	5.42
bc06	33.53	4	11.46	5.87
bc05	35.53	4	11.61	5.69
bc03	39.58	3	13.38	6.72
bc02	41.60	3	13.71	6.78
bc01	43.45	5	14.30	7.06
bc00	44.84	4	14.88	7.41

APPENDIX 5. PLUS-MINUS ANALYSIS

Note that the absence of a T- indicates that the T+ term and depth are a result of extrapolation.

LINE 1: MELROSE-BANGLEY				
SITE	DISTANCE (km)	T- (s)	T+ (s)	DEPTH (km)
12	24.08	1.25	0.43	1.57
12a	25.22	1.65	0.40	1.47
13	25.94	1.93	0.32	1.18
14	28.79	2.89	0.41	1.51
15	29.97	3.23	0.45	1.65
15a	31.24	-	0.41	1.14
16	32.55	-	0.54	1.51
17	34.15	-	0.62	1.72
18	36.40	-	0.65	1.80
19	38.31	-	0.57	1.58
20	40.70	-	0.72	2.00

LINE 2: MELROSE-RATHO				
SITE	DISTANCE (km)	T- (s)	T+ (s)	DEPTH (km)
55	-6.23	-	0.39	2.24
33	-1.90	-	0.50	2.88
00	-1.24	-	0.54	3.09
01	1.31	-	0.48	2.77
02	3.68	-	0.49	2.84
03	5.91	-	0.48	2.77
04	7.89	-	0.40	2.32
05	9.83	-	0.38	2.20
06	11.80	-	0.46	2.65
07	13.47	-	0.38	2.20
08	15.75	-	0.37	2.10
09	17.68	-	0.41	2.33
10	20.04	-	0.37	2.14
11	22.15	-2.41	0.40	2.28
12	23.83	-1.91	0.41	2.38
13	24.00	-1.61	0.50	2.88
13a	26.81	-0.94	0.40	2.31
14	27.98	-0.52	0.45	2.58
15	29.92	0.13	0.37	2.15
16	32.95	1.12	0.59	3.39
17	34.24	1.58	0.56	3.24
18	35.86	2.06	0.55	3.17
19	38.20	2.89	0.55	3.14
20	40.07	3.42	0.53	3.03
21	42.11	4.15	0.49	2.84

LINE 3: RATHO-MOFFAT			
SITE	DISTANCE (km)	TIME DIFF. (s)	DEPTH DIFF. (km)
21	32.57	-0.03	0.22
22	34.27	-0.07	0.43
23	36.37	-0.15	0.98
24	37.93	-0.17	1.07
25	41.08	-0.30	1.89
26	42.32	-0.25	1.60
27	44.31	-0.30	1.94
28	46.13	-0.34	2.15
29	48.25	-0.31	2.00
30	50.41	-0.31	1.97
31	52.01	-0.01	0.08
34	58.31	-0.03	0.22
35	60.54	-0.13	0.85
36	62.75	-0.01	0.08
37	63.64	-0.04	0.28
38	66.39	-0.03	0.18

LINE 4: GLENLUCE-TORMITCHELL				
SITE	DISTANCE (km)	T- (s)	T+ (s)	DEPTH (km)
01	2.05	-	0.21	1.43
02	4.08	-	0.28	1.93
03	5.58	-	0.34	2.38
04	8.34	-	0.29	2.02
05	10.01	-	0.29	2.01
06	11.30	-	0.28	1.95
6a	12.68	2.16	0.21	1.48
07	13.98	1.84	0.22	1.56
08	16.44	1.04	0.23	1.88
8a	17.25	0.71	0.22	1.76
09	18.17	0.42	0.26	2.13
10	20.28	-0.34	0.31	2.55
11	22.72	-1.21	0.24	1.95
12	23.96	-1.69	0.28	2.26
13	26.20	-2.41	0.27	1.84
15	30.46	-	0.31	2.09
16	32.27	-	0.26	1.80
17	34.75	-	0.30	2.08
18	35.85	-	0.28	1.93
00	38.58	-	0.27	1.82
33	40.05	-	0.29	2.01
44	42.26	-	0.25	1.71
66	45.88	-	0.48	3.25
77	48.16	-	0.49	3.38
88	50.00	-	0.51	3.50
00	-0.47	-	0.21	1.48
33	-1.87	-	0.25	1.73
44	-3.18	-	0.25	1.76

APPENDIX 6. RAYTRACING RESULTS

This appendix compares times computed by raytracing with the observed values. A (+) value for a discrepancy indicates a computed time that is later than the observed.

Discrepancies are arranged by line and then shotpoint. Ray codes show the type of first arrival and the causal layer: a0 - direct arrivals; a1 - headwaves from a sedimentary refractor; a2 - headwaves from crystalline basement. An agreement of the times to within 0.03 s is considered "good".

LINE 2, MELROSE SHOT.

Station number	Code	Discrepancy (s)
mr01	a0	+ 0.05
mr02	a0	0.00
mr03	a0	+ 0.03
mr04	a1	0.00
mr05	a1	0.00
mr06	a1	0.00
mr07	a1	+ 0.03
mr08	a1	+ 0.02
mr09	a1	+ 0.01
mr10	a1	+ 0.04
mr11	a2	- 0.05
mr12	a2	- 0.03
mr13	a2	- 0.03
mr14	a2	0.00
mr15	a2	- 0.01
mr16	a2	0.00
mr17	a2	- 0.01
mr18	a2	+ 0.02
mr19	a2	- 0.01
mr20	a2	+ 0.04
mr21	a2	+ 0.02

LINE 2, RATHO SHOT.

Station number	Code	Discrepancy (s)
ra28	a0	- 0.04
ra27	a0	+ 0.02
ra26	a1	0.00
ra25	a1	+ 0.01
ra24	a1	+ 0.02
ra23	a1	0.00
ra22	a1	- 0.07
ra21	a2	+ 0.04
ra20	a2	0.00
ra19	a2	+ 0.03
ra18	a2	+ 0.02
ra17	a2	+ 0.03
ra16	a2	- 0.01
ra15	a2	+ 0.02
ra14	a2	- 0.01
ra13	a2	- 0.06
ra12	a2	+ 0.02
ra11	a2	+ 0.06
ra10	a2	- 0.01
ra09	a2	- 0.03
ra08	a2	- 0.01
ra07	a2	- 0.02
ra06	a2	- 0.06
ra05	a2	- 0.02
ra04	a2	- 0.08
ra03	a2	- 0.05
ra02	a2	- 0.04
ra01	a2	- 0.02
ra00	a2	- 0.03
ra33	a2	- 0.01
ra55	a2	- 0.03

LINE 4, GLENLUCE SHOT.

Station number	Code	Discrepancy (s)
gt01	a0	+ 0.01
gt02	a0	- 0.02
gt03	a0	- 0.02
gt04	a0	+ 0.02
gt05	a0	+ 0.02
gt06	a0	0.00
gt07	a0	+ 0.02
gt08	a1	+ 0.06
gt09	a1	- 0.03
gt10	a1	0.00
gt11	a1	+ 0.01
gt12	a1	- 0.03
gt13	a1	0.00
gt14	a1	- 0.02
gt15	a2	- 0.02
gt16	a2	0.00
gt17	a2	+ 0.01
gt18	a2	+ 0.02
gt19	a2	+ 0.03
gt20	a2	+ 0.01
gt21	a2	+ 0.02
gt22	a2	- 0.01
gt23	a2	0.00
gt24	a2	0.00

LINE 4, TORMITCHELL SHOT.

Station number	Code	Discrepancy (s)
tm18	a1	- 0.01
tm17	a1	- 0.04
tm16	a1	0.00
tm15	a1	- 0.01
tm14	a1	- 0.02
tm13	a2	+ 0.01
tm12	a2	0.00
tm11	a2	+ 0.03
tm10	a1	- 0.02
tm09	a1	- 0.03
tm08	a1	- 0.03
tm07	a1	0.00
tm06	a1	+ 0.05
tm05	a1	0.00
tm04	a1	+ 0.02
tm03	a1	- 0.01
tm02	a1	- 0.02
tm01	a1	+ 0.04
tm00	a1	+ 0.03
tm33	a1	0.00
tm44	a1	- 0.01

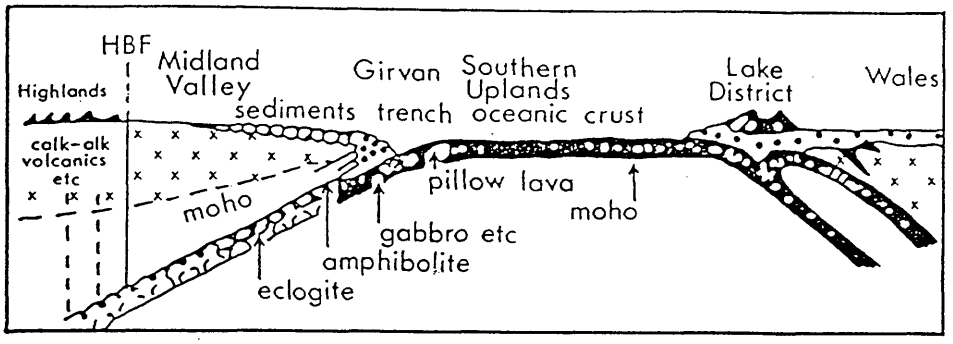

Figure 1.1a Model for the closure of the Iapetus Ocean proposed by Dewey (1969).

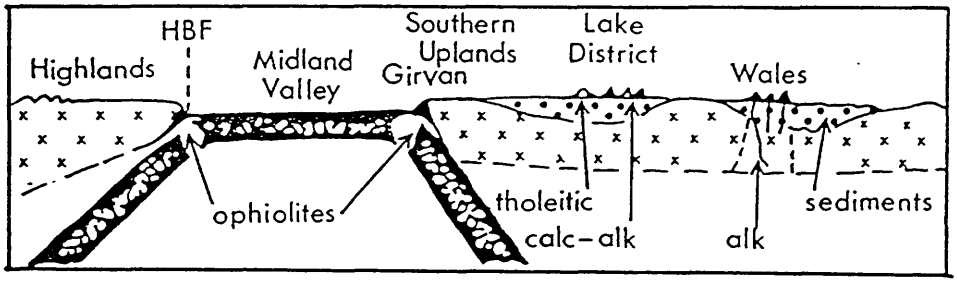

Figure 1.1b Gunn's (1973) model for the closure of the Iapetus Ocean.

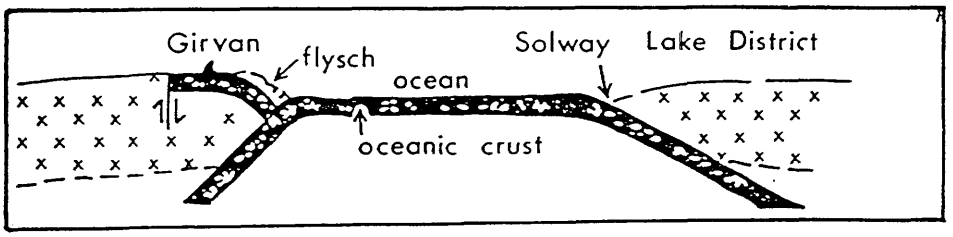

Figure 1.1c Church & Gayer (1973) model for the Iapetus Ocean.

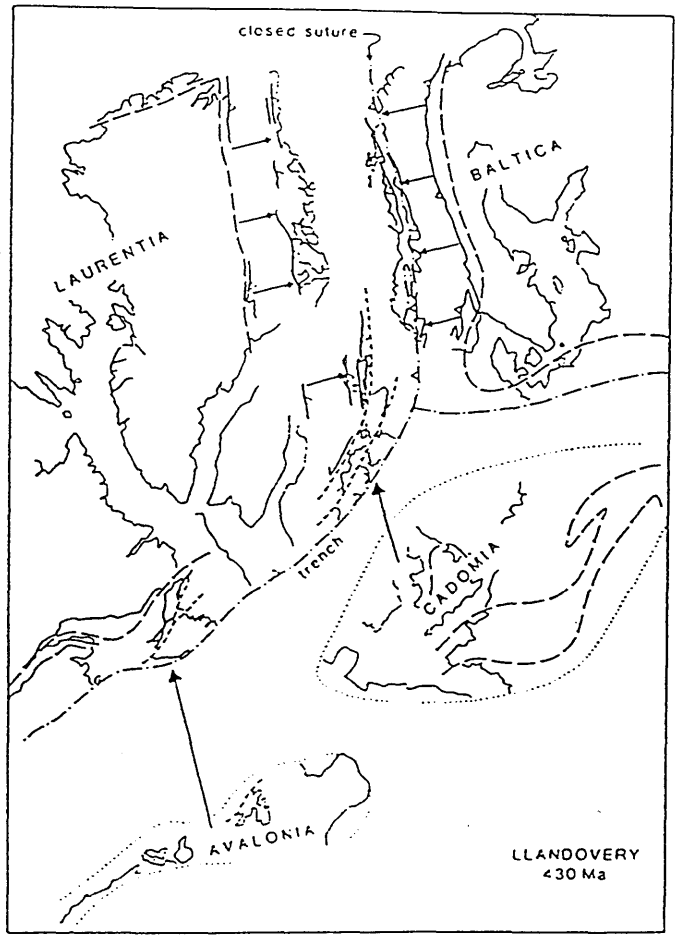

Figure 1.1d Reconstruction of the N Atlantic caledonides in Llandovery time (430 Ma). Collision has already taken place between Baltica and Laurentia. Cadomia has yet to collide with N Britain-S Baltica and Avalonia with the Appalachians (after Soper and Hutton 1984).

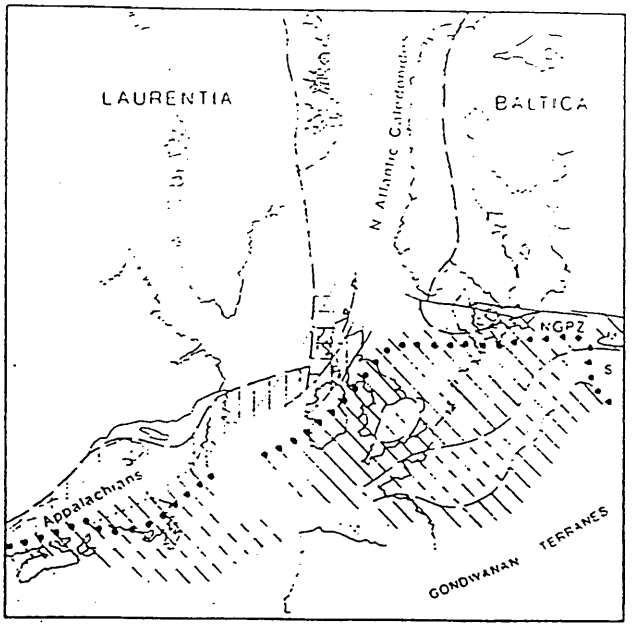

Figure 1.1e Pre-Atlantic reconstruction showing the Y-shaped configuration of the Caledonian-Appalachian orogen:horizontal shading, N Atlantic Caledonides; vertical shading, limit of Appalachian accreted terranes; diagonal shading, late Caledonian and Acadian deformation; small dots, possible locus of major mid-Palaeozoic sinistral strike-slip; large dots, northern limit of Gondwana-derived terranes (after Soper 1988).

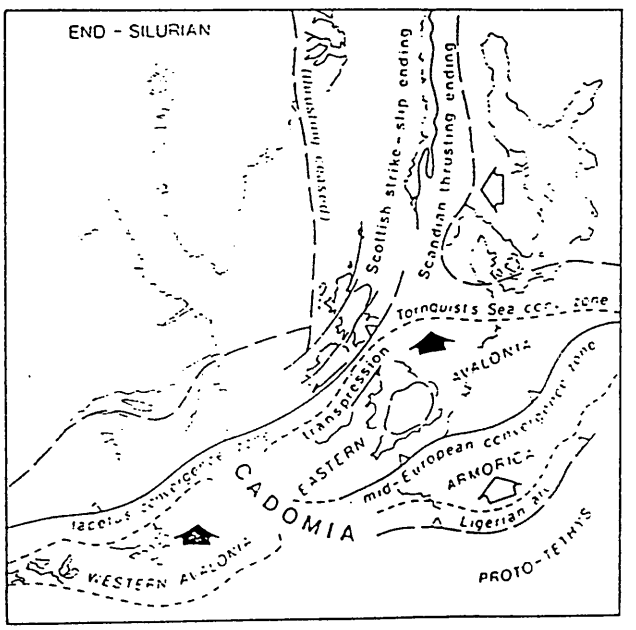

Figure 1.1f Reconstruction of the Caledonides at about the time of the Siluro-Devonian boundary (after Soper 1988).

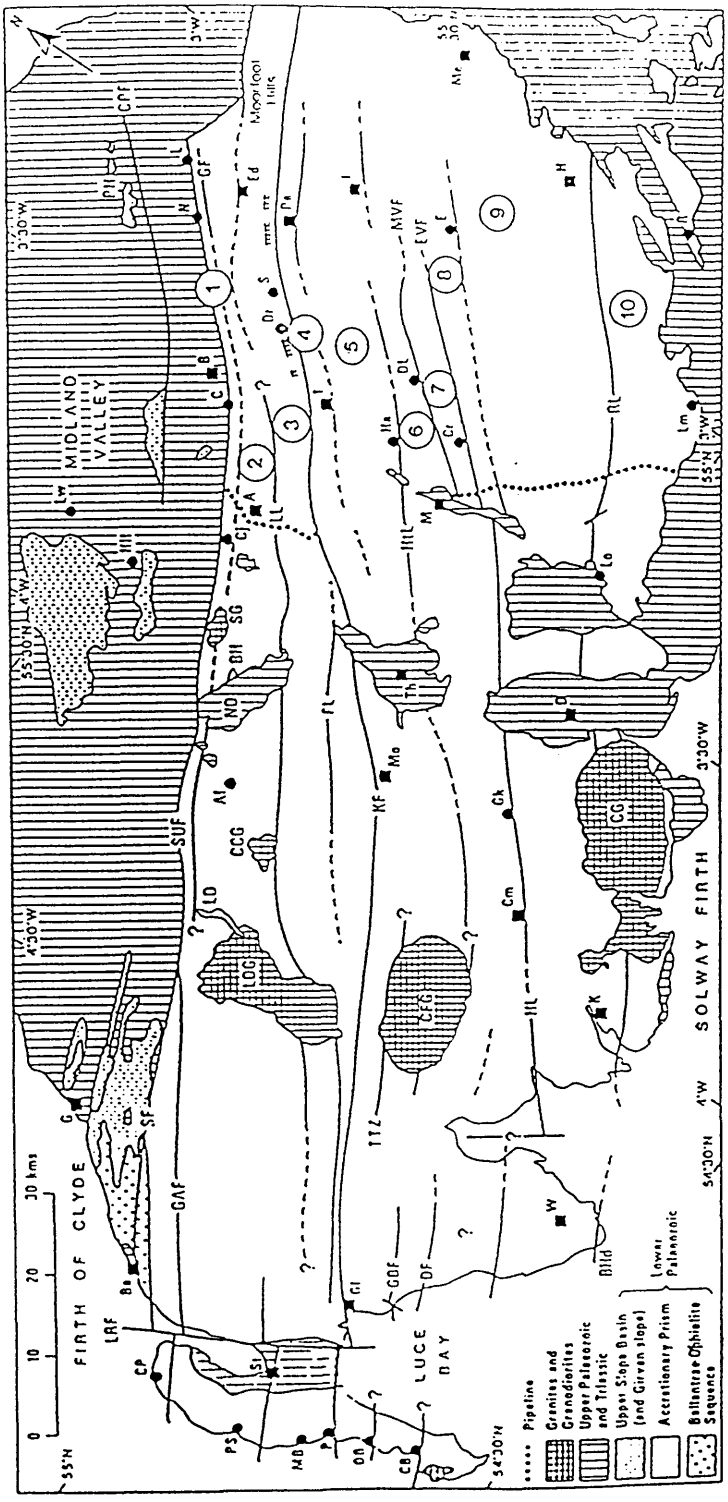

Figure 1.2a Geological map of the Southern Uplands. Major reverse faults separate tracts with distinctive stratigraphic sequences. Numbers refer to tract number, solid lines show major faults; dashed lines show inferred continuations of faults (after Leggett *et al.* 1979b). Abbreviations are explained on the following page.

Faults

CPF Carmichael-Pentland fault
DF Drumlair fault
EVF Ettrick Valley fault
FL Fardingmulloch line
GAF Glan App fault
GBF Gillespie Burn fault
GF Grassfield fault
HL Hawick line
HtL Hartfell line
KF Kibledores fault
KT Killantringan thrust
LL Leadhills line
LRF Loch Ryan fault
MVF Moffat Valley fault
RL Riccarton line
SF Stinchar fault
SUF Southern Uplands fault
TTZ Talnotry Thrust zone

Place names

A Abington
Af Glen afton dam
B Biggar
Ba Ballantrae
BH Bail Hill
BHd Burrow Head
C Coulter
CB Clanyard Bay
Cj Crawfordjohn
Cm Crossmichael
CoB Coldingham
CP Corsewall Point
Cr Craigmichen
D Dumfries
DB Drumbreddan Bay
DL Dobbs Linn
Dr Drummelzier
E Ettrickbridgend
Ed Eddleston
Ey Eyemouth
G Girvan
Gk Glenkiln
GL Glenluce
H Hawick
Ha Hartfell
I Innerleithein
K Kirkcudbright
L Leadburn
La Lauder
LD Loch Doon
M Moffat
MB Morroch Bay
Me Melrose
Mo Moniaive
N Noblehouse
ND Nithsdale
P Portayew
Pe Peebles
PS Portslogan
R Riccarton
S Stobo
St Stranraer
T Talla-Tweedsmuir
Th Thornhill
W Whithorn

Devonian granites

CCG Cairnsmore of Carsphairn
CFG Cairnsmore of Fleet
CG Criffel
LDG Loch Doon
SG Spango Granite

Abbreviations for Figure 1.2a

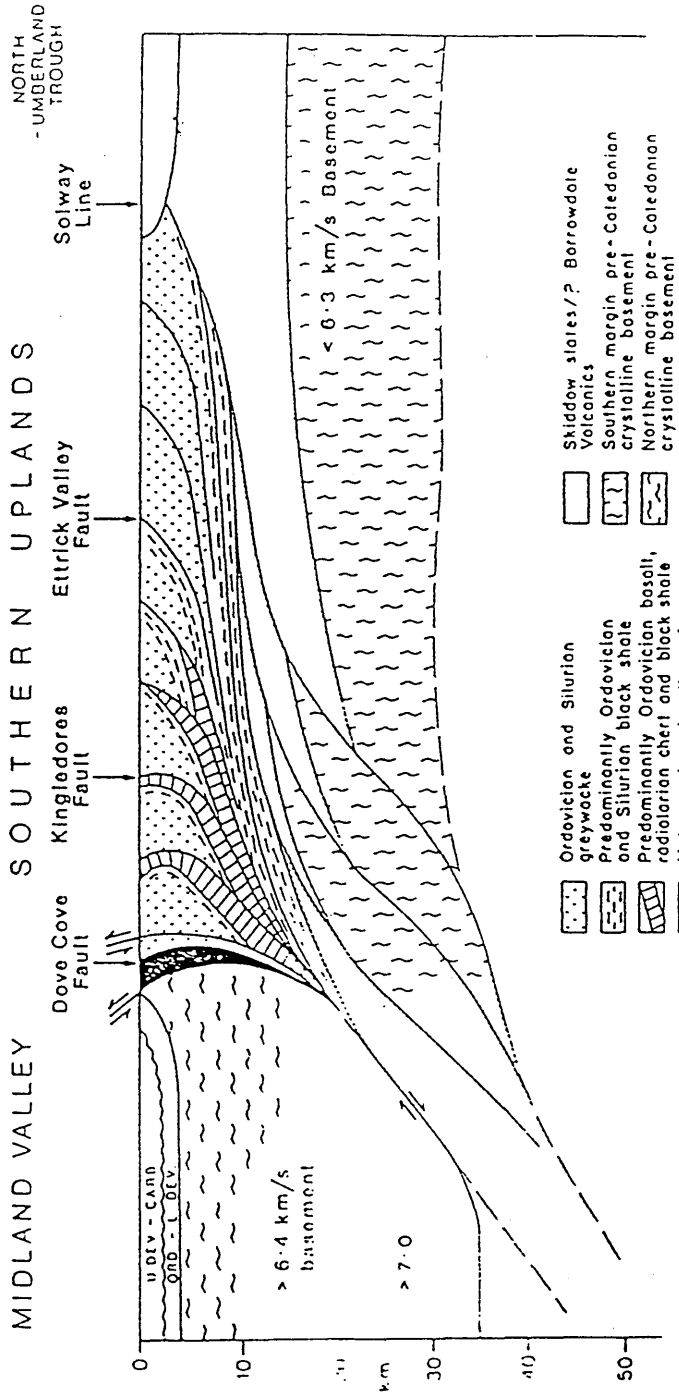

Figure 1.2b Simplified model for the crustal structure of the Southern Uplands (after Leggett *et al.* 1983).

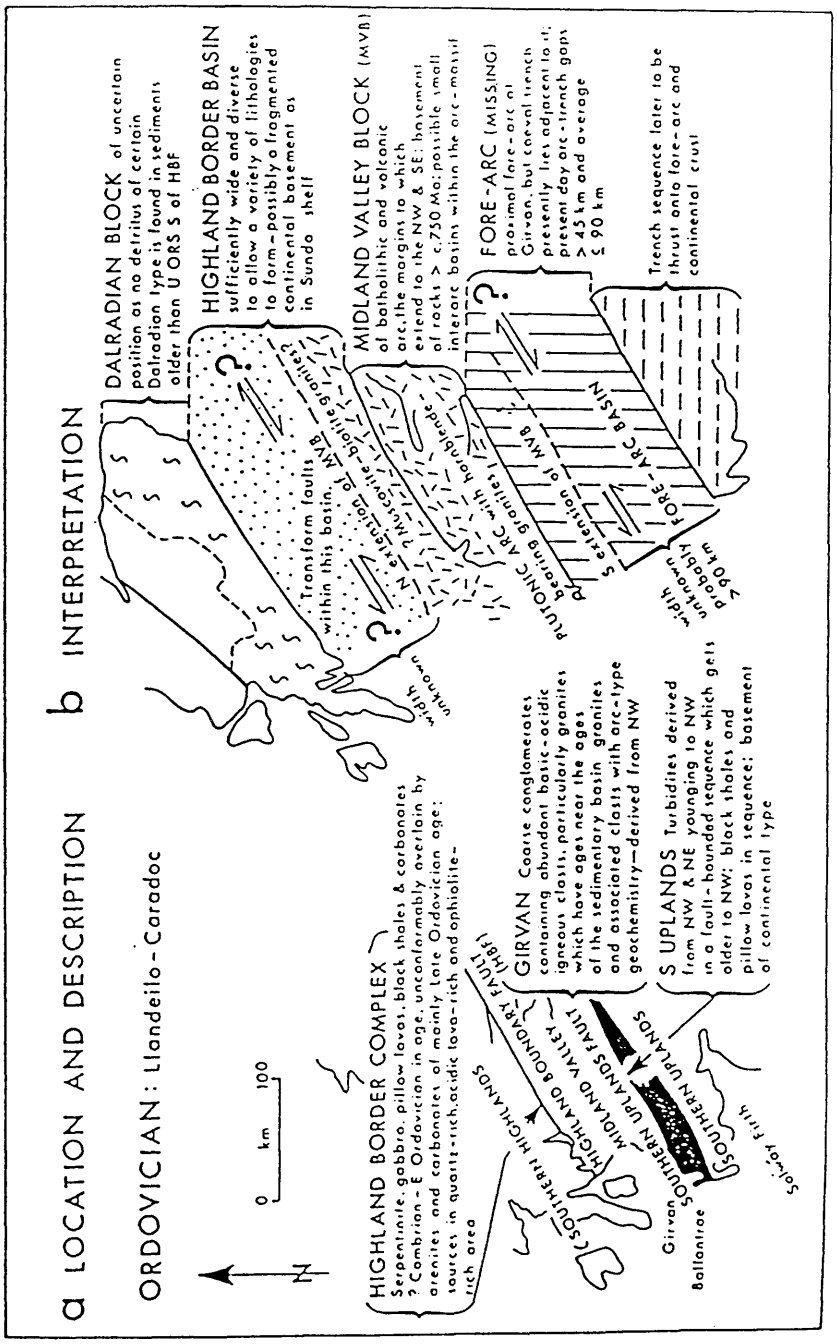

Figure 1.2c Distribution of (a) outcrops of Ordovician rocks and (b) tectonic elements in Ordovician times (after Bluck 1984).

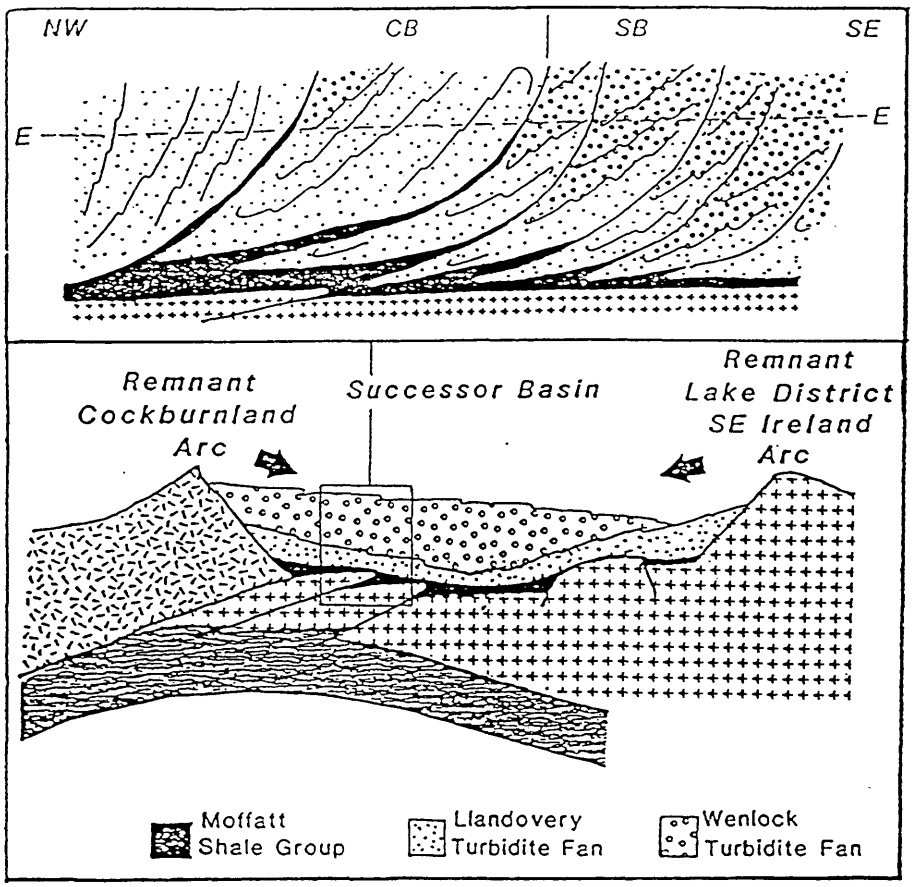

Figure 1.2d Simplified alternative model for Central belt (CB) and Southern belt (SB) of the Southern Uplands (E-E = approximate erosion level). Bottom sketch illustrates infill of Silurian successor basin (after Murphy and Hutton 1986).

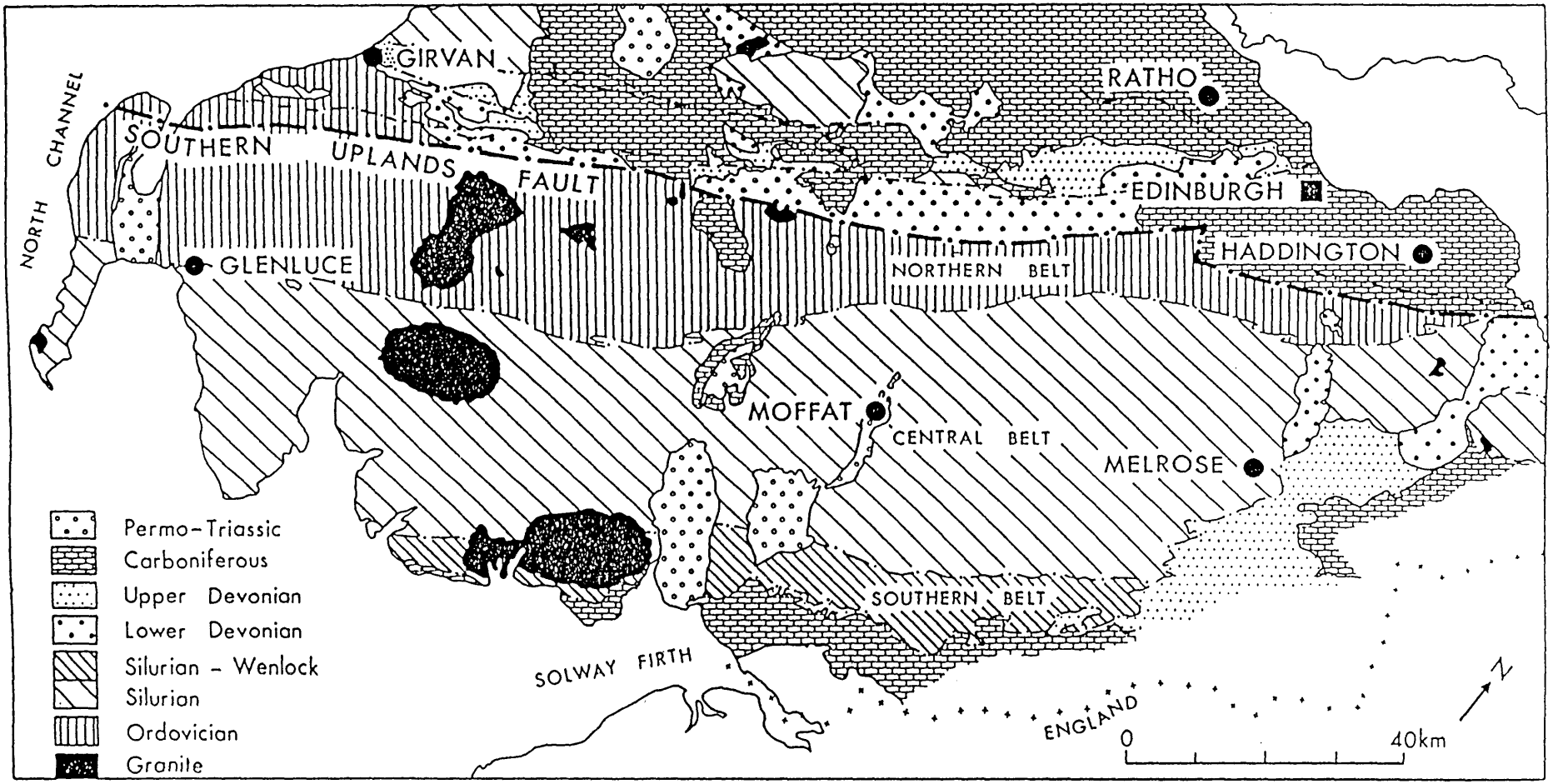

Figure 1.3 Geological map of the Southern Uplands.

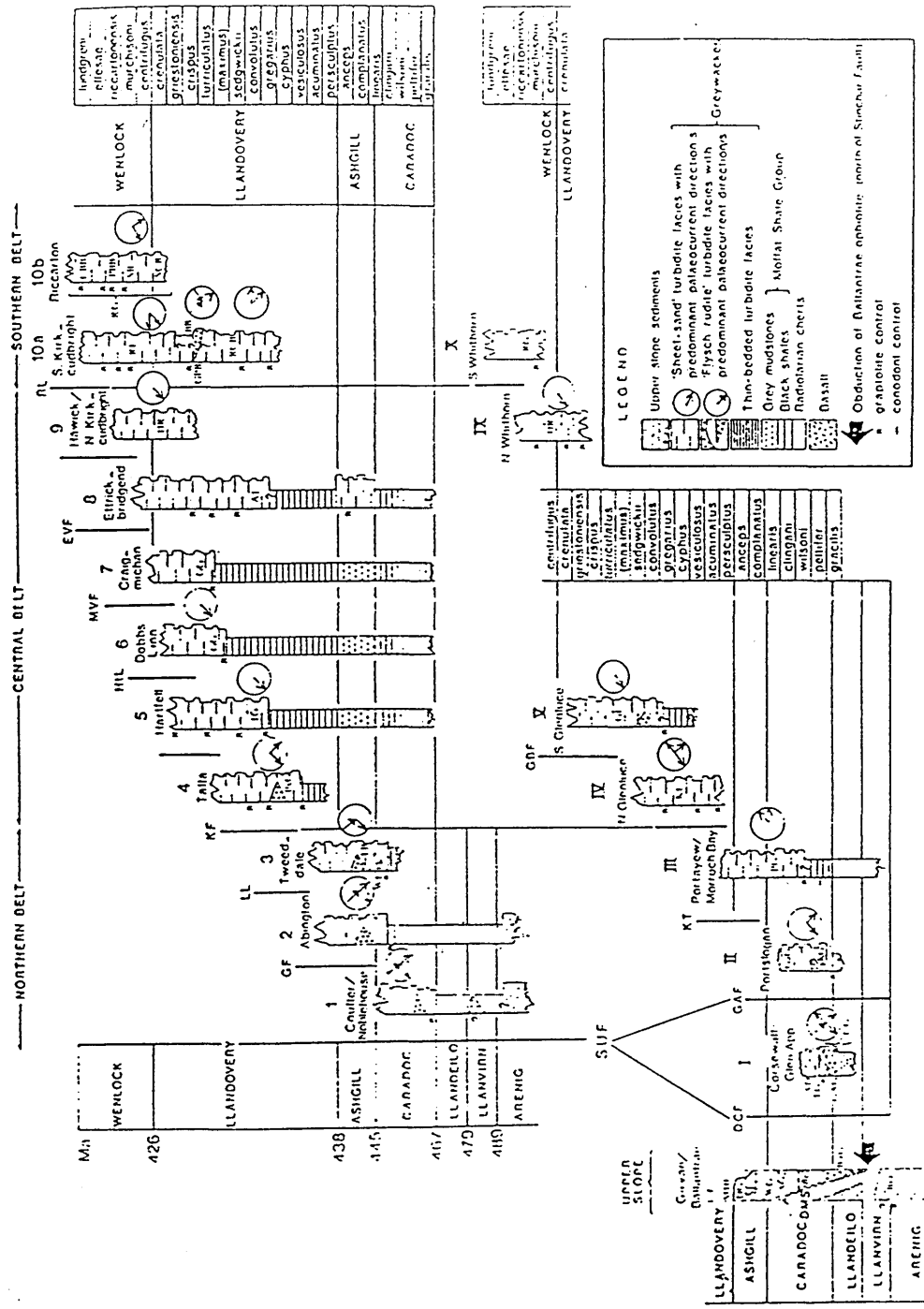

Figure 1.4 Time-stratigraphic diagram showing representative stratigraphic sequences for fault slices in two traverses across the Southern Uplands from the SUF in the north to the unconformable Upper Palaeozoic cover in the south (after Leggett *et al.* 1982).

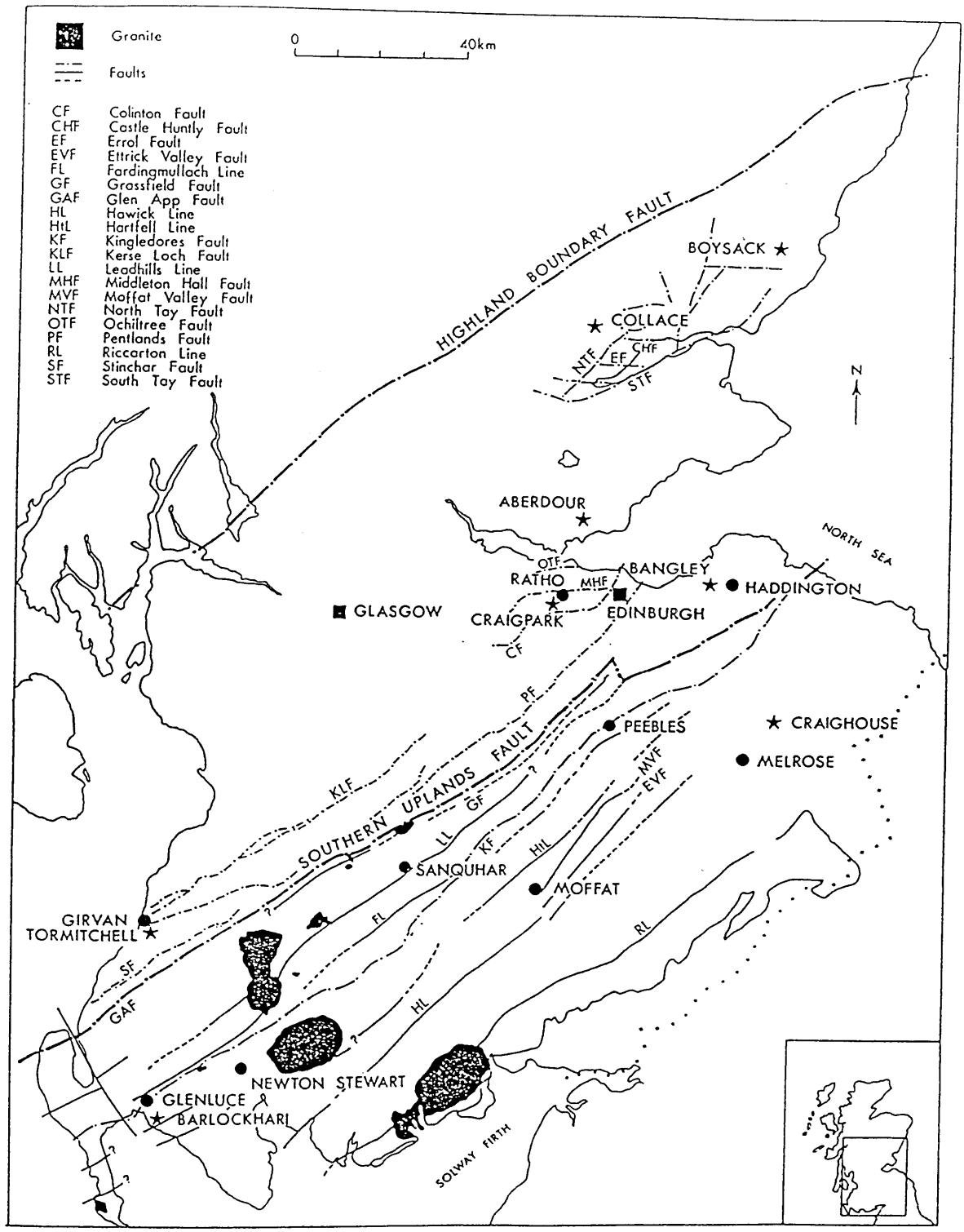

Figure 1.5 Principal faults crossed by the profiles in the Midland Valley and Southern Uplands. Experiment seismic sources shown by stars.

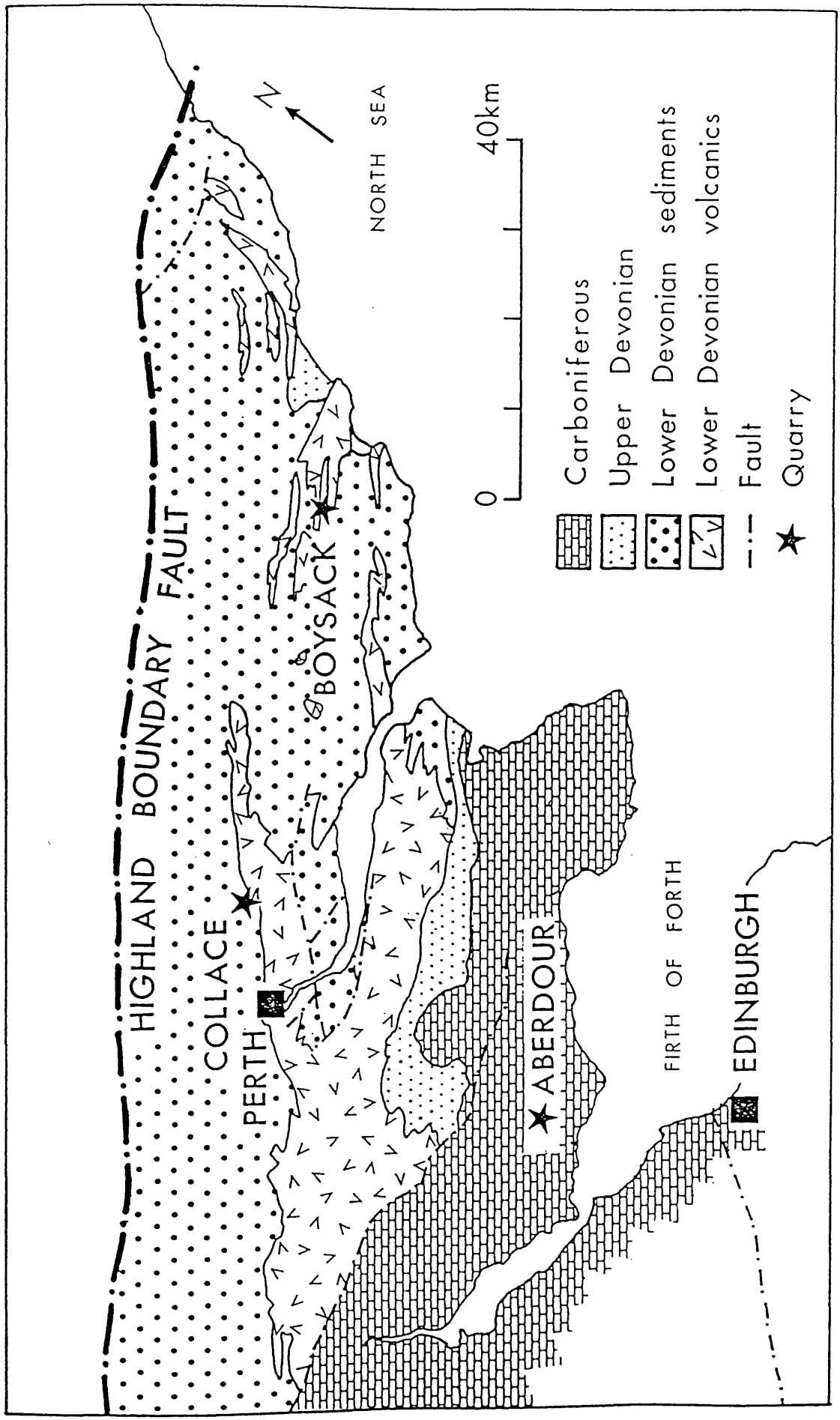

Fig. 1.6 Geology of the Strathmore Syncline, the Midland Valley of Scotland.

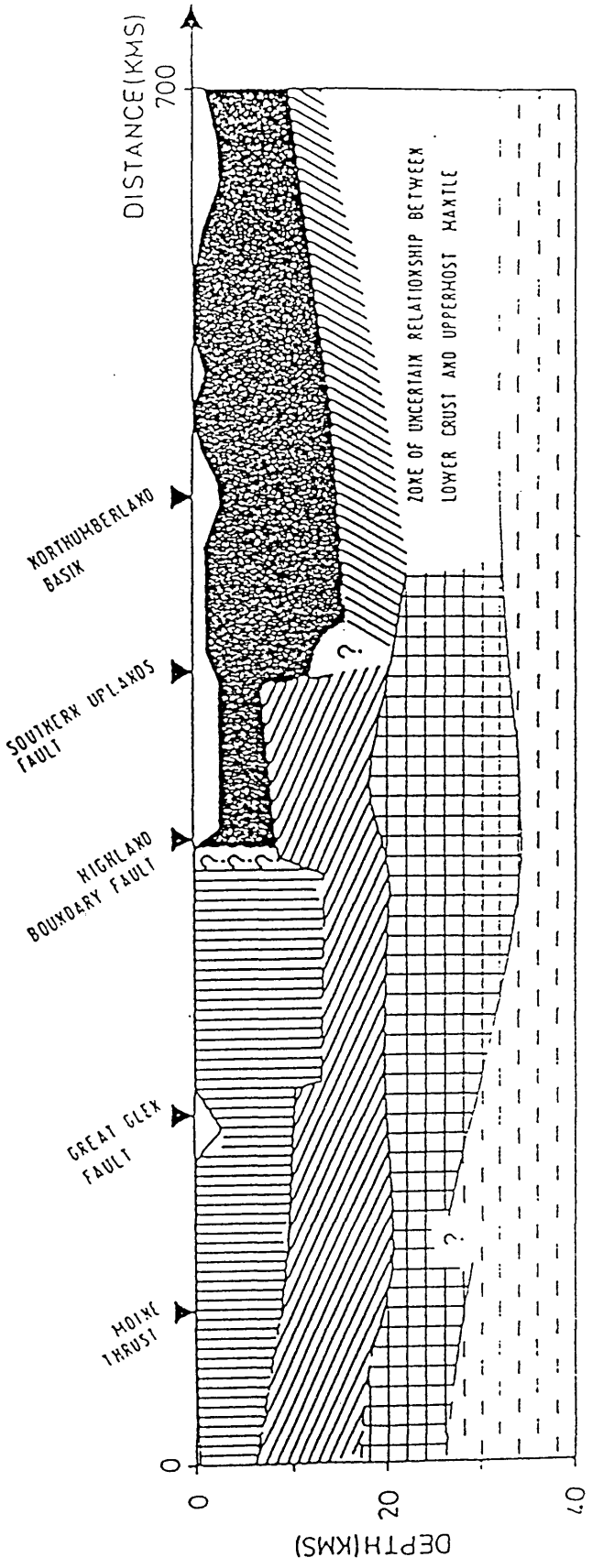

Figure 1.7 Cross-section of the crust and Moho of northern Britain from the LISPB profile (after Bamford 1979).

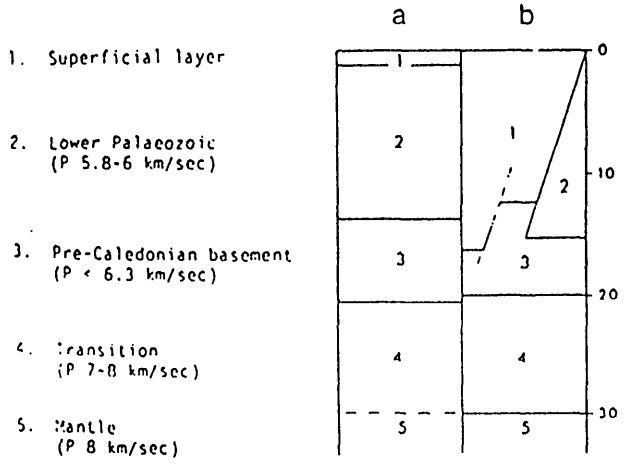

1. Superficial layer
2. Lower Palaeozoic (P 5.8-6 km/sec)
3. Pre-Caledonian basement (P < 6.3 km/sec)
4. Transition (P 7-8 km/sec)
5. Mantle (P 8 km/sec)

	Density g/cc	Velocity km/sec (P waves)	Magnet-ization emu/cc	Resistivity ohm m
1. Lower Palaeozoic greywacke, shale (a = graphitic), spilite	2.73	5.5 to 6.0	10^{-3} to 10^{-4}	10^{3} to 10^{4} (a) 10
2. Late Caledonian granite	2.62	.. ..	.. ..	10^{3} to 10^{4}
3. Pre-Palaeozoic "basement" high grade metamorphic rocks gneiss, schist, granulite (= b)	2.7 to 2.9	6.4	10^{-3} to (b) 10^{-3}	.. .. (a) 10
4. Lower crust more basic that 3; anorthositic	2.8 to 2.9	7.0	above Curie pt. temp.	10^{3} to 10^{4}
5. Mantle	3.2	8.0	.. ..	?

Boundary between 1 and 3 shows Caledonian structural relief.
Boundary between 3 and 4 presumed gradational.

Figure 1.8 Comparison between models proposed for the crustal structure of the Southern Uplands, a. Bamford (1979), b. Powell (1971), (after Craig 1983).

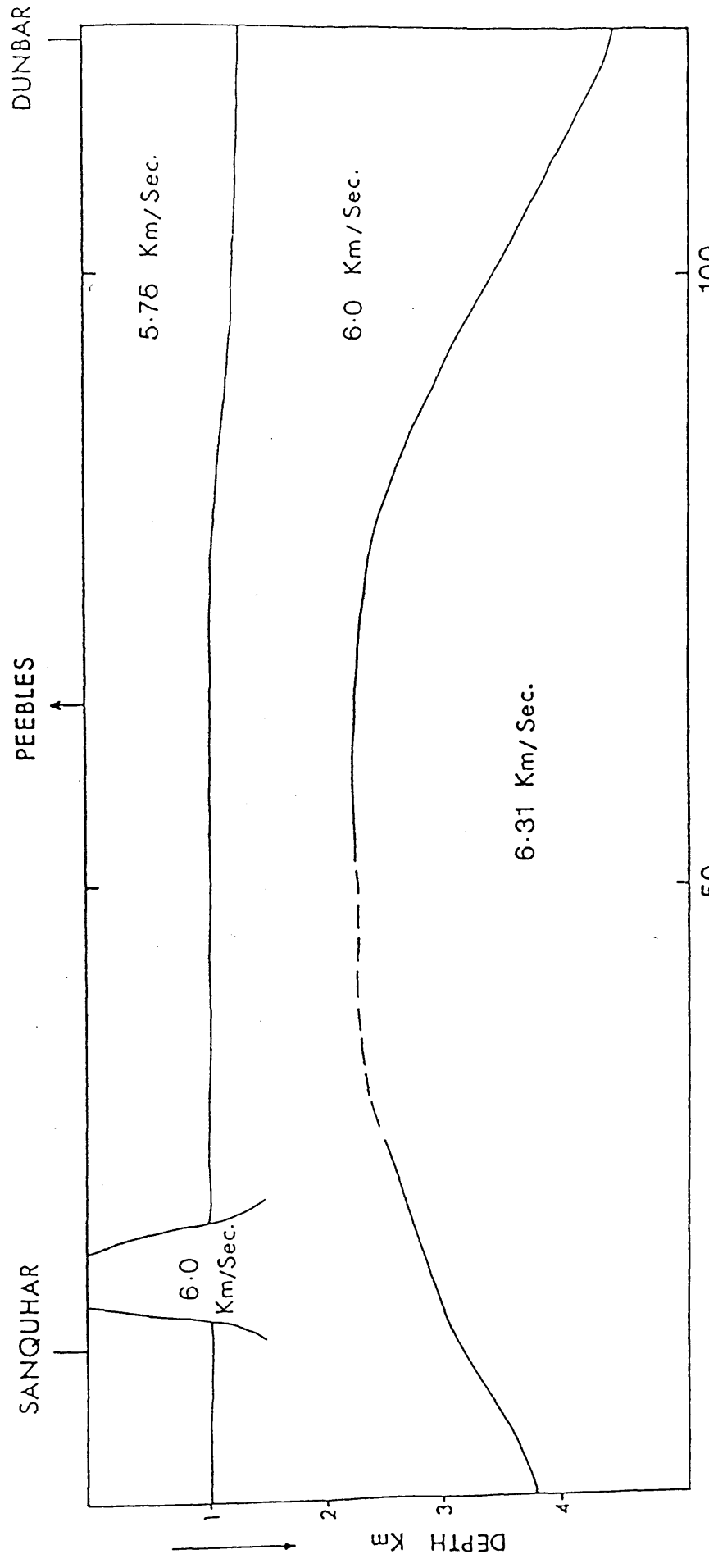

Figure 1.9 Upper crustal velocity structure along the SUSP profile in the Southern Uplands (after Al-Mansouri 1986).

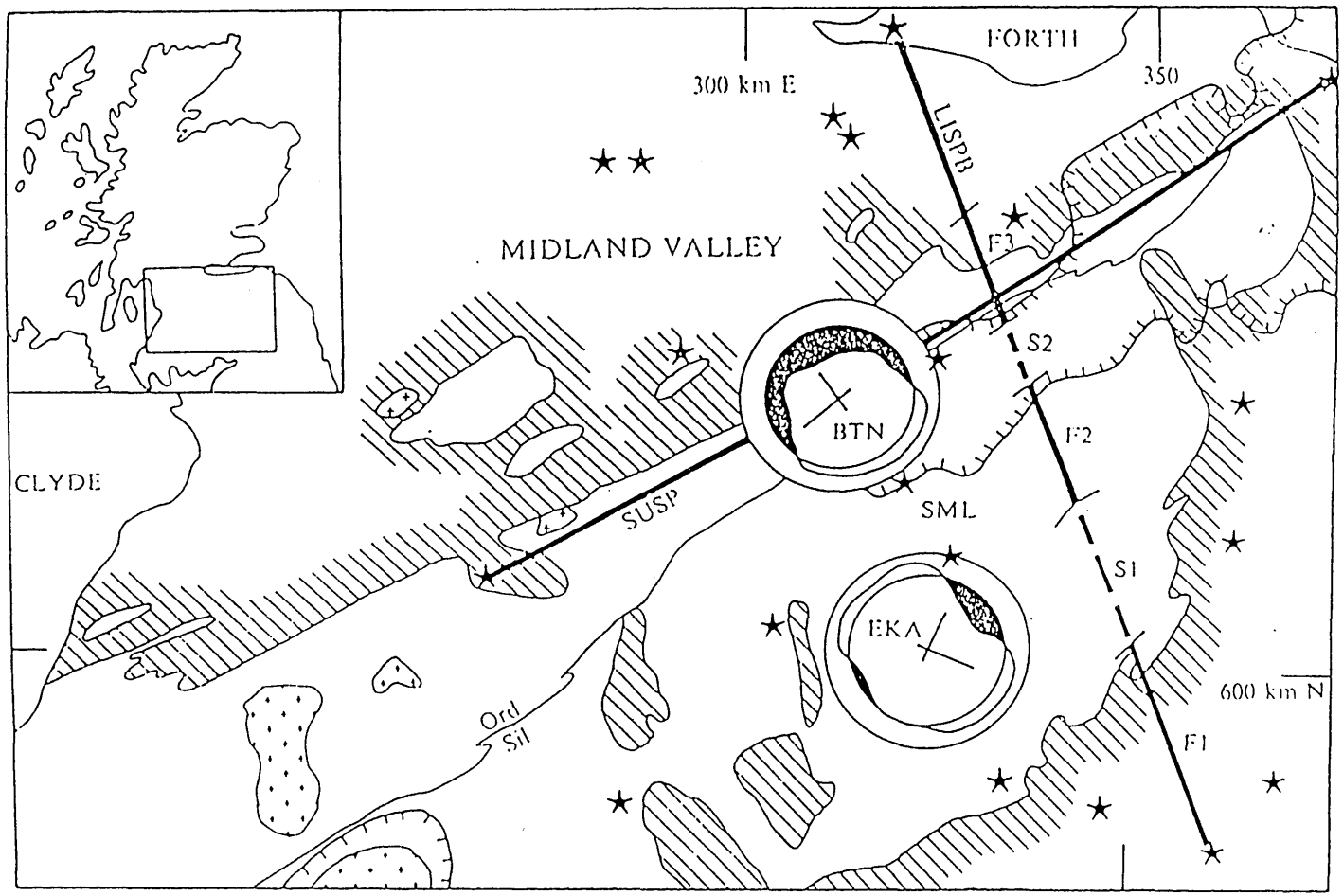

Figure 1.10 Location of previous seismic work in southern Scotland. On the LISPB profile, E and 2 identify shot positions and F1-3, S1-2, locate high and low velocity blocks. SUSP is the Southern Uplands Seismic Profile. Seismological arrays at Eskdalemuir (EKA) and Broughton (BTN). Lower Palaeozoic rocks is limited by shading, plusses indicate granites. Polar plots are of apparent velocity vs direction with scale rings at 5.5 km/s (outer) and 6.0 km/s (inner) so black area represents area where velocity is greater than 6.0 km/s (after Hall *et al.* 1983).

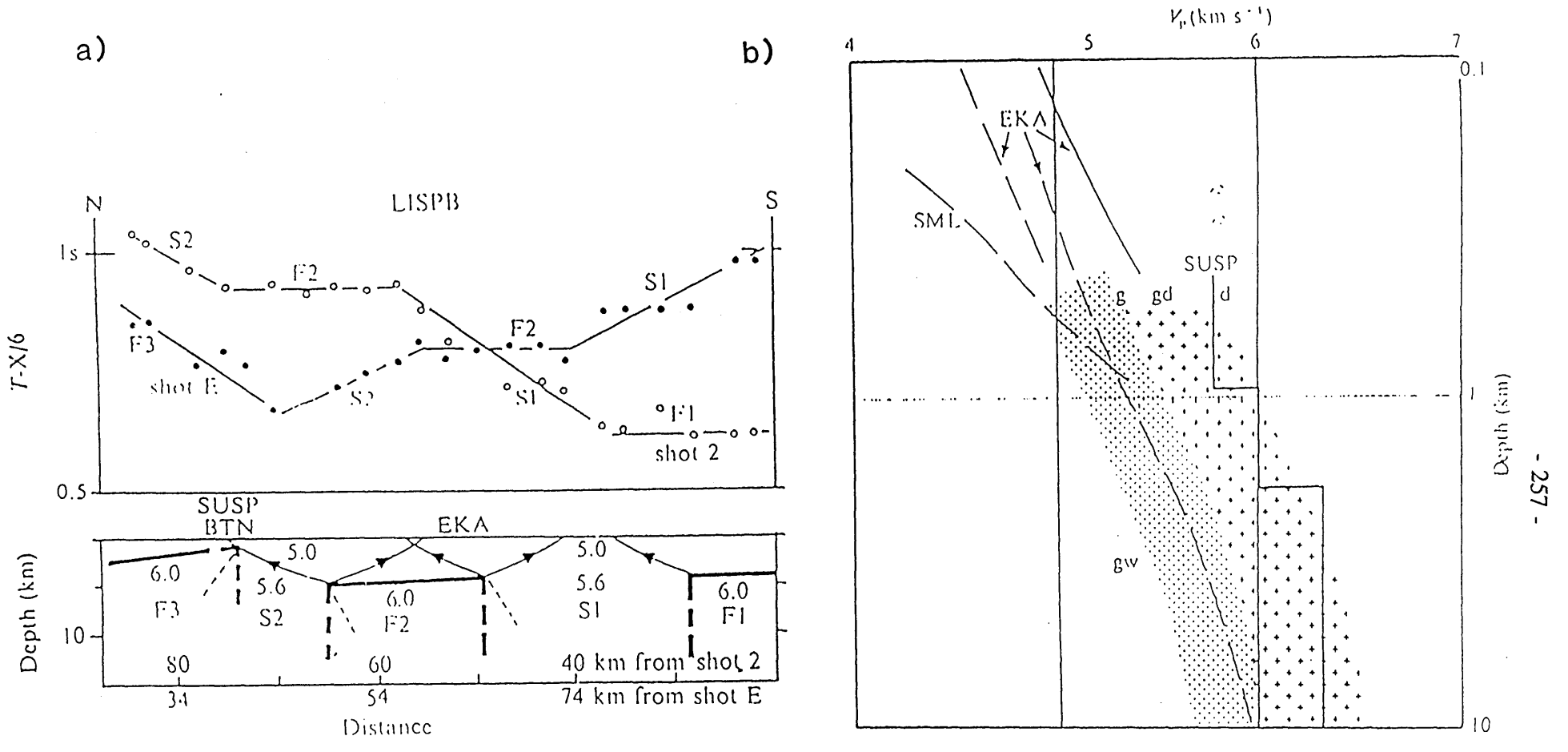

Figure 1.11 a) LISPB time-distance data from the Southern Uplands, reduction velocity is 6.0 km/s. Structural model shows velocity distribution containing fast (F) and slow (S) blocks which give rise to the corresponding segments on the time-distance plot. b), velocity-depth plot for the Southern Uplands. solid lines show along-strike velocities and dashed lines across-strike velocities. EKA-Eskdalemuir seismic array, SML is an array study at Saint Mary's Loch in the S2 slow block. Dotted area, (gw), represents velocity field for plutonic rocks, g - granite, gd - granodiorite, d - diorite. SUSP- Southern Uplands Seismic Profile (after Hall *et al.* 1983).

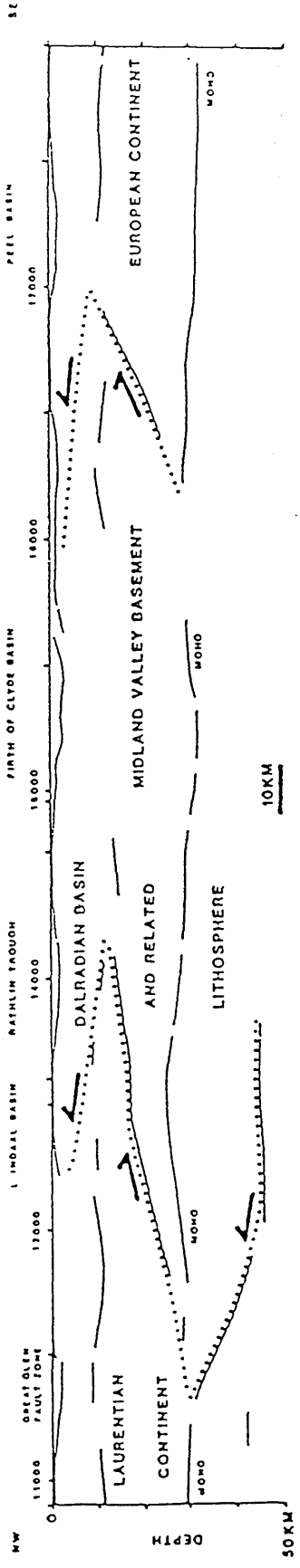

Figure 1.12 Summary of main features of the WINCH profile; dotted lines show position of inferred boundaries of major lithospheric units (after Hall *et al.* 1984).

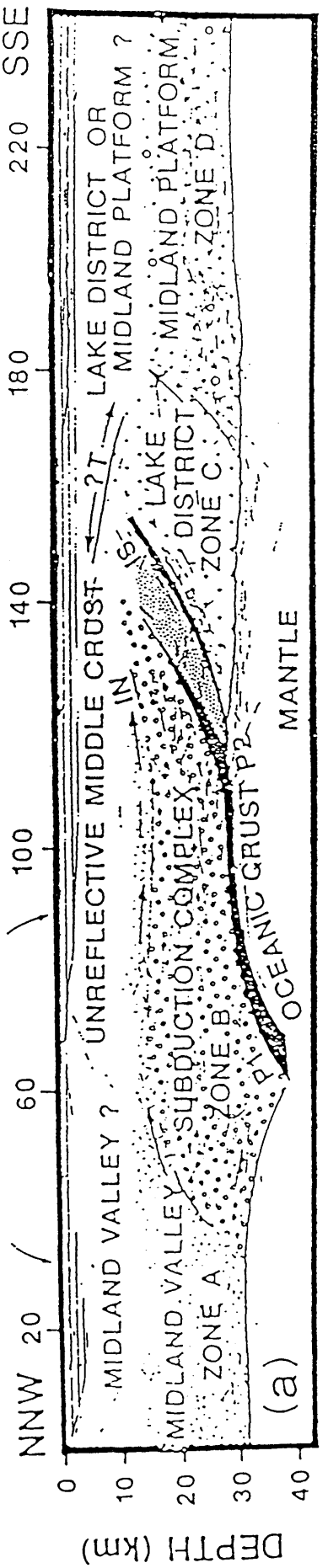

Figure 1.13 Geological interpretation of the NEC migrated depth section (after Freeman *et al.* 1988).

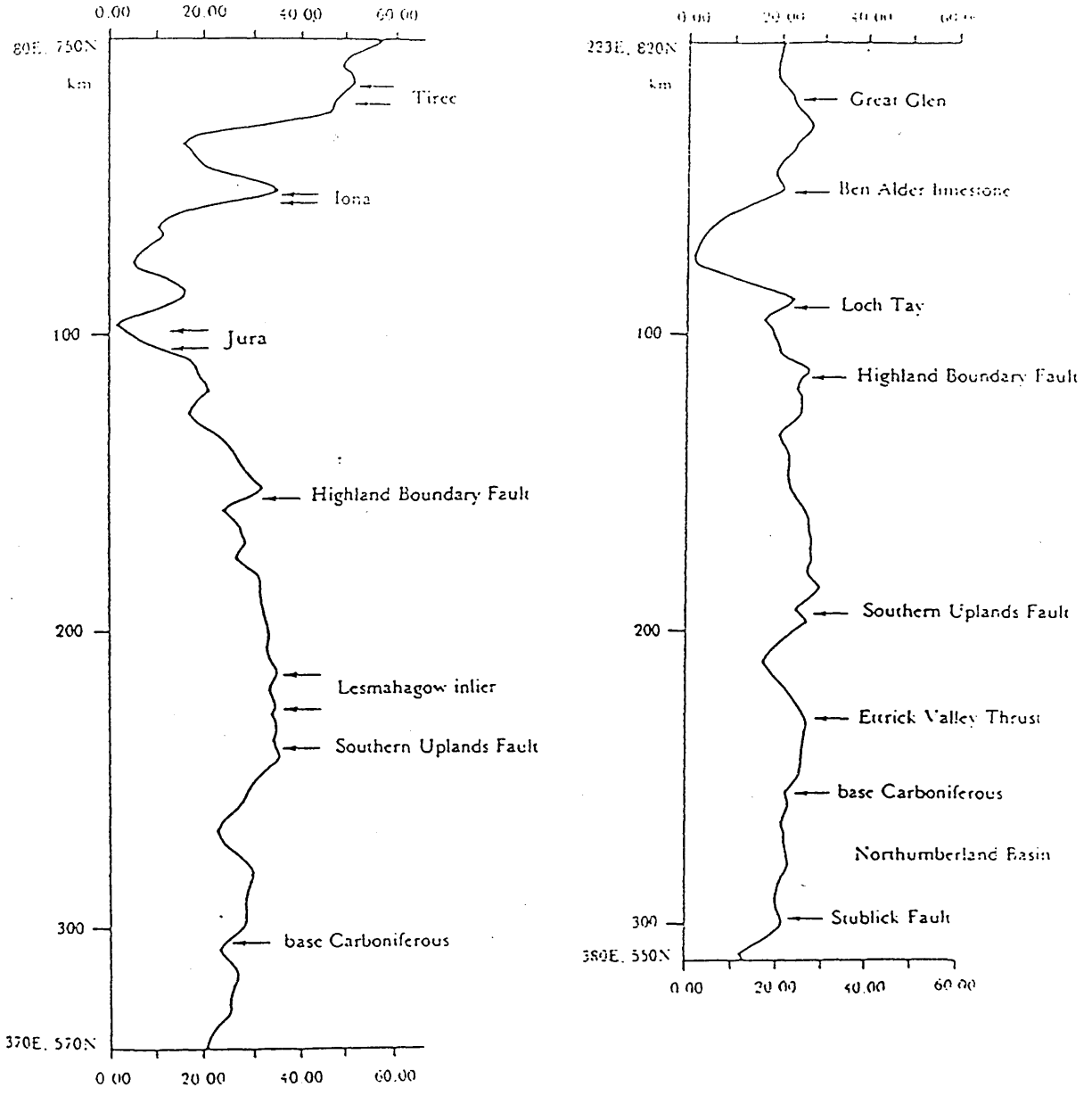

Figure 1.14 Stripped isostatic anomaly profiles across Scotland (after Hipkin and Hussain 1983).

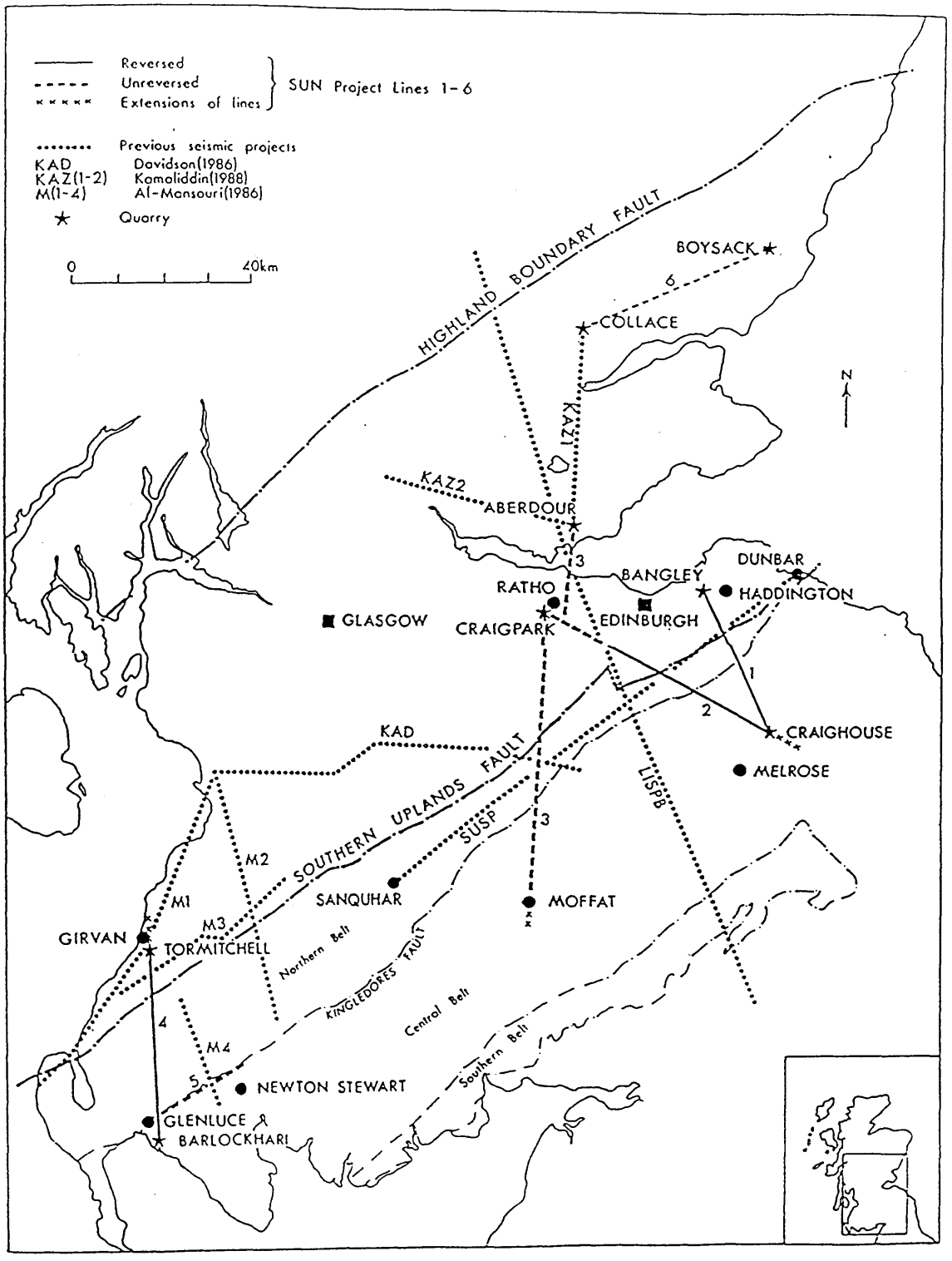

Fig. 2.1 Profiles recorded during the SUN project, with those of previous relevant seismic projects.

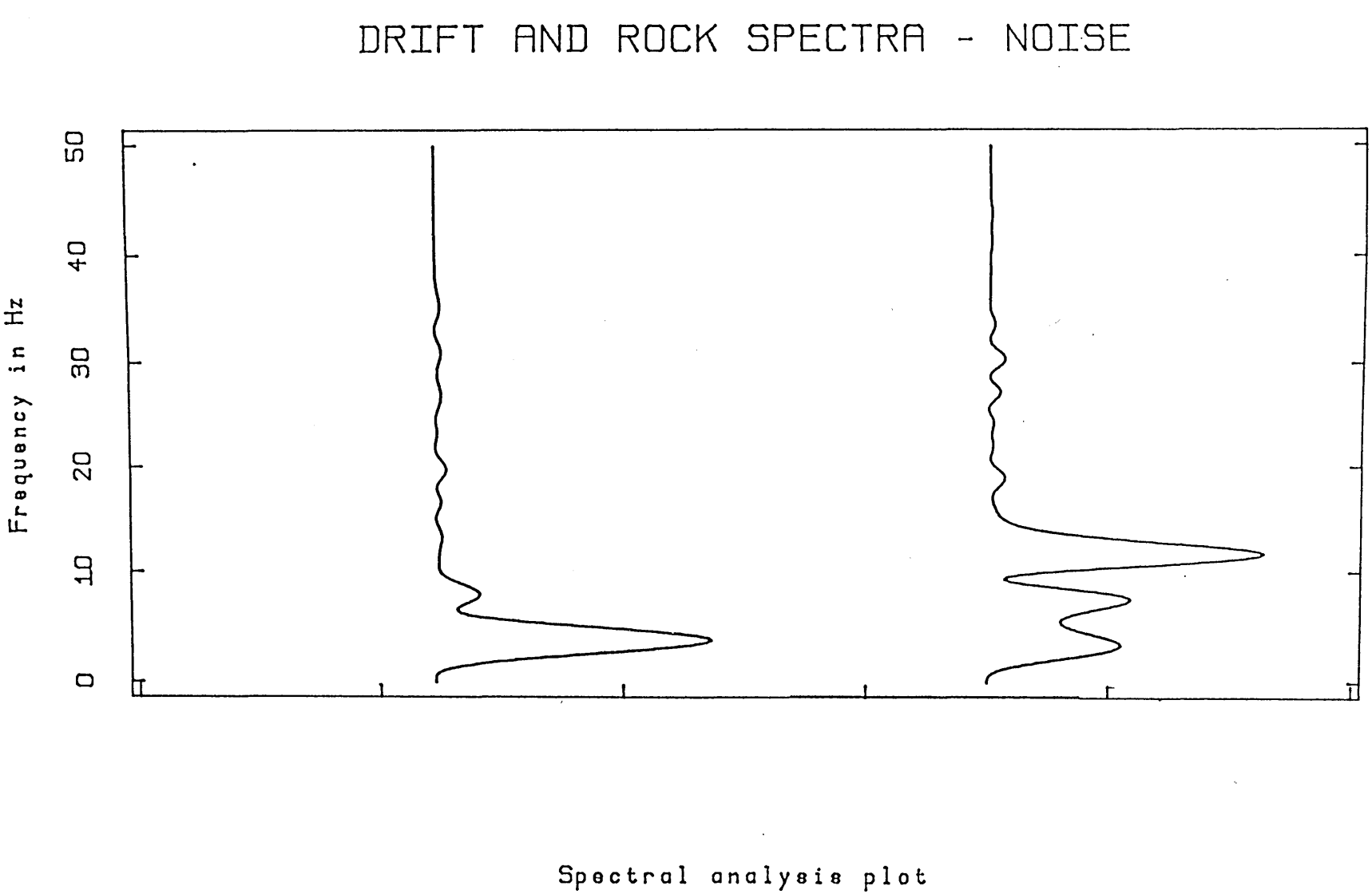

Fig. 2.2a Comparison of noise frequency spectra between a drift and rock site.

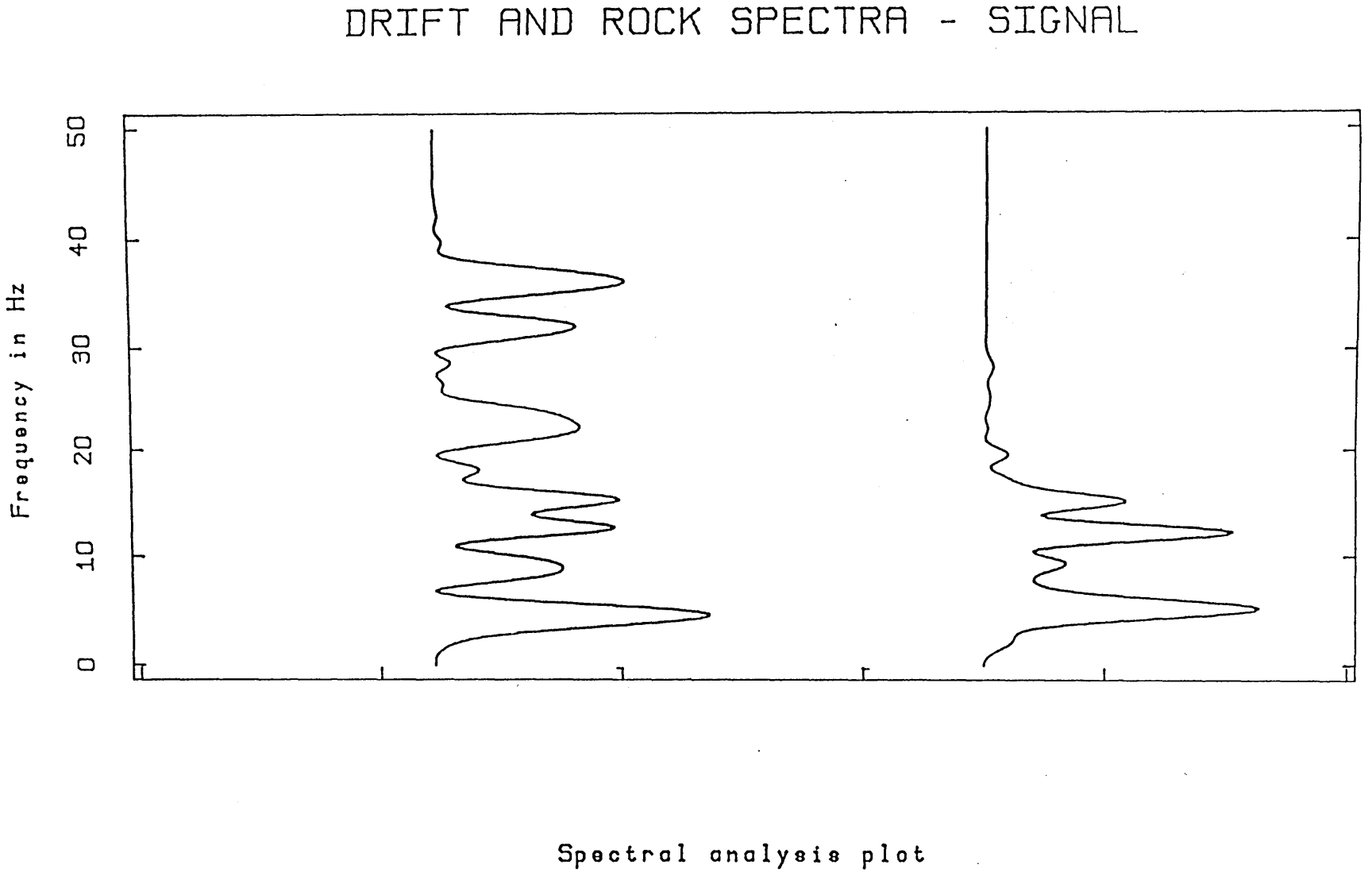

Fig. 2.2b Comparison of signal frequency spectra between a drift and rock site.

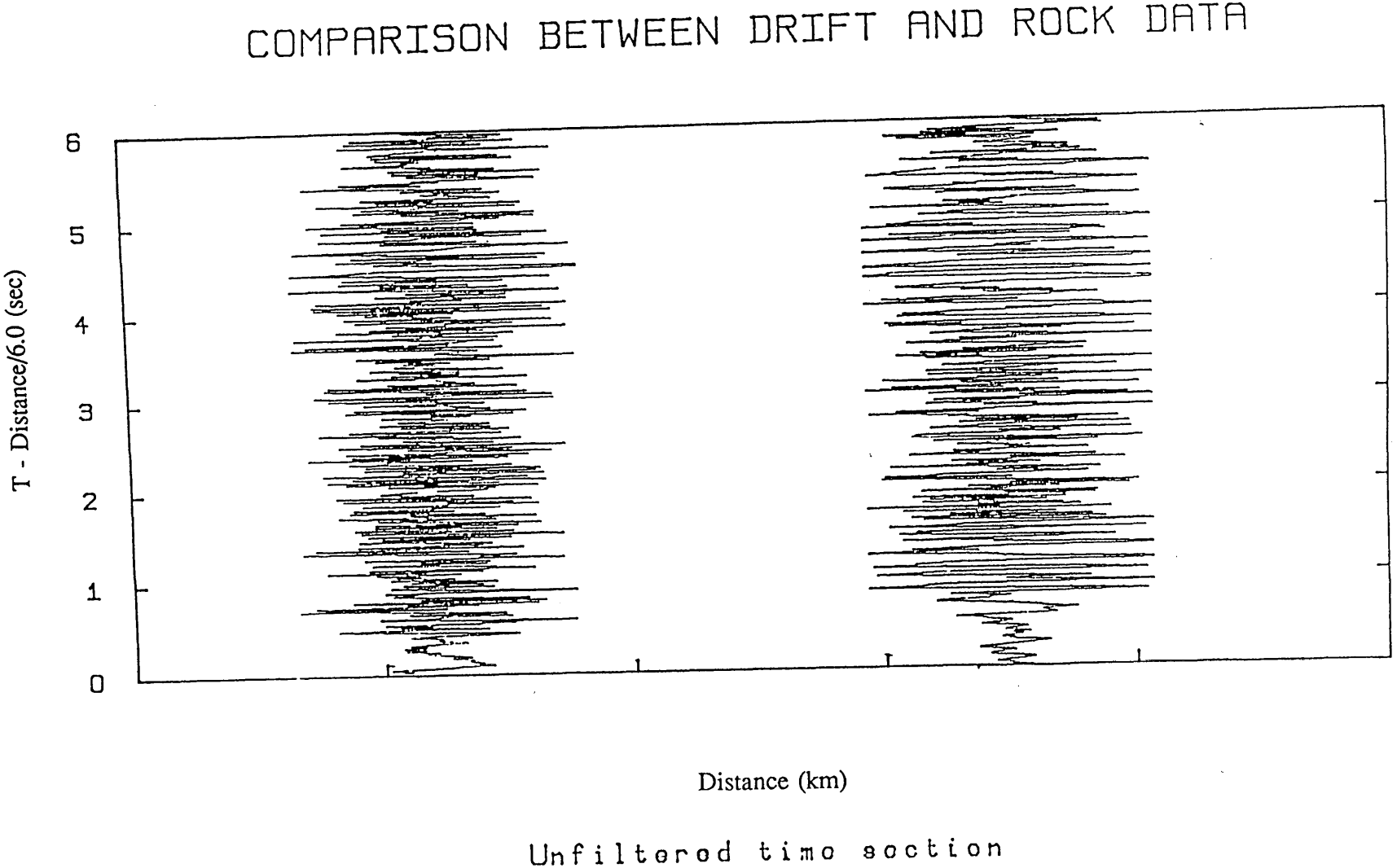

Fig. 2.2c Unfiltered data analysed in Figures 2.2 a and b.

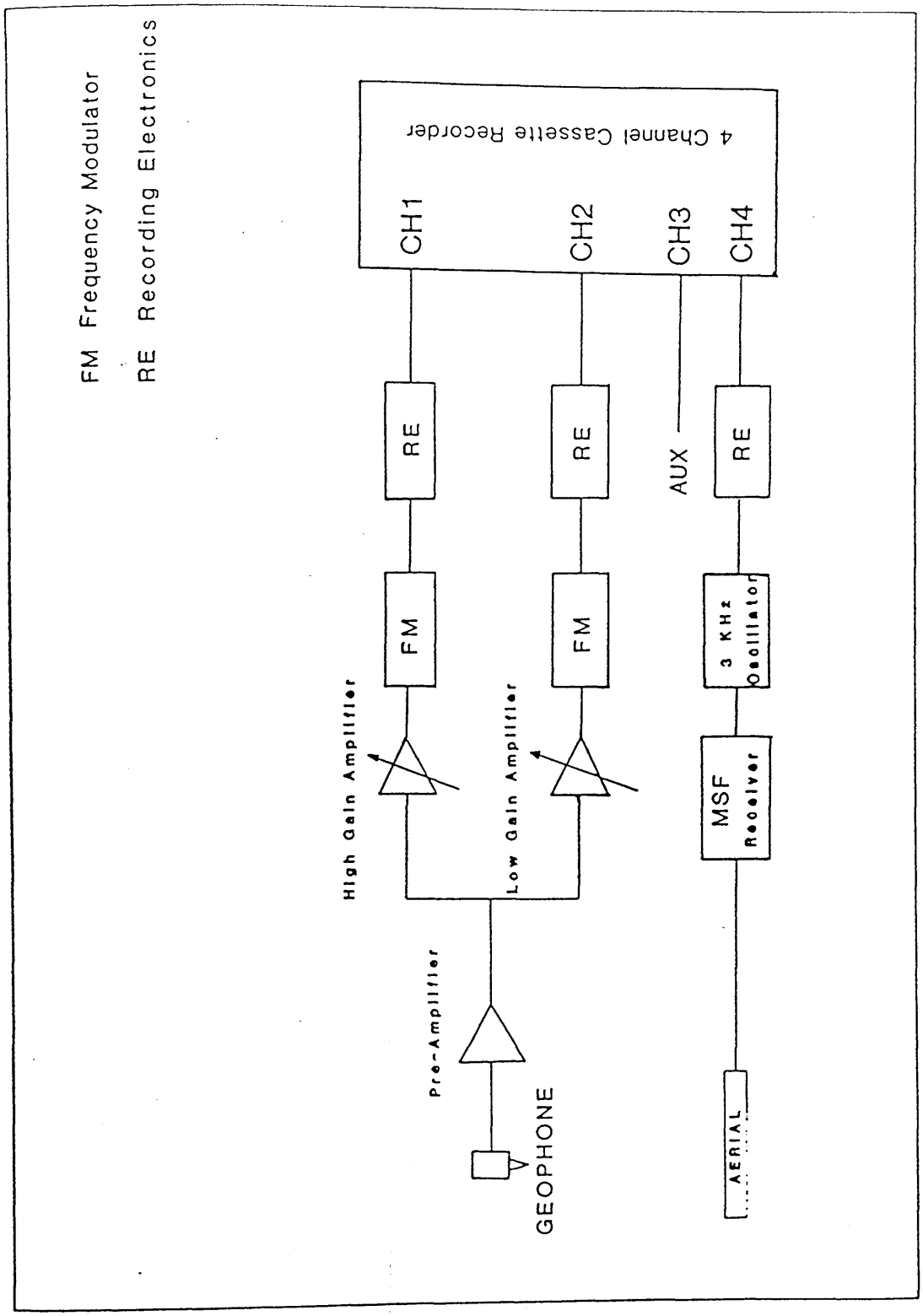

Fig. 2.3 Block diagram showing the recording arrangement of the Glasgow FM "Mark 2" recorder system.

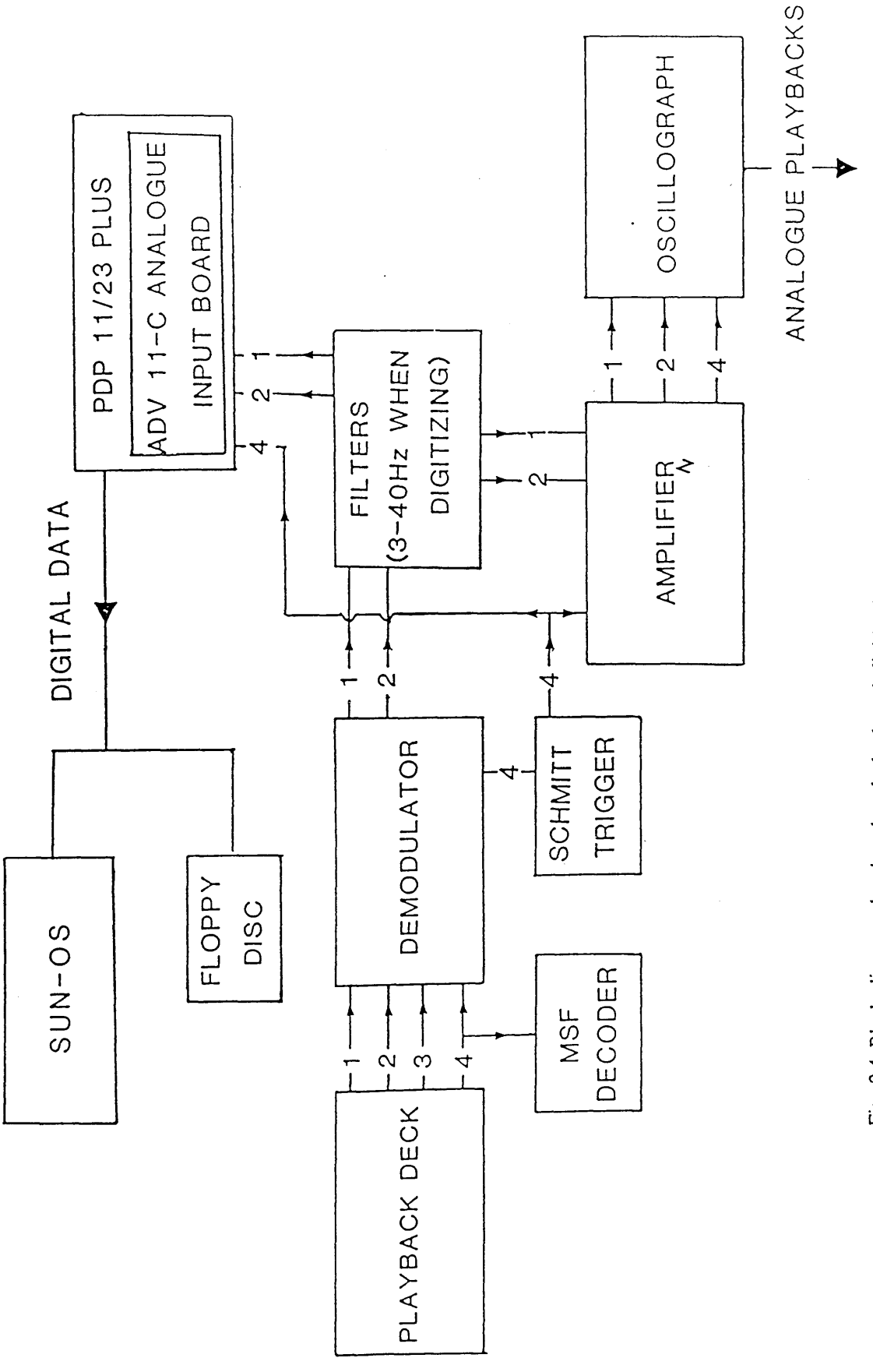

Fig. 2.4 Block diagram showing the playback and digitization system of the Glasgow FM "Mark 2" recorder system.

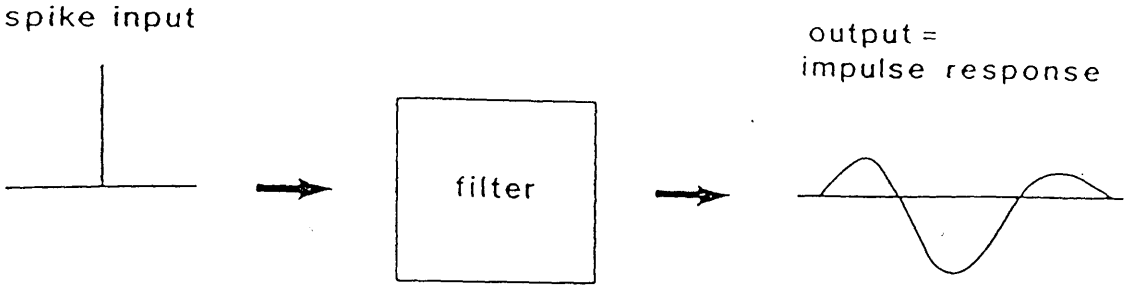

Fig. 3.1 The concept of the impulse response of a filter, which defines the operation of a filter (after Kearey & Brooks 1984).

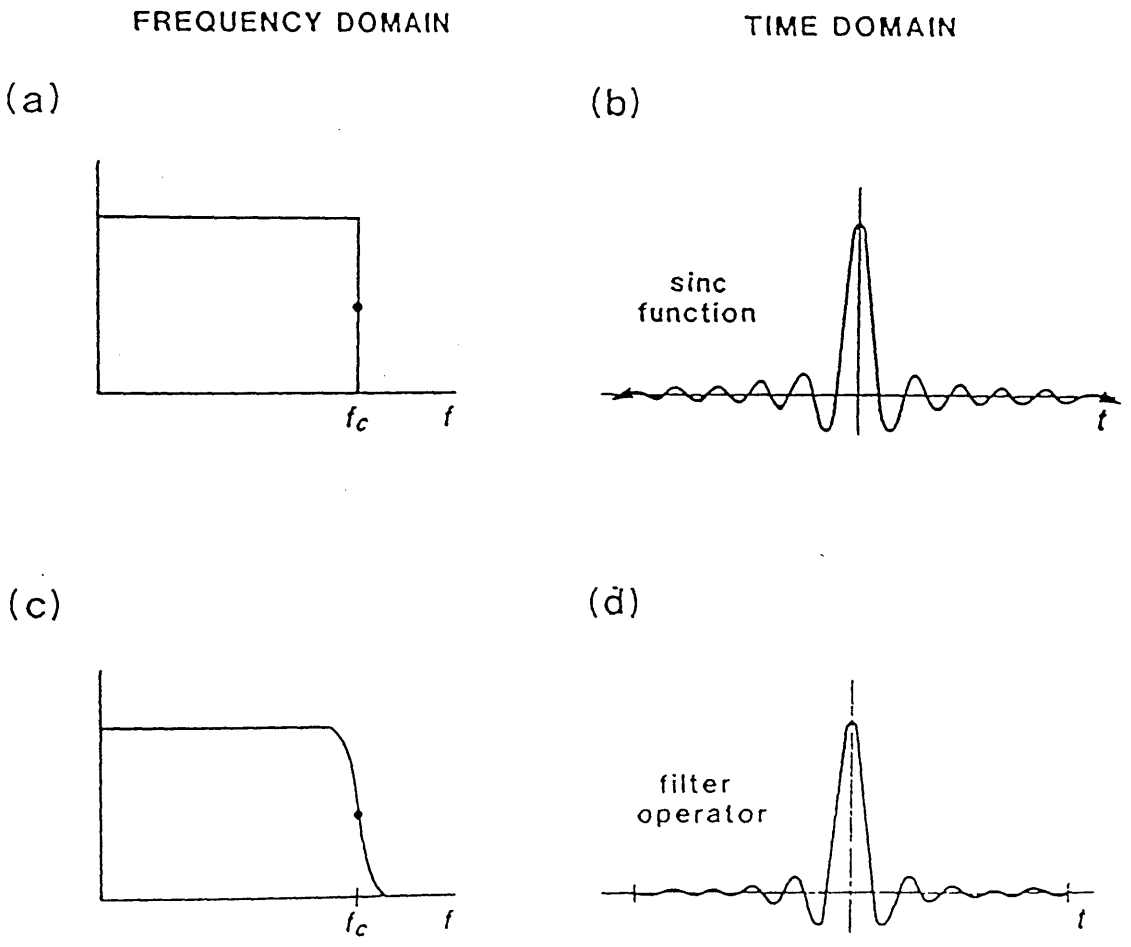

Fig 3.2 Design of a low-pass filter, a) amplitude spectrum, b) impulse response of infinitely long ideal lowpass filter, c) frequency response of a realizable lowpass filter operator of finite length, d) lowpass filter with a ramped cut-off (after Kearey & Brooks 1984).

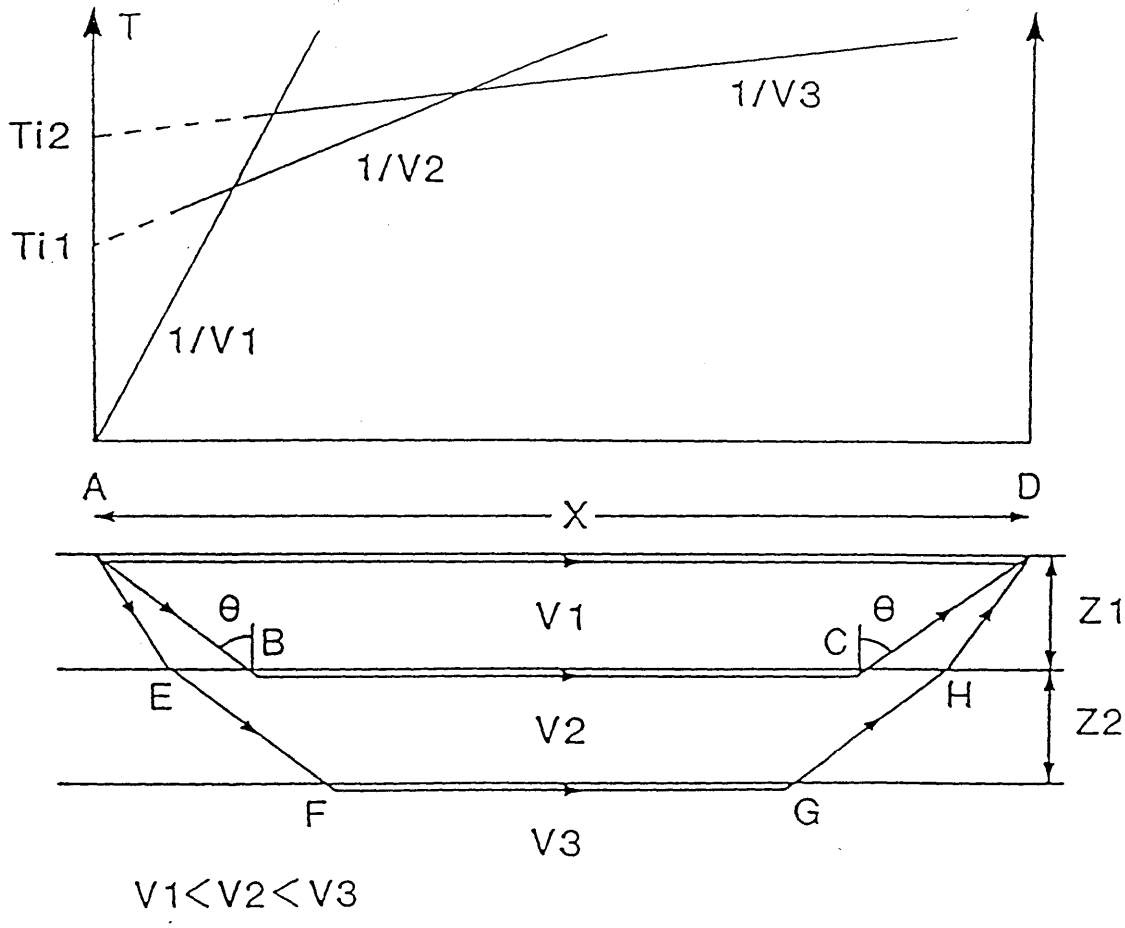

Fig. 3.3 Principles of the refraction method. The top part represents the time-distance graph and bottom represents the equivalent ray model.

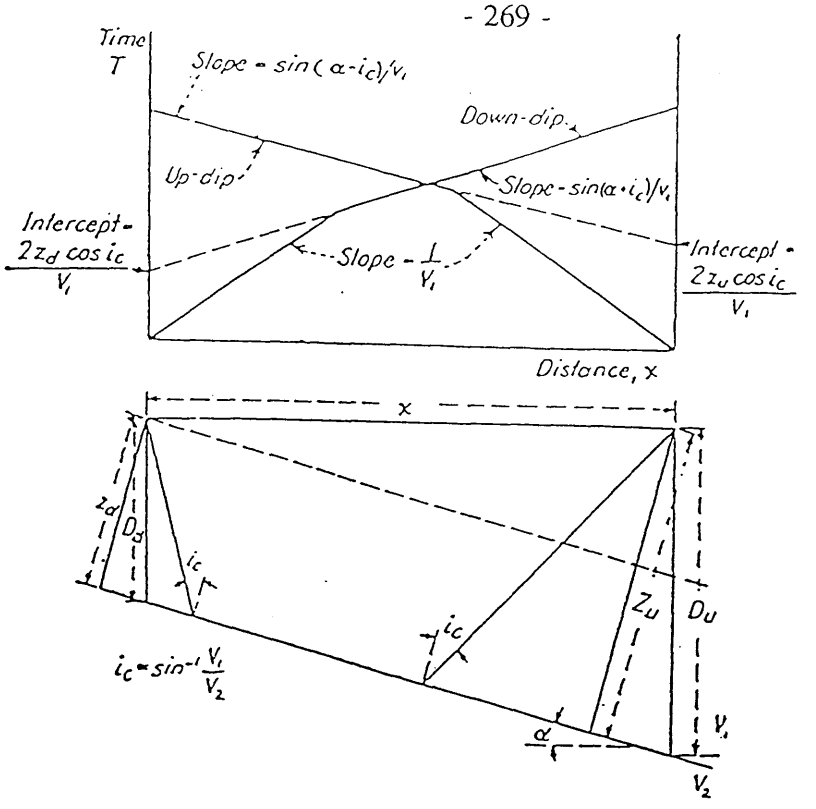

Fig. 3.4 Refraction at a dipping interface (after Dobrin 1960). See text for explanation of formulae.

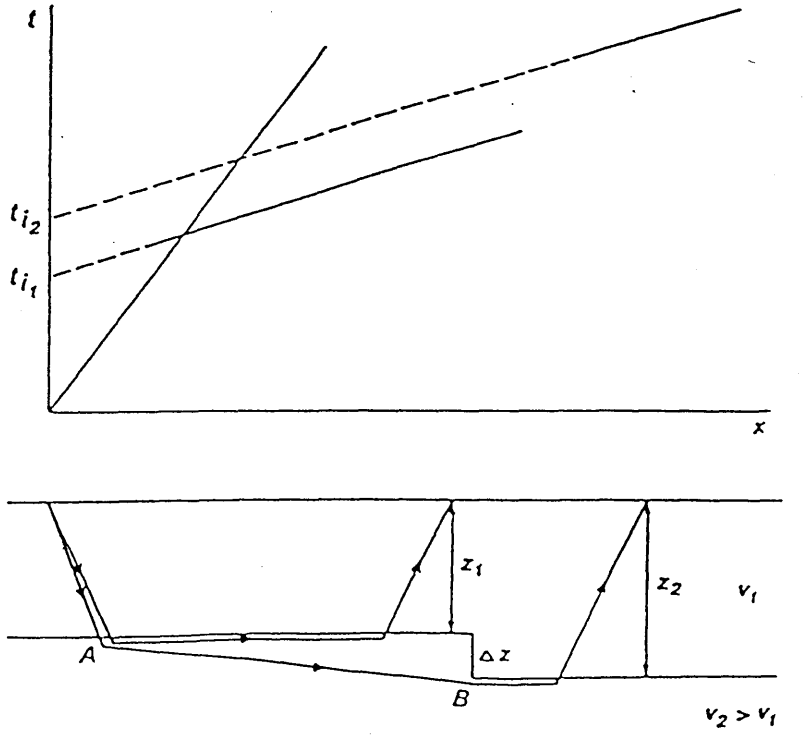

Fig. 3.5 Effect of a fault on refracted rays (after Kearey & Brooks 1984).

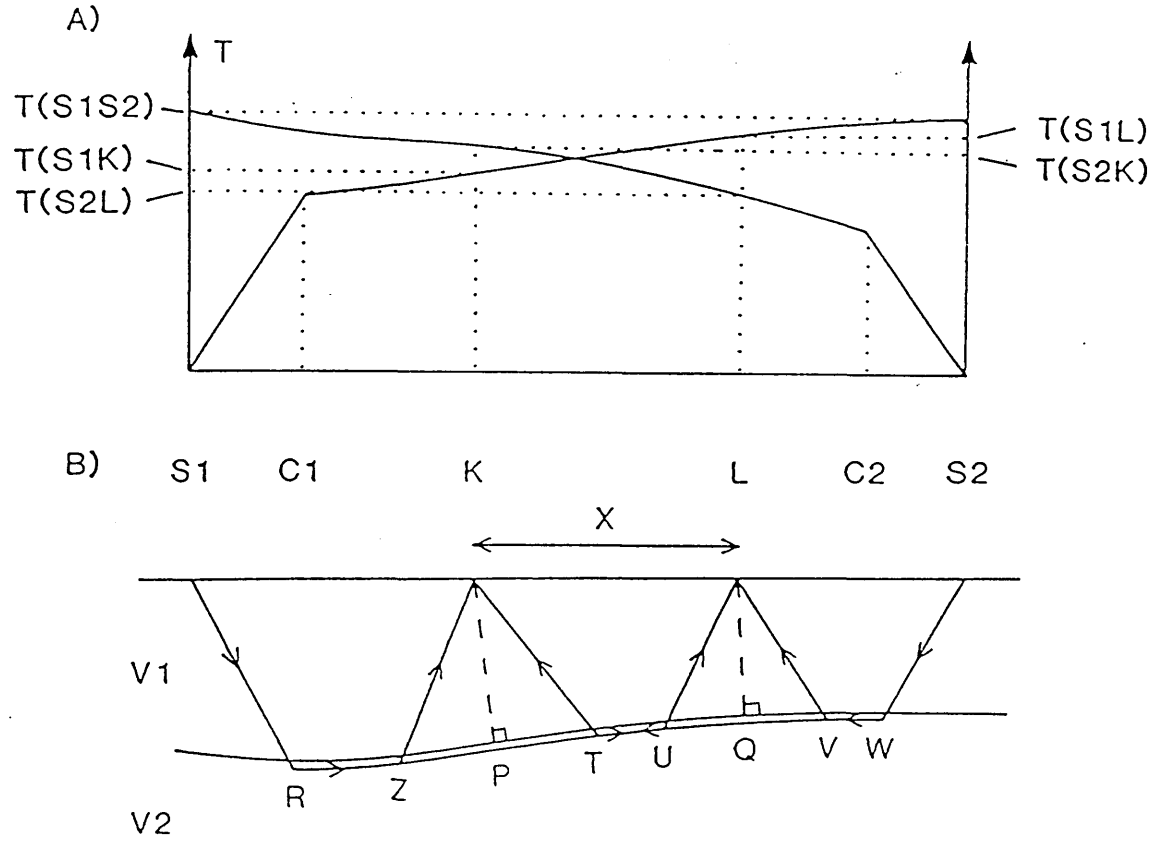

Fig. 3.6 The plus-minus method of refraction; A), travel-time curves B), ray-paths from end shots (S1, S2) to intermediate receivers (K, L). After Dentith 1987.

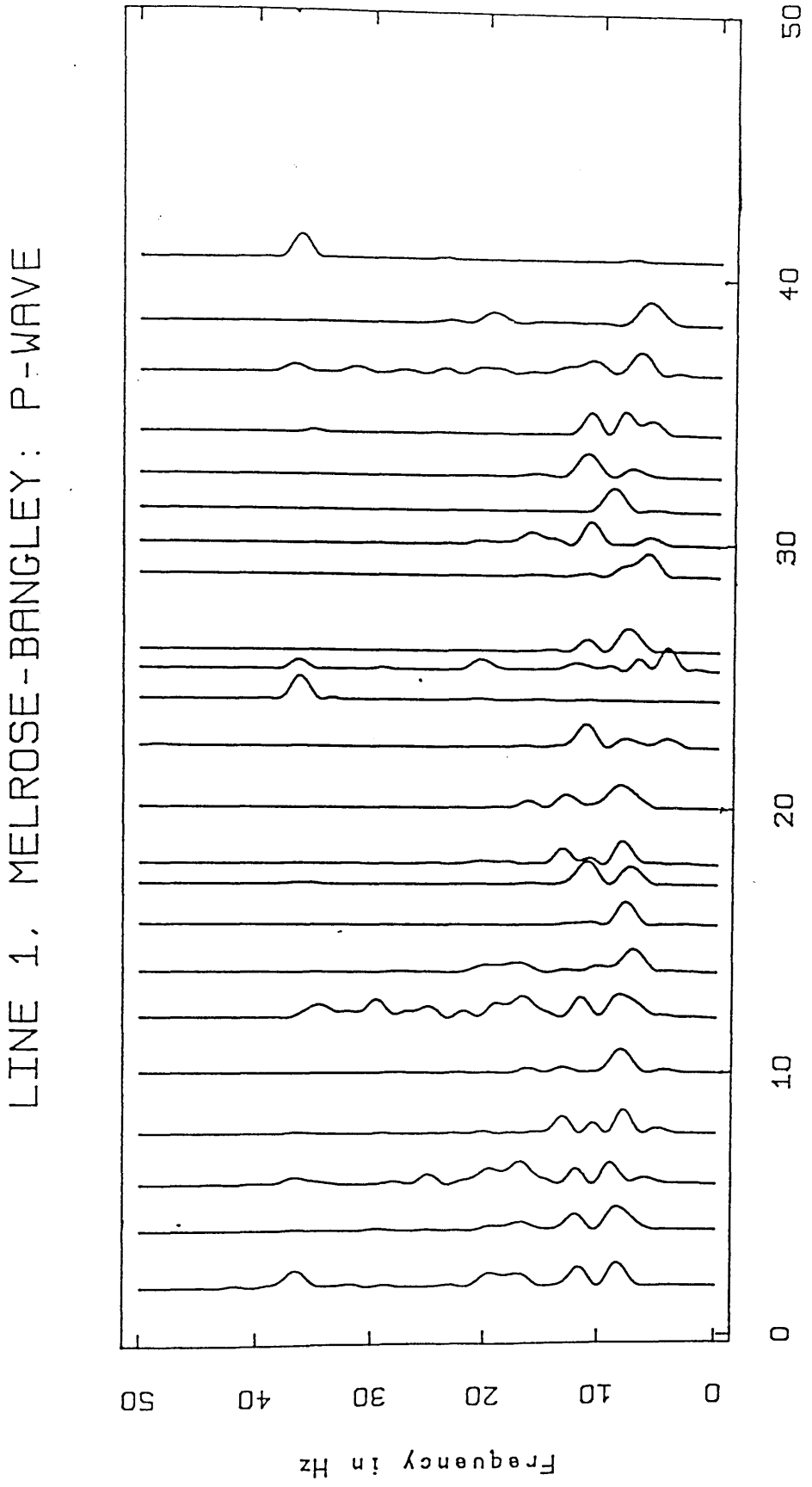

Fig. 4.1 Spectral analysis for line 1 (Melrose shot).

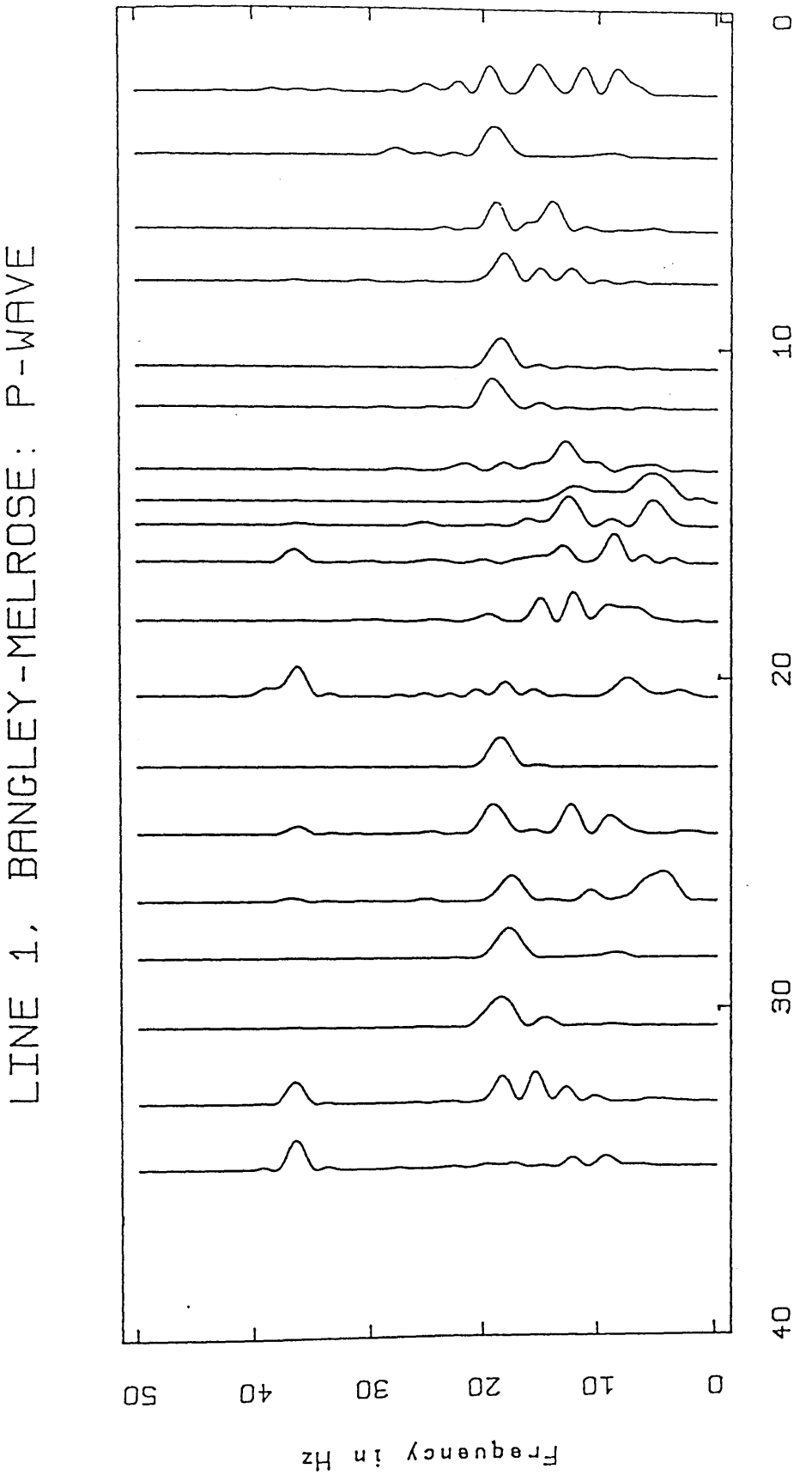

Fig. 4.2 Spectral analysis for line 1 (Bangley shot).

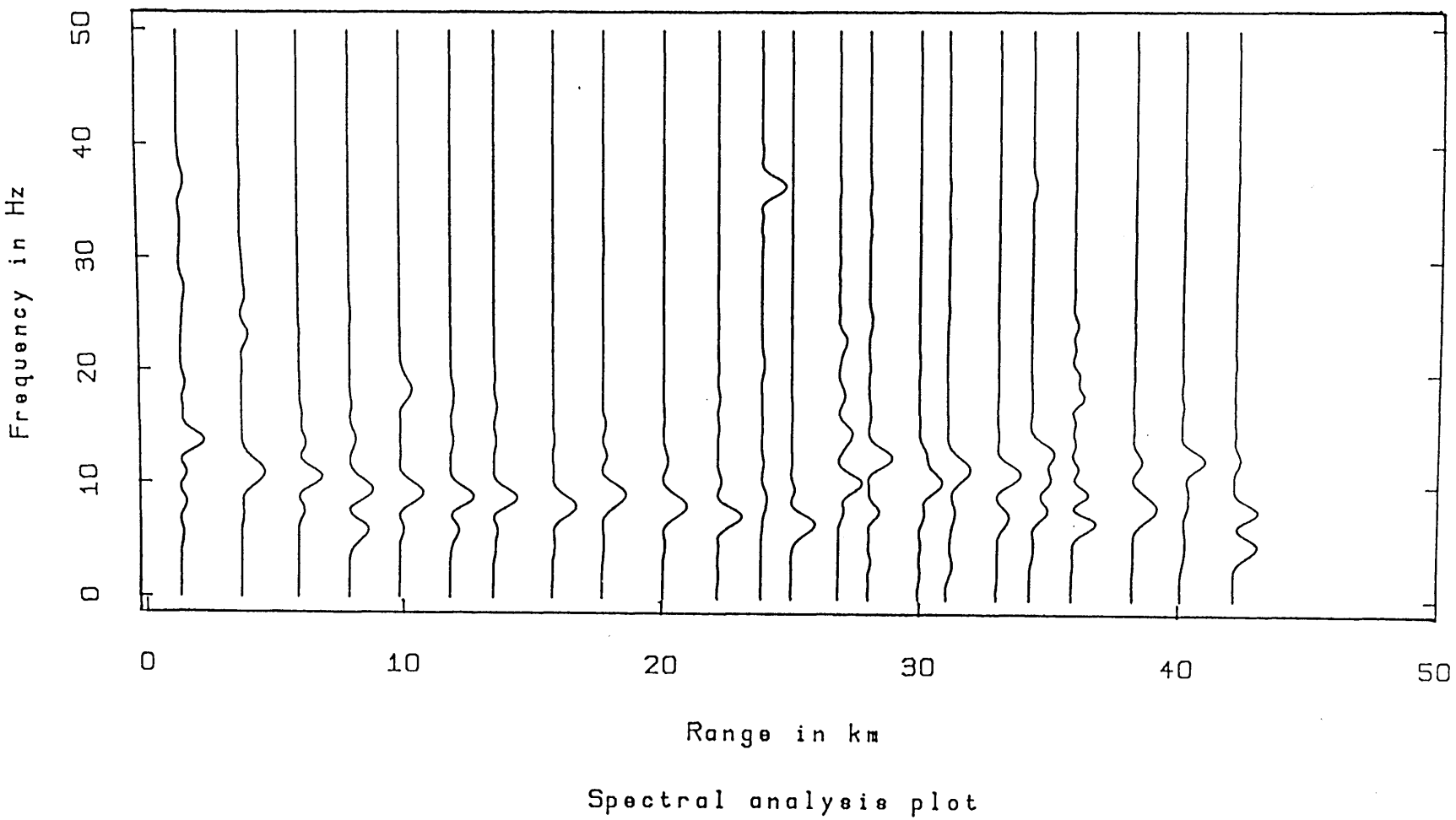

Fig. 4.3 Spectral analysis for line 2 (Melrose shot).

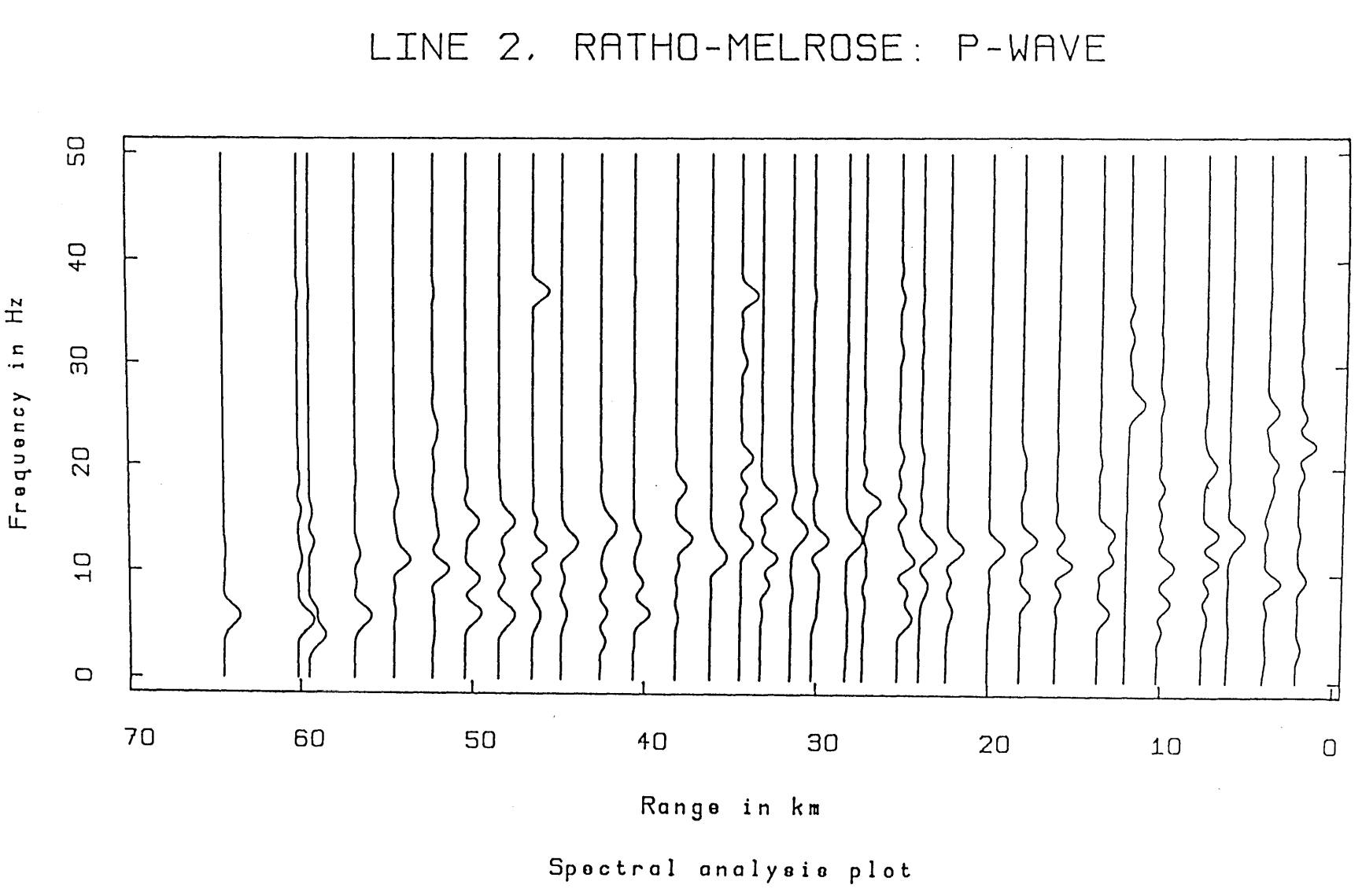

Fig. 4.4 Spectral analysis for line 2 (Ratho shot).

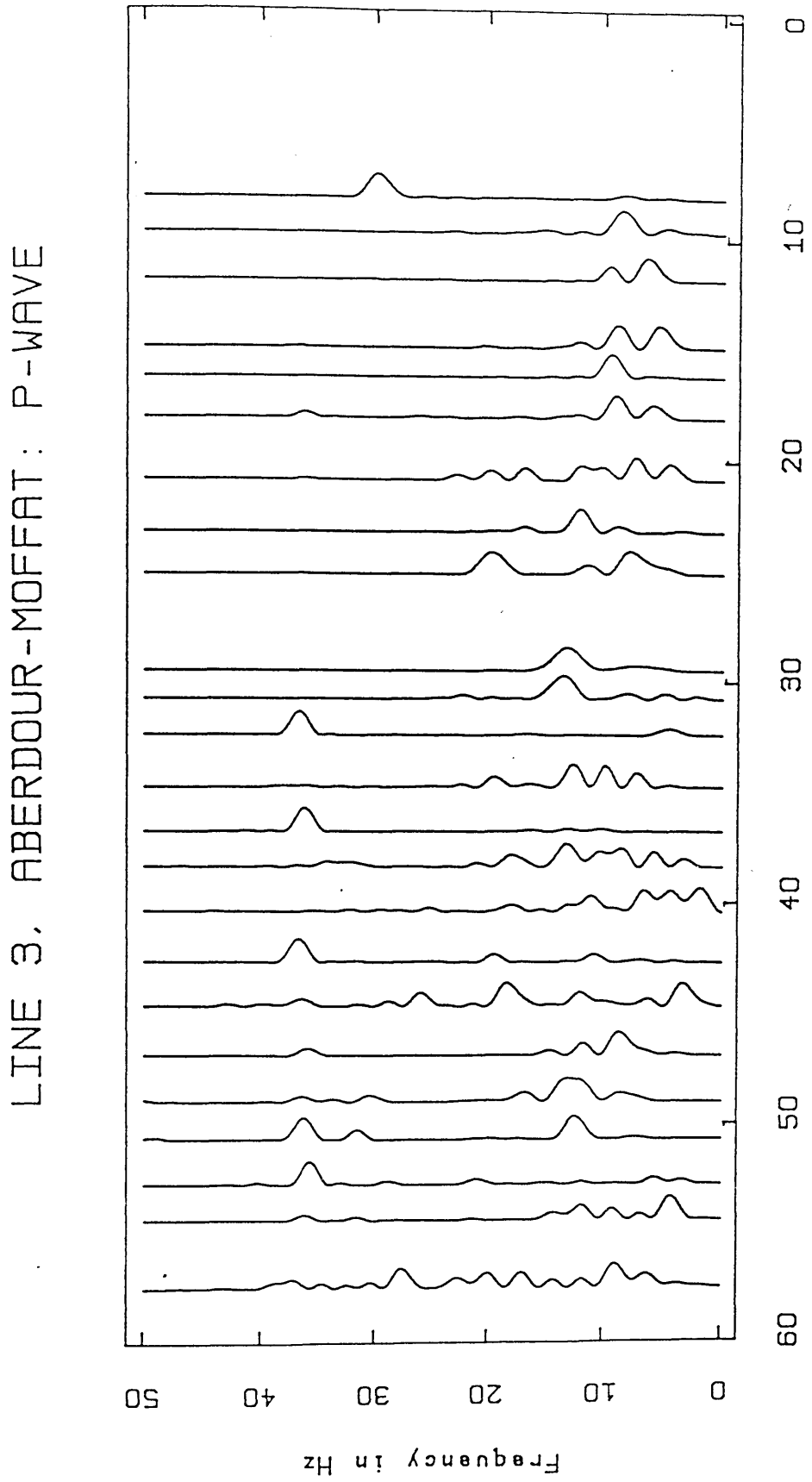

Fig. 4.5 Spectral analysis for line 3 (Aberdour shot).

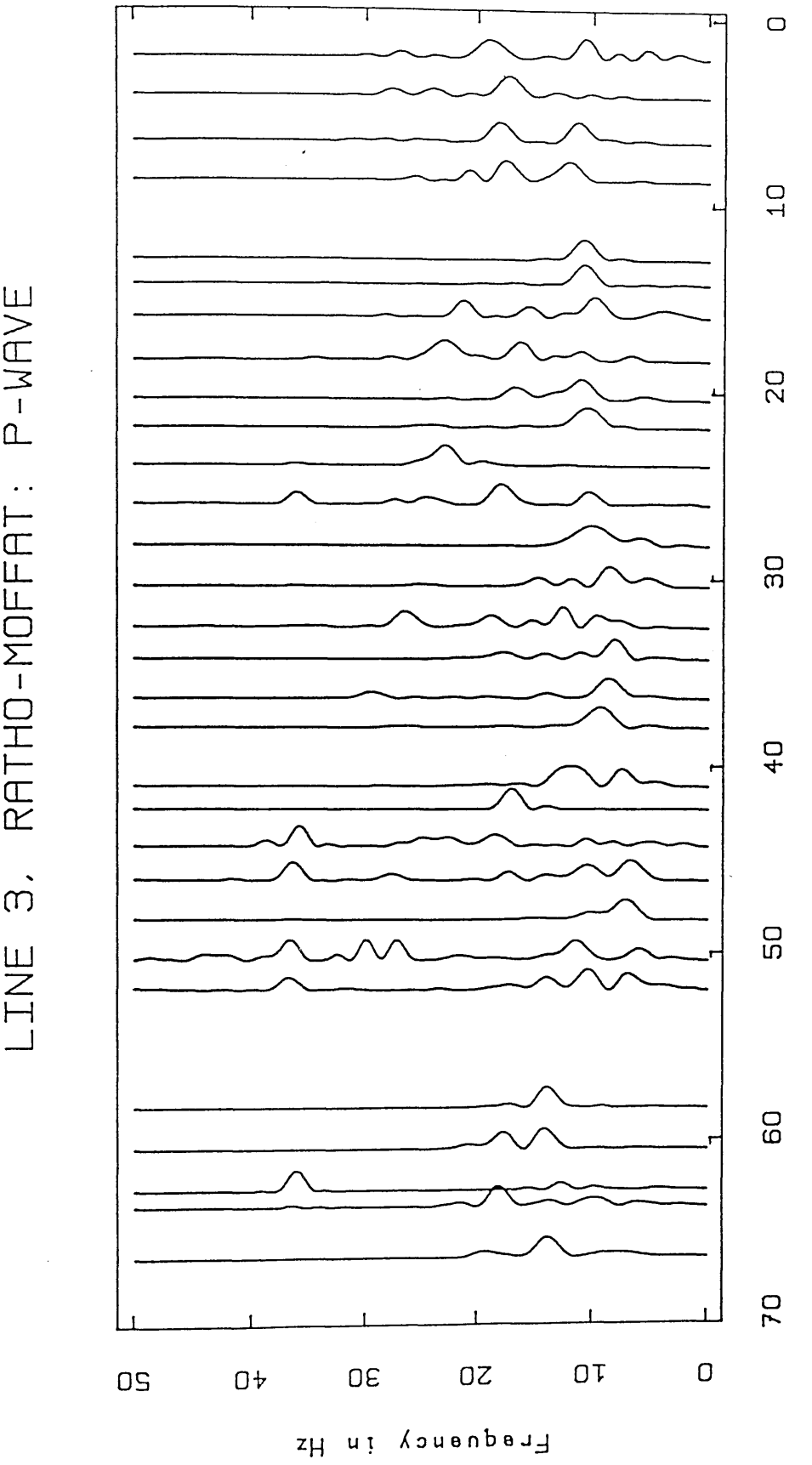

Fig. 4.6 Spectral analysis for line 3 (Ratho shot).

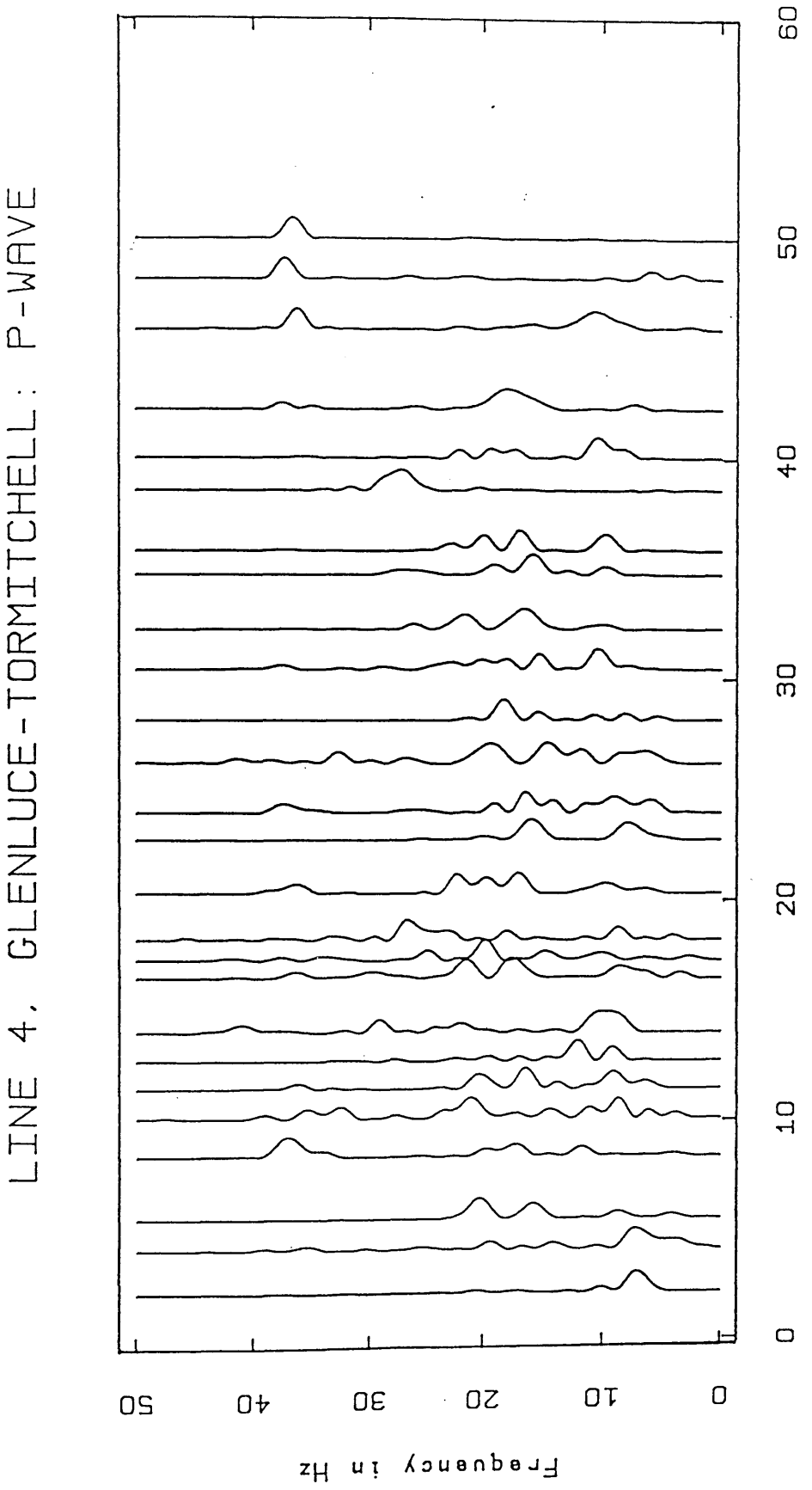

Fig. 4.7 Spectral analysis for line 4 (Glenluce shot).

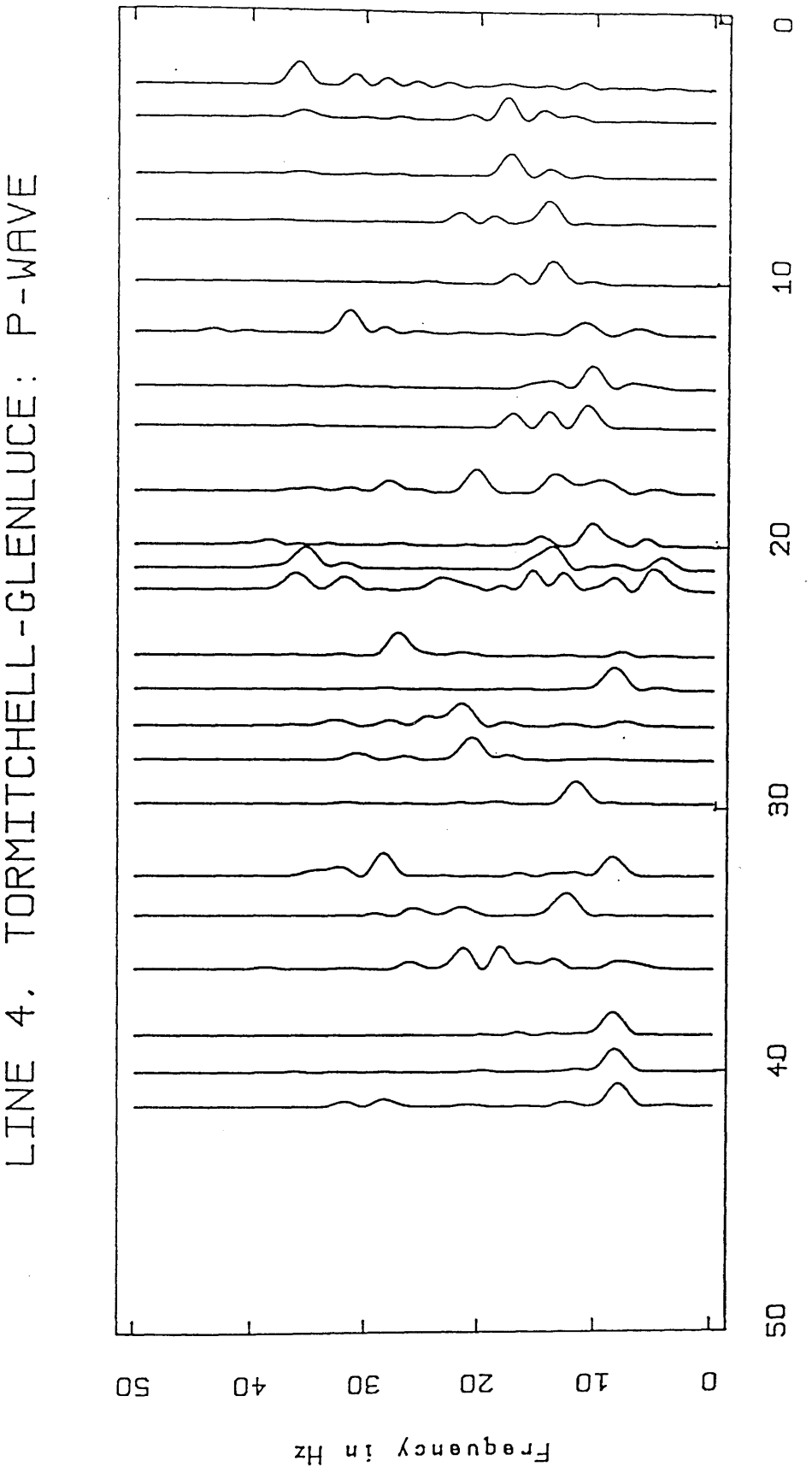

Fig. 4.8 Spectral analysis for line 4 (Tormitchell shot).

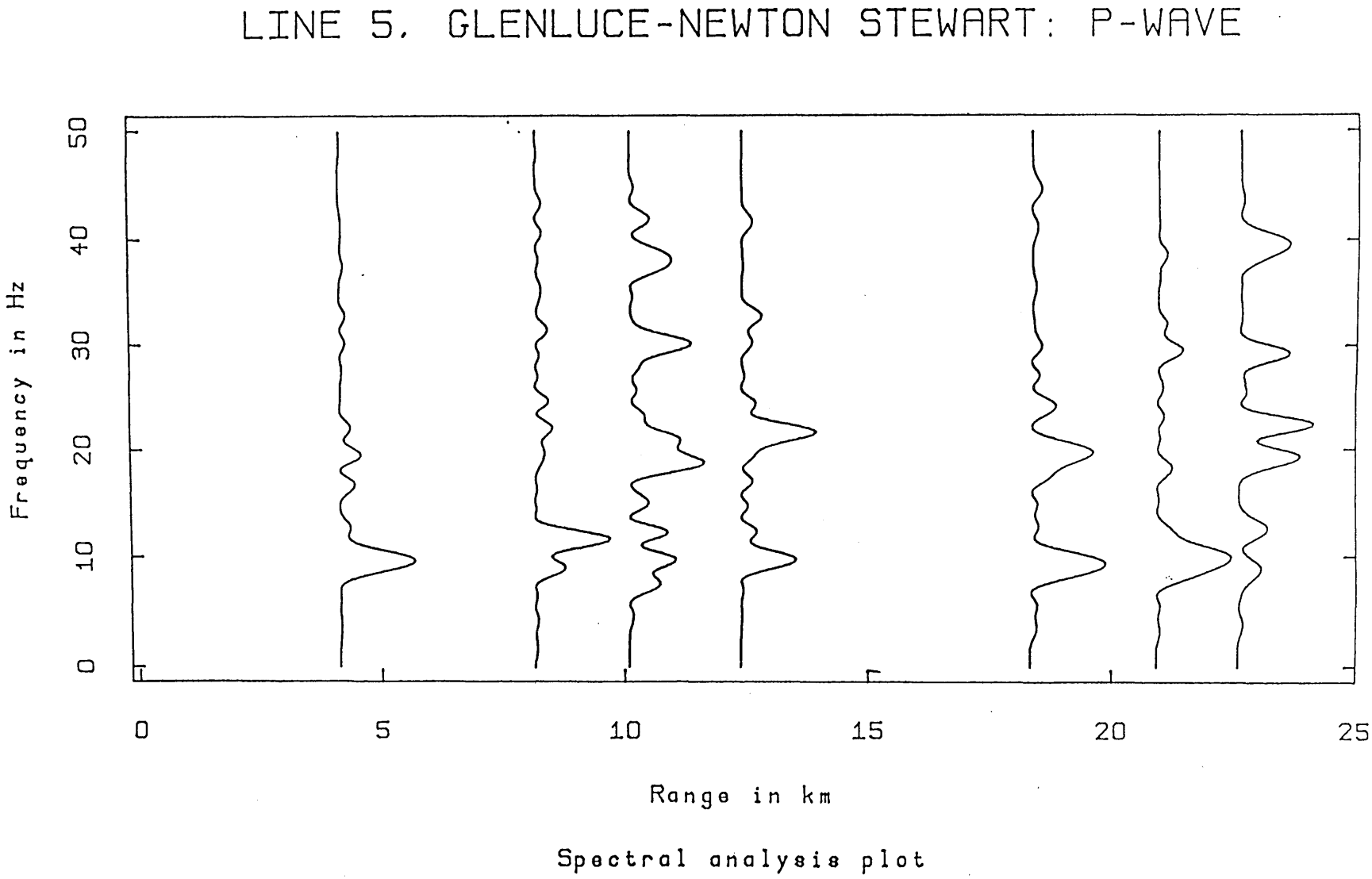

Fig. 4.9 Spectral analysis for line 5 (Glenluce shot).

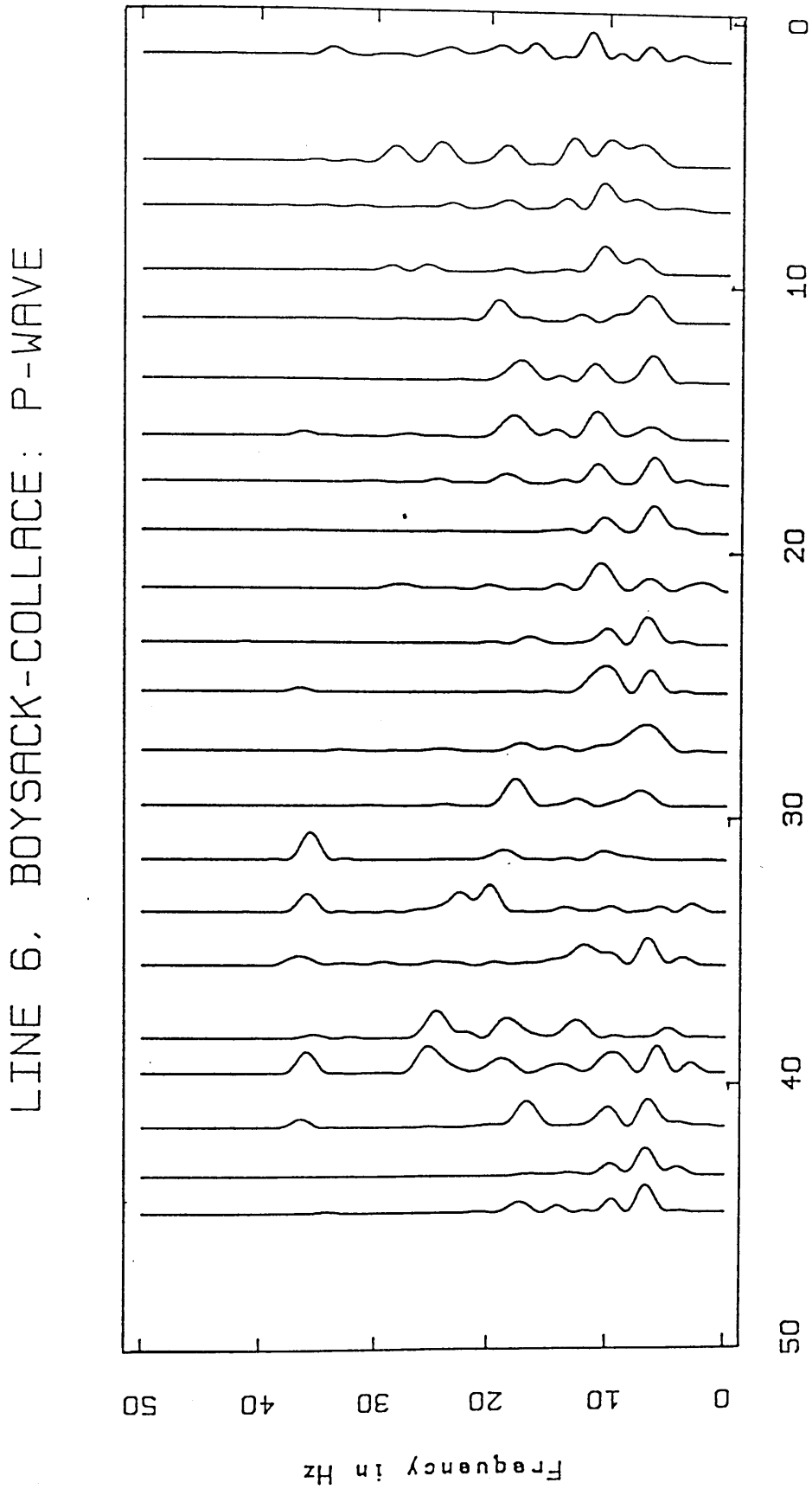

Fig. 4.10 Spectral analysis for line 6 (Boysack shot).

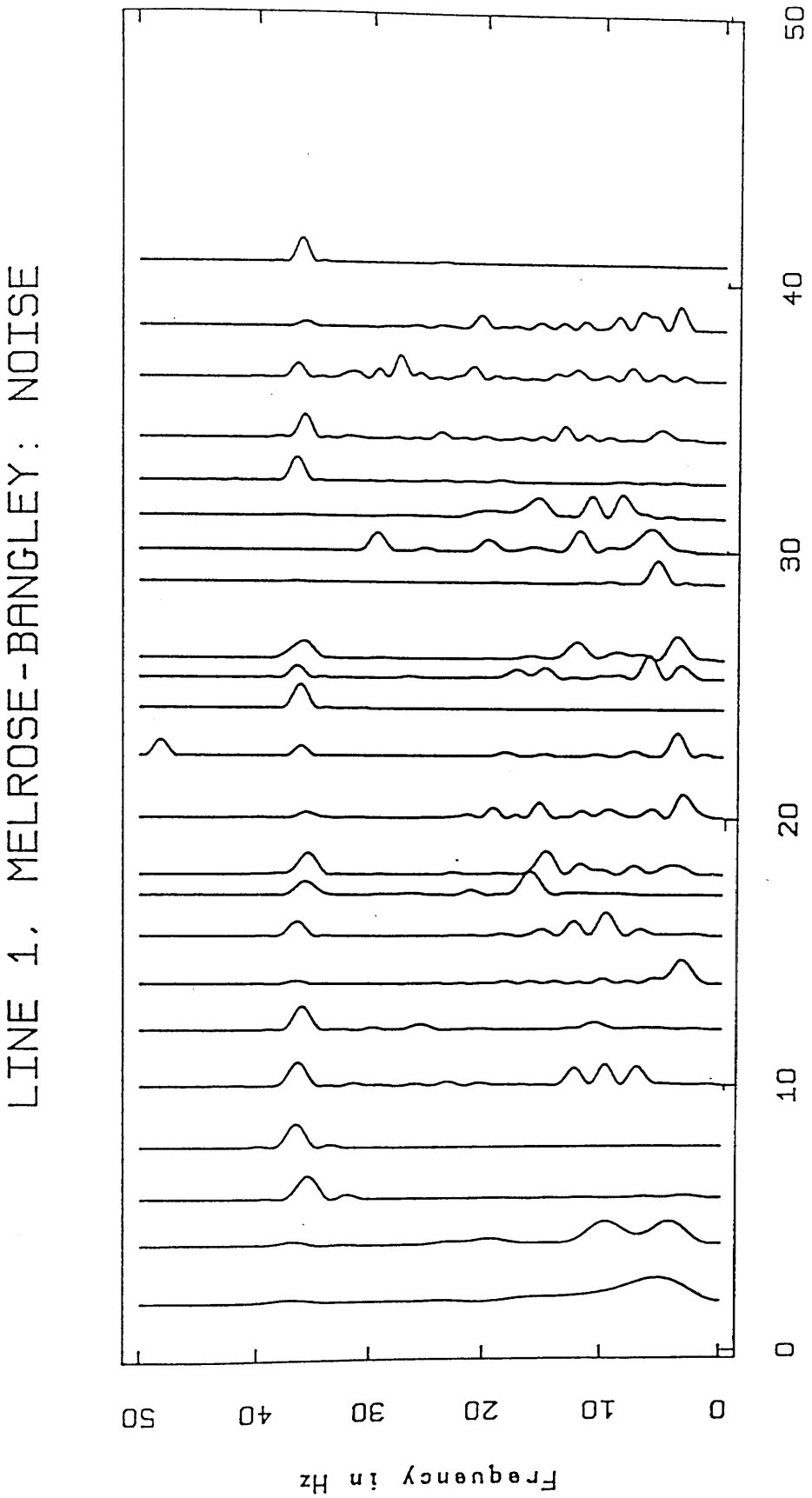

Fig. 4.11 Spectral analysis for line 1 (noise).

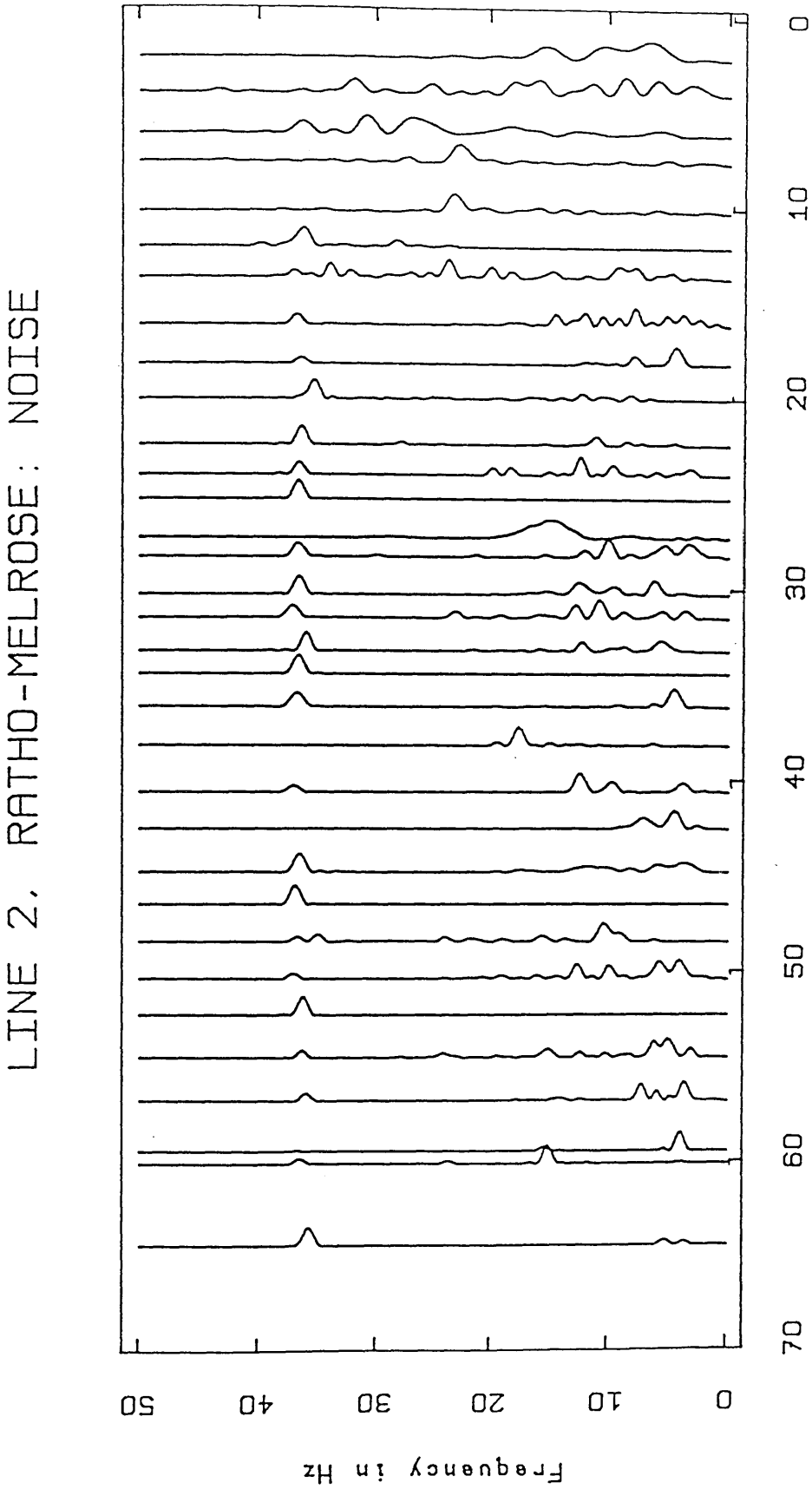

Fig. 4.12 Spectral analysis for line 2 (noise).

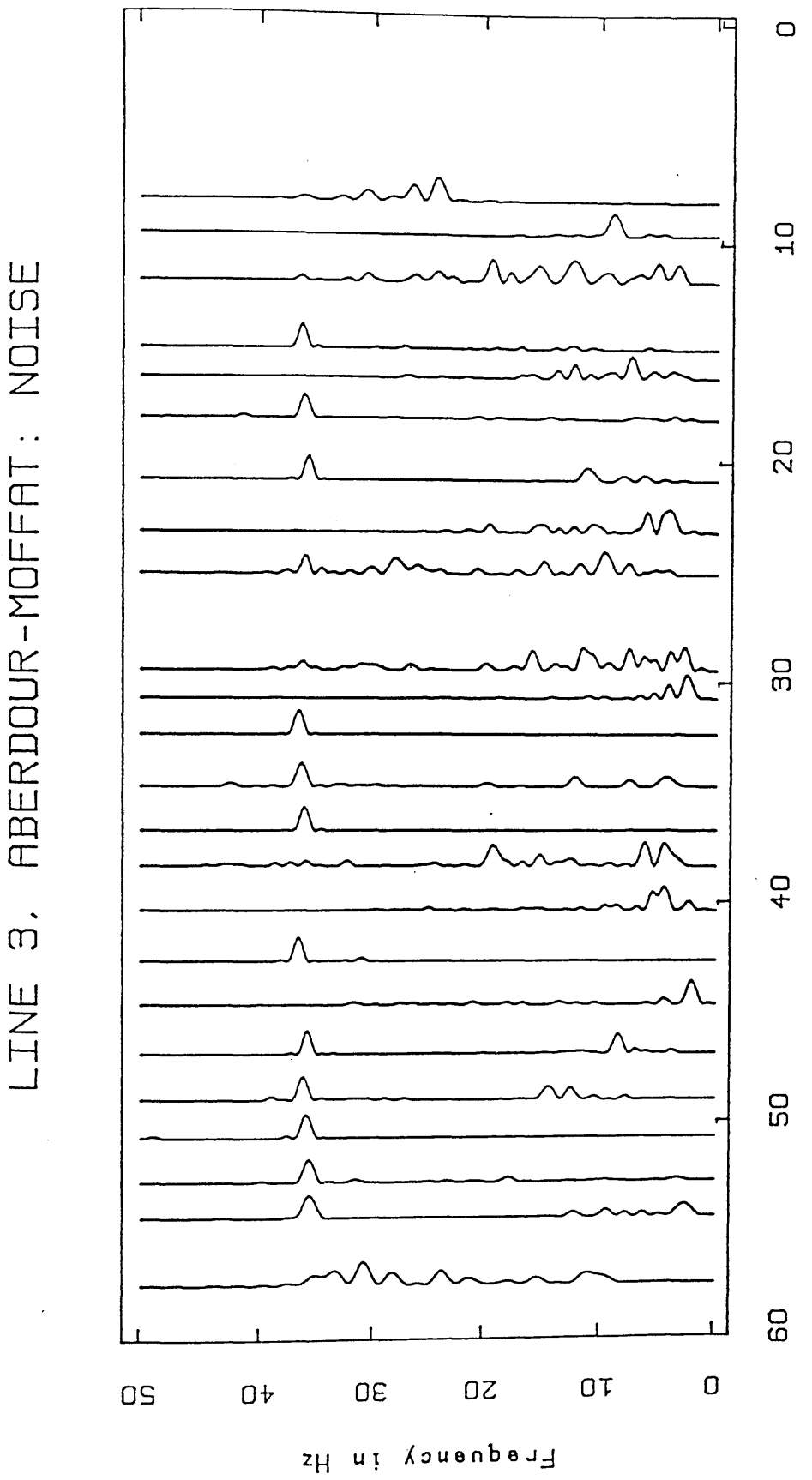

Fig. 4.13 Spectral analysis for line 3 (noise).

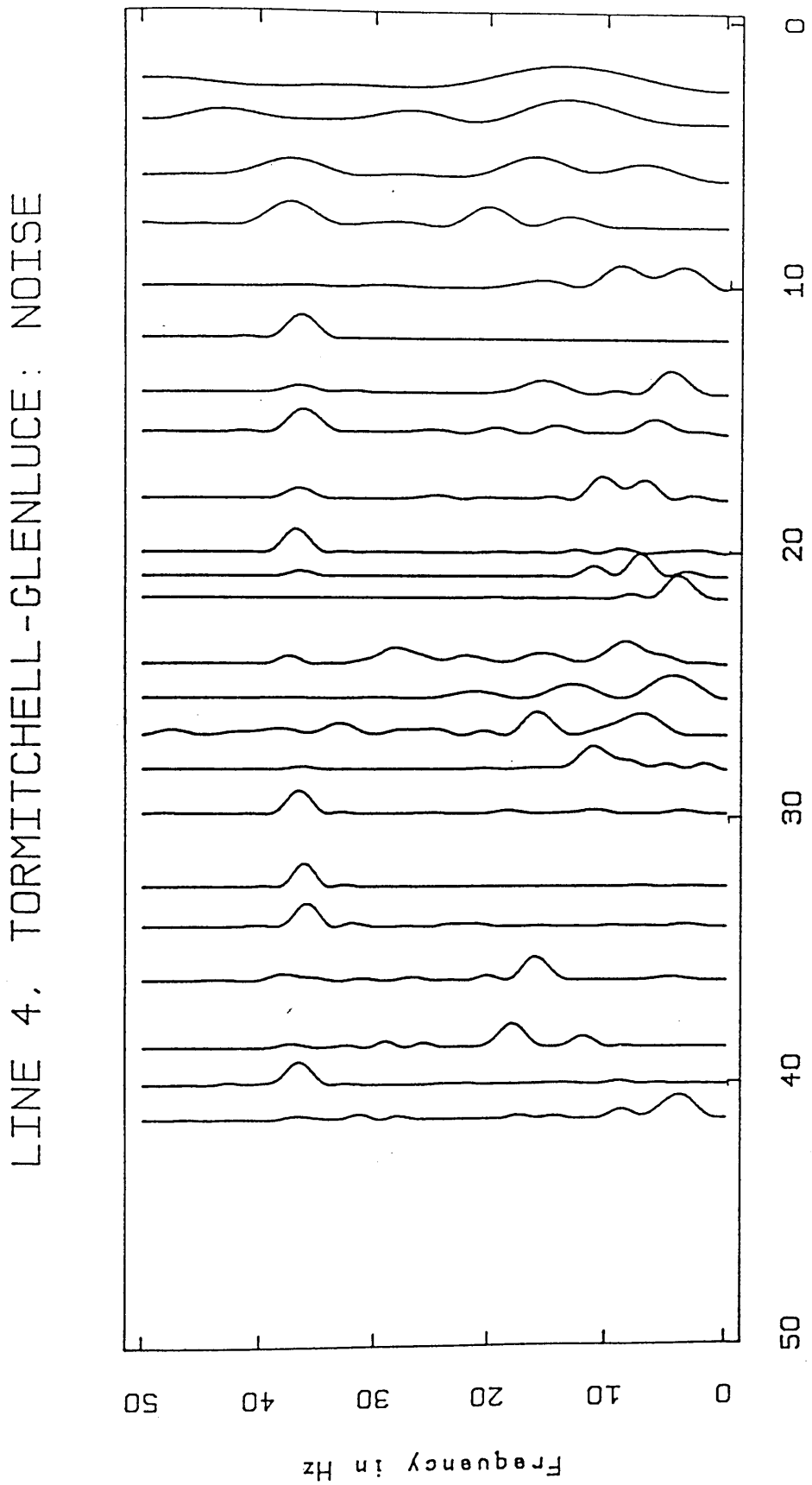

Fig. 4.14 Spectral analysis for line 4 (noise).

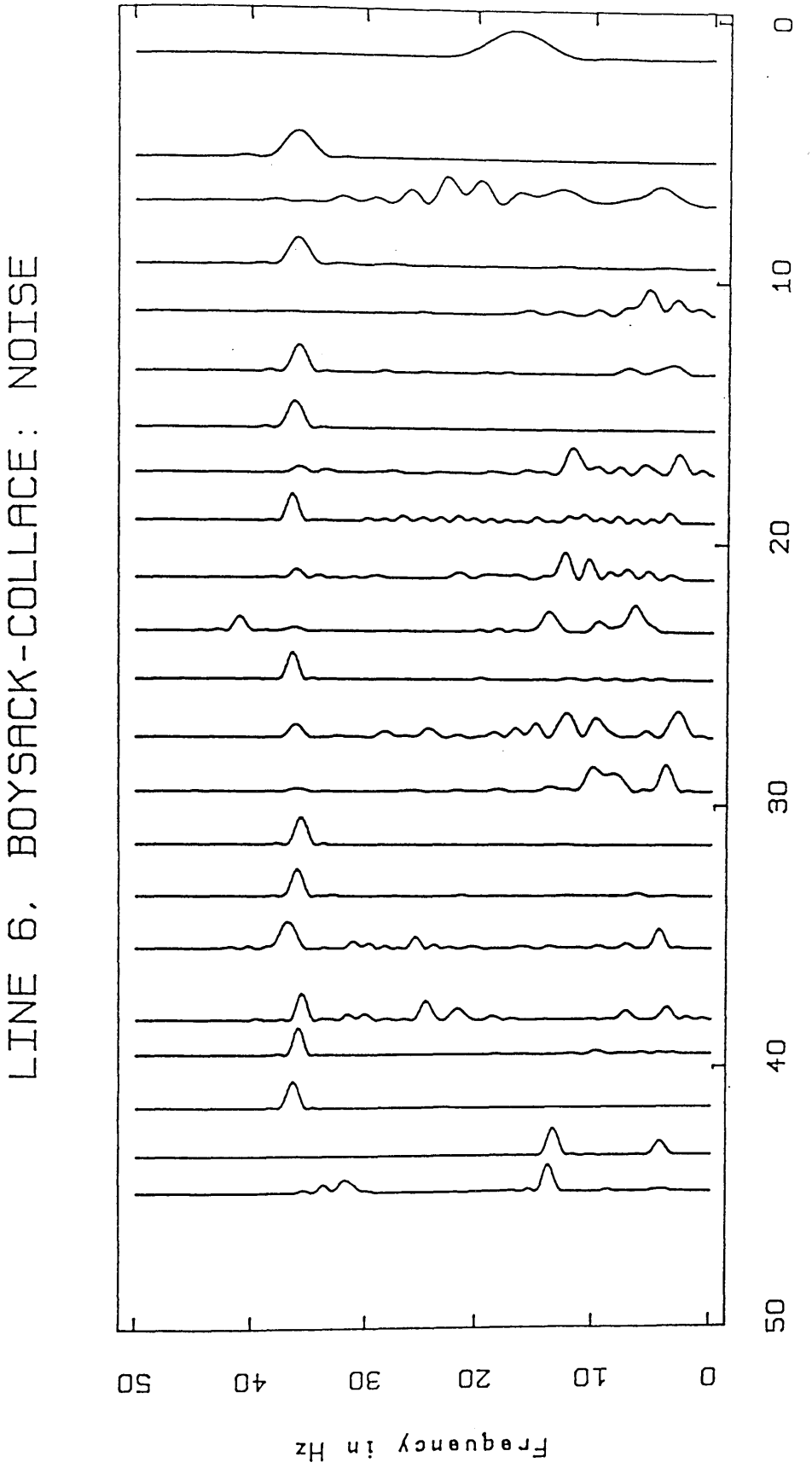

Fig. 4.15 Spectral analysis for line 6 (noise).

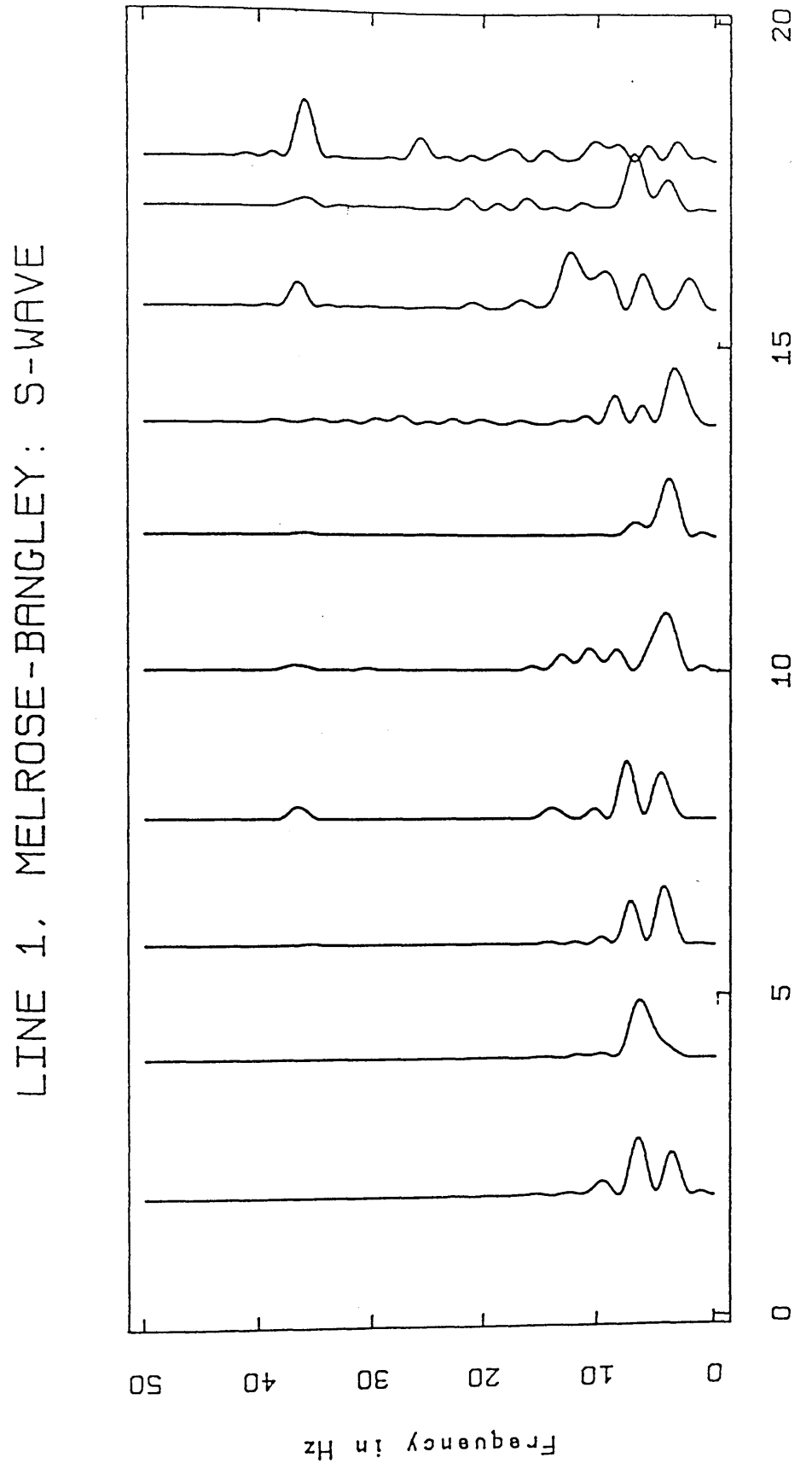

Fig. 4.16 Spectral analysis for line 1, Melrose shot (S-wave).

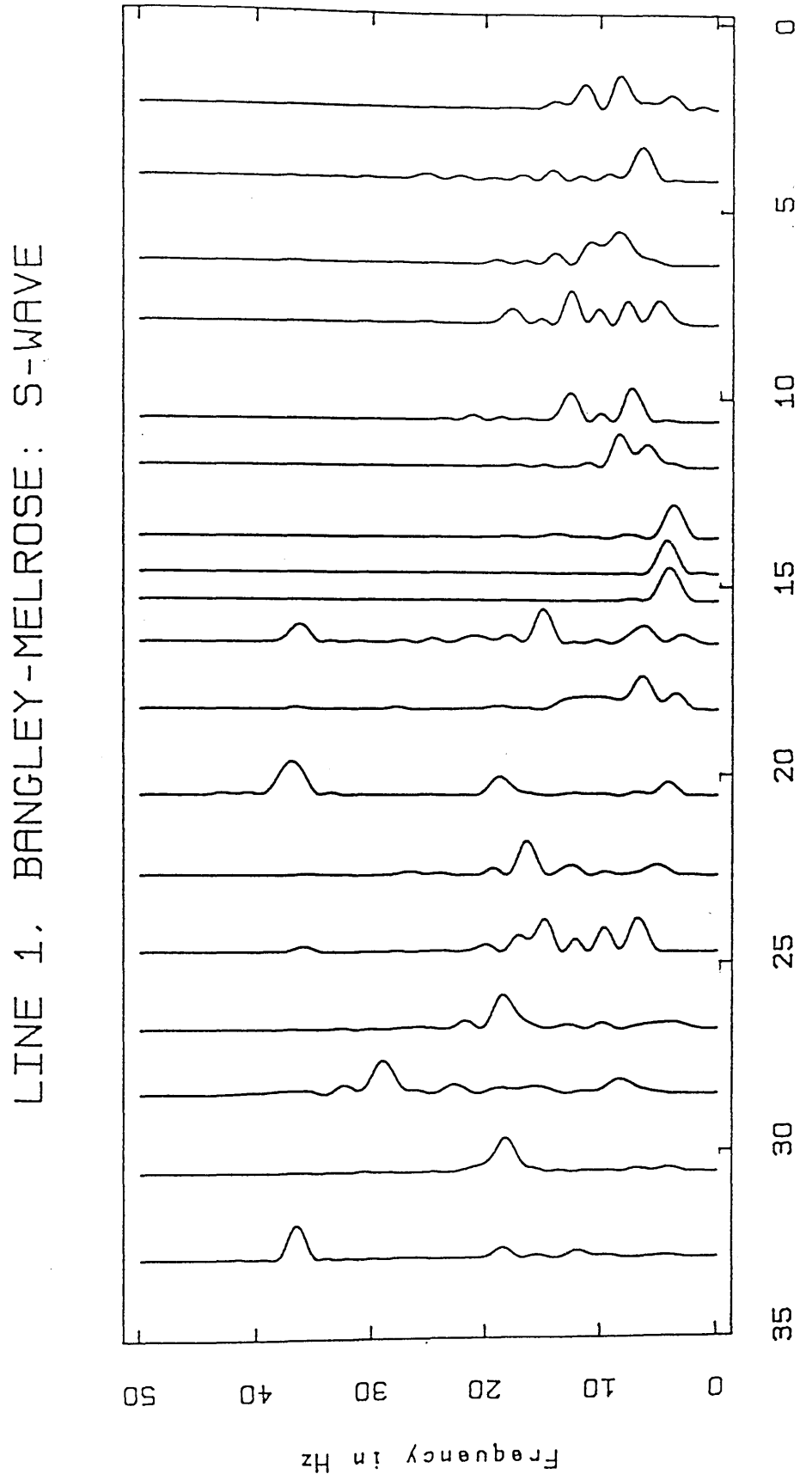

Fig. 4.17 Spectral analysis for line 1, Bangley shot (S-wave).

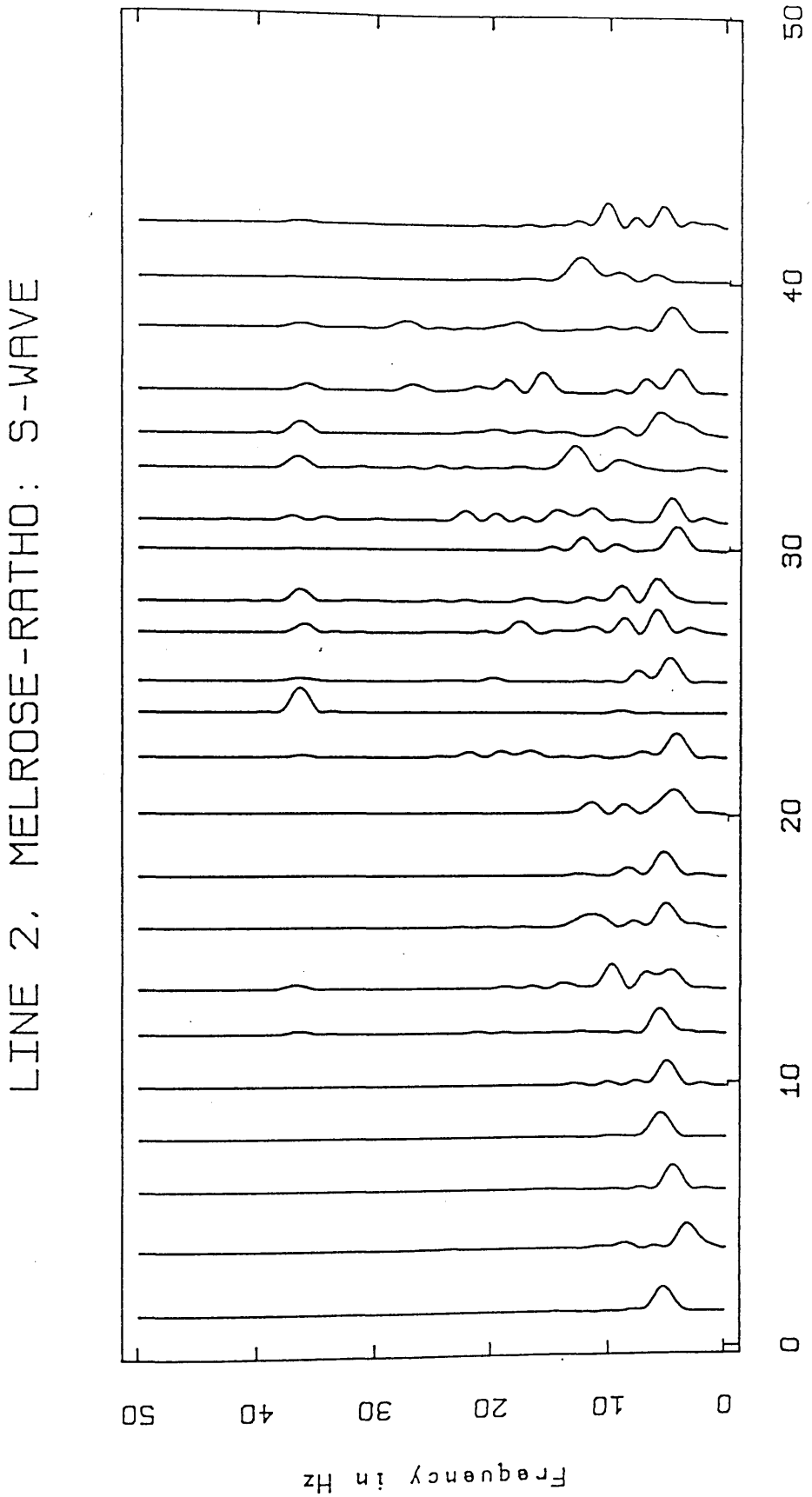

Fig. 4.18 Spectral analysis for line 2, Melrose shot (S-wave).

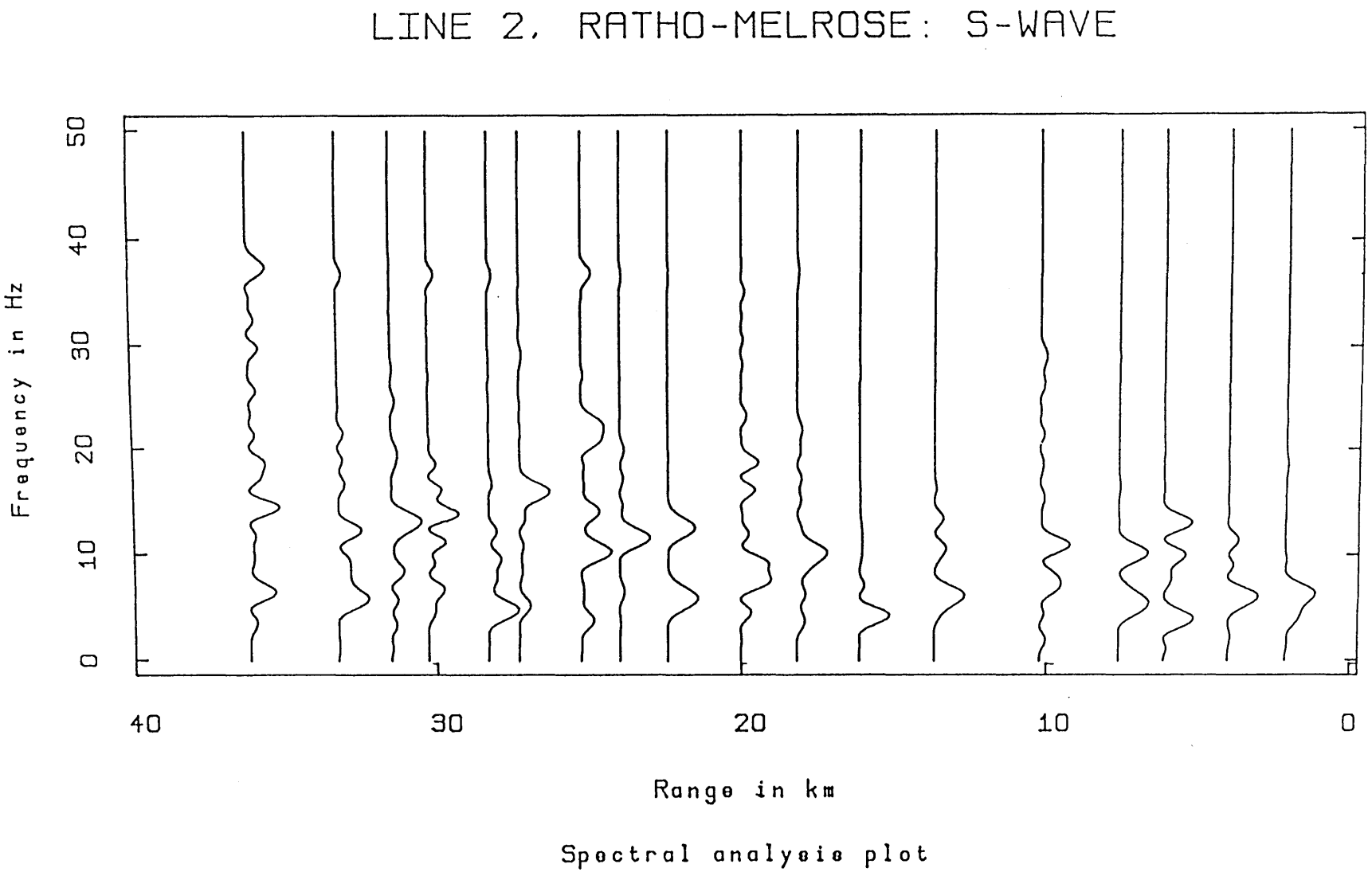

Fig. 4.19 Spectral analysis for line 2, Ratho shot (S-wave).

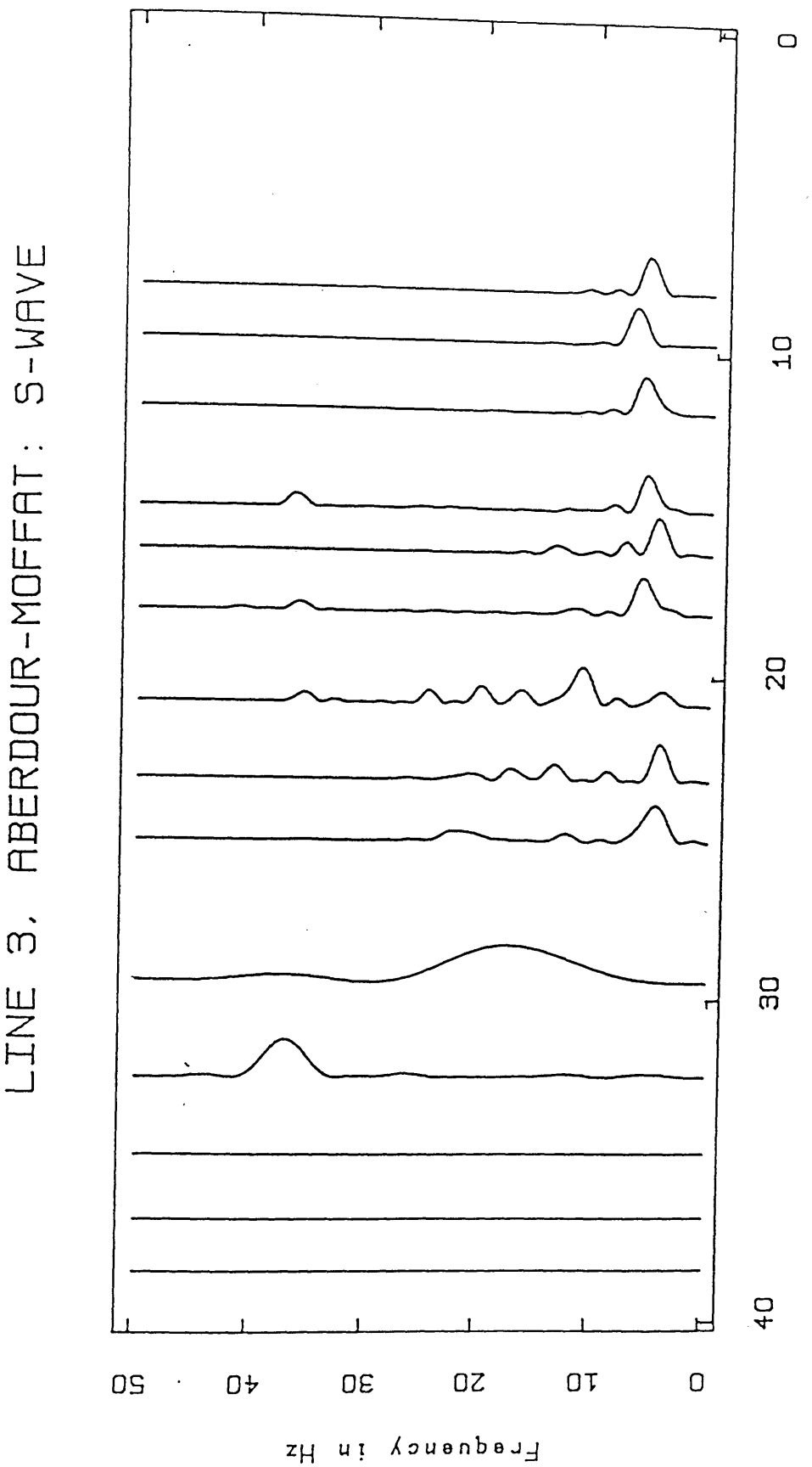

Fig. 4.20 Spectral analysis for line 3, Aberdour shot (S-wave).

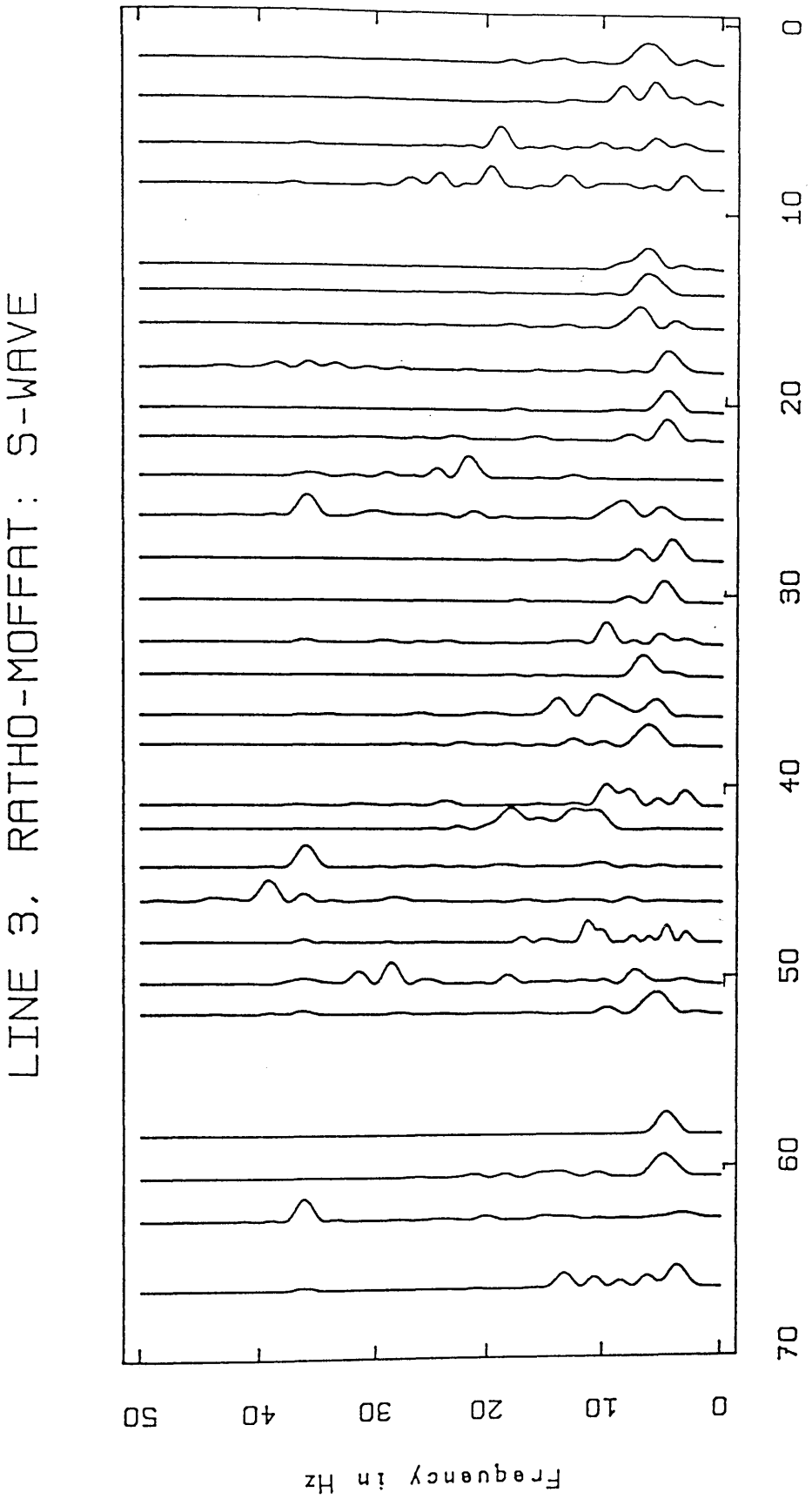

Fig. 4.21 Spectral analysis for line 3, Ratho shot (S-wave).

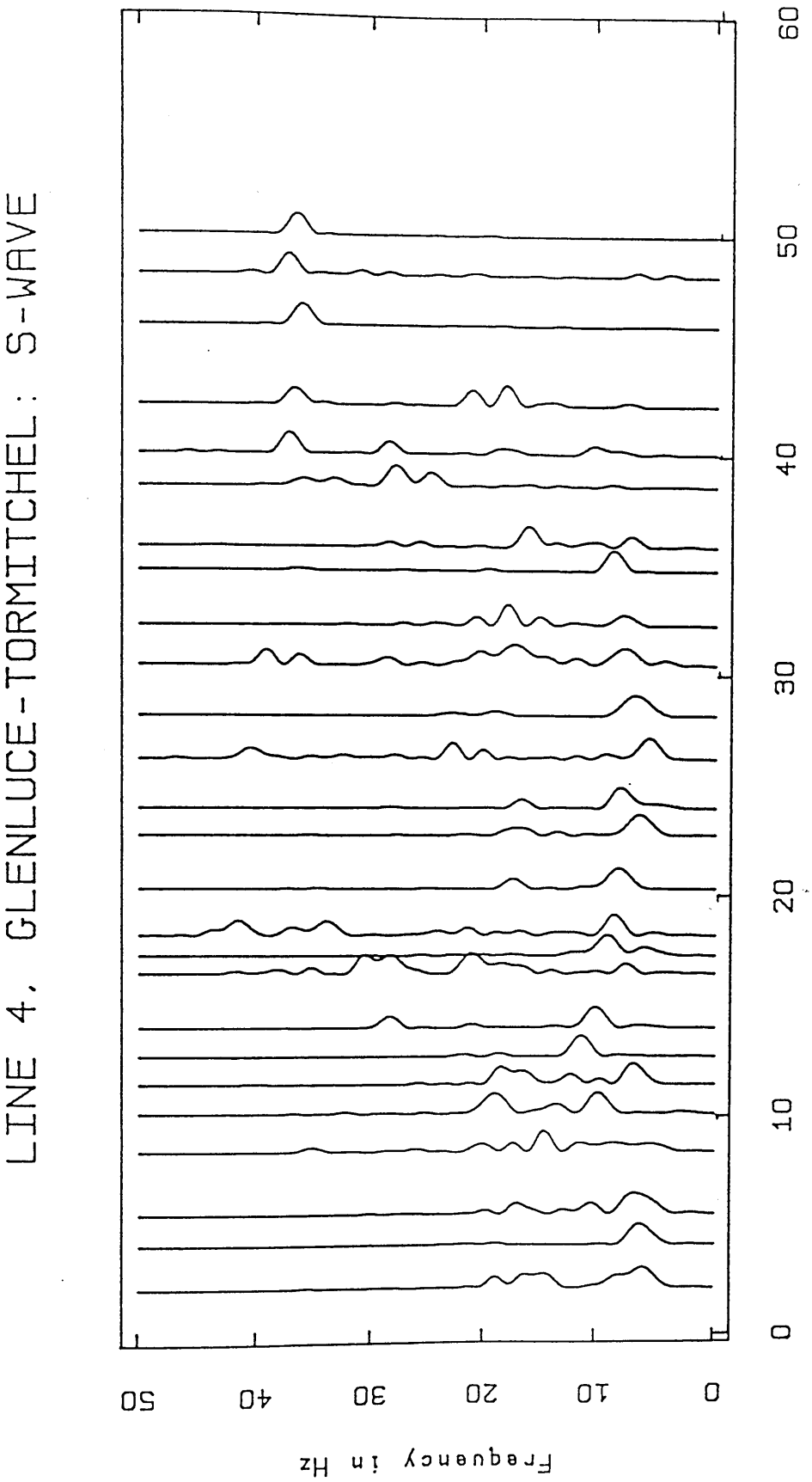

Fig. 4.22 Spectral analysis for line 4, Glenluce shot (S-wave).

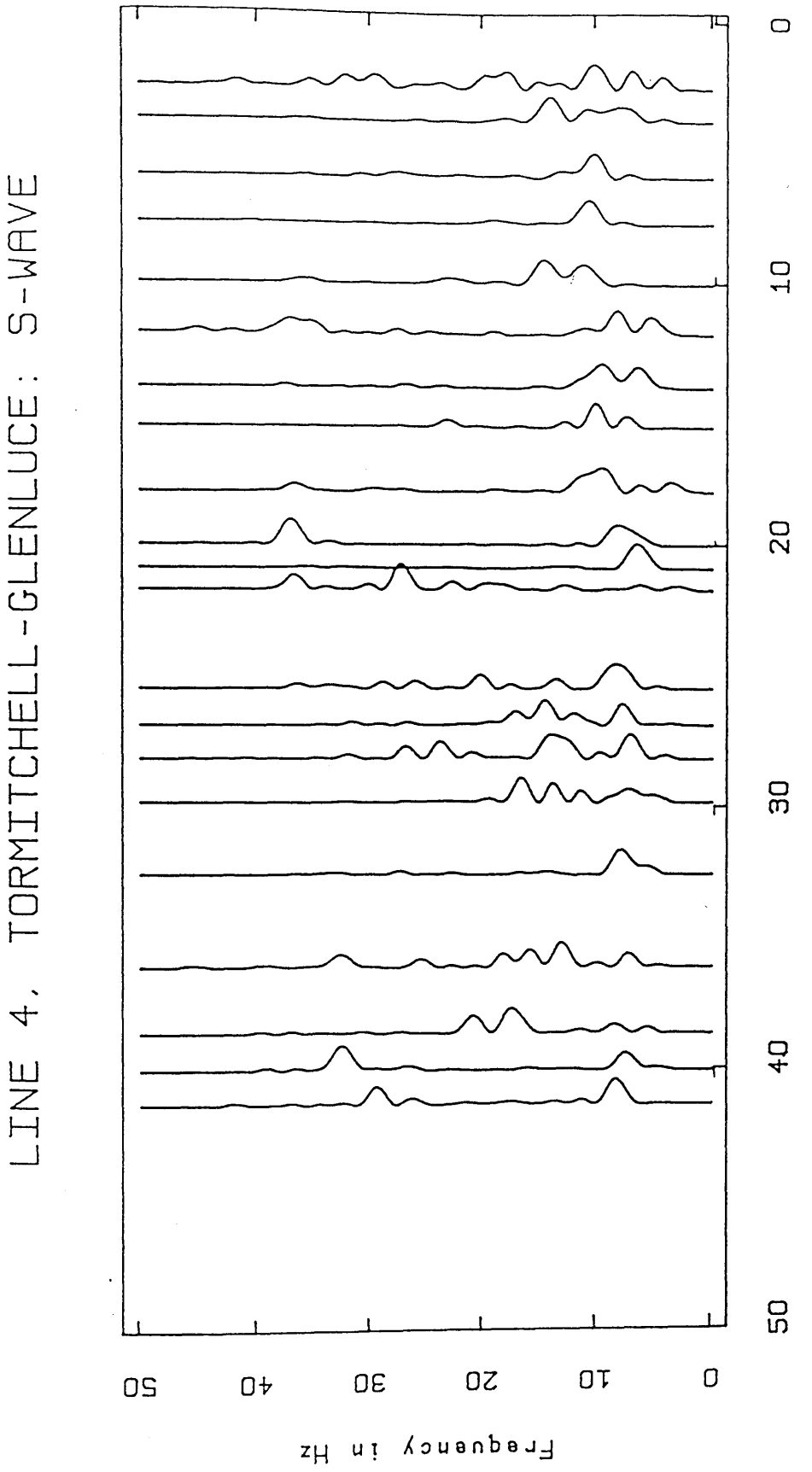

Fig. 4.23 Spectral analysis for line 4, Tormitchell shot (S-wave).

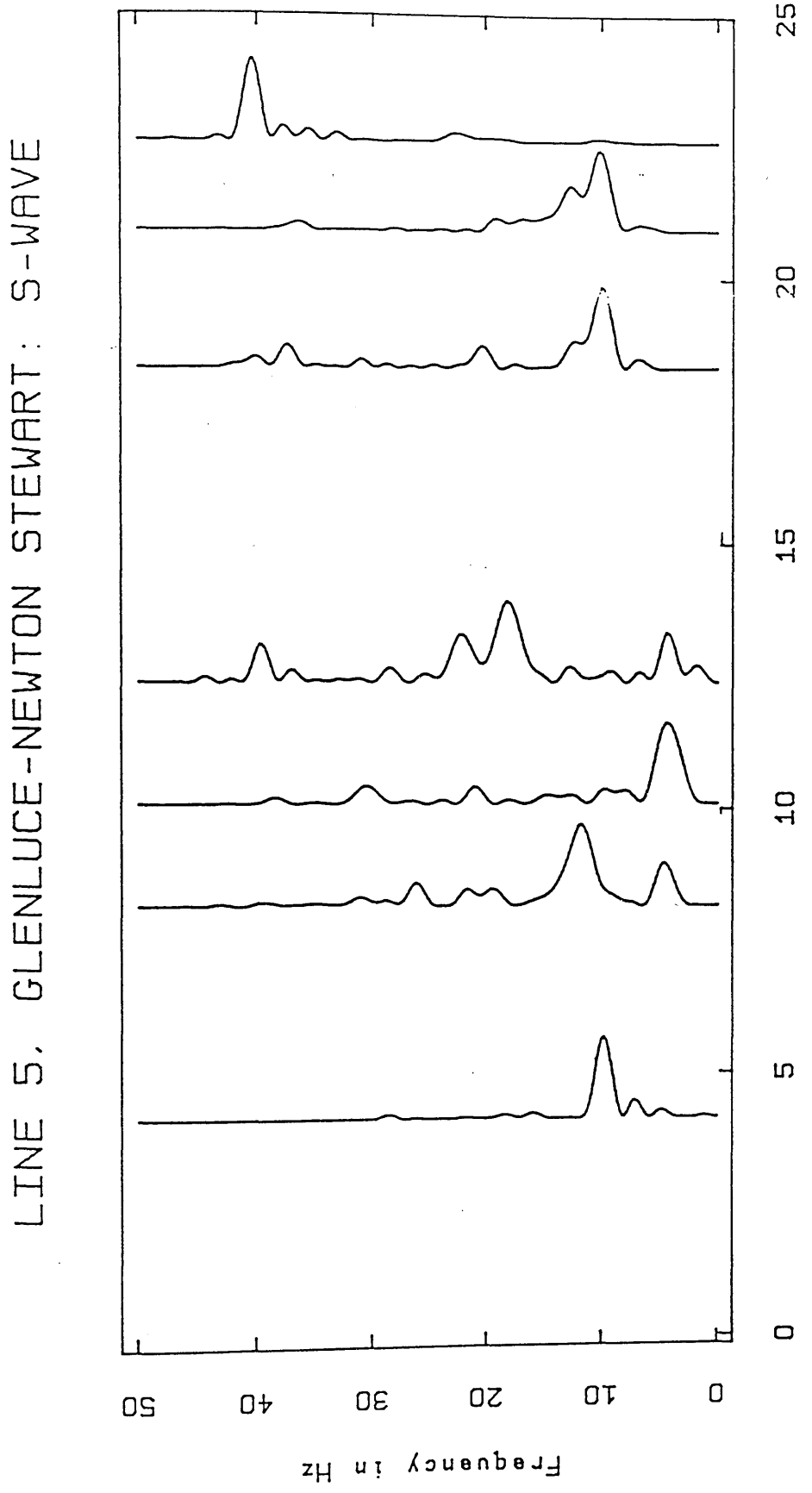

Fig. 4.24 Spectral analysis for line 5, Glenluce shot (S-wave).

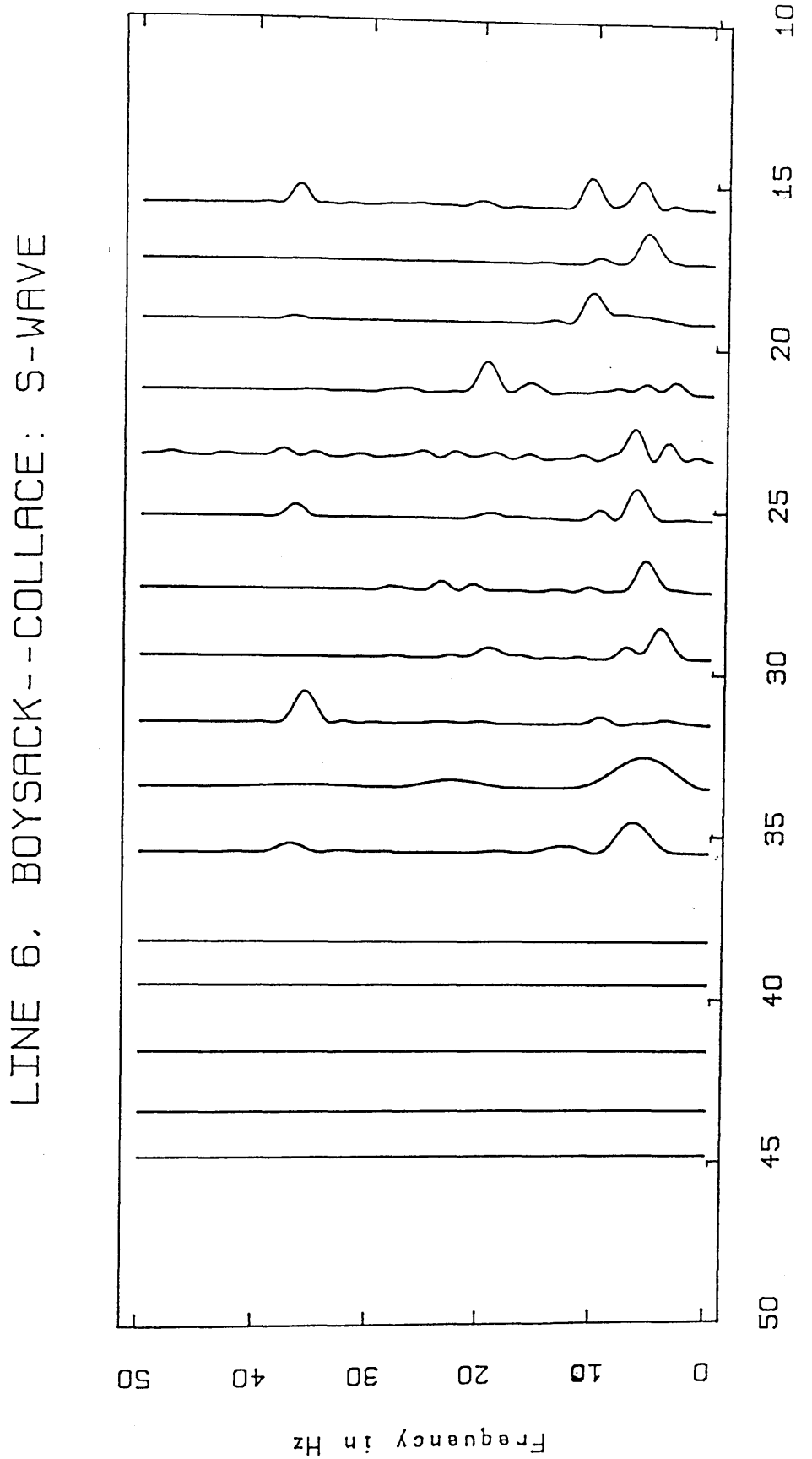

Fig. 4.25 Spectral analysis for line 6, Boysack shot (S-wave).

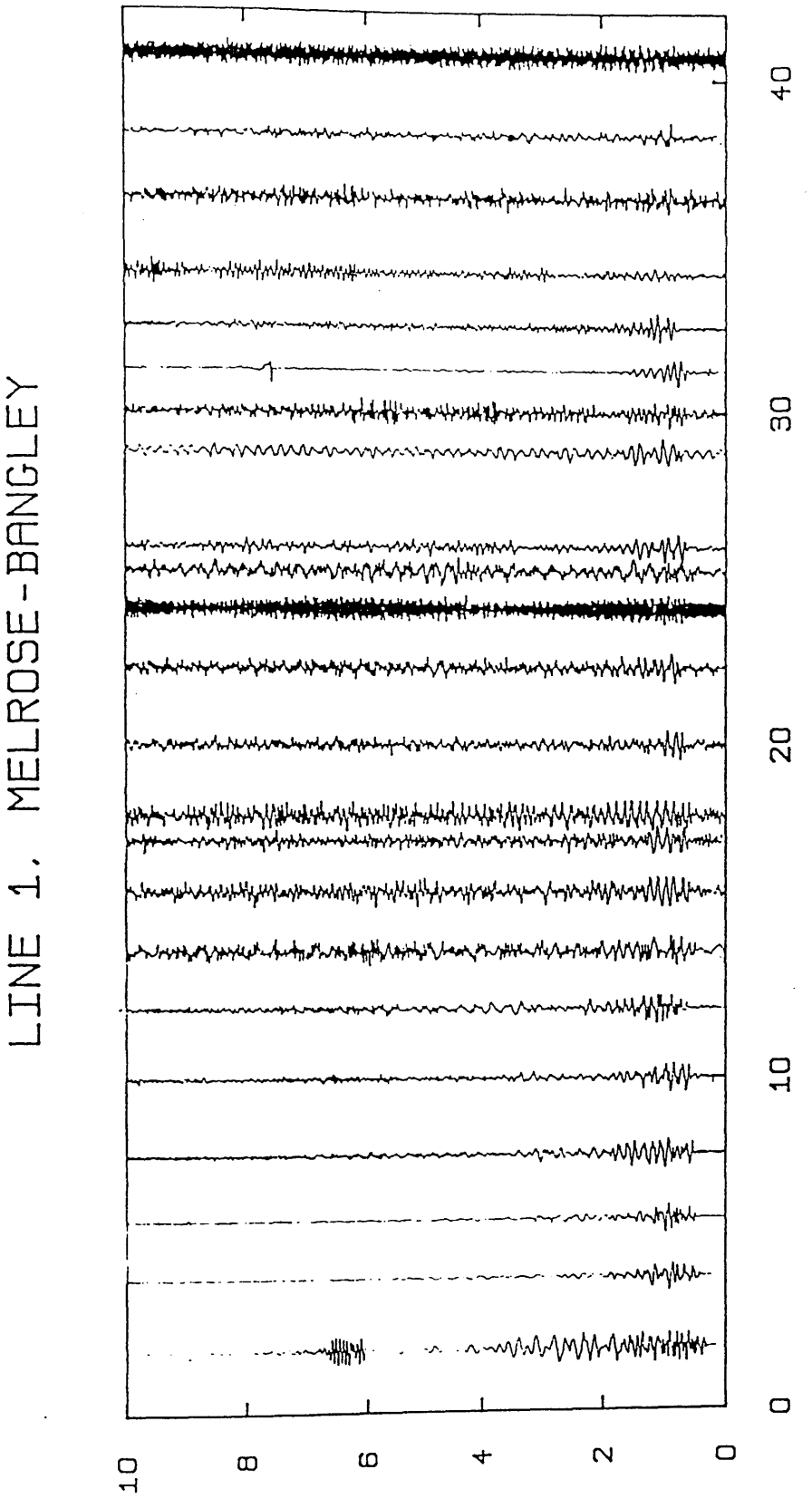

Fig. 4.26a Unfiltered section line 1 (Melrose shot).

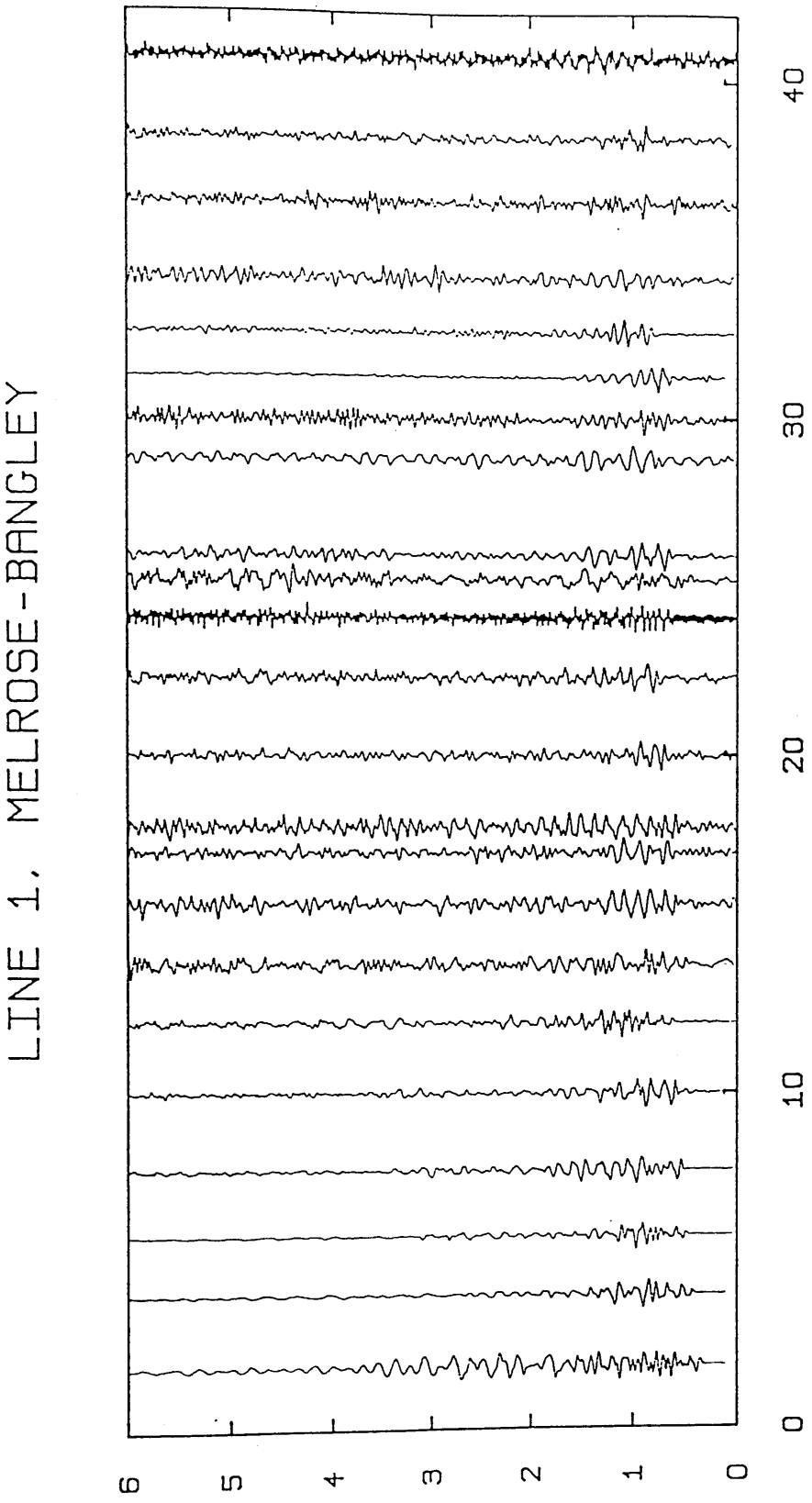

Fig. 4.26b Filtered section line 1, P-wave (Melrose shot).

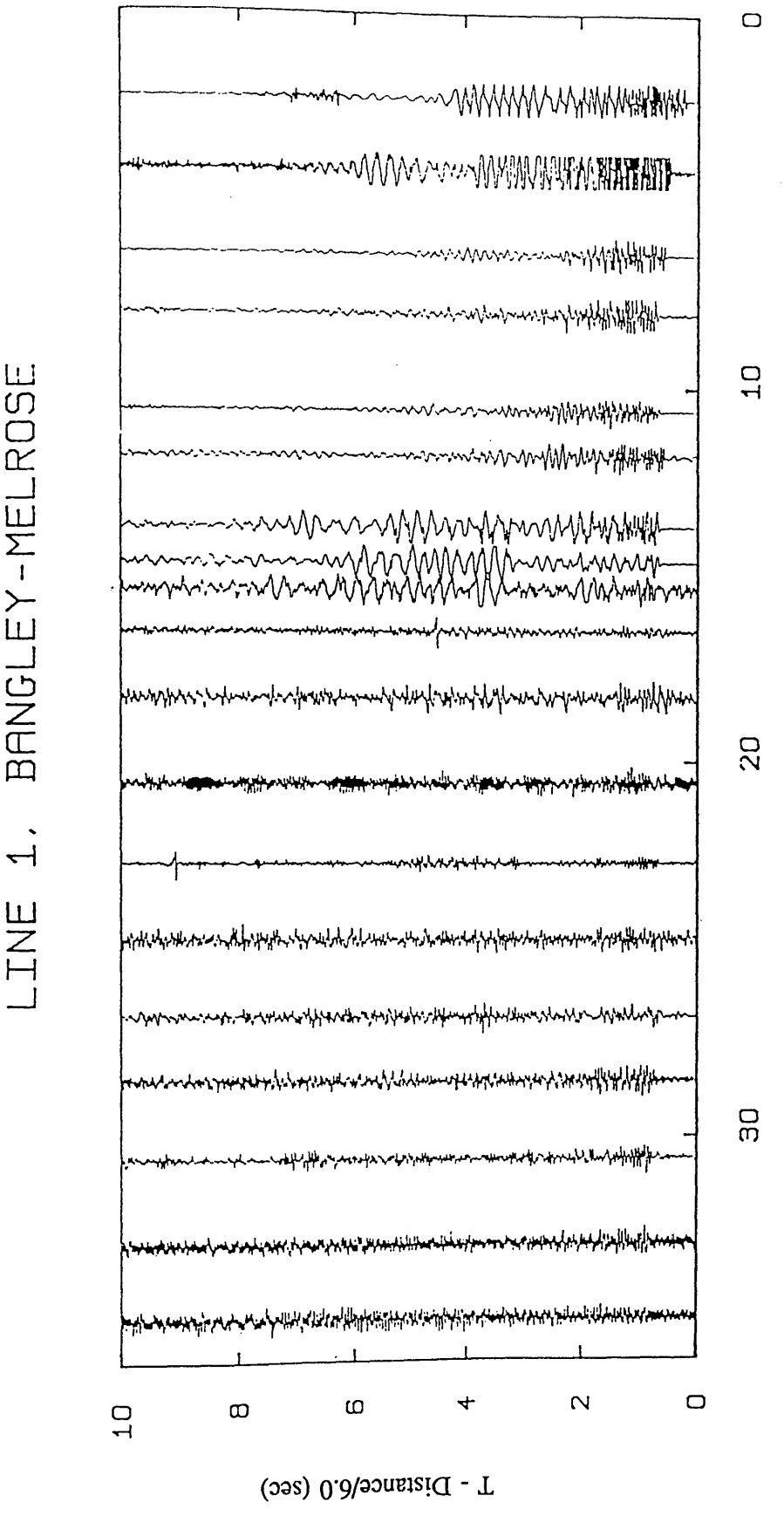

Fig. 4.27a Unfiltered section line 1 (Bangley shot).

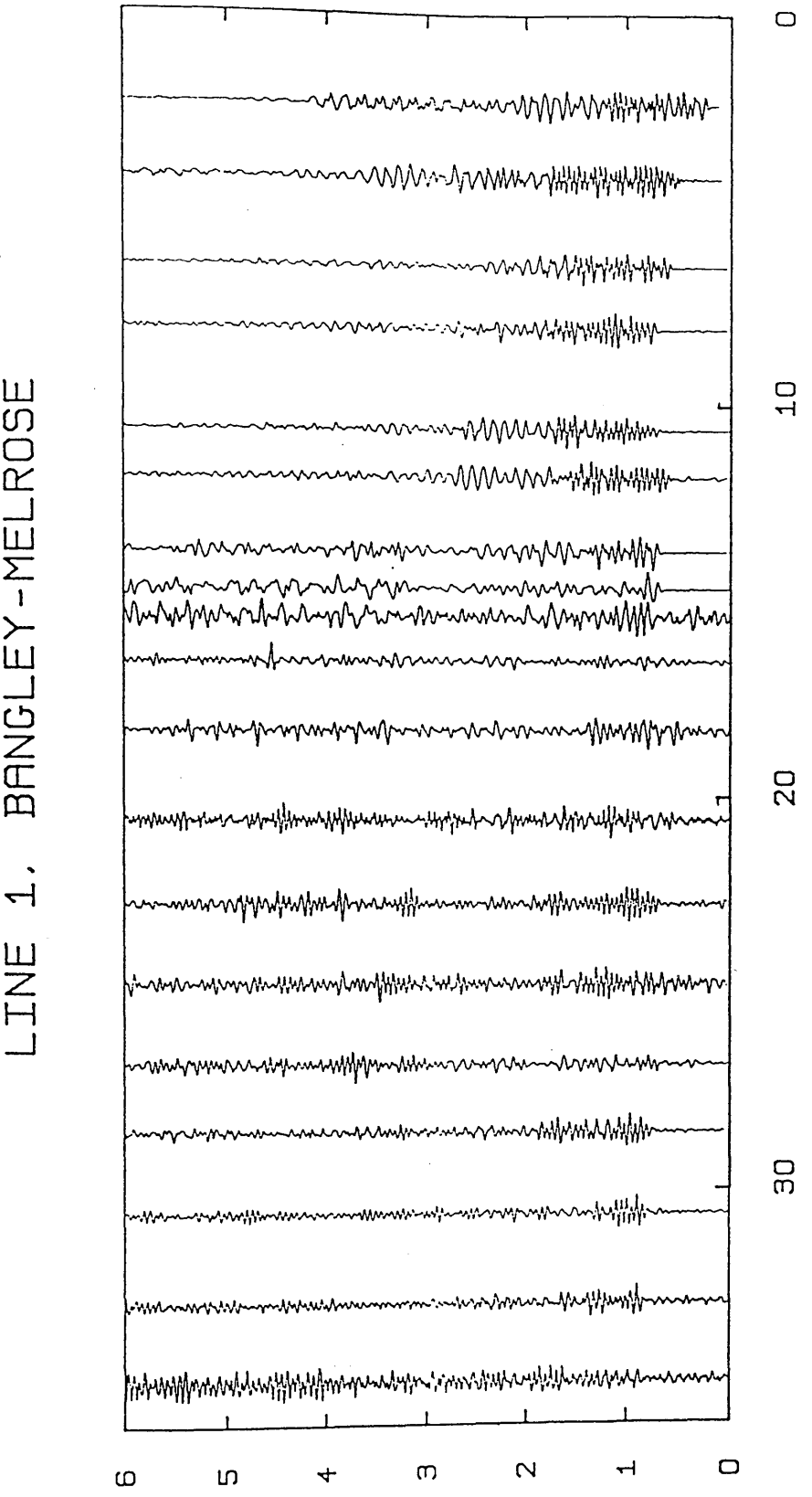

Fig. 4.27b Filtered section line 1, P-wave (Bangley shot).

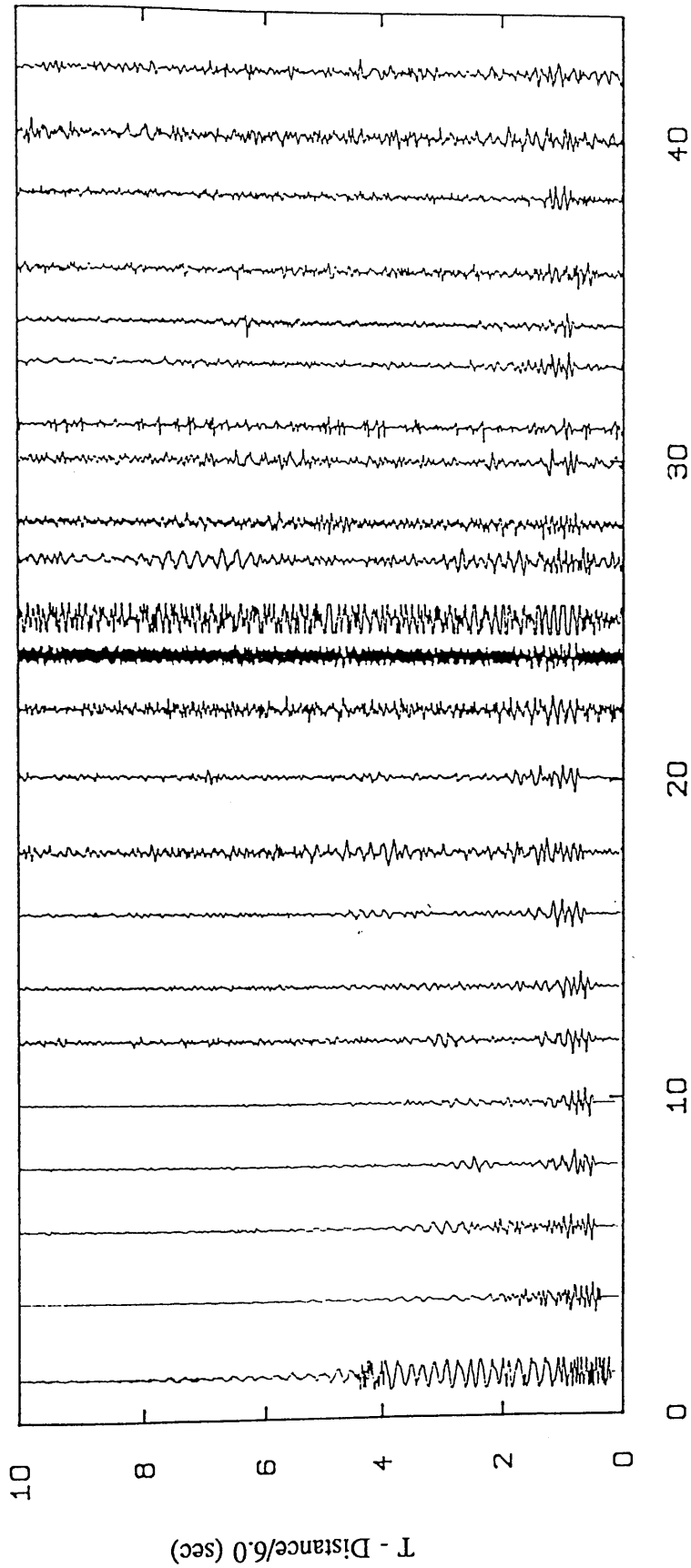

Fig. 4.28a Unfiltered section line 2 (Melrose shot).

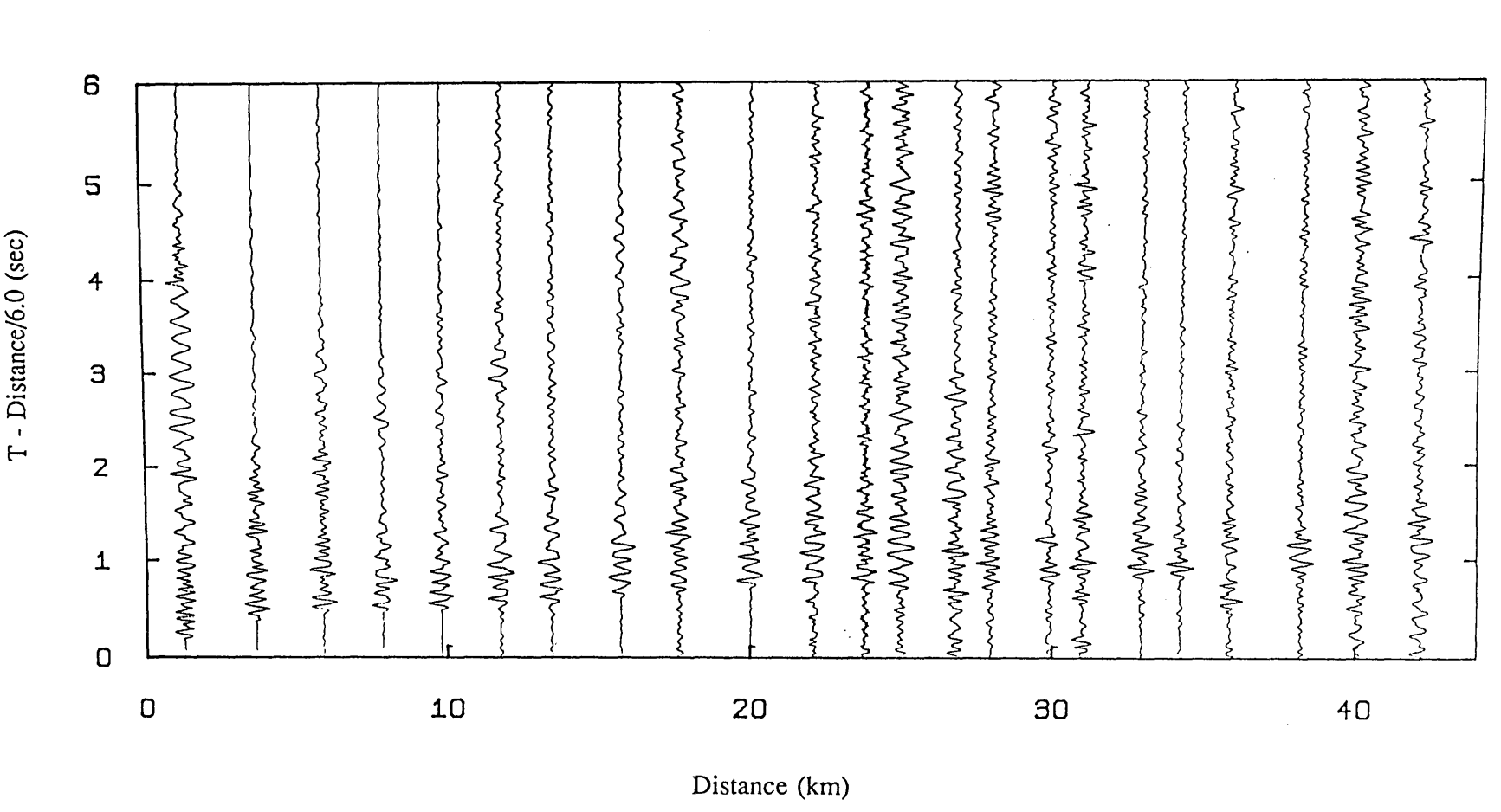

Fig. 4.28b Filtered section line 2, P-wave (Melrose shot).

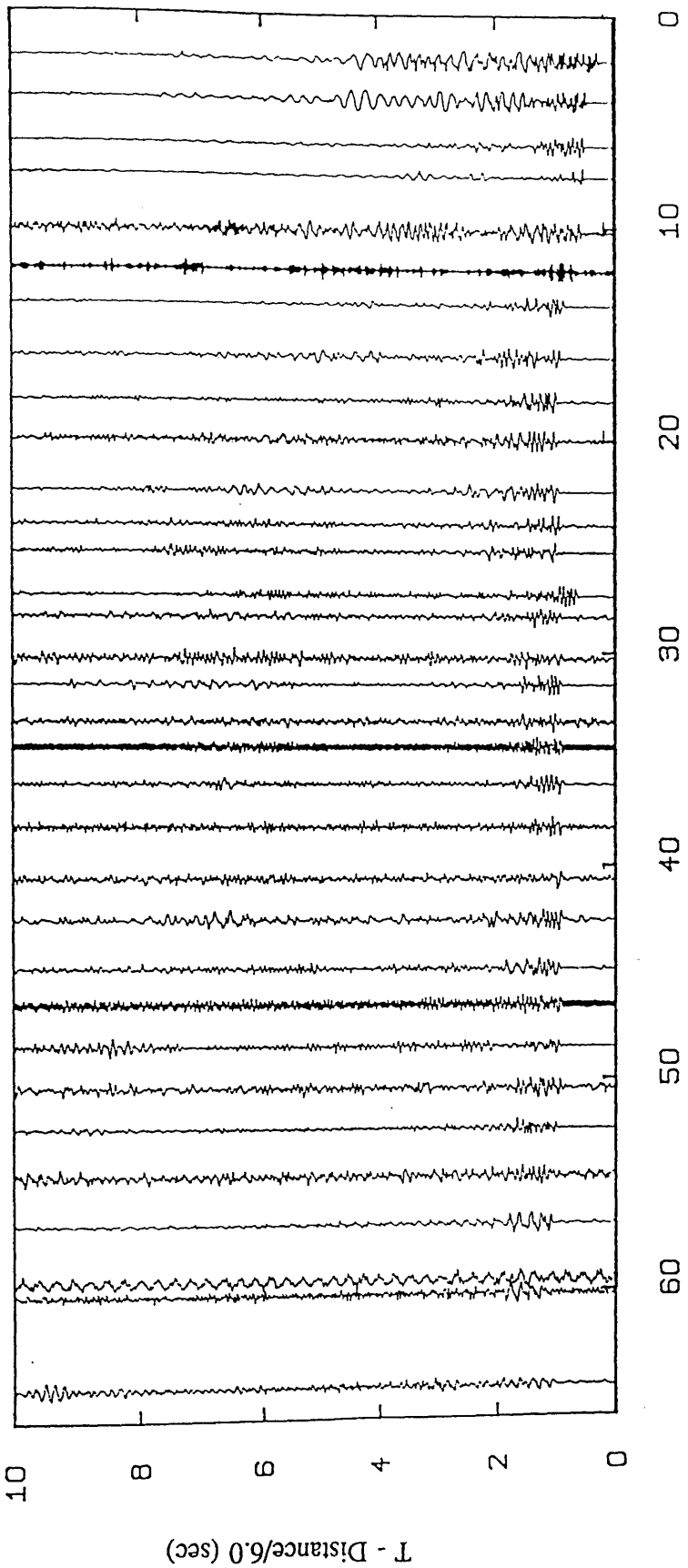

Fig. 4.29 Unfiltered section line 2 (Ratho shot).

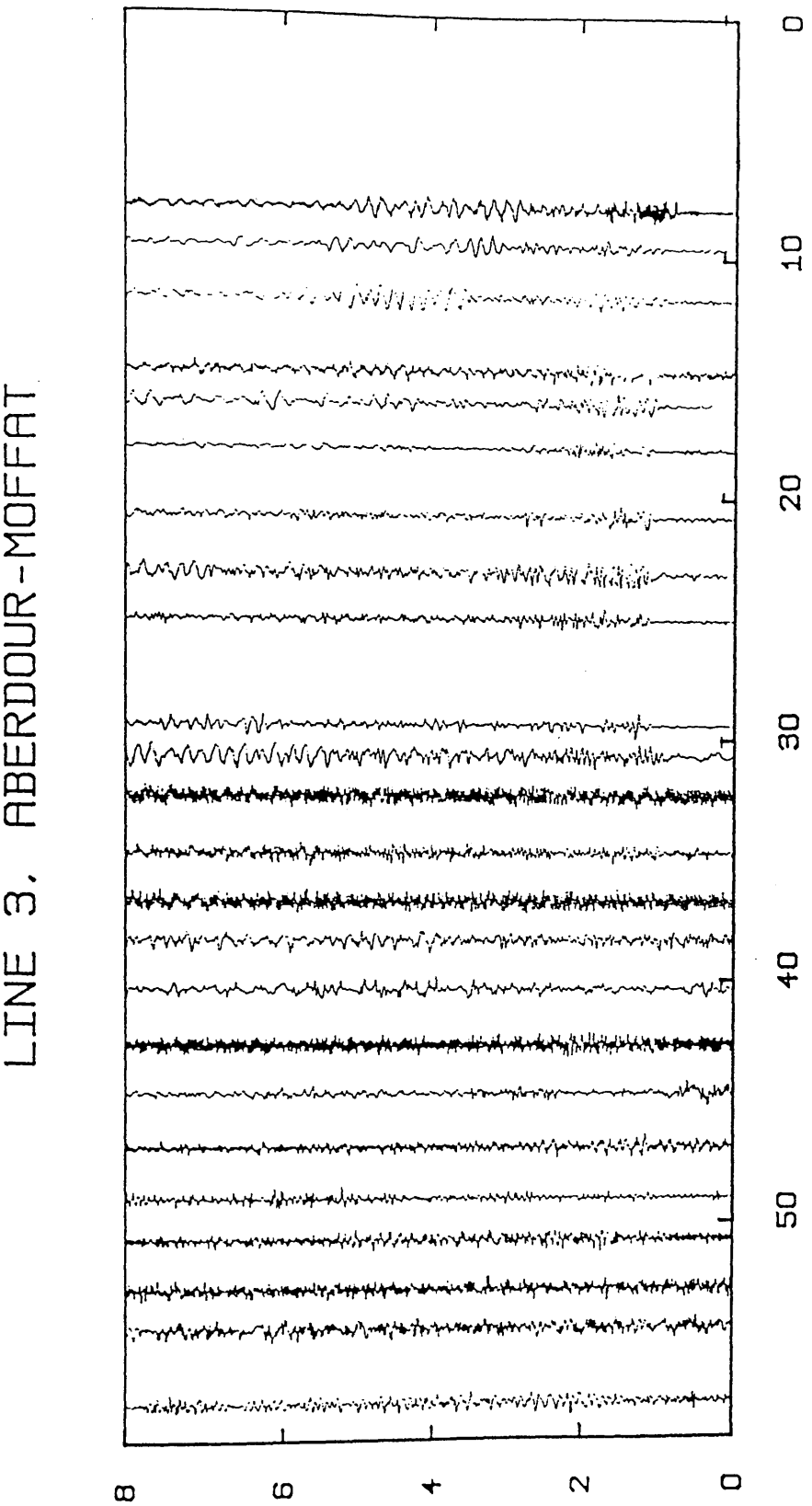

Fig. 4.30a Unfiltered section line 3 (Aberdour shot).

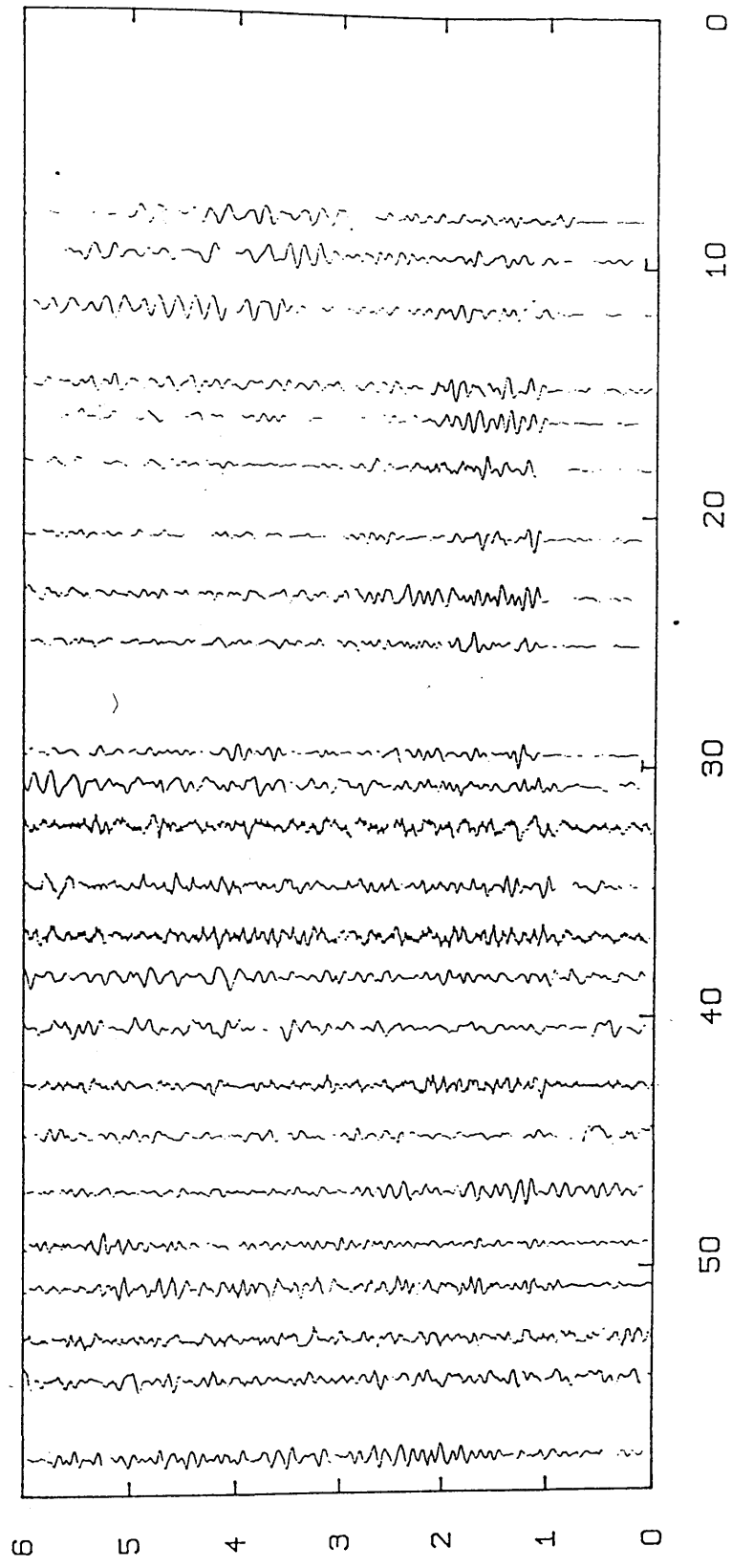

Fig. 4.30b Filtered section line 3, P-wave (Aberdour shot).

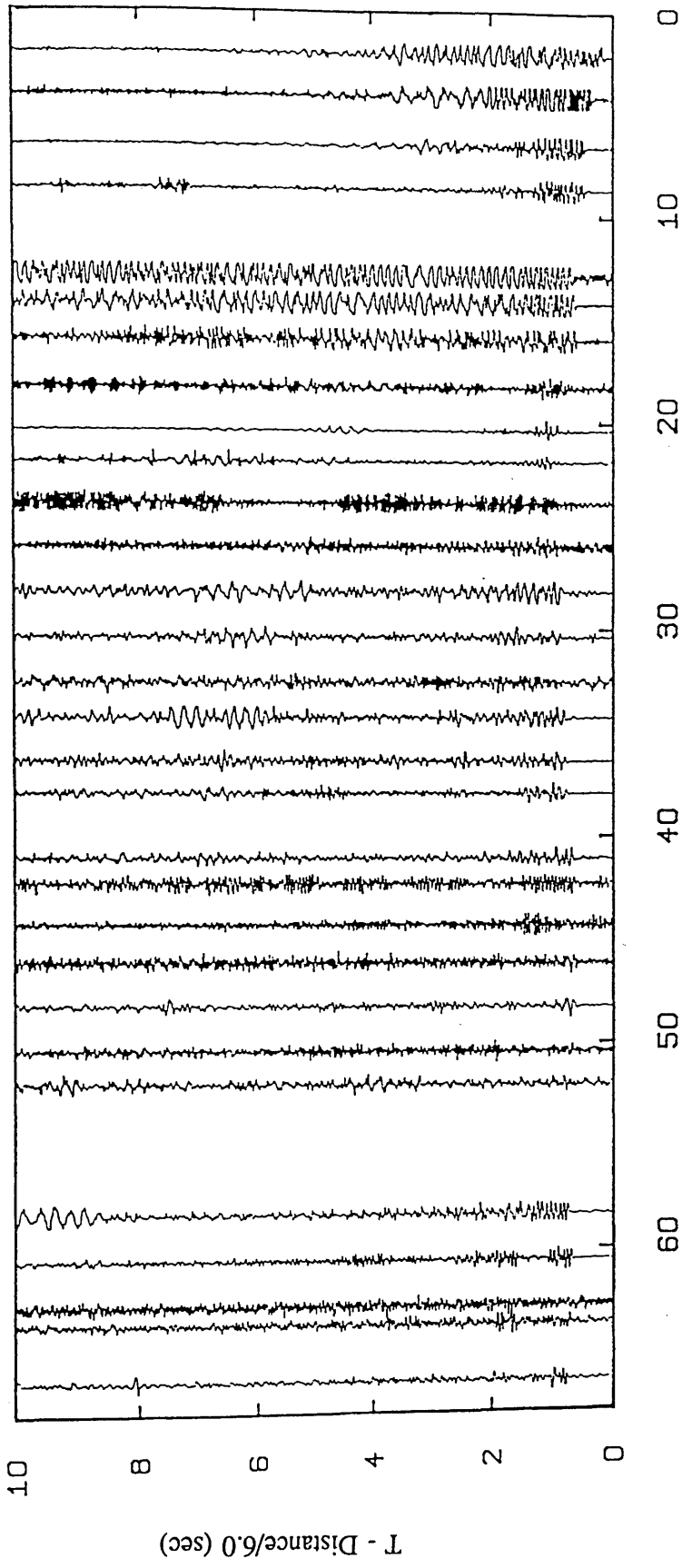

Fig. 4.31a Unfiltered section line 3 (Ratho shot).

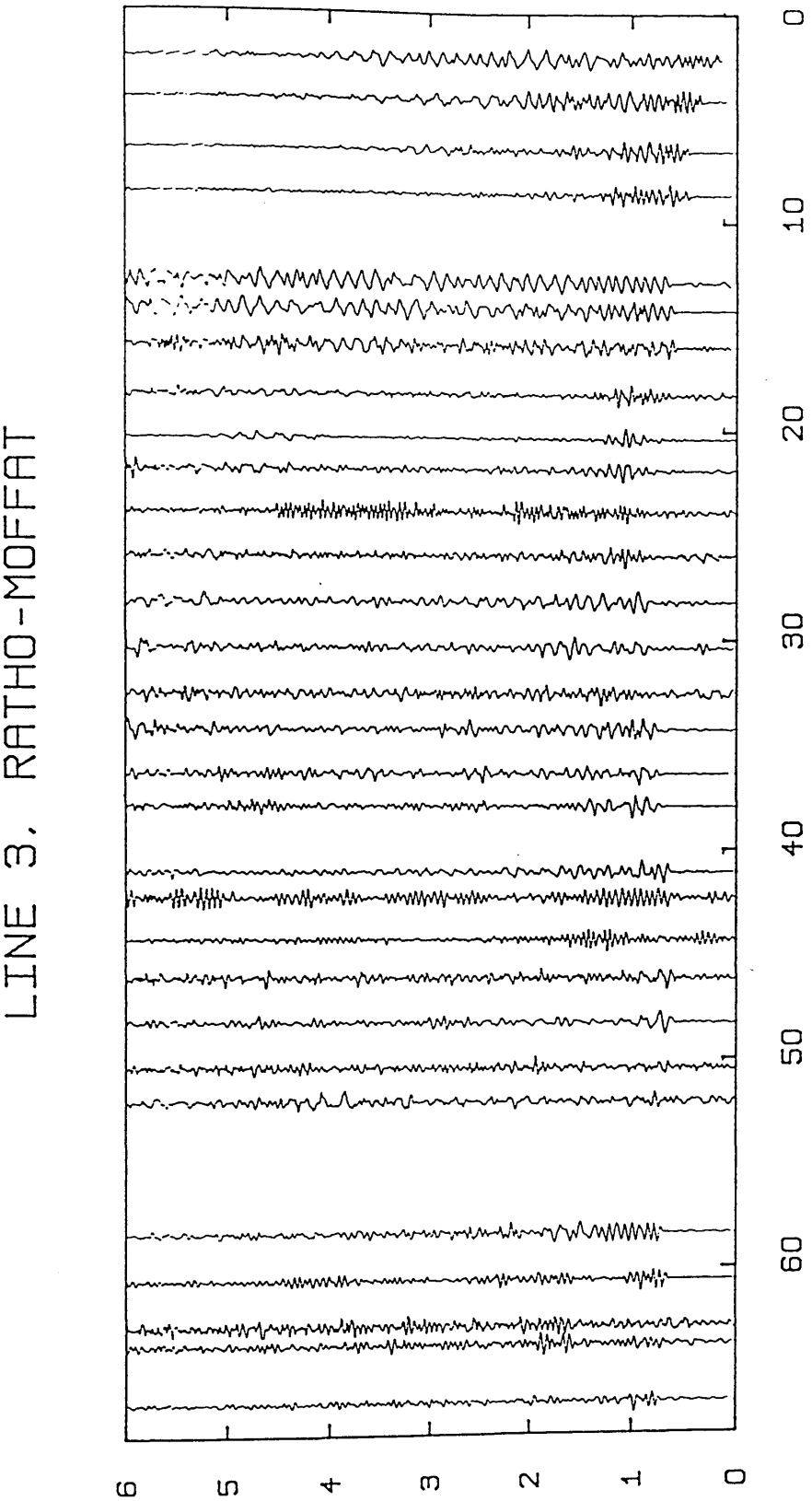

Fig. 4.31b Filtered section line 3, P-wave (Ratho shot).

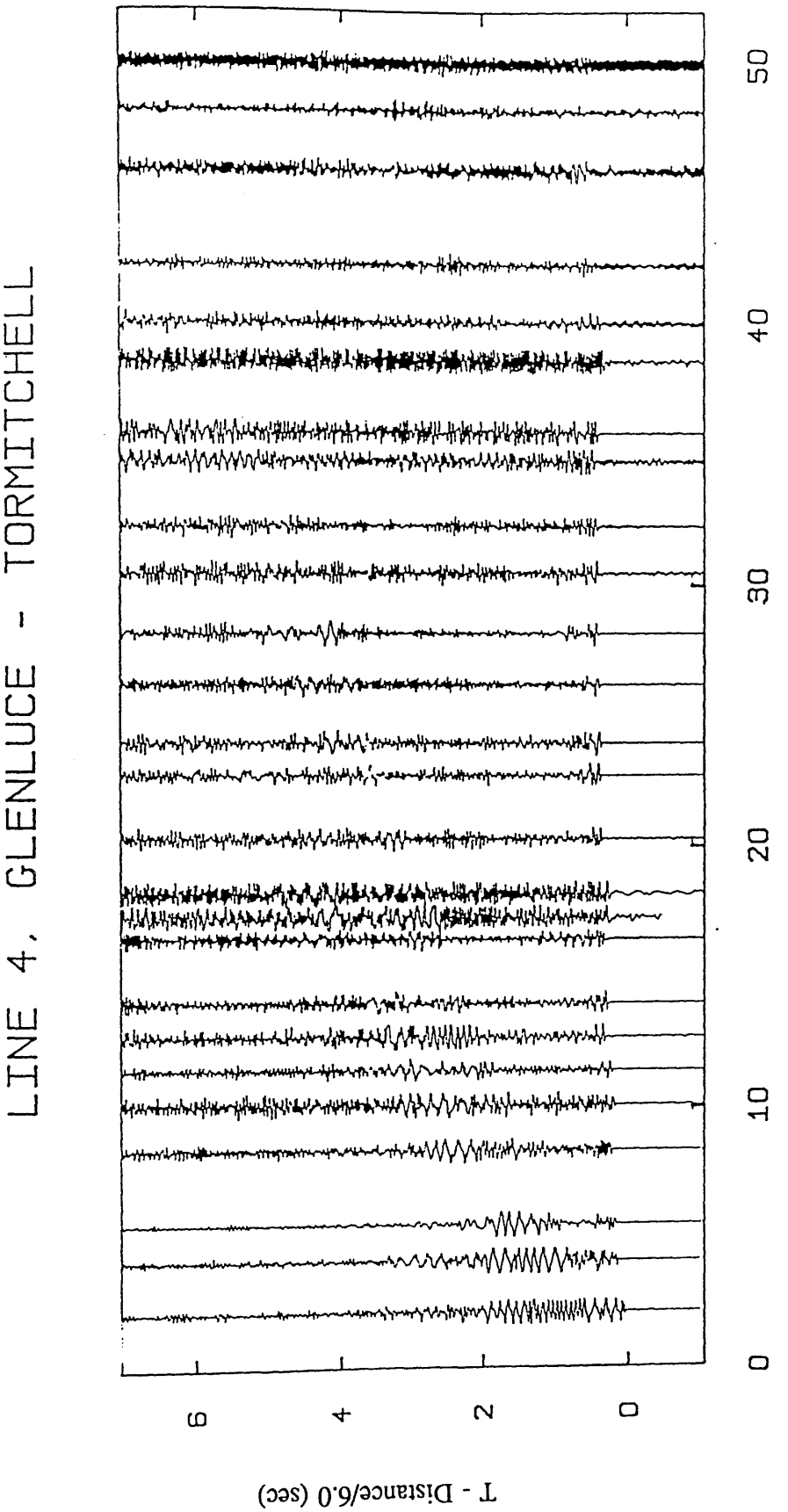

Fig. 4.32 Unfiltered section line 4 (Glenluce shot).

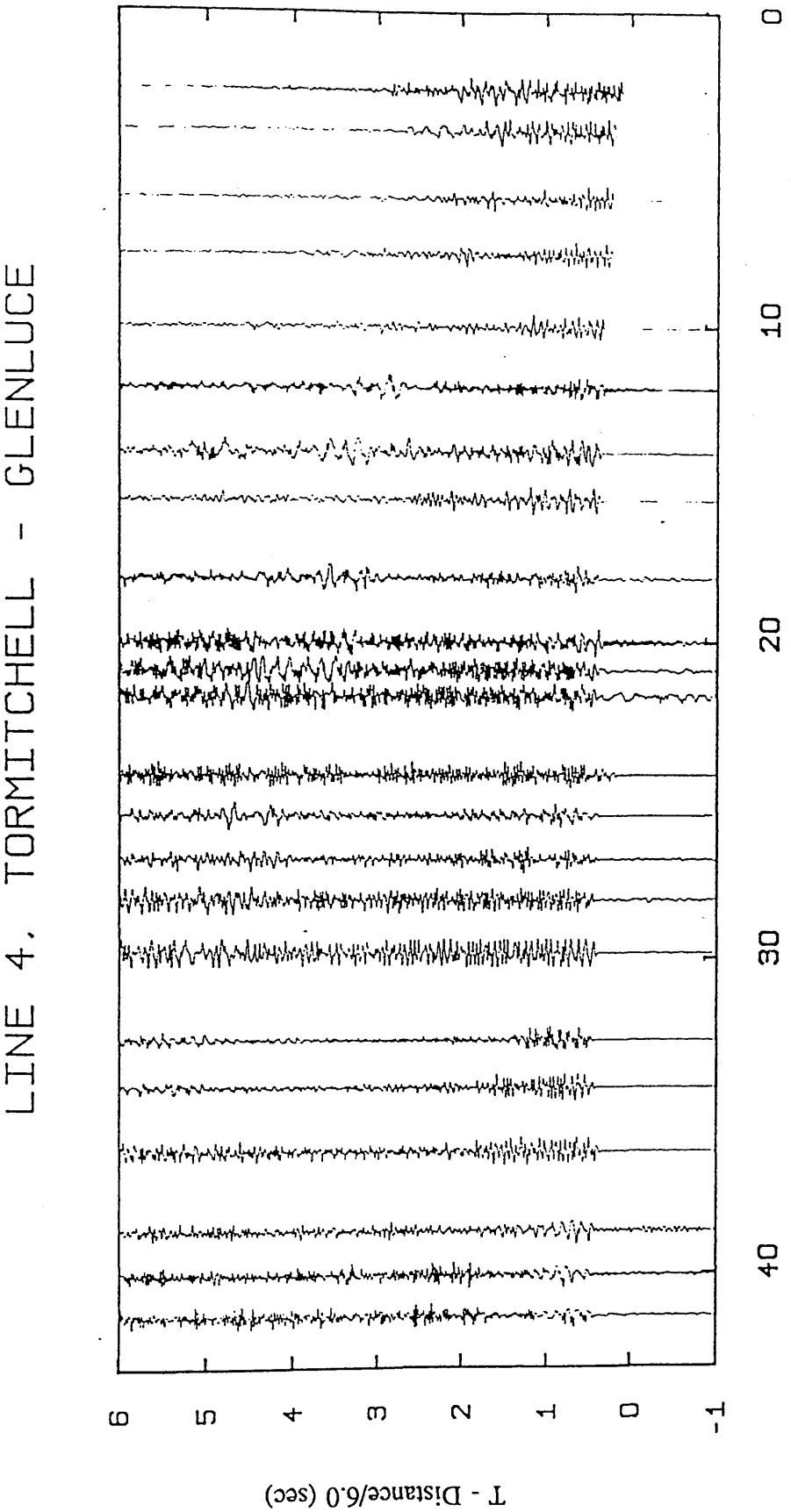

Fig. 4.33a Unfiltered section line 4 (Tormitchell shot).

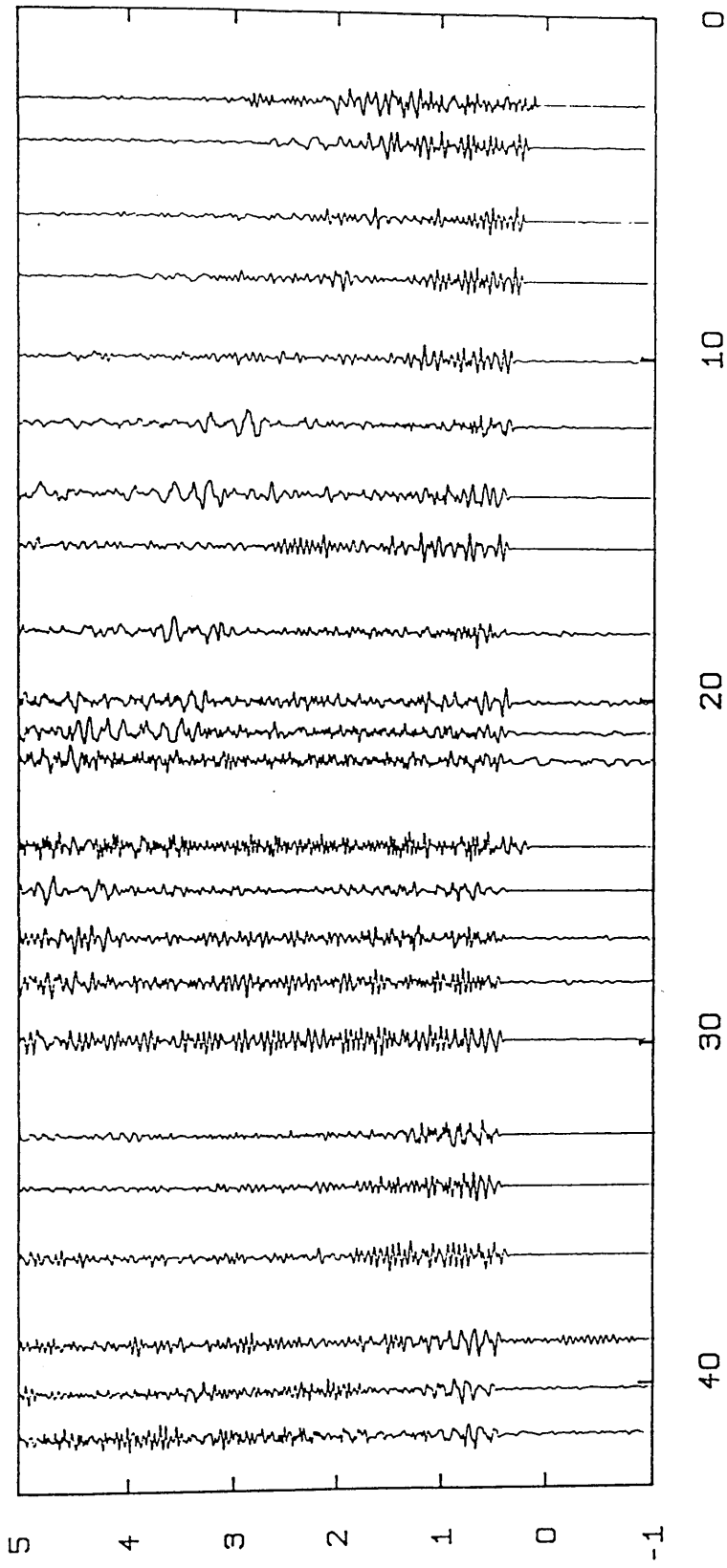

Fig. 4.33b Filtered section line 4, P-wave (Tormitchell shot).

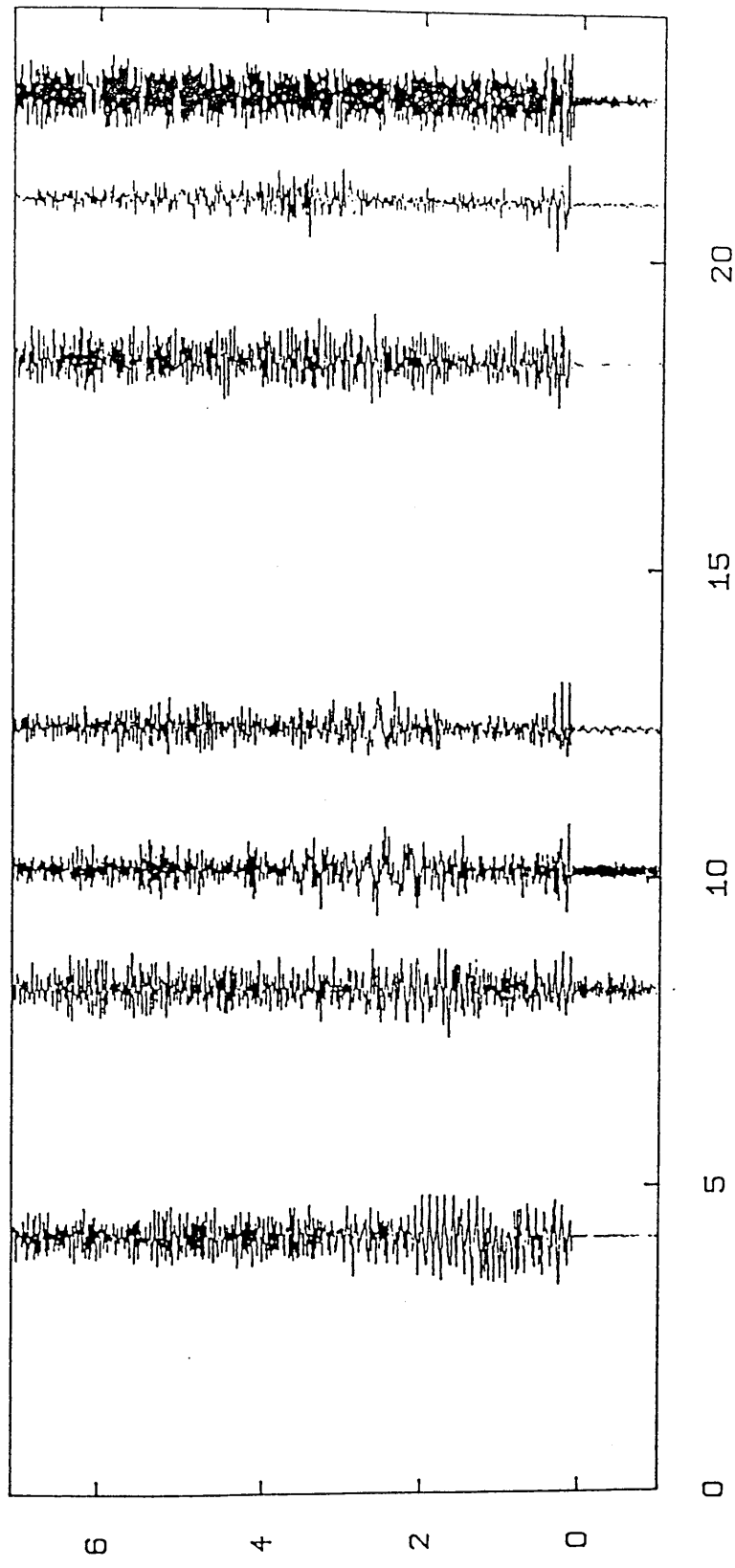

Fig. 4.34 Unfiltered section line 5 (Glenluce shot).

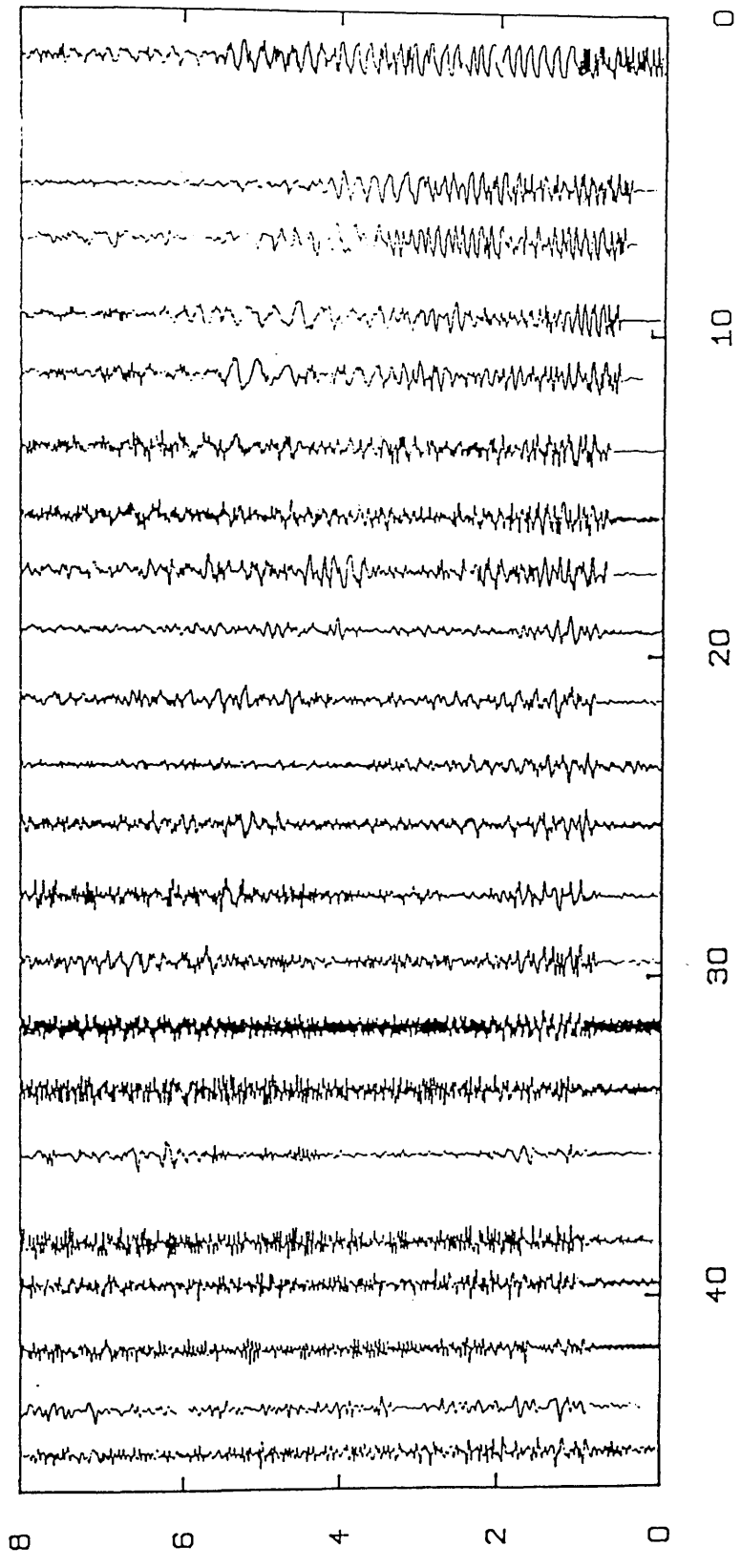

Fig. 4.35 Unfiltered section line 6 (Boysack shot).

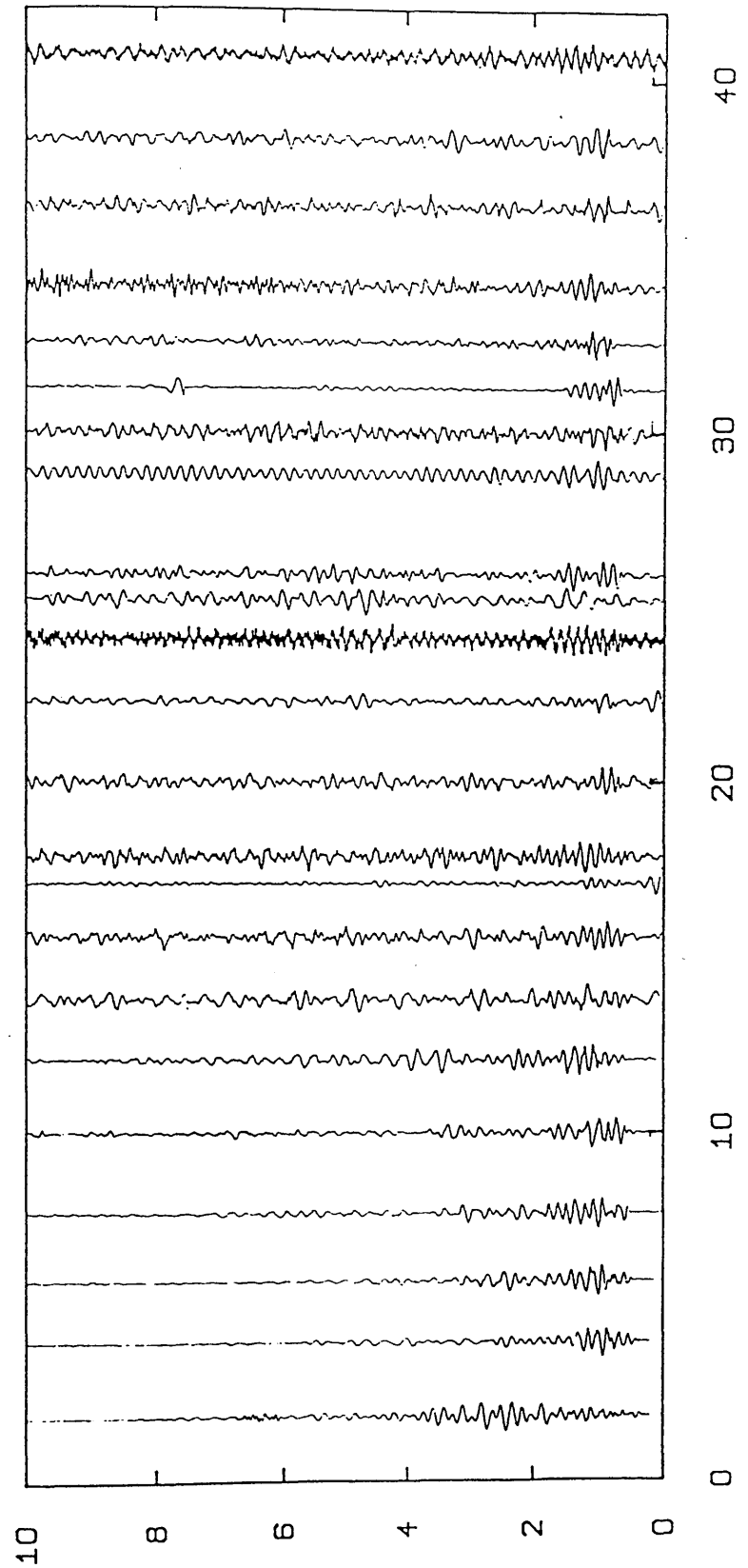

Fig. 4.36 Filtered section line 1, S-wave (Melrose shot).

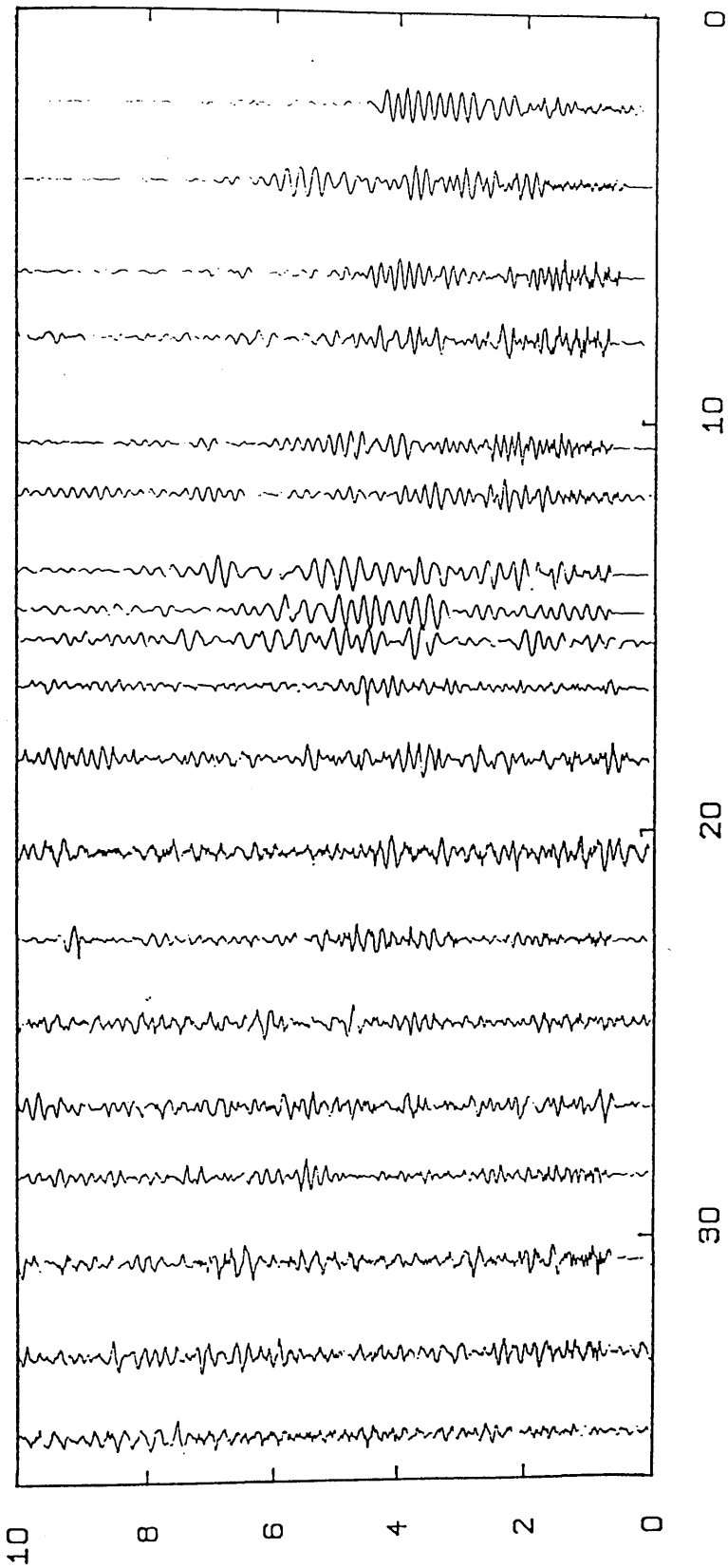

Fig. 4.37 Filtered section line 1, S-wave (Bangley shot).

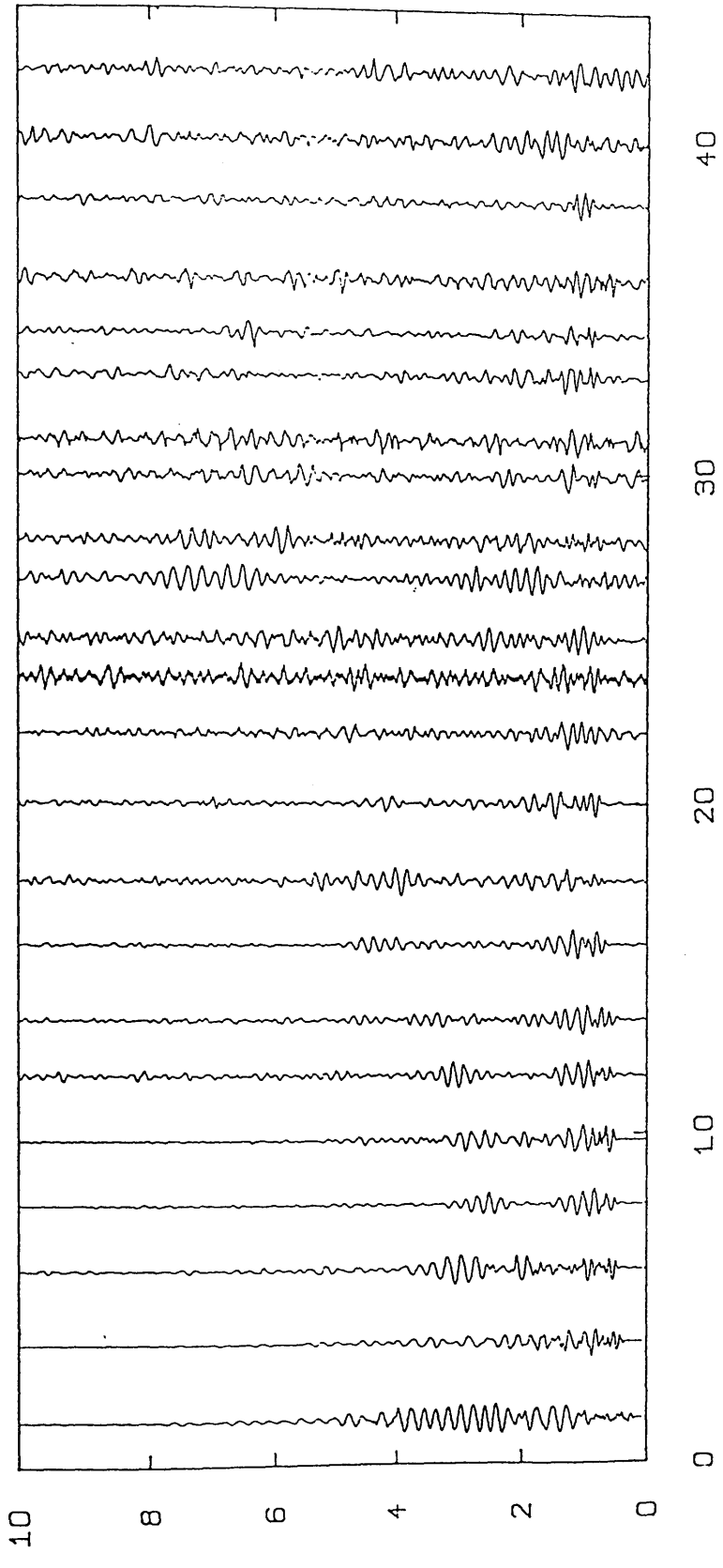

Fig. 4.38 Filtered section line 2, S-wave (Melrose shot).

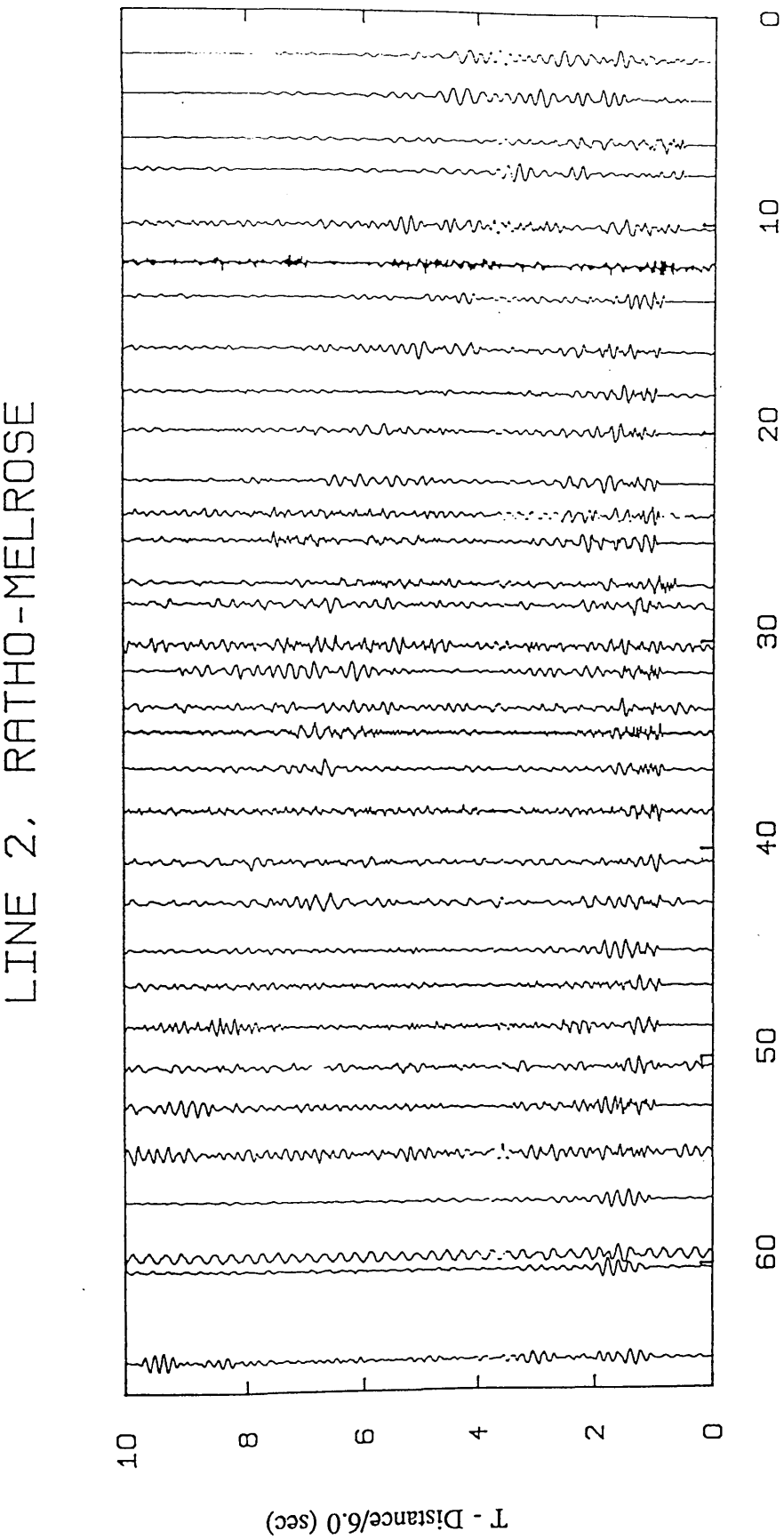

Fig. 4.39 Filtered section line 2, S-wave (Ratho shot).

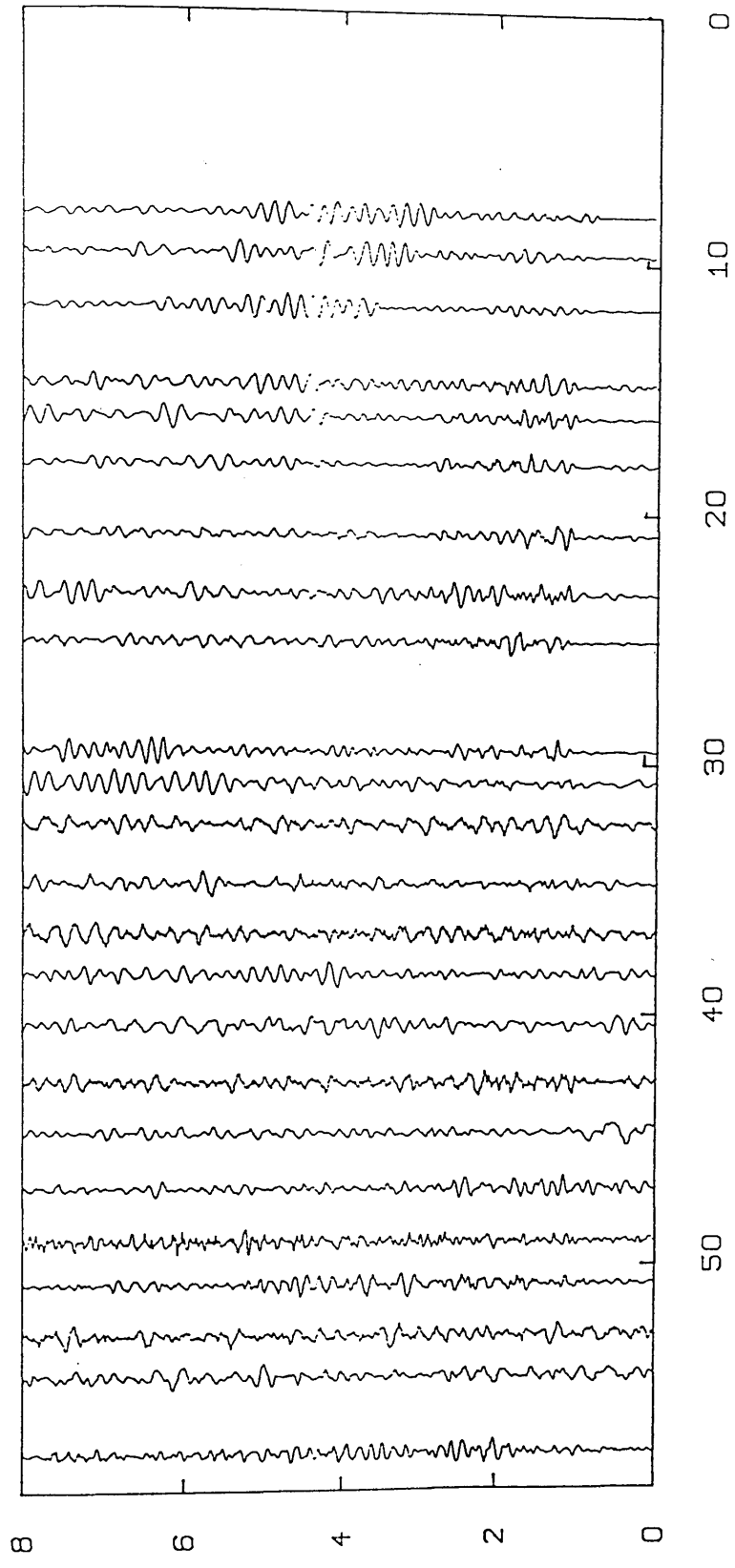

Fig. 4.40 Filtered section line 3, S-wave (Aberdour shot).

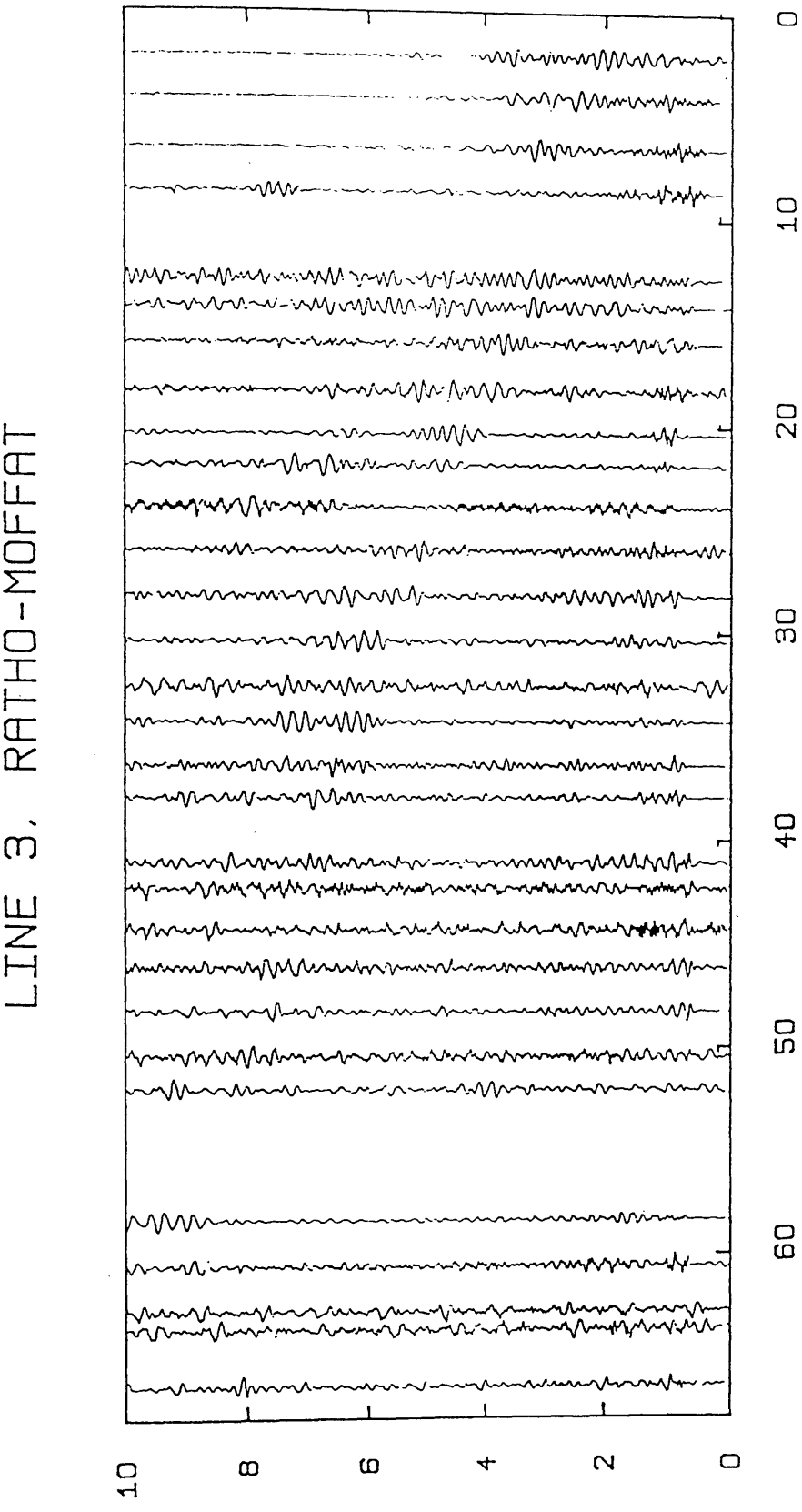

Fig. 4.41 Filtered section line 3, S-wave (Ratho shot).

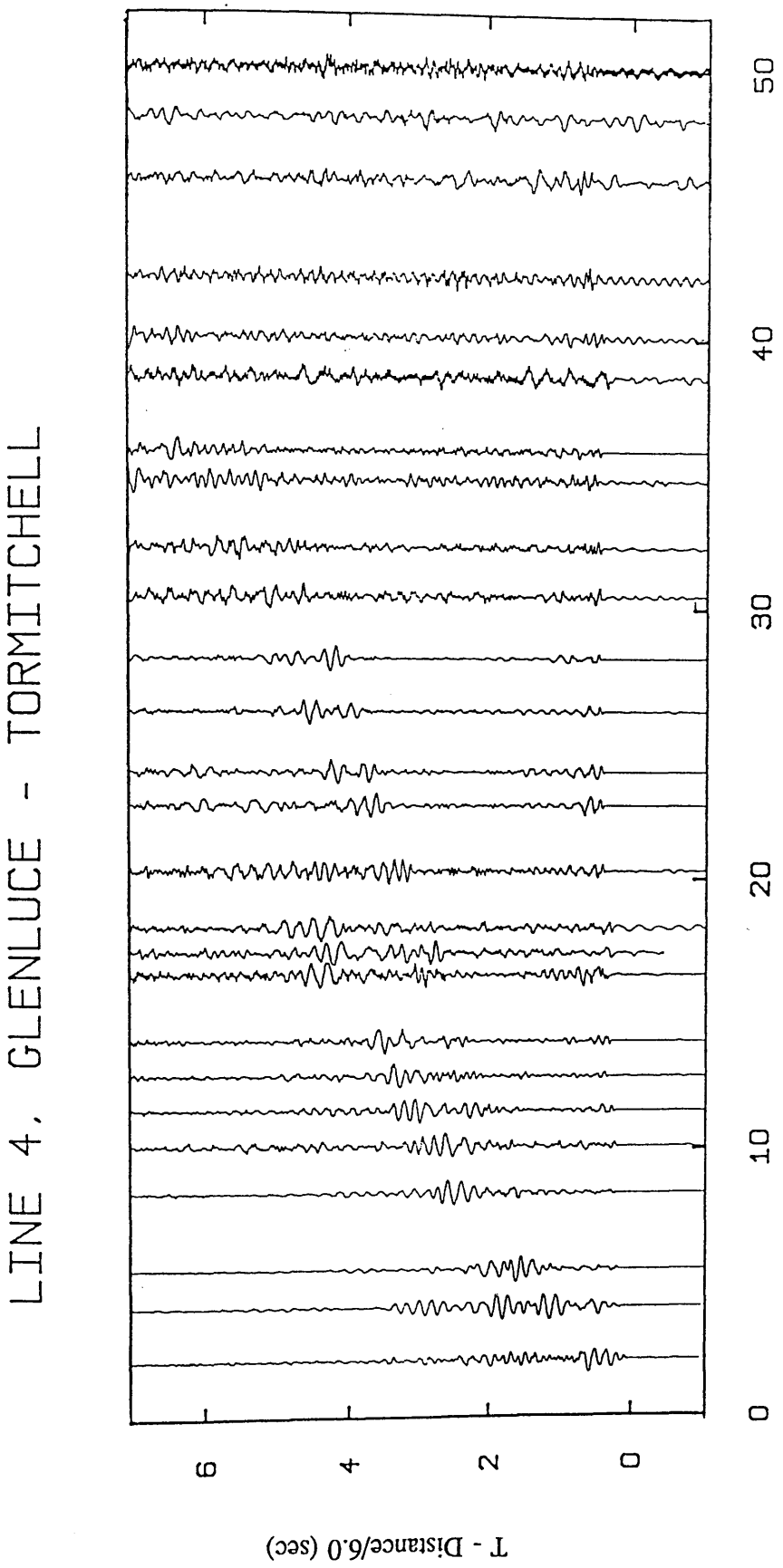

Fig. 4.42a Filtered section line 4, S-wave (Glenluce shot).

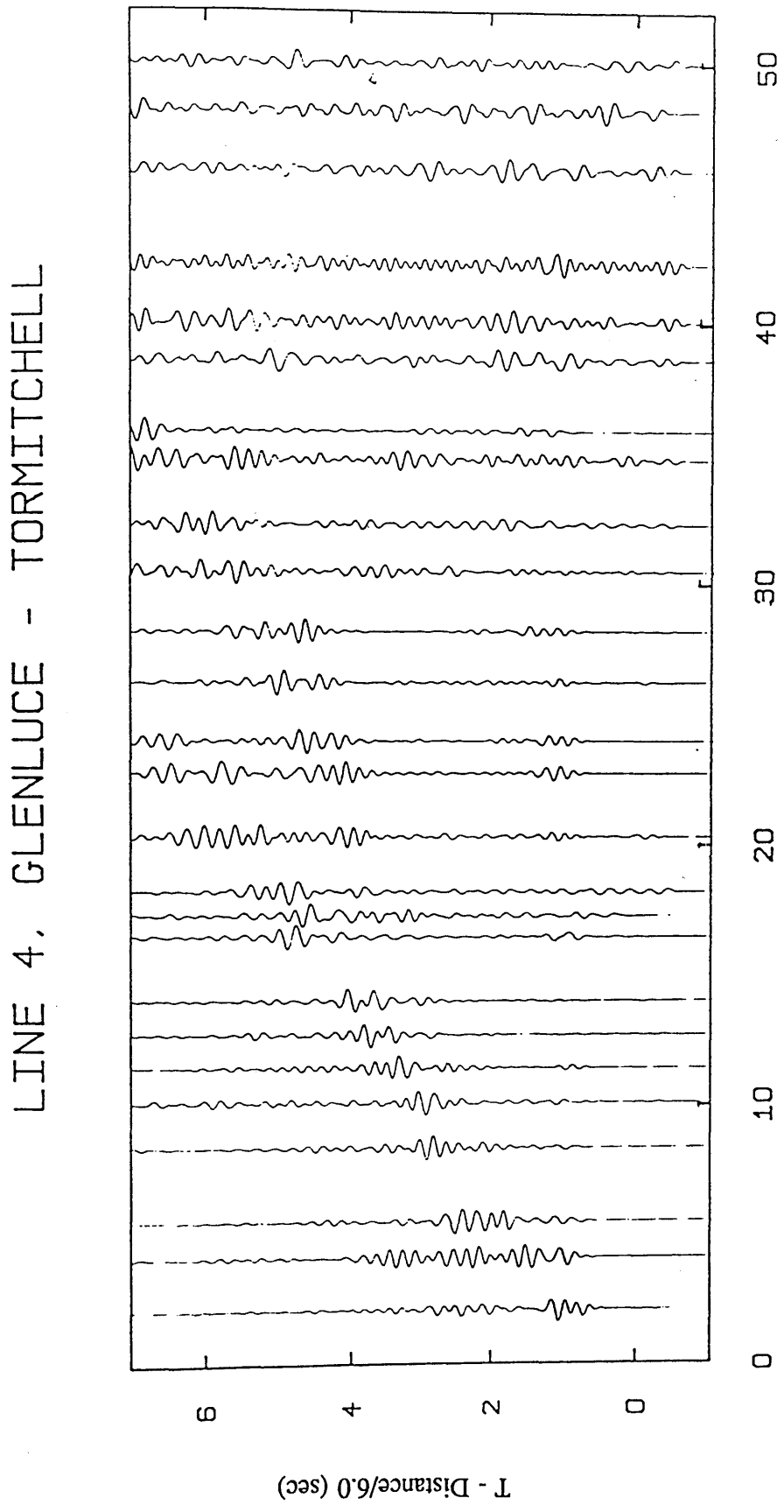

Fig. 4.42b Filtered section line 4, S-wave (Glenluce shot).

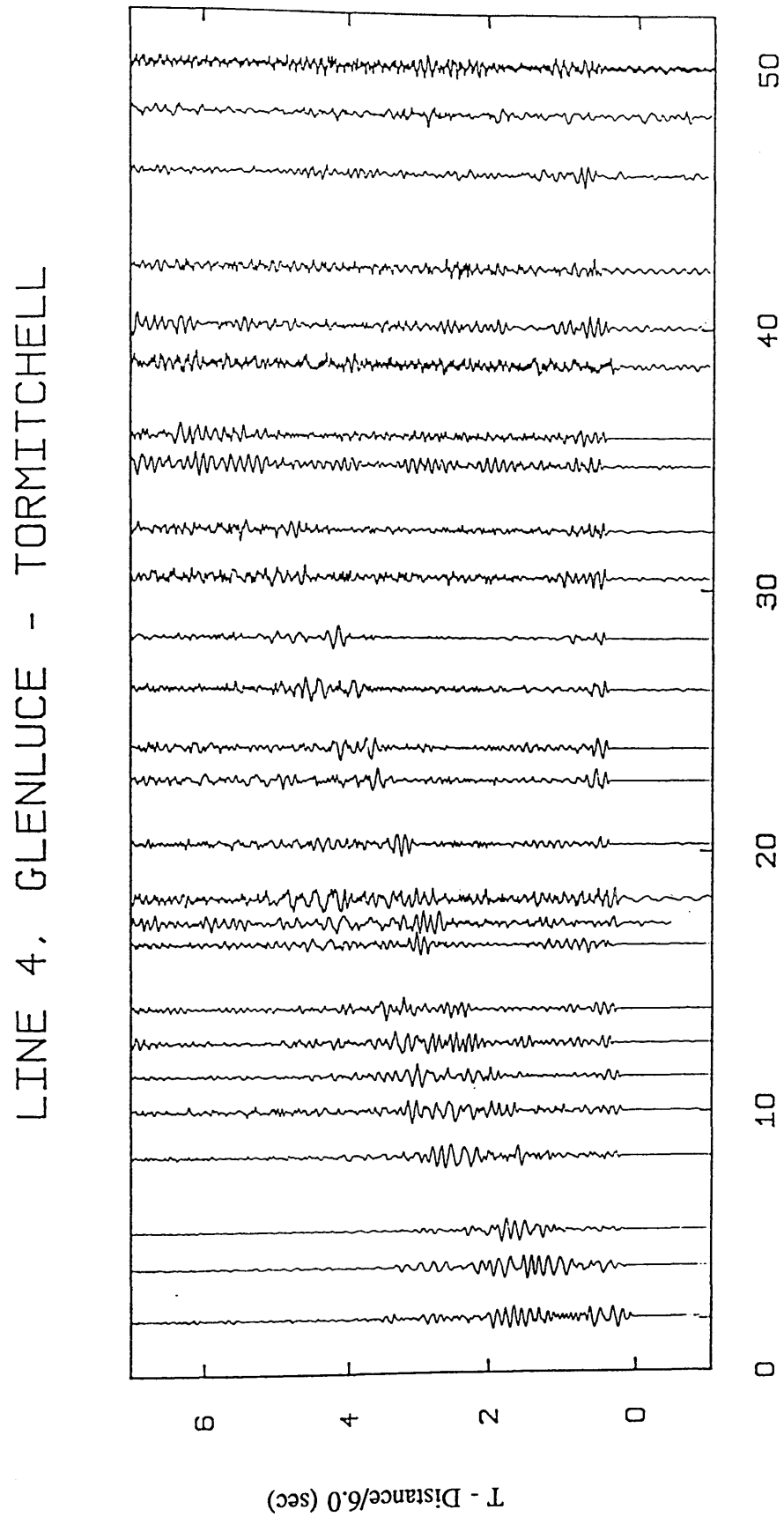

Fig. 4.42c Filtered section line 4, S-wave (Glenluce shot).

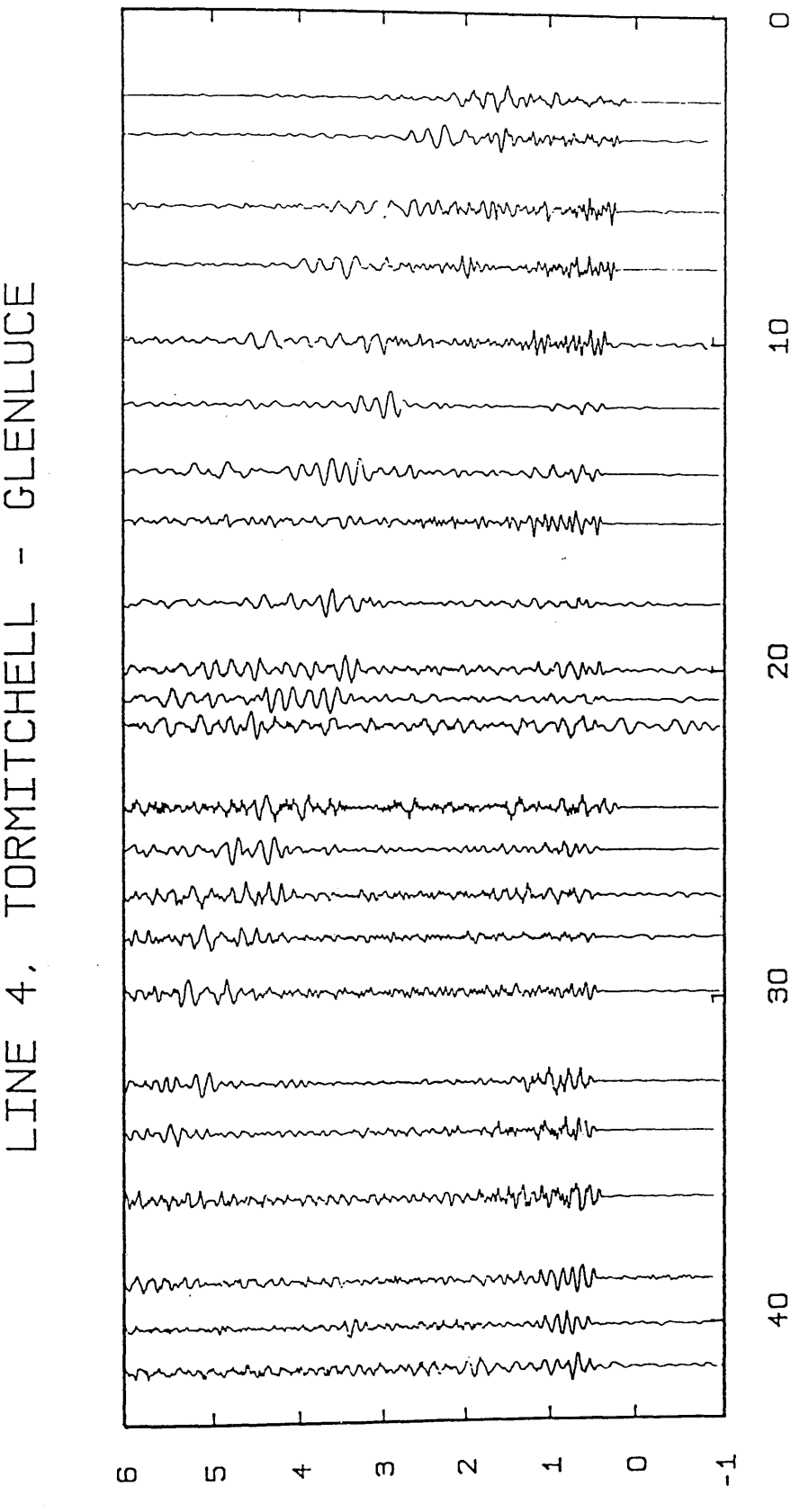

Fig. 4.43 Filtered section line 4, S-wave (Tormitchell shot).

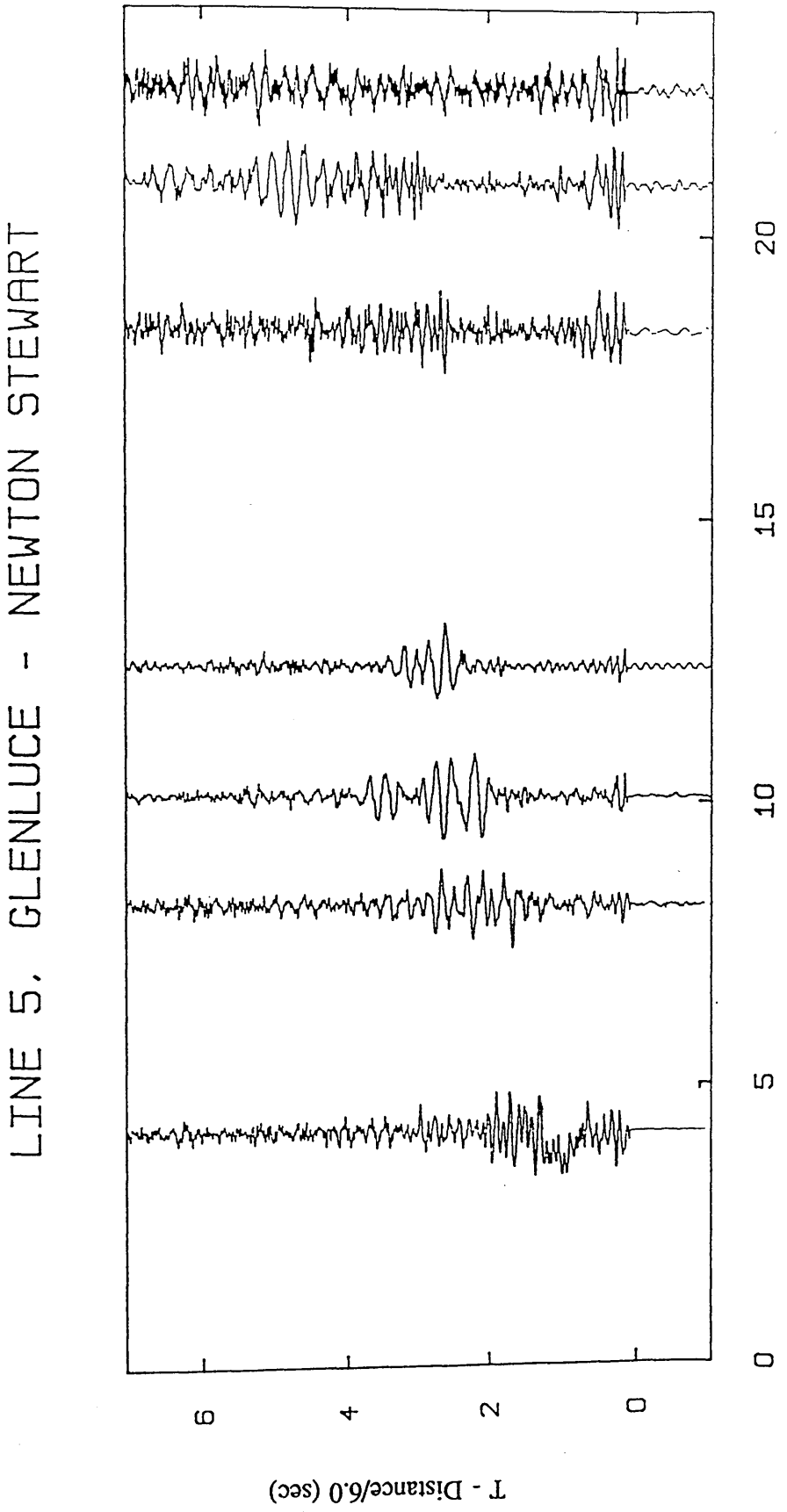

Fig. 4.44 Filtered section line 5, S-wave (Glenluce shot).

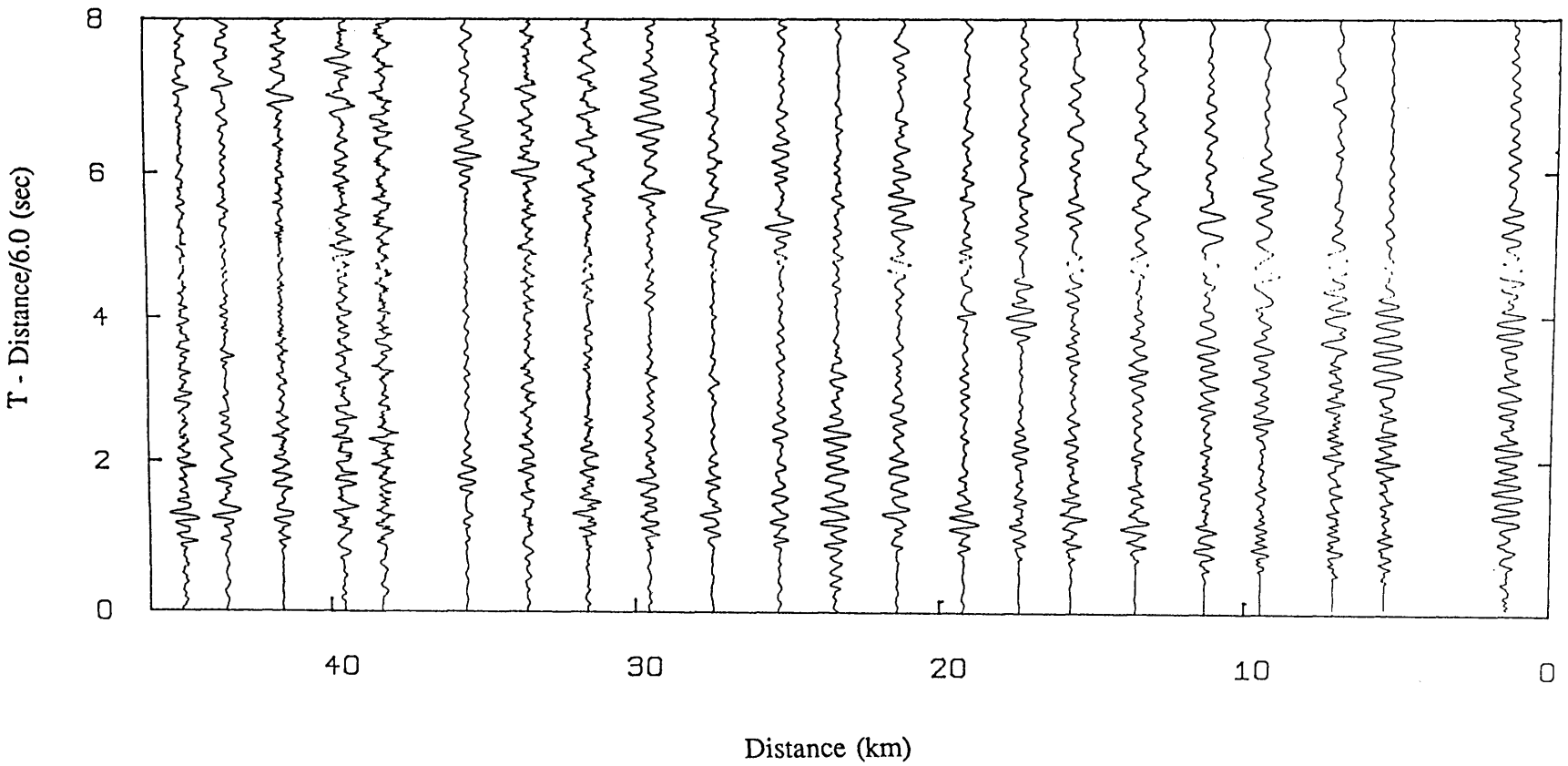

Fig. 4.45 Filtered section line 6, S-wave (Boysack shot).

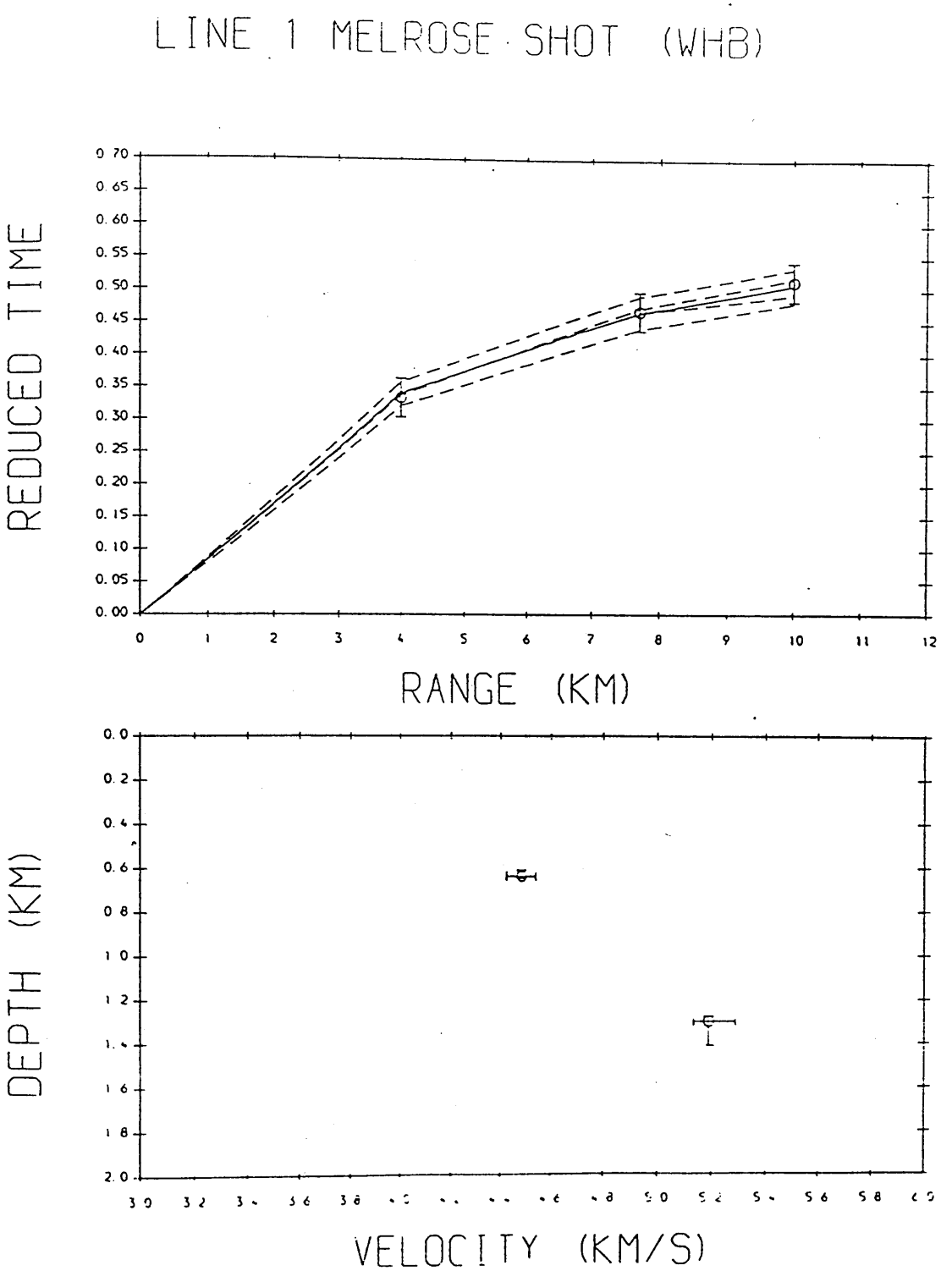

Fig. 5.1 Time-distance data and velocity-depth results from WHB inversion; line 1 (Melrose shot). Reduction velocity is 6.0 km/s.

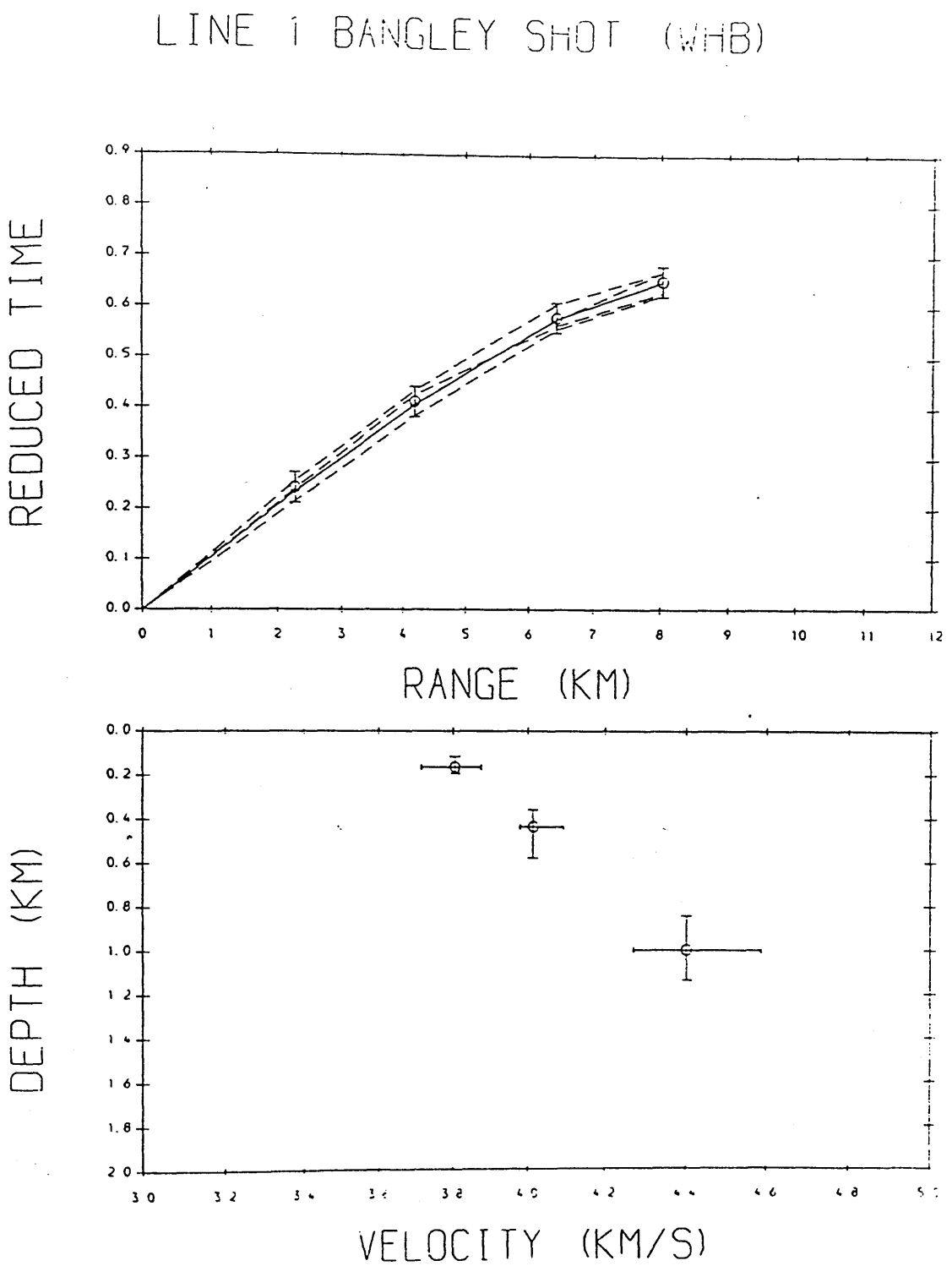

Fig. 5.2 Time-distance data and velocity-depth results from WHB inversion; line 1 (Bangley shot). Reduction velocity is 6.0 km/s.

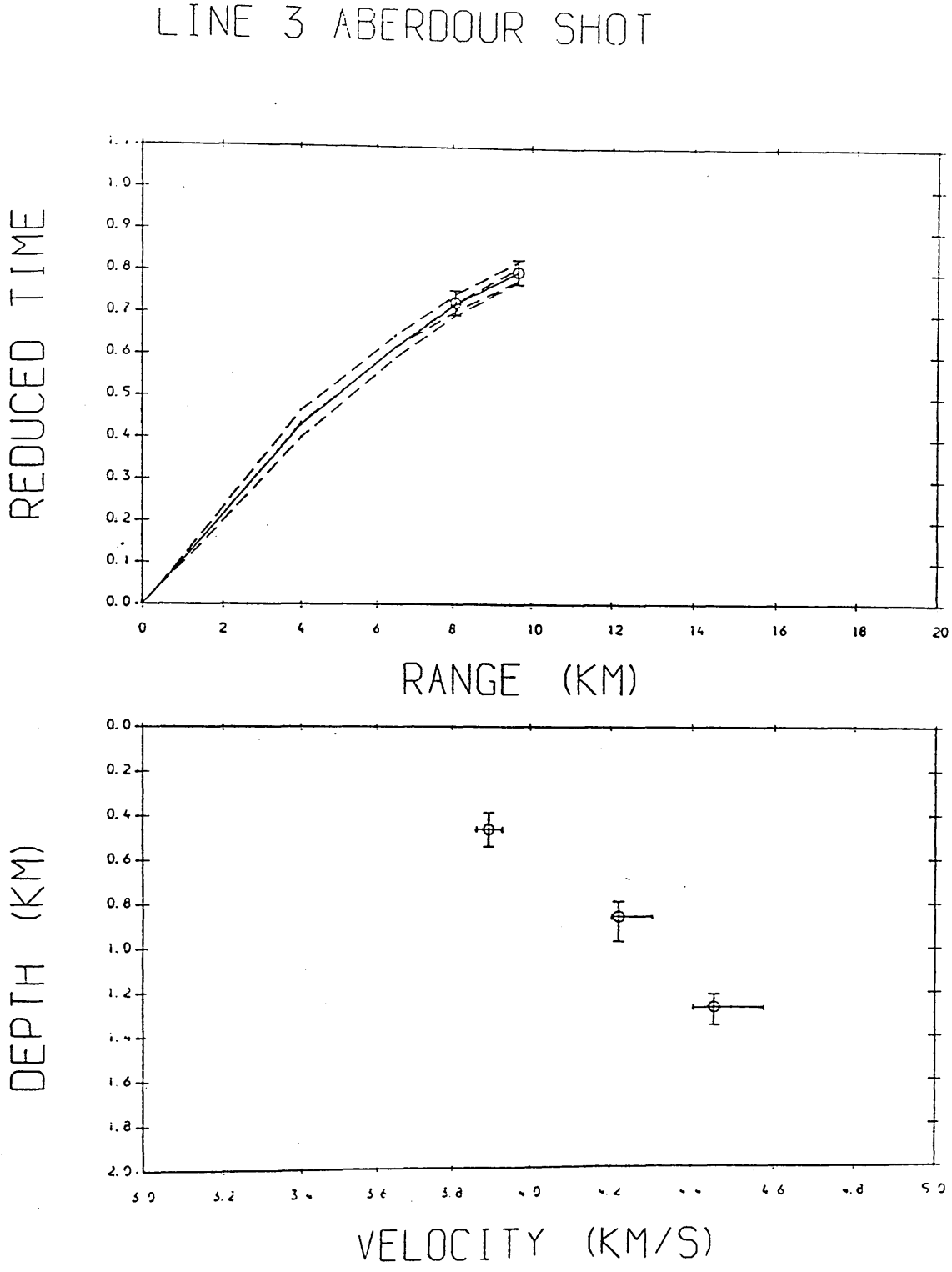

Fig. 5.3 Time-distance data and velocity-depth results from WHB inversion; line 3 (Aberdour shot). Reduction velocity is 6.0 km/s.

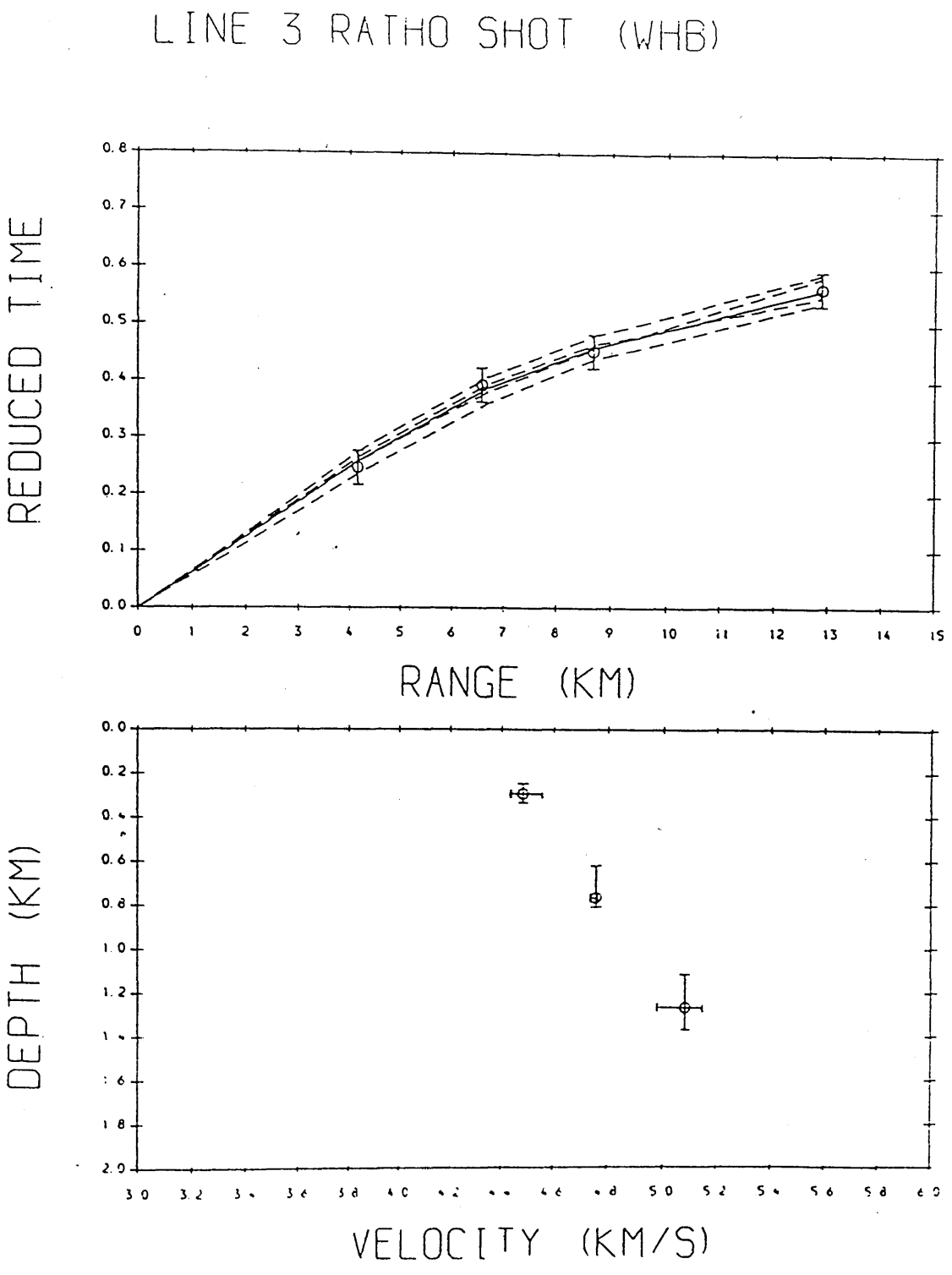

Fig. 5.4 Time-distance data and velocity-depth results from WHB inversion; line 3 (Ratho shot). Reduction velocity is 6.0 km/s.

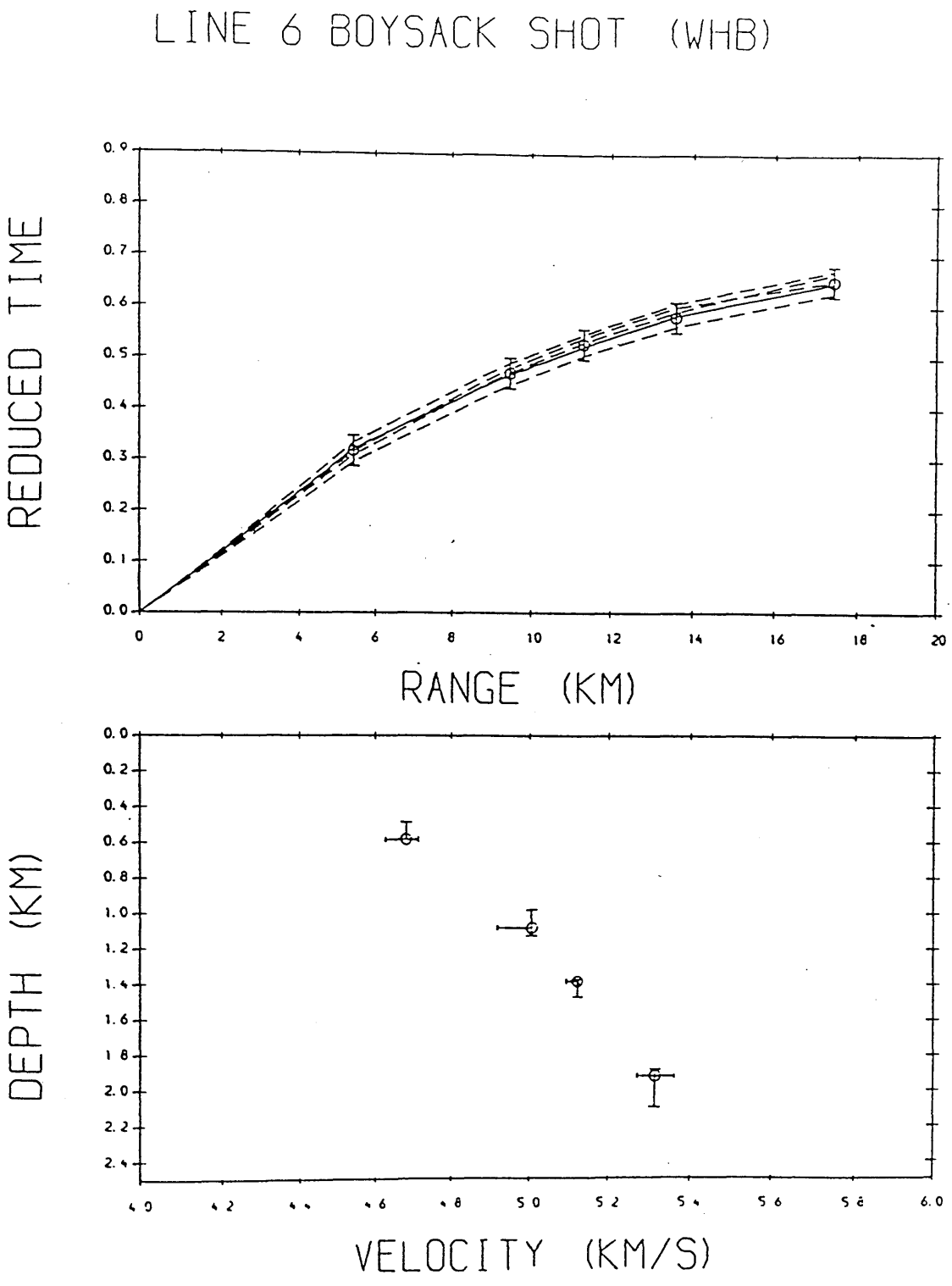

Fig. 5.5 Time-distance data and velocity-depth results from WHB inversion; line 3 (Boysack shot). Reduction velocity is 6.0 km/s.

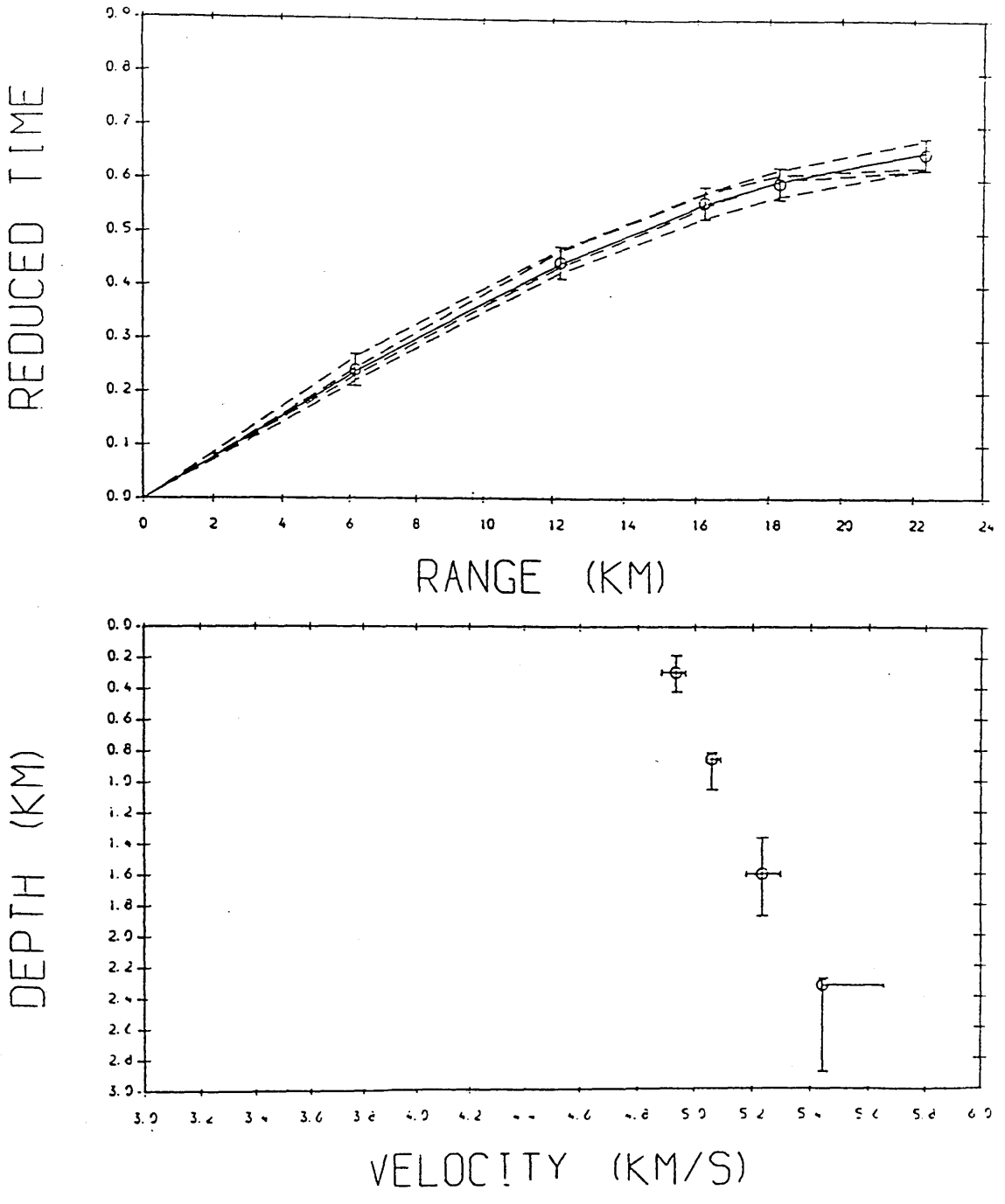

Fig. 5.6 Time-distance data and velocity-depth results from WHB inversion; line 6 (Collace shot). Reduction velocity is 6.0 km/s.

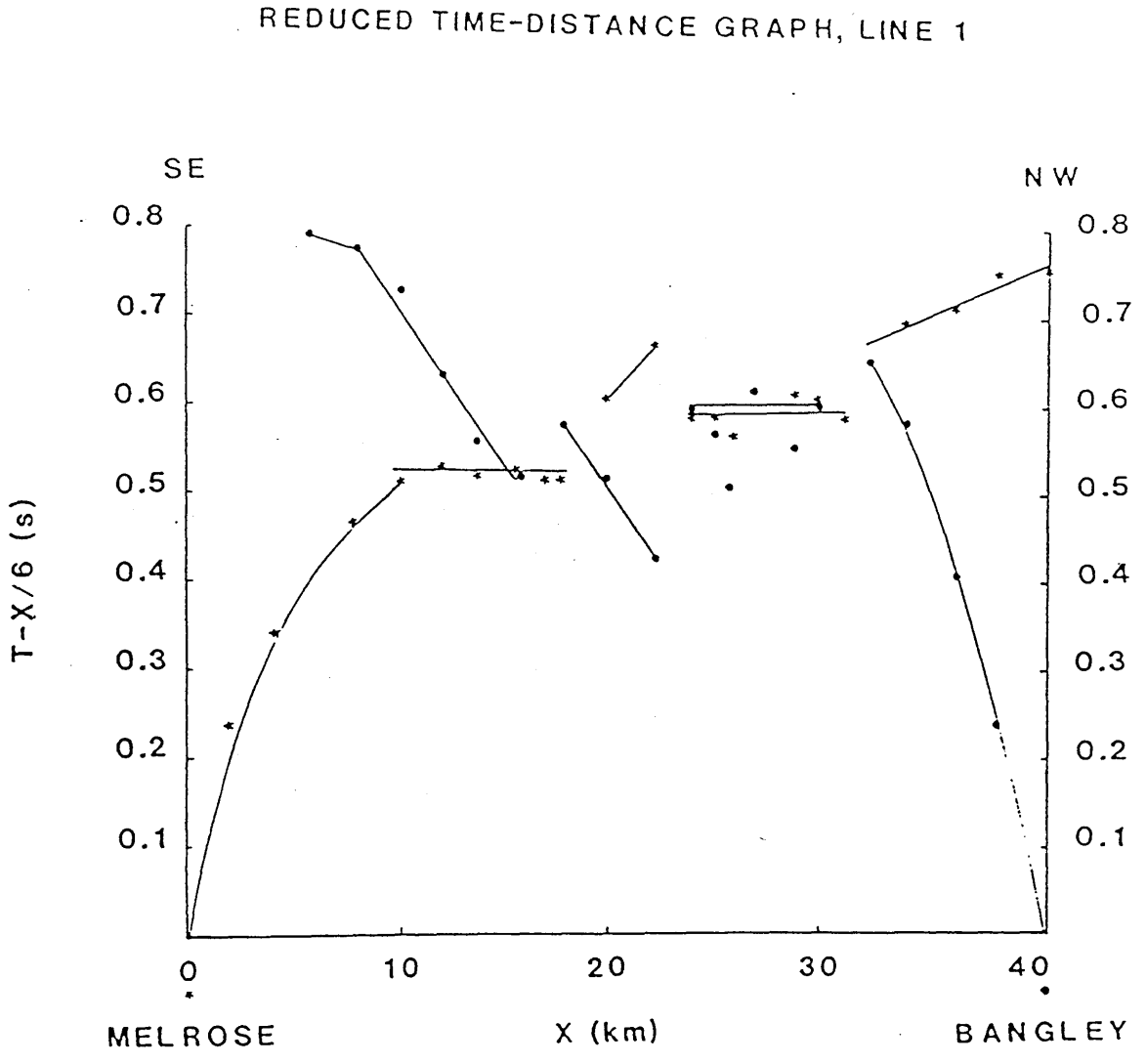

Fig. 5.7 Reduced time-distance graph for line 1.

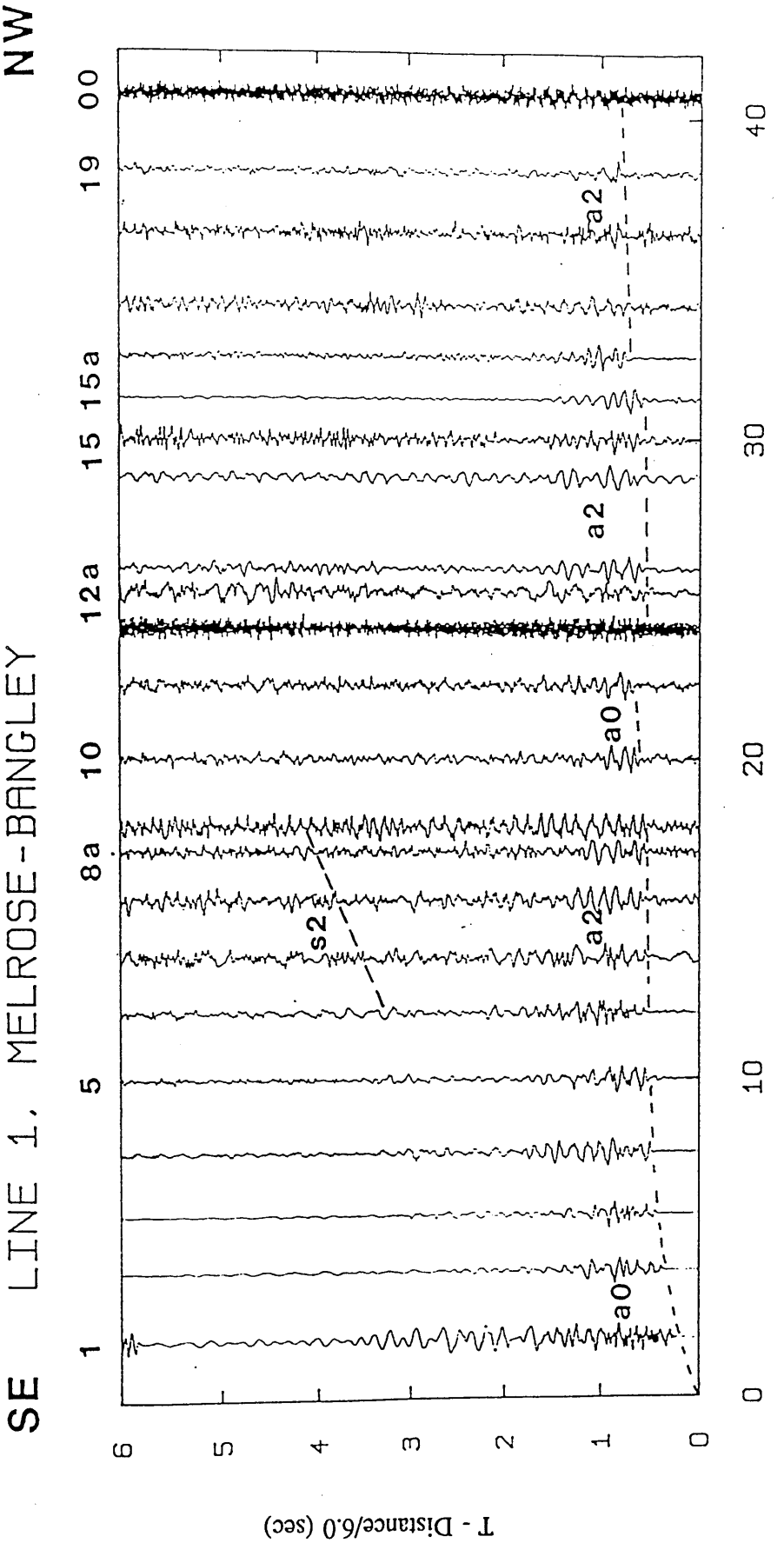

Fig. 5.8 Unfiltered seismic section for line 1 (Melrose shot), interpreted.

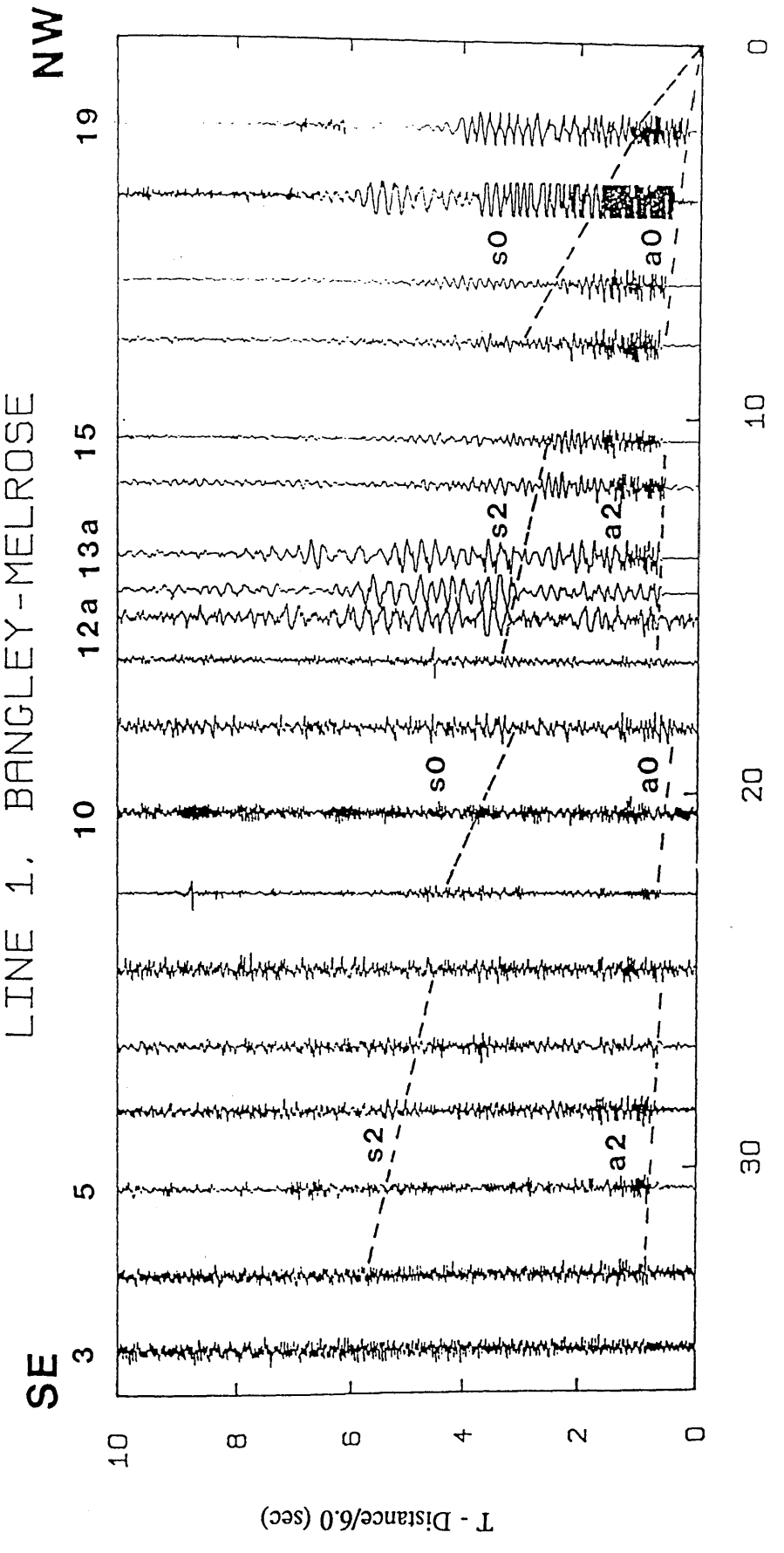

Fig. 5.9 Unfiltered seismic section for line 1 (Bangley shot), interpreted.

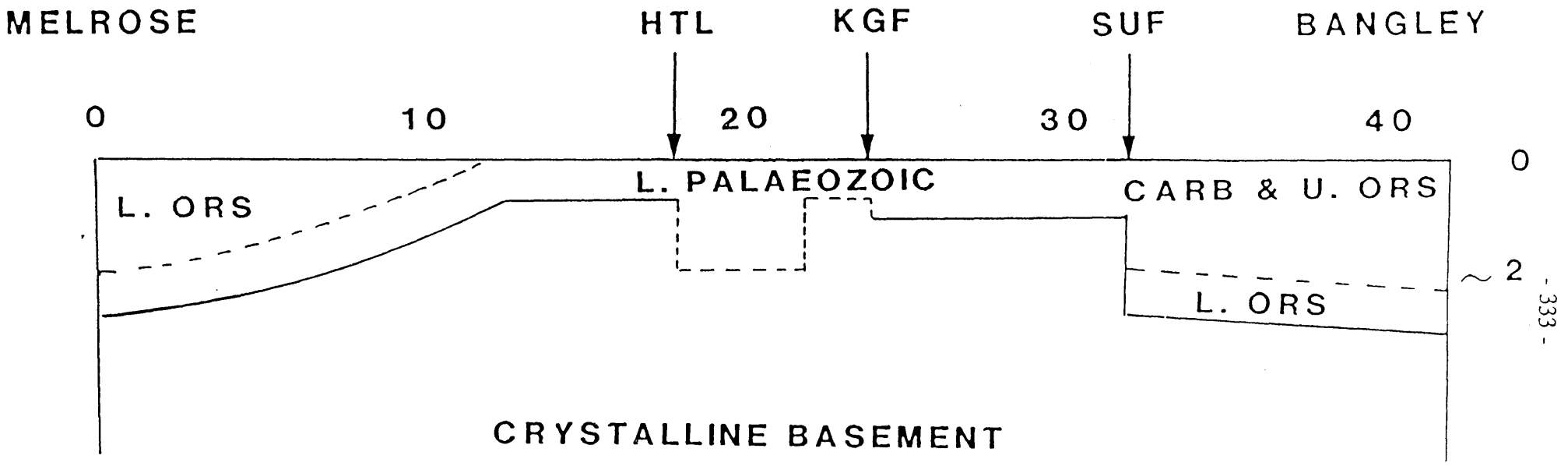

SCHEMATIC DEPTH SECTION ALONG LINE 1

Fig. 5.10 Schematic depth section showing a possible planar layer interpretation for line 1. HTL=Hartfell Line, KGF=Kingledores Fault, SUF= Southern Uplands Fault.

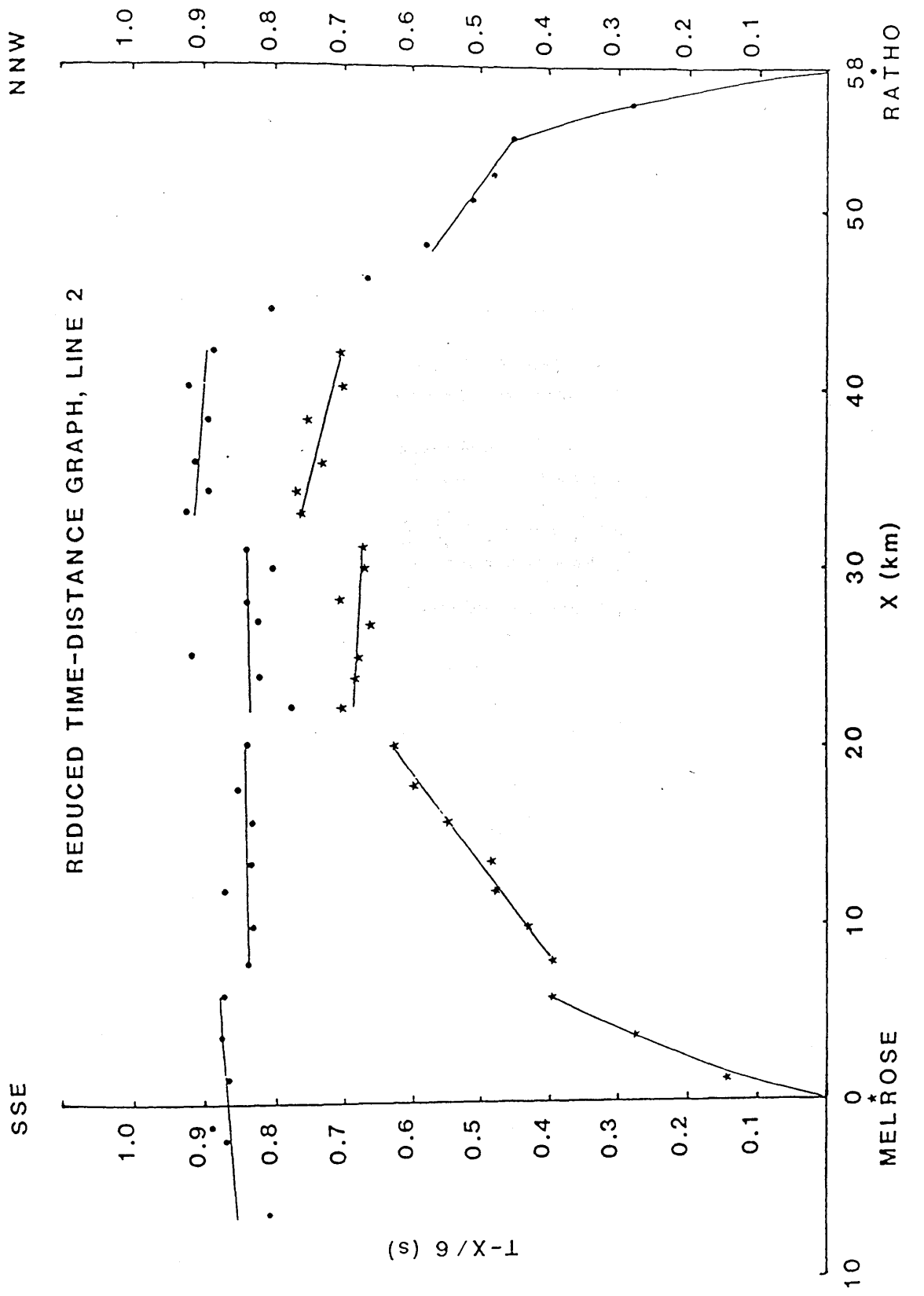

Fig. 5.11 Reduced time-distance graph for line 2.

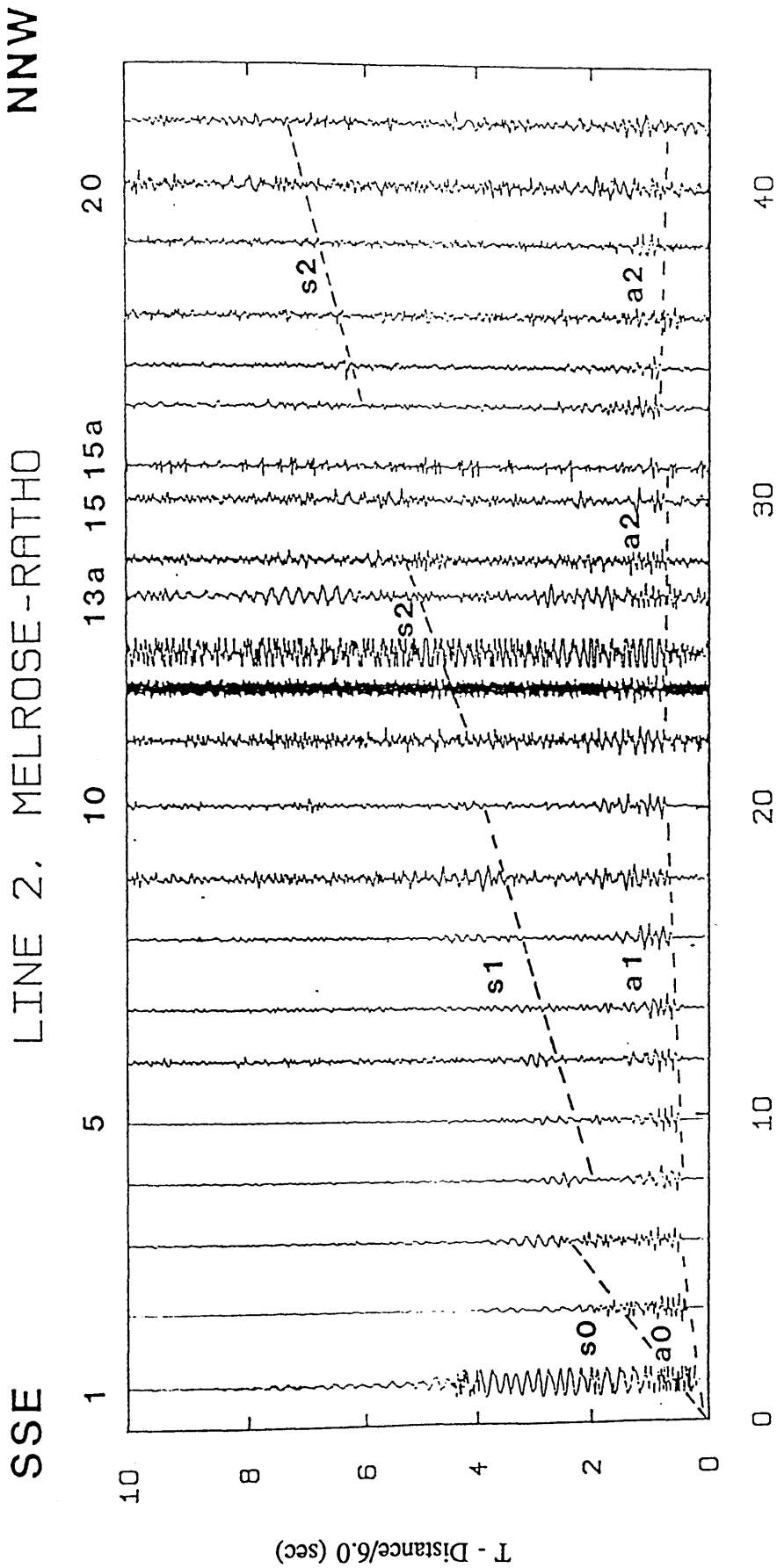

Fig. 5.12 Unfiltered seismic section for line 2 (Melrose shot), interpreted.

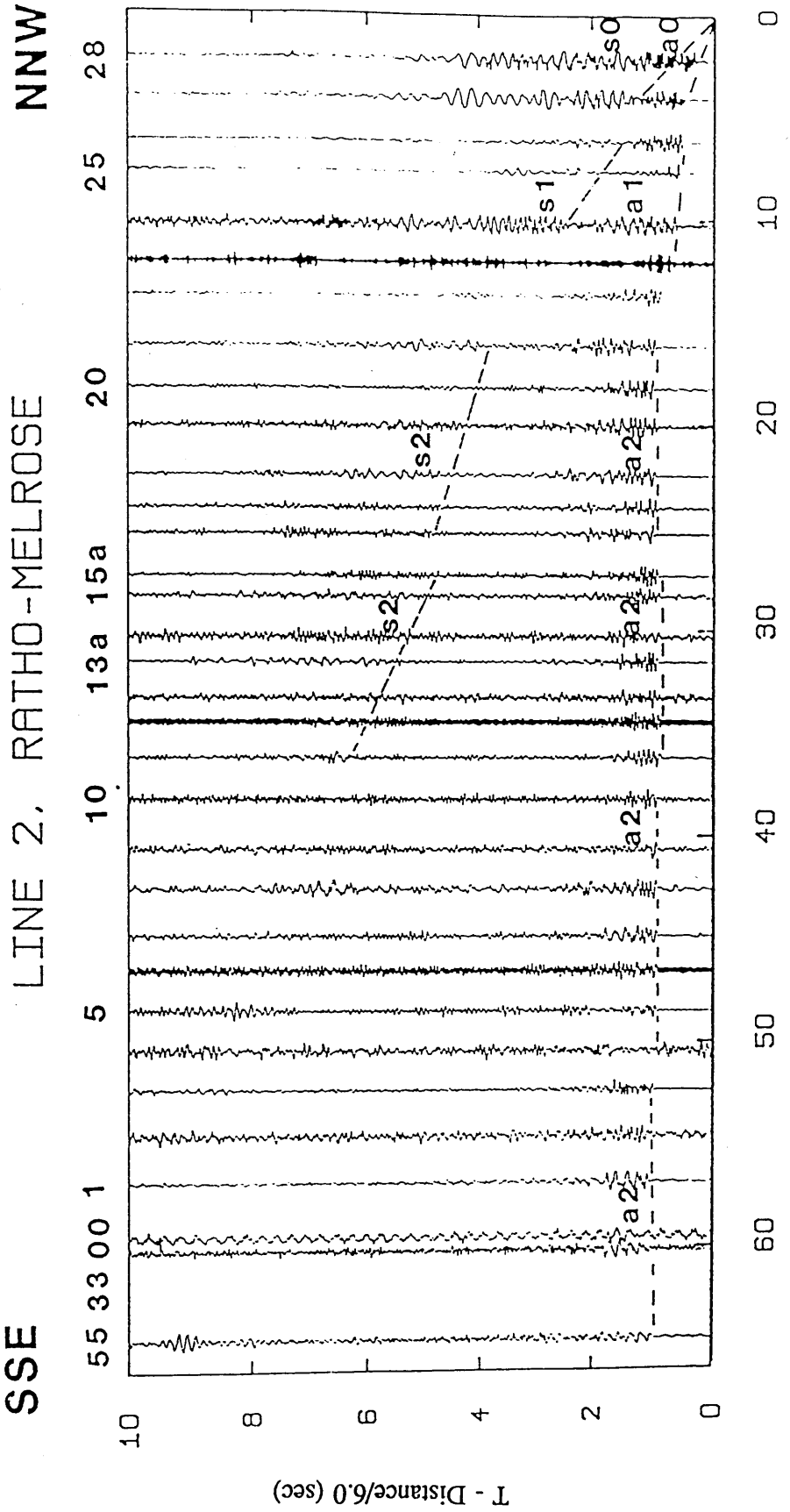

Fig. 5.13 Unfiltered seismic section for line 2 (Ratho shot), interpreted.

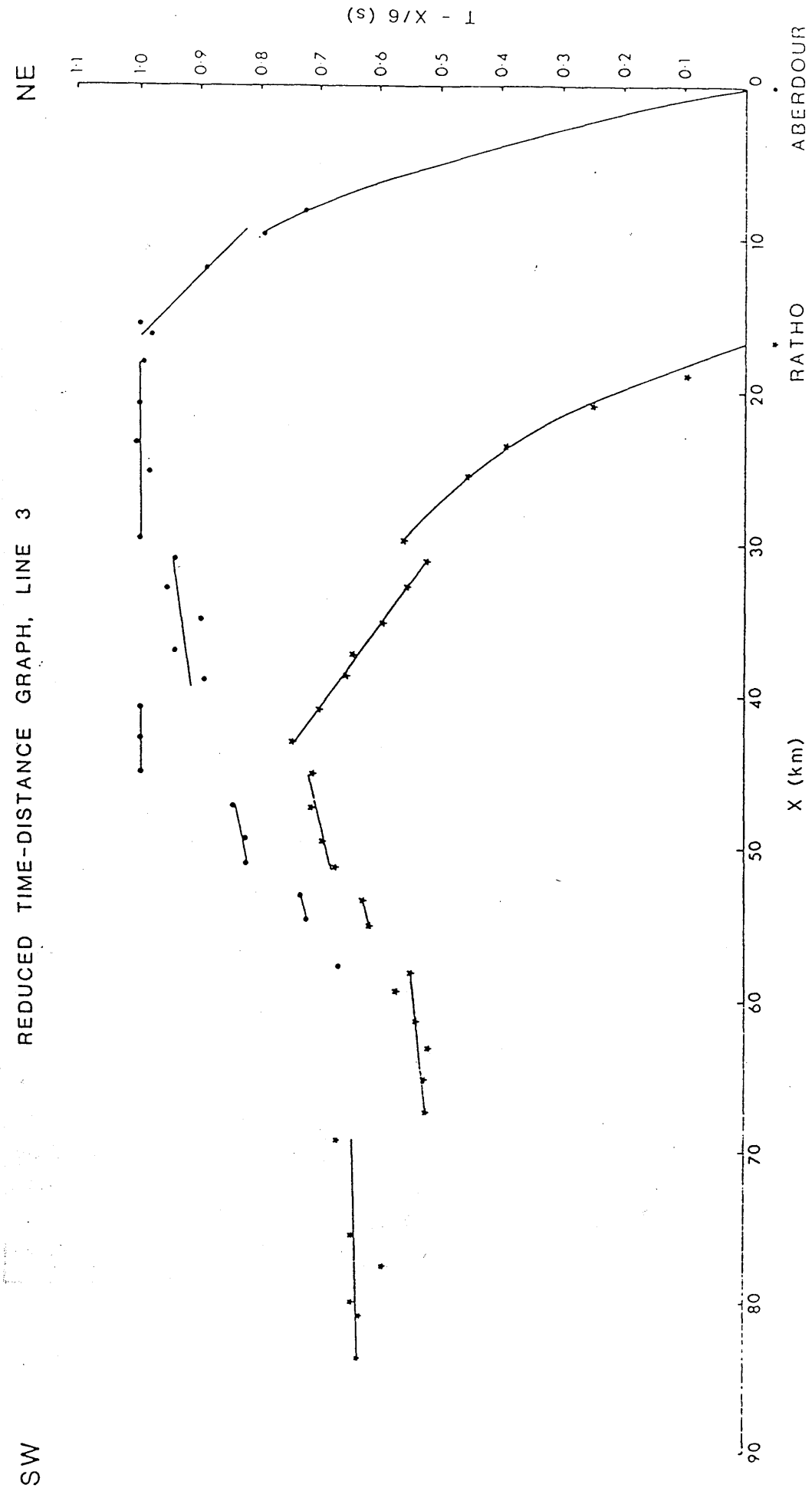

Fig. 5.14 Reduced time-distance graph for line 3.

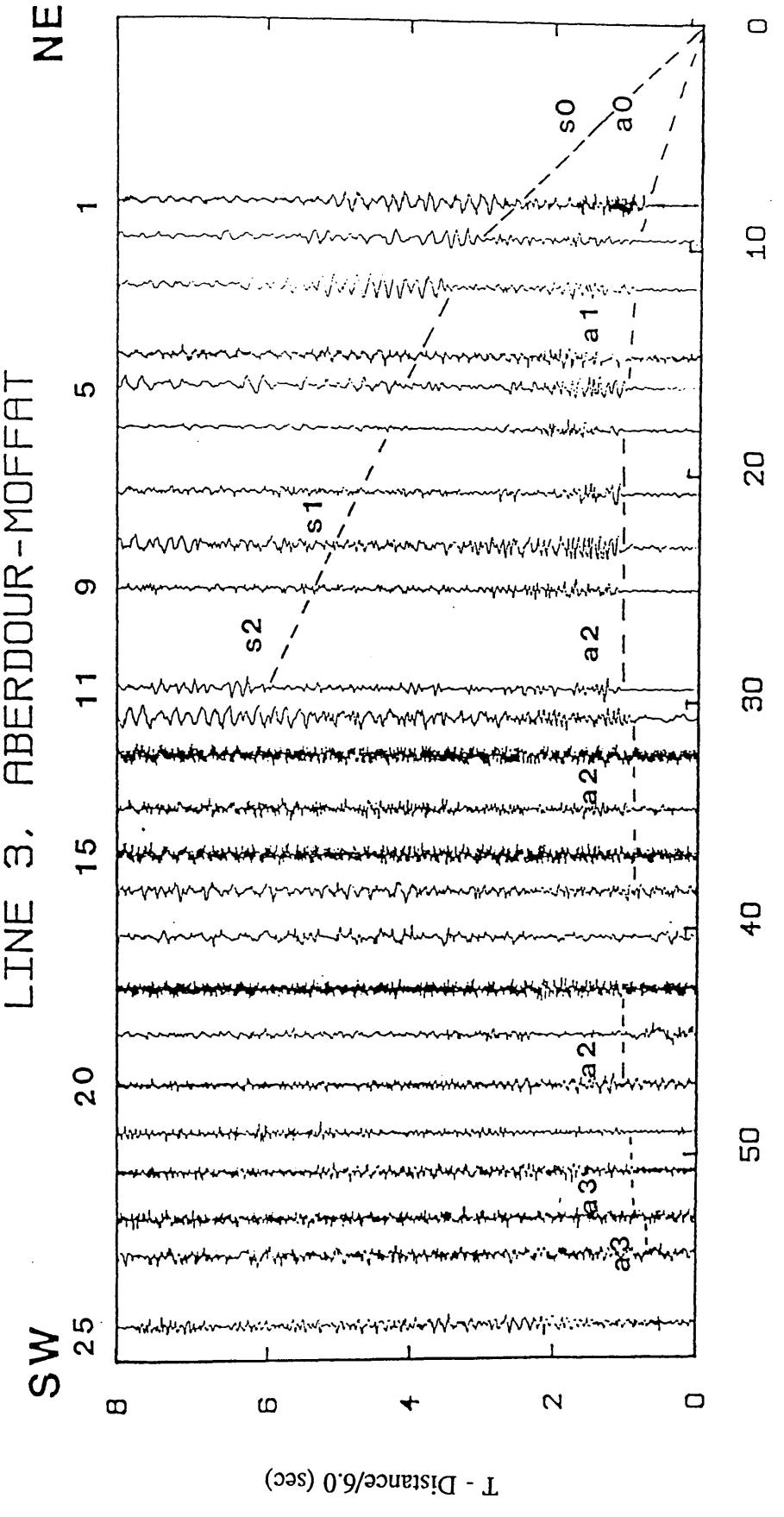

Fig. 5.15 Unfiltered seismic section for line 3 (Aberdour shot), interpreted.

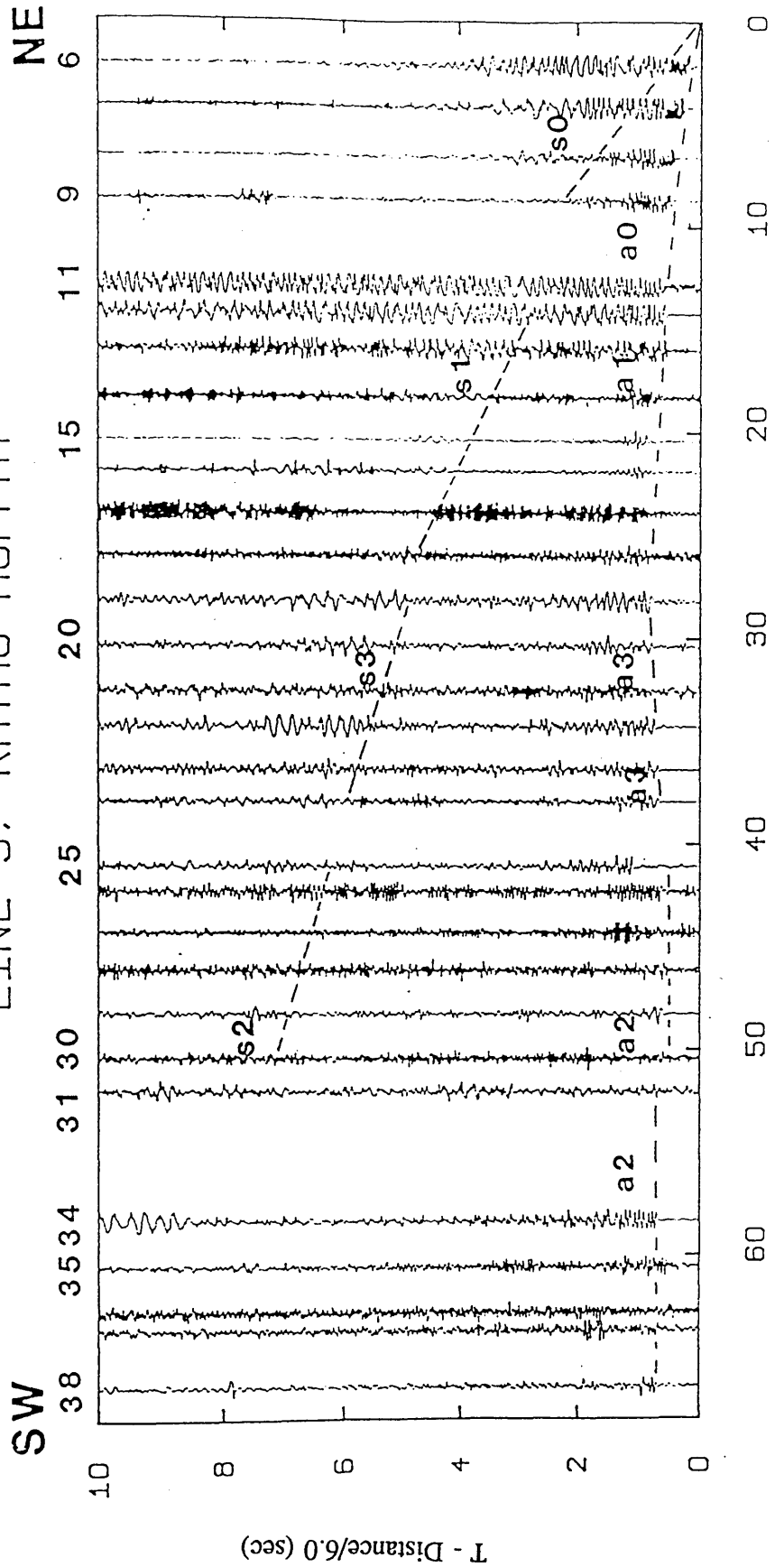

Fig. 5.16 Unfiltered seismic section for line 3 (Ratho shot), interpreted.

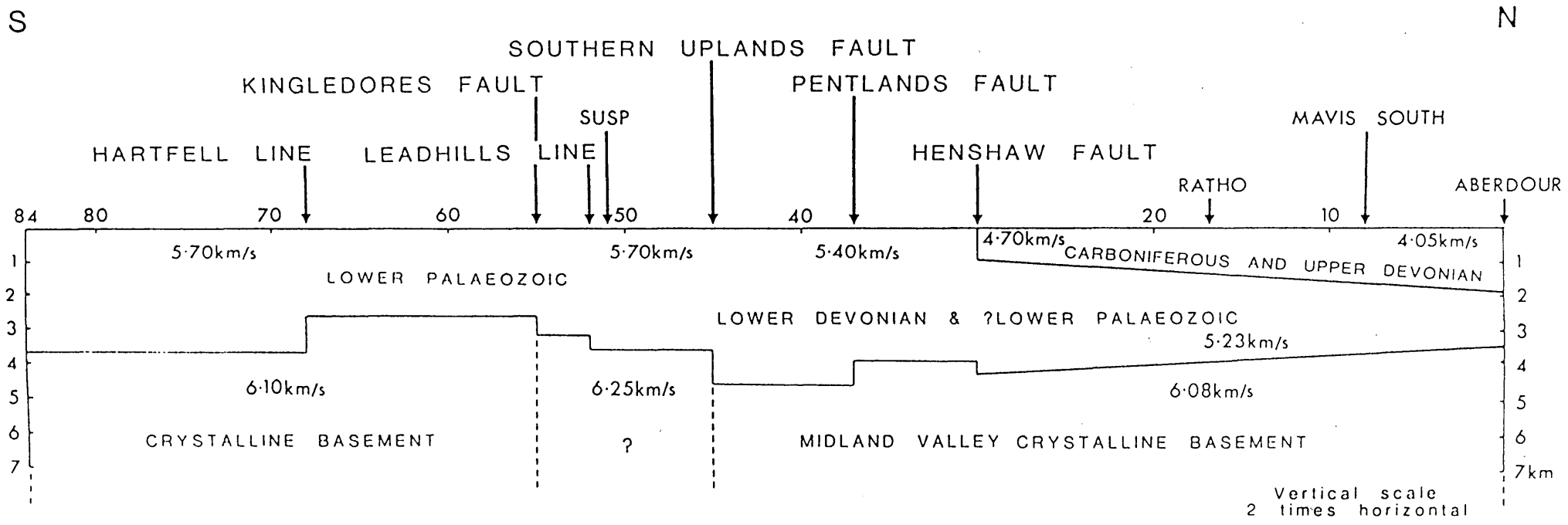

PLANAR LAYER INTERPRETATION, LINE 3

Fig. 5.17 Geological model along line 3 derived from planar layer interpretation. P-wave velocities are indicated. 4.05 km/s is the top layer velocity measured from Aberdour while 4.70 km/s is the top layer velocity when measured from Ratho.

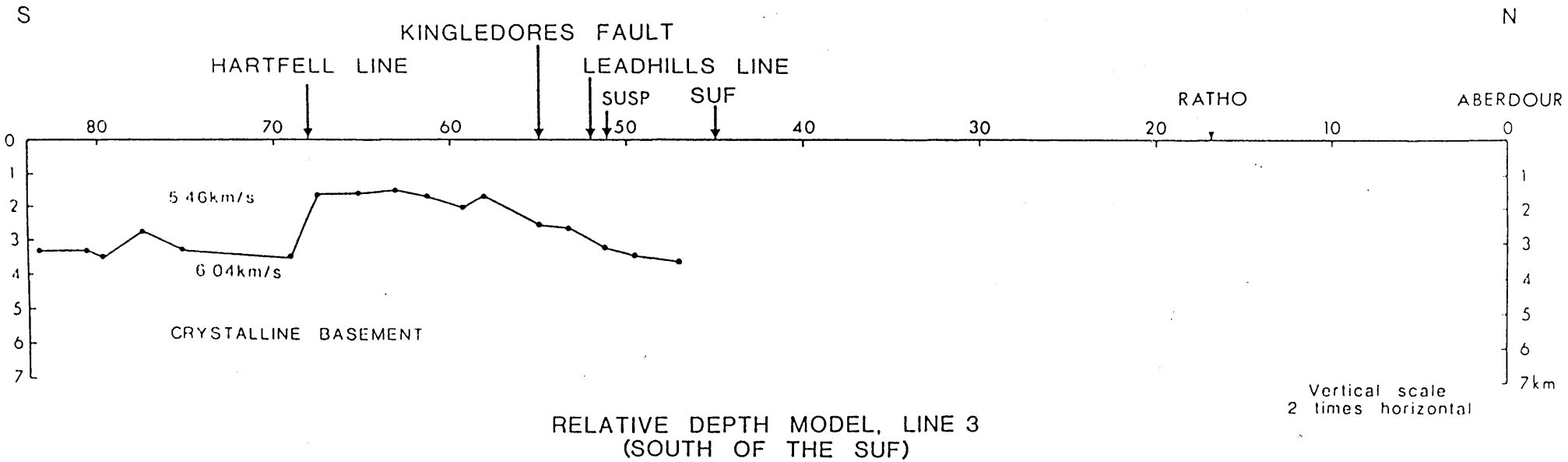

RELATIVE DEPTH MODEL, LINE 3
(SOUTH OF THE SUF)

Fig. 5.18 The adapted "Plus-minus" interpretation along line 3.

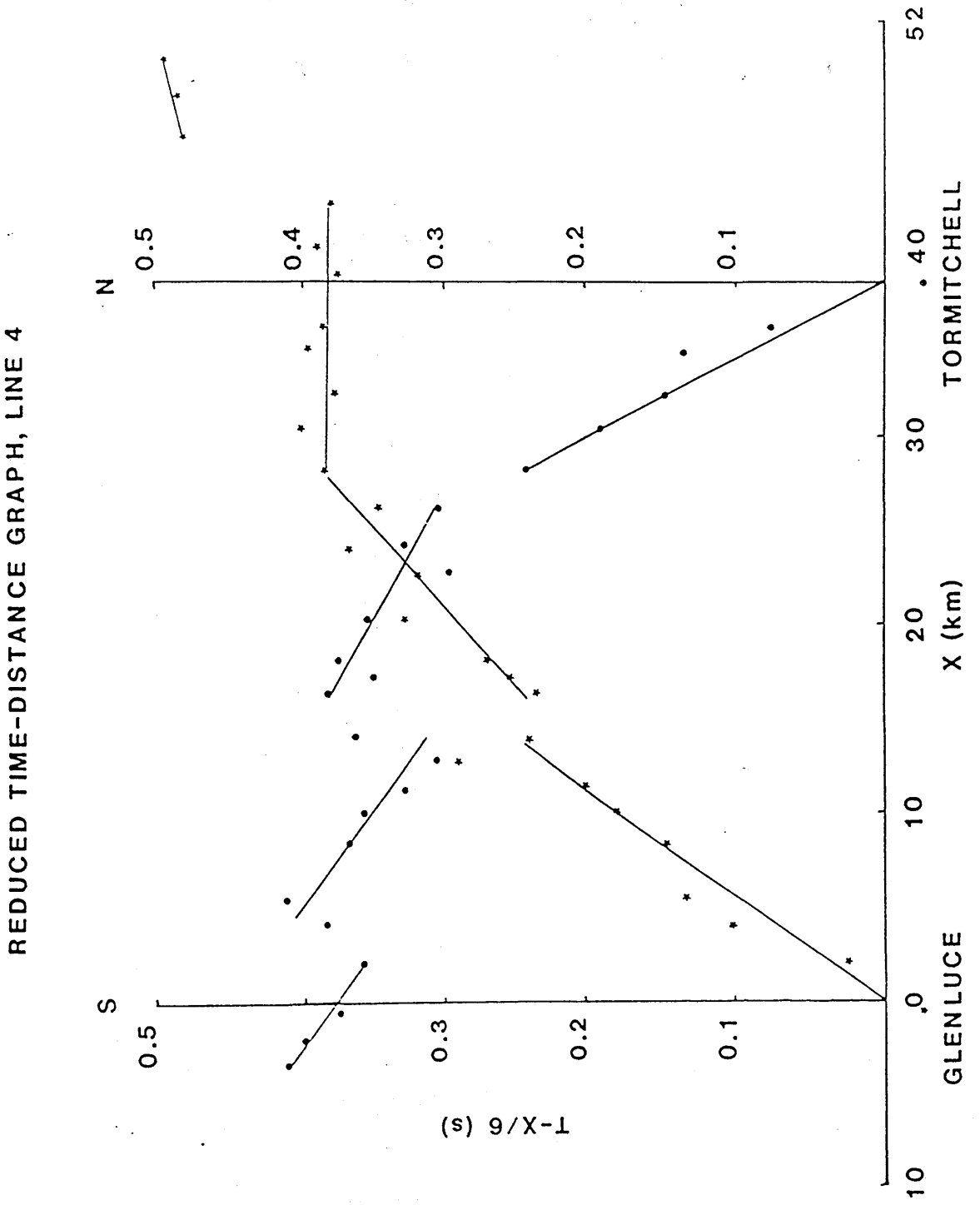

Fig. 5.19 Reduced time-distance graph for line 4.

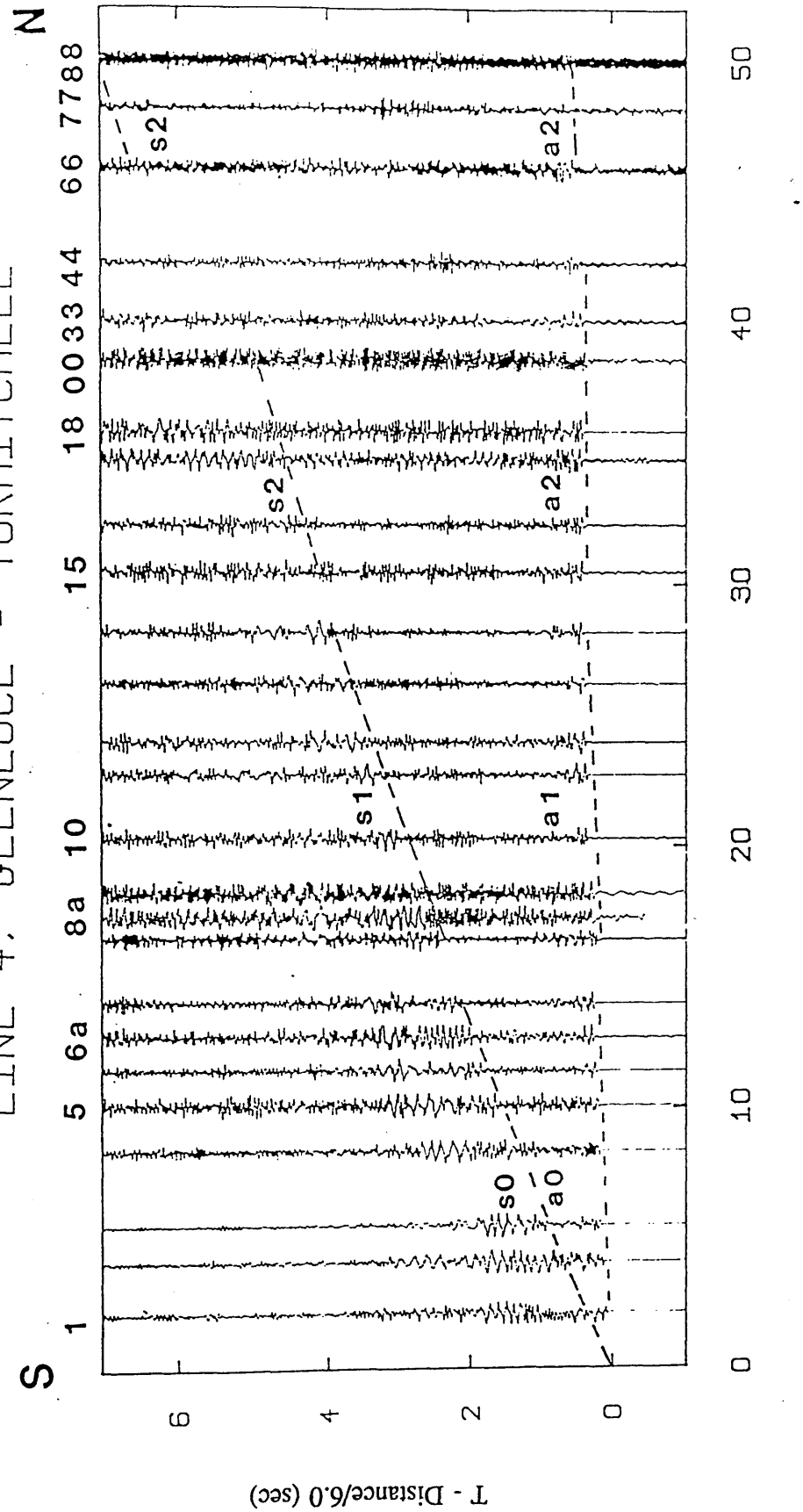

Fig. 5.20 Unfiltered seismic section for line 4 (Glenluce shot), interpreted.

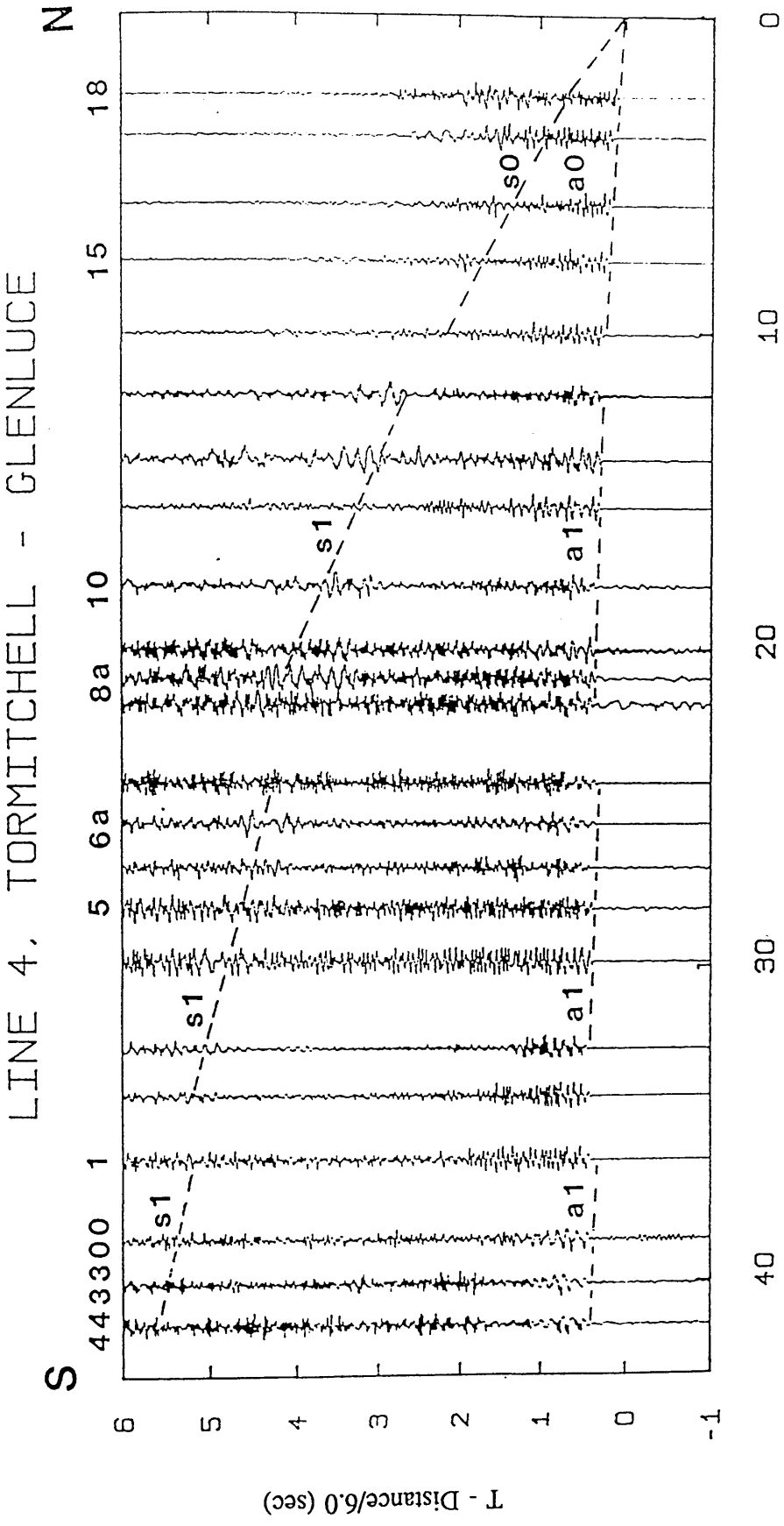

Fig. 5.21 Unfiltered seismic section for line 4 (Tormitchell shot), interpreted.

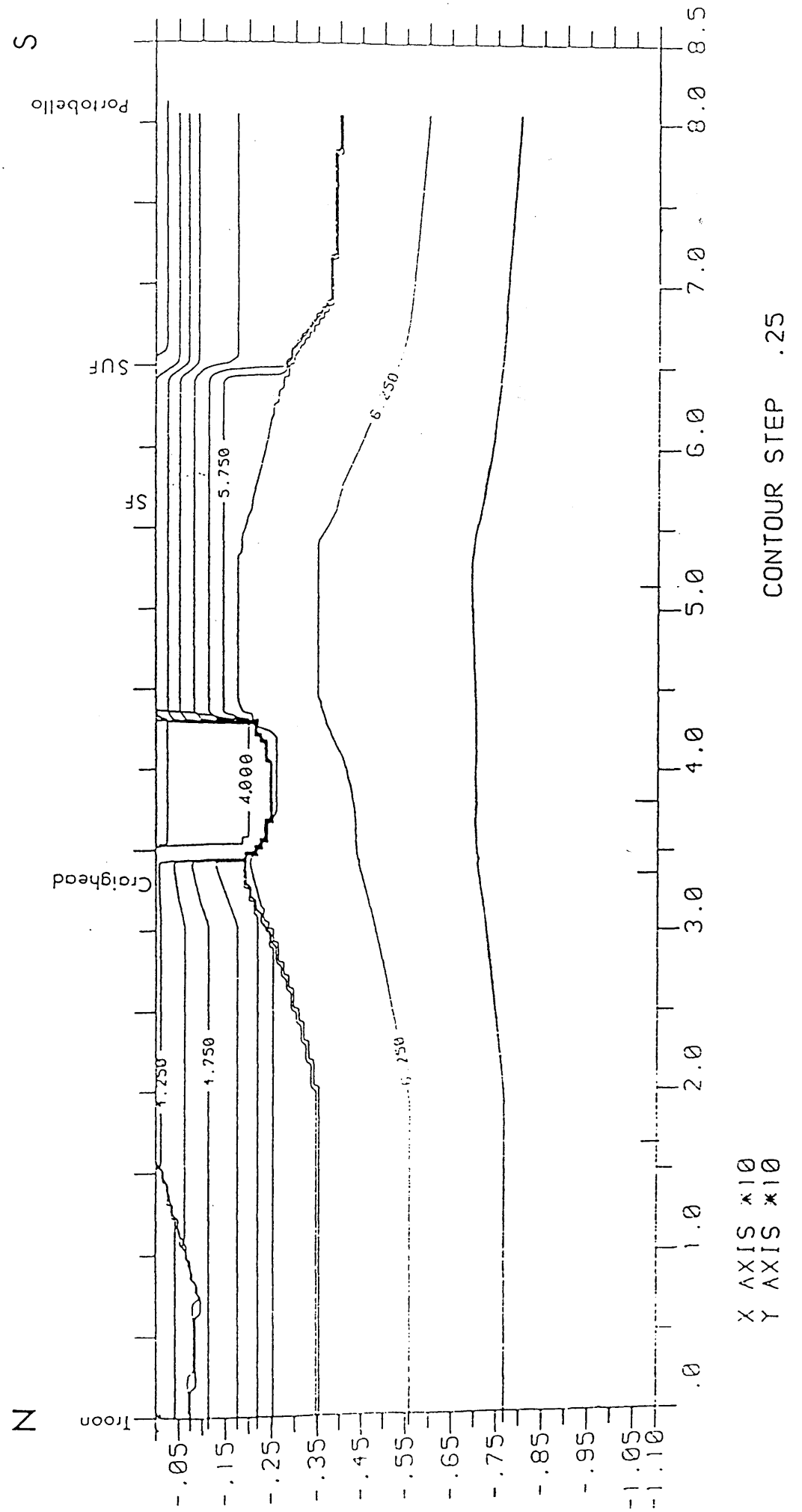

Fig. 5.22 Upper crustal velocity structure along line M1. See Fig. 2.1 for the location of M1. Adapted from Al-Mansouri (1986). Contours are of P-wave velocity.

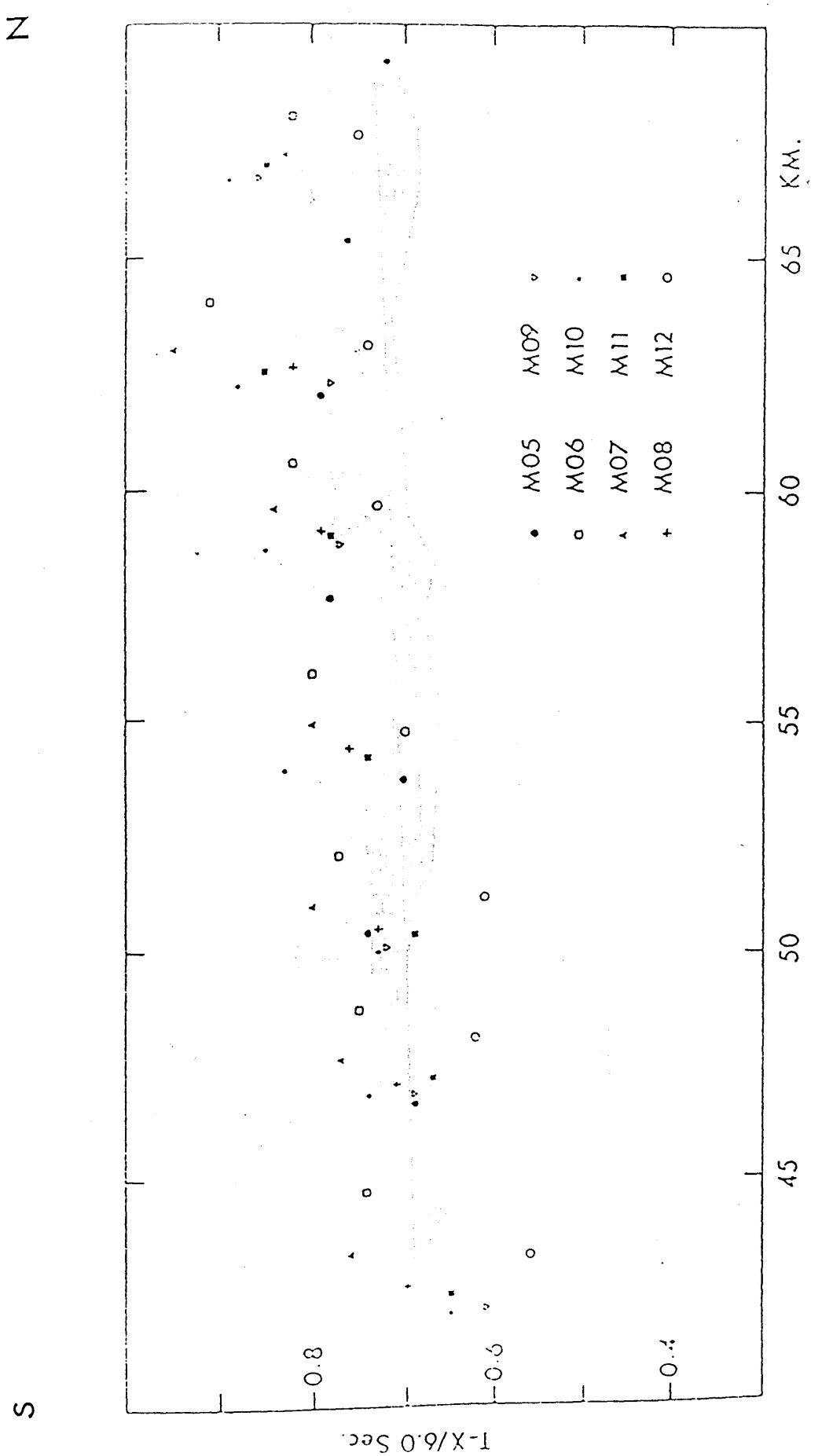

Fig. 5.23 Reduced time-distance plot of first arrivals of marine explosive shots of the Caledonian Suture Seismic Project, recorded across the Galloway area, along line M4 (see Fig. 2.1). After Al-Mansouri (1986). M05-M12 are the successive shotpoints.

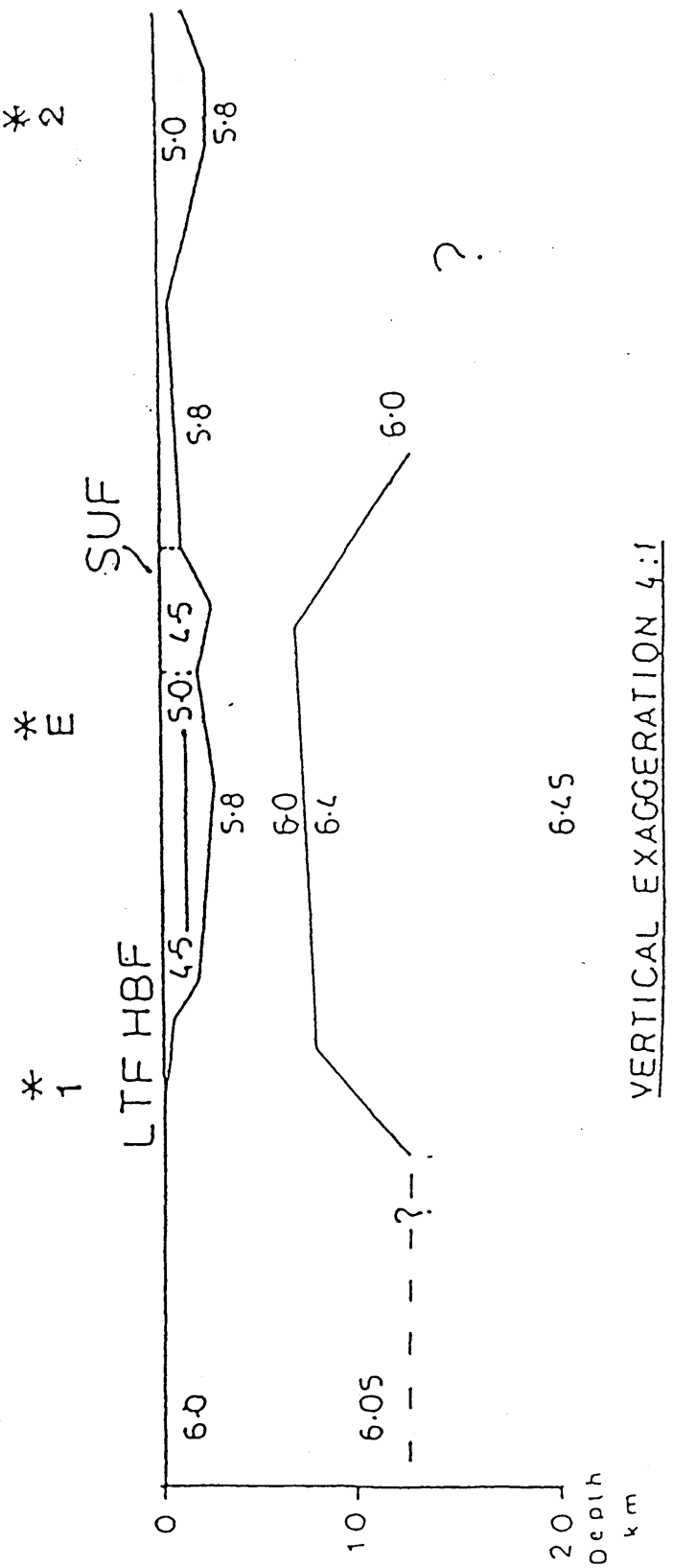

Fig. 5.24 P-wave velocity distribution and upper crustal structure of the LISPB project across Scotland. After Bamford *et al.* (1977).

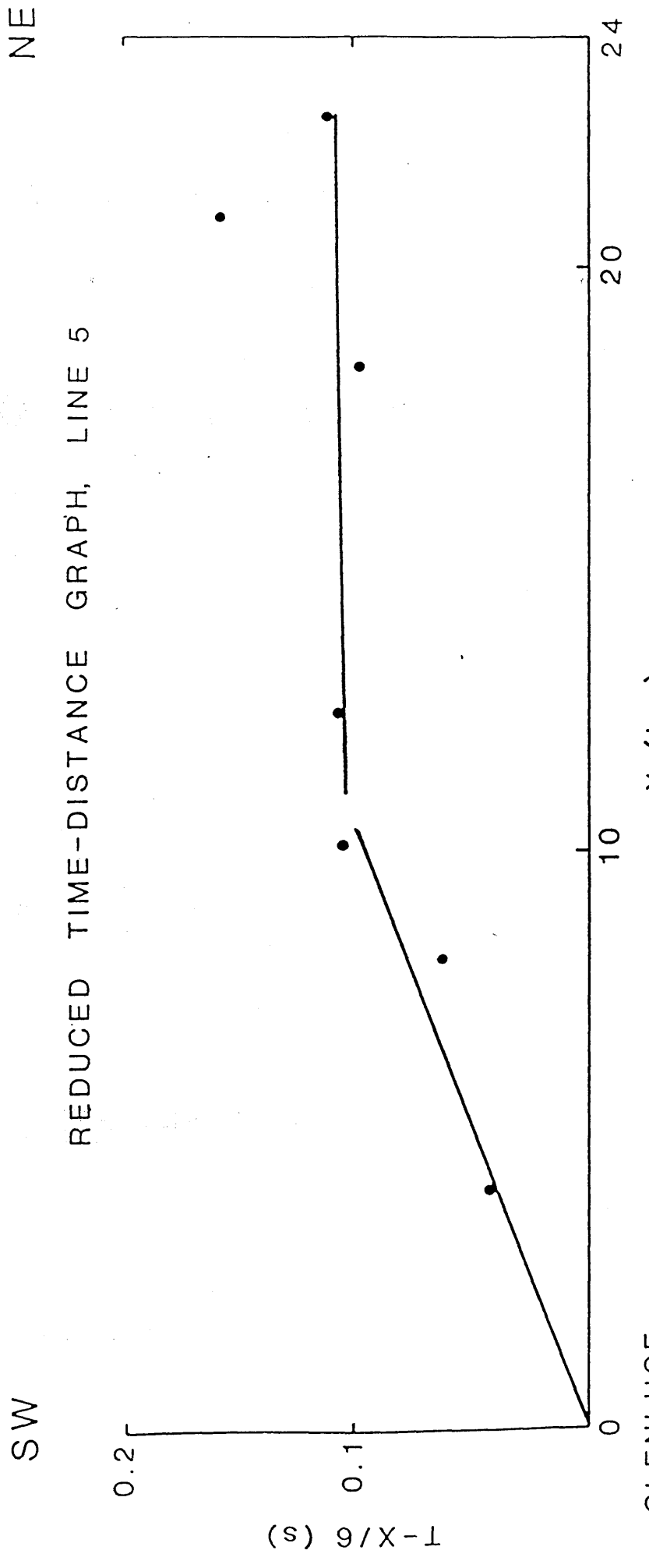

Fig. 5.25 Reduced time-distance graph for line 5.

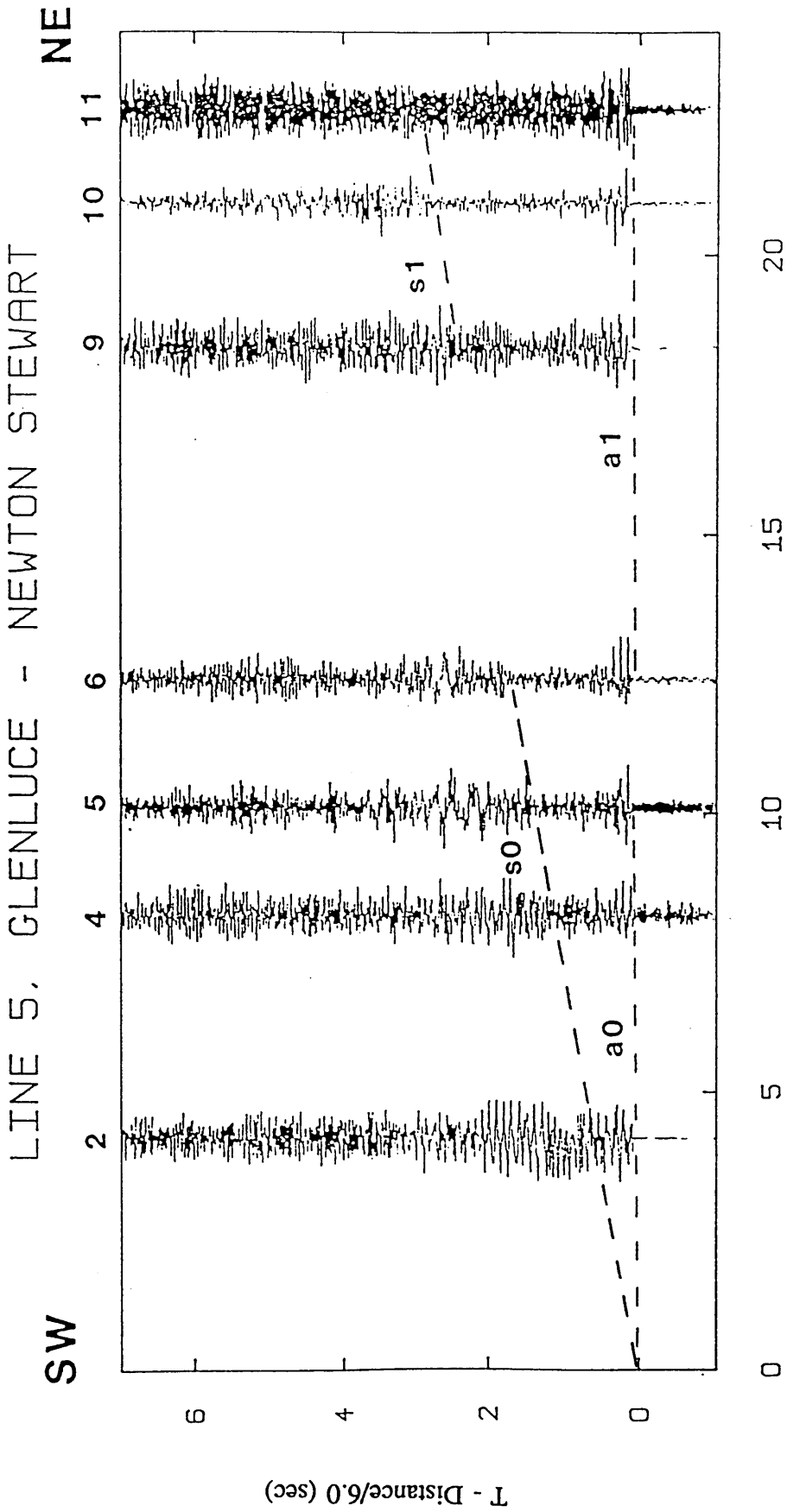

Fig. 5.26 Unfiltered seismic section for line 5 (Glenluce shot), interpreted.

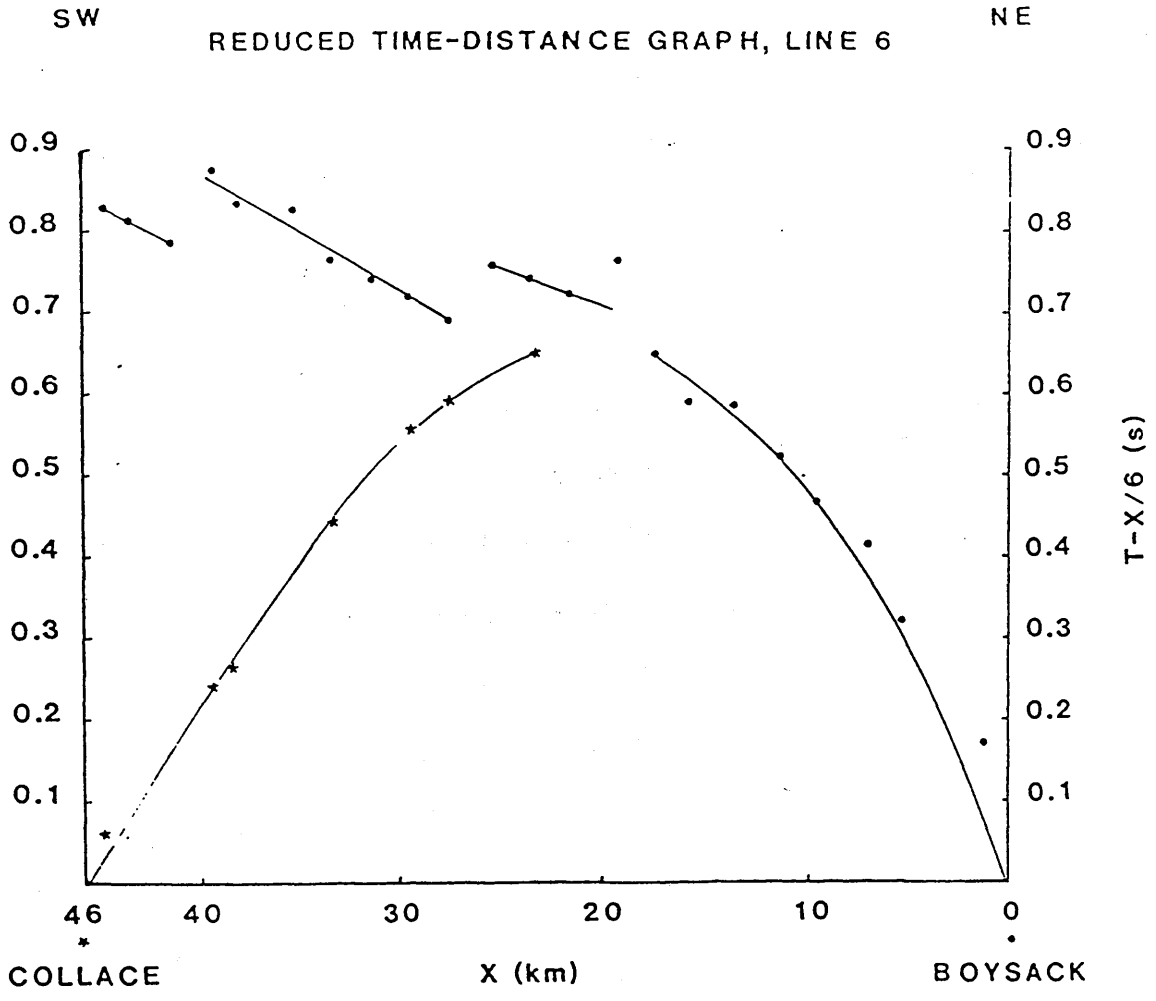

Fig. 5.27 Reduced time-distance graph for line 6.

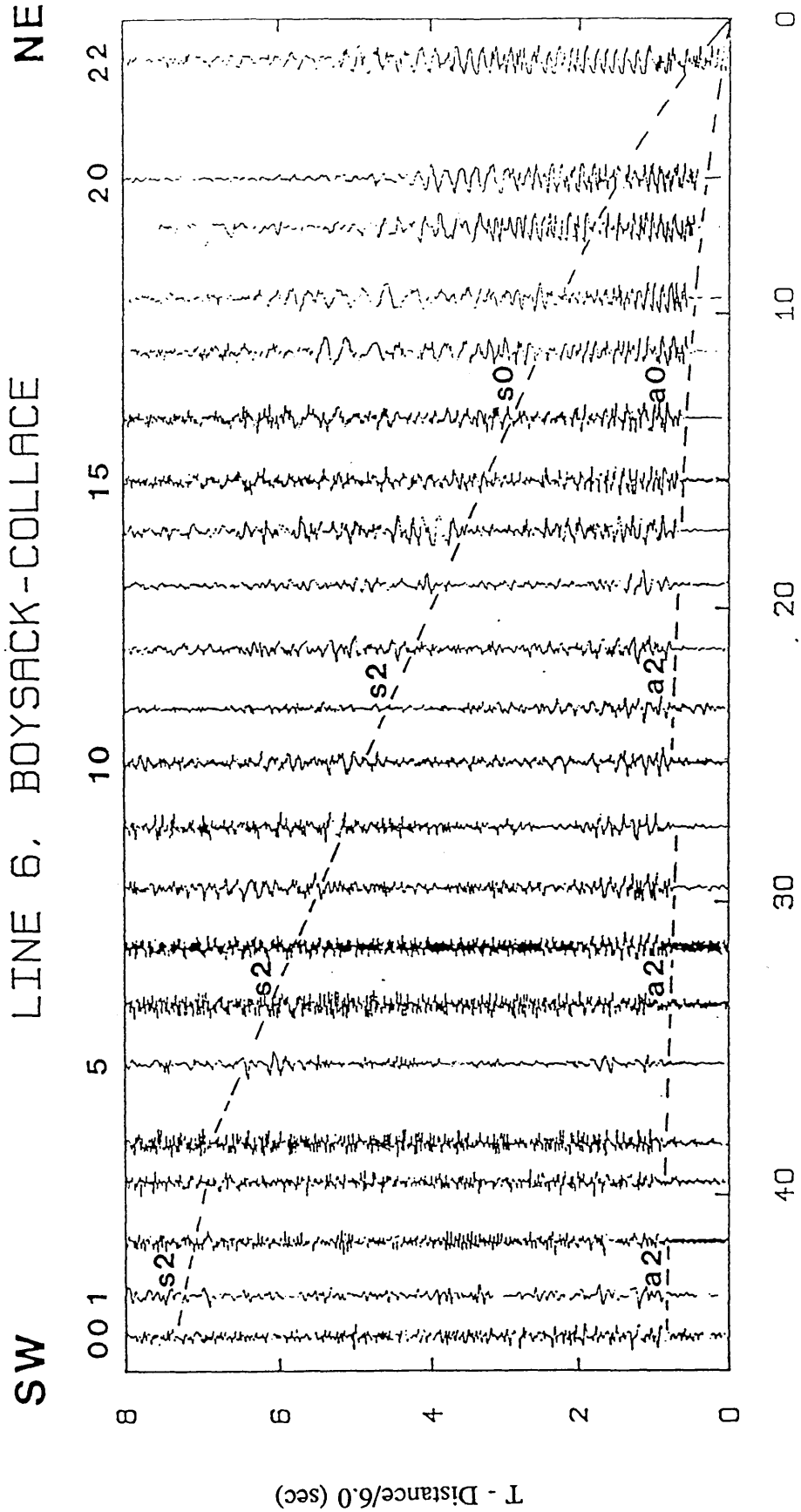

Fig. 5.28 Unfiltered seismic section for line 6 (Boysack shot), interpreted.

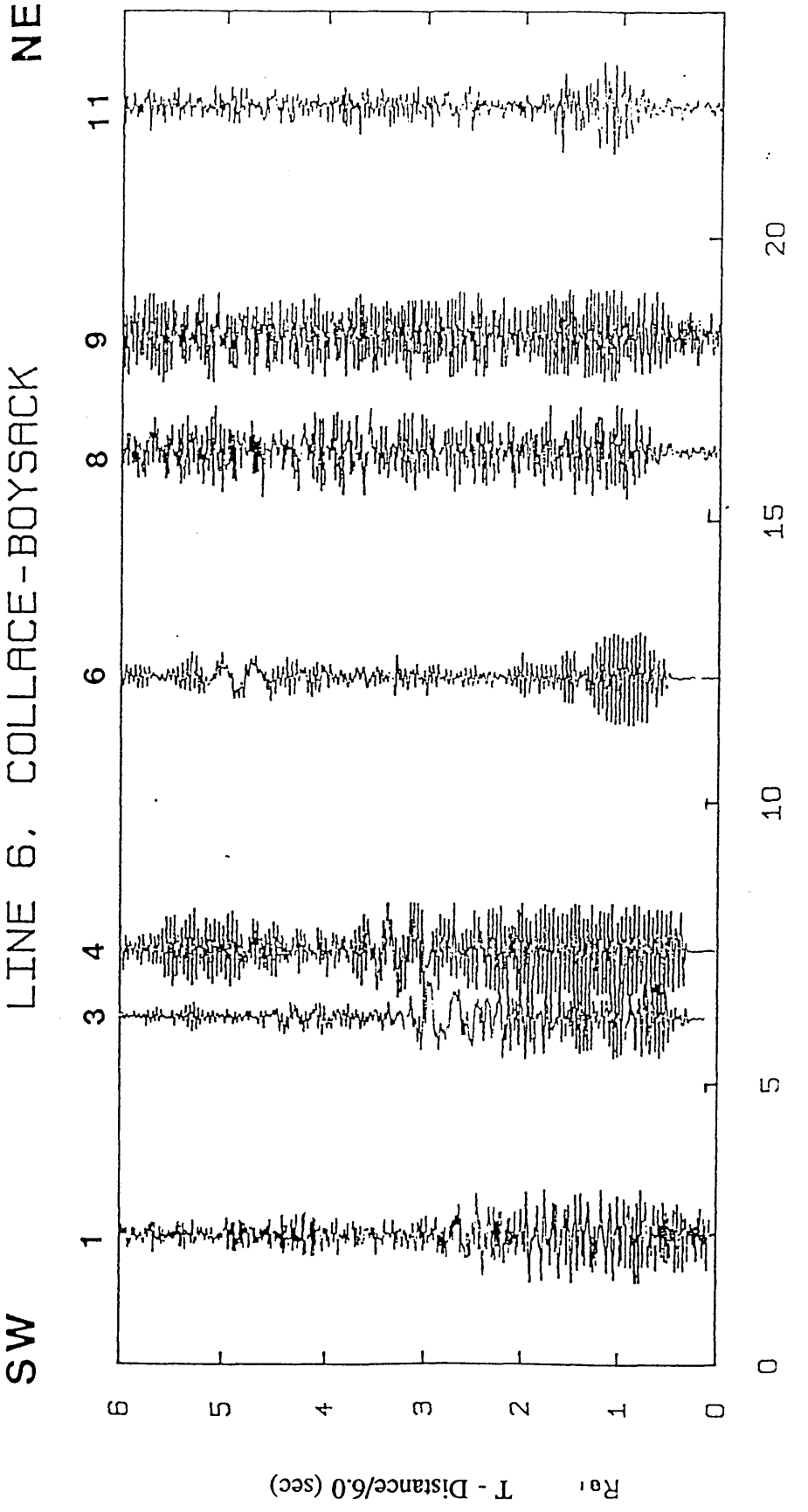

Fig. 5.29 Unfiltered seismic section for line 6 (Collace shot).

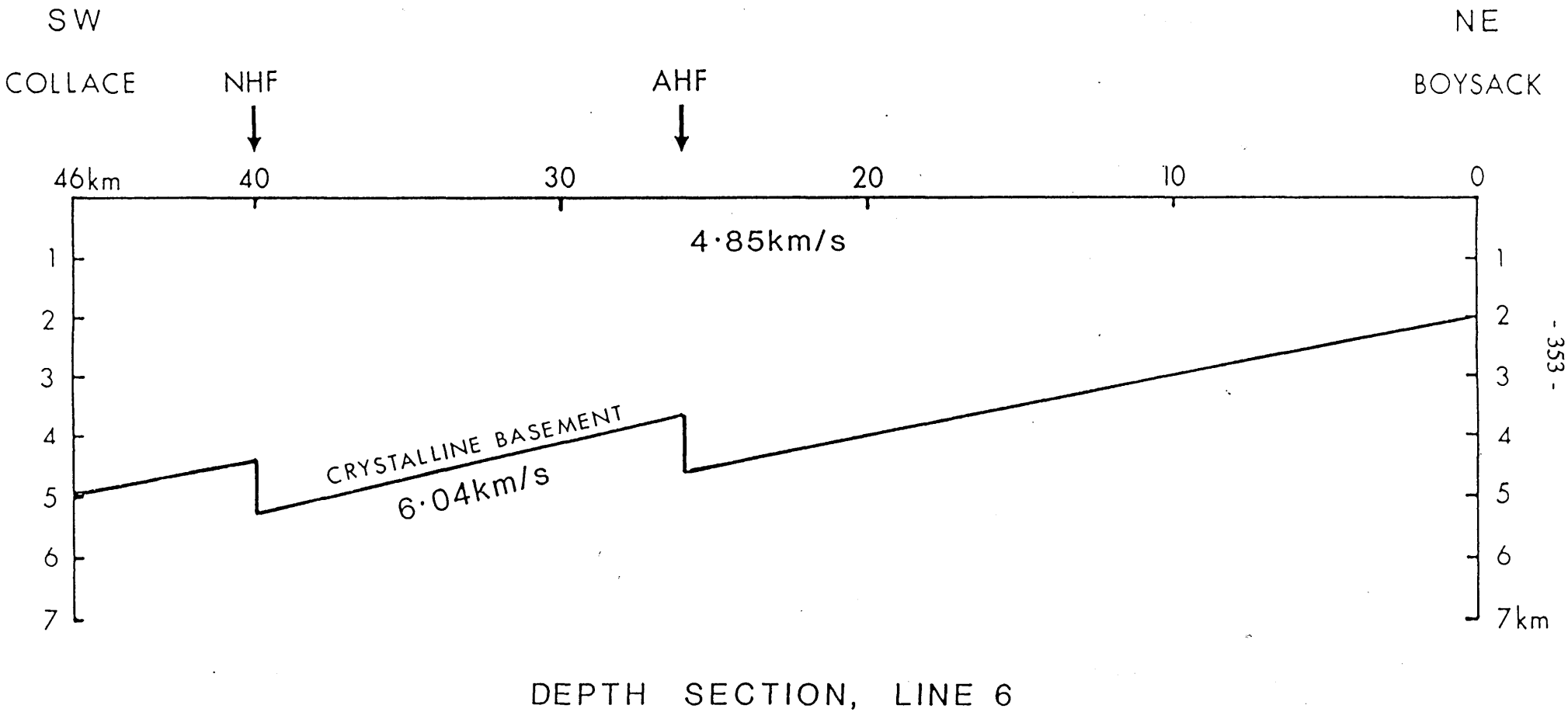

DEPTH SECTION, LINE 6

Fig. 5.30 Depth model along line 6. AHF and NHF are the Auchterhouse and Northballo Faults.

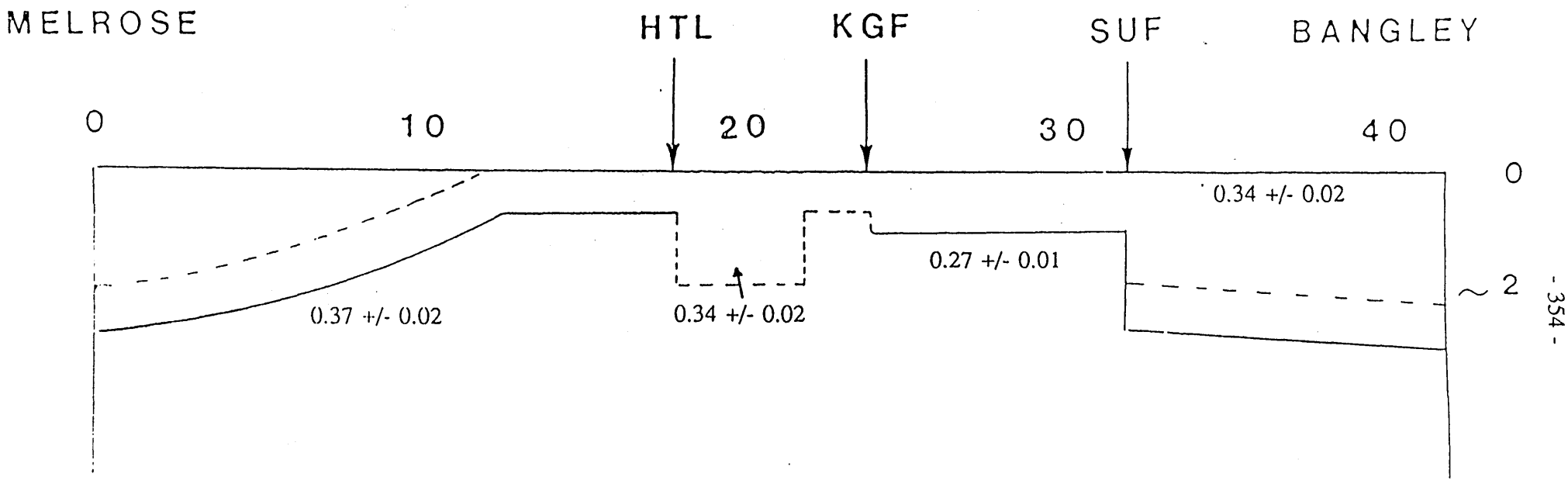

SCHEMATIC DEPTH SECTION ALONG LINE 1

Fig. 5.31 Possion's ratio distribution along line 1.

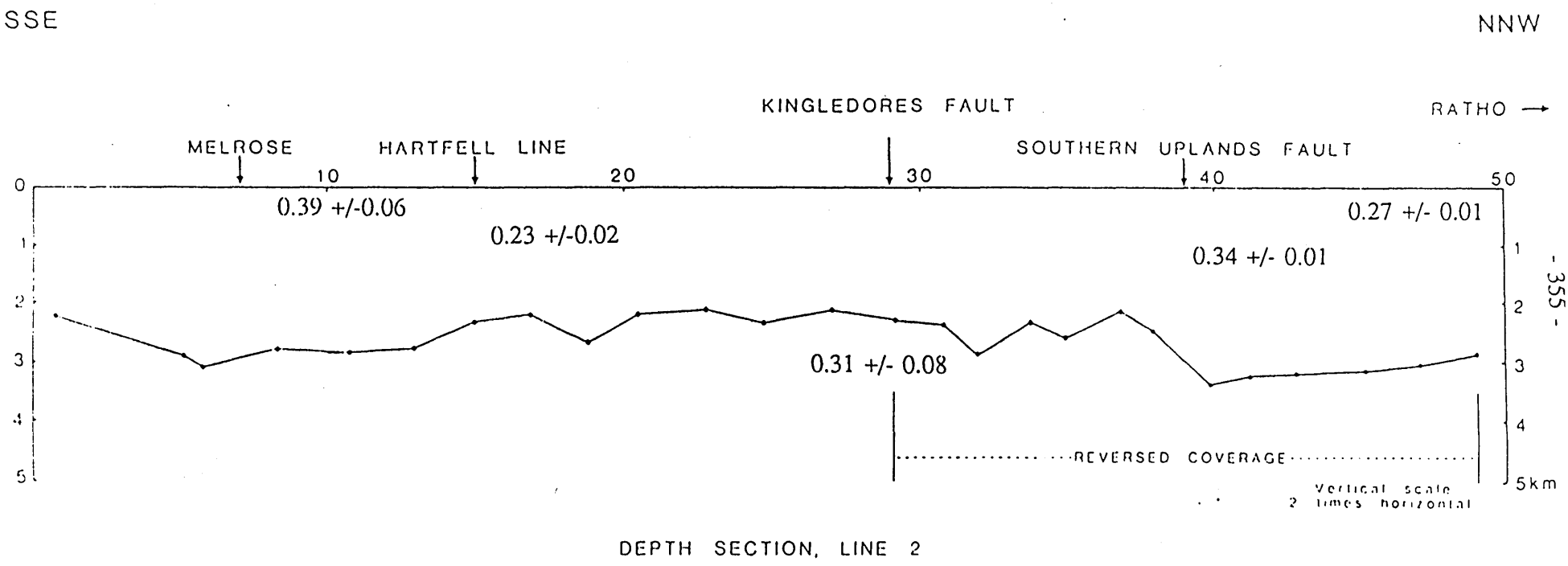

DEPTH SECTION, LINE 2

Fig. 5.32 Possion's ratio distribution along line 2.

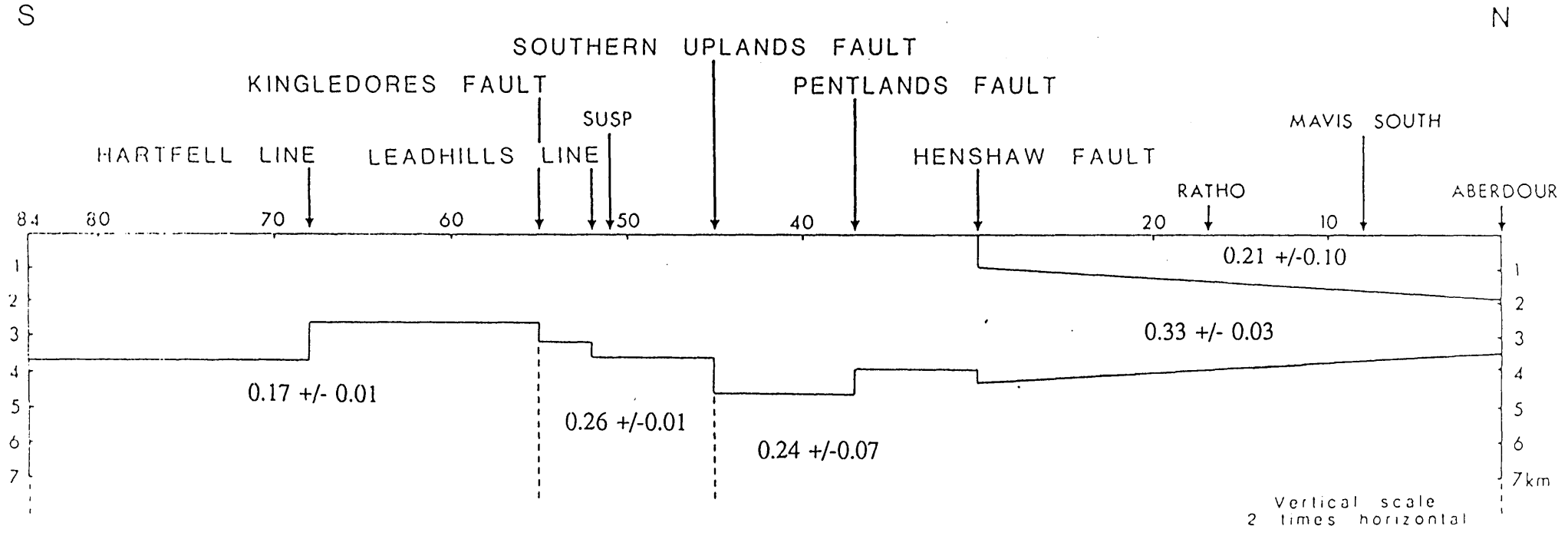

PLANAR LAYER INTERPRETATION, LINE 3

Fig. 5.33 Possion's ratio distribution along line 3.

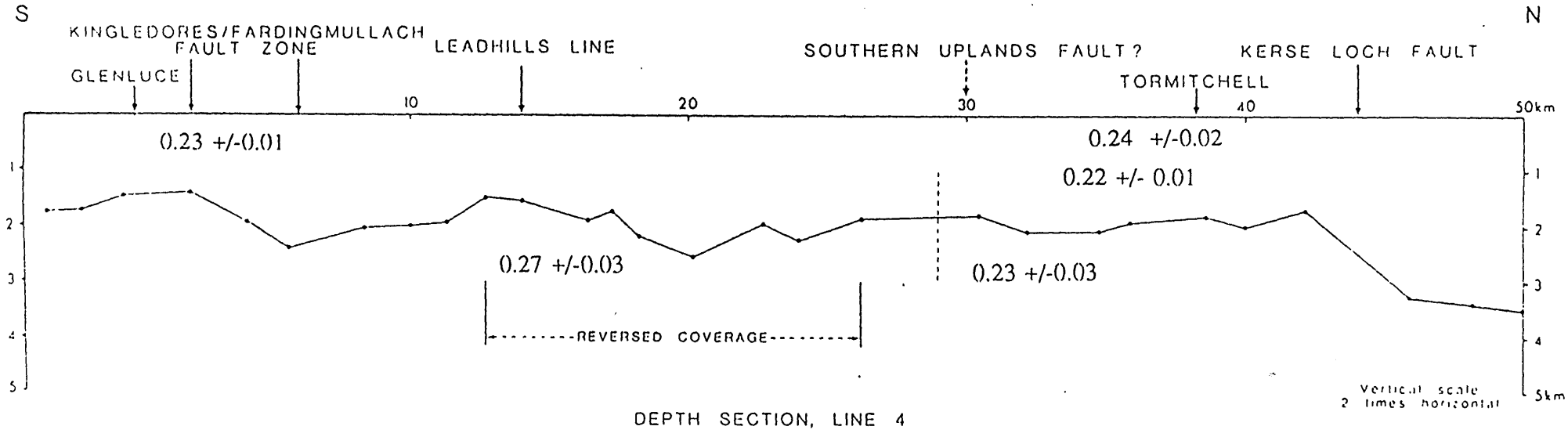

Fig. 5.34 Possion's ratio distribution along line 4.

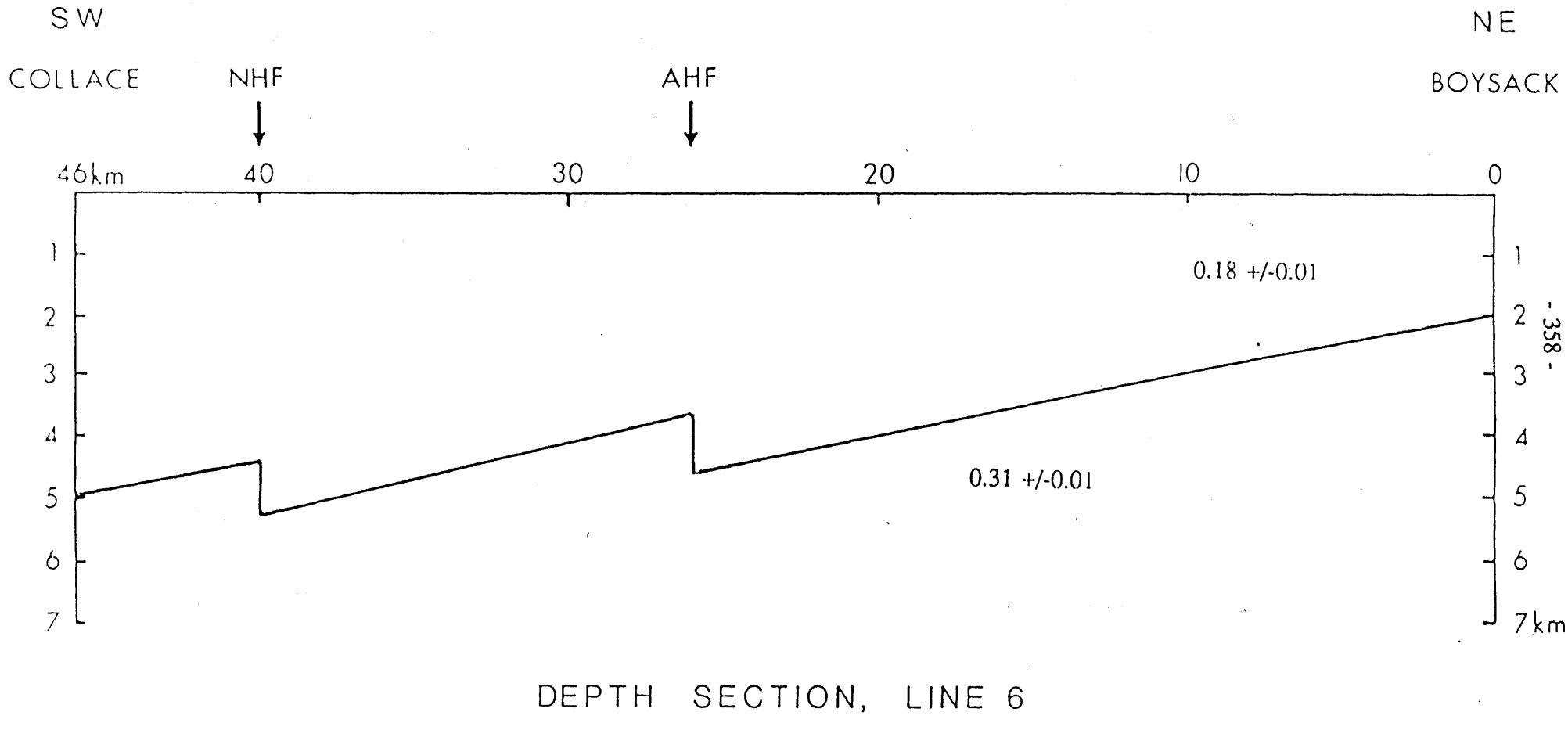

DEPTH SECTION, LINE 6

Fig. 5.35 Possion's ratio distribution along line 6.

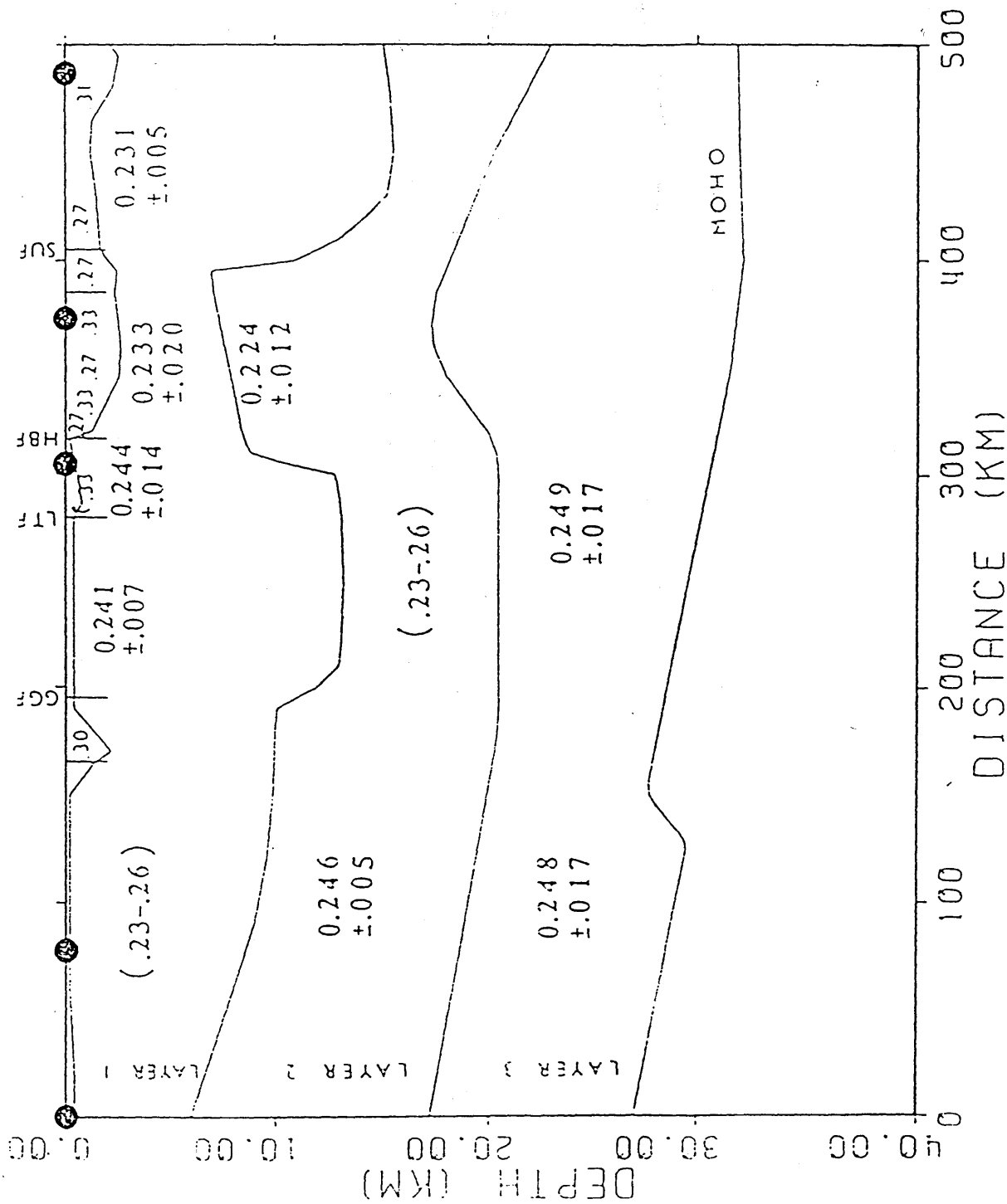

Fig. 5.36 Possion's ratio distribution in northern Britain. After Assumpcao & Bamford (1978).

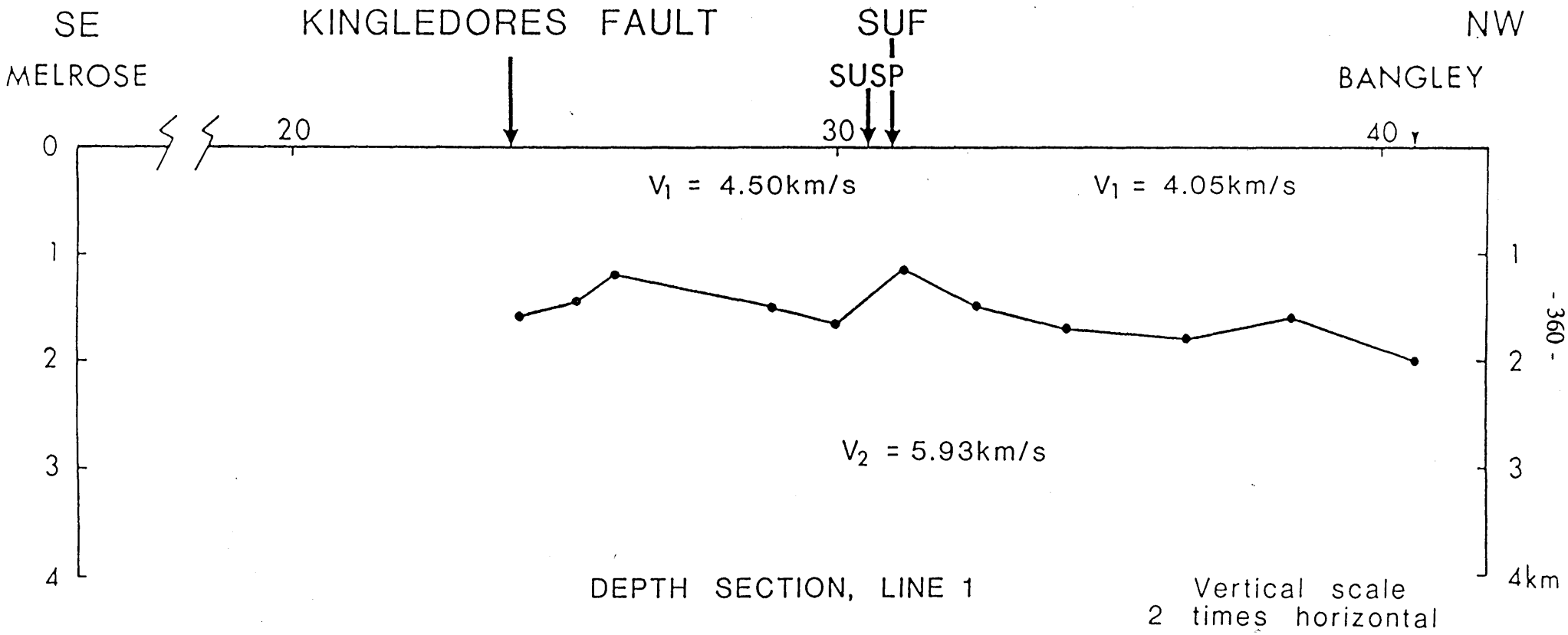

Fig. 5.37 Plus-minus depth section along line 1.

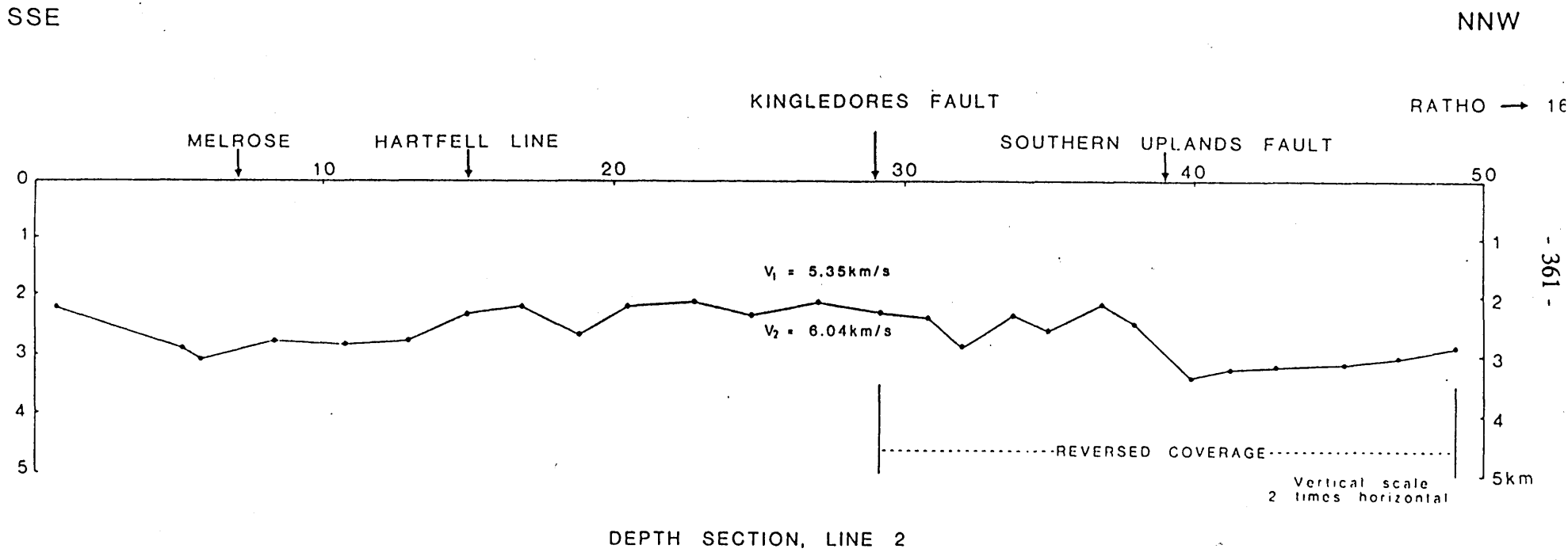

Fig. 5.38 Plus-minus depth section along line 2.

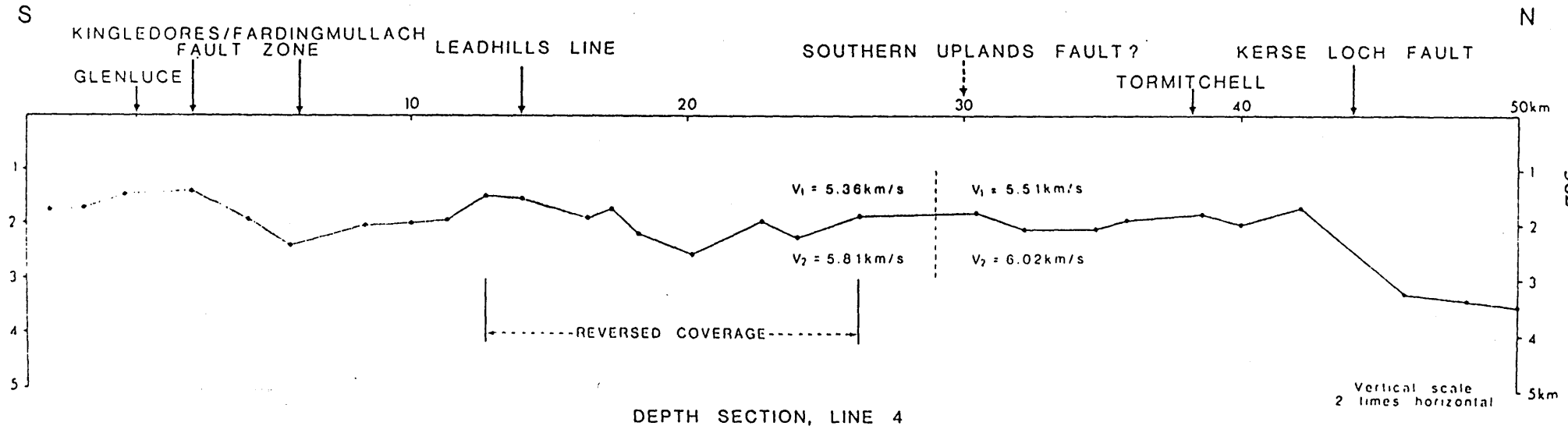

DEPTH SECTION, LINE 4

Fig. 5.39 Plus-minus depth section along line 4.

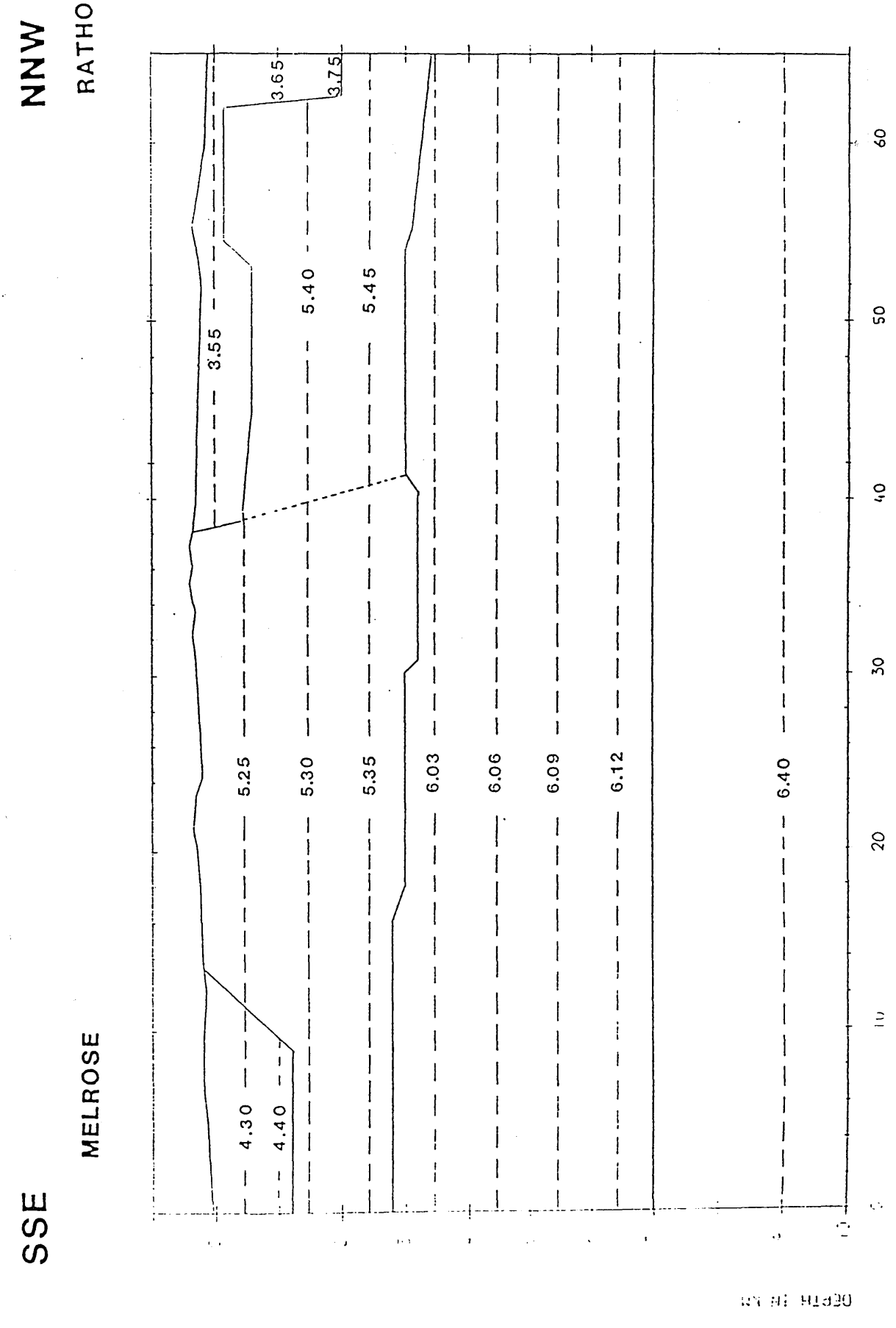

Fig. 5.40 P-wave velocity model along line 2 derived by raytracing.

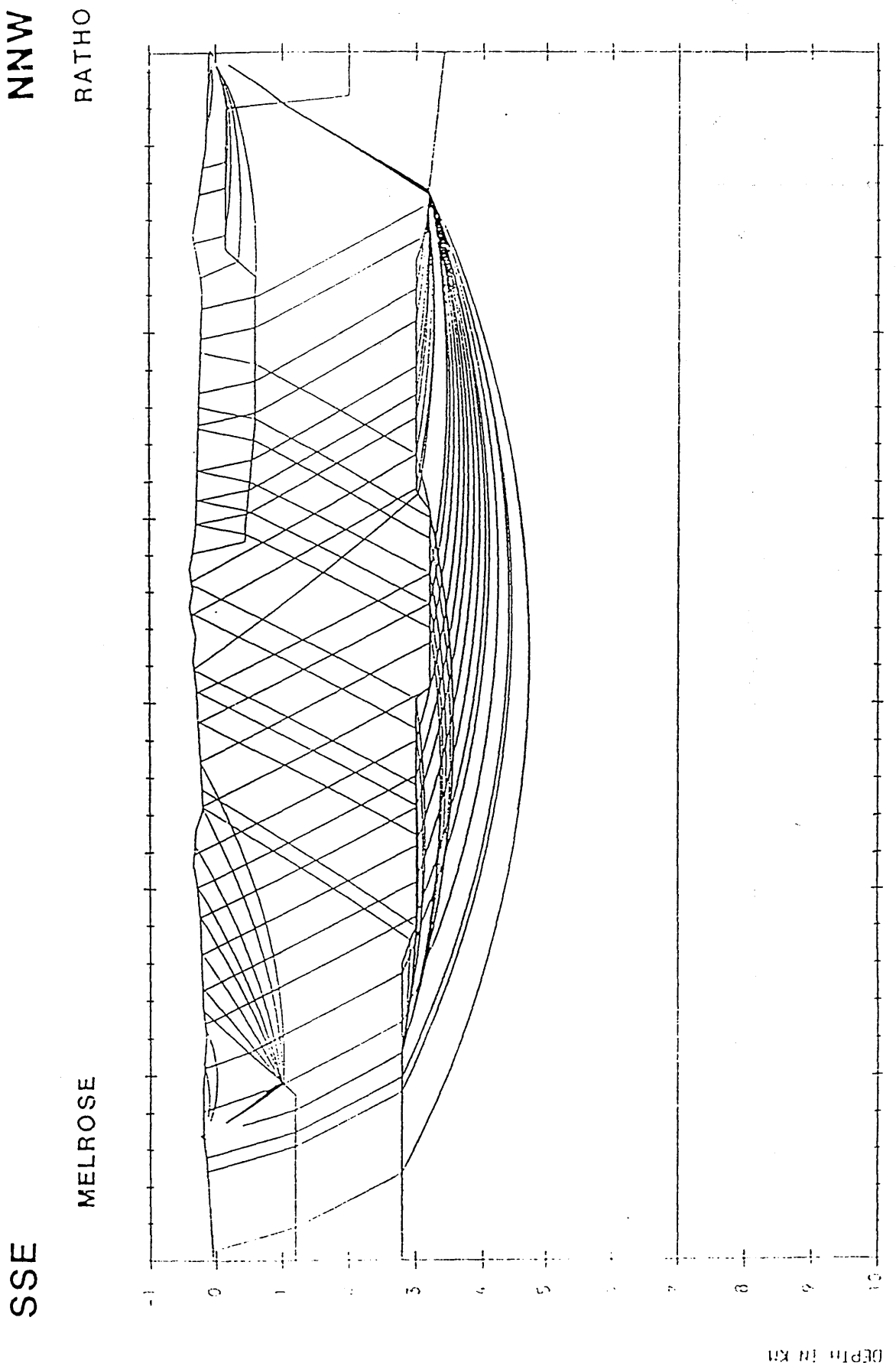

Fig. 5.41 Ray-paths used in the calculation of travel-times along line 2. Shotpoints are denoted (*).

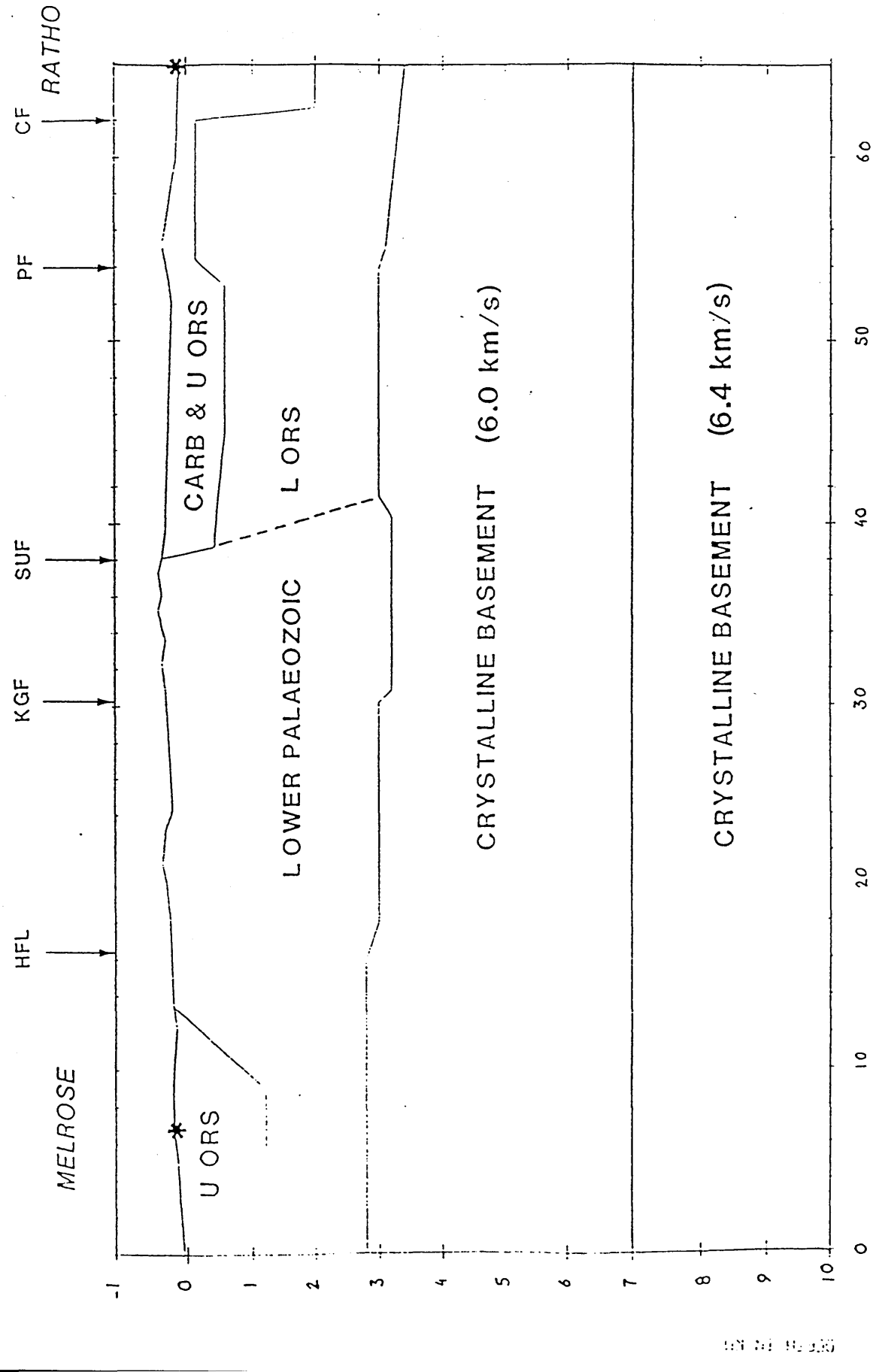

Fig. 5.42 Geological model along line 2 derived by raytracing. CF- Colinton Fault, HFL-Hartfell Line, KGF-Kingledores Fault, PF-Pentland Fault, SUF-Southern Uplands Fault.

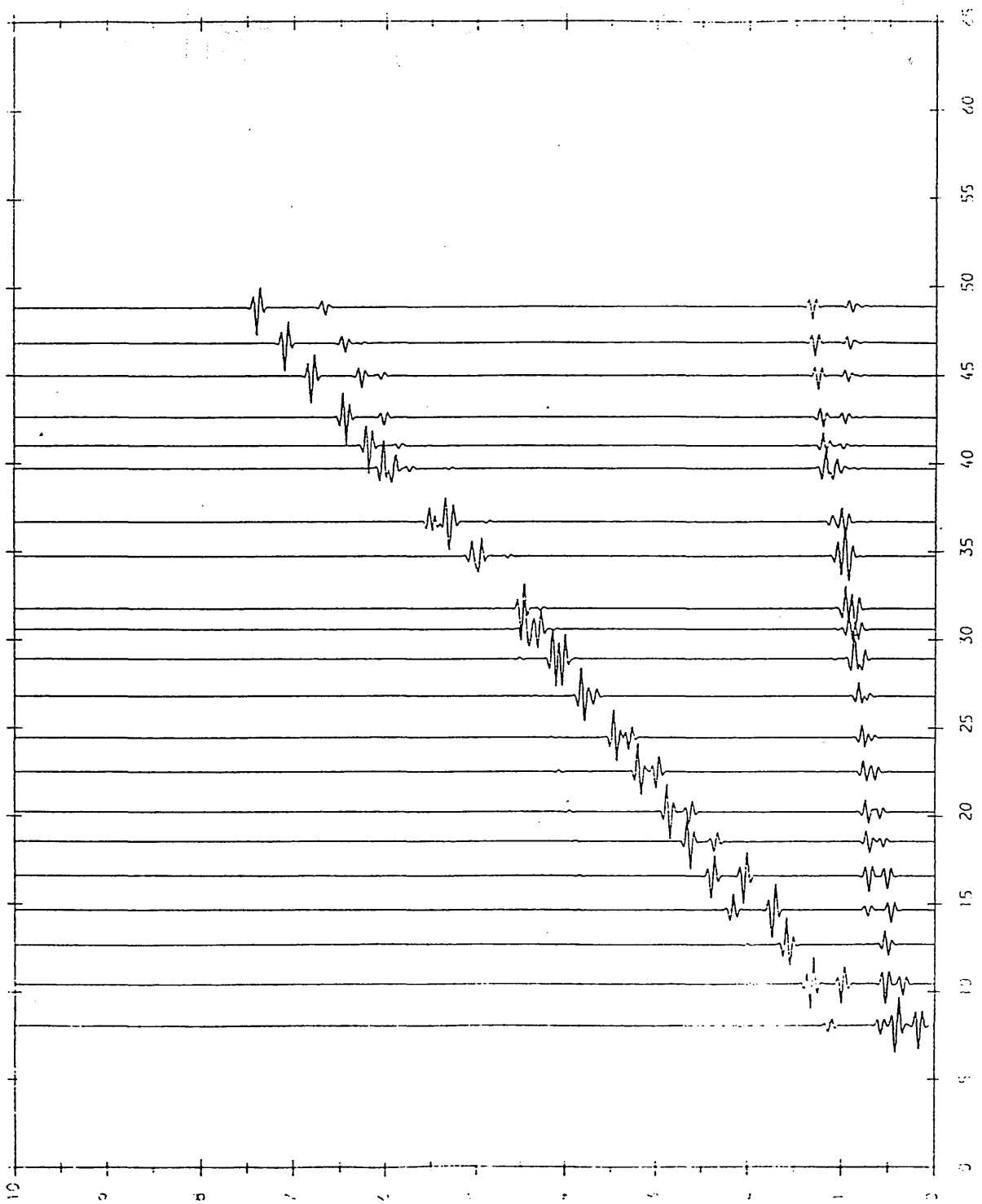

Fig. 5.43 Synthetic seismograms obtained along line 2, Melrose shot.

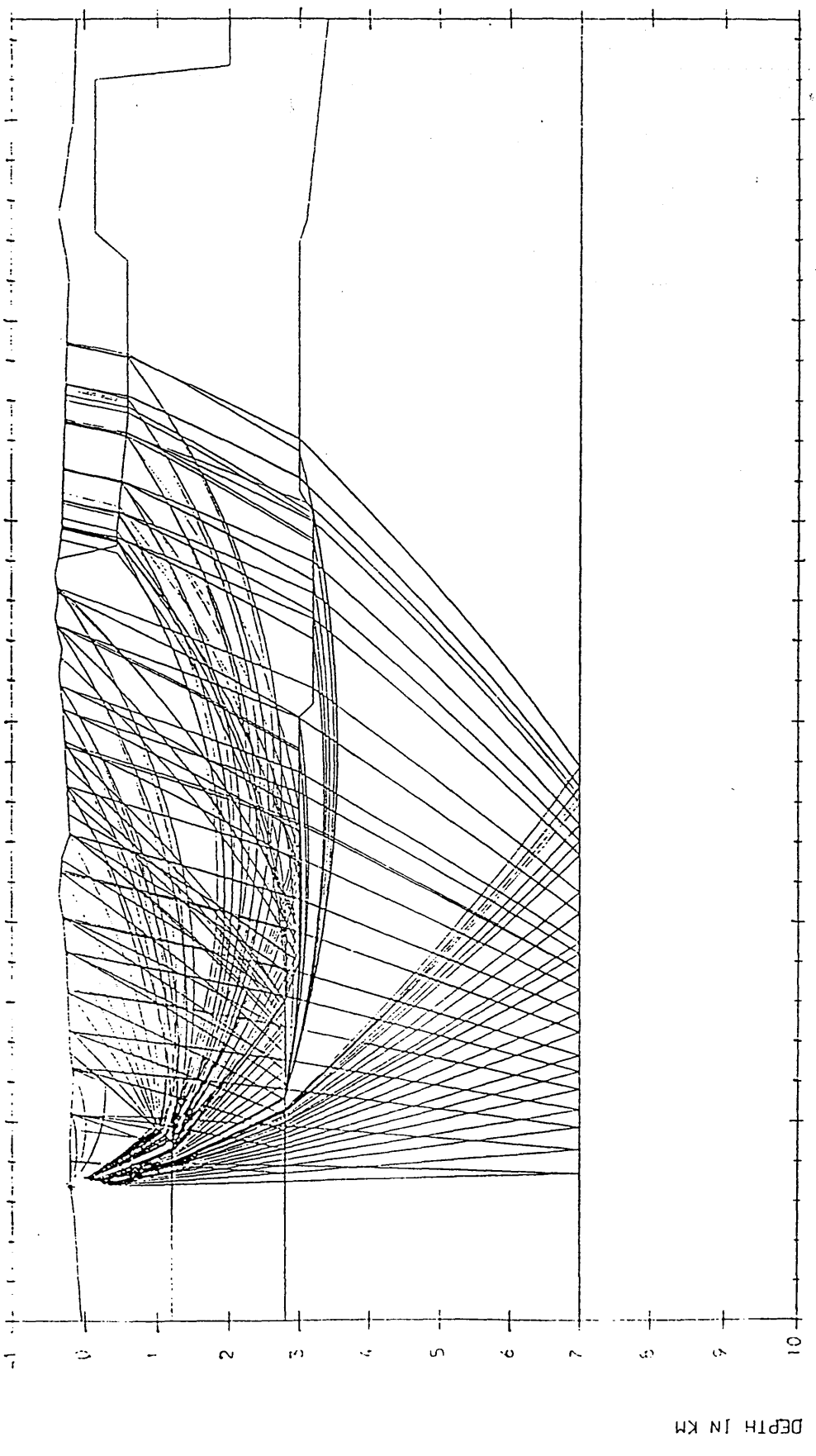

Fig. 5.44 Rays used to calculate the synthetic seismograms of Fig. 5.43.

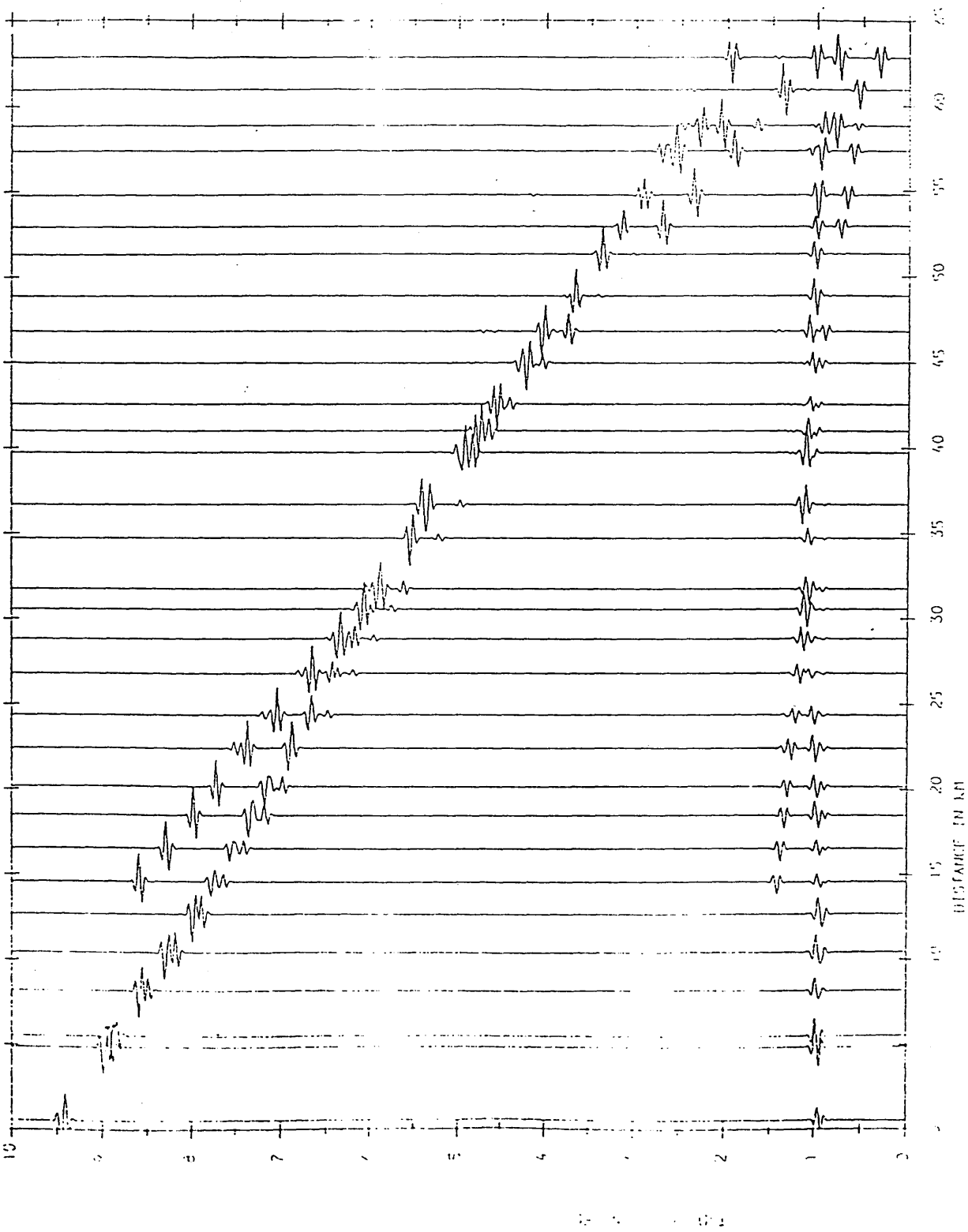

Fig. 5.45 Synthetic seismograms obtained along line 2, Ratho shot.

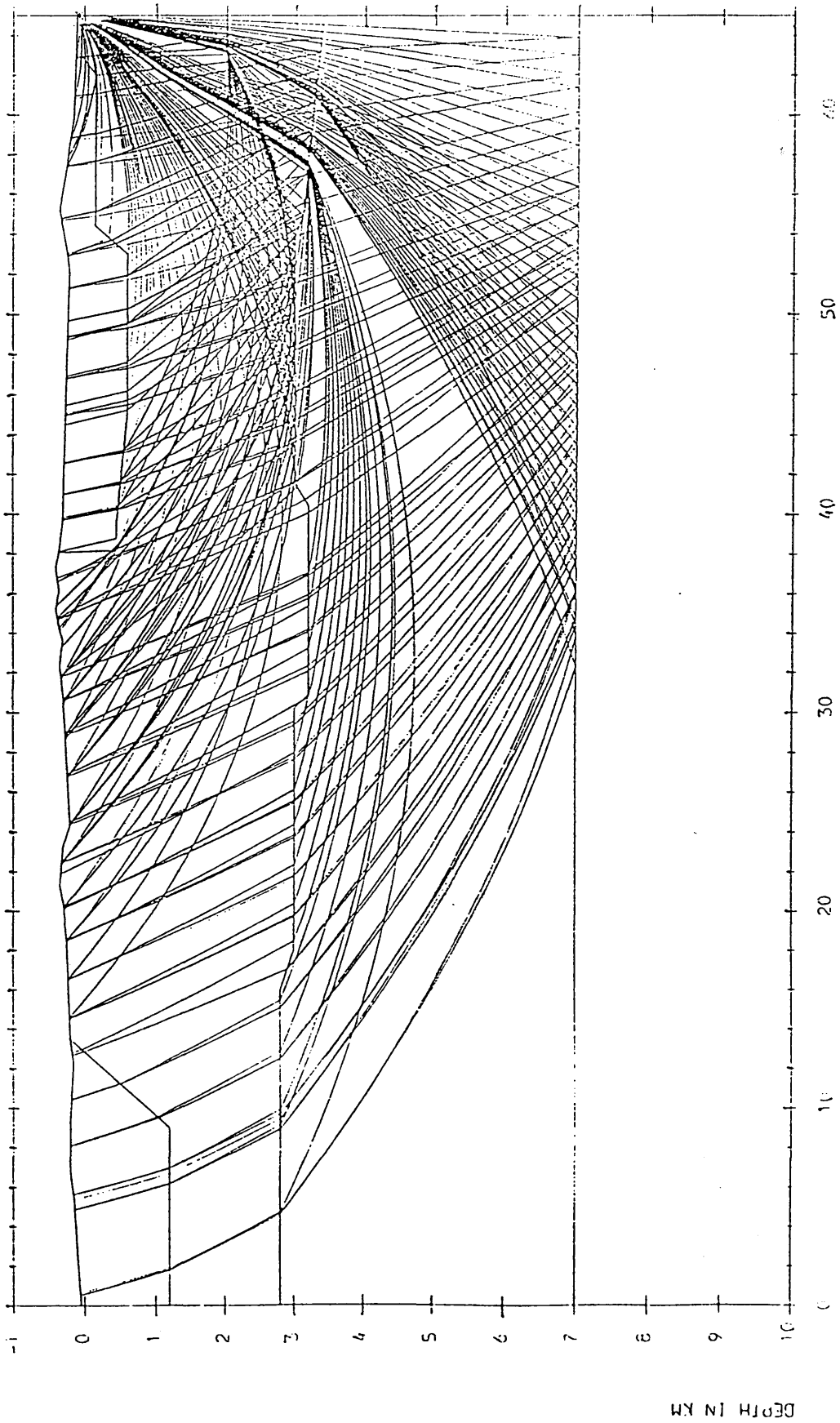

Fig. 5.46 Rays used to calculate the synthetic seismograms of Fig. 5.45

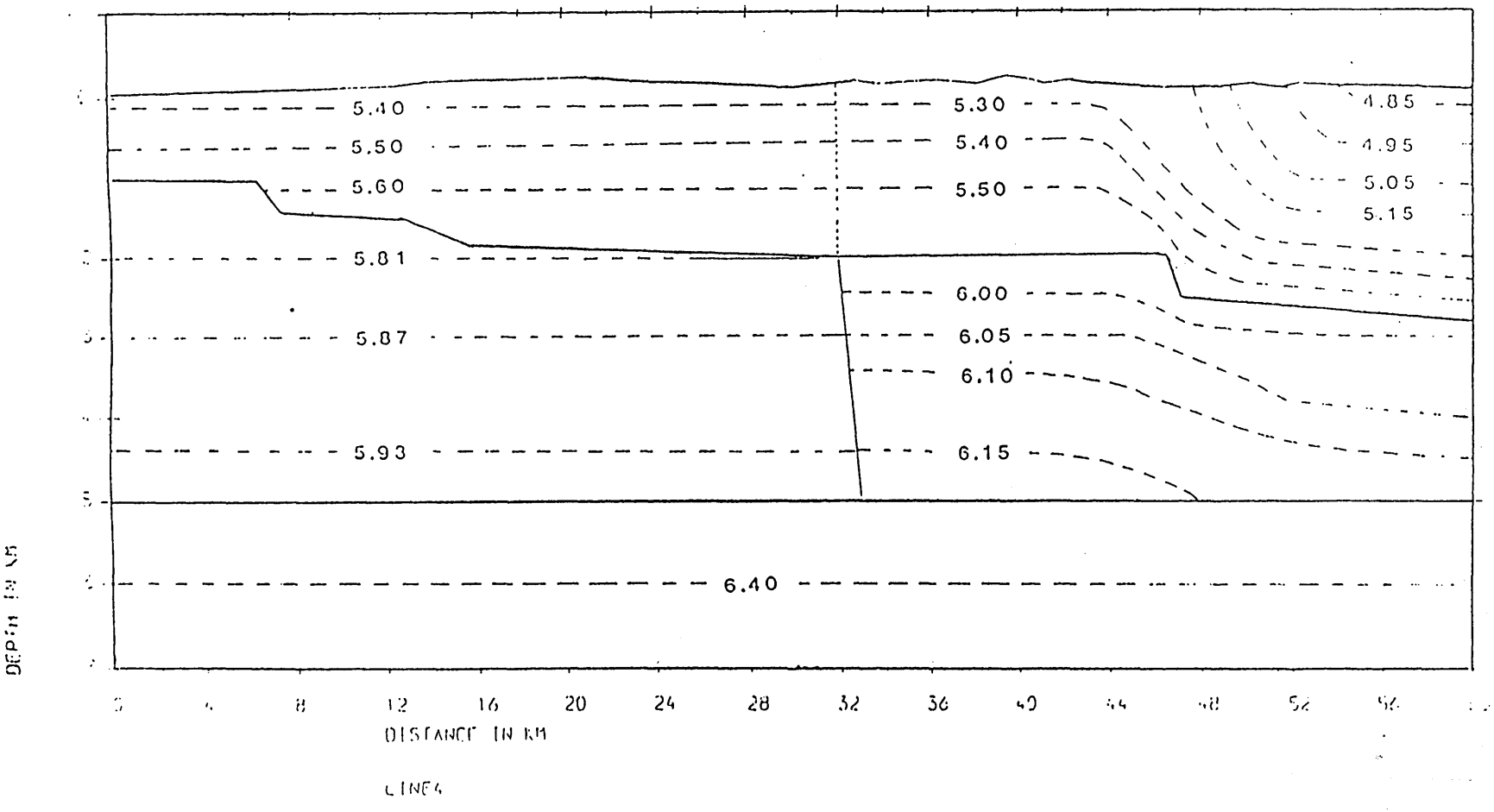

Fig. 5.47 P-wave velocity model along line 4 derived by raytracing.

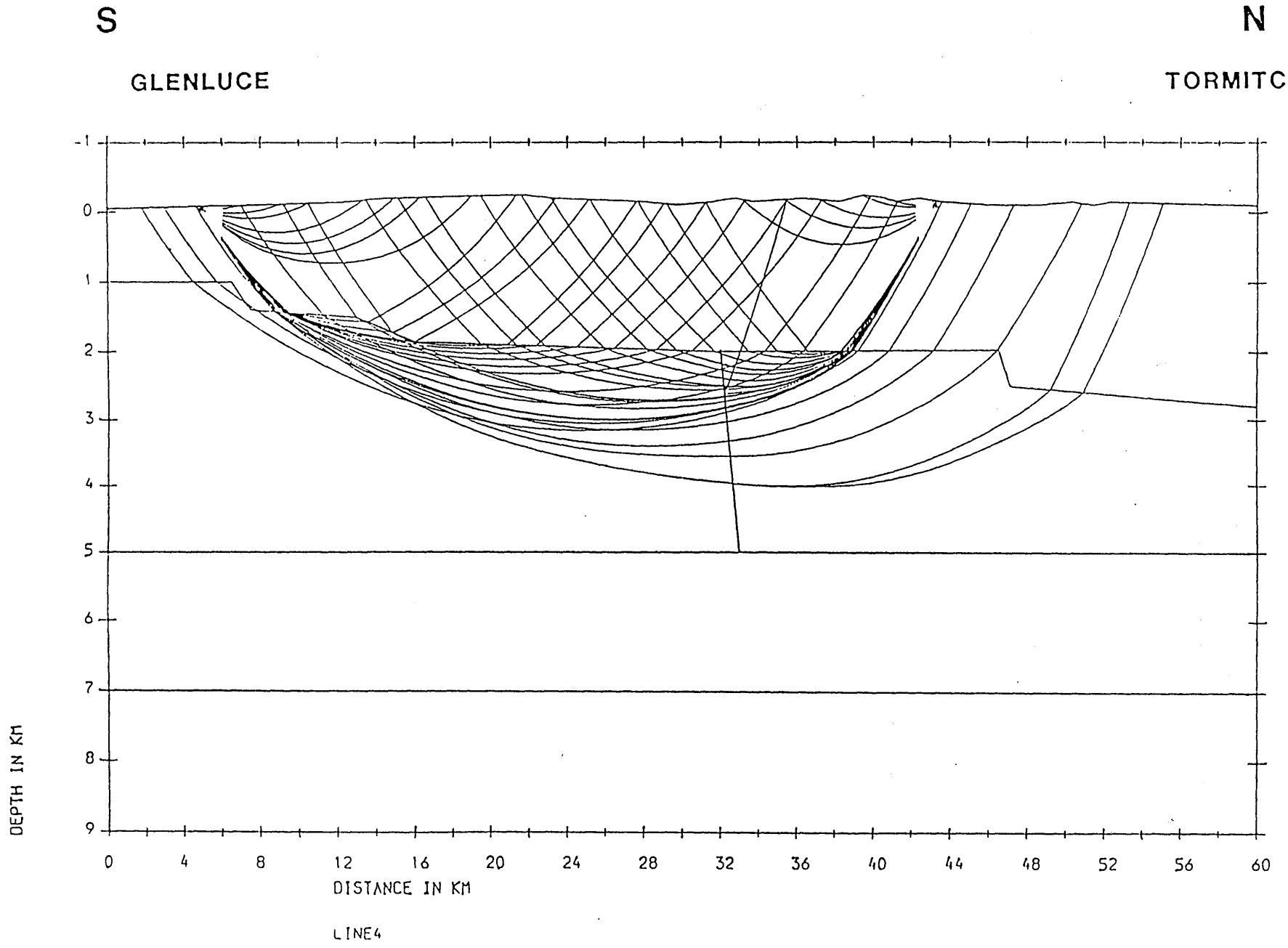

Fig. 5.48 Ray-paths used in the calculation of travel-times along line 4. Shotpoints are denoted (*).

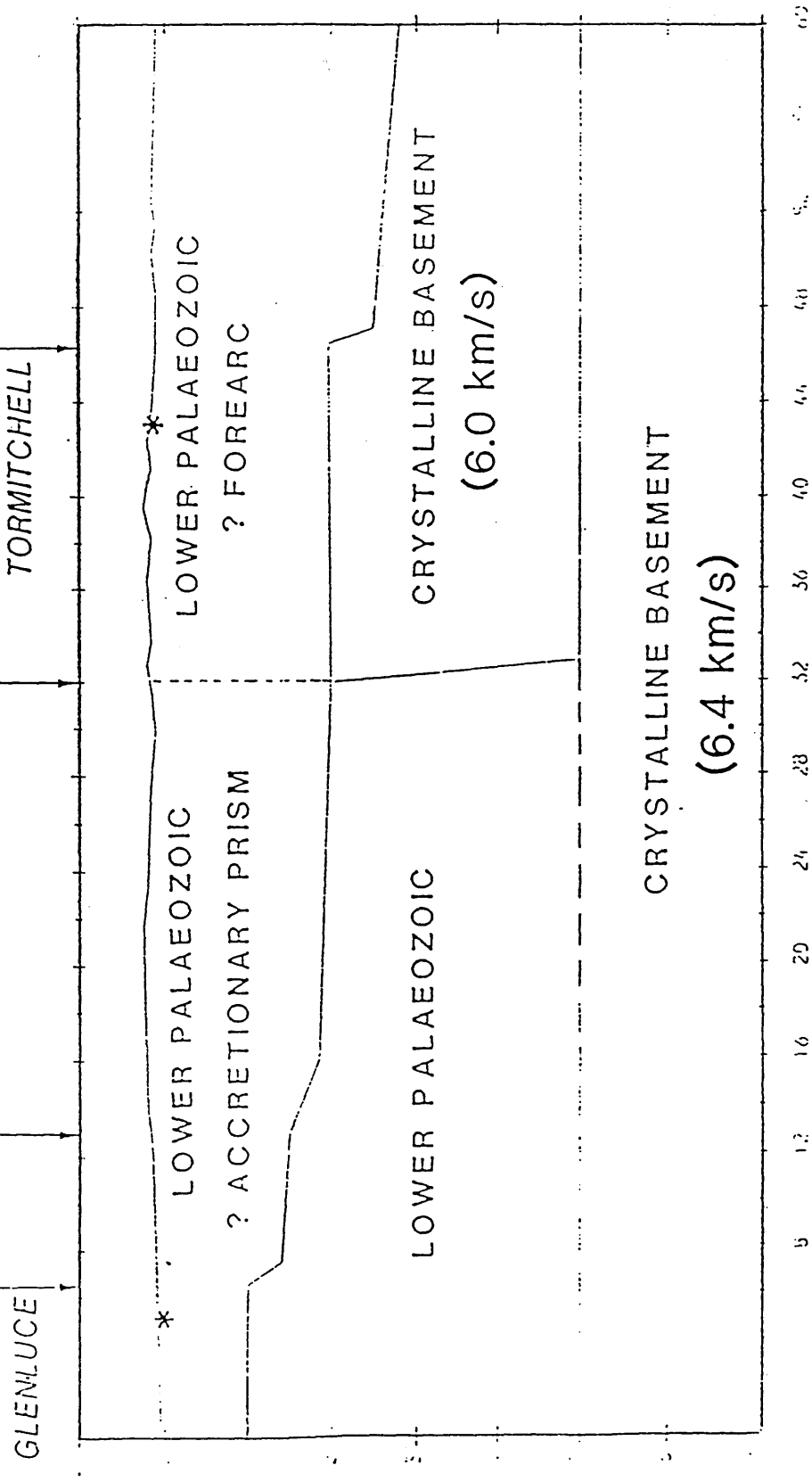

Fig. 5.49 Geological model along line 4 derived by raytracing. KGF- Kingledores Fault, KLF-Kerse Loch Fault, LHL-Leadhills Line, SUF- Southern Uplands Fault.

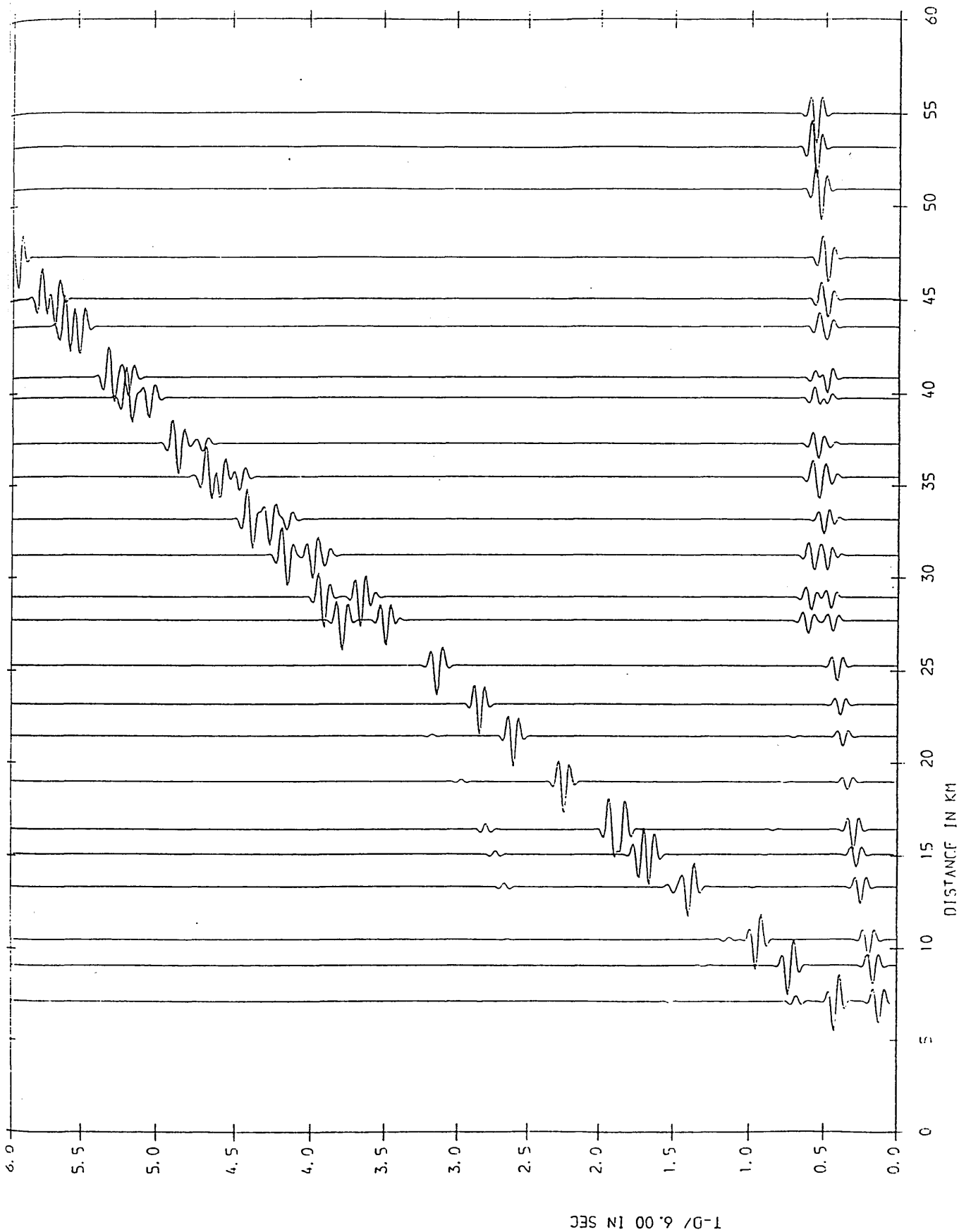

Fig. 5.50 Synthetic seismograms obtained along line4, Glenlucc shot.

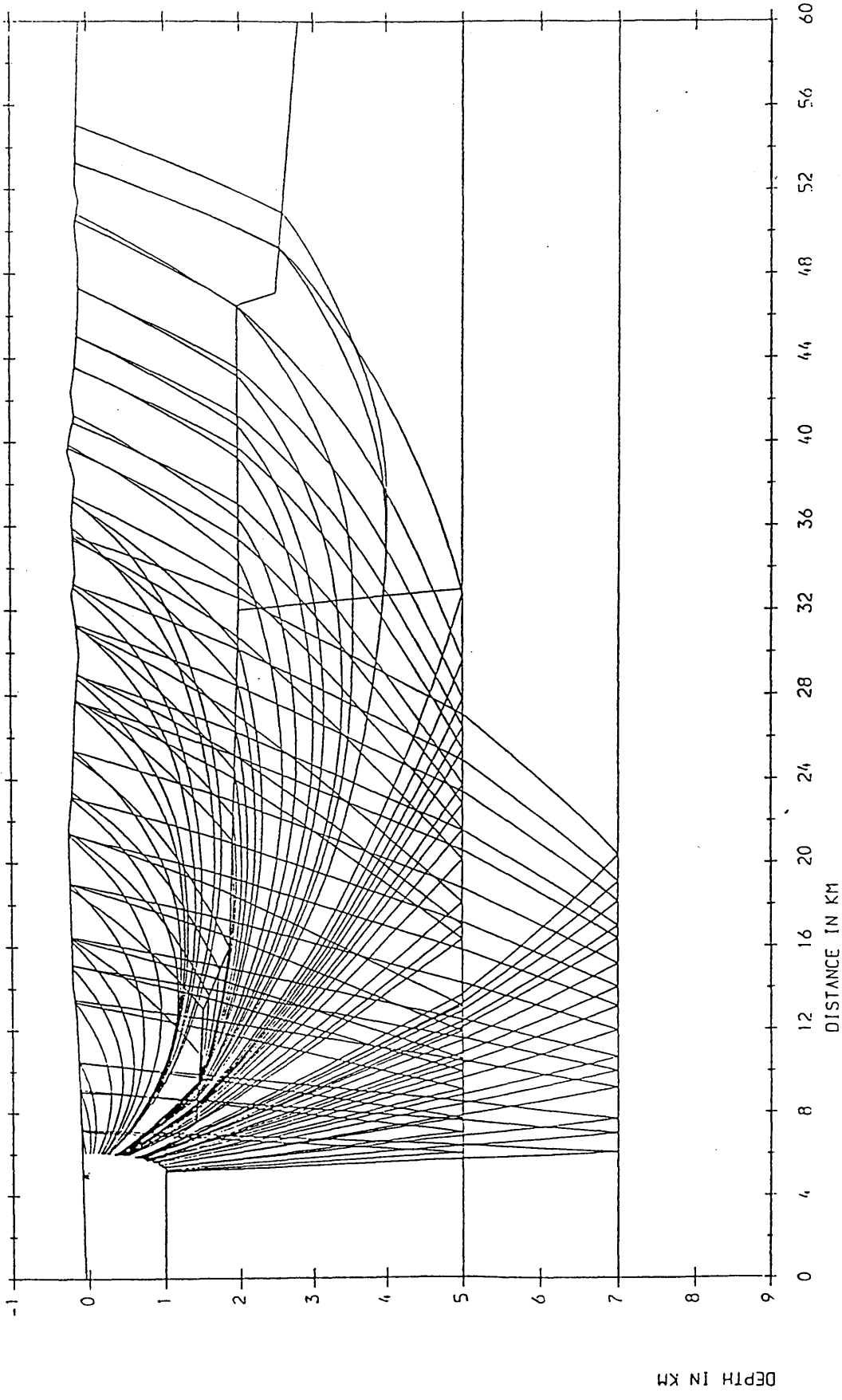

Fig. 5.51 Rays used to calculate the synthetic seismograms of Fig. 5.50.

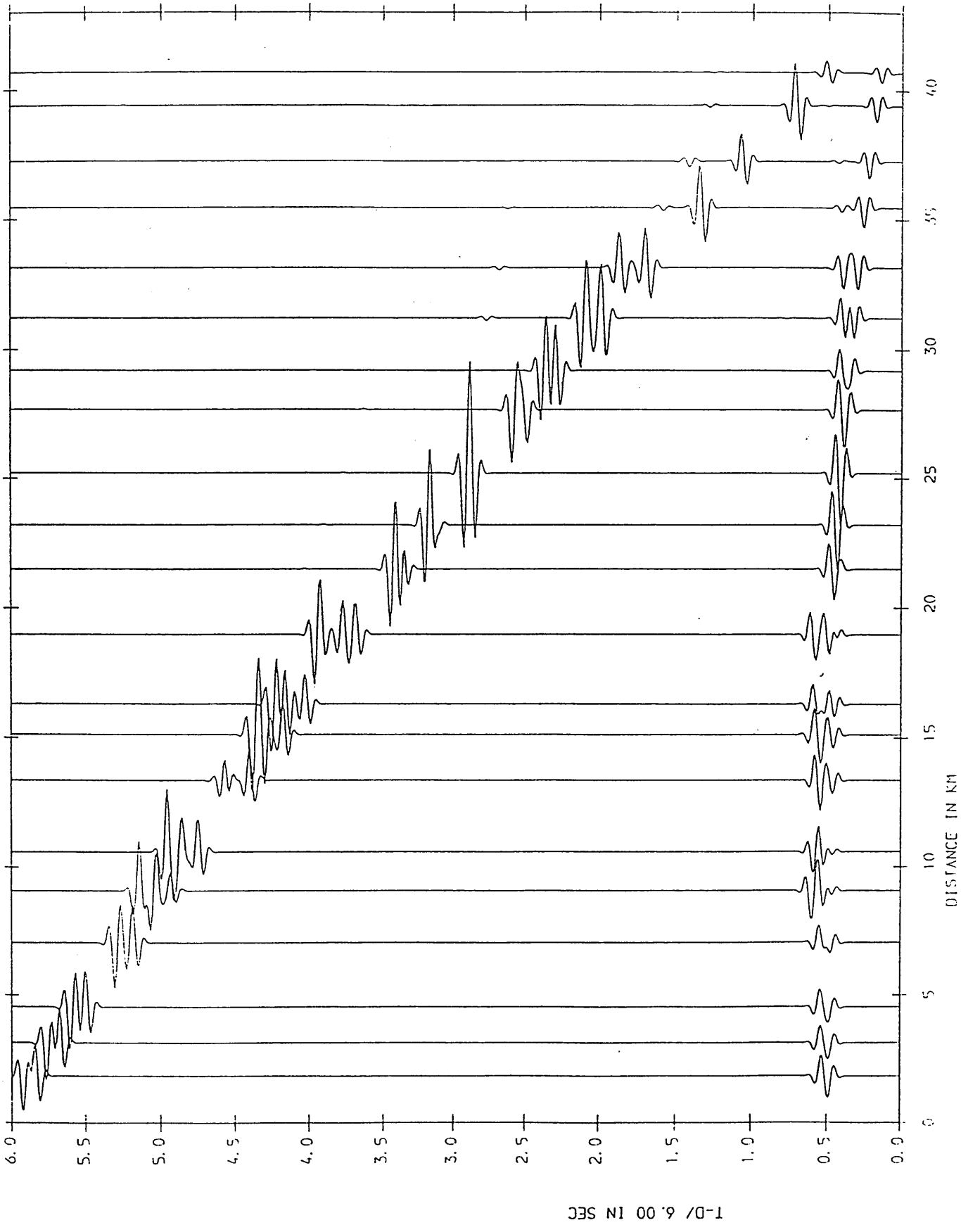

Fig. 5.52 Synthetic seismograms obtained along line 4, Tormitchell shot.

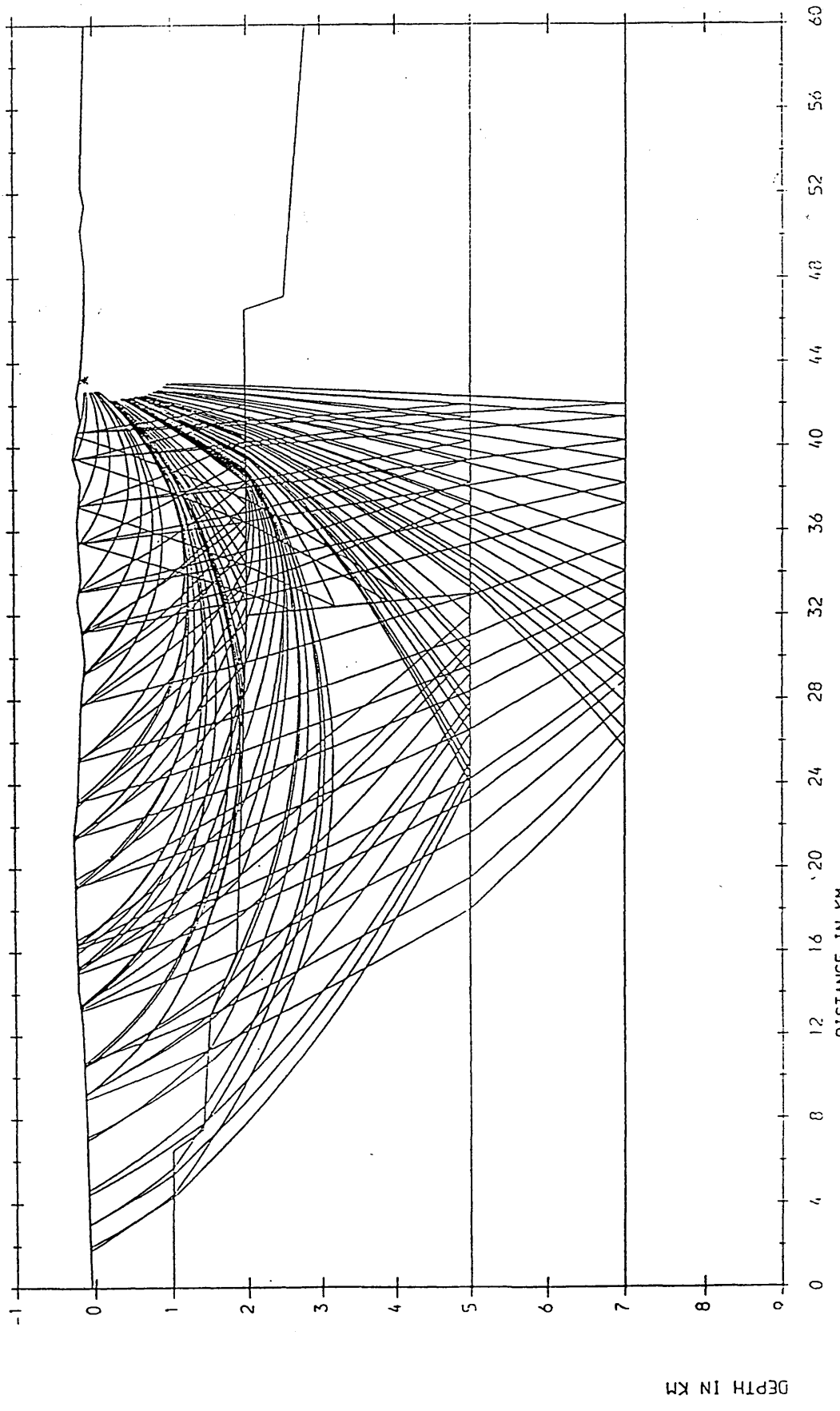

Fig. 5.53 Rays used to calculate the synthetic seismograms of Fig. 5.52.